

Thermohydraulic relationships for advanced water cooled reactors



INTERNATIONAL ATOMIC ENERGY AGENCY

IAEA

April 2001

The originating Section of this publication in the IAEA was:

Nuclear Power Technology Development Section
International Atomic Energy Agency
Wagramer Strasse 5
P.O. Box 100
A-1400 Vienna, Austria

THERMOHYDRAULIC RELATIONSHIPS FOR ADVANCED
WATER COOLED REACTORS
IAEA, VIENNA, 2001
IAEA-TECDOC-1203
ISSN 1011-4289

© IAEA, 2001

Printed by the IAEA in Austria
April 2001

FOREWORD

This report was prepared in the context of the IAEA's Co-ordinated Research Project (CRP) on Thermohydraulic Relationships for Advanced Water Cooled Reactors, which was started in 1995 with the overall goal of promoting information exchange and co-operation in establishing a consistent set of thermohydraulic relationships which are appropriate for use in analyzing the performance and safety of advanced water cooled reactors. For advanced water cooled reactors, some key thermohydraulic phenomena are critical heat flux (CHF) and post CHF heat transfer, pressure drop under low flow and low pressure conditions, flow and heat transport by natural circulation, condensation of steam in the presence of non-condensables, thermal stratification and mixing in large pools, gravity driven reflooding, and potential flow instabilities.

Thirteen institutes co-operated in this CRP during the period from 1995 to 1999.

The IAEA acknowledges the strong efforts of the following persons in preparing this report: N. Aksan (Paul Scherrer Institute, Switzerland), F. D'Auria (University of Pisa, Italy), D.C. Groeneveld (AECL Research, Canada), P.L. Kirillov (Institute of Physics and Power Engineering, Russian Federation) and D. Saha (Bhabha Atomic Research Centre, India). The IAEA officers responsible for this publication were A. Badulescu and J. Cleveland of the Division of Nuclear Power.

EDITORIAL NOTE

The use of particular designations of countries or territories does not imply any judgement by the publisher, the IAEA, as to the legal status of such countries or territories, of their authorities and institutions or of the delimitation of their boundaries.

The mention of names of specific companies or products (whether or not indicated as registered) does not imply any intention to infringe proprietary rights, nor should it be construed as an endorsement or recommendation on the part of the IAEA.

CONTENTS

CHAPTER 1. INTRODUCTION	1
1.1. Overview of advanced water cooled reactors.....	1
1.2. Background for the co-ordinated research project	4
1.3. Objectives	5
1.4. Participants.....	5
1.5. Summary of activities within the co-ordinated research project	6
1.6. Structure of this report.....	6
References to Chapter 1	6
CHAPTER 2. THERMOHYDRAULIC PHENOMENA OF INTEREST TO ADVANCED WATER COOLED REACTORS	9
References to Chapter 2	13
CHAPTER 3. A GENERAL CHF PREDICTION METHOD FOR ADVANCED WATER COOLED REACTORS	15
Nomenclature	15
3.1. Introduction	16
3.2. CHF mechanisms.....	18
3.2.1. General	18
3.2.2. DNB (departure from nucleate boiling)	18
3.2.3. Helmholtz instability.....	19
3.2.4. Annular film dryout	19
3.2.5. Unstable or periodic dryout	20
3.2.6. Slow dryout.....	20
3.3. CHF database.....	20
3.3.1. General	20
3.3.2. Tube database.....	22
3.3.3. Bundle database	24
3.4. CHF prediction methodology	24
3.4.1. General	24
3.4.2. Analytical models	26
3.4.3. Empirical CHF prediction methods	26
3.4.4. Application to bundle geometries	28
3.5. Recommended CHF prediction method for advanced water-cooled reactors	30
3.5.1. Tubes.....	30
3.5.2. Rod bundles	31
3.5.3. Correction factors.....	31
3.6. Assessment of accuracy of the recommended prediction methods	37
3.6.1. CHF look up table assessment	37
3.6.2. Accuracy of bundle CHF prediction methods	37
3.6.3. Impact of accuracy of CHF model on cladding temperature prediction.....	39
3.7. CHF concerning accident conditions.....	39
3.7.1. General	39
3.7.2. Effect of the axial/radial node size.....	39
3.7.3. Transient effects on CHF	42

3.8. Recommendations and final remarks	42
References to Chapter 3	43
CHAPTER 4. GENERAL FILM BOILING HEAT TRANSFER PREDICTION METHODS FOR ADVANCED WATER COOLED REACTORS	
	49
Nomenclature	49
4.1. Introduction	50
4.2. Description of post-CHF phenomena	52
4.2.1. General	52
4.2.2. Transition boiling	53
4.2.3. Minimum film boiling temperature	55
4.2.4. Flow film boiling	56
4.3. Film boiling data base	60
4.3.1. General	60
4.3.2. Tube and annuli	61
4.3.3. Bundle	61
4.4. Overview of film boiling prediction methods	61
4.4.1. General	61
4.4.2. Pool film boiling equations	66
4.4.3. Film boiling models	70
4.4.4. Flow film boiling correlations	75
4.4.5. Look-up tables for film boiling heat transfer in tubes	86
4.5. Recommended/most recent film boiling prediction methods	88
4.5.1. Pool film boiling	88
4.5.2. Flow film boiling	89
4.5.3. Radiation heat transfer in film boiling	90
4.5.4. Correlations for single phase heat transfer to superheated steam	91
4.5.5. Application to rod bundles	91
4.6. Application to film boiling prediction methods codes	93
4.6.1. General	93
4.7. Conclusions and final remarks	94
References to Chapter 4	95
CHAPTER 5. PRESSURE DROP RELATIONSHIPS	
	109
Nomenclature	109
5.1. Introduction	110
5.2. Survey of situations where pressure drop relationships are important	111
5.2.1. Distinction between core and system approach	113
5.2.2. Geometric conditions of interest	113
5.3. Correlations for design and analysis	115
5.3.1. Components of pressure drop	115
5.3.2. Configurations	117
5.3.3. Friction pressure drop correlations	118
5.3.4. Local pressure drop	128
5.3.5. Importance of void fraction correlations	132
5.3.6. Review of previous assessments	134

5.3.7. Proposed assessment procedure for diabatic vertical flow	142
5.3.8. Results of assessment.....	142
5.4. Comparisons of correlations as they stand in codes	146
5.4.1. Physical models in system codes	147
5.5. Final remarks	149
References to Chapter 5	151
CHAPTER 6. REMARKS AND FUTURE NEEDS	163
References to Chapter 6	165
APPENDICES I–XIX	
APPENDIX I: ACTIVITIES CONTRIBUTED TO THE CRP BY THE RESEARCH GROUPS AT THE PARTICIPATING INSTITUTES	169
APPENDIX II: THE 1995 LOOK-UP TABLE FOR CRITICAL HEAT FLUX IN TUBES	175
APPENDIX III: CHF PREDICTION FOR WWER-TYPE BUNDLE GEOMETRIES	183
APPENDIX IV: AECL LOOK-UP TABLE FOR FULLY DEVELOPED FILM-BOILING HEAT-TRANSFER COEFFICIENTS ($\text{kW m}^{-2} \text{K}^{-1}$)	190
APPENDIX V: IPPE TABLE OF HEAT TRANSFER COEFFICIENTS FOR FILM BOILING AND SUPERHEATED STEAM FOR TUBES	241
APPENDIX VI: CIAE METHOD FOR DETERMINING FILMBOILING HEAT TRANSFER	271
APPENDIX VII: TWO-PHASE VISCOSITY MODELS FOR USE IN THE HOMOGENEOUS MODEL FOR TWO-PHASE PRESSURE DROP	273
APPENDIX VIII: TWO-PHASE PRESSURE DROP CORRELATIONS BASED ON THE MULTIPLIER CONCEPT	274
APPENDIX IX: DIRECT EMPIRICAL TWO-PHASE PRESSURE DROP CORRELATIONS.....	281
APPENDIX X: FLOW PATTERN SPECIFIC PRESSURE DROP CORRELATIONS FOR HORIZONTAL FLOW	283
APPENDIX XI: FLOW PATTERN SPECIFIC PRESSURE DROP FOR VERTICAL UPWARD FLOW	288
APPENDIX XII: INTERFACIAL FRICTION MODELS GIVEN BY SOLBRIG (1986).....	291

APPENDIX XIII:	SLIP RATIO MODELS FOR CALCULATION OF VOID FRACTION.....	294
APPENDIX XIV:	$K\beta$ MODELS FOR THE CALCULATION OF VOID FRACTION.....	295
APPENDIX XV:	DRIFT FLUX MODELS FOR THE CALCULATION OF VOID FRACTION.....	296
APPENDIX XVI:	MISCELLANEOUS EMPIRICAL CORRELATIONS FOR VOID FRACTION.....	304
APPENDIX XVII:	COMPILATION OF DATA.....	305
APPENDIX XVIII:	DETAILED RESULTS OF ASSESSMENT OF VOID FRACTION CORRELATIONS	310
APPENDIX XIX:	DETAILED RESULTS OF ASSESSMENT OF FLOW PATTERN DATA	319
ANNEX A:	INTERNATIONAL NUCLEAR SAFETY CENTER DATABASE	331
ANNEX B:	PREPARED METHODOLOGY TO SELECT RANGES OF THERMOHYDRAULIC PARAMETERS.....	335
CONTRIBUTORS TO DRAFTING AND REVIEW		343

Chapter 1

INTRODUCTION

1.1. OVERVIEW OF ADVANCED WATER COOLED REACTORS

In the second half of the 20th century nuclear power has evolved from the research and development environment to an industry that supplies 17% of the world's electricity. In these 50 years of nuclear development a great deal has been achieved and many lessons have been learned. At the end of 1998, according to data reported in the Power Reactor Information System, PRIS, of the IAEA, there were 434 nuclear power plants in operation and 34 under construction. Over eight thousand five hundred reactor-years of operating experience had been accumulated.

Due to further industrialization, economic development and projected increases in the world's population, global energy consumption will surely continue to increase into the 21st century. Based on IAEA's review of nuclear power programmes [IAEA (1998)] and plans of Member States, several countries, especially in the Far East, are planning to expand their nuclear power capacity considerably in the next 15–20 years.

The contribution of nuclear energy to near and medium term energy needs depends on several key issues. The degree of global commitment to sustainable energy strategies and recognition of the role of nuclear energy in sustainable strategies will impact its future use. Technological maturity, economic competitiveness and financing arrangements for new plants are key factors in decision making. Public perception of energy options and related environmental issues as well as public information and education will also play a key role in the introduction of evolutionary designs. Continued vigilance in nuclear power plant operation, and enhancement of safety culture and international co-operation are highly important in preserving the potential of nuclear power to contribute to future energy strategies.

To assure that nuclear power remains a viable option in meeting energy demands in the near and medium terms, new reactor designs, aimed at achieving certain improvements over existing designs are being developed in a number of countries. Common goals for these new designs are high availability, user-friendly features, competitive economics and compliance with internationally recognized safety objectives.

The early development of nuclear power was to a large extent conducted on a national basis. However, for advanced reactors, international co-operation is playing an important role, and the IAEA promotes international co-operation in advanced reactor development and application. Various organizations are involved, including governments, industries, utilities, universities, national laboratories, and research institutes.

Worldwide there is considerable experience in nuclear power technology and especially in light water reactor (LWR) and heavy water (HWR) technology. Of the operating plants, 346 are LWRs totaling 306 GW(e) and 31 are HWRs totaling 15 GW(e). The experience and lessons learned from these plants are being incorporated into new water cooled reactor designs. Utility requirements documents have been formulated to guide these activities by incorporating this experience with the aim of reducing costs and licensing uncertainties by establishing a technical foundation for the new designs.

The full spectrum of advanced water cooled reactor designs or concepts covers different types of designs — evolutionary ones, as well as innovative designs that require substantial development efforts. A natural dividing line between these two categories arises from the necessity of having to build and operate a prototype or demonstration plant to bring a concept with much innovation to commercial maturity, since such a plant represents the major part of the resources needed. Designs in both categories need engineering, and may also need research and development (R&D) and confirmatory testing prior to freezing the design of either the first plant of a given line in the evolutionary category, or of the prototype and/or demonstration plant for the second category. The amount of such R&D and confirmatory testing depends on the degree of both the innovation to be introduced and the related work already done, or the experience that can be built upon. This is particularly true for designs in the second category where it is entirely possible that all a concept needs is a demonstration plant, if development and confirmatory testing is essentially completed. At the other extreme, R&D, feasibility tests, confirmatory testing, and a prototype and/or demonstration plant are needed in addition to engineering. Different tasks have to be accomplished and their corresponding costs in qualitative terms are a function of the degree of departure from existing designs. In particular, a step increase in cost arises from the need to build a reactor as part of the development programme (see Figure 1.1).

Advanced design	Evolutionary design
Different types of new nuclear plants are being developed today that are generally called advanced reactors. In general, an advanced plant design is a design of current interest for which improvement over its predecessors and/or existing designs is expected. Advanced designs consist of evolutionary designs and designs requiring substantial development efforts. The latter can range from moderate modifications of existing designs to entirely new design concepts. They differ from evolutionary designs in that a prototype or a demonstration plant is required, or that insufficient work has been done to establish whether such a plant is required.	An evolutionary design is an advanced design that achieves improvements over existing designs through small to moderate modifications, with a strong emphasis on maintaining proven design features to minimise technological risks. The development of an evolutionary design requires at most engineering and confirmatory testing.
	Innovative design
	An innovative design is an advanced design which incorporates radical conceptual changes in design approaches or system configuration in comparison with existing practice. Substantial R&D, feasibility tests, and a prototype or demonstration plant are probably required.

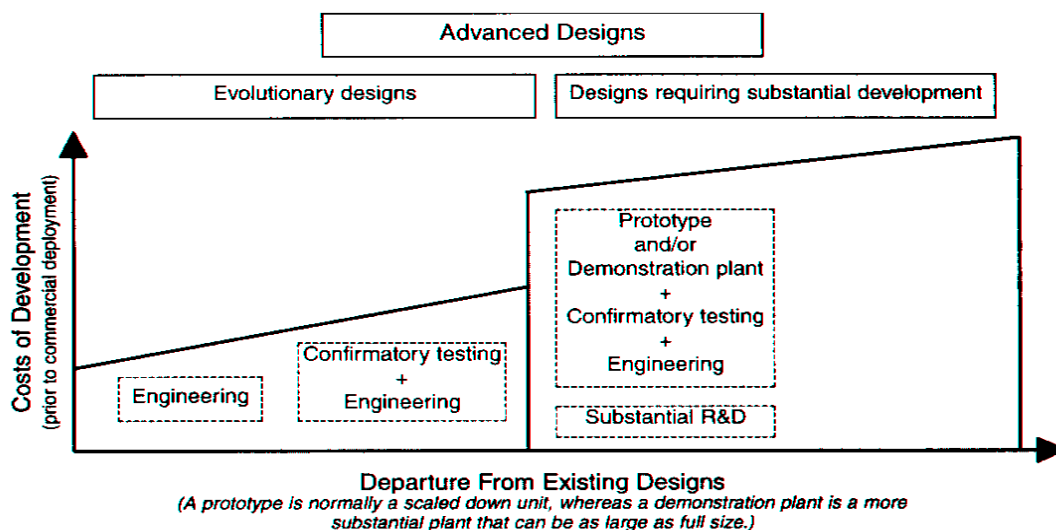


Figure 1.1. Efforts and development costs for advanced designs versus departure from existing designs (Terms are excerpted from IAEA-TECDOC-936).

Large water cooled reactors with power outputs of 1300 MW(e) and above, which possess inherent safety characteristics (e.g. negative Doppler and moderator temperature coefficients, and negative moderator void coefficient) and incorporate proven, active engineered systems to accomplish safety functions are being developed. Other designs with power outputs from, for example, 220 MW(e) up to about 1300 MW(e) which also possess inherent safety characteristics and which place more emphasis on utilization of passive safety systems are also being developed. Passive safety systems are based on natural forces such as convection and gravity, making safety functions less dependent on active systems and components like pumps and diesel generators. Table 1.1 presents a list of advanced water cooled reactors under development¹.

TABLE 1.1. SURVEY OF ADVANCED WATER COOLED REACTOR DESIGNS UNDER DEVELOPMENT

	Name	Type	Power, MW(e)	Supplier/designer	Design status ¹
Evolutionary, large-size plants	APWR	PWR	1300	Westinghouse, USA& Mitsubishi, Japan	Conceptual design
	ABWR	BWR	1300	General Electric, USA in co-operation with Hitachi and Toshiba, Japan	Detailed design
	BWR 90	BWR	1200	ABB Atom, Sweden	Detailed design
	EP1000 ³	PWR	1000	Westinghouse, USA, Genesi, Italy, EUR	Basic design
	EPR	PWR	1545	Nuclear Power International (NPI)	Basic design
	ESBWR ²	BWR	1190	General Electric, USA	Preliminary design
	KNGR	PWR	1350	Korea Electric Power Corp., Republic of Korea	Basic design
	Sizewell C	PWR	1250	National Nuclear Corp. (NNC), UK	Conceptual design
	System 80+	PWR	1350	ABB Combustion Engineering, USA	Detailed design
	SWR 1000	BWR	1000	Siemens, Germany	Conceptual design
	WWER-1000(V-392)	PWR	1000	Atomenergoprojekt/Gidropress, Russia	Basic design
	CP-1300	PWR	1300	Korea Advanced Institute of Science and Technology, Republic of Korea	Conceptual design
	CANDU 9	HWR	900–1300	Atomic Energy of Canada, Ltd	Detailed design
Evolutionary, medium-size plants	AC-600	PWR	600	China National Nuclear Corp. (CNNC) China	Conceptual design
	AP-600	PWR	600	Westinghouse, USA	Detailed design
	HSBWR	BWR	600	Hitachi Ltd., Japan	Basic design
	MS-600	PWR	600	Mitsubishi, Japan	Detailed design
	WWER-640 (V-407)	PWR	640	Atomenergoprojekt/Gidropress, Russia	Detailed design
	CANDU 6	HWR	670	Atomic Energy of Canada, Ltd.	Detailed design
	AHWR ⁴	HWR	220	Bhabha Atomic Research Centre, India	Basic design
Design concepts requiring substantial development	ISIS	PWR	300	Ansaldo Spa., Italy	Conceptual design
	JPSR	PWR	630	Japan Atomic Energy Research Institute (JAERI), Japan	Design study
	PIUS	PWR	650	ABB Atom, Sweden	Basic design
	SPWR	PWR	600	Japan Atomic Energy Research Institute (JAERI), Japan	Conceptual design
	VPBER-600	PWR	630	OKBM, Russia	Conceptual design

¹ The design status classification refers to the IAEA (1997a), Terms for Describing New, Advanced NPPs.

² ESBWR (and JSBWR in Japan) is an enlarged version of GE's SBWR design.

³ EP 1000 (in Europe) represents an enlarged version of AP-600.

⁴ Boiling light water cooled, heavy water moderated.

¹ For detailed descriptions of these designs see IAEA (1997c and 1997d).

1.2. BACKGROUND FOR THE CO-ORDINATED RESEARCH PROJECT

The nuclear industry and regulatory bodies have developed thermohydraulics codes for predicting the performance of water cooled reactors under normal, transient and accident conditions. These codes are used for plant design, evaluation of safety margin, establishment of emergency procedures and operator training. These codes essentially solve mass, momentum and energy balance equations and include detailed representations of thermohydraulic relationships and thermophysical properties.

Extensive validation programmes have been carried out to demonstrate the applicability of the codes to plants, considering the stated objectives. These have been conducted in national and international contexts at four levels, involving the use of:

- fundamental experiments;
- separate effects test facilities (SETF);
- integral test facilities (ITF);
- plant data.

Experimental data have been extensively compared with code predictions including International Standard Problems of the OECD Committee on the Safety of Nuclear Installations (CSNI) and IAEA standard problem exercises.

The present situation in relation to the development, validation and use of system codes, can be summarized as follows:

- the codes have reached an acceptable degree of maturity though the reliable application is still limited to the validation domain;
- the use of qualified codes is more and more requested for assessing the safety of existing reactors, and for designing advanced reactors;
- code validation criteria and detailed qualification programmes have been established [OECD-NEA-CSNI (1989, 1987, 1994 and 1996b)];
- methodologies to evaluate the ‘uncertainty’ (i.e. the error) in the prediction of nuclear plant behaviour by system codes have been proposed and are being tested;
- problems like user effect (i.e. influence of code users on the predictions) [OECD-NEA-CSNI (1995)] nodalization qualification, quantification of code accuracy (i.e. ranking of the error in the comparison between measured and calculated trend), have been dealt with and experience is currently available;
- relevant activities have been recently completed that are coordinated by the OECD Committee on the Safety of Nuclear Installations (CSNI). These include:
 - the state of the art report on themalhydraulics of emergency core cooling [OECD-NEA-CSNI (1989)];
 - the set-up of the ITF code validation matrix [OECD-NEA-CSNI (1987, 1992 and 1996b)];
 - the set-up of the SETF code validation matrix including the identification and the definition of the phenomena that must be predicted by codes [OECD-NEA-CSNI (1994)];
 - the characterization of relevant plant status;
 - the lessons learned from the execution of the International Standard Problem exercises [OECD-NEA-CSNI (1996a and 1996b)].

Clearly the performance of these codes is dependent on the accuracy and consistency of the representations of the thermohydraulic relationships and thermophysical properties data contained in the codes.

On the recommendation of the IAEA's International Working Group on Advanced Technologies for Water Cooled Reactors (IWG-ATWR) a Coordinated Research Project (CRP) to establish a thermophysical properties database for light and heavy water reactor materials was organized with the objective to collect and systematize a thermophysical properties database for reactor materials under normal operating, transient and accident conditions. This CRP has been completed with the publication of IAEA (1997b). Also, on the recommendation of the IWG-ATWR, the CRP on Thermohydraulic Relationships for Advanced Water Cooled Reactors began in January 1995 with a duration of 4-years.

1.3. OBJECTIVES

The objectives of the CRP are (i) to systematically list the requirements for thermohydraulic relationships in support of advanced water cooled reactors during normal and accident conditions, and provide details of their database where possible and (ii) to recommend and document a consistent set of thermohydraulic relationships for selected thermohydraulic phenomena such as CHF and post-CHF heat transfer, pressure drop, and passive cooling for advanced water cooled reactors.

Key collaborative activities of the participating institutes within the CRP include:

- preparation of internationally peer reviewed and accepted prediction methods for CHF, post CHF heat transfer and pressure drop;
- establishment of a base of non-proprietary data and prediction methods available on the Internet.

1.4. PARTICIPANTS

The participating institutes and chief scientific investigators are:

Atomic Energy of Canada Ltd (AECL), Canada (D.C. Groeneveld)
China Institute of Atomic Energy (CIAE), China (Hanming Xu and Yuzhou Chen)
Nuclear Research Institute (NRI), Czech Republic (J. Macek)
Forschungszentrum Karlsruhe (FZK), Germany (F.J. Erbacher and X. Cheng)
Bhabha Atomic Research Centre (BARC), Mumbai, India (D. Saha)
University of Pisa, Italy (F. D'Auria)
Ente per le Nuove tecnologie, l'Energia e l'Ambiente (ENEA), Italy (S. Cevolani)
Korea Atomic Energy Research Institute (KAERI), Republic of Korea (M.K. Chung)
Korea Advanced Institute of Science and Technology (KAIST), Republic of Korea (S.H. Chang)
Institute of Physics and Power Engineering (IPPE), Russia (P. Kirillov)
Paul Scherrer Institute (PSI), Switzerland (N. Aksan)
Middle East Technical University, Turkey (O. Yesin)
Argonne National Laboratory, United States of America (J. Roglans-Ribas)

The programme has been co-ordinated through annual meetings of the chief scientific investigators from the participating institutes.

1.5. SUMMARY OF ACTIVITIES WITHIN THE CO-ORDINATED RESEARCH PROJECT

Brief summaries of CRP related activities contributed to the CRP by the research groups at the participating institutes are given in Appendix I.

1.6. STRUCTURE OF THIS REPORT

This chapter provides a brief discussion of the background for this CRP, the CRP objectives and lists the participating institutes. Chapter 2 provides a summary of important and relevant thermohydraulic phenomena for advanced water cooled reactors on the basis of previous work by the international community. Chapter 3 provides details of the database for critical heat flux, and recommends a prediction method which has been established through international co-operation and assessed within this CRP. Chapter 4 provides details of the database for film boiling heat transfer, and presents three methods for predicting film boiling heat transfer coefficients developed by institutes participating in this CRP. Chapter 5 compiles a range of pressure drop correlations, and reviews assessments of these relations and the resulting recommendations. Chapter 6 provides general remarks and conclusions, and comments on future research needs in thermohydraulics of advanced water cooled reactors.

Nomenclature is provided at the beginning of each chapter for which it is necessary, and references are provided at the end of each chapter. Chapter appendices present relevant information in more detail. The report contains two annexes. Annex A identifies the contents of a base of thermohydraulics data which has been contributed by institutes participating in the CRP and made openly available on the internet site which is maintained by International Nuclear Safety Center at Argonne National Laboratory. Annex B discusses a methodology to select the range of interest for parameters affecting CHF, film boiling and pressure drop in advanced water cooled reactors.

REFERENCES TO CHAPTER 1

IAEA, 1998, Energy, Electricity and Nuclear Power Estimates for the Period up to 2020, Reference Data Series No. 1, Vienna.

IAEA, 1997a, Terms for Describing New, Advanced Nuclear Power Plants, IAEA-TECDOC-936, Vienna.

IAEA, 1997b, Thermophysical Properties of Materials for Water Cooled Reactors, IAEA-TECDOC-949, Vienna.

IAEA, 1997c, Status of Advanced Light Water Cooled Reactor Designs: 1996, IAEA-TECDOC-968, Vienna.

IAEA, 1997d, Advances in Heavy Water Reactor Technology, IAEA-TECDOC-984, Vienna.

OECD-NEA-CSNI, 1987, CSNI Code Validation Matrix of Thermal-Hydraulic Codes for LWR LOCA and Transients, Report No. 132, Paris.

OECD-NEA-CSNI, 1989, Thermohydraulics of Emergency Core Cooling in Light Water Reactors, a State-of-the-Art Report, (SOAR) by a Group of Experts of the NEA Committee on the Safety of Nuclear Installations, Report No. 161, Paris.

OECD-NEA-CSNI, 1992, Wolfert, K., Glaeser, H., Aksan, N., CSNI validation matrix for PWR and BWR Codes, RL(92)12 (Proc. CSNI-Specialists Mtg on Transient Two-Phase flow, Aix-en-Provence), M. Reocreux, M.C. Rubinstein, eds.

OECD-NEA-CSNI, 1994, Aksan N., et al., Separate Effects Test Matrix for Thermal-Hydraulic Code Validation, R(93)14, Part 1 and Part 2, Volume I: Phenomena Characterization and Selection of Facilities and Tests, Volume 2: Facility and Experiments Characteristics.

OECDNEA-CSNI, 1995, Städtke H., User on the transient system code calculations, R(94)35.

OECD-NEA-CSNI, 1996a, Annunziato A., et al., CSNI Integral Test Facility Validation Matrix for the Assessment of Thermal-Hydraulic Codes for LWR LOCA and Transients, R(96)17.

OECD-NEA-CSNI, 1996b, Lessons Learned from OECD/CSNI ISP on Small Break LOCA, R(96)20, OECD/GD(97)10.

Chapter 2

THERMOHYDRAULIC PHENOMENA OF INTEREST TO ADVANCED WATER COOLED REACTORS

This chapter will provide a short summary on the important and relevant thermal-hydraulic phenomena for advanced water cooled reactor designs in addition to the relevant thermal-hydraulic phenomena identified for the current generation of light water reactors (LWRs). The purpose of these relevant phenomena lists is that they can provide some guidance in development of research plans for considering further code development and assessment needs, and for the planning of experimental programs.

All ALWRs incorporate significant design simplifications, increased design margins, and various technical and operational procedure improvements, including better fuel performance and higher burnup, a better man-machine interface using computers and improved information displays, greater plant standardization, improved constructability and maintainability, and better operator qualification and simulator training.

Design features proposed for the ALWRs include in some cases the use of passive, gravity-fed water supplies for emergency core cooling and natural circulation decay heat removal. This is the case, for example, for the AP600 and ESBWR. Further, natural circulation cooling is used for the ESBWR core for all conditions. Both plants also employ automatic depressurization systems (ADSs), the operation of which are essential during a range of accidents to allow adequate emergency core coolant injection from the lower pressure passive safety systems. The low flow regimes associated with these designs will involve natural circulation flow paths not typical of current LWRs. These ALWR designs emphasize enhanced safety by means of improved safety system reliability and performance. These objectives are achieved by means of safety system simplification and reliance on immutable natural forces for system operation. Simulating the performance of these safety systems is central to analytical safety evaluation of advanced LWRs with passive safety systems.

Specifically, the passive safety principles of the next generation ALWR designs include:

- (1) low volumetric heat generation rates,
- (2) reliance solely on natural forces, such as gravity and gas pressurization, for safety system operation,
- (3) dependence on natural phenomena, such as natural convection and condensation, for safety system performance.

The engineered safety features which incorporate these passive safety principles achieve increased reliability by means of system redundancy, minimization of system components, non-reliance on external power sources, and integral long term decay heat removal and containment cooling systems. In the design of the current generation of operating reactors, redundancy and independence have been designed into the protection systems so that no single failure results in loss of the protection function. Since the new ALWR designs incorporate significant changes from the familiar current LWR designs and place higher reliance on individual systems, a thorough understanding of these designs is needed with respect to system interactions. These interactions may occur between the passive safety systems e.g. the core makeup tanks and accumulators in the AP600, and the ADS system and

isolation condensers in the ESBWR. In addition, there is a close coupling in both plant designs between the reactor coolant system and the containment during an accident.

It can also be noted that in order to fully profit from the safety benefits due to the introduction of the passive safety systems, the behaviour of plants in which engineering safety features involving active components have been replaced with completely passive devices must be carefully studied to ensure the adequacy of the new design concepts for a wide spectrum of accident conditions. In fact, choice of passivity is an advantage in reducing the probability of the wrong operator interventions, especially in the short-term period after an accident, although passive systems require more sophisticated modelling techniques to ascertain that the natural driving forces that come into play can adequately accomplish the intended safety functions. Hence, there is also the need for an in-depth study of the basic phenomena concerning the design of ALWRs which make use of passive safety features.

Thermalhydraulic phenomena relevant to the evolutionary type ALWRs can be considered the same as those valid for the current generation LWRs. A suitable review of applicable phenomena can be found in [OECD-NE-CSNI (1987, 1989, 1994 and 1996)] and [NUREG (1987)]. For completeness, the list is reported in Table 2.1. A limited specific research activity in this area appears necessary, if one excludes new domains like Accident Management and special topics like instability in boiling channels where the interest is common to the present generation reactors.

In the case of advanced cooled reactors the foreseeable relevant thermalhydraulic phenomena can be grouped into two categories [see OECD-NEA-CSNI (1996)]:

- a) phenomena that are relevant also to the present generation reactors (Table 2.1)
- b) new kinds of phenomena and/or scenarios.

For the category a) the same considerations apply as for the evolutionary ALWRs and the phenomena of concern are therefore well documented in [OECD-NEA-CSNI (1987 and 1989)] and [NUREG (1987)]. However, it has to be noted that significance of various phenomena may be different for the passive and advanced reactors. Nevertheless, it is believed that the data base, understanding and modelling capabilities acquired for the current reactors are adequate for phenomena in category a.

Phenomena of the category b can be subdivided into three classes:

- b1) phenomena related to the containment processes and interactions with the reactor coolant system
- b2) low pressure phenomena
- b3) phenomena related specifically to new components, systems or reactor configurations

In current generation LWRs the thermalhydraulic behaviour of the containment system and of the primary system are studied separately. This is not any more possible in most of the new design concepts; suitable tools must be developed to predict the performance of the integrated system.

A speciality common to almost all the advanced design reactors is the presence of devices that depressurize the primary loop essentially to allow the exploitation of large amount of liquid at atmospheric pressure and to minimize the risk of high pressure core melt.

TABLE 2.1. RELEVANT THERMALHYDRAULIC PHENOMENA IDENTIFIED FOR THE CURRENT GENERATION REACTORS*

0	BASIC PHENOMENA	1 Evaporation due to Depressurisation 2 Evaporation due to Heat Input 3 Condensation due to Pressurisation 4 Condensation due to Heat Removal 5 Interfacial Friction in Vertical Flow 6 Interfacial Friction in Horizontal Flow 7 Wall to Fluid Friction 8 Pressure Drops at Geometric Discontinuities 9 Pressure Wave Propagation
1	CRITICAL FLOW	1 Breaks 2 Valves 3 Pipes
2	PHASE SEPARATION/VERTICAL FLOW WITH AND WITHOUT MIXTURE LEVEL	1 Pipes/Plena 2 Core 3 Downcomer
3	STRATIFICATION IN HORIZONTAL FLOW	1 Pipes
4	PHASE SEPARATION AT BRANCHES	1 Branches
5	ENTRAINMENT/DEENTRAINMENT	1 Core 2 Upper Plenum 3 Downcomer 4 Steam Generator Tube 5 Steam Generator Mixing Chamber (PWR) 6 Hot Leg with ECCI (PWR)
6	LIQUID-VAPOUR MIXING WITH CONDENSATION	1 Core 2 Downcomer 3 Upper Plenum 4 Lower Plenum 5 Steam Generator Mixing Chamber (PWR) 6 ECCI in Hot and Cold Leg (PWR)
7	CONDENSATION IN STRATIFIED CONDITIONS	1 Pressuriser (PWR) 2 Steam Generator Primary Side (PWR) 3 Steam Generator Secondary Side (PWR) 4 Horizontal Pipes
8	SPRAY EFFECTS	1 Core (BWR) 2 Pressuriser (PWR) 3 Once-Through Steam Generator Secondary Side (PWR)
9	COUNTERCURRENT FLOW/ COUNTERCURRENT FLOW LIMITATION	1 Upper Tie Plate 2 Channel Inlet Orifices (BWR) 3 Hot and Cold Leg 4 Steam Generator Tube (PWR) 5 Downcomer 6 Surgeline (PWR)
10	GLOBAL MULTIDIMENSIONAL FLUID TEMPERATURE, VOID AND FLOW DISTRIBUTION	1 Upper Plenum 2 Core 3 Downcomer 4 Steam Generator Secondary Side
11	HEAT TRANSFER: NATURAL OR FORCED CONVECTION SUBCOOLED/NUCLEATE BOILING DNB/DRYOUT POST CRITICAL HEAT FLUX RADIATION CONDENSATION	1 Core, Steam Generator, Structures 2 Core, Steam Generator, Structures 3 Core, Steam Generator, Structures 4 Core, Steam Generator, Structures 5 Core 6 Steam Generator, Structures
12	QUENCH FRONT PROPAGATION/REWET	1 Fuel Rods 2 Channel Walls and Water Rods (BWR)
13	LOWER PLENUM FLASHING	
14	GUIDE TUBE FLASHING (BWR)	
15	ONE AND TWO PHASE IMPELLER-PUMP BEHAVIOUR	
16	ONE AND TWO PHASE JET-PUMP BEHAVIOUR (BWR)	
17	SEPARATOR BEHAVIOUR	
18	STEAM DRYER BEHAVIOUR	
19	ACCUMULATOR BEHAVIOUR	
20	LOOP SEAL FILLING AND CLEARANCE (PWR)	
21	ECC BYPASS/DOWNCOMER PENETRATION	
22	PARALLEL CHANNEL INSTABILITIES (BWR)	
23	BORON MIXING AND TRANSPORT	
24	NONCONDENSABLE GAS EFFECT (PWR)	
25	LOWER PLENUM ENTRAINMENT	

* This table is applicable to LWRs and is expected to be applicable to WWERs as well.

TABLE 2.2. RELEVANT THERMALHYDRAULIC PHENOMENA OF INTEREST IN THE ADVANCED WATER COOLED DESIGN REACTORS

b1. Phenomena occurring due to the interaction between primary system and containment		
1. Behaviour of large pools of liquid:	–	thermal stratification – natural/forced convection and circulation – steam condensation (e.g. chugging, etc.) – heat and mass transfer at the upper interface (e.g. vaporization) – liquid draining from small openings (steam and gas transport)
2. Tracking of non-condensibles (essentially H ₂ , N ₂ , air):	–	effect on mixture to wall heat transfer coefficient – mixing with liquid phase – mixing with steam phase – stratification in large volumes at very low velocities
3. Condensation on the containment structures:	–	coupling with conduction in larger structures
4. Behaviour of containment emergency systems (PCCS, external air cooling, etc.):	–	interaction with primary cooling loops
5. Thermofluidynamics and pressure drops in various geometrical configurations:	–	3-D large flow pths e.g. around open doors and stair wells, connection of big pipes with pools, etc. – gasliquid phase separation at low Re and in laminar flow – local pressure drops
b2. Phenomena occurring at atmospheric pressure		
6. Natural circulation:	–	interaction among parallel circulation loops inside and outside the vessel – influence of non-condensables
7. Steam liquid interaction:	–	direct condensation – pressure waves due to condensation
8. Gravity driven reflood:	–	heat transfer coefficients – pressure rise due to vaporization – consideration of a closed loop
9. Liquid temperature stratification:	–	lower plenum of vessel – downcomer of vessel – horizontal/vertical piping
b3. Phenomena originated by the presence of new components and systems or special reactor configurations		
10. Behaviour of density locks:	–	stability of the single interface (temperature and density distribution) – interaction between two density locks
11. Behaviour of check valves:	–	opening/closure dynamics – partial/total failure
12. Critical and supercritical flow in discharge pipes and valves:	–	shock waves – supercritical flow in long pipes – behaviour of multiple critical section
13. Behaviour of Isolation Condenser	–	low pressure phenomena
14. Stratification of boron:	–	interaction between chemical and thermohydraulic problems – time delay for the boron to become effective in the core

In this case, the phenomena may be similar (or the same) as those reported for current generation LWRs (Table 2.1) but the range of parameters and their safety relevance can be much different.

In addition to the concerns specific to light-water-cooled reactors, the following concerns are specific to HWRs:

- I. Thermalhydraulics related to short fuel bundles located in long HWR-type horizontal channels, and on-line fuelling,
 - II. Thermalhydraulics related to radial and axial pressure-tube creep.
- Finally, the presence of new systems or components and some geometric specialities of advanced design reactors require the evaluation of additional scenarios and phenomena.

A list of identified phenomena belonging to subclasses b1, b2 and b3 is given in Table 2.2.

REFERENCES TO CHAPTER 2

OECD-NEA-CSNI, 1987, CSNI Code validation Matrix of Thermal-Hydraulic Codes for LWR LOCA and Transients, Rep. No. 132, Paris, France.

OECD-NEA CSNI, 1989, Thermohydraulics of Emergency Core Cooling in Light Water Reactors, a State-of-the-Art Report, (SOAR) by a Group of Experts of the NEA Committee on the Safety of Nuclear Installations, Rep. No. 161, Paris.

OECD-NEA-CSNI, 1994, Aksan, N., D'Auria, F., Glaeser, H., Pochard, R., Richards, C., Sjöberg, A., Separate Effects Test Matrix for Thermal-Hydraulic Code Validation, R(93)14, Vol. I: Phenomena Characterization and Selection of Facilities and Tests; Vol. 2: Facility and Experiments Characteristics.

OECD-NEA-CSNI, 1996, Aksan, N., D'Auria, F., Relevant Thermalhydraulic Aspects of Advanced Reactor Design, CSNI Status Report OCDE/GD(97)8, Paris.

NUREG, 1987, Compendium of ECCS Research for Realistic LOCA Analysis, USNRC Rep. 1230, Washington, DC.

Chapter 3

A GENERAL CHF PREDICTION METHOD FOR ADVANCED WATER COOLED REACTORS

NOMENCLATURE

C	Constant	-
CHF	Critical heat flux	kW/m ²
C _p	Specific heat	kJ/(kg °C)
D _e , D _{hy}	Hydraulic equivalent diameter	m
D _{he}	Heated equivalent diameter	m
D	Tube inside diameter	m
d	Fuel element diameter	m
E	Entrainment rate	kg/(m ² s)
g	Acceleration due to gravity	m/s ²
G	Mass flux	kg/(m ² s)
H	Enthalpy	kJ/kg
h	Heat transfer coefficient k	W/(m ² °C)
K, F	Correction factor	-
L _{sp}	Distance to upstream spacer plane	m
L	Heated length	m
P	Pressure	kPa
p	Element pitch	m
q	Surface heat flux	kW/m ²
T	Temperature	°C
U	Velocity	m/s
X	Quality	-
Z	Axial co-ordinate	m

GREEK SYMBOLS

α	Void fraction	-
δ	Inter element gap	m
ϕ	Surface heat flux	kW/m ²
λ	Latent heat of evaporation	kJ/kg
ρ	Density	kg/m ³
σ	Surface tension	N/m
y	Dimensionless mass flux	-
ΔH	Local subcooling, $h_s - h$	kJ/kg
ΔX	Bundle quality imbalance	-
ΔT	Local subcooling, $T_s - T$	°C
θ	Angle	degrees

SUBSCRIPTS

a	Actual value
avg	Average value
b	Bubble, bulk, boiling
BLA	Boiling length average

c	Critical, convection
CHF	Critical heat flux
DO	Dryout
f	Saturated liquid value
fg	Difference between saturated vapour and saturated liquid value
h, H	Heated
hom	Homogeneous
g	Saturated vapour
I, in	Inside, inlet
l	Liquid
m	Maximum
max.	Maximum
min	Minimum
nu	Non-uniform AFD
P/B	Pool boiling
o	Outside, outlet
rad	Radiation
s	Saturation value
sub	Subcooling
U	Uniform (AFD)
v	Vapour

ABBREVIATIONS

AFD	Axial flux distribution
BLA	Boiling length average
CHF	Critical heat flux
c/s	Cross section
DNB	Departure from nucleate boiling
DO	Dryout
FB	Film boiling
PDO	Post-dryout
RFD	Radial flux distribution

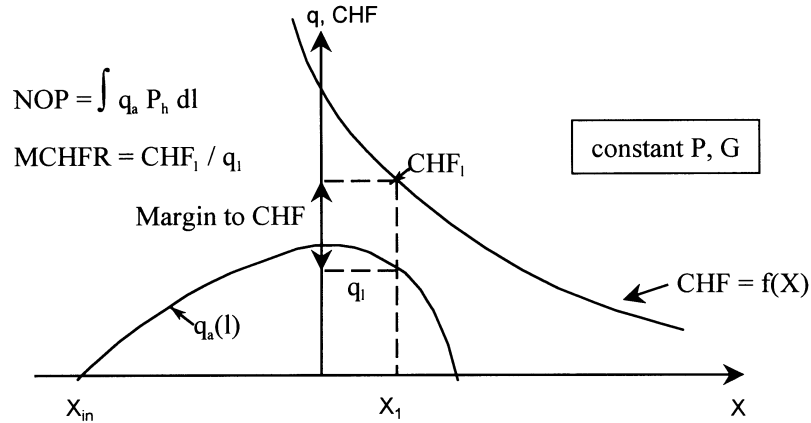
3.1. INTRODUCTION

The objective of this chapter is to recommend a validated CHF prediction method suitable for the assessment of critical power at both normal operating conditions and accident conditions in Advanced Water Cooled Reactors (AWCRs). This method can be implemented into systems codes such as RELAP, CATHARE, CATHENA as well as subchannel codes such as COBRA, ASSERT and ANTEO. The requirement of this prediction method has been discussed in more detail in previous CRP RCM meetings and expert meetings.

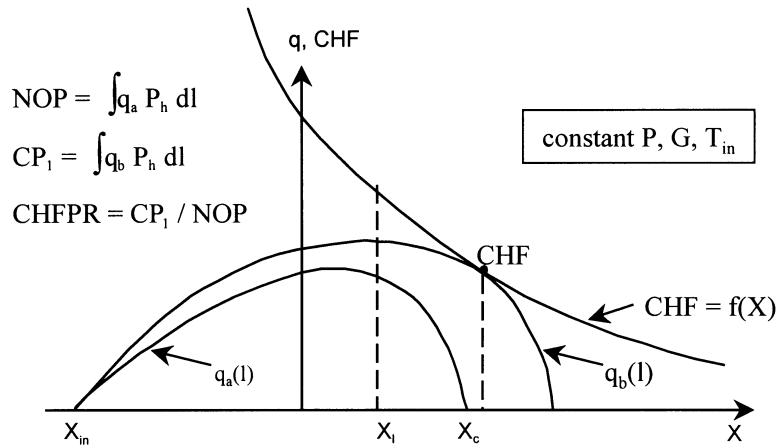
The two main applications for CHF predictions are:

- (i) to set the operating power with a comfortable margin to avoid CHF occurrence. This margin to CHF can be expressed in terms of Minimum Critical Heat Flux Ratio (MCHFR, ratio of CHF to local heat flux for the same pressure, mass flux and quality), Minimum Critical Heat Flux Power Ratio (MCHFPR, the ratio of power at initial CHF occurrence to the operating power for the same pressure mass

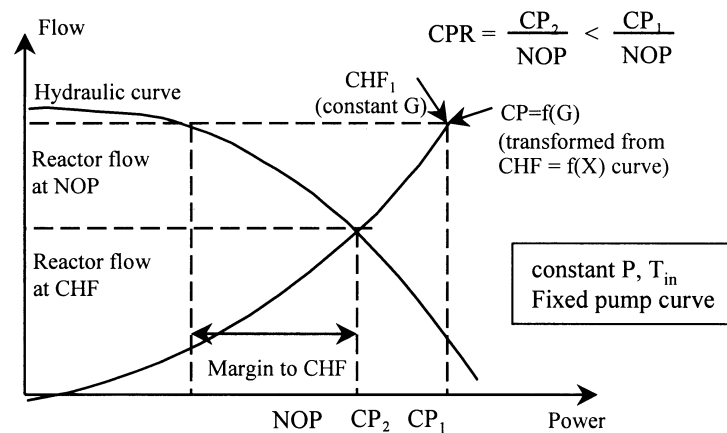
flux and inlet temperature), or Minimum Critical Power Ratio (MCPR, the ratio of reactor or fuel channel power at initial dryout occurrence to normal operating power for the same system, pressure and inlet temperature); the definition of these ratios is illustrated in Fig. 3.1. A detailed discussion has been provided by Groeneveld (1996). Most CHF prediction methods address this concern; these prediction methods provide best-estimate values of the *initial CHF* occurrence in a reactor core or fuel bundle.



(a) Schematic representation of definition of MCHFR



(b) Schematic representation of definition of MCHFPR



(c) Schematic representation of definition of MCPR

FIG. 3.1. Definition of margins to CHF as defined by MCHFR, MCHFPR and MCPR.

- (ii) to evaluate the thermalhydraulic and neutronic response to CHF occurrence in a reactor core. This requires knowledge of how CHF spreads in the reactor core, which in turn requires a best-estimate prediction of the *average CHF* for a section of the core and/or prediction of the variation of fuel surface area in dryout as a function of power.

This chapter is subdivided as follows: Section 3.2 discusses various CHF mechanisms, followed by a description of the CHF database in Section 3.3. In Section 3.4, CHF prediction methodologies are reviewed for both tubes and bundle geometries, ranging from correlations, subchannel codes, analytical models and look up tables. In Section 3.5, the recommended prediction methods for CHF in AWCRs are described, together with correction factors to account for various CHF separate effects. The assessment of the accuracy of the recommended prediction method when applied to steady state conditions is described in Section 3.6. Finally in Section 3.7 the prediction of CHF during transients such as LOCAs, flow and power transients are discussed.

The topic of CHF has been extensively researched during the past 30 years. Excellent reviews may be found in text books by Collier (1981), Tong (1965), Tong and Weisman (1996), Hewitt (1970) and Hetsroni (1982), and review articles by Bergles (1977), Tong (1972), Groeneveld and Snoek (1986), Weisman (1992) and Katto (1994).

3.2. CHF MECHANISMS

3.2.1. General

In forced convective boiling, the boiling crisis² occurs when the heat flux is raised to such a high level that the heated surface can no longer support continuous liquid contact. This heat flux is usually referred to as the critical heat flux (CHF). It is characterized either by a sudden rise in surface temperature caused by blanketing of the heated surface by a stable vapour layer, or by small surface temperature spikes corresponding to the appearance and disappearance of dry patches. The CHF normally limits the amount of power transferred, both in nuclear fuel bundles, and in conventional boilers. Failure of the heated surface may occur once the CHF is exceeded. This is especially true for highly subcooled CHF conditions. At high flows and positive dryout qualities, the post-dryout heat transfer is reasonably effective in keeping the heated surface temperatures at moderate levels, and operation in dryout may be sustained safely for some time.

In flow boiling the CHF mechanisms depend on the flow regimes and phase distributions, which in turn are controlled by pressure, mass flux and quality. For reactor conditions of interest, the flow quality generally has the strongest effect on CHF: the CHF decreases rapidly with an increase in quality. The change in CHF with pressure, mass flux and quality is illustrated in the tables of Appendix II. The following sections describe the CHF mechanisms encountered at different qualities and flow conditions.

3.2.2. DNB (departure from nucleate boiling)

- (i) *Nucleation induced.* This type of CHF is encountered at high subcooling (negative flow qualities) where heat is transferred very efficiently by nucleate boiling. Here the bubbles grow and collapse at the wall; between the bubbles some convection will take place.

² Other terms used to denote the boiling crisis: burnout, dryout, departure from nucleate boiling (DNB).

The CHF (or DNB) occurs at very high surface heat fluxes. It has been suggested [Collier (1981); Tong (1972)] that the CHF occurrence is due to the spreading of a drypatch following microlayer evaporation under a bubble and coalescence of adjacent bubbles although no definite proof of this is yet available. The occurrence of CHF here only depends on the local surface heat flux and flow conditions and is not affected by the upstream heat flux distribution. The surface temperature excursion occurring once CHF is exceeded is very rapid (fast dryout) and usually results in a failure of the heated surface.

- (ii) *Bubble clouding.* In subcooled and saturated nucleate boiling (approximate quality range: from -5% to $+5\%$) the number of bubbles generated depends on the heat flux and bulk temperature. The bubble population density near the heated surface increases with increasing heat flux and a so-called bubble boundary layer [Tong (1965), Weismann (1983)] often forms a short distance away from the surface. If this layer is sufficiently thick it can impede the flow of coolant to the heated surface. This in turn leads to a further increase in bubble population until the wall becomes so hot that a vapour patch forms over the heated surface. This type of boiling crisis is also characterized by a fast rise of the heated surface temperature (fast dryout). Physical failure of the heated surface frequently occurs under these conditions.

3.2.3. Helmholtz instability

In saturated pool boiling, the CHF is limited by the maximum vapour removal rate. Zuber's theory of CHF [as reported by Hsu and Graham (1976)] assumes the heated surface to be covered by a rising vapour column with countercurrent liquid jets flowing downwards to compensate for the removal of liquid by evaporation. Ultimately at very high heat flux levels (vapour removal rates) the relative velocity between liquid and vapour will be so high that an unstable flow situation is created, resulting in a CHF condition. This was recognized by Kutateladze (1952) who based his hydrodynamic theory of the boiling crisis on this instability. A similar situation can be considered at very low flow rates or flow stagnation conditions. This type of CHF is accompanied by a rapid rise in surface temperature (fast dryout).

3.2.4. Annular film dryout

In the annular dispersed flow regime (high void fraction and mass flow) the liquid will be in the form of a liquid film covering the walls and entrained droplets moving at a higher velocity in the core. Continuous thinning of the liquid film will take place due to the combined effect of entrainment and evaporation. Near the dryout location the liquid film becomes very thin and due to the lack of roll waves (which normally occur at higher liquid film flow rates) entrainment is suppressed. If the net droplet deposition rate does not balance the evaporation rate the liquid film must break down. The temperature rise accompanying this film breakdown is usually moderate (stable dryout). The liquid film breakdown may be promoted by one of the following mechanisms:

- (i) *Thermocapillary effect:* If a significant amount of heat is transferred by conduction through the liquid film and the interface is wavy, the temperature of the liquid vapour interface will have a maximum in the valley of the wave and large surface tension gradients will be present. The surface tension gradients tend to draw liquid to areas of high surface tension. Under influence of this "thermocapillary effect" the liquid film

will eventually break down in the valley of the wave. This mechanism is thought to be important at low flows and high qualities.

- (ii) *Nucleation induced film breakdown*: Hewitt et al. (1963) noticed that nucleation and surface evaporation could occur simultaneously in the annular flow regime. If the liquid film thickness is close to the maximum bubble size, then the bubble may rupture the liquid vapour interface and a momentary drypatch could occur. At high heat flux levels the liquid film may be prevented from rewetting this spot by the high drypatch temperatures. This mechanism will only occur for local heat flux spikes, or a highly non-uniform axial heat flux distribution.

3.2.5. Unstable or periodic dryout

The critical heat flux can be considerably reduced due to the hydrodynamic characteristics of the experimental equipment. Flow oscillations are frequently encountered in parallel channels, channels experiencing slug flow or in systems having a compressible volume near the inlet. During an oscillation the velocity at the wall is periodically slowed down, thus permitting the boundary layer to become superheated which may lead to a premature formation of a drypatch. Unstable dryouts are accompanied by an oscillation in surface temperature.

3.2.6. Slow dryout

During a slow dryout the heated surface does not experience the usual dryout temperature excursions; instead, a gradual increase in surface temperature with power is observed. A slow dryout is usually encountered in flow regimes where the phases are distributed homogeneously such as froth flow or highly dispersed annular flow at high mass velocities ($>2.7 \text{ Mg m}^{-2} \text{ s}^{-1}$) and void fractions $>80\%$. At these conditions liquid-wall interaction is significant thus limiting the temperature rise at dryout. Calculations based on cooling by the vapour flow only indicate that post-CHF temperatures are below the minimum film boiling (Leidenfrost) temperature; hence depositing droplets may wet the surface thus increasing the heat transfer coefficient.

3.3. CHF DATABASE

3.3.1. General

Since the CHF usually limits the power output in water cooled reactors, accurate values of CHF are required. The CHF has been measured extensively in simple geometries such as directly heated tubes. Such measurements have helped us to understand the CHF mechanisms. However to obtain accurate values of the CHF at reactor conditions of interest, experiments in test sections closely simulating the reactor fuel bundles are required. Such experiments are very expensive; e.g., CHF tests in Canada alone have cost over 30 million dollars over the past 20 years.

To reduce the expense and complexity of CHF testing of full-scale fuel bundles with high pressure steam-water, low-latent-heat modeling fluids have been used. Freons have been used successfully in many heat transfer laboratories as a modeling fluid for simulating the CHF of water. Reliable CHF predictions for water can be made based on CHF measurements in Freons at considerably lower pressures (e.g. 1.56 MPa in Freon-12 compared to 10 MPa in water), temperatures (e.g. 50°C in Freon-12 compared to 300°C in water) and powers (e.g.

685 kW in Freon-12 compared to 10 MW in water), resulting in cost savings of around 80% compared to equivalent experiments in water.

In Sections 3.3.2 and Section 3.3.3, the available databases will be discussed. Particular attention is given to the CHF data in tubes as:

- (i) the tube database is most complete and covers a much wider range of flow conditions than any other geometry, and
- (ii) bundle geometries can be broken down into subchannels (see Section 3.4.4) which are traditionally assumed to behave as tubes with correction factors applied to account for subchannel specific effects.

TABLE 3.1. RANGES OF CONDITIONS COVERED BY VARIOUS SETS IN THE AECL DATABANK

References	Diameter (mm)	Length (m)	Pressure (MPa)	Mass Flux ($\text{Mg.m}^{-2}.\text{s}^{-1}$)	Dryout Quality (-)	Inlet Subcooling (kJ.kg^{-1})	Critical Heat Flux (MW.m^{-2})	No. of Data
Alekseev [Kirillov, 1992]	10.0	1.000–4.966	9.80–19.6	0.216–7.566	-0.866–0.944	57–1398	0.134–4.949	1108
Becker et al. [1962, 1963]	3.94–20.1	0.400–3.750	0.22–8.97	0.100–3.183	-0.069–1.054	-50–1640	0.278–7.477	2664
Becker et al. [1965]	3.93–37.5	0.216–3.750	1.13–9.91	0.160–5.586	-0.005–0.993	-16–2711	0.503–6.620	1343
Becker and Ling [1970]	2.40–36.0	0.500–1.880	3.05–7.10	0.093–2.725	0.207–0.903	371–1065	1.026–5.130	116
Becker et al. [1971]	10.0	1.000–4.966	3.00–20.0	0.156–8.111	-0.866–1.061	26–1414	0.135–5.476	1496
Bennett et al. [1965]	9.22–12.6	1.524–5.563	6.61–7.48	0.624–5.844	0.026–0.948	21–691	0.590–3.300	201
Bergelson [1980]	8.00	0.241–0.400	0.17–3.08	1.927–7.078	-0.295–0.090	96–853	3.511–14.57	336
Bergles [1963]	0.62–6.21	0.011–0.155	0.14–0.59	1.519–24.27	-0.137–0.111	25–534	4.957–44.71	117
Bertoletti et al. [1964]	4.90–15.2	0.050–2.675	4.88–9.88	1.051–3.949	-0.083–0.774	-28–769	0.199–7.503	386
Borodin and MacDonald [1984]	8.92	3.690–3.990	8.20–10.4	1.194–6.927	0.105–0.570	31–456	0.542–2.304	465
Cheng et al. [1983]	12.3	0.370–0.740	0.10–0.69	0.050–0.400	0.187–1.227	42–210	0.331–2.115	150
De Bortoli et al. [1958]*	4.57–7.77	0.229–0.589	6.90–13.8	0.651–6.726	0.052–0.768	0–874	1.609–5.805	54
Dell et al. [1969]	6.17	0.914–5.512	6.90	1.329–4.136	0.144–0.779	79–365	0.493–3.340	82
Era et al. [1967]	5.98	1.602–4.800	6.78–7.05	1.105–3.015	0.374–0.952	-1211–565	0.109–1.961	163
Griffel [1965]	6.22–37.5	0.610–1.972	3.45–10.3	0.637–18.58	-0.209–0.592	45–1209	1.401–8.107	402
Griffel [1965] SRL data	6.35–25.4	0.597–1.105	0.41–8.41	0.664–11.39	-0.253–0.484	66–1224	3.186–11.83	85
Groeneveld [1985]	10.0	1.000–2.000	7.90–20.0	0.282–2.805	-0.097–0.805	622–1733	1.133–5.479	118
Hassid et al. [1967]	2.49–2.51	1.590–2.391	2.94–6.09	0.369–3.858	-0.035–0.838	0–467	1.427–3.433	238
Hewitt et al. [1965]	9.30	0.229–3.048	0.10–0.21	0.091–0.301	0.161–1.083	-41–383	0.144–4.013	442
Jens and Lottes [1951]	5.74	0.625	3.45–13.8	1.302–10.60	-0.464–0.150	279–1310	2.965–11.92	48
Judd and Wilson [1967]	11.3	1.829	6.86–13.9	0.674–3.428	0.016–0.776	33–730	0.593–2.669	49
Kirillov et al. [1984]	7.71–8.09	0.990–6.000	6.37–18.1	0.494–4.154	-0.494–0.981	7–1537	0.110–7.700	2470
Landislaw [1978]	4.00	0.200	0.42–1.00	0.884–5.504	-0.051–0.01	104–638	1.860–4.631	136
Lee and Obertelli [1963]*	5.59–11.5	0.216–2.007	4.14–11.0	0.678–4.421	0.000–0.910	9–690	1.104–8.107	295

TABLE 3.1. (CONT.)

References	Diameter (mm)	Length (m)	Pressure (MPa)	Mass Flux ($\text{Mg.m}^{-2}.\text{s}^{-1}$)	Dryout Quality (-)	Inlet Subcooling (kJ.kg^{-1})	Critical Heat Flux (MW.m^{-2})	No. of Data
Lee [1965]*	9.25–11.8	0.841–3.658	6.45–7.17	1.961–5.722	-0.002–0.462	12–584	1.000–4.306	274
Lee [1966]	14.1–44.7	0.635–1.524	8.24–12.6	0.332–3.410	-0.110–0.780	60–451	0.871–3.738	435
Leung et al. [1990]	5.45	2.511	5.03–9.71	1.168–9.938	0.210–0.578	6–316	0.656–3.058	66
Leung et al. [1990]	8.94	2.490	7.03–9.58	1.956–7.611	0.106–0.414	13–229	0.904–2.328	39
Lowdermilk et al. [1958]	4.00–4.80	0.119–0.991	0.10	0.027–4.866	0.030–1.236	317–331	0.167–9.525	113
Matzner [1963]*	12.8	1.930	6.86	0.933–1.978	0.075–0.592	54–947	1.686–3.372	25
Matzner et al. [1965]	10.2	2.438–4.877	6.89	1.193–9.560	0.008–0.693	48–1183	0.643–4.041	99
Mayinger [1967]	7.00	0.560–0.980	1.92–10.2	2.233–3.734	0.098–0.405	-239–314	0.924–5.618	128
Menegus [1959]***	3.6–92.4	-	0.19–6.80	0.006–13.70	-0.21–0.000	0–600	1.56–11.70	129
Nguyen and Yin [1975]	12.6	2.438–4.877	6.65–8.40	0.930–3.838	0.216–0.738	52–413	0.677–2.024	56
Rudzinski [1992]**	8.00	1.745	3.07–10.1	1.232–7.832	0.038–0.727	19–495	1.388–4.512	106
Smolin et al. [1962, 1964]	3.84–10.8	0.776–4.000	7.84–19.6	0.498–7.556	-0.132–0.795	5–1329	0.230–5.652	666
Smolin et al. [1979]	3.84–16.0	0.690–6.050	2.94–17.7	0.490–7.672	-0.136–0.789	4–1362	0.245–5.626	3009
Snoek [1988]	11.9	1.500	9.46–9.61	0.980–5.060	0.034–0.543	-481–356	0.423–3.037	33
Swenson [1962]*	10.5	1.753–1.803	13.8	0.678–1.763	0.178–0.502	41–565	0.587–1.063	25
Tapucu [1992]**	8.00	0.940–1.840	0.49–3.01	0.876–4.061	0.164–0.779	31–809	1.193–4.680	68
Thompson and Macbeth [1964]+	1.02–37.5	0.025–3.660	0.10–19.0	0.010–18.58	-0.820–1.577	0–1659	0.113–21.42	2356
Tong [1964]	6.22–12.9	0.380–3.660	5.17–13.8	0.678–14.00	0.002–0.502	5–1060	0.587–6.139	266
Yin et al. [1988]	13.4	3.658	1.03–21.2	1.938–2.081	0.075–0.431	0–493	0.583–1.864	287
Zenkevich et al. [1969]	3.99–15.1	0.250–6.000	5.88–19.6	0.498–9.876	-1.652–0.964	2–1644	0.136–14.76	5641
Zenkevich et al. [1971]	7.80–8.05	7.000–20.00	6.86–17.7	1.008–2.783	0.262–0.876	18–1549	0.470–1.283	392
Zenkevich [1974]++	4.80–12.6	1.000–6.000	5.89–19.6	0.497–6.694	-0.221–0.969	5–1381	0.230–4.740	840
Overall	0.62–92.4	0.011–20.00	0.10–21.2	0.006–24.27	-1.652–1.577	-1211–2711	0.109–44.71	28 017

* These data have already been included in Thompson and Macbeth's compilation.

** These data are used for validation only.

*** These data have not been used since the heated-length values of channels were not provided.

+ Duplicated data of Becker (1963) have been removed.

++ Duplicated data of Zenkevich et al. (1969) have been removed.

3.3.2. Tube database

Table 3.1 lists a summary of data collected jointly by AECL and IPPE, and used in the development of the CHF prediction methods, including the CHF look up table [Groeneveld et al. (1996)]. Figure 3.2(a) shows that the conditions covered, although extensive, do leave open several gaps in the data. The non-proprietary part of the CHF databank, containing over 30 000 CHF data, obtained in directly heated tubes, has recently been deposited in the International Nuclear Safety Center Database at Argonne National Laboratory, described in Annex A.

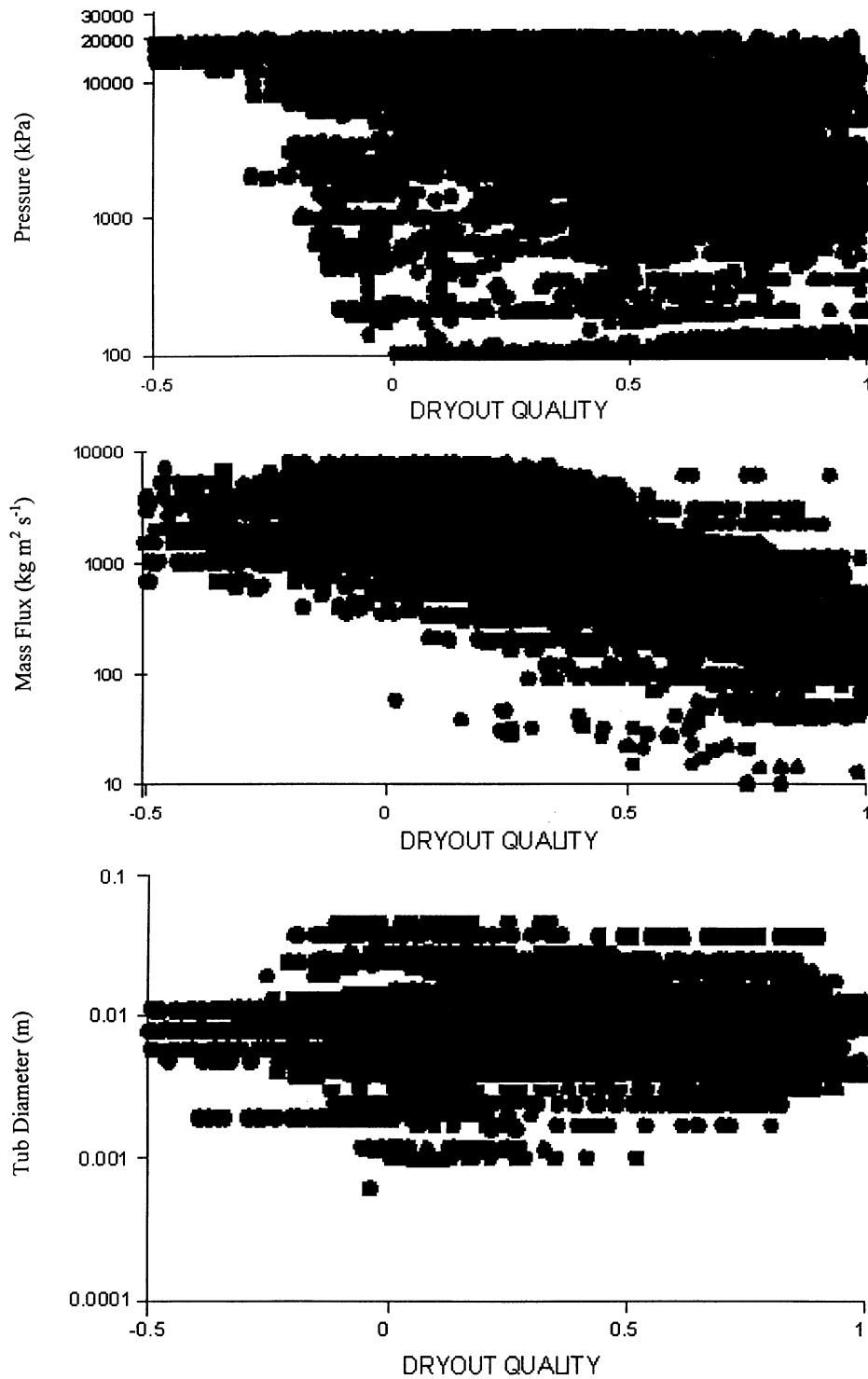


FIG. 3.2(a). Ranges of test conditions for the combined AECL-IPPE tube-CHF data bank.

The parameters controlling the CHF in tubes (for steady state conditions, and a uniform heat flux distributions) are:

- (i) Primary: thermodynamic quality, mass velocity, pressure and diameter
- (ii) Secondary: heated length, surface roughness, conductivity and tube wall thickness.

As the secondary parameters usually have a insignificant effect on CHF for conditions of interest, they may be ignored.

3.3.3. Bundle database

A large number of CHF experiments in bundles have been performed ranging from crude simulations of fuel bundles (e.g. annuli or 3-rod bundles) to full-scale simulations of actual fuel bundles. The following parameters have been found important in controlling CHF in fuel bundles:

- (i) Flow parameters (pressure, mass flow, and quality). This includes cross section average flow conditions (this is usually reported) and distribution of flow parameters (i.e. distribution of enthalpy and flow across a bundle as evaluated by subchannel codes or other empirical means).
- (ii) Bundle geometric parameters (number of rods, rod spacing, unheated flow boundary and heated length).
- (iii) Rod bundle spacing devices and CHF enhancement devices (grids, appendages and mixing vanes) and their axial spacing.
- (iv) Heat flux distribution (axial and radial heat flux distributions, and flux tilt across elements).

A number of surveys of bundle CHF data have been made. However because of the proprietary nature of bundle CHF data, these reviews are usually restricted as most bundle data (especially the recent ones) are unavailable or can only be obtained under special agreements. An earlier paper by Hughes (1974) provides a compilation of bundle CHF data sources. A more recent example of the ranges of conditions covered by specific bundle data sets is given in Figure 3.2(b) for the WWER bundle geometry [Macek (1998)], as can be seen the coverage is reasonably wide. However, as most bundle experiments still use fixed thermocouples, the reliability of the experimental CHF data as representing the initial occurrence of CHF may well be too optimistic (i.e. overpredicts the CHF). The more advanced sliding thermocouple technique (Schenk, 1990) has demonstrated that large differences (up to 20%) in bundle CHF can occur around the circumference of the most critical rod at the axial location corresponding to the initial CHF.

3.4. CHF PREDICTION METHODOLOGY

3.4.1. General

Because of the many possible fuel bundle geometric shapes, a wide range of possible flow conditions and the various flux distributions for AWCRs, it is impossible to predict the CHF for all cases with a single CHF prediction method and a reasonable degree of accuracy. The complexity of predicting the CHF in a nuclear fuel bundle may be best understood by first considering the prediction of CHF of a simplest experimental setup; a uniformly heated tube cooled internally by a fluid flowing at a steady rate vertically upwards. Here the CHF is a function of the following independent variables:

$$CHF = f(L_H, D_e, G, \Delta H_{in}, P, E) \quad (3.1)$$

where E takes into account the effect of the heated surface, i.e. surface roughness, thermal conductivity and wall thickness.

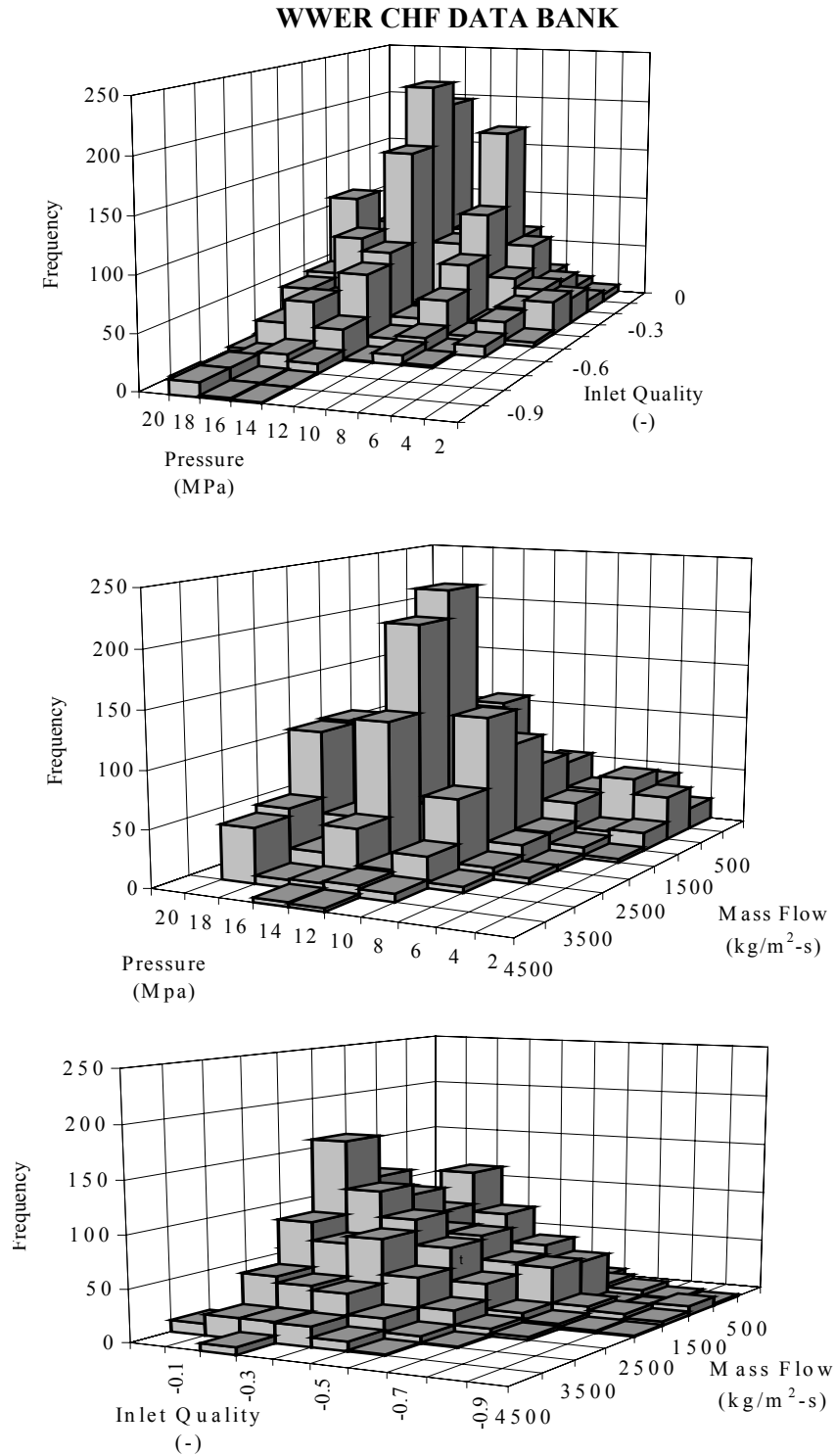


FIG. 3.2(b). Ranges of test conditions covered by the WWER CHF databank.

Despite the simplicity of the experimental setup, over 400 correlations for CHF in tubes are currently in existence. The present proliferation of correlations illustrates the complex state-of-the-art in predicting the CHF phenomenon even for a simple geometry at steady-state flow conditions. The complexity in predicting the CHF increases significantly for fuel bundle geometries during severe transients, when additional parameters characterizing the transient are required. This demonstrates the need to categorize the important CHF-controlling parameters and their ranges of interest. A methodology to categorize these parameters for thermalhydraulic parameters of interest has been proposed in Annex B.

In the following sections, analytical CHF prediction methods are discussed in Section 3.4.2, followed by empirical prediction methods in Section 3.4.3 which include empirical correlations as well as the CHF look up table. In Section 3.4.4 the application of CHF prediction methods to bundle geometries is described.

3.4.2. Analytical models

Analytical CHF models are based on the physical mechanisms and satisfy the conservation equations. They generally require a two-fluid model approach but occasionally must use a three-field approach (e.g. dispersed annular flow). Although the models have been improved significantly and usually predict the correct asymptotic trends, the evaluation process is complex and time-consuming. Furthermore, because of our limited understanding of the mechanisms involved, and the lack in measurements of interfacial parameters, the models are still less accurate than empirical correlations over the range of their database. An excellent review of the analytical CHF models has been presented by Weisman (1992). The most common CHF models that have met with some success are:

Annular film dryout model. This model is based on a mass balance on the liquid film in annular flow, and postulates that CHF corresponds to the depletion of the liquid film. Equations for droplet entrainment and deposition have been proposed. The model provides a reasonable predictions of CHF for the annular flow at medium to high pressures and flows and void fractions exceeding 50% [Hewitt and Hall-Taylor (1970)].

Bubbly layer model. This model postulates that CHF occurrence in the lower quality regime first occurs when the bubble layer covering the heated surface, becomes so thick and saturated with bubbles that liquid mixing between the heated surface and the cooler core liquid becomes insufficient. This model as proposed by Weisman and Pei (1983); and Ying and Weisman (1986) appear to predict the CHF with reasonable accuracy at high pressure, high flow and low quality conditions.

Helmholtz instability model. In pool boiling, the boiling crisis is reached when the flow of vapour leaving the heated surface is so large that it prevents a sufficient amount of liquid from reaching the surface to maintain the heated surface in the wet condition. The phenomenon that limits the inflow of liquid is the Helmholtz instability, which occurs when a counter-current flow of vapour and liquid becomes unstable. Zuber (1959) and Kutateladze (1952) have derived equations for the CHF based on the Helmholtz instability theory- their predictions agree with the CHF values measured in pool boiling systems. For very low flows, a modified version of this model as expressed by the Zuber-Griffith CHF correlation ($CHF_{PB}(1 - \alpha)$) appears reasonable for up- and down flow at flows less than $0.1 \text{ Mg.m}^{-2}.\text{s}^{-1}$ and $\alpha < 0.8$. However for $\alpha > 0.8$ this correlation significantly underpredicts the CHF. At these conditions the $1 - \alpha$ correction is not recommended [Griffith et al. (1977)].

3.4.3. Empirical CHF prediction methods

Empirical CHF prediction methods may be subdivided into those based on inlet conditions and those based on local cross-sectional average (CSA) conditions.

3.4.3.1. Inlet-conditions-type prediction methods

These prediction methods are all in the form of empirical correlations, based on CSA inlet conditions (P , G , T_{in} or ΔH_{in}) and usually assume the “overall power” hypothesis. This hypothesis states that, for a given geometry and inlet conditions, the critical power N_{DO} (power corresponding to the first occurrence of CHF for that geometry) is independent of axial or radial heat flux distribution or

$$N_{DO} = f(P_{in}, G_{in}, T_{in}, c / s, L_H) \quad (3.2)$$

This will permit the use of CHF correlations derived from uniformly heated bundle data for the prediction of dryout power in non-uniformly heated bundles of identical geometry (i.e. identical cross section and heated length).

This technique is a reasonable one for obtaining a first estimate of dryout power; it gives reasonable estimate of dryout power in the annular flow regime for symmetric flux profiles and form factors ($=q_{max}/q_{avg}$) close to unity. However it is not recommended for form factors significantly different from unity.

This approach can also be used to predict the critical power of fuel channels with a fixed cross section, heated length, axial flux distribution (AFD) and radial flux distribution (RFD), irrespective of the form factor. If the experimental AFD and RFD represent the worst flux shapes from a CHF point of view, then the empirical correlations can be used for lower-bound predictions.

The Inlet-Conditions-Method cannot be used for predicting the location and magnitude of the CHF except when CHF initially occurs at the downstream end.

3.4.3.2. Local-conditions-type prediction methods

This type of prediction methods follow the local-conditions hypothesis which states that the local CHF is dependent only on the local conditions and not on upstream history. In principle, the local conditions hypothesis is sound if it is based on the true local conditions (which must include radial distribution of void, liquid and vapour velocity, liquid temperature and turbulent velocity fluctuation near the wall). Hence ideally

$$CHF = f(P, G, X_{DO}, c / s) \quad (3.3)$$

In practice only the local cross section average pressure, flow and quality are known and the assumption

$$CHF = f(\alpha(r), T_l(r), U_l(r), U_v(r), U_l'(r), \dots, P, (c / s)) \quad (3.4)$$

that is often made. The local conditions approach, or variations thereof, is probably the most common method for predicting CHF. This form is more convenient than Eq. 3.1 since it depends on fewer parameters and permits the prediction of the location of CHF. One complication with this method is its ability (or lack of it) to account for the effect of AFD.

Two methods are frequently used to account for the effect of a non-uniform AFD on CHF: the boiling-length-average (BLA) approach, and the F-factor approach [Tong (1965, 1972), Kirillov and Yushenko (1996)]. The F-factor approach tends to modify CHF correlations designed for uniform heating, while in the boiling-length-average (or BLA) heat flux approach the heat flux distribution is modified. Lahey and Moody (1977) have shown that the two techniques are similar, yield similar answers and are reasonably successful in predicting the CHF for various non-uniform AFDs. Section 3.5.3.6 will describe the recommended approach for correcting for the effect of AFD.

Local conditions based empirical correlations. The large majority of the CHF prediction methods proposed are of this type. It is conservatively estimated that there are over 400 empirical correlations of this type proposed in the literature for directly heated tubes. Their main disadvantage is their limited range of application.

CHF table look up method. Since most empirical correlations and analytical models have a limited range of application, the need for a more general technique is obvious. As a basis of the generalized technique the local conditions hypothesis was used for the reasons given in Section 3.4.3.2. The initial attempt to construct a standard table of CHF values for a given geometry was made by Doroshchuk (1975), using a limited database of 5000 data. The CHF table approach, which is basically a normalized databank, has been continued at CENG-Grenoble, University of Ottawa, IPPE, and Chalk River using a much more extensive database (30 000 data). The recently completed International CHF table look up method [Groeneveld et al. (1996)] provides CHF values for water cooled tubes, at discrete values of pressure (P), mass flux (G), and quality (X), covering the ranges of 0.1–20 MPa, 0–7500 kg.m⁻².s⁻¹ (zero flow refers to pool-boiling conditions) and –50 to 100% vapour quality (negative qualities refer to subcooled conditions). Linear interpolation between table values is used for determining CHF. Extrapolation is usually not needed as the table covers a range of conditions much wider than any other prediction method. The CHF look up table and its derivation are presented in Appendix II.

Compared to other available prediction methods, the tabular approach has the following advantages: (i) greater accuracy, (ii) wider range of application, (iii) correct asymptotic trend (iv) requires less computing time and (v) can be easily updated if additional data become available. Although tabular techniques were initially developed for tubular geometries, and have been successfully used in subchannel codes, their greatest potential for application is in predicting the consequences of postulated Loss of coolant-Accidents (LOCA). To apply the tables to transient heat transfer in bundles requires the use of adjustment factors to correct for geometry, flux shape, and possibly transient effects. Here the advantages of the tabular technique (wide range of application, greater accuracy and more efficient in computing) are particularly important to the user.

Although promising, the look up table approach has certain disadvantages such as (i) it is a purely empirical prediction method and hence it does not reflect any of the physics, and (ii) could introduce erroneous trends if the underlying database is subject to experimental errors. Despite these reservations, the look up table approach is currently considered to be more accurate than other prediction methods for the CHF for most situations of interest.

3.4.4. Application to bundle geometries

Prediction of the critical power in untested fuel bundle geometries remains unreliable. Effects of flux distribution, grid spacers and bundle array dimensions are not well understood. The

next two approaches are commonly used, while the third one has more recently been proposed and an alternative.

- (1) *Empirical approach*: The empirical CHF predictions methods use cross-sectional average conditions to predict the CHF or critical power and are designed for tubes or bundles. For bundles for which experimental data can be obtained (using an electrically heated fuel bundle simulator, having a fixed axial and radial flux distribution) a variant of the following methodology is frequently employed:
 - obtain sufficient data for deriving an empirical CHF correlation for conditions of primary interest;
 - extrapolate the empirical correlations (which are usually based on a given axial and radial flux distribution) to other flux distributions of interest using the change in CHF as predicted by (i) subchannel codes (see below) or (ii) empirical methods to account for changes in the upstream flux shape (as described in the previous section);
 - similarly extrapolate to other conditions not tested in the full scale simulation tests using trends observed in simpler geometries, or as predicted by subchannel codes.
- (2) *Subchannel approach*: The subchannel approach is basically different from the empirical approach as it predicts the axial variation in flow and enthalpy for each subchannel. It is particularly useful for bundles for which no direct experimental data are available. The following methodology is normally followed for bundle CHF prediction based on the subchannel analysis approach:
 - employ subchannel codes to predict the flow and enthalpy predictions across the bundle
 - employ subchannel CHF models (basically modified tube CHF prediction methods) for predicting the initial CHF occurrence anywhere in the bundle.

Two definitions of subchannels are currently in use. The conventional approach defines subchannel boundaries by lines between rod centre and is used in subchannel codes such as ASSERT [Carver et al. (1993)], COBRA [Owen 1971)]; ANTEO [Cervolani (1995)] or HAMBO [Bowring (1967)]. The rod centered approach defines subchannel boundaries by lines of zero stress between rods and is used primarily to predict CHF in the annular flow regime [using Hewitt and Hall-Taylor's (1970)] annular flow model or an equivalent CHF correlation. A thorough review of subchannel prediction methods is presented by Weisman (1975).

- (3) *Enthalpy imbalance approach*. An alternative to the subchannel approach has been described by McPherson (1971) (applied to various bundle geometries contained in pressure tubes), Bobkov (1995, 1997) (applied to excentric annuli and bundle subchannels), and Leung (1997) (applied to 37 element bundle CHF predictions). This approach, which was recently reviewed by Kirillov et al. (1996b), considers the differences in enthalpy rise rates among bundle subchannels, and based on this defines a quality imbalance, ΔX for that bundle. This quality imbalance (a variation of this is the enthalpy imbalance number specified by McPherson(1971)) represents the difference in qualities between the cross section average bundle quality and the maximum bundle subchannel quality for a given cross-section. The difficulty is in predicting the ΔX value; no general expression for the enthalpy imbalance is yet available but ad hoc expressions for specific bundle geometries have been proposed. In general,

$\Delta H = f(\delta / d, \Delta X_{\max})$ where δ / d is the element gap/diameter ratio, and ΔX_{\max} is the maximum quality imbalance, which depends on the difference between the subchannel enthalpy of the critical subchannel for zero cross flow and the cross-sectional average enthalpy. Once a general expression for ΔX is found (this may well require a fit of a randomly-generated database using a subchannel code) the bundle CHF can be obtained from the tube CHF look up table [Groeneveld et al. (1996)] for the critical subchannel. In equation form this bundle CHF methodology is as follows:

$$CHF_{bundle}(P, G, X) = CHF_{tube}(P, G, X_0) \cdot K_1 \cdot K_3 \cdot K_4 \cdot K_5 \quad (3.5)$$

where:

$X_0 = X + \Delta X$ and K_1, K_3 , etc. are correction factors described in Section 3.5.3. The impact of flow imbalance on CHF is usually assumed to be negligible or assumed to be incorporated in ΔX .

3.5. RECOMMENDED CHF PREDICTION METHOD FOR ADVANCED WATER COOLED REACTORS

To provide precise predictions of CHF for advanced water cooled reactors fuel bundles is a nearly impossible task as advanced water cooled reactors designs include a variety of bundle cross sections as well as element spacer designs. This section therefore will recommend a generic approach of predicting CHF in untested bundle geometries. The basis of almost any generic bundle prediction method is a tube CHF prediction method, because (i) the parametric trends with P , G , and X are similar in tubes and in bundles, and (ii) tube CHF prediction methods are generally used in subchannel codes to predict the CHF in bundles.

In this section we will first discuss the recommended tube CHF prediction method and will subsequently describe how this method can be used for predicting the CHF in bundle geometries.

3.5.1. Tubes

The recommended CHF prediction is the recently published CHF look up table for tube [Groeneveld et al. (1996)] which was based on cooperation of several international groups, notably AECL in Canada and IPPE in Russia. This CHF prediction method is a slight modification from previous tables [Groeneveld et al. (1993)], has been validated independently by others as described in Section 3.6.1 and has resulted into better CHF predictions compared to other existing CHF correlations, both in accuracy and range of validity. Groeneveld et al. (1996) have presented a complete description of the new table including its derivation, and accuracy with respect to the world database, and a comparison with other widely used CHF prediction methods.

3.5.2. Rod bundles

The tube CHF look up [Groeneveld et al. (1996), see also Appendix II] needs to be converted into a prediction method for bundle geometries. To do this, two approaches may be used:

- (1) Subchannel based approach, as described in Section 3.4.4 item 2, and
- (2) Cross-sectional average bundle approach as described in Section 3.4.4 item 3.

Ideally a subchannel code should be used to predict the CHF for bundle geometry. Several subchannel codes are currently in existence [see review article by Weisman (1975) for more details] but their validation tends to be limited to a narrow range of bundle geometries and flow conditions for which their constitutive relations have been tuned to agree with the experimental database. With time this limitation is expected to be resolved as more appropriate constitutive relations are being derived and the robustness of the codes is continuously being improved.

In both of the above approaches the CHF needs to be modified to account for bundle specific or subchannel specific effects. The following correction factor methodology is adopted to evaluate the bundle or subchannel CHF:

$$CHF_{bundle} = CHF_{table} \times K_1 \times K_2 \times K_3 \times K_4 \times K_5 \times K_6 \times K_7 \times K_8 \quad (3.6)$$

where

CHF_{bundle} is cross section average value of the heat flux at which the CHF first occurs at the cross-section, CHF_{table} is the CHF value for a tube as found in the look up table for the same cross-sectional average values of P and G, and K_1 to K_8 are correction factors to account for specific bundle effects. Note that the form of this equation implies that all correction factors are independent. Many factors are somewhat interdependent, but these interdependencies are assumed to be second order effects unless indicated otherwise in the following sections. The correction factors are described in Section 3.5.3.

3.5.3. Correction factors

Table 3.2 lists the most common bundle specific or subchannel specific effects which are expected to affect the CHF. As these effects are not reflected by the database for the tube look up table, correction factors have been derived. Table 3.3 lists approximate relationships for the correction factors. The sections below elaborate on the more important correction factors.

3.5.3.1. Diameter

Experiments in tubes have shown a strong effect of tube diameter on CHF. A number of investigators have discussed this effect. Recently Wong (1996) has made a thorough systematic study of this effect and concluded that the original approach using the equation:

$$K_1 = \frac{CHF_D}{CHF_{D=8mm}} = \left(\frac{D}{8}\right)^n \quad (3.7)$$

where

n is between $-1/3$ and $-1/2$ and appears to be valid for the majority of the data. Slight improvements could be made by assuming $n = f(P, G, X)$ but the improvements were minor and limited to the range of experimental data on which the new n -function was based. Cheng and Erbacher (1997) have recently performed additional experiments in Freon and noticed that the change in CHF with diameter according to Eq. 3.7 appears to valid (with $n \sim -1/2$) for diameters equal or smaller than 8 mm but no effect of diameter (or a very small effect) on CHF was observed for diameters greater than 8 mm. Note that Cheng's data were obtained primarily at subcooled or low quality conditions. Kirillov and Yushenka (1996) also noted disagreements in the diameter effect on CHF for negative qualities but the general agreement for $D \leq 8\text{mm}$ with n between $-1/3$ and $-1/2$. Despite this disagreement, the recommendation by Groeneveld (1996) using $n = -1/2$, and subsequently confirmed by Wong (1996), appears to be a simple compromise which agrees reasonably with the bulk of the available data.

Although K_1 was derived empirically from tube data, the diameter correction factor has been applied directly to subchannels as well where the D_{hy} is used. Because of lack of data on CHF in various sizes of subchannels, the validity of the approach as applied to subchannels has not been confirmed.

TABLE 3.2. CHF SEPARATE EFFECTS ENCOUNTERED IN FUEL BUNDLES

GENERAL	DETAILS OF SEPARATE EFFECTS
Global Flow Area Effects:	<ul style="list-style-type: none"> - n-rod bundle where $n \gg 3$ and all subchannels identical except corners or cold-wall-adjacent subchannels (e.g., square or triangular arrays of subchannels) - n-rods where $n \gg 3$ and adjacent subchannels are generally not equal (e.g. 37-rod bundle geometries inside round tubes)
Subchannel Effects	<ul style="list-style-type: none"> - Subchannel size/shape (similarity to tube) - Cold wall effect - Distorted subchannels (due to bowing, clad strain, pressure tube creep) - Misaligned bundles (CANDU case)
Length Effects	Similar to appendage effects
Spacers/Bundle Appendages Effects	<ul style="list-style-type: none"> - mixing grids - attached spacers/ bearing pads/ endplates (CANDU)
Flow Orientation Effects	<ul style="list-style-type: none"> - Vertically upward - Vertically downward - Horizontal
Axial/Radial Flux Distribution Effects	<ul style="list-style-type: none"> - Axial flux distribution (flux peaking/global flux distribution) - Radial Flux Distribution (global RFD effect, cold wall effect, flux tilt across an element)
Flow Parameter Effects	- mass flow (incl. zero flow or pool boiling / flow stagnation case)
Transient Effects	<ul style="list-style-type: none"> - Power/Flow/Pressure transients - Combined transients
Effect of Fluid Type	<ul style="list-style-type: none"> - Light water - Heavy water - Modelling fluids (Freons) in conjunction with a CHF Fluid-to-fluid modelling technique

TABLE 3.3. SUMMARY OF CORRECTION FACTORS APPLICABLE TO THE CHF LOOK-UP TABLE

FACTOR	FORM	COMMENTS
K ₁ , Subchannel or Tube-Diameter Cross-Section Geometry Factor	For $2 \leq D_{hy} \leq 25$ mm: $K_1 = (0.008/D_{hy})^{1/2}$ For $D_{hy} > 25$ mm: $K_1 = 0.57$	Includes the observed diameter effect on CHF. This effect is slightly quality dependent.
K ₂ , Bundle-Geometry Factor	$K_2 = \min[1, (0.5 + 2 \delta / d) \exp(-0.5 x^{1/3})]$	This is a tentative expression, an empirically derived factor is preferred. K ₂ is also a weak function of P, G and X.
K ₃ , Mid-Plane Spacer Factor for a 37-element Bundle	$K_3 = 1 + A \exp(-B L_{sp} / D_{hy})$ $A = 1.5 K_L^{0.5} (G / 1000)^{0.2}$ $B = 0.10$	This factor has been validated over a limited range of spacer geometries.
K ₄ , Heated-Length Factor	For $L / D_{hy} \geq 5$: $K_4 = \exp[(D_{hy} / L) \exp(2 \alpha_h)]$ $\alpha_h = X \rho_f / [X \rho_f + (1 - X) \rho_g]$	Inclusion of α_h correctly predicts the diminishing length effect at subcooled conditions.
K ₅ , Axial Flux Distribution Factor	For $X \leq 0$: $K_5 = 1.0$ For $X > 0$: $K_5 = q_{loc}/q_{BLA}$	Tong's F-factor method (1972) may also be used within narrow ranges of conditions.
K ₆ , Radial or Circumferential Flux Distribution Factor	For $X > 0$: $K_6 = q(z)_{avg} / q(z)_{max}$ For $X \leq 0$: $K_6 = 1.0$	Tentative recommendation only and to be used with well-balanced bundle. May be used for estimating the effect of flux tilts across elements. Otherwise method of Yin (1991) is recommended.
K ₇ , Flow-Orientation Factor	$K_7 = 1 - \exp(-(T_l / 3)^{0.5})$ where $T_l = \left(\frac{1 - X}{1 - \alpha} \right)^2 \frac{f_L G^2}{g D_{hy} \rho_f (\rho_f - \rho_g) \alpha^{0.5}}$ f_L is the friction factor of the channel	This equation was developed by Wong and Groeneveld (1990) based on a balance of turbulent and gravitational forces. The void fraction is evaluated with the correlation of Premoli et al. (1970).
K ₈ , Vertical Low-Flow Factor	$G < -400$ kg.m ⁻² .s ⁻¹ or $X < 0$: $K_8 = 1$ $-400 < G < 0$ kg.m ⁻² .s ⁻¹ : Use linear interpolation between table value for upward flow and value predicted from $CHF = CHF_{G=0, X=0} (1 - \alpha_{hom}) C_l$	For $\alpha_h < 0.8$: $C_l = 1.0$ For $\alpha_{hom} \geq 0.8$: $C_l = \frac{0.8 + 0.2 \rho_f / \rho_g}{\alpha_{hom} + (1 - \alpha_{hom}) \rho_f / \rho_g}$ Minus sign refers to downward flow. G=0, X=0 refers to pool boiling.

3.5.3.2. Bundle

Prediction of the critical power in untested fuel bundle geometries such as many of the proposed advanced water cooled reactor fuel bundles has a higher uncertainty especially if the flux distribution, grid spacer shape and bundle array dimensions are different from those tested previously. The most reliable approach aside from ad hoc testing, is to employ a subchannel analysis as described in Section 3.4.5 (at a limited range of conditions of interest) to valuate the bundle CHF analytically, and to derive a bundle correction factor expressed as

$K_2 = \text{CHF}_{\text{bundle}}/\text{CHF}_{\text{table}}$ for use inside a systems code. In the absence of any test data Eq. 3.8 is the simplest one available and follows the correct asymptotic trends.

$$K_2 = \text{Min}[1.0, (0.5 + 2\delta/d)\exp(-0.5 x^{1/3})] \quad (3.8)$$

Note that further work in this area is required and that the approach based on the enthalpy imbalance as embodied in Equation 3.5 [Kirillov (1996b)] is the most promising

$$K_2 = \frac{\text{CHF}_{\text{tube-table}}(P, G, X + \Delta X)}{\text{CHF}_{\text{tube-table}}(P, G, X)} \quad (3.9)$$

one. This would then simply change the bundle correction factor to the form of Equation 3.9, but requires an empirical expression for ΔX (see also Section 3.4.4 item 3 and the references of Appendix III for further details).

3.5.3.3. Spacer

A number of researchers have investigated the effect of spacing devices on CHF or critical power. Figure 3.3 shows the various types of spacers used in these studies. In general a significant increase in local CHF was observed just downstream of the spacers. This increase usually decays slowly with distance downstream as illustrated in Fig. 3.4. The increase is primarily due to the higher turbulence level of the two-phase flow, which can strongly suppress the occurrence of CHF and the improved intersubchannel mixing. In experiments on CANDU fuel bundles, this increase in CHF is most pronounced just downstream of spacer planes and bundle junctions, where increases in local CHF of over 150% have been observed.

The strong CHF-enhancement effect has been confirmed by others, e.g. Tong (1972). It has been expressed by the enhancement factor:

$$K_3 = 1 + A \exp\left(-B \frac{L_{sp}}{D_{hy}}\right) \quad (3.10)$$

where

$A = 1.5 K^{0.5} (0.001G)^{0.2}$ (K is the pressure loss coefficient of the spacing device) and $B = 0.1$ were proposed by Groeneveld (1989).

Subsequent studies at CRL and IPPE have noted that using the pressure loss coefficient itself may not be sufficient because of the apparent insensitivity of the CHF enhancement to streamlining of the grid spacer, and an expression using the flow blockage area may be more appropriate [Kirillov (1997)]. Note that these values will still be approximations as the shape of the spacer and the element gap are also important parameters.

In bundles the length factor is no longer needed as this effect is already incorporated in the spacer correction factor (hence $K_4 = 1$).

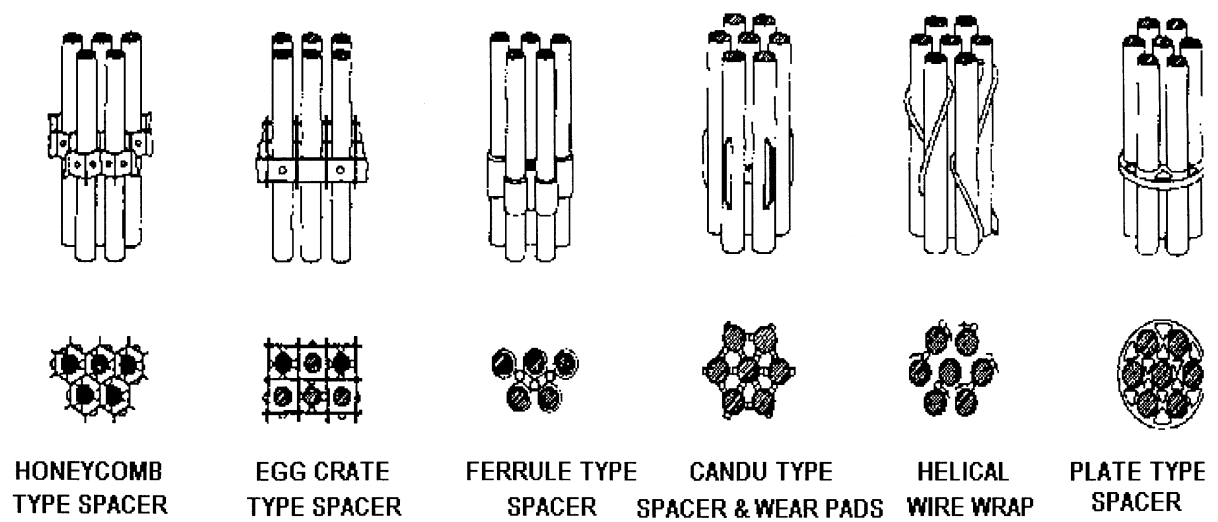


FIG. 3.3. Different types of rod spacing devices.

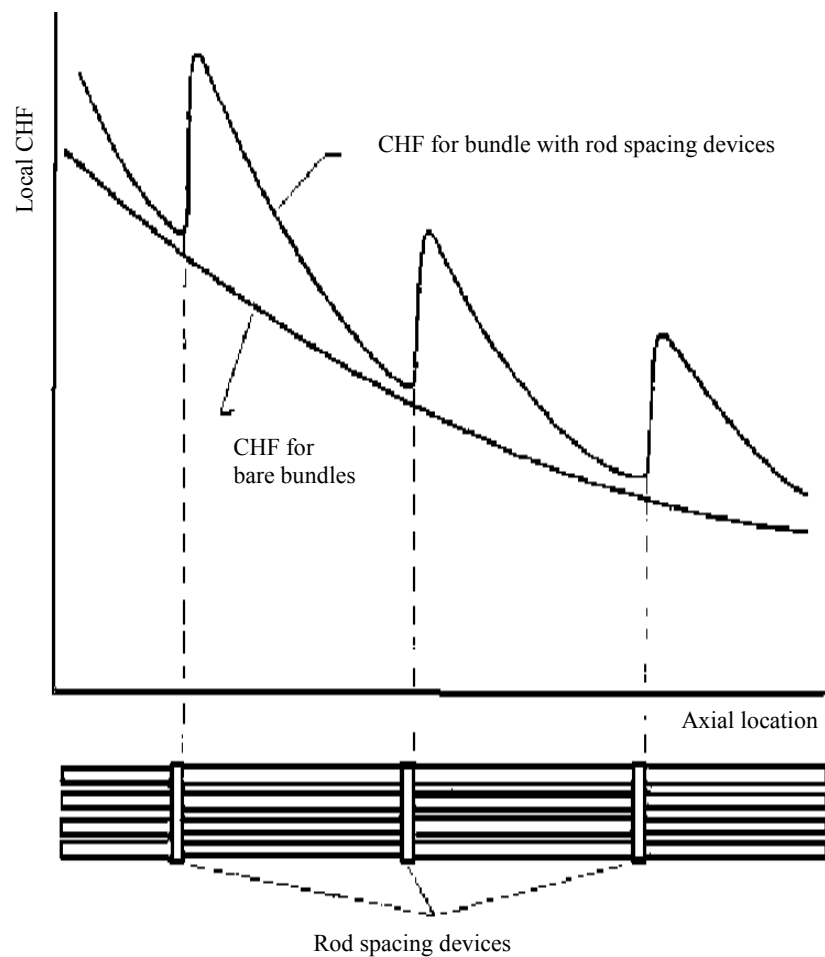


FIG. 3.4. Exponential decaying CHF enhancement downstream of a spacing device.

3.5.3.4. Axial flux distribution

Many experimenters have studied the effect of axial flux distribution (AFD) on critical power [e.g. Collier (1981); Tong (1972); Todreas and Rohsenow (1965); Groeneveld (1975), Kirillov (1997)]. The common observation in all these studies is that the AFD has a strong effect on the CHF in the annular flow regime but this effect tends to disappear altogether for the DNB-type of CHF. The effect of AFD on CHF can be accounted for by using the boiling-length-average (BLA) heat flux instead of the local heat flux. The BLA heat flux is defined as:

$$q_{BLA} = \frac{1}{L_B} \int_{L_x=0}^{L_x=x_{DO}} \phi dL \quad (3.11)$$

$$L_B = \frac{G H_{fg} D_{he}}{4 X_{DO} q_{BLA}} \quad (3.12)$$

where the BLA heat flux has been incorporated in the AFD correction factor K_5 defined as:

$$\begin{aligned} K_5 &= \rho_{local} / \rho_{BLA} & \text{for } X > 0.0 \\ K_5 &= 1.0 & \text{for } X \leq 0.0 \end{aligned}$$

3.5.3.5. Radial flux distribution

The ideal tool for evaluating the RFD effect on dryout power or CHF is a reliable subchannel code. Subchannel codes can also consider the effect of flux tilt across elements by accounting for the different heat flux values around the circumference of a fuel pin. However subchannel codes are complex, expensive to run and have usually a limited range validity. Hence a more empirical approach is often preferred. The RFD correction factor falls between two extreme values: (i) for open bundles where the subchannel flow and enthalpy imbalance is small, and the maximum heat flux controls the initial occurrence of CHF. For such a case K_2 is close to unity (or ΔX is close to zero) and K_6 is approximately equal to $q_{avg}(z)/q_{max}(z)$, where q_{max} represents the maximum heat flux for the subchannel and q_{avg} is the cross section average heat flux, and (ii) for very tight bundles ($\delta/D \leq 0.1$) where the communication between subchannels is severely hampered and K_6 (if used in conjunction with K_2 as expressed by Equation 3.8) depends also on the subchannel and flow imbalance. For this case a technique for obtaining a K_6 value based on RFD was proposed by Yin et al. (1991), but this still requires knowledge of the RFD corresponding to simultaneous CHF occurrence across the bundle (this could possibly be obtained from subchannel codes). However if the K_2 value is obtained from Equation 3.9 (based on ΔX), no further correction for K_6 beyond the q_{avg}/q_{max} value is required.

3.5.3.6. Flow orientation

The effect of orientation is important for CANDU reactors, where the fuel channels are oriented horizontally, and for conventional boilers, where many of the boiler tubes are inclined. The approach taken is to correct the vertical flow CHF by a penalty factor to account for the deleterious effects of flow stratification. For fully stratified flow, the CHF = 0 (i.e. $K_7=0$), while for a flow regime unaffected by flow stratification, $CHF_{ver} = CHF_{hor}$ or $K_7 = 1.0$. Using a mechanistically based flow regime map [e.g. Taitel and Dukler (1975)]

permits the determination of the mass flux threshold G_1 , corresponding to the onset of complete flow stratification (where liquid no longer touches the top of the channel, i.e. the CHF = 0) and the mass flux threshold G_2 , corresponding to the first noticeable effect of stratification on the phase distribution. Table 3.3 shows a simple expression for the correction factor K_7 having the correct asymptotic trends. A more rigorous expression for the flow stratification correction factor was derived by Wong et al. (1990), based on both the flow regime and a force balance on the phases. Their expression for the correction factor K_7 resulted in accurate predictions of the CHF in horizontal flow in various fluids over a wide range of conditions.

3.6. ASSESSMENT OF ACCURACY OF THE RECOMMENDED PREDICTION METHODS

3.6.1. CHF look up table assessment

The CHF look up table described in Section 3.5.1 and presented in Appendix II as well as earlier versions of the look up table have been assessed extensively. The most recent assessment was made at KAIST, Korea, by Baek et al. (1996) using their database. Their assessment confirms the error statistics reported by Groeneveld et al. (1996), and confirms the improved prediction capability compared with the 1986 AECL-University of Ontario (UO) Look-up Table [Groeneveld et al. (1986)]. In addition the distribution of CHF data and the error distribution of the CHF look up table as a function of pressure, flow and quality intervals are given in Table 3.4.

Earlier assessments by Smith (1986) and Weaver (1995) indicated the suitability of the table look up approach and has resulted in its use in systems codes such as CATHARE [Bestion (1990)], THERMOHYDRAULIK [Ulrych (1993)], ASSERT [Kiteley (1991), Carver (1993)] and RELAP [Weaver (1995)]. Assessments were also made by Aksan et al. (1995) and Faluomi and Aksan (1997) where an earlier version of the look up table (CHF-UO table) was compared to other leading CHF correlations and the impact of the differences in CHF predictions on nuclear plant transients of interest was assessed.

3.6.2. Accuracy of bundle CHF prediction methods

As indicated in the previous sections, the prediction of bundle CHF is much more difficult than the tube-based predictions. In addition the database has a much greater uncertainty because of the relatively crude fixed thermocouple technique for detecting initial CHF occurrence. Prediction accuracy for a well tested bundle geometry is usually quite reasonable (frequently within 5% at a 2σ confidence level for a given inlet conditions) but this is due to the fine-tuning of the correlation/subchannel code with empirically derived coefficients. For new AWCR geometries the accuracy is significantly reduced and could well be greater than 10% at 2σ .

An independent assessment was made by Chun et al. (1997) of the CHF look up table as a prediction method for bundles in conjunction with a subchannel code (COBRA-IV-1). They compared the look up table with six leading CHF prediction methods [Biasi et al. (1967)]; W-3, EPRI-1 as referred to by Chun et al. (1997); Katto and Ohno (1984); and two CHF models [Weisman and Ying (1985); Lin et al. (1989)]. They concluded that, for AWCR design applications, in the absence of a database, the look up table has the greatest potential as a general predictor for CHF in rod bundles. The CHF look up table has also been used and assessed in conjunction with the ASSERT subchannel code [Carver (1993,1995)] and the ANTEO subchannel code [Cervolani (1995)].

For specific bundle geometries a bundle specific look up table can be used. Good success has been reported with the recent IPPE bundle CHF look up table for WWER geometries. This table is reproduced in Appendix III where a brief description of its potential use is also provided.

TABLE 3.4. ERROR-DISTRIBUTION TABLE FOR LOCALIZED RANGES OF FLOW CONDITIONS

Pressure Range (kPa)		100 to 1000				1000 to 5000				5000 to 8000			
Mass Flux Range (kg.m ⁻² .s ⁻¹)		Quality Range				Quality Range				Quality Range			
		-0.5- -0.1	-0.1- 0.2	0.2- 0.5	0.5- 1	-0.5- -0.1	-0.1- 0.2	0.2- 0.5	0.5- 1	-0.5- -0.1	-0.1- 0.2	0.2- 0.5	0.5- 1
0 to 1000	No. of Data	0	1	55	523	0	0	87	1755	0	1	141	776
	Avg. Error (%)	0	31.9	4.7	0.4	0	0	-8.1	-3.5	0	4.6	-1.0	-1.4
	Rms Error (%)	0	31.9	16.7	8.8	0	0	10.2	7.2	0	4.6	5.4	5.9
	No. of Data Set	0	1	4	5	0	0	7	8	0	1	12	15
1000 to 3000	No. of Data	0	0	115	21	0	45	766	416	2	454	1340	747
	Avg. Error (%)	0	0	12.3	2.1	0	-2.5	-2.7	-1.9	-4.2	0.0	0.7	0.0
	Rms Error (%)	0	0	25.7	18.5	0	4.1	10.2	10.8	4.2	10.4	4.4	8.2
	No. of Data Set	0	0	6	4	0	5	10	8	2	17	22	15
3000 to 4500	No. of Data	0	1	33	0	1	67	248	0	0	486	493	0
	Avg. Error (%)	0	14.3	9.9	0	13.3	1.2	4.8	0	0	1.9	0.3	0
	Rms Error (%)	0	14.3	20.1	0	13.3	12.7	12.0	0	0	9.9	3.8	0
	No. of Data Set	0	1	2	0	1	7	7	0	0	18	19	0
4500 to 6000	No. of Data	0	0	0	0	0	34	28	0	6	228	126	0
	Avg. Error (%)	0	0	0	0	0	4.9	5.7	0	3.0	1.0	2.1	0
	Rms Error (%)	0	0	0	0	0	10.3	11.9	0	8.3	5.3	5.6	0
	No. of Data Set	0	0	0	0	0	7	5	0	3	13	9	0
6000 to 8000	No. of Data	0	0	0	0	0	19	22	0	0	95	15	0
	Avg. Error (%)	0	0	0	0	0	24.9	11.9	0	0	7.2	9.6	0
	Rms Error (%)	0	0	0	0	0	61.9	17.3	0	0	11.0	12.3	0
	No. of Data Set	0	0	0	0	0	3	2	0	0	9	5	0
Pressure Range (kPa)		8000 to 12 000				12 000 to 16 000				16 000 to 20 000			
0 to 1000	No. of Data	0	27	249	535	0	178	621	388	32	154	333	215
	Avg. Error (%)	0	1.3	1.8	-0.6	0	-0.6	1.2	0.7	1.5	-0.3	0.2	0.7
	Rms Error (%)	0	5.0	11.9	8.4	0	6.1	6.1	10.4	4.8	4.4	5.0	8.9
	No. of Data Set	0	5	12	13	0	7	13	10	3	8	9	8
1000 to 3000	No. of Data	3	671	1457	216	86	1234	1763	15	135	570	1031	16
	Avg. Error (%)	3.8	0.4	2.5	3.1	-0.4	1.2	1.8	-4.2	1.1	0.7	-0.5	0.3
	Rms Error (%)	4.7	4.8	9.1	10.7	5.2	4.7	6.0	5.3	5.5	4.1	4.8	3.8
	No. of Data Set	3	18	23	12	8	15	13	4	8	9	9	3
3000 to 4500	No. of Data	3	538	392	0	25	513	337	0	59	255	272	3
	Avg. Error (%)	3.2	1.4	0.2	0	2.2	2.5	-0.4	0	2.3	4.6	1.3	-6.7
	Rms Error (%)	3.7	4.7	6.2	0	5.6	5.7	5.2	0	6.4	8.6	5.7	10.6
	No. of Data Set	2	18	12	0	3	10	8	0	5	9	8	2
4500 to 6000	No. of Data	0	272	193	0	28	221	124	0	14	134	106	0
	Avg. Error (%)	0	0.9	0.9	0	4.0	4.1	3.5	0	0.9	6.6	2.6	0
	Rms Error (%)	0	5.6	7.8	0	5.4	6.9	6.4	0	1.6	9.3	5.9	0
	No. of Data Set	0	12	10	0	3	9	7	0	3	7	7	0
6000 to 8000	No. of Data	0	143	124	0	0	47	18	0	6	34	9	0
	Avg. Error (%)	0	4.9	3.6	0	0	6.2	-1.8	0	-1.5	7.5	-2.7	0
	Rms Error (%)	0	13.6	8.3	0	0	14.9	3.6	0	1.9	12.1	6.0	0
	No. of Data Set	0	11	7	0	0	6	3	0	2	6	5	0

3.6.3. Impact of accuracy of CHF model on cladding temperature prediction

CHF prediction methods are usually integrated in reactor safety codes and are used to predict the cladding temperature. This brings up the concern whether the same CHF prediction method is used for maximum cladding temperature prediction and for predicting the hydraulics response in a channel (see Section 3.7.1 for more details). Various investigators have considered the sensitivity of the CHF model in their codes on the cladding temperature transient. Belsito and D'Auria (1995) used an earlier version of the CHF look up table [Groeneveld et al. (1986)] and concluded that the discrepancies between pre-test and post-test analysis is due to the uncertainty in the boundary conditions and the calculation of the pressure at CHF.

3.7. CHF CONCERNING ACCIDENT CONDITIONS

3.7.1. General

In the previous discussion of CHF prediction methods it was assumed that the prediction of the initial occurrence of CHF is of paramount importance (as it is for setting the operating power for a reactor). However to predict the proper thermalhydraulic/neutronic response (they are linked) to a more massive occurrence of CHF across the core, knowledge of how CHF occurrence spreads across the reactor core is required. This will permit an evaluation of how much of the heat generated by the fuel is used for evaporation (usually 100% for saturated boiling if the CHF has not been exceeded), and how much is used for heating up the fuel (this could be close to 100% during fast transients where the fuel cladding has just experienced CHF and is heating up to the corresponding film boiling temperature). Systems codes ideally should be based on this more detailed (3-D) approach of evaluating the spread of CHF occurrence (or drypatch size) across the core.

The drypatch size predictions depends directly on the choice of the time steps, axial node size and size of nodes across the core. Detailed experiments on 37-rod fuel bundle simulators using sliding thermocouples [Schenk et al. (1990)] have clearly indicated that it requires a significant rise in power (10–25%) just to spread the CHF around one element, while the same measurements indicated that fuel element supports (spacers, endplates, grids) usually have a large local impact (~100–200%) on CHF (e.g. see Section 3.5.3).

A number of papers have been published where an assessment was made of the implementation impact of the CHF look up table [Faluomi and Aksan (1997); Aksan et al. (1995); Weaver (1991)]. They generally confirm the difficulty of individual CHF correlations in following the complex CHF variations with flow conditions.

3.7.2. Effect of the axial/radial node size

It is now known that CHF is strongly affected by fuel element supports such as grid spacers (which frequently are equipped with mixing vanes), and spacers/endplates in CANDU reactors. Increases in CHF of over 100% (for the same local flow conditions) due solely to the presence of an upstream fuel rod support have been measured. This increase in CHF decreases exponentially with distance downstream from the rod spacer as shown by Equation 3.10. The net impact of this depends on the specifics of the bundle geometry and rod support type: decreases in CHF by up to 50% over a distance of 12 cm have been measured [Doerffer

(1996)]. It is recommended to use as small an axial node length as practically possible (less than 5 cm) for those types of safety analysis where the size of the drypatch is important.

CHF does not occur simultaneously across a bundle, and in fact even across a 37 element bundle, it requires typically 50% increase power (for the same local flow conditions P, G and X) to have the CHF spread across the half the bundle geometry, and over 100% to spread across the whole geometry. Figures 3.5 and 3.6 [D'Auria (1997)] also illustrate the non-uniformity in CHF occurrence as measured in the LOBI and BETHSY test facilities [Faluomi and Aksan (1997)]; for square array bundle geometries. This limits the use of a 1-D system code in representing the CHF behaviour and its impact on void generation and neutron flux behaviour for PHWR.

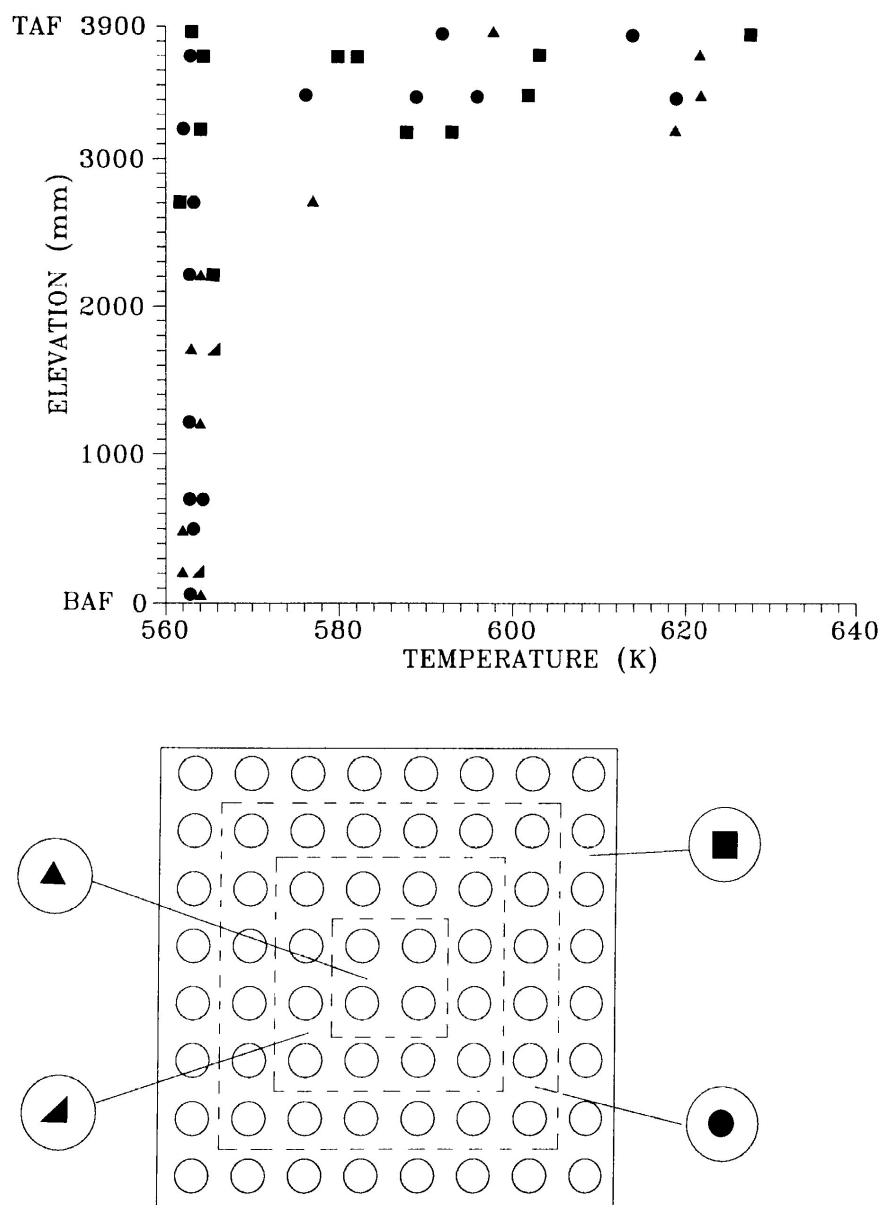


Figure 3.5. Axial and radial distribution of rod surface temperatures during initial CHF occurrence measured in the LOBI small break LOCA experiment BL-34.

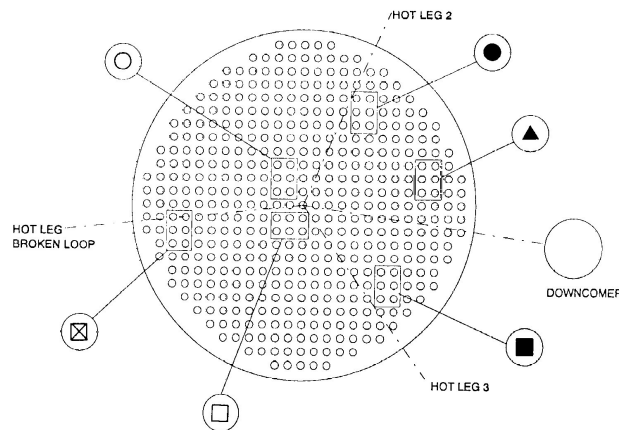
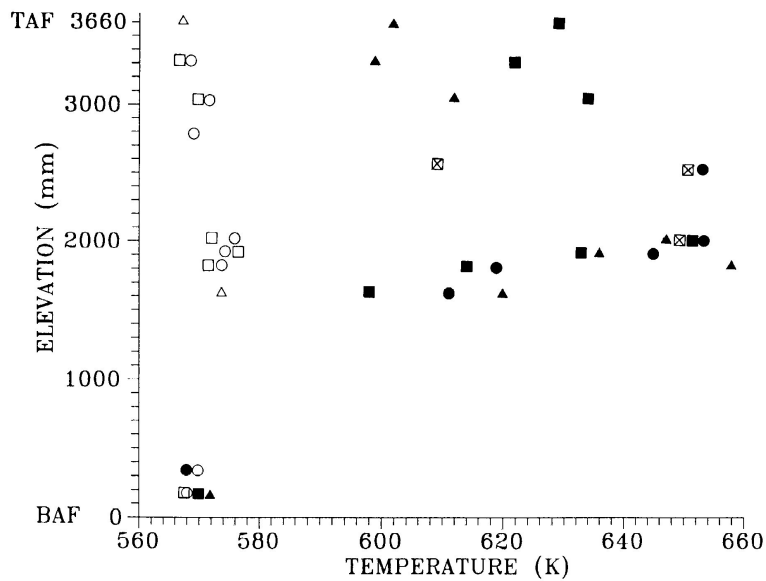


Figure 3.6. Axial and radial distribution of rod surface temperatures during initial CHF occurrence measured in the BETHSY small break LOCA experiment.

Three possible options are proposed to resolve the concerns of properly representing the thermalhydraulic/neutronic response to massive CHF occurrence.

- (1) use subchannel codes to evaluate the spread of CHF occurrence in a core across a fuel cell or bundle;
- (2) predict the *average* (not initial) CHF for a fuel cell or bundle and use this for predicting the fraction of fuel in dryout (this requires knowledge of the variation in flow conditions among fuel bundle/fuel cell);
- (3) use subchannel codes and/or experimental data to relate the bundle/core drypatch fraction to heat flux beyond the initial CHF occurrence and use this in systems code calculations to predict the thermalhydraulic and neutronic response.

The choice of which option is appropriate depends on the application, the availability of relevant data and the type of subchannel and systems code.

3.7.3. Transient effects on CHF

3.7.3.1. Flow transient

During a LOCA or pump rundown scenario, the flow decay phase can frequently be characterized by $G = G_0 e^{-t/C_1}$, during which time CHF will occur. The impact of the flow transient on CHF depends strongly on the flow decay constant C_1 : This permits a subdivision of the transients into:

- (i) slow transients, where the channel transit time is much smaller than the flow decay time constant C_1 . These are mild transients, which can be considered as pseudo-steady-state cases. Here, the CHF is assumed to be unaffected by the flow transient. For normal reactor flow conditions, the core transit time is roughly about 1 sec.
- (ii) fast transients where the transit time is greater than the flow decay time constant C_1 . Here the CHF is expected to be affected noticeably by the transient and any effect due to AFD is considered secondary.

As a first order approximation, it may be assumed that for $1/G (dG/dt) < 0.1$ (i.e. a decay time constant $C_1 > 10$ seconds) no effect of the transient on CHF is noticeable and the BLA heat flux (or any other methods which correctly account for upstream AFD) should be used. For a time constant C_1 of 1 second or less, however, the BLA effect is no longer relevant as it is overshadowed by transient effects. It is generally assumed that the CHF is enhanced during fast transients but no reliable predictions are available. The assumption that $CHF_{\text{transient}} = CHF_{\text{steady state}}$ for the same instantaneous local flow conditions is frequently made.

3.7.3.2. Power transients

Power transients will also accompany a LOCA. The power transient can be either in the form of a power decay, or a power spike. The easiest methodology for representing the power change is by employing the “Lagrangian” approach. The similarity between the variation in upstream heat flux as experienced by a fluid parcel while travelling along a non-uniformly heated channel, and the change in heat flux experienced by a fluid particle during a power transient can be used in evaluating the impact of a power transient on CHF [see also Chang (1989)]. If the fluid is in the annular flow regime (void fractions $>60\%$), a methodology similar to the BLA approach can be used, provided that the time a fluid particle sees a change in heat flux is transformed properly into an equivalent AFD. A previous study of axial flux spikes [Groeneveld (1975)] has shown that a BLA-type of approach can handle flux spikes with a magnitude of 2–3 times the average heat flux.

3.8. RECOMMENDATIONS AND FINAL REMARKS

- (1) Based on the arguments presented in Sections 3.4-3.6, the CHF look-up table as presented in Appendix II is currently recommended for use as the reference prediction method for CHF in advanced water-cooled reactors. As an alternative for fuel bundles in which the rods are arranged in a triangular array, the WWER-based look-up table of Appendix III is recommended.
- (2) For new bundle geometries, and in the absence of any relevant bundle CHF data, corrections for radial and axial flux shapes should be applied to account for differences between CHF values in tubes and bundle or bundle subchannels. These corrections can

best be obtained from a reliable subchannel code; without the complexity of a subchannel code, the method of applying correction factors based on element spacing, axial and radial flux distribution may be utilised.

- (3) Supercritical water is currently being considered as a coolant medium for several Advanced Water Cooled Reactor concepts. The heat transfer characteristics of reactor cores cooled by supercritical water needs further investigation. Specifically the pseudo-CHF and post-CHF behaviour of supercritical water has received very little attention in the literature.
- (4) Over 90% of the CHF literature is concerned with the prediction of initial CHF. There are currently no expressions for determining the average CHF or the spread of CHF available, even though this can be very important for predicting the thermalhydraulic and neutronic response to massive CHF occurrence during severe LOCAs. The methodology described in Section 3.7 may be used for evaluating the average CHF or the size of the drypatch.
- (5) As shown in Figure 3.2 there exists currently a scarcity of CHF data at low flows/low qualities and at or high flows/high qualities. In addition relatively little is known of the effect of fast flow and power transients on CHF. Additional experiments are required to improve our knowledge of CHF in these areas.

REFERENCES TO CHAPTER 3

ADORNI, N., et al., 1966, Heat Transfer Crisis and Pressure Drop with Steam-Water Mixtures: Experimental Data with 7-Rod Bundles at 50 and 70 kg/cm², CISE Report R170.

AKSAN, S.N., D'AURIA, F., FALUOMI, V., 1995, "A comparison and assessment of some chf prediction models used in thermalhydraulic systems codes", paper presented at First Research Coordination Mtg on Thermalhydraulic Relationships for Advanced Water-Cooled Reactors, IAEA-RC-574.

BAEK, W.-P., KIM, H.-C., CHANG, S.H., 1996, An Independent Assessment of Groeneveld et al.'s 1995 CHF Look up Table, Nuclear Engineering and Design.

BECKER, K.M., FLINTA, J., NYLUND, O., 1967, "Dynamic and static burnout studies for the full-scale Marviken fuel elements in the 8 MW Loop FRIGG" (Proceedings, Symp. on Two-Phase Flow Dynamics, Eindhoven, Netherlands), Vol. 1, 461–474.

BELSITO, S., D'AURIA, F., 1995, Comparison of Advanced Computer Codes in the Simulation of CHF Occurrence in the PKF Facility, Report on Expert Group Meetings on CHF and Post-CHF Heat Transfer, New Orleans, IAEA-CT-2991 and 2992.

BERGLES, A.E., 1977, Burnout in boiling heat transfer. Part II: Subcooled and low quality forced-convection systems, Nuclear Safety **18** 2 154–167.

BESTION, B., 1990, The physical closure laws in the CATHARE code, Nuclear Eng. Design **124** 229–245.

BEZRUKOV, Y.A., ASTACHOV, V.I., SALII, L.A., 1974, "Study of CHF in rod bundles for WWER type reactors", Proc. Thermophysical Mtg TF-74, Moscow (57–66).

BEZRUKOV, Y.A., ASTACHOV, V.I., BRANTOV, V.G., 1976, Experimental study and statistical analysis of CHF data for WWER type reactors, *Teploenergetika* **2** 80–82.

BOBKOV, V.P., VINOGRADOV, V.N., ZYATNINA, O.A., KOZINA, N.V., 1995, A method of evaluating the critical heat flux in channels and cells of arbitrary geometries, *Thermal Engineering* **42** 3 (221–231).

BOBKOV, V.P., VINOGRADOV, V.N., ZYATNINA, O.A., KOZINA, N.V., 1997, Considerations in describing burnout in rod bundles, *Thermal Engineering* **44** 3 (2–7).

BOWRING, R.W., 1967, HAMBO, A Computer Programme for the Subchannel Analysis and Burnout Characteristics of Rod Clusters, Part I. General Description, UKAEA Rep. AEEW-R524.

BURCK, E., HUFSCHMIDT, W., DE CLERQ, E., 1968, Der Einfluss Kuenstlicher Rauigkeiten auf die Erhoehung der Kritischen Waermestromdichte von Wasser in Ringspalten bei erzweigener Konvektion, EUR 4040d.

CARVER, M.B., KITELEY, J.C., ZHOU, R.Q.N., JUNOP, S.V., 1993, Validation of ASSERT Subchannel Code for Standard and Non-Standard Geometries, ARD-TD-454P, 2nd Int. Seminar on Subchannel Analysis, EPRI, Palo Alto.

CHANG, S.H., LEE, K.W., GROENEVELD, D.C., 1989; Transient-effects modeling of critical heat flux, *Nuclear Eng. Design* **133** 51–57.

CHUN, T.H., HWANG, D.H., BAEK, W.P., CHANG, S.H., 1997, “Assessment of the look-up table method for bundle CHF predictions with a subchannel code” (Proc. ISSAC-4 Mtg Tokyo).

CERVOLANI, S., 1995, “Description and validation of ANTEO, an optimized PC code for the thermohydraulic analysis of fuel element bundles” (Proc. 2nd Regional Mtg on Nuclear Energy in Central Europe, Portoroz, Slovenia).

CHENG, X., ERBACHER, F.J., 1997, this publication, Chapter 3.

COLLIER, J.G., 1972 and 1981, *Convective Boiling and Condensation*, McGraw-Hill, London.

D'AURIA, F., 1997, this publication, Figures 3.5 and 3.2.

DEBORTOLI, R.A., GREEN, S.J., LETOURNEAU, B.W., TROY, M., WEISS, A., 1958, Forced-Convection Heat Transfer Burnout Studies for Water in Rectangular Channels and Round Tubes at Pressures Above 500 Psia, Westinghouse Electric Corp. Rep. WAPD-188.

DOERFFER, S., GROENEVELD, D.C., SCHENK, J.R., 1996, "Experimental study of the effects of flow inserts on heat transfer and critical heat flux", (Proc. 4th Int. Conf. on Nuclear Engineering, New Orleans, Vol. 1 — Part A (41–49).

DOROSHCHUK, V.E., LEVITAN, L.L., LANTZMAN, F.P., Investigation into Burnout in Uniformly Heated Tubes, ASME Publication 75-WA/HT-22.

DURANT, W.S., TOWELL, R.H., MIRSHAK, S., 1965, "Improvement of Heat Transfer to Water Flowing in an Annulus by Roughening the Heated Wall", Chem. Engrg. Progress Symposium Series **6** 60 106–113.

FALUOMI, V., AKSAN, S.N., 1997, "Analysis and assessment of some selected CHF models as used in Relap5/Mod3 code", (Proceedings Fifth Int. Conf. on Nuclear Engineering (ICONE 5), Nice, France).

GASPARI, G.P., HASSID, A., VANOLI, G., 1969, "An experimental investigation on the influence of radial power distribution on critical heat flux in a nuclear rod cluster", (Proc. European Two-Phase Flow Group Mtg, Karlsruhe).

GASPARI, G.P., et al., 1968, Heat Transfer Crisis and Pressure Drop with Steam Water Mixtures: Further Experimental Data with Seven Rod Bundles, CISE Rep. R-208.

GROENEVELD, D.C., et al., 1996, The 1996 look-up table for critical heat flux in tubes, Nuclear Eng. Design **163** 1–23.

GROENEVELD, D.C., 1996, On the definition of critical heat flux margin, Nuclear Eng. Design **163** 245–247.

GROENEVELD, D.C., LEUNG, L.K.H., 1989, "Tabular approach to predicting critical heat flux and post-dryout heat transfer", Proc. 4th Int. Top. Mtg on Nuclear Reactors Thermalhydraulics, Karlsruhe), Vol 1, 109–114.

GROENEVELD, D.C., YOUSEF, W.W., 1980, "Spacing devices for nuclear fuel bundles: A survey of their effect on CHF, post-CHF heat transfer and pressure drop", (Proc. ANS/ASME/NRC Int. Top. Mtg on Nuclear Reactor Thermal-Hydraulics, Saratoga Springs), NUREG/CP-0014, Vol. 2, 1111–1130.

GROENEVELD, D.C., 1975, The Effect of Short Flux Spikes on the Dryout Power", Atomic Energy of Canada Ltd Rep. AECL-4927.

GROENEVELD, D.C., 1974, "The occurrence of upstream dryout in uniformly heated channels", (Proc. Fifth Int. Heat Transfer Conf.), Vol. IV (265–269).

GROENEVELD, D.C., 1972, The Thermal Behaviour of a Heated Surface at and Beyond Dryout", Atomic Energy of Canada Ltd Rep. AECL-4309.

GROENEVELD, D.C., SNOEK, C.W., 1986, "A comprehensive examination of heat transfer correlations suitable for reactor safety analysis", Multiphase Science and Technology, Volume II (181–274).

GROENEVELD, D.C., et al., 1986a, "Analytical and experimental studies in support of fuel channel critical power improvements", Proc. Canadian Nuclear Society Annual Mtg, Toronto.

GROENEVELD, D.C., et al., 1992, "CHF fluid-to-fluid modelling studies in three laboratories using different modelling fluids", (Proc. NURETH-5, Salt Lake City), Vol. 2, 531–538.

HERON, R.A., et al., 1969, Burnout Power and Pressure Drop Measurements on 12-ft., 7-rod Clusters Cooled by Freon-12 at Ispra, UKAEA Rep. AEEW-R655.

HETSRONI, G., 1982, "Handbook of multiphase systems", Hemisphere, McGraw-Hill.

HEWITT, G.F., HALL-TAYLOR, N.S., 1970, Annular Two-Phase Flow, Pergamon Press, Oxford.

HEWITT, G.F., KEARSEY, H.A., LACEY, P.M.C., PULLING, D.J., 1963, Burn-Out and Nucleation in Climbing Film Flow, UKAEA Rep. AERE-R437.

HSU, Y.Y., GRAHAM, R.W., 1976, Transport Processes in Boiling and Two Phase Systems, McGraw-Hill.

HUGHES, E.D., et al., 1974, A compilation of rod array critical heat flux data sources and information", Nuclear Engrg. & Design **30** 20–35.

JENSEN, A., MENNOV, G., 1974, Measurement of Burnout, Film Flow and Pressure Drop in a Concentric Annulus 3500 x 26 x 17 mm With a Heated Rod and Tube, European Two-Phase Flow Group Meeting, Harwell, UK.

KATTO, Y., 1994, Critical heat flux, Int. J Multiphase Flow **20** (53–90).

KIRILLOV, P.L., YUSHENKO, S.S., 1996, "Diameter effect on CHF", Second Research Coordination Meeting, IAEA Coordinated Research Program on Thermalhydraulic Relationships for Advanced Water-Cooled Reactors, Vienna, Austria.

KIRILLOV, P.L., BOBKOV., V.P., SMOGALEV, I.P., VINOGRADOV, V.N., 1996, Prediction of Critical Heat Flux in Channels Relevant to Water Cooled Reactors, IAEA Contract 8219R1.

KIRILLOV, P.L., BOBKOV. V.P., 1997, Working Material Related to the WWER-type Bundle CHF Look-up Table, Presented at the Third Research Coordination Meeting, Coordinated Research Program on Thermalhydraulic Relationships for Advanced Water-Cooled Reactors, Obninsk, Russia.

KITELEY, J.C., CARVER, M.B., LINER, Y., BROMLEY, B.P., MCCracken, I.K., 1991, "ASSERT-IV thermalhydraulics subchannel analysis code simulation of dryout power and pressure drop in a horizontal 37-rod bundle fuel channel including the effect of pressure tube creep", Proc. 16th Annual CNA Nuclear Simulation Symp. St. John, New Brunswick.

KRUZHILIN, G.N., 1949, Experimental data on heat transfer boiling at natural convection", Izvestiya Akademii Nauk SSSR, Otdel Technik. Nauk **5** (701–702).

KUNSEMILLER, D.F., 1965, Multi-Rod, Forced Flow Transition and Film Boiling Measurements, General Electric Rep. GEAP-5073.

KUTATELADZE, S.S., 1952, Heat Transfer in Boiling and Condensation, USAEC Rep. AEC-tr-3770.

- KUTATELADZE, S.S., BORISHANSKII, V.M., 1966, A Concise Encyclopedia of Heat Transfer, Pergamon Press.
- KYMALAINEN, O., et al., 1993, "Heat flux distribution from a volumetrically heated pool with high Rayleigh number", (Proc. NURETH-6 Conf. Grenoble), Vol. 1 (47–53).
- LAHEY, R.T., GONZALEZ-SANTOLO, J.M., 1977, "The effect of non-uniform axial heat flux on critical power", Paper C219/77 presented at the Inst. of Mech. Engineers Conf. on Heat and Fluid Flow in Water Reactor Safety, Manchester.
- LAHEY, R.T., Jr., MOODY, F.J., 1977, The Thermal Hydraulics of a Boiling Water Nuclear Reactor, ANS Monograph.
- LIN, W., LEE, C.H., PEI, B.S., 1989, An improved theoretical critical heat flux model for low quality flow", Nuclear Technol. **88** (294–306).
- LEE, D.H., OBERTELLI, J.D., 1963, An Experimental Investigation of Forced Convection Boiling in High Pressure Water, UKAEA Rep. AEEW-R213.
- LEUNG, L.K.H., 1997, AECL Report.
- MACEK, J., 1998, Private Communication.
- MCPHERSON, G.D., 1971, The Use of the Enthalpy Imbalance Number in Evaluating the Dryout Performance of Fuel Bundles, AECL Rep. AECL-3968.
- NORMAN, W.S., MCINTYRE, V., 1960, Heat transfer and liquid film on a vertical surface, Trans. Inst. Chem. Engineers **38** 301–307.
- PARK, H., DHIR, V. K., et al., 1994, Effect of external cooling on the thermal behavior of a boiling water reactor vessel lower head, Nuclear Technol. V. **108** 2 266–282.
- POLOMIK, E.E., 1967, Transition Boiling, Heat Transfer Program, Final Summary Report on Program for Feb. 63–Oct. 67, General Electric Report GFAP-5563.
- ROWE, D.S., 1971, COBRA III, A Digital Computer Program for Steady State and Transient Thermal-Hydraulics Analysis of Rod-Bundle Nuclear Fuel Elements, Battelle-Northwest Report BNWL-B-82.
- SCHENK, J.R., GROENEVELD, D.C., 1990, "Measurement of thermohydraulic parameters inside multi-element bundles", Proc. Int. Symp. on Multi-Phase Flow, Miami.
- SMITH, R.A., 1986, Boiling Inside Tubes: Critical Heat Flux for Upward Flow in Uniformly Heated Tubes, ESDU Data Item No. 86032, Engineering Science Data Unit International Ltd, London.
- SULATSKI, A.A., EFIMOV, V.K., GRANOVSKY, V.S., 1997, "Boiling crisis at the outer surface of WWR vessel", Proc. Int. Symp. on the Physics of Heat Transfer in Boiling and Condensation, Moscow (263–268).

- TAITEL, Y., DUKLER, A.E., 1975, A Model for Predicting Flow Regime Transitions in Horizontal and Near Horizontal Gas/Liquid Flow, ASME 750WA/HT829 (1975); AIChE J. **22** (1976) 47855.
- TIPPETS, F.E., 1962, "Critical Heat Fluxes and Flow Patterns in High Pressure Boiling Water Flows", ASME Paper 62-WA-162 presented at the Winter Annual Meeting of the ASME, New York.
- TODREAS, N.E., ROHSENOW, W.M., 1965, The Effect of Non-uniform Axial Heat Flux Distribution, Rep. 9843-37, M.I.T. Dept. of Mech. Engineering.
- TONG, L.S., HEWITT, G.F., 1972, Overall Viewpoint of Flow Boiling CHF Mechanisms, ASME paper 72-HT-54.
- TONG, L.S., 1972, Boiling Crisis and Critical Heat Flux, USAEC Rep. TID-25887.
- TONG, L.S., WEISMAN, J., 1996, Thermal Analysis of Pressurized Water Reactors, Third Edn, American Nuclear Society.
- TONG, L.S., 1965, Boiling Heat Transfer and Two-Phase Flow, John Wiley & Sons.
- TOWELL, R.H., 1965, Effect of Spacing on Heat Transfer Burnout in Rod Bundles, Report DP-1013.
- ULRYCH, G., 1993, "CHF table applications in KWV PWR design", Paper presented at the Int. Workshop on CHF Fundamentals — CHF Table Improvements, Braunschweig.
- WATERS, E.O., FITZSIMMONS, D.E., 1963 DNB varies with rod spacing in 19-rod bundles, Nucleonics (96-101).
- WEAVER, W.L., RIEMKE, R.A., WAGNER, R.J., JOHNSON, G.W., 1991, "The RELAP5/MOD3 code for PWR safety analysis", (Proc. NURETH-4". 4th Int. Top. Mtg on Nuclear Reactor Thermalhydraulics, Karlsruhe", Vol. 2 (1221-1226).
- WEISMAN, J., BOWRING, R.W., 1975, Methods for detailed thermal and hydraulic analysis of water-cooled reactors, Nuclear Science Engineer. **57** (255-276).
- WEISMAN, J., 1992, The current status of theoretically based approaches to the prediction of the critical heat flux in flow boiling, Nuclear Technol. **99** (1-21).
- WEISMAN, J., PEI, B.S., 1983, Prediction of critical heat flux in flow boiling at low quality conditions, Int. J. Heat Mass Transfer **26** (1463).
- WEISMAN, J., YING, S.H., 1985, A theoretical based critical heat flux prediction for rod bundles, Nucl. Eng. Design **85** (239-250).
- YING, S.H., WEISMAN, J., 1986, Prediction of critical heat flux in flow boiling at intermediate qualities, Int. J. Heat Mass Transfer **29** (1639).
- WONG, Y.L., GROENEVELD, D.C., CHENG, S.C., 1990, CHF predictions in horizontal tubes, Int. J. Multiphase Flow **16** (123).
- ZUBER, N., 1959, Hydrodynamic Aspects of Boiling Heat Transfer, Atomic Energy Commission Report AECU-4439.

Chapter 4

GENERAL FILM BOILING HEAT TRANSFER PREDICTION METHODS FOR ADVANCED WATER COOLED REACTORS

NOMENCLATURE

A	area of surface
C_p	specific heat
C	concentration
D	hydraulic diameter
d	drop diameter
F	empirical function
G	mass flux
g	acceleration of gravity
h	enthalpy
l	length
Nu	Nusselt number
P	pressure
Pr	Prandtl number
q	heat flux
Re	Reynolds number
r	latent heat of evaporation
S	velocity slip ratio; pitch of rod bundles
T	temperature
t	time
V	specific volume
X	mass quality
X_a	actual quality

GREEK SYMBOLS

Π	perimeter
ΔT_{\min}	$\Delta T_{\min} = T_{\min} - T_s$
α	heat transfer coefficient
ε	emissivity
λ	thermal conductivity
λ_c	critical wave length
ϕ	void fraction
μ	dynamic viscosity
ρ	density
σ	surface tension
σ_o	Stefan-Boltzman constant
Θ	inclination angle in degrees

SUBSCRIPTS

a	actual
c	critical
cr, CHF	critical heat flux
e	equilibrium
f	front of wetting
g	gas (vapour)
h	hydraulic; heat
ℓ	liquid
min	minimum
Q	quench
s	saturation
st	stabilisation
sub	subcooled
tot	total
TB	transition boiling
v	vapour
vd	vapour-to-drop
w	wall
wv	wall-to-vapour
wd	wall-to-drop

ABREVIATIONS

AWCR	advanced water cooled reactor
CHF	critical heat flux
CRP	coordinating research project
DFFB	dispersed film flow boiling
ECC	emergency cooling of core
IAFB	inverted annular film boiling
LOCA	loss of coolant accident
LWR	light water reactor
MFBT	minimum film boiling temperature
MHF	minimum heat flux
PDO	post-dryout heat transfer
QF	quench front
RCM	research coordination meeting

4.1. INTRODUCTION

Post-CHF (or post-dryout) heat transfer is encountered when the surface temperature becomes too high to maintain a continuous liquid contact, and the surface becomes covered by a continuous or intermittent vapour blanket. Post-CHF heat transfer includes transition boiling, where intermittent wetting of the heated surface takes place, and film boiling, where the heated

surface is too hot to permit liquid contact. The boundary between these post-CHF heat transfer modes is the minimum film boiling temperature, or T_{MFB} . Due to the poor heat transport properties of the vapour, high heated surface temperatures are often encountered during film boiling.

Although nuclear reactors normally operate at conditions where dryout does not occur, accidents can be postulated where dryout occurrence is possible. The most serious of the postulated accidents is thought to be the loss-of-coolant accident (LOCA) caused by a rupture in the primary coolant system. Accurate prediction of the consequences of a LOCA requires precise calculation of fuel-coolant heat transfer during (i) the blowdown phase (when the fuel channel is voided), and (ii) the subsequent emergency-core-cooling (ECC) phase. Although the time-in-dryout may be short, nevertheless this interval, when the primary mode of heat transfer is film boiling, can be of crucial importance in maintaining core integrity.

The post-CHF cladding temperature can be predicted from empirical correlations or from theoretical models. Since theoretical models are rather complex and the physical mechanisms on which they are based are not yet fully understood, predictions are usually based on empirical correlations. The main three methodologies considered by IPPE, AECL and CIAE have been presented in this chapter.

Film boiling heat transfer has been extensively investigated during the past 30 years. Excellent reviews may be found in text books by Tong (1965), Collier (1980), Delhay et al. (1981), Strykovitch et al. (1982), a handbook by Hetsroni (1982), and articles by Ganic et al. (1977), Mayinger (1978), Tong (1978), Sergeev (1978, 1987), Groeneveld and Snoek (1986), Groeneveld (1992), Yadigaroglu (1989), Sakurai (1990a), Andreoni and Yadigaroglu (1994) and in the proceedings of the 1st International Symposium on Fundamental Aspects of Post-CHF Heat Transfer (1984).

The objective of this chapter is to review and recommend film boiling prediction methods suitable for the assessment of LOCAs and other disruptive accidents in AWCs and for implementation into systems codes such as RELAP, CATHARE, and CATHENA, as well as subchannel codes such as COBRA, ASSERT, and MIF. The requirements for this prediction method have been discussed in more detail in CRP RCM meetings and expert meetings.

This chapter is subdivided as follows:

- (i) Section 4.2 discusses the mechanisms of the post-CHF heat transfer;
- (ii) Section 4.3 describes the film boiling data base in tubes and rod bundles;
- (iii) Section 4.4 provides an overview of the prediction methodology for film boiling heat transfer;
- (iv) Section 4.5 presents the recommended prediction methods for film boiling heat transfer;
- (v) Section 4.6 discusses the film boiling prediction methodologies used in reactor safety codes; and
- (vi) Section 4.7 provides final remarks related to the use of film boiling prediction methods in the thermal analysis of advanced water cooled reactors.

4.2. DESCRIPTION OF POST-CHF PHENOMENA

4.2.1. General

Post-CHF heat transfer is encountered when the surface temperature becomes too high to maintain a continuous liquid contact. As a result the heated surface becomes covered by a continuous vapour blanket as is the case in the film boiling regime, or an intermittent vapour blanket, as is the case in the transition boiling regime. The boundary between these post-CHF heat transfer modes is the minimum film boiling temperature, or T_{MFB} .

Post-CHF heat transfer is initiated as soon as the critical heat flux condition is exceeded; it persists until quenching or rewetting of the surface occurs. Depending on the particular scenario and flow conditions present, various heat transfer modes of the boiling curve of Fig. 4.1 may be distributed along a heated surface, or a series of heat transfer modes can succeed each other in time at the same location as is the case during transients.

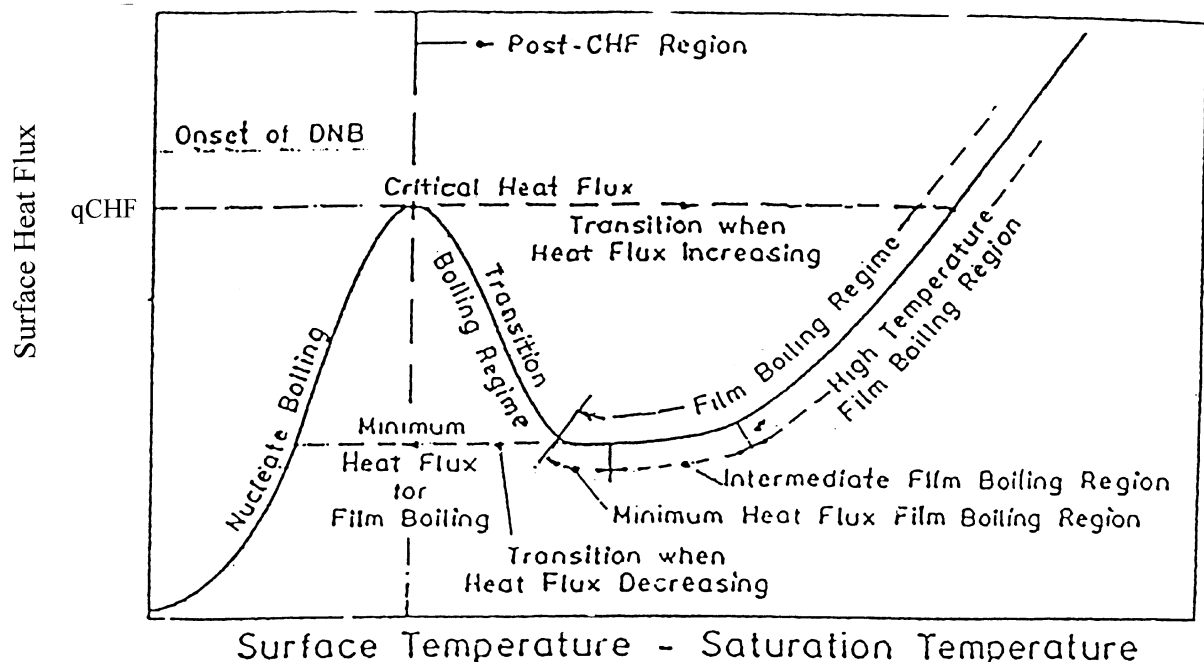


FIG. 4.1. Typical boiling curve.

The occurrence of film boiling depends on surface temperature and flow conditions. Figure 4.2 is a three-dimensional representation of the variation of the heat flux with wall temperature and quality at constant mass flux and pressure, the so-called boiling surface concept described by Nelson (1975) and Collier (1980). The flow quality introduces a third dimension to the problem that was not present in pool boiling. This 3-D boiling surface or map shows the nucleate, transition and film boiling surfaces (regimes) as well as the critical and minimum heat flux lines for a given pressure and mass flux.

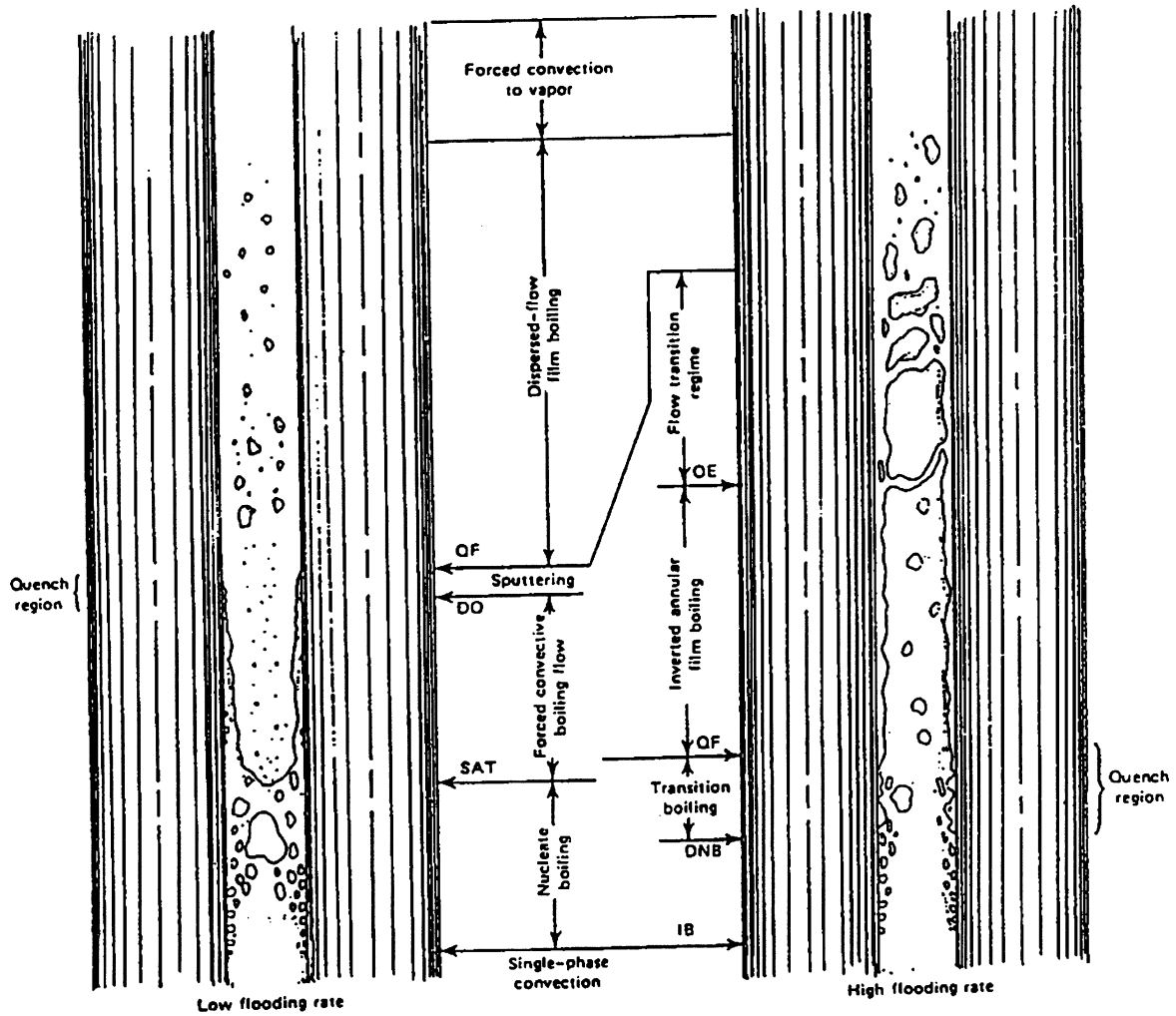


FIG. 4.3. Post-CHF reflooding heat transfer modes [Yadigaroglu, 1978]

The transition boiling section of the boiling curve is bounded by the critical heat flux (Fig. 4.3) and the minimum heat flux. The critical heat flux has been extensively studied and can be predicted by a variety of correlations. The minimum heat flux has undergone less study; it is known to be affected by flow, pressure, fluid properties and heated surface properties and will be discussed in Section 4.2.3.

At surface temperatures in excess of the CHF temperature, the heated surface will be partially covered with unstable vapour patches, varying with space and time. Ellion (1954) studied forced convective transition boiling in subcooled water and observed frequent replacement of vapour patches by liquid. Although this may seem similar to transition pool boiling as described above, the introduction of the convective component will improve the film boiling component by reducing the vapour film thickness and changing the heat transfer mode, whether dry or wet, from free convection to forced convection. This will result in an increase in q_{\min} and also can increase ΔT_{mfb} (if ΔT_{mfb} is hydrodynamically controlled). For low qualities and subcooled conditions the slope of the transition boiling is always negative, just as in pool boiling.

The amount of heat transfer in the transition boiling region is primarily governed by liquid-solid contact. At the critical heat flux point the contact-area (or time) fraction F is close to unity and, therefore, the liquid contact heat flux q_ℓ is close to the CHF. The value of F strongly decreases with increasing wall temperature. In the high quality region for example, most of the heat transferred during transition boiling will be due to droplet-wall interaction. Initially, at surface temperatures just in excess of the boiling crisis temperature, a significant fraction of the droplets will deposit on the heated surface but at higher wall superheats the vapour repulsion forces become significant in repelling most of the droplets before they can contact the heated surface. The repelled droplets will contribute to the heat transfer by disturbing the boundary layer sufficiently to enhance the heat transfer to the vapour.

The periodic contacts between liquid and heated surface in the transition boiling region of the boiling curve result in the formation of both large amounts of vapour, which forces liquid away from the surface, and creates an unstable vapour film or blanket. Because of this, the surface heat flux and the surface temperature can experience variations both with time, and position on a heater. However, the average heat transfer coefficient decreases as the temperature increases, because the time of contact between the liquid and the heater surface is decreased.

To gain a better understanding of the transition boiling mechanism, the phenomena occurring at the interface between fluid and a heated surface (i.e. the mechanism of fluid-solid contact including the frequency of this contact; heat transfer in the contact areas; time history of such contact) need to be considered. Comprehensive reviews of these phenomena have been presented by Kalinin et al. (1987) and Auracher (1987, 1990).

Transition boiling has received less attention than nucleate or film boiling. Only in recent years has the interest in this boiling regime increased because of its potential importance during a LOCA in a nuclear reactors. Overviews of the mechanisms and prediction methods for transition boiling have been provided by Bankoff and Mehra (1962), Groeneveld and Fung (1976), Auracher (1987, 1990), Winterton (1982), Groeneveld and Snoek (1986) and Johannsen (1991).

4.2.3. Minimum film boiling temperature

The minimum film boiling temperature (T_{MFB}) separates the high temperature region where inefficient film boiling or vapour cooling takes place, from the lower-temperature region, where much more efficient transition boiling occurs. It thus provides a limit to the application of transition boiling and film boiling correlations. Knowledge of the minimum film boiling temperature is particularly important in reactor safety assessments.

A large number of terms have been used for the minimum film boiling temperature or T_{MFB} . They include rewetting temperature, quench temperature, Leidenfrost temperature, film boiling collapse temperature and others.

During quenching of a surface (such as emergency core cooling), rewetting commences at the minimum film boiling temperature and, as a rule, rapidly proceeds until nucleate boiling is established at a much lower wall temperature. Predicting the minimum film boiling temperature as a function of the system parameters is thus very important since heat transfer coefficients on

either side of the minimum film boiling temperature can differ by orders of magnitude. Generally, T_{MFB} is defined as the temperature at the minimum heat flux.

The T_{MFB} also represents a temperature boundary beyond which surface properties and surface conditions generally do not affect the heat transfer. Wettability or contact angle although important in nucleate and transition boiling, are not applicable in the film boiling regime, and conduction along the surface becomes less important when nucleate and film boiling no longer occur side-by-side.

Two theories have been proposed for the analytical prediction of the minimum film boiling temperature. One theory says that the minimum temperature is a thermodynamic property of the fluid (i.e. maximum liquid temperature) and thus is primarily a function of pressure. The other theory suggests that rewetting commences due to hydrodynamic instabilities which depend on the velocities, densities, and viscosities of both phases as well as the surface tension at the liquid-vapour interface. During fast transitions, where insufficient time is available to fully develop the hydrodynamic forces, rewetting is expected to be thermodynamically controlled while for low flows and low pressures, where sufficient time is available and the volumetric expansion of the fluid near the wall is large, rewetting is more likely to be hydrodynamically controlled. Once rewetting has occurred locally, the rewetting front can then propagate at a rate which is primarily controlled by axial conduction. These theories can be modified to include the thermal properties of the surface.

There is no general consensus on the effect of the various system parameters on the minimum film boiling temperature under forced convective conditions. These effects are included in correlations for the minimum temperature which have been tabulated by Groeneveld and Snoek (1986).

4.2.4. Flow film boiling

4.2.4.1. General

Film boiling is generally defined as that mode of boiling heat transfer where only the vapour phase is in contact with the heated surface. The term film boiling was originally applied to pool boiling where the stagnant liquid was separated from the heated surface by a vapour film. The term has been used in forced convective boiling to refer to conditions where the liquid does not contact the heated surface but is usually in one of the following forms:

- (i) a dispersed spray of droplets, normally encountered at void fractions in excess of 80% (liquid-deficient or dispersed flow film boiling regime);
- (ii) a continuous liquid core (surrounded by a vapour annulus which may contain entrained droplets) usually encountered at void fractions below 40% (inverted annular film boiling or IAFB regime); or
- (iii) a transition between the above two cases, which can be in the form of an inverted slug flow for low to medium flow.

Figure 4.3 illustrates the above flow regimes. Of these, the dispersed flow film boiling (DFFB) regime is most commonly encountered and has been well studied. Its heated surface temperature is moderate while in the inverted annular and the inverted slug flow regimes, excessive surface temperatures are frequently encountered.

Radiation heat transfer, although unimportant in transition boiling, becomes increasingly important in film boiling, particularly at low flows, low void fractions and surface temperatures in excess of 700°C.

The main parameters controlling the film boiling heat transfer are: pressure, equilibrium quality (or subcooling), and mass flux. At low flows, strong non-equilibrium effects can be present which will need to be considered. In addition at locations just downstream of (or “just subsequent to” during fast transients) the CHF or quench occurrence, upstream/history effects are important. These effects frequently are not included in film boiling models [see also Gottula et al. (1985); Shiralkar et al. (1980); Kirillov et al. (1982)].

Due to the high surface temperatures frequently encountered during film boiling with water, studies using cryogenic and refrigerant fluids and pool boiling studies have been extensively employed to improve our understanding of film boiling and to extract parametric trends and derive correlations.

Reviews of the film boiling literature have been prepared separately for the higher quality DFFB regime [Mayinger (1978); Collier (1981); Groeneveld (1975a & 1977); Andreoni and Yadigaroglu (1994)]; the IAFB regime [Groeneveld (1984, 1992); Andreoni and Yadigaroglu (1974)] and for pool film boiling [Hsu (1972); Kalinin (1987)].

4.2.4.2. Inverted annular film boiling

IAFB refers to the film boiling type characterized by a vapour layer separating the continuous liquid core from the heated surface. Figure 4.3 (RHS) shows schematically the phase distribution during IAFB. IAFB resembles pool film boiling superficially, but the actual heat transfer mechanisms are considerably more complex.

In the inverted annular flow regime few entrained droplets are present while the bulk of the liquid is in the form of a continuous liquid core which may contain entrained bubbles. At dryout the continuous liquid core becomes separated from the wall by a low viscosity vapour layer which can accommodate steep velocity gradients. However, the velocity distribution across the liquid core is fairly uniform. Once a stable vapour blanket has formed, the heat is transferred from the wall to the vapour and subsequently from the vapour to the wavy liquid core. Initially, for very thin vapour films, heat transfer from the wall to the liquid is primarily by conduction across a laminar vapour film. When the vapour film thickness increases, turbulent flow will occur in the film, and the liquid-vapour interface becomes agitated. Heat transfer across the wavy vapour-liquid interface takes place by forced convection. This mode of heat transfer is much more efficient than the single-phase convective heat transfer between a smooth wall and the vapour; hence it is assumed that the bulk of the vapour is at or close to the liquid core temperature (i.e. saturation temperature). The low-viscosity, low-density vapour-flow experiences a higher acceleration than the dense core flow. This results in an increased velocity differential across the interface which may lead to liquid entrainment from the wavy interface. It may also lead to more interaction of the liquid core with the heated surface through dry collisions and will increase the turbulence level in the vapour annulus. The resulting increase in wall-vapour and wall-core heat transfer will lower the wall temperature; if the wall temperature drops below the minimum film boiling temperature rewetting may occur. Rewetting can also occur at higher temperatures if it is caused by a propagating rewetting front.

Modeling of IAFB requires proper relationships for the interfacial heat and momentum transfer between the superheated vapour blanket and the subcooled or saturated liquid core. The net interfacial heat transfer determines the rate of vapour generation and, therefore, the film thickness.

The heat transfer process in IAFB can be considered by the following heat flux components:

- (i) convective heat transfer from the wall to vapor ($q_{w,v}$);
- (ii) radiation heat transfer from the wall to liquid (q_{rad});
- (iii) heat transfer from vapor to the vapor-liquid interface ($q_{v,i}$);
- (iv) heat transfer from the vapor-liquid interface to the liquid core ($q_{i,l}$).

In the case of subcooled film boiling, the last heat flux component is used for both vaporization and reducing liquid subcooling. For saturated liquid, $q_{i,l}$ is used only for vaporization, thus increasing the vapor film thickness more rapidly.

A significant increase in heat transfer coefficient with an increase in liquid subcooling has generally been observed in pool film boiling and flow film boiling [e.g. see Groeneveld (1992)]. The effect of subcooling on the film boiling heat transfer coefficient may be explained as follows: heat is transferred primarily by conduction across a thin vapour film to the interface (convection and radiation may also be significant). Here a fraction of the heat received is used for heating up the liquid core, while the remainder is used for evaporation. Higher subcoolings results in less evaporation, and hence a thinner vapour film, which consequently increases the heat transfer coefficient h . During tests on heated bodies immersed in water, Bradfield (1967) observed that subcooled film boiling with subcoolings less than 35°C resulted in a calmer interface with a wavelike motion compared to saturated boiling. Most experimental studies show an increase in h with an increase in X_e at the high mass velocities ($G > 1000 \text{ kg/m}^2\text{s}$ at $P > 6 \text{ MPa}$ [Stewart (1981); Laperriere and Groeneveld (1984)] and $G > 100 \text{ kg/m}^2\text{s}$ at $P = 0.1 \text{ MPa}$, [Fung (1981)]) although at times this increase in h may not be evident near zero qualities. At lower mass velocities, a decrease in h ($=q_w/(T_w - T_s)$) with an increase in X_e is frequently observed. The above effect is due to the gradual thickening of the vapour film with increasing X_e . This will increase the resistance to conduction heat transfer which may still be dominant at low G and X_e values. It also increases the convective heat transfer coefficient, defined as $h_c = q/(T_w - T_v)$. Since at low flows the vapour temperature T_v may rise significantly above saturation, the T_w may still increase despite the increase in h_c . At high mass velocities ($G > 2000 \text{ kgm}^{-2}\text{s}^{-1}$) T_v is usually near saturation and h generally increases with X_e . With an increase in quality or void fraction the IAFB regime breaks up at void fraction of about 30–60% and the transition to the DFFB regime occurs.

The recent reviews on IAFB published by Groeneveld (1992), Johannsen (1991) and Hammouda (1996) include description or tabulations of new or modified models for IAFB heat transfer related to reflood heat transfer of water-cooled nuclear reactors. These reviews are based on publications by Analytis et al. (1987), Klyugel et al. (1986), Mosaad (1986), Hsu et al. (1986), Wang et al (1987,1988), Yan (1987), and Lee et al. (1987).

4.2.4.3. Slug flow film boiling

Slug flow film boiling is usually encountered at low flows and void fractions which are too high to maintain inverted annular film boiling but too low to maintain dispersed flow film

boiling. In tubes, it is formed just downstream of the inverted annular flow regime when the liquid core breaks up into slugs of liquid in a vapour matrix. The prediction of the occurrence of slug flow during bottom flooding ECC is important because of the change in heat transfer rate long before the arrival of the quench front.

Several theories for the break-up of the IAFB regime have been proposed. Data of Chi (1967) suggest that the liquid core will break up into slugs which are equal in length to the most unstable wavelength of interfacial waves. Subcooling tends to stabilize the liquid-vapour interface, and thus inhibits the formation of slug flow. Smith (1976) assumes the location of slug flow to correspond to the point of minimum heat transfer coefficient in the film boiling region. In doing so, he is suggesting that if the vapour velocity is high enough to break up the liquid core, then it is also high enough to considerably improve the heat transfer coefficient. Kalinin (1969) observed another possible mechanism for the onset of slug flow in transient tests. Immediately after the introduction of liquid to their test section, the sudden increase in void due to vapour generation at the leading edge of the liquid caused a back pressure which decelerated the flow. The higher pressure and lower flow rate caused a decrease in vaporization and the flow surges forward. The cycle was repetitive with a liquid slug separating from the liquid core with each cycle.

4.2.4.4. Dispersed flow film boiling (DFFB)

The DFFB regime is characterized by the existence of discrete liquid drops entrained in a continuous vapor flow. This flow regime may be defined as dispersed flow film boiling, liquid deficient heat transfer, or mist flow. It is of importance in nuclear reactor cores for off-normal conditions such as the blowdown or ECCS phase of a LOCA, as well as in steam generators.

The DFFB regime usually occurs at void fractions in excess of 40%. No exact lower-bound value for the onset of DFFB is available as the transition from IAFB or slug flow film boiling is likely to be gradual. According to Levitan and Borevskiy (1989), the beginning of the dispersed regime is determined by the following correlation

$$X_{ad} = (2.7 \pm 0.3) \left(\frac{\rho_\ell \cdot \sigma}{G^2 \cdot d} \right)^{1/4} \left(\frac{\rho_v}{\rho_\ell} \right)^{1/3} \quad (4.1)$$

where

X_{ad} represents the onset of annular dispersed flow.

In the DFFB regime the vapour temperature is controlled by wall-vapour and vapour-droplet heat exchange. Due to the low superheat of the vapour near the dryout location or rewetting front the vapour droplet heat exchange is small and most of the heat transferred from the wall is used for superheating the vapour. At distances further downstream, however, an "equilibrium" vapour superheat can be reached, i.e. the amount of heat transferred from the wall to the vapour may approximately balance the amount of heat absorbed by the droplets (from the vapour) and used for evaporation of the droplets.

Near the heated surface the heat exchange between vapour and droplets is enhanced due to the temperature in the thermal boundary layer being well above that of the vapour core [Cumo and Farello (1967)]. If the temperature of the heated surface is below the minimum temperature, some wetting of the wall may occur resulting in an appreciable fraction of the droplets being evaporated [Wachters (1965)]. At temperatures above the minimum temperature only dry collisions can take place (collisions where a vapour blanket is always present between surface and droplet). Little heat transfer takes place to small droplets which resist deformation and bounce back soon following a dry collision [Wachters (1965); Bennett et al. (1967)]. However, the dry collisions disturb the boundary layer thus improving the wall-vapour heat transfer. Larger droplets are much more deformable and tend to spread considerably thus improving both the wall-vapour and vapour-droplet heat exchange [Cumo and Farello (1967); Wachters (1965)]. This spreading may lead to a breakup into many smaller droplets if the impact velocity is sufficiently high [McGinnis and Holman (1969)]. The vapour film thickness separating the stagnated droplets from the heated surface is difficult to estimate but must be greater than the mean free path of the vapour molecules in order to physically separate the liquid from the heated surface.

Attempts to evaluate the direct heat flux to the droplets due to interaction with the heated surface have resulted in the postulation of many simplifying assumptions, e.g. Bailey (1972), Groeneveld (1972), Plummer et al. (1976). These assumptions may be questionable when applied to liquid deficient cooling. However, due to lack of direct measurement of droplet-wall interaction during forced-convective film boiling conditions no other approach can be taken.

The heat flux encountered during DFFB can be partitioned as follows:

- (i) Heat transfer from wall to liquid droplets which reach the thermal boundary layer without wetting the wall (dry collisions) — q_{wdd} ;
- (ii) Heat transfer from wall to liquid droplets which temporarily wet wall (wet collisions) — q_{wdw} ;
- (iii) Convective heat transfer from wall to vapor — q_{wv} ;
- (iv) Convective heat transfer from steam to droplets in the vapor core — q_{vd} ;
- (v) Radiation heat transfer from wall to liquid droplets — q_{rad} ;
- (vi) Radiation heat transfer from wall to vapor — q_{rad} .

The most important unknown in DFFB is the thermal non-equilibrium or vapour superheat. The vapour superheat increases with heat flux (its main driving force) and decreases with interfacial area and interfacial drag. Both the interfacial area and the interfacial drag are dependent hydrodynamic parameters controlled by the dynamics of interfacial shear, droplet generation, break-up, and coalescence mechanisms, and evaporation history. There are basic difficulties in determining experimentally important parameters such as the interfacial drag coefficient. Since the spectrum of droplet sizes may vary from case to case, and the closure laws depend on droplet diameter, the formulation of universally valid closure laws is difficult. This has been investigated in more detail analytically and experimentally by Andreoni and Yadigaroglu (1991, 1991a, 1992), and Kirillov and Smogalev (1973).

4.3. FILM BOILING DATA BASE

4.3.1. General

Because of the importance of film boiling heat transfer and reactor accident analysis, there has been a significant interest in providing a good film boiling data base for reactor

conditions of interest. The high CHF and generally low heat transfer coefficients in film boiling results in high surface temperatures and this restricts the range of conditions at which measurements are feasible under steady state conditions. Hence many of the earlier experimental data were obtained in cryogenics and refrigerants, in temperature controlled systems [Smith (1976); Ellion (1954)] or from transient tests [Newbold et al. (1976); Cheng and Ng (1976); Fung (1977)]. However, a novel approach has been developed at Chalk River for obtaining subcooled film boiling data [Groeneveld and Gardiner (1978)]. Using the so-called hot-patch technique steady-state subcooled and low-quality film boiling data can be obtained in a heat flux controlled system at heat flux levels well below the CHF. This approach has permitted a much more extensive study of film boiling especially at IAFB conditions [e.g. Stewart (1981); Fung (1981); LaPerriere and Groeneveld (1984); Gottula et al. (1985); Johannsen (1991)].

4.3.2. Tube and annuli

Tables 4.1 and 4.2 summarize the test conditions of film boiling data obtained in tubes and annuli, respectively. Although the coverage is extensive, there is still a scarcity of film boiling data at low pressures and low flows. Recent data obtained by CIAE have helped to resolve this lack of data [Chen and Chen (1998)].

4.3.3. Bundle

Table 4.3 summarizes the film boiling data available for rod bundles. Many other bundle data have been obtained but these are inaccessible because of their potential commercial value and because of licensing concerns. The film boiling bundle data base is more limited than the CHF bundle data base because of the higher temperatures which makes testing much more difficult. The hot patch approach, used successfully in tubes, cannot be used in bundles and this further restricts this data base.

4.4. OVERVIEW OF FILM BOILING PREDICTION METHODS

4.4.1. General

Accurate prediction of the wall temperature in the film boiling regime is of vital importance in accident analysis of the core and steam generators of advanced water cooled reactors. The following four methods for estimating the film boiling heat transfer are commonly used:

- (i) Semi-theoretical equations for pool film boiling (Section 4.4.2);
- (ii) Semi-theoretical models to predict flow film boiling. They are based on the appropriate constitutive equations, some of which are empirical in nature;
- (iii) Purely empirical correlations for flow film boiling, which do not account for any of the physics, but instead assume a forced convective type correlation;
- (iv) Phenomenological equations for flow film boiling, which account for the thermal non-equilibrium and attempt to predict the “true” vapour quality and the vapour temperature.

Because of the proliferation of film boiling prediction methods (there are currently over 20 film boiling models available and well over 50 correlations) tabular methods have recently been proposed. Tabular methods are well accepted for the prediction of CHF and are based more closely on experimental data. They will be discussed in Section 4.4.5.

TABLE 4.1. EXPERIMENTAL DATA ON FILM BOILING IN TUBES

Year	Reference	P, MPa	G, kg/m ² s	d, mm	L m	X	q, MW/m ²	T _w , °C	n, number of points	Notes
1950	Mc Adams	0.8 - 24	70 - 230	3.3			0.03 - 0.54			L/d=14.7 - 80
1960	Hemann	2.1 - 10.3	190 - 1070	2.5 - 8.4			0.16 - 0.92			L/d=36 - 100
1961	Collier	0.1 - 7.4	580 - 1380	4.3 - 61			0.16 - 0.41			L/d=35 - 170
1961	Parker	0.2	50 - 100	25.4	0.5	0.89 - 1.0	0.01 - 0.06			rewetting of wall
1961	Swenson	20.7	949 - 1356	14		0.08 - 0.98	0.297 - 0.581	379 - 499		
1963	Miropolskiy	3.9 - 21.6	398 - 2100	8	1.5	-2.43 - 3.42	0.07 - 2.33		5500	
1964	Bertoletti	7	1000 - 4000	5; 9		0.4 - 0.90	0.1 - 1.60			unstable temperature
1965	Bishop et al.	16.6 - 21.5	2000 - 3377	2.5 - 5.1		0.07 - 0.91	0.905 - 1.92	390 - 610		
1967	Bennett et al.	6.89	380 - 5180	12.6		0.229 - 1.48	0.383 - 2.07	454 - 840		
1967	Era et al.	6.89 - 7.28	1090 - 3020	6		0.456 - 1.24	0.20 - 1.65	295 - 630		
1967	Herkenrath et al.	14 - 20.5	693 - 3556	10 - 20		-0.117 - 1.32	0.253 - 1.666	374 - 592		
1967	Mueller	6.9	700 - 1000	15.7		0.62 - 1.0	0.5 - 0.85			
1967	Polomik	6.9	700 - 1350	15.7		0.8 - 1.0	0.55 - 1.10			
1969	Brevi	5	470 - 3000	6.5; 9.3		0.40 - 1.0	0.38 - 1.5			
1969	Kutucukcuoglu	1 - 3.3		7 - 14			0.03 - 0.57			L/d= 50, 150
1970	Lee	14 - 18	1000 - 4000		9; 13	0.3 - 0.7	0.3 - 1.4			heated by sodium
1971	Keays	6.9	700 - 4100	12.7		0.15 - 0.90	0.8 - 1.5			cosine heat flux distribution

TABLE 4.1. (CONT.)

Year	Reference	P, MPa	G, kg/m ² s	d, mm	L, m	X	q, MW/m ²	T _w , °C	n number of points	Notes
1972	Bailey	17.8	668 - 2690	12.7		0.391 - 0.95	372 - 454			U-tube
1973	Sutherland	6.9	24 - 175	38			0.016 - 0.063			L/d=120 - 220
1974	Grachev et al.	7 - 14	350 - 1000	11.12	2.1-9.0	0.35 - 1.3	0.05 - 0.3		414	heated by sodium
1975	Janssen et al.	0.683 - 7.07	16.6 - 1024	12.6		0.584 - 1.63	0.034 - 0.997	341 - 727		
1981	Fang	0.089 - 0.145	50 - 495	11.8 - 11.9		-0.026 - 0.138	0.025 - 0.257	362-1148		
1982	Stewart, Groeneveld	1.94 - 9.05	114 - 2810	8.9	1.71	-0.12 - 0.736	0.064 - 0.459	306 - 780	1023	
1983	Becker et al.	2.98 - 20.1	4.96 - 3110	10 ÷ 24.7		-0.042 - 1.65	0.083 - 1.29	279 - 722		
1983	Borodin	8.2 - 8.34	1350 - 6870	8.9		0.133 - 1.07	0.90 - 2.7	378 - 720		
1983	Chen and Nijihawan	0.226 - 0.419	18.7 - 69.5	14.1		0.072 - 0.838	0.0027 - 0.088	229 - 648		
1983	Laperriere	3.95 - 9.63	962 - 4510	9		-0.119 - 0.597	0.069 - 0.736	308 - 781		
1985	Gottula et al.	0.290 - 0.79	1.21 - 19.3	15.7		0.319 - 0.87	0.003 - 0.044	175 - 789		
1987	Remizov et al.	4.9 - 19.6	350 - 3000	10	1.5-10.2	0 - 2.48	0 - 1.28		37298	
1988	Chen, Fu, Chen	0.15 - 1.02	100 - 512	7; 12	0.99				38	
1988	Mosaad	0.11	100 - 500	9	0.28	-0.12 - 0			2100	
1988	Swinnerton et al.	0.2 - 1.92	200 - 1000	9.75	0.92	0 - 0.46	0.005 - 0.5		273	
1989	Chen Yu-Zhou et al.	0.41 - 6	47.6 - 1462	12	2.2	-0.05 - 0.24	0.028 - 0.260			
1996(b)	Chen and Chen	0.1-6.0	23-1462	6.8; 12	1.2-2.6	-0.05-1.36	0.015-0.49		3568	

TABLE 4.2. EXPERIMENTAL DATA ON FILM BOILING IN ANNULI

Year	Reference	P, Mpa	G, kg/m ² s	d _i , mm	L, m	X	q, MW/m ²	T _w , °C	n number of points	Notes
1961	Polomik	5.5 - 9.7	1000 - 2560			0.15 - 1.0	0.6 - 2.2			d _e = 1.52; 3.05
1964	Bennett	3.5 - 6.9	700 - 2700			0.2 - 1.0	0.6 - 1.8			
1967	Era	7	800 - 3800			0.3 - 1.0	0.13 - 1.0			d _e = 2; 5 spacers
1969	Groeneveld	4.1 - 8.3	1350 - 4100				0.5 - 1.4			two heated sections separated by unheated section
1971	Polomik	6.9	350 - 2700			0.15 - 0.65	0.75 - 2.3			d _e = 3.3 spacers
1971	Era	5	600 - 2200			0.2 - 0.9	0.2 - 0.6			d _e = 3 uniformly and nonuniformly heated
1980	OKB Hidropress Report No 431-0-047	1.5 - 15.9	8.9 - 148	9.1 d _o = 15.5	3.24	0.5 - 1.96	0.03 - 0.275		1154	

TABLE 4.3. EXPERIMENTAL DATA ON FILM BOILING IN ROD BUNDLES

Year	Reference	P, MPa	G, kg/m ² s	d _r , mm	S, mm	L, m	n, number of rods	X	q, MW/m ²	n number of points	Notes
1963	Matzner	6.9	700 - 2700				19	0.17 - 0.60	0.8 - 2.35		d _e = 8.3 mm, mainly stable temperature
1964	Hench	4.1 - 9.7	390 - 2700				2	0.2 - 0.9	0.45 - 1.9		d _e = 10.3 mm
1965	Kunsemiller	4.1 - 9.7	390 - 1350				3	0.3 - 0.7	0.55 - 1.0		d _e = 11.2 mm
1966	Adorni	5 - 5.5	800 - 3800				7	0.2 - 0.9	0.2 - 1.5		mainly stable temperature
1968	Matzner	3.4 - 8.3	700 - 1400				19	0.23 - 0.38			d _e = 6.7 mm segmented bundle
1970	Groeneveld et al.	6.3	1100 - 2200	15.2	16.2	0.5	3	0.3 - 0.6	0.033 - 1.16	160	inpile test trefoil
1971	Mc Pherson	10.9 - 2.17	700 - 4100				28	0.28 - 0.53	0.6 - 1.45		d _e = 7.8 mm mainly stable temperature
1973	Groeneveld and Mc Pherson	6.8 - 10.2	630 - 1350	13.8	14.8 - 15.8	0.5	36	0.35 ÷ 1	0.08 - 1.2		inpile test T _w = 650°C
1976	OKB Hidropress Report No 213-0-084	1 - 6	130 - 700	9.1		1.75	7	0.6 - 1.24	0.1 - 0.35	301	d _e = 2.5 mm spacers

4.4.2. Pool film boiling equations

4.4.2.1. Horizontal surfaces

Pool film boiling from a horizontal surface has been investigated for over 50 years, and can be reasonably well represented by analytical solutions. Most pool film boiling and low flow film boiling prediction methods [e.g. Bromley (1950); Borishanskiy (1959, 1964); Berenson (1961)] are of the following form:

$$\alpha = C \cdot \left[\frac{\lambda_v^3 \cdot r^* \cdot \rho_v (\rho_\ell - \rho_v)}{\mu_v \cdot \Delta T} \right]^{1/4} \cdot F(U, l) + \alpha_{rad}(\epsilon, T_W, T_S) \quad (4.2)$$

where

r^* is an equivalent latent heat and includes the effect of vapour superheat, sometimes expressed as $r^* = r + 0.5(C_p)_v \Delta T$. The velocity effect on the heat transfer coefficient is taken into account by the F-function. The symbol l represents either a characteristic length (e.g. diameter) of the surface or the critical wave length which is usually defined as:

$$l = \sqrt{\frac{\sigma}{g(\rho_\ell - \rho_v)}} \quad (4.3)$$

Other relations for pool film boiling have been proposed by Epstein and Hauser (1980), Klimenko (1981), Dhir (1990), and Sakurai (1990a, 1990b). Table 4.4 gives the correlations for the film boiling heat transfer on horizontal surfaces in pool boiling based on the following dimensional groups

$$Nu = \alpha l / \lambda_v \quad (4.4)$$

$$Ra = \frac{g \cdot l^3 \cdot (\rho_\ell - \rho_v)}{\rho_v \cdot \nu_v^2} \cdot Pr \quad (4.5)$$

4.4.2.2. Vertical surfaces

Saturated pool film boiling on vertical surfaces has been investigated experimentally and theoretically by many researchers including Hsu, and Westwater (1960), Suryanarayana, and Merte (1972), Leonardo, and Sun (1976), Andersen (1976), Bui, and Dhir (1985). Frequently equations similar as those for horizontal surfaces are proposed for vertical surfaces; the main difference is usually in the constant C in front of the equation and the characteristic length. Sakurai (1990a, 1990b, 1990c) developed new equations for film boiling heat transfer on surfaces with different configurations. In particular, correlations for vertical plates and tubes, spheres and horizontal plates were derived by the same procedure as that used for horizontal cylinders. The latter was derived by slightly modifying the corresponding analytical solution to get agreement with the experimental results.

TABLE 4.4. CORRELATIONS FOR FILM BOILING HEAT TRANSFER ON HORIZONTAL SURFACES IN POOL BOILING

References	Correlations	Notes
1	2	3
Chang 1959	$Nu = 0.295 \left(Ra \cdot \frac{r^*}{C_p \cdot \Delta T} \right)^{1/3} \quad (1)$ <p>where</p> $Ra = gl^3(\rho_v - \rho_\ell)Pr/\rho_v \nu_v^2 \quad (2)$ $l = \sqrt{\sigma/g(\rho_v - \rho_\ell)} \quad (3)$ $r^* = r + 0.5 \left(C_p \right)_v \Delta T \quad (4)$	Laminar flow in vapor film.
Berenson 1961	$Nu = 0.672 \left(Ra \cdot \frac{r^*}{C_p \cdot \Delta T} \right)^{1/2} \quad (5)$	Laminar flow in vapor film; Ra, l, and r* according to Eqs. 2, 3 and 4.
Frederking et al. 1966	$Nu = 0.20 \left(Ra \cdot \frac{r^*}{C_p \cdot \Delta T} \right)^{1/3} \quad (6)$	Turbulent film boiling; Ra, l, and r* according to Eqs. 2, 3 and 4.
Hamill Baumeister, 1967 (cited by Klimenko 1981)	$Nu = 0.648 \left(Ra \cdot \frac{r^*}{C_p \cdot \Delta T} \right)^{1/4} \quad (7)$ $r^* = r + 0.95 \left(C_p \right)_v \Delta T \quad 7.1$	Turbulent film boiling; Ra and l according to Eqs. 2 and 3.
Clark, 1968 (cited by Klimenko 1981)	$Nu = 0.612 \left(Ra \cdot \frac{r^*}{C_p \cdot \Delta T} \right)^{1/2} \quad (8)$	Turbulent film boiling; Ra, l, and r* according to Eqs. 2, 3 and 4.

TABLE 4.4. (CONT.)

1	2	3
Lao, 1970 (cited by Klimenko 1981)	$Nu = 185Ra \cdot \left(\frac{r}{C_p \cdot \Delta T} \right)^{-0.09} \quad (9)$ $l = 2\pi\sqrt{[6\sigma/g(\rho_\ell - \rho_v)]} \quad (10)$	Turbulent film boiling; Ra, r^* according to Eqs. 2 and 4.
Klimenko 1981	$Nu = 0.19Ar^{1/3} Pr^{1/3} \cdot f_1 \left(\frac{r}{C_{pv} \cdot \Delta T} \right) \quad (11)$ <p>Here</p> $Ar = \frac{g \cdot l^3 \cdot (\rho_\ell - \rho_v)}{\rho_v \cdot \nu_v^2} < 10^8 \quad (12)$ $f_1 \left(\frac{r}{C_{pv} \cdot \Delta T} \right) = \begin{cases} 1 & \text{for } \frac{r}{C_{pv} \cdot \Delta T} < 1.4 \\ 0.89 \cdot \left(\frac{r}{C_{pv} \cdot \Delta T} \right)^{1/3} & \text{for } \frac{r}{C_{pv} \cdot \Delta T} > 1.4 \end{cases} \quad (13)$	Laminar flow in vapor film; l according to Eq. 3

TABLE 4.4. (CONT.)

1	2	3
Klimenko 1981	$Nu = 0.0086 Ar^{1/2} Pr^{1/3} \cdot f_2 \left(\frac{r}{C_{pv} \cdot \Delta T} \right) \quad (14)$ <p>Here $Ar \geq 0.8$</p> $f_2 \left(\frac{r}{C_{pv} \cdot \Delta T} \right) = \begin{cases} 1 & \text{at } \frac{r}{C_{pv} \Delta T} < 2 \\ 0.71 \left(\frac{r}{C_{pv} \cdot \Delta T} \right)^{1/2} & \text{at } \frac{r}{C_{pv} \Delta T} > 2 \end{cases} \quad (12)$	Turbulent film boiling.
Granovsky et al 1992	$Nu = 0.031 \cdot (\lg A)^{3.5} \varphi^{2/3} \quad (13)$ $A = \frac{(Ar)^*}{\left(\frac{C_p \cdot \Delta T}{r^* \cdot Pr} \right)^2 + \frac{C_p \cdot \Delta T}{r^* \cdot Pr}} \quad (14)$ $(Ar)^* = \frac{g \cdot l^3 \cdot \rho_v (\rho_l - \rho_v)}{\mu_v^2} \quad (15)$ $\varphi = \alpha_{\text{film}} / (\alpha_{\text{film}} + \alpha_{\text{rad}}) \quad (16)$	Turbulent film boiling; l and r^* according to Eq. 3 and 4.

4.4.2.3. Downward-facing surfaces

Recent experiments by Kaljakin et al. (1995) on curved down-facing surfaces have demonstrated that in many cases the heat transfer coefficient prediction for pool film boiling or for low mass velocities can be based on the modified Bromley formula (1950):

$$\alpha_x = \beta \sqrt{\frac{\lambda_v^3 \rho_v g \cdot (\rho_\ell - \rho_v) r^*}{\mu_v \Delta T \cdot x}} \quad (4.6)$$

where

$\beta = 0.8 + 0.0022\Theta$; Θ is a surface inclination angle, in degrees;
 $\Delta T = T_w - T_s$; is a characteristic length along the vessel surface, and
 r^* is defined as in Equation 4.2.

Eq. 4.6 is reportedly valid for a pressure range of about 0.1 – 0.2 MPa.

4.4.3. Flow film boiling models

4.4.3.1. General

The first flow film boiling models were developed for the DFFB regime. In these models, all parameters were initially evaluated at the dryout location. It was assumed that heat transfer takes place in two steps: (i) from the heated surface to the vapour, and (ii) from the vapour to the droplets (see also Section 4.2.4.4). The models evaluate the axial gradients in droplet diameter, vapour and droplet velocity, and pressure, from the conservation equations. Using a heat balance, the vapour superheat was then evaluated. The wall temperature was finally found from the vapour temperature using a superheated-steam heat transfer correlation. Improvements to the original model have been made by including droplet-wall interaction, by permitting a gradual change in average droplet diameter due to the break-up of droplets, and by including vapour flashing for large pressure gradients.

Subsequent to the development of models for the DFFB regime, models have also been developed for the IAFB regime. They are basically unequal-velocity, unequal-temperature (UVUT) models which can account for the non-equilibrium in both the liquid and the vapour phase. Most of the models are based on empirical relationships to predict interfacial heat and momentum transfer. Advanced thermalhydraulic codes employ similar models to simulate the post-CHF region. Universal use of film boiling models is still limited because of unresolved uncertainties in interfacial heat transfer, interfacial friction and liquid-wall interactions, as well as the difficulty in modelling the effect of grid spacers.

4.4.3.2. IAFB regime

A large number of analytical models have been developed to simulate the IAFB conditions [e.g. Analytis and Yadigaroglu (1987); Kawaji and Banerjee (1987); Denham (1983); Seok and Chang (1990); Chan and Yadigaroglu (1980); Takenaka (1989); Analytis (1990); de Cachard (1995); Mosaad (1988), Mosaad and Johannsen (1989); Hammouda, Groeneveld, and Cheng (1996)]. The salient features of many of these models have been

tabulated by Groeneveld (1992) and Hammouda (1996). Table 4.5 provides an overview of some of the current IAFB models. The majority is based on two-fluid models and employ some or all of the assumptions listed below:

- (i) at the quench front the liquid is subcooled and the vapour is saturated;
- (ii) vapour will become superheated at the down stream of the quench front;
- (iii) both the vapour and liquid phases at the interface are at saturation;
- (iv) the interfacial velocity is taken as the average of the vapour and liquid velocities;
- (v) there is no entrainment of vapour in a liquid core or of the liquid in the vapor film;
- (vi) the vapour film flow and the liquid core flow are both turbulent.

The above assumptions clearly indicate differences from the classical Bromley-type analysis for pool film boiling, and there is no smooth transition between these two cases.

The main challenge in implementing IAFB models into two-fluid codes resides in the proper choice of the interfacial heat and momentum exchange correlations. Interfacial heat exchange enhancements may be due to turbulence in the film, violent vaporization at the quench front, liquid contacts with the wall near the quench front, upstream grid spacers or approaching quench front, and the effect of the developing boundary layer in the vapour film. The large amount of vapour that may be generated right at the quench front (release of the heat stored in the wall due to quenching) must also be taken into account. Reflooding experiments clearly show an exponential decay of the heat transfer coefficient with distance from the quench front for a length extending some 20 or 30 cm above the quench front.

The constitutive relations employed are based on the simplifying assumptions. In general, there are too many adjustable parameters and assumptions made by different authors which results in a multitude of IAFB models. A part of the reason is the difficulty in verifying the proposed interfacial relationships with experimental-based values. Despite this, relatively good agreement was reported by the model developers between their model prediction and the experimental data, but no independent review of their models was ever made.

During high-subcooling film boiling the vapour film at the heated surface is very thin over most of the IAFB length. Here the prediction methods or models tend to overpredict the wall temperature, presumably because the conduction-controlled heat transfer across a very thin film was not properly accounted for.

4.4.3.3. DFFB regime

Significant non-equilibrium between the liquid and vapor phases is usually present in the DFFB regime, except for the high mass velocities. Mixture models are intrinsically not able to predict this non-equilibrium and hence the need for two-fluid models. As the interfacial heat transfer is easier to determine either experimentally or analytically for the DFFB regime vs. the IAFB regime, these models tend to be somewhat more accurate than those simulating IAFB.

As discussed in Section 4.2 the heat transfer in DFFB is a two-step process, i.e. (i) wall to vapour heat transfer and (ii) vapour to entrained droplets heat transfer. Enhancement of heat transfer due to the interaction of the droplets with the heated wall are usually small except for low wall superheats, near the T_{MFB} , where transition boiling effects become important.

TABLE 4.5. SUMMARY OF IAFB MODELS

	CHARACTERISTICS	REFERENCES							
		Analytis, Yadigaroglu (1987)	Avdeev (1986)	Chen Yu (1986)	Mosaad, Johannsen (1989)	Fung, Groeneveld (1982)	Groeneveld, Chen, Hammomuda (1991)	Hsu et al (1982)	Klugel, Kabanov (1986)
1.	Dimensional (1D – one-dimensional; 2D - two-dimensional)	1D	1D	1D	1D	1D	1D	2D	1D
2.	Flow Structure (h – homogeneous; t – two fluids)	t	t	t	t	t	t	t	t
3.	Vapour Generation								
3.1	from liquid surface	+	+	+	+	+	+	+	+
3.2	evaporation of drops in a vapour film	–	–	+	–	–	–	–	+
3.3	evaporation of drops on a wall	–	–	–	–	–	–	–	+
3.4	wall-liquid interaction	–	–	–	–	–	–	+	–
4.	Vapour Film								
4.1	flow regime (<i>l</i> – laminar; <i>t</i> – turbulent)	<i>t</i>	<i>t</i>	<i>t</i>	<i>t</i>	<i>l, t</i>	<i>l, t</i>	<i>t</i>	<i>l, t</i>
4.2	presence of drops	–	–	–	–	–	–	–	+
4.3	boundary of liquid (<i>s</i> – smooth; <i>w</i> – wavy)	<i>w</i>	<i>s</i>	<i>s</i>	<i>w</i>	<i>s</i>	<i>s</i>	<i>w</i>	<i>s</i>
4.4	Radiation through a vapour film	+	–	+	+	–	+	+	+
5.	Central Flow								
5.1	1 – one phase flow; 2 – two-phase flow	1	1	1	1	1	1	1	2
5.2	flow regime (<i>l</i> – laminar; <i>t</i> – turbulent)	<i>l, t</i>	<i>l, t</i>	<i>t</i>	<i>t</i>	<i>t</i>	<i>t</i>	<i>t</i>	<i>t</i>
6.	Accuracy by author (%)		20-25		RMS 12			11	
7.	Verification								
7.1	Pressure, MPa	1	1-20	<1	0.1-8	0.1		2; 4	
7.2	Velocity, m/s	0.025	0.85	0.1	0.1	0.2			
		–	–	–	–	–			
		0.17	73	10	10	0.3			
7.3	Subcooling, K	< 70	5-200		20-60	< 20			

TABLE 4.6. SUMMARY OF DFFB MODELS

1	CHARACTERISTICS	REFERENCES								
		Andreani, Yadigaroglu (1991)	Barzoni, Martini (1982)	Chen Yu (1994)	Chen, Ozkaynak, Sundaram (1979)	Forslund, Rohsenow (1968)	Ganich, Rohsenow (1977)	Groeneveld, Delorme (1976)	Jones, Zuber (1977)	Kudriavtzev et al. (1987)
1	2	3	4	5	6	7	8	9	10	11
1.	Dimensional (1D – one-dimensional; 2D - two-dimensional; 3D - three-dimensional)	2D, 3D	1D	1D	1D	1D	1D	1D	1D	2D
2.	Flow Structure (h – homogeneous; dv - drops + vapour)	dv	h	dv	dv	dv	dv	h	dv	h
3.	Scheme of Heat Transfer*	II	I	II	II	III	III	I	II	II
4.	Effects									
4.1	Deposition of drops	+	–	–	–	+	+	–	–	–
4.2	Spectrum of drops	+	–	–	–	–	+	–	–	–
4.3	Effect of drops on transport properties of medium	+	–	+	–	–	–	–	–	+
4.4	Slip	+	–	–	–	–	+	+	–	–
4.5	Radiation	–	–	+	–	–	–	–	–	–
5.	Accuracy by author (%)		RMS 12.3		15			RMS 6.93		
6.	Verification									
6.1	Pressure, MPa			0.1-6			0.7 - 21.5			
6.2	Mass Flux, kg/m ² ·s			24 - 1000				130 - 5200		
6.3	Quality			0.05 - 1.4				0.08 - 1.6		

* Scheme of Heat Transfer

I - heat transfer wall to vapour

II - I + wall to droplet

III - I + II + wall to drops.

TABLE 4.6. (CONT.)

1	CHARACTERISTICS	REFERENCES										
		Marinov, Kabanov (1977)	Moose, Ganic (1982)	Nishikawa et al. (1982, 1981)	Saha (1980)	Sergeev (1976)	Tong, Young (1974)	Varone, Rohsenow (1986)	Vojtek (1982)	Welb, Chen J. (1986)	Whalley et al. (1982)	Yoder, Rohsenow (1983)
1	2	12	13	14	15	16	17	18	19	20	21	22
1.	Dimensional (1D – one-dimensional; 2D - two-dimensional; 3D - three-dimensional)	1D	1D	1D	1D	1D	1D	1D	1D	1D	1D	1D
2.	Flow Structure (h – homogeneous; dv - drops + vapour)	h	dv	dv	dv	dv	dv	dv	h	dv	dv	dv
3.	Scheme of Heat Transfer*	II	III	III	III	II	II	III	II	II	II	II
4.	Effects											
4.1	Deposition of drops	–	+	+	–	–	–	+	+	–	–	–
4.2	Spectrum of drops	–	+	–	–	–	+	–	–	–	+	+
4.3	Effect of drops on transport properties of medium	–	–	–	–	–	–	+	–	+	–	–
4.4	Slip	+	–	–	–	–	+	–	–	–	–	+
4.5	Radiation	–	–	+	–	+	–	–	–	–	–	–
5.	Accuracy by author (%)			20		RMS 10				24	30 - 60	
6.	Verification											
6.1	Pressure, MPa					1-18			3-12	0.1-7		
6.2	Mass Flux, kg/m ² ·s			400 - 1600		100 - 1500			300 - 1400	12 - 100		
6.3	Quality								0.3 - 0.1	0 - 0.99		

* Scheme of Heat Transfer

I - heat transfer wall to vapour

II - I + wall to droplet

III - I + II + wall to drops.

At high mass velocities, the droplet size is small, the interfacial area is large and the interaction between the vapor and droplets is sufficiently intensive to keep the vapor temperature close to the saturation temperature. Here a Dittus-Boelter type equation, based on the volumetric flow rate and vapour properties, provides a reasonable estimate of the overall heat transfer coefficient, and an analytical model is not required.

A large number of models have been developed for the DFFB regime. The first DFFB models were developed for the liquid deficient regime by the UKAEA [Bennett (1967)] and MIT [Lavery and Rohsenow (1967)]. In these models, all parameters were initially evaluated at the dryout location. The models evaluated at the axial gradients in droplet diameter, vapour and drop velocity, and pressure, from the conservation equations. Using a heat balance, the vapour superheat was then evaluated. The wall temperature was finally found from the vapour temperature using a superheated-steam heat transfer correlation. Bailey (1972), Groeneveld (1972), and Plummer et al. (1976) have suggested improvements to the original model by including droplet-wall interaction, by permitting a gradual change in average droplet diameter due to the break-up of droplets, and by including vapour flashing for large pressure gradients. Additional expressions for the vapour generation rate have also been suggested by Saha (1980), and Jones and Zuber (1977).

The various models tend to have the same basic structure but differ in the choice of interfacial relationships and separate effects. The following variants have been used in the models:

- (i) droplet size: based on various Weber number criteria for the initial droplet size and for subsequent break-up; Weber number may be ignored; subsequent droplet break-up is often ignored
- (ii) droplet size distribution: various assumptions have been made, e.g. constant size, gaussian distribution
- (iii) droplet drag force: depends on drag coefficient and assumed shape of the droplet
- (iv) interfacial heat transfer: depends on phase velocity differential: various equations are possible
- (v) droplet-wall heat transfer q_{dw} : this may be expressed by a separate heat flux $q_{dw} = 0$ or $q_{dw} = f(T_w - T_{SAT})$; may be ignored ($q_{dw} = 0$) or may be incorporated by enhancement of the convective heat transfer.

Despite these variants the agreement between the predictions of most DFFB models is quite good at steady-state conditions, and medium flows and pressures ($G = 0.3\text{--}6 \text{ Mgm}^{-2}\text{s}^{-1}$, $P = 5\text{--}10 \text{ MPa}$).

Details of the models and the equations on which they are based may be found in Andreoni and Yadigaroglu (1994), Groeneveld and Snoek (1986), Chen and Cheng (1994), and Hammouda (1996). Table 4.6 provides an overview of the major features of the DFFB models.

4.4.4. Flow film boiling correlations

4.4.4.1. IAFB correlations

For the IAFB regime many equations have been proposed, including the classic Bromley (1950) equation for the vertical surface, the Ellion (1954) equation, the Hsu and

Westwater (1960) equation, the modified Bromley equation for pool film boiling: [Leonard (1978); Hsu (1975)], and various other ones. Groeneveld (1984, 1992) later updated by Hammouda (1996) have tabulated the proposed equations for IAFB. None of the proposed prediction method appears to have a wide range of application as far as flow conditions is concerned or as far as geometry is concerned. Most are derived for tube flow or for pool boiling conditions and none has been derived for application in a bundle geometry equipped with rod spacing devices. Hence caution should be exercised before applying them to AWCs.

4.4.4.2. DFFB correlations

4.4.4.2.1. Correlations based on equilibrium conditions

Most of the equilibrium-type equations for film boiling are variants of the single-phase Dittus-Boelter type correlation. These equations were empirically derived or simply assume that there is no non-equilibrium and hence use the same basic prediction method as for superheated steam except that the Reynolds number is usually based on the homogeneous (no slip) velocity. These equations usually have a very limited range of application, or are valid only for the high mass velocity regime where non-equilibrium effects are small. The most common correlations of this type are tabulated in Table 4.7. Among these the Dougall Rohsenow (1963), the Miropolskiy (1963) and the Groeneveld (1973) equations are the more popular ones. The latter two are both based on Miropolskiy's Y-factor as defined in Table 4.7. This factor is particularly significant at lower pressures and qualities. Groeneveld optimized his coefficients and exponents based on a separate data base for tubes, annuli and bundles.

4.4.4.2.2. Phenomenological equations based on non-equilibrium conditions

Phenomenological equations attempt to predict the degree of non-equilibrium between the liquid and vapour phase. These equations are a compromise between the empirical correlations discussed in the previous section and the film boiling models described in Section 4.4.3. The phenomenological equations generally predict an equilibrium vapour superheat corresponding to fully developed flow and based on local equilibrium conditions. They generally do not require knowledge of upstream conditions, such as location of the quench front. An overview of the phenomenological film boiling equations is given in Table 4.8.

The non-equilibrium equations are based on film boiling data for water and have been developed by Groeneveld and Delorme (1976), Plummer et al. (1977), Chen et al. (1977, 1979), Saha (1980), Sergeev (1985a), Nishikawa (1986). Most of them use the of the Dittus-Boelter type equation e.g. Equation 4.7:

$$Nu_v = \frac{\alpha \cdot D}{\lambda_v} = a \cdot Re_v^b \cdot Pr_v^c \quad (4.7)$$

where

a, b, and c are constants and α is the two-phase heat transfer coefficient in a tube with an inside diameter D.

TABLE 4.7. EMPIRICAL FLOW FILM BOILING HEAT TRANSFER CORRELATIONS

References	Correlations	Ranges of Parameters		
		P MPa	G kg/m ² ·s	X
Collier 1962	$q \cdot [D^{0.2} / (G \cdot X)^{0.8}] = c_0 [(T_w - T_s)^m]$ where $c_0 = [\exp(0.01665 \cdot G)] / 389$; $m = 1.284 \div 0.00312 \cdot G$; $T_w - T_s < 200^\circ\text{C}$; $[G] \text{--kg/m}^2 \cdot \text{s}$; $[D] \text{--m}$; $[q] \text{--kW/m}^2$; $[T] \text{--K or } ^\circ\text{C}$; $q \cdot [D^{0.2} / (G \cdot X)^{0.8}] = 0.018 (T_w - T_s)^{0.921}$ where $T_w - T_s < 200^\circ\text{C}$; $[G] \text{--kg/m}^2 \cdot \text{s}$; $[D] \text{--m}$; $[q] \text{--kW/m}^2$; $[T] \text{--K or } ^\circ\text{C}$; $\text{Nu}_w = 0.076 \{ \text{Re}_w [X + (\rho_v / \rho_\ell) (1 - X)] (\rho_w / \rho_v) \}^{0.8} \text{Pr}_w^{0.4}$	7.03	>1000	0.15-1
Collier 1962	$q \cdot [D^{0.2} / (G \cdot X)^{0.8}] = 0.018 (T_w - T_s)^{0.921}$ where $T_w - T_s < 200^\circ\text{C}$; $[G] \text{--kg/m}^2 \cdot \text{s}$; $[D] \text{--m}$; $[q] \text{--kW/m}^2$; $[T] \text{--K or } ^\circ\text{C}$; $\text{Nu}_w = 0.076 \{ \text{Re}_w [X + (\rho_v / \rho_\ell) (1 - X)] (\rho_w / \rho_v) \}^{0.8} \text{Pr}_w^{0.4}$	7.03	<10 ⁶	0.15-1
Swenson et al. 1961	$\text{Nu}_w = 0.076 \{ \text{Re}_w [X + (\rho_v / \rho_\ell) (1 - X)] (\rho_w / \rho_v) \}^{0.8} \text{Pr}_w^{0.4}$	20.6	945-1350	
Miropolskiy 1963	$\text{Nu} = 0.023 \text{Re}_v^{0.8} \text{Pr}_w^{0.8} [X + (\rho_v / \rho_\ell) (1 - X)]^{0.8} \cdot y$ where $y = 1 - 0.1 [(\rho_\ell / \rho_v) - 1] (1 - X)^{0.4}$; $\text{Nu} = \alpha_s \cdot d / \lambda_v$; $\text{Re}_v = G \cdot D / \mu_v$; $0.23 \leq q \leq 1.16 \text{ MW/m}^2$; $8 \leq D \leq 24 \text{ mm}$; $\text{Nu} = 0.0203 \{ \text{Re} [X + (\rho_v / \rho_\ell) (1 - X)]^{0.8} \text{Pr}^{0.4}$	3.9-21.6	800-4550	
Dougall 1963	$\text{Nu} = 0.0203 \{ \text{Re} [X + (\rho_v / \rho_\ell) (1 - X)]^{0.8} \text{Pr}^{0.4}$	<3.5	1660-3650	<0.5
Bishop et al. 1964	$\text{Nu}_w = 0.098 \{ \text{Re}_w (\rho_w / \rho_v) [X + (\rho_v / \rho_\ell) (1 - X)] \}^{0.83} \text{Pr}_w^{0.83} (\rho_v / \rho_\ell)^{0.5}$ (6)	16.8-21.9	1350-3400	0.1-1

TABLE 4.7. (CONT.)

References	Correlations	P MPa	G kg/m ² ·s	X
Bishop et al. 1964	$Nu_v = 0.055 \{Re_v (\rho_\ell / \rho_v) [X + (\rho_v / \rho_\ell) (1 - X)]\}^{0.82} Pr_w^{0.96} (\rho_v / \rho_\ell)^{0.35} (1 + 26.9 \cdot D/L) \quad (7)$	16.8-21.9	350-3400	0.1-1
Bishop et al. 1965	$Nu_\ell = 0.0193 Re_\ell^{0.8} Pr_\ell^{1.23} (\rho_v / \rho_\ell)^{0.068} [X + (\rho_v / \rho_\ell) (1 - X)]^{0.68} \quad (8)$	4.08-21.9	700-3140	0.07-1
Bishop et al. 1965	$Nu_\ell = 0.033 Re_\ell^{0.8} Pr_\ell^{1.25} (\rho_v / \rho_\ell)^{0.197} [X + (\rho_v / \rho_\ell) (1 - X)]^{0.738} \quad (9)$	4.08-21.9	700-3140	0.07-1
Tong 1965	$Nu_w = 0.005 (D \cdot G / \mu_w)^{0.8} Pr_w^{0.5} \quad (10)$	>700	>14	<0.1
Quin 1966	$Nu_v = 0.023 \{Re_v [X + (\rho_v / \rho_\ell) (1 - X)]\}^{0.8} Pr_w^{0.4} (\mu_v / \mu_\ell)^{0.14} \quad (11)$	6.9	1150	0.72-0.79
Kon'kov et al. 1967	$Nu = 0.019 \cdot \{Re_v [X + (\rho_v / \rho_\ell) (1 - X)]\}^{0.8} Pr_w$ where $0.29 \leq q \leq 0.87 \text{ MW/m}^2$; $D = 8 \text{ mm}$;	2.94-19.6	500-4000	-
Henkenrath et al. 1967	$Nu_w = 0.06 \{Re_w [X + (\rho_v / \rho_\ell) (1 - X)] (\rho_v / \rho_\ell) Pr_w\}^{0.8} (G/1000)^{0.4} (P/P_{cr})^{2.7} \quad (13)$	14.2-22.3	750-4100	0.1-1
Brevi et al. 1969	$Nu_\ell = 0.0089 (Re_\ell X / \varphi)^{0.84} Pr_\ell^{0.333} [(1 - X_{cr}) / (X - X_{cr})]^{0.124} \quad (14)$ where φ - void fraction.	5.06	500-3000	0.4-1
Lee 1970	$T_w - T_s = 1915 \cdot \left[\frac{q}{G \left(X + \frac{1-X}{4.15} \right)} \right]^2 \quad (15)$ q- W/m ²	14.2-18.2	1000-4000	0.30-0.75

TABLE 4.7. (CONT.)

References	Correlations	P MPa	G kg/m ² s	X
Slaughterbeck et al. 1973	$\text{Nu}_v = 1.604 \cdot 10^{-4} \{ \text{Re}_v [X + (\rho_v / \rho_\ell) (1 - X)] \}^{0.838} \text{Pr}_w^{1.81} q^{0.278} (\lambda_v / \lambda_{cr})^{-0.508}$ <p>(16)</p> <p>where $[q]$-Btu·h⁻¹·ft⁻²;</p>	6.88-20.2	1050-5300	0.12-0.9
Groeneveld 1973	$\text{Nu}_v = 0.052 \text{Re}_v^{0.668} \text{Pr}_w^{1.26} [1 - 0.1 (\rho_\ell / \rho_v - 1)]^{0.4} (1 - X)^{0.41-1.06}$ <p>(17)</p> <p>where $\text{Nu}_v = \alpha_s D / \lambda_v$; $\text{Re}_v = (G D / \mu_v) [X + (\rho_v / \rho_\ell) (1 - X)]$ $0.03 \leq q \leq 2 \text{MW} \cdot \text{m}^{-2}$; $2.5 \leq D \leq 12.8 \text{ mm}$; annuli.</p>	0.07-21.5	130-4000	-0.12-3.09
Cumo et al. 1974	$\text{Nu}_v = 0.0091 \text{Re}_v^{1.154}$ <p>(18)</p>			
Tong, and Young 1974	$q = q_{cr} + 0.023 (T_w - T_v) (\lambda_w / d) (G_w D / \mu_v)^{0.8} \text{Pr}^{0.333}$ <p>(19)</p>	4.05-10.1	400-5150	0.20-1.65
Mattson 1974	$\alpha_s D / \lambda_v = 3.28 \cdot 10^{-4} \{ \text{Re}_v^{1.15} [X + (\rho_v / \rho_\ell) (1 - X)] \}^{0.777}$ $\text{Pr}_{v,w}^{1.69} q^{0.18} (\lambda_v / \lambda_\ell)^{-0.294}$ <p>(20)</p> <p>where D is equivalent hydraulic diameter, ft; $[\lambda]$-Btu·h⁻¹·ft⁻¹·F⁻¹; $[q]$-Btu·h⁻¹·ft⁻²;</p>	6.9-22	710-5170	0.1-0.9
Mattson 1974	$\alpha_s D / \lambda_v = 1.6 \cdot 10^{-4} \{ \text{Re}_v [X + (\rho_v / \rho_\ell) (1 - X)] \}^{0.838} \text{Pr}_{v,w}^{1.81} q^{0.278} (\lambda_v / \lambda_\ell)^{-0.508}$ <p>(21)</p> <p>where D is equivalent hydraulic diameter, ft; $[\lambda]$-Btu·h⁻¹·ft⁻¹·F⁻¹; $[q]$-Btu·h⁻¹·ft⁻²;</p>	<20.8	710-5170	0.1-0.9

TABLE 4.7. (CONT.)

References	Correlations	P MPa	G kg/m ² s	X
Groeneveld 1975 (a)	$\text{Nu}_v = 1.09 \cdot 10^{-3} \{ \text{Re}_v [X + (\rho_v / \rho_\ell)(1 - X)] \}^{0.989} \text{Pr}_{v,w}^{1.41} Y^{1.15}$ <p>where</p> $Y = [1 - 0.1(\rho_\ell / \rho_v - 1)^{0.4} (1 - X)^{0.4}]$ <p>$0.12 \leq q \leq 2.1 \text{ MW} \cdot \text{m}^{-2}$; $2.5 \leq D \leq 25 \text{ mm}$; Tubes;</p>	6.8-21.5	700-5300	0.1-0.9
Groeneveld 1975 (a)	$\text{Nu}_v = 1.85 \cdot 10^{-4} \text{Re}_v [X + (\rho_v / \rho_\ell)(1 - X)] \text{Pr}_w^{1.57} Y^{1.12} q^{0.131}$ <p>where</p> $Y = [1 - 0.1(\rho_\ell / \rho_v - 1)^{0.4} (1 - X)^{0.4}]$ <p>$[q] \text{ - Btu} \cdot \text{h}^{-1} \cdot \text{ft}^{-2}$; Tubes;</p>	5.5-21.5	700-5300	0.1-0.9
Groeneveld 1975 (a)	$\text{Nu}_v = 7.75 \cdot 10^{-4} \{ \text{Re}_v [X + (\rho_v / \rho_\ell)(1 - X)] \}^{0.902} \text{Pr}_w^{1.47} Y^{1.54} q^{0.112}$ <p>where</p> $Y = [1 - 0.1(\rho_\ell / \rho_v - 1)^{0.4} (1 - X)^{0.4}]$ <p>$[q] \text{ - Btu} \cdot \text{h}^{-1} \cdot \text{ft}^{-2}$; Tubes and annuli</p>	3.4-21.5	700-5300	0.1-0.9
Groeneveld 1975 (a)	$\text{Nu}_v = 3.27 \cdot 10^{-3} \{ \text{Re}_v [X + (\rho_v / \rho_\ell)(1 - X)] \}^{0.901} \text{Pr}_w^{1.32} Y^{1.5}$ <p>where</p> $Y = [1 - 0.1(\rho_\ell / \rho_v - 1)^{0.4} (1 - X)^{0.4}]$ <p>$[q] \text{ - Btu} \cdot \text{h}^{-1} \cdot \text{ft}^{-2}$; Tubes and annuli</p>	3.4-21.5	700-5300	0.1-0.9
Campolunghi et al. 1975	$\text{Nu}_w = 0.038 [\text{Re}_w \text{Pr}_w (x/\phi) (\rho_w / \rho_v) (G / 1000)]^{0.4} (P/P_{\text{cr}})^{2.7}$			X_{cr} to 1
Vorob'ev et al. 1981	$\text{Nu}_w = 0.0228 \{ \text{Re}_w [X + (\rho_v / \rho_\ell)(1 - X)] \}^{0.8} \text{Pr}_w^{0.4} [(1 - X_{\text{cr}})/(X - X_{\text{cr}})]^{0.28}$ <p>$[(G \cdot \pi / q) (\rho_v / \rho_\ell)]^{-0.004} \cdot (v_v / v_w)^{0.686}$</p> <p>where</p> <p>$2 \leq q \leq 1 \text{ MW} \cdot \text{m}^{-2}$; $D = 10 \text{ mm}$;</p> <p>v_v and v_w is specific vapor volume at saturation and wall temperatures.</p>	9.8-17.6	350-1000	X_{cr} to 1

TABLE 4.7. (CONT.)

References	Correlations	P MPa	G kg/m ² s	X
Remizov 1987	$\alpha_s = \frac{14.5 + 0.0296 \cdot G}{(X + 0.001) - X_{cr}} - (5400 - 9.38G)(X - X_{cr}) + 1400$ <p>(28)</p> <p>where $[\alpha_s] = W \cdot m^2 \cdot K$; $0.2 \leq q \leq 0.7 \text{ MW} \cdot m^{-2}$; $D = 10 \text{ mm}$; And for narrow range data P is 16.0-18.0MPa</p> $(\alpha_s)' = \alpha_s \frac{2}{\sqrt{q \cdot 10^{-5}}}$ <p>(29)</p> <p>where $[q] = W \cdot m^{-2}$</p>	7-14	350-700	X_{cr} to 1

TABLE 4.8. NON-EQUILIBRIUM PDO HEAT TRANSFER CORRELATIONS

References	Correlations	Ranges of Parameters		
		P MPa	G kg/m ² ·s	X
Plummer 1976	<p> $\text{Nu}_v = \frac{\alpha_{wv} D}{\lambda_v} = 0.023 \text{Re}_v^{0.8} \cdot \text{Pr}_v^{1/3} \cdot F$ </p> <p>or</p> <p> $\alpha_{wv} = 0.023 \frac{\lambda_v}{D} \cdot \left\{ \frac{GD}{\mu_v} \left[X_a + S(1 - X_a) \frac{\rho_v}{\rho_\ell} \right]^{0.8} \right\} \cdot \text{Pr}^{1/3} \cdot \left(\frac{\mu_v}{\mu_{wv}} \right)^{0.14} \left[1 + 0.3 \left(\frac{D}{L + 0.01D} \right)^{0.7} \right]$ </p> <p>where</p> <p>L is a length from CHF section and S is a slip ratio, which is given as</p> <p> $S = 1 + 0.5 \left[\frac{(\rho_\ell / \rho_v)^{0.205}}{(GD / \mu_\ell)^{0.016}} - 1 \right] \times \left(1 - K \frac{X_e - X_{cr}}{1 - X_{cr}} \right)^\gamma$ </p> <p>where</p> <p>$\gamma = A/K^B$ and K is the degree of non-equilibrium</p> <p> $K = C_1 \ln \left[G \cdot \left(\frac{D}{\rho_v \sigma} \right)^{1/2} (1 - X_{cr})^5 \right] + C_2$ </p> <p>for water A=2.5; B=0.264; C₁=0.07 and C₂=0.40.</p>			

TABLE 4.8. (CONT.)

References	Correlations	P MPa	G kg/m ² ·s	X
Groeneveld and Delorme 1976	<p>(3)</p> $Nu_f = 0.008348 \{ (G \cdot D / \mu_v)^{0.8} [X_a + (\rho_v / \rho_\ell) (1 - X_a)] \}^{0.8774} P_f^{0.6112}$ <p>X_a can be found from $(h_{va} - h_{ve})/r = \exp(-\tan \psi)$ where $h_{va} = h_{l,s} + X_a r$ $\psi = f(P, G, X, q)$ where the functional relationships may be found in Groeneveld and Delorme 1976 the subscript “f” refers to the temperature between wall and bulk of vapour flow; $0.03 \leq q \leq 2 \text{ MW} \cdot \text{m}^{-2}$, $5 \leq D \leq 20 \text{ mm}$;</p>	0.7-2.15	130-4000	-0.12-3.09
Marinov 1977	<p>(4)</p> $Nu_v = 0.023 (G \cdot d / \mu_v)^{0.8} [X + (\rho_v / \rho_\ell) (1 - X)]^{0.8} Pr_w^{0.8}$ <p>for the wall surface temperature from $T_w = T_v + (q / \alpha_v)$ $0.06 \leq q \leq 0.75 \text{ MW} \cdot \text{m}^{-2}$; $D = 12 \text{ mm}$;</p>	0.1 - 7	30-850	0.65-1.1

TABLE 4.8. (CONT.)

References	Correlations	P MPa	G kg/m ² ·s	X
Remizov and Sergeev 1987	<p>Method of calculation of T_w from the differential equation:</p> $\frac{dX_a}{dX} = 1.75m\lambda_v \left(\rho_v/\rho_\ell\right)^2 (G/q)^2 x^2 [(1 - X_a)/X_a][(X - X_a)/X_a]^n \quad (5)$ <p>where m and n are the functions of D; ΔT; X_a is found from boundary conditions $X = X_{cr}$ and $T_v = T_s$; The wall temperature $T_w = T_v + q/\alpha_n$, is defined from $(h_v - h_\ell)/r = (X - X_a)/X_a \rightarrow h_v$; where α_n is calculated from the correlation $Nu_v = 0.028 Re_v^{0.8} Pr_v^{0.4} (\rho_w/\rho_v)^{1.15}$, at $q < 1 \text{ MW} \cdot \text{m}^{-2}$.</p>	5-18	100-1000	$X > X_{cr}$

The equations are based on a vapour Reynolds number which is usually based on the actual quality X_a instead of the equilibrium quality X_e . Some of the equations [e.g. Plummer et al. (1977)] also permit slip to exist between the phases as shown in Equation 4.8:

$$Re_v = \frac{G \cdot D}{\mu_v} \left[X_a + S \cdot (1 - X_a) \frac{\rho_v}{\rho_\ell} \right] \quad (4.8)$$

where S is the slip ratio which in this case depends on the degree of non-equilibrium.

However most of the phenomenological equations are based on the assumption of homogeneous flow. Further details of the equations are provided in Table 4.8.

The main difference between the various phenomenological equations is primarily in the relation between the equilibrium quality X_e and the actual quality X_a . For example Groeneveld and Delorme (1976) recommended the following relationship:

$$[X_e/X_a] - \max(1, X_e) = \exp(-\tan\psi) \quad (4.9)$$

where

$$\psi = f(Re_{v, \text{hom}}, P, q, X_e)$$

The non-equilibrium correlation developed by Plummer et al. (1977) was based an expression for $(X_a - X_{do})/(X_e - X_{do}) = f(G)$ while Tong and Young (1974) expressed $X_a/X_e = f(X_e, G)$ and Chen et al. (1977) expressed $X_a/X_e = f(P, T_w)$. Plummer based his equation on data for water, nitrogen and freon-12 and takes into account the wall-to-drop heat transfer α_{wd} as well. The heat flux from the wall to vapor and from the wall to droplets is given as,

$$q = \alpha_{wv}(T_w - T_v) + \alpha_{wd}(T_w - T_s) \quad (4.10)$$

where the heat transfer coefficient to the vapour α_{wv} is given in Table 4.8 and the wall-to-droplet heat transfer coefficient α_{wd} is given as,

$$\alpha_{wd} = \frac{\lambda_v}{\delta_f} (1 - \phi) \exp\left(-2 \frac{D}{L}\right) \quad (4.11)$$

and $\delta_f = 1.2 \cdot 10^{-4}$ and the void fraction ϕ is based on the actual quality.

Sergeev's method (1978, 1985a, 1985b, and 1987) evaluates the wall temperature and is valid for $G \leq 1000 \text{ kg/m}^2 \cdot \text{s}$; $P = 3 \div 18 \text{ MPa}$; $X > X_{cr}$; $\Delta T = T_w - T_s \leq 500^\circ\text{C}$. It is based on a known critical quality and the assumptions that:

- (i) the radiation heat transfer coefficient is small.
- (ii) the interaction of drops with a wall is insignificant.
- (iii) the heat transfer coefficient can be found from a single-phase convection equation (e.g. see Section 4.5.4).

The relation between X_e and X_a can be found by solving the following differential equation:

$$\frac{dX_a}{dX_e} = C \cdot m \frac{\lambda_v}{\sigma \cdot \rho_\ell} \cdot \frac{G^2 \Pi_w}{\sum_j \Pi_{th}} \cdot X_a (1 - X_a) \left(\frac{X_e - X_a}{X_a} \right)^n \quad (4.12)$$

where

C is an empirical constant; $C = 1.5$ for tubes, rod bundles, and annuli at the PDO regime on two surfaces; $C = 3$ for annuli at the PDO regime on one surface. Besides, m and n are functions of pressure; Π_w and Π_{th} are the wetted and thermal channel perimeters. Eq. 4.12 can be integrated from X_{cr} (at $T_{va} \equiv T_s$) to the given channel section for given X_e . This method has been used for tubes, annuli (with a gap of 2 mm and more) and rod bundles (without heat transfer enhancement due to spacing devices).

4.4.5. Look-up tables for film boiling heat transfer in tubes

The high interest in film boiling heat transfer over the past 30 years has led to a proliferation of filmboiling models and prediction methods, many of them film-boiling-regime specific, applicable only over the range of test conditions investigated by the individual investigator. Hence it has become increasingly more difficult to select film boiling prediction methods which can be used with confidence over a wide range of conditions and geometries as will be encountered in AWCs. In addition, these prediction methods, particularly the models and phenomenological equations, are very time consuming even with the use of fast computers. This is because of (i) frequent iteration, (ii) the large number of equations involved, and (iii) evaluation of many different fluid properties during each iteration.

To simplify the film boiling prediction process, and to make it more universally applicable, the film boiling table look-up method has been developed. This approach is similar to the CHF table look-up method, and is basically a methodology which is based on a combination of all available film boiling data and predicted values covering a very wide range of conditions. It contains a tabulation of normalized heat transfer coefficients for fully developed film boiling at discrete values of pressure, mass flux, quality, and heat flux. Because the world's film boiling data base still has significant gaps, particularly at conditions where experiments are difficult (i.e. high surface temperatures), the tables are based partially on extrapolation using the observed trends from the better film boiling models or correlations and of known asymptotic trends. Ideally the tabulated heat transfer coefficient should be based on the wall superheat with respect to the actual vapour temperature, but since this temperature is almost always difficult to evaluate, the equilibrium vapour temperature or the saturation temperature are usually used as reference temperatures.

The look-up table method for film boiling was first suggested by Groeneveld (1988) and has since been refined into an improved method [Leung et al. (1997)], based on over 15 000 film boiling data for a wider range of conditions. Leung's most recent look-up table is given in Appendix IV (Table IV.I), where the fully developed heat transfer coefficient with respect

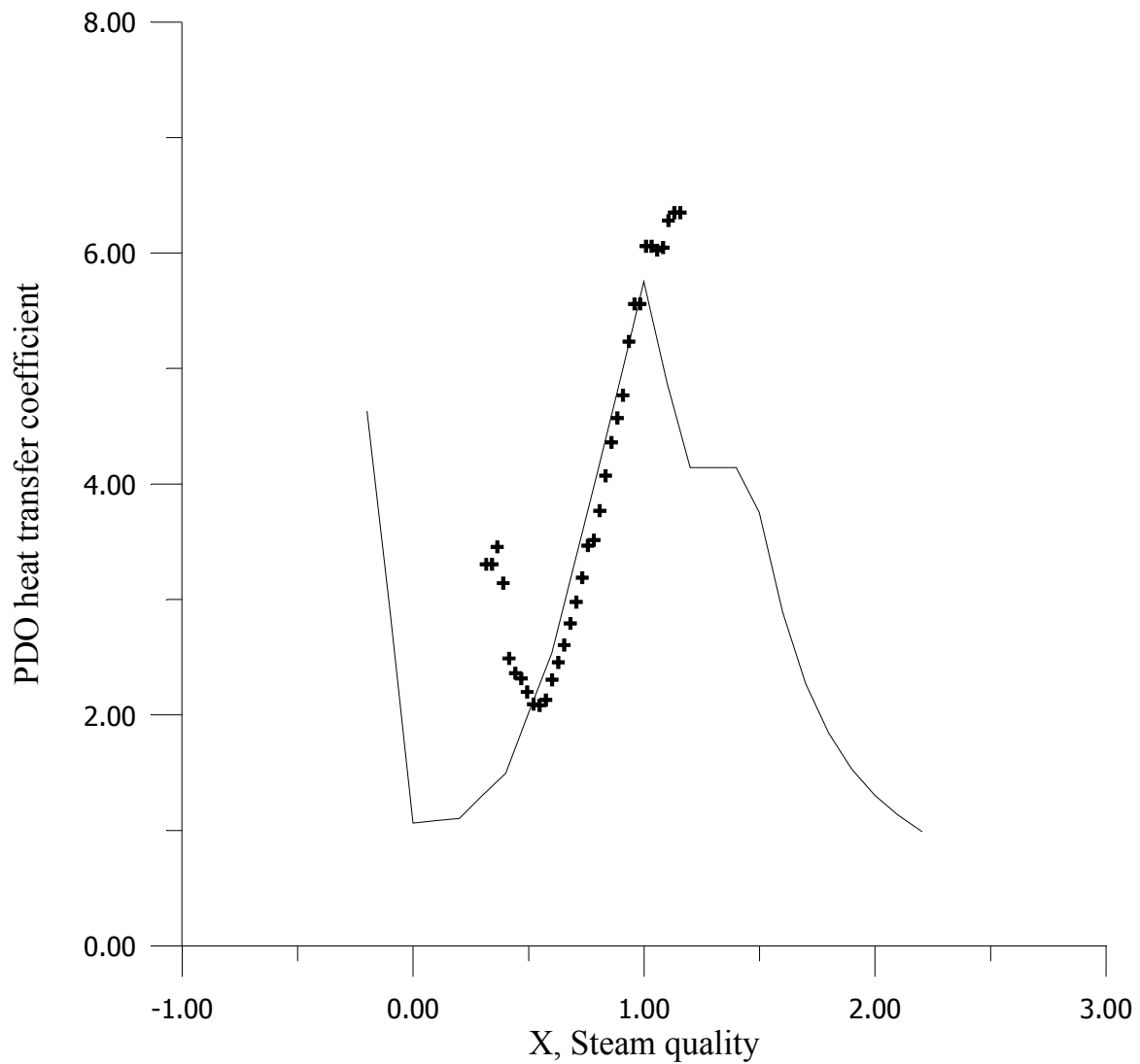


FIG. 4.4. PDO heat transfer coefficient as a function of steam quality; $P=16$ MPa, $G=1000$ $\text{kg}/(\text{m}^2\text{s})$, $q=0.6$ MW/m^2 ; the line presents the look-up table-1999 values, the pluses are experimental points.

to the equilibrium vapour temperature is tabulated for discrete values of mass velocities (0 to 7 $\text{Mgm}^{-2}\text{s}^{-1}$ in 12 steps), pressures (0.1 to 20 MPa in 14 steps), quality (-0.2 to $+1.2$ in 11 steps) and heat flux (0.05 to 3 MWm^{-2} in 9 steps). In the development of this table the developing heat transfer coefficients close to the dryout point or quench point were not used, as these values depend on prior history which is different in accident scenarios (where film boiling prediction methods are most often applied) then in steady state conditions. This table was compared extensively with the data base and the rms error was 6.73% in surface temperature. The error and data distribution for Leung's table [Appendix IV (Table IV.II)] show significant gaps in the data base at low flows and medium pressures. Some of these gaps in the data have since been partially filled by the CIAE [Chen and Chen (1998)].

Recently Kirillov et al.(1996) have taken parts of the Leung/Groeneveld table, experimental data and combined them with measurements and predictions from the Sergeev et al.(1985a) model, and added a gradual transition between. Their heat transfer coefficients

were tabulated for pressures of 0.1 to 20 MPa, mass flux values of 250 to 2000 kgm⁻²s⁻¹, thermodynamic qualities from -0.2 to +2.2 in intervals of 0.1 and heat flux values of 0.2, 0.6 and 1.0 MWm⁻² and is presented in Appendix V. Kirillov however defined his heat transfer coefficient based on a saturation temperature but extended his tabulated values up to thermodynamic qualities of 2.2, which corresponds to equilibrium bulk steam temperatures over 1000 °C at low pressures. This representation suppresses the effect of mass velocities, particularly at the highest qualities as can be seen in Appendix V. An example of the variation of the heat transfer coefficient is shown in Fig. 4.4.

Chen and Chen (1994) measured film boiling at low flows and low to medium pressures, and noted the presence of strong inlet effects at these conditions. Subsequently Chen and Chen (1998) proposed a new method for predicting the film boiling heat transfer based on finding the Plummer (1976) non-equilibrium factor $K = (X_a - X_c)/(X_e - X_c)$ which is a function only of P , G , and X_c . The K value can be derived using the method of Appendix VI. This permits the vapour temperature to be found from iteration after which, using a pure steam heat transfer equation, the heat transfer coefficient and wall temperature can be found. The table is suitable for finding the heat transfer coefficient in the developing heat transfer region downstream of the CHF location. This method differs significantly from those discussed above as it requires also knowledge of the critical quality; as expected this will improve the prediction accuracy particularly for the low flow cases where developing non-equilibrium effects are significant (the Leung table look-up method does not predict the developing heat transfer, only fully developed heat transfer coefficients were used in its development). For low flow Chen's data and table, as presented in Appendix VI [Chen and Chen (1998)] make a significant contribution as they fill a gap in both the data base and in our understanding of the non-equilibrium effects during low flow film boiling. However in many cases the non-equilibrium is still an inferred value as actual vapour temperature measurements are difficult to measure and have only been obtained successfully over very limited conditions.

The above table prediction methods partially complement each other but can result in significantly different predictions. These differences in predictions need to be resolved and work is in progress to wards this.

4.5. RECOMMENDED/MOST RECENT FILM BOILING PREDICTION METHODS

4.5.1. Pool film boiling

There is a general agreement that the modified Bromley equation for film boiling may be used for horizontal surfaces:

$$\alpha_{FB} = 0.62 \cdot \left[\frac{\lambda_v^3 \rho_v (\rho_\ell - \rho_v) \cdot r \cdot g}{\Delta T_s \cdot \mu_v} \cdot \frac{1}{2\pi} \sqrt{\frac{g(\rho_\ell - \rho_v)}{\sigma}} \right]^{1/4} \quad (4.13)$$

For vertical surfaces, changes to the constant in front of the equation and the characteristic length are required as indicated in Section 4.4.2.

4.5.2. Flow film boiling

4.5.2.1. Film boiling table

Because of the large number of film boiling methods presently available, it would be desirable to have more universal prediction method. The bundle look-up table method appears to be a more promising approach because of the following reasons:

- (i) simplicity
- (ii) correct asymptotic, and parametric trends
- (iii) most universal method with the best overall fit to the fully developed film boiling data base
- (iv) with modifications now being introduced, it can be used to account for effects such as geometry, spacer devices etc.

A similar approach has recently been adopted for predicting the CHF in safety analysis [e.g. in RELAP and CATHARE (Section 3.6.1)]. The current look-up tables do not yet properly account for the developing flow effects, in particular as it is encountered during accident scenarios, but a combination of the approach proposed by Chen and Chen (1998) and an appropriate transformation from a time dependent heat transfer coefficient [e.g. $\alpha = f(t - t_c)$] to a length dependent heat transfer coefficient [$\alpha = f(z - z_c)$] is expected to resolve this shortcoming. Current work in progress will also account for the effects of upstream flow obstructions (such as grids or endplates), which are known to have a significant desuperheating effect.

The film boiling look-up table and other film-boiling prediction-methods are least reliable in areas where data are unavailable, and this is particularly true if strong non-equilibrium effects are present. At high flow this problem disappears and the equilibrium-type correlations will apply, i.e. the equations of Table 4.8 will apply but with the vapour temperature based on equilibrium conditions ($T_v = \min [T_{sat}, T_b]$).

The film boiling look-up table method has been used for the following applications

- (i) as a normalized database for validation of film boiling models;
- (ii) as an alternative to film boiling models which cover only limited ranges of flow conditions.

For application in AWCR condition, correction factors may eventually be incorporated in the look-up table to account for the effects of the heat flux distribution and transmissions. They are not available at present. The mechanistic models may also be used to account for these effects [e.g.: Analytis and Yadigaroglu (1987); Analytis (1989, 1990) and Chen and Chen (1997)].

4.5.2.2. Inverted annular film boiling

The film-boiling prediction methods are least accurate for the IAFB regime. The data base coverage in IAFB is much more sparse compared to DFFB. Upstream effects, prior history effects and spacer effects will affect the heat transfer prediction. No properly validated

method covering all conditions of interest is available for this regime. At the low flow end of the IAFB regime the pool boiling prediction method will provide a lower-bound prediction. The look-up table method for the IAFB regime is based both on experimental data (where available) and on the model of Hammouda and Groeneveld (1996).

4.5.2.3. Dispersed flow film boiling

High mass flux

The prediction accuracy for flow film boiling is most accurate at high mass-velocities ($G > \sim 3 \text{ Mgm}^{-2}\text{s}^{-1}$) where non-equilibrium effects are unimportant. For these conditions existing equations for heat transfer to superheated steam may be used. Section 4.5.4 presents some of these equations. The film boiling look-up tables (Appendix IV, Table IV.I and Appendix V) at high mass velocities are based primarily on single phase heat transfer equations.

Low mass flux

At low mass velocities non-equilibrium effects become significant and the prediction accuracy reduces. Also the effect spacers will complicate the prediction accuracy. Further work on the look-up table is required as the recent data of Chen and Chen (1994) has not yet been used in updating the AECL look-up table. The upstream history effect is also more important at these conditions as film boiling may never become fully developed; a method such as the one suggested by Chen and Chen (1998) may need to be combined or incorporated in the look-up table. No single validated prediction method is available covering all conditions of the low mass velocity DFFB regime.

4.5.3. Radiation heat transfer in film boiling

The radiation heat transfer coefficient is usually evaluated separately and added to the convection heat transfer coefficient, i.e.:

$$\alpha = \alpha_{\text{conv}} + \alpha_{\text{rad}} \quad (4.14)$$

It should be noted that the radiation heat transfer is particularly significant for the IAFB regime. In this case, the heat transfer at the wall-to-liquid radiation is expressed according to Siegel and Howell (1972) as,

$$\alpha_{\text{rad}} = 5.67 \cdot 10^{-8} \frac{(T_w + T_s)(T_w^2 + T_s^2)}{\frac{1}{\epsilon_w} + \frac{1}{\epsilon_\ell \sqrt{\phi - 1}} - 1} \quad (4.15)$$

where:

T_w and T_s are the surface and the saturation temperatures, respectively in K; ϵ_w and ϵ_ℓ are respectively the emissivity of the heated surface and the liquid.

At $T_w \leq 700$ °C the radiation heat transfer is relatively small for the DFFB regime. Nevertheless, it is added to the convection heat transfer coefficient. The following simple two-gray-plane method may be used:

$$\alpha_{\text{rad}} = 5.67 \cdot 10^{-8} \frac{(T_w + T_s)(T_w^2 + T_s^2)}{\frac{1}{\epsilon_w} + \frac{1}{\epsilon_v} - 1} \quad (4.16)$$

The emissivity of the heated surface ϵ_w is dependent on both surface material and surface temperature. The surface emissivity is affected by oxidation, particularly for Zr with thin ZrO_2 coatings, while the vapour emissivity can be indirectly affected by the droplet concentration.

4.5.4. Correlations for single phase heat transfer to superheated steam

Single phase heat transfer to superheated steam is important as it provides an asymptotic value to the film boiling heat transfer for cases when the actual quality approached 1.0 . A number of tube-based correlations have been proposed; all of them are of the Dittus-Boelter type and give similar predictions. The following two equations are frequently used:

- (i) Miropolskiy (1975) equation, valid for $P = 4 - 22$ MPa, $G = 0.4 - 2$ $\text{Mgm}^{-2}\text{s}^{-1}$ and $\rho_w/\rho_v = 0.5 - 0.9$, range of $\text{Re} = 10^5 - 2 \times 10^6$

$$\text{Nu}_v = \alpha_v \cdot D / \lambda_v = 0.028 \text{Re}_v^{0.8} \cdot \text{Pr}_v^{0.4} (\rho_w / \rho_v)^{1.15} \quad (4.17)$$

where

$$\text{Re}_v = G \cdot X \cdot D / \mu_v$$

- (ii) Colborn equation:

$$\text{Nu}_v = 0.023 \text{Re}_v^{0.8} \cdot \text{Pr}_v^{0.4} (T_{va} / T_w)^{0.5} \quad (4.18)$$

4.5.5. Application to rod bundles

Virtually all film boiling prediction methods are based on correlations derived for tubes. Applying them to the prediction of fuel-bundle cladding temperatures is common practice; in doing so the following bundle-specific factors should be considered:

- (i) bundle enthalpy and flow imbalance
- (ii) heat transfer enhancement downstream of grids or spacers

- (iii) adjacent wet surface or cold wall
- (iv) narrow gaps between elements
- (v) change in wall friction in dry portion of bundle (resulting in higher flow in dry subchannels)
- (vi) non-circular subchannel cross section shape
- (vii) presence of axial dry-streaks in partially dry bundles.

Reactor safety computer codes may account for some but not all of the above effects. Bundle enthalpy and flow imbalance can be evaluated using subchannel codes (see also Section 3.4.4) to predict the flow conditions in individual subchannels. The flow conditions, in turn, will permit the evaluation of the local CHF as described in Chapter 3. When the heat flux of a rod surface facing a given subchannel exceeds the local CHF, both the wall-fluid heat transfer coefficient and the wall friction factor will be reduced drastically. By keeping track of the circumferential drypatch fraction (CDF) and the axial drypatch length (ADL) for each rod facing each subchannel, the flow and enthalpy distribution as well as the distribution in film-boiling heat transfer coefficient can be evaluated. This will permit the evaluation of the fuel temperature distribution and the prediction of the extent of fuel melting. The above approach is being incorporated in some of the subchannel codes to permit a detailed prediction of the cladding temperature distribution.

As was noted also in Chapter 3, the change in geometry from tubes to bundles considerably complicates the thermalhydraulic analysis. Aside from the cross-section differences, the global and local effects of the grid or spacers on the wall heat transfer, quench behaviour and interface mass and energy transport are usually unknown, or at best are included via an empirical fix for each grid spacer configuration. In general (grid) spacers can have the following effects:

- (viii) promotes rewetting downstream of the grid due to the larger turbulence level (i.e. encourages multiple quench fronts)
- (ix) acts as a cooling fin
- (x) causes desuperheating of the vapour
- (xi) results in an increase of interfacial area by breaking up the droplets or liquid core
- (xii) homogenizes the flow.

No satisfactory models are available to model the film boiling heat transfer in bundles equipped with grid spacers and hence most of the codes neglect the presence of the spacer grids. This is despite the fact that experimental studies by Yao et al. (1982), Yoder et al. (1983), Lee et al. (1984), Ihle et al. (1984) and others have demonstrated the beneficial effect of grid spacers, particularly during a reflooding phase where grid spacer can considerably reduce cladding temperatures.

4.6. APPLICATION TO FILM BOILING PREDICTION METHODS CODES

4.6.1. General

Most system analysis codes used in LWR and HWR safety analysis represent the core or bundle by an equivalent tube. Bundle specific effects as discussed in Section 4.5.4 above are frequently ignored. Also the axial node size used is frequently so large that it skips the transition boiling IAFB region. Thus the details of spatial variation of the heat flux cannot be considered properly, unless the size of the nodes is drastically reduced.

4.6.1.1. RELAP

Different geometrical configurations (more than 10) can be accommodated in the RELAP5 code. For each of these, various options for heat transfer modes and correlations are available. Here reference is made to the “default” geometry, that is a standard cylinder externally cooled, [see RELAP5 (1995)].

In the reference geometry, at least three types of flow patterns are distinguished, namely, inverted annular flow, slug flow and dispersed flow. The mechanisms of the wall-to-fluid heat transfer include conduction across a vapor film, convection to flowing vapor, convection between vapor and the droplets, and radiation across the vapor film.

For pool film boiling and IAFB conditions where forced convection is not important, the Bromley (1950) equation is basically adopted in this case. However, the Berenson (1961) wave length concept was introduced in this equation, together with a factor to account for the void fraction effect, and a correction for the liquid subcooling proposed by Sudo and Murao (1975). For higher vapour velocities, the wall-vapour heat transfer coefficient is predicted using the well-known Dittus-Boelter type correlation for single phase heat transfer. The Analytis and Yadigaroglu (1987) model has also been implemented in RELAP5/MOD 2 and was reported to successfully predict reflooding transients [Analytis (1989, 1990)].

Radiation heat transfer will be evaluated using Sun’s (1976) methodology by considering the radiative heat transfer between wall-to-liquid, wall-to-vapor, and vapor-to-liquid and their respective emissivities.

4.6.1.2. CATHARE

In the CATHARE code the heat transfer from the wall across the vapour film is predicted with either

- (xiii) Bromley-type equation modified to account for the effect of subcooling,
- (xiv) a pure heat conduction equation,
- (xv) Dittus-Boelter type equation, used primarily at higher vapor velocities and void fractions, and
- (xvi) natural convective equations at high void fraction and low velocities.

If in doubt which equation applies, the maximum predicted heat transfer coefficient should be used. Further details of the CATHARE equations can be found in Groeneveld (1982), Bestion (1990) and Groeneveld and Rousseau (1982). The radiation from wall to both phases is modeled using equations proposed by Deruaz and Petitpain (1976), which strictly speaking are applicable only for DFFB.

4.7. CONCLUSIONS AND FINAL REMARKS

- (1) The prediction of film boiling heat transfer is much more complex than that of CHF. Aside from requiring a 4th parameter (heat flux) in the look-up table, non-equilibrium effects should also be considered, especially in the region just down stream of the quench, near flow obstructions, and at low flows.
- (2) Current film boiling models and correlations appear to be flow regime specific. No single prediction method can currently provide a satisfactory prediction for both the IAFB and the DFFB regime.
- (3) All film boiling prediction methods are derived or validated based on data obtained in directly heated tubes. They have generally not been validated for bundle geometries experiencing severe transients. Effects such as differences in flow cross sections (subchannels vs. tubes), presence of narrow gaps and cold walls are usually not accounted for.
- (4) Fuel bundles are equipped with bundle appendages (as in HWRs) or grid spacers. These appendages have a CHF and heat transfer enhancing effect, as well as a desuperheating effect thus reducing the non-equilibrium. They also result in having multiple quench fronts. Current film boiling prediction methods usually ignore these important effects.
- (5) The current proliferation of film boiling prediction methods, and their limited range of validity, has reinforced the need for universal prediction methods. Several such prediction methods are now under development.
- (6) Despite the ever increasing speed of computers, the evaluation of film boiling temperatures is still time-intensive requiring coarse nodalization. The main reasons for this are: (i) frequent iteration, (ii) the large number of equations involved, and (iii) evaluation of many different fluid properties during each iteration. Table look-up methods vastly simplify this prediction process, and permit direct evaluation of the film boiling heat transfer coefficient.
- (7) Caution should be exercised when extrapolating steam heat-transport properties to high temperatures ($>1500^{\circ}\text{C}$). In addition to the uncertainty in extrapolating to high temperatures, the dissociation of steam will also affect the steam properties.
- (8) The film boiling prediction methods discussed in this chapter were based primarily on steady state conditions. Transient can have a significant effect on film boiling. Aside from affecting the region over which film boiling will occur (by affecting the CHF) IAFB or pool film boiling can be destabilized, possibly resulting in a momentary return to transition boiling. Increases in heat transfer coefficient of 10–40 times have been recorded due to small pressure pulses or by passing through shock waves.

- (9) During the past three years progress has been made in developing look-up tables for film boiling heat transfer. This has been embodied in this chapter. No final recommendation for any specific prediction method for film boiling has been made as work on combining the most promising methods into a single, fully validated method is still in progress.
- (10) The table prediction methods discussed previously partially complement each other but can result in significantly different predictions. Further research activities to resolve these differences in prediction methods are currently in progress.
- (11) Table IV.I (see Appendix IV) and Table V.I (see Appendix V) contain values for film boiling heat transfer for all heat flux values including those where the heat flux value is below the CHF but above the minimum heat flux. The data base for these table usually comes from the “hot patch” type of experiments or from predictions of models.
- (12) The differences between the three main prediction methods for film boiling heat transfer appear exaggerated as the reference temperatures of the heat transfer coefficients differ; a table based only on surface temperature will result in a convergence of these prediction methods.
- (13) The heat transfer coefficient α_s applied in Table 4.1 and Fig. 4.4 is referred to a temperature difference $(T_w - T_s)$. This results in seeming absence of the mass flux effect on the heat transfer intensity at high qualities. However, such definition of α_s is convenient for engineering calculations. It is preferred to use only the value T_s as the reference temperature because that allows to simplify considerably the prediction of the FFB heat transfer coefficient. It should be borne in mind that the recalculation between the values of α_s and α_v leads to $\alpha_s/\alpha_v = (T_w - T_v)/(T_w - T_s)$ improper results and the distortion of function $\alpha_s(G)$. During recalculation $\alpha_s \rightarrow \alpha_v$ we discovered that the effect is negligible and $\alpha_s \neq G^{0.8}$. The calculation was carried out by the method based on Miropolsky's work (1975) where it was found that $Nu \approx Re^{0.8}$ and $\alpha_v \approx G^{0.8}$. Two FFB heat transfer regimes should be distinguished: 1) PDO (post-CHF) heat transfer, 2) before-CHF heat transfer. At the present time it is not obvious yet whether the heat transfer correlations will be the same for both regimes or not. The FFB heat transfer prediction in a rod bundle is performed by both the CHF look-up table for bundles and the LUT for FFB in tubes with appropriate correction factors.

REFERENCES TO CHAPTER 4

- ADORNI, N., 1966, Heat Transfer Crisis and Pressure Drop with Steam-Water Mixtures: Experimental Data with Seven Rod Bundles at 50 and 70 kg/sm², CISE R-170.
- ANALYTIS, G.Th., 1989, Implementation of a Consistent Inverted Annular Flow Model in RELAP5/MOD2, Trans. ANS 60, 670–671.
- ANALYTIS, G.Th., 1990, Implementation and Assessment of an Inverted Annular Flow Model in RELAP5, ICAP Meeting, Madrid.

- ANALYTIS, G.Th., YADIGAROGLU, G., 1987, Analytical modelling of inverted annular film boiling, Nucl. Eng. Design V. 99 201–212.
- ANDERSEN, J., 1976, Low-Flow Film Boiling Heat Transfer on Vertical Surfaces, AJChE Symp. Ser., V.73 (2–6).
- ANDREONI, M., YADIGAROGLU, G., 1991a, Study of Two-Dimensional Effects on DFFB by Eulerian-Lagrangian Model, Proc. of the 27th ASME/ANS National Heat Transfer Conf., July 28–31, Minneapolis.
- ANDREONI, M., YADIGAROGLU, G., 1991b, A Mechanistic Eulerian-Lagrangian Model for DFFB, in Phase-Interface Phenomena in Multiphase Flow, Hemisphere Publ. (Hewitt, G.F., Mayinger, F., Eds), London.
- ANDREONI, M., YADIGAROGLU, G., 1992, Effect of the Cross-sectional Droplet Distribution in DFFB at Low Mass Flux, Proc. NURETH-5 3, 823–831.
- ANDREONI, M., YADIGAROGLU, G., 1994, Prediction methods for dispersed flow film boiling, Int. J. of Multiphase Flow **20** 1–51.
- AURACHER, H., 1987, Partielles Filmsieden in Zweiphasenstromungen, Fortschritt-Ber. VDI, R. 3, No 142, VDI-Verl., Dusseldorf.
- AURACHER, H., 1990, Transition Boiling, Proc. 9th Int. Heat Transfer Conf., Jerusalem 1 (69–90).
- AVDEEV, A.A., 1986, Heat transfer and pressure drop at film subcooled boiling in channels, Teploenergetika **4** 39–42 (in Russian).
- BAILEY, N.A., 1972, Dryout and Post Dryout Heat Transfer at Low Flow in a Single Tube Test Section, Europ. Two-Phase Group Meeting, Riso.
- BANKOFF, S.G., MEHRA, V.S., 1962, A quenching theory for transition boiling, Ind. Eng. Chem. Fund. **1** 38–40.
- BARZONI, G., MARTINI, R., 1982, Post-dryout Heat Transfer: an Experimental Study in Vertical Tube and a Simple Theoretical Method, Proc. 7th Int. Heat Transfer Conference, Munich **5** 401–410.
- BECKER, K.M., 1983, An Experimental Investigation of Post Dryout Heat Transfer, Dep. of Nucl. Reactor Engn., Royal Institute of Technology, Stockholm, KHT-NEL-33.
- BENNETT, A.W., 1964, Heat Transfer to Mixtures of High Pressure Steam and Water in an Annulus, Rep. AERE-R-4352.
- BENNETT, A.W., HEWITT, G.F., KEARSEY, H.A., KEEYS, R.K.F., 1967, Heat Transfer to Steam Water Mixtures Flowing in Uniformly Heated Tubes in which the Critical Heat Flux has been Excluded, Rep. AERE-R-5373.
- BERENSON, P.J., 1961, Film boiling heat transfer from a horizontal surface, J. Heat Transfer **83** 3 (351–358).

- BERENSON, P.J., 1962, Experiments on pool-boiling heat transfer, *Int. J. Heat Mass Transfer* **5** (985–999).
- BERTOLETTI, S., 1961, Heat Transfer and Pressure Drop with Steam-Water Spray, Rep. CISE R-36.
- BESTION, D., 1990, The physical closure laws in the CATHARE code, *Nucl. Eng. Des.* **124**.
- BISHOP, A.A., SANDBERG, R.O., TONG, L.S., 1964, High Temperature Supercritical Pressure Water Loop. Part V: Forced Convection Heat Transfer to Water After the Critical Heat Flux at High Supercritical Pressures, WCAP-2056 (Pt. 5).
- BISHOP, A.A., SANDBERG, R.O., TONG, L.S., 1965, Forced Convection Heat Transfer at High Pressures After the Critical Heat Flux, ASME Paper 65-HT-31.
- BORISHANSKIY, V.M., KUTATELADZE, S.S., 1959, Reference Book on Heat Transfer, Gosenergoizdat, Moscow (in Russian).
- BORISHANSKIY, V.M., FOKIN, B.S., 1964, “Heat transfer film pool boiling at natural convection”, *Heat Transfer in Single and Two-Phase Flows*, Energija, Moscow, 221–235 (in Russian).
- BRADFIELD, W.S., 1967, On the effect of subcooling on wall superheat in pool boiling, *J. Heat Transfer* **89** 3 (87–88).
- BREVI, R., CUMO, M., PALMIERI, A., PITIMADA, D., 1969, Heat Transfer Coefficient in Post Dryout Two-Phase Mixtures, *Europ. Two-Phase Group Meeting*, Karlsruhe.
- BROMLEY, L.A., 1950, Heat transfer in stable film boiling, *Chem. Eng. Progress* **46** 5.
- BUI, T.D., DHIR, V.K., 1985, Transition boiling heat transfer on a vertical surface, *J. Heat Transfer* **107** (756–763).
- CAMPOLUNGI, F., CUMO, M., FERRARI, G., 1975, On the thermal design of steam generators for LMFBRs, *Trans. ANS* **20** (137–139).
- CHAN, K.C., YADIGAROGU, G., 1980, Calculations of Film Boiling Heat Transfer Above the Quench Front During Reflooding, *Proc. 19th Nat. Heat Transfer Conf., Orlando* **7** (65–72).
- CHANG, YAN-PO, 1959, Wave theory of heat transfer in film boiling, *J. Heat Transfer* **81** 1 (1–12).
- CHEN, Y., FU, X., CHEN, S.P., 1988, “Experimental and analytical study of inverted annular film boiling of water”, *Experimental Heat Transfer Fluid Mechanics and Thermodynamics* (Shah, R. K. et al., Eds.), Elsevier (1438–1443).
- CHEN, YU., CHEN, H.Y., 1994, A Model of Dispersed Flow Film Boiling Heat Transfer of Water, *Proc. 10th Int. Heat Transfer Conference, Brighton* **7** 18-FB-3 (419–424).

CHEN YUZHOU, CHENG, P., WANG, J.W., YANG, M., 1989a, Experimental Results of Subcooled and Low Quality Film Boiling Heat Transfer of Water in Vertical Tubes at Moderate Pressure, Proc. NURETH-4, Karlsruhe (1105–1110).

CHEN, YUZHOU, 1989b, Experimental Measurement of the Minimum Film Boiling of Flow Water in Multiphase Flow and Heat Transfer (Chen, X., Veziroglu, T.N., Tien, C.L., Eds) 393–400.

CHEN, J.C., OZKAYANAK, F.T., SUNDARAM, R.K., 1979, Vapor Heat Transfer in Post-CHF Region Including the Effect of Thermodynamic Non-Equilibrium, Nucl. Eng. Design **51** (143–155).

CHEN, J.C., SUNDARAM, R.K., OZKAYNAK, F.T., 1977, A Phenomenological Correlation for Post-CHF Heat Transfer, Rep. NUREG-0237.

CHEN Y.Z., CHEN, H.Y., 1994, “An experimental investigation of thermal non-equilibrium in dispersed flow film boiling of water”, Proc. Int. Conf. on New Trends in Nuclear System Thermohydraulics, Pisa **1** (31–38).

CHEN Y., CHEN, H., 1996a, Forced convection heat transfer to steam in tubes with different diameters, Chinese J. Engineering Thermophysics **17** (107–110).

CHEN Y., CHEN, H., 1996b, “Experimental results of steady-state film boiling of forced flowing water”, Paper presented at 2nd Research Co-ordination, Vienna.

CHEN Y., CHEN, H., 1997, “Assessment of RELAP5/MOD2.5 with steady-state dispersed flow film boiling experiments”, Proc. 5th Topical Meeting on Nuclear Thermal Hydraulics, Operation and Safety.

CHEN Y.Z., CHEN, H.Y., Aug 1998, “A tabular method for prediction of the heat transfer during saturated film boiling of water in a vertical tube”, Proc. 11th Int. Heat Transfer Conf. Seoul, Rep. of Korea.

CHENG, S.C., NG, W., 1976, Transition boiling heat transfer on forced vertical flow via a high thermal capacity heating process, Lett. Heat and Mass Transfer **3** (333–342).

CHENG, S.C., RAGHEB, H., 1979b, Transition boiling data of water on Inconel surface under forced convection, Int. J. Multiphase Flow **5** (281–291).

CHI, J.W.H., 1967, Slug flow and film boiling of hydrogen, J. Spacecraft and Rockets **4** (1329–1332).

CLARK, J.A., 1968; Cryogenic heat transfer, Advances in Heat Transfer **5**.

COLLIER, J.G., et al., 1961, Heat Transfer to Mixtures of High Pressure Steam and Water in an Annulus. Pt. I: Single Phase Experiments: Superheated Steam, AERE-R 3653.

COLLIER, J.G., et al., 1962, Heat Transfer and Fluid Dynamic Research as Applied to Fog Cooled Power Reactors, AECL-1631.

COLLIER, J.G., 1980, Convective Boiling and Condensation”, McGraw-Hill, London.

COLLIER, J.G., 1981, "Post dryout heat transfer", Two-Phase Flow and Heat Transfer in the Power and Process Industries (Bergles, A.E., Collier, J.G., Delhaye, J.M., Hewitt, G.F., Mayinger, F., Eds) Hemisphere Publishing Corporation (282–324).

CUMO, M., FARELLO, G.E., 1967, "Heated wall droplet interaction for two phase flow heat transfer in liquid deficient region", Proc. Symp. on Two Phase Flow Dynamics, Eindhoven, vol. II (1325–1357).

CUMO, M., URBANI, G.C., 1974, Post-burnout Heat Transfer, CNEN/RT/ING.

DE CACHARD, F., 1995, "Development, Implementation and Assessment of Specific, Two-Fluid Closure Laws for IAFB", Proc. NURETH-7, Saratoga Springs **1** 4 (166–191).

DELHAYE, J.M., GIOT, M., RIETHMULLER, M.L., 1981, Thermohydraulics of Two-Phase Systems for Industrial Design and Nuclear Engineering, Hemisphere Publishing Co.

DENHAM, M.K., 1983, IAFB and Bromly Model, Rep. AEEW-1590.

DERUAZ, R., PETITPAIN, B., 1976, "Modelling of heat transfer by radiation during reflooding in a PWR", OECD Spec. Meet. on the Behavior of Water Reactor Fuel Elements under Accident Conditions, Spain.

DHIR, V.K., 1990, "Nucleate and transition boiling heat transfer under pool and external flow conditions", Proc. 9th Int. Heat Transfer Conf., Jerusalem, 139–155.

DOUGALL, R.S., ROHSENOW, W.M., 1963, Film Boiling on the Inside of Vertical Tubes with Upward Flow of Fluid at Low Qualities, MIT-TR-9079-26.

ELLION, M.E., 1954, A Study of the Mechanism of Boiling Heat Transfer, IPL-20-88, Cal. Inst. Technol.

EPSTEIN, M., HAUSER, G.M., 1980, Subcooled forced convection film boiling in the forward stagnation region of a sphere or cylinder, Int. J. Heat & Mass Transfer **23** 2 (179–189).

ERA, A., 1967, Heat Transfer Data in the Liquid Deficient Region for Steam-Water Mixtures at 70 kg/sm² Flowing in Tubular and Annular Conduits, CISE R-184.

ERA, A., GASPARI, G.P., PEOTTI, M., ZAVATARELLI, Z., 1971, "Post dryout heat transfer measurements in an annulus with uniform and non-uniform axial heat flux distribution", Europ. Two-Phase Group Meeting, Riso.

FORSLUND, R.P., ROHSENOW, W.M., 1968, Dispersed flow film boiling, J. Heat Transfer, Trans. ASME **90**, 399–407.

FREDERKING, T.H., WU, Y.C., CLEMENT, B.W., 1966, Effects of interfacial instability film boiling of saturated liquid helium-i above a horizontal surface, AIChE J. **12** (238–244).

FUNG, K.K., 1977, Forced Convective Transition Boiling, MSc Thesis, University of Toronto.

FUNG, K.K., 1981, Subcooled and Low Quality Film Boiling of Water in Vertical Flow at Atmospheric Pressure, PhD Thesis, University of Ottawa; ARNL Rep. NUREG/CR-2461.

FUNG, K.K., GROENEVELD, D.C., 1982, "A Physical Model of Subcooled and Low Quality Film Boiling of Water in Vertical Flow at Atmosphere Pressure", Proc. 7th Int. Heat Transfer Conf. Munich, 381–386

GANIC, E.N., ROHSENOV, W.M., 1977, Dispersed flow heat transfer, Int. J. Heat Mass Transfer **20**, 8 (855–866).

GOTTULA, R.P., et al., 1985, Forced Convective, Nonequilibrium, Post-CHF Heat Transfer Experiment Data and Correlation Comparison Rep., NUREG/CR-3193 (1985).

GRACHEV, N.S., IVASHKEVITCH, A.A., KIRILLOV, P.L., PROHOROVA, V.A., TURCHIN, N.M., 1974, "DNB in Steam Generators Sodium-Water and PDO Heat Transfer", Proc. USA-USSR Seminar on Development of Sodium Cooled Fast Breeder Reactor Steam Generators, Los Angeles (302–331).

GRANOVSKI, V.S., SULATZKY, A.A., HABENSKI, V.B., SHMELEV, S.M., 1992, Film boiling heat transfer from a horizontal surface, Inzhenerno-fizicheskiy Zhurnal **63** 3, 259–269 (in Russian).

GROENEVELD, D.C., THIBODEAU, M., MCPHERSON, G.D., 1970, Heat Transfer Measurements on Trefoil Fuel Bundles in the Post-Dryout Regime with Data Tabulation, AECL-3414.

GROENEVELD, D.C., 1972, The Thermal Behaviour of a Heated Surface and Beyond Dryout, AECL-4309.

GROENEVELD, D.C., 1973, Post-Dryout Heat Transfer at Reactor Operating Conditions, AECL-4513.

GROENEVELD, D.C., MCPHERSON, G.D., 1973, In Reactor Post-Dryout Experiments with 36-Element Fuel Bundles, AECL-4705.

GROENEVELD, D.C., 1975a, PDO Heat Transfer: Physical Mechanisms and a Survey of Prediction Methods, Nucl. Eng. Design **32** 3, 283.

GROENEVELD, D.C., 1975b, The Effect of Short Flux Spikes on the Dryout Power, , Chalk River, Rep., AECL-4927.

GROENEVELD, D.C., DELORME, G.G.J., 1976, Prediction of thermal non-equilibrium in the post-dryout regime, Nucl. Eng. Design **36**, 17–26.

GROENEVELD, D.C., FUNG, K.K., 1976, Forced Convective Transition Boiling — Review of Literature and Comparison of Prediction Methods, Rep. AECL-5543.

GROENEVELD, D.C., GARDINER, S.R.M., 1977, Post-CHF Heat Transfer under Forced Convective Conditions in Thermal and Hydraulic Aspects of Nuclear Reactor Safety 1, Light Water Reactors, 43–47 (Jones, O.C. et al., Eds).

GROENEVELD, D.C., GARDINER, S.R.M., 1978, A method of obtaining flow film boiling data for subcooled water, *Int. J. Heat & Mass Transfer* **21**, 664–665

GROENEVELD, D.C., 1982, Prediction Methods for Post-CHF Heat Transfer and Superheated Steam Cooling Suitable for Reactor Accident Analysis, Rep. DRE/STT/SETRE/82-4-E/DGR, CEA-CENG.

GROENEVELD, D.C., ROUSSEAU, J.C., 1982, “CHF and Post-CHF heat transfer: An assessment of prediction methods and recommendations for reactor safety codes”, NATO Advanced Research Workshop of Two-Phase Flows and Heat Transfer, Aug. 31–Sep. 3, Germany, Vol. 1, 203–238.

GROENEVELD, D.C., 1984, “An inverted annular and low quality film boiling: a state-of-art report”, *Int. Workshop on Fundamental Aspects of PDO Heat Transfer*, Salt Lake City.

GROENEVELD, D.C., SNOEK, C.W., 1986, “A comprehensive examination heat transfer correlations suitable for reactor safety analysis”, *Multiphase Science and Technology* (Hewitt, G.F. et al eds.) 181–271.

GROENEVELD, D.C., October 1988, “Recent Developments in Thermalhydraulic Prediction Methods”, *Proc. Int. Top. Mtg on Thermalhydraulics and Nuclear Reactors*, Seoul.

GROENEVELD, D.C., 1992, A Review of Inverted Annular and Low Quality film Boiling, Post-dryout Heat Transfer (Hewitt, Delhaye, Zuber, Eds), CRC Press (327–366).

HAMMOUDA, N., GROENEVELD, D.C., CHENG, S.C., 1996, Two-fluid Modelling of Inverted Annular Film Boiling.

HAMMOUDA, N., 1996, Subcooled Film Boiling in Non-Aqueous Fluids, PhD Thesis, University of Ottawa.

HEINEMANN, J.B., 1960, An Experimental Investigation of Heat Transfer to Superheated Steam in Round and Rectangular Channels, ANL-6213

HENCH, G.E., 1964, Multi-Rod (Two Rod) Transition and Film Boiling in Forced Convection Heat Transfer to Water at 1000 psia, GEAP-4721.

HERKENRATH, H., MÖRK-MÖRKENSTEIN, P., JUNG, U., WECKERMANN, F.J., 1967, Wärmeübergang an Wasser bei Erzwungener Stromung in Druckbereich von 140 bis 250 Bar, EUR-3658d.

HETSRONI, G., 1982, Handbook of Multiphase Systems, Hemisphere Publising Co/McGraw-Hill.

HSU, Y.Y., WESTWATER, J.W., 1960, Approximate theory for film boiling on vertical surfaces, *Chem. Eng. Prog. Symp. Ser.* **56**, 15–24.

HSU, Y.Y., 1972, “A Review of film boiling at cryogenic temperatures”, *Advances in Cryogenic Engineering*, Vol. 17 (361–381).

HSU, Y.Y., 1975, "A Tentative Correlation for the Regime of Transient Boiling and Film Boiling During Reflood", Proc. 3rd Water Reactor Safety Review Meeting.

HSU, C.C., GUO, Z.C., YAN, A., BI, H.R., 1986, "Low pressure and subcooled water flow film boiling research by visual method", 4th Miami Int. Symp. On Multi-Phase Transport and Particulate Phenomena, Miami Beach.

HSU, CHI-CHUN, YANG, YAN-HUA, CHEN, F., 1989, "Two-dimensional mathematical model and numerical study of IAFB heat transfer", Proc. NURETH-4, Karlsruhe, 1099–1104.

IHLE, P. et al, 1984, "Grid Spacer Effects in Reflooding Experiments Using Rod Bundles of Different Fuel Rod Simulator Design", First Int. Workshop on Fundamental Aspects of Post-Dryout Heat Transfer, Salt Lake City, Utah, 1984, NUREG/CP-0060.

JANSSEN, E., KERVINEN, J.A., 1975, Film Boiling and Rewetting, NEDO-20975.

JOHANNSEN, K., 1991, Low quality transition and inverted annular flow film boiling of water: an updated review, *Experim. Thermal and Fluid Science* **4**, 497–509.

JONES, O.C., ZUBER, N., 1977. Post-CHF heat transfer: A non-equilibrium, relaxation model. ASME paper 77-HT-79.

KALININ, E.K., 1969, "Investigation of the Crisis of Film Boiling in Channels, a Two-Phase Flow and Heat Transfer in Rod Bundles", ASME Ann. Mtg Los Angeles (89–94).

KALININ, E.K., BERLIN, I.I., KOTYUK, V.V., 1987, Transition boiling heat transfer, *Advances in Heat Transfer* **18**, 241–323.

KALJAKIN, S.G., GRABEZHNAJA, V.A., GRACHEV, N.S., 1995, "Experimental studies for the computer code verification in supporting corium retention in WWER vessel", Thermophysics-90/Thermophysical Aspects of WWER Safety (Proc. Int. Symp. Obninsk 2), 210–221 (in Russian).

KAWAJI, M., BANERJEE, S., 1987, Application of a multifield model to reflooding of a hot vertical tube: Part 1 — Model structure and interfacial phenomena", *J. Heat Transfer, Trans. ASME* **109**, 204–211.

KEEYS, R.K.F., RALPH, G.C., ROBERTS, 1971, Post Burnout Heat Transfer in High Pressure Steam-Water Mixtures in a Tube with Cosine Heat Flux Distribution, AERE-R-6411.

KIRILLOV, P.L., SMOGALEV, I.P., 1973, Effect of droplet size on mass transfer in two-phase flow", *Teplofizika Vysokikh Temperatur* **11**, 1312–1313 (in Russian).

KIRILLOV, P.L., KOKOREV, B.V., REMIZOV, O.V., SERGEEV, V.V., 1982, "PDO Heat Transfer", Proc. 7th Int. Heat Transfer Conf., Munich 4, 437–442.

KIRILLOV, P.L., et al., 1996, The Look-Up Table for Heat Transfer Coefficient in Post-Dryout Region for Water Flowing in Tubes (the 1996-Version), Preprint FEI-2525, Institute of Physics and Power Engineering, Obninsk (in Russian).

- KLIMENKO, V.V., 1981, Film boiling on horizontal plate- new correlation, *Int. J. Heat Mass Transfer* **24** 1, 69–79.
- KLYUGEL, E.V., KABANOV, L.P., 1986, Film boiling with wetting of heated surfaces, *Therma. Eng.* **33**, 218–221.
- KON'KOV, A.S., ZUPERMAN, D.A., 1967, The experimental investigation of heat transfer to moisture steam, *Teploenergetika* **3**, 54–56 (in Russian).
- KUNSEMILLER, D.F., 1965, Multi-Rod Forced Flow Transition and Film Boiling Measurements, GEAP-5073.
- KUDRYAVTSEVA; A.A., YAGOV; V.V., ZUDIN, YU,B., 1987, A method of calculating thermohydraulic characteristics of dispersed film boiling regime, *Teploenergetika* **10**, 65-69 (in Russian).
- LAO, Y.J., BARRY, R.E., BALZHISER, R.E., 1970, “Study of film boiling a horizontal plate”, *Proc. 4th Int. Heat Transfer Conf. Paris* 5, B 3.10.
- LAPERRIERE, A., GROENEVELD, D.C., 1984, "A study of low quality film boiling at high pressures and flows", *AIChE Symposium Series* 236, **80**, 440–445.
- LAVERTY, W.F., ROHSENOW, W.M., 1967, Film Boiling of Saturated Liquid Nitrogen Flowing in a Vertical Tube, *J. Heat Transfer* **89**, 90–98.
- LEE, D.H., 1970, “Studies of heat transfer and pressure drop relevant to subcritical once-through evaporators”, *Proc. Symp. on Progress in Sodium-cooled Fast Reactor Engineering*, Monaco.
- LEE, D.H., SHEEN, H.J., CHO, S.K., ISSAPOUR, I., 1984, “Measurement of droplet dynamics across grid spacer in mist cooling of subchannel of PWR”, *Proc. First Int. Workshop on Fundamental Aspects of Post-Dryout Heat Transfer*, Salt Lake City, NUREG/CP-0060.
- LEE, Y., KIM, K.H., 1987, Inverted Annular Flow Boiling, *J. Multiphase Flow* **13**, 345–355
- LEONARD, J., SUN, K.H., 1976, “Low flow film boiling heat transfer on vertical surfaces; empirical formulations and applications to BWR LOCA analysis”, *AJChE Symp.* **73**, 7–13.
- LEONARD, J., SUN, K.H., ANDERSEN, J., 1978, Calculation of Low Flow Film Boiling Heat Transfer for BWR LOCA Analysis, GE Rep. NEDO-20566-1.
- LEUNG, L.K.H., HAMMOUDA, N., GROENEVELD, D.C., 1997, “A look-up table for film-boiling heat transfer coefficients in tubes with vertical upward flow”, *Proc. Eighth Int. Top. Mtg on Nuclear Reactor Thermal-Hydraulics*, Kyoto, Japan, Sept. 30–Oct. 4.
- LEVITAN, L.L., BOREVSKY, L.YA., 1989, “Holographia Steam-Water Flow”, Moscow Energoatomizdat.
- MARINOV, M.J., KABANOV, L.P., 1977, Study of PDO heat transfer at low pressure and low mass flux, *Teploenergetika* **7**, 81–83 (in Russian).

MATTSON, R.J., CONDIE, K.G., BENGSTON, S.J., OBENCHAIN, C.F., 1974, "Regression analysis of post-CHF flow boiling data", Proc. 5th Heat Transfer Int. Conf. Tokyo 4, B.3.8, 115–119.

MATZNER, B., 1963, Experimental Studies of Boiling Fluid Flow and Heat Transfer at Elevated Pressures, Columbia University Monthly Progress Report MPR-XIII-2–63.

MATZNER, B., GASTERLINE, G.E., KOKOLIS, S., 1968, Critical Heat Flux and Flow Stability in a 9 ft. 19-rod Test Section Simulating a Setting of Short Discrete Rod Bundles, Columbia University Topical Report, No 10.

MAYINGER, F., LANGER, R., 1978, "PDO heat transfer", Proc. 6th Int. Heat Transfer Conf., Toronto 6, 181.

MCADAMS, W.H., et al., 1950, Heat transfer to superheated steam at high pressure, Trans. ASME 72, 421–428.

MCGINNIS, F.K., HOLMAN, J.P., 1969, Individual droplet heat-transfer rates for splattering on hot surfaces, Int. J. Heat Mass Transfer **12**, 95–108.

MCPHERSON, G.D., MATZNER, B., GASTERLINE, F., GASTERLINE, J.E., WIKHAMMER, G.A., 1971, "Dryout and post- dryout behaviour of a 28-element fuel bundle", American Nucl. Society Winter Meeting, Miami Beach.

MIROPOLSKIY, Z.L., 1963, Heat transfer at film boiling steam-water mixture in tubes, Teploenergetika **5**, 49–52 (in Russian).

MIROPOLSKIY, Z.L., 1975, heat transfer to superheated steam at heat supply and heat removal", Teploenergetika **3**, 75–78 (in Russian).

MOOSE, R.A., GANIC, E.N., 1982, On the calculation of wall temperatures in the post-dryout heat transfer region, Int. J. Multiphase Flow **8**, 525–542.

MOSAAD, M., 1986, "A theoretical analysis of film boiling heat transfer from vertical surfaces to subcooled liquid", 4th Miami Int. Symp. On Multi-Phase Transport and Particulate Phenomena, Miami Beach.

MOSAAD, M., 1988, Subcooled Film Boiling Transfer to Flowing Water in Vertical Tube, Thesis, Techn. Univ. Berlin, Berlin.

MOSAAD, M., JOHANNSEN, K., 1989; "A new correlation for subcooled and low quality film boiling heat transfer of water at pressures from 0.1 to 8 Mpa". Proc. 4th Int. Top. Mtg on Nuclear Reactor Thermal-Hydraulics, Karlsruhe.

MUELLER, R.E., 1967, Film Boiling Heat Transfer Measurements in a Tubular Test Section, EURAEC-1871/GEAP-5423.

NELSON, R., 1975, "The heat transfer surface technique", LOCA Heat Transfer Workshop, Idaho Falls, Idaho.

NEWBOLD, F.J., RALPH, J.C., WARD, J.A., 1976, "Post dryout heat transfer under low flow and low quality conditions," Paper presented at the European Two Phase Flow Group Meeting, Erlangen.

NIJHAWAN, S., CHEN, J.C., SUNDERAM, R.K., LONDON, E.J., 1980, Measurements of vapour superheat in post-critical heat flux boiling, *J. Heat Transfer* **102**, 465–470.

NISHIKAWA, K., YOSHIDA, S., MORI, H., TAKAMATSU, H., 1986, PDO heat transfer to freon in a vertical tube at high subcritical pressure, *Int. J. Heat Mass Transfer* **29**, 1245–1251.

QUIN, F.P., 1966, Forced Flow Heat Transfer to High Pressure Water beyond the Critical Heat Flux, ASME Paper 66-WA/HT-36.

PARKER, Y.D., GROSH, R.Y., 1962, Heat Transfer to a Mist Flow, ANL-6291.

PLUMMER, D.N., GRIFFITH, P., ROHSENOW, W.M., 1976, "Post-Critical Heat Transfer to Flowing Liquid in a Vertical Tube," Presented at the 16th National Heat Transfer Conference, 76-CSME/CSCHE-13, St. Louis.

POLOMIK, E.E., LEVY, S., SAWOCHKA, S.G., 1961, Heat Transfer Coefficients with Annular Flow During Once Through Boiling of Water to 100% Quality at 800, 1000 and 1400 psia, GEAP-3703.

POLOMIK, E.E., 1971, Deficient Cooling 7th Quarterly Report, GEAP-10221-7.

REMIZOV, O.V., 1978, Study of temperature operating conditions of heat generating surface at crisis, *Teploenergetika* **2**, 16–21 (in Russian).

REMIZOV, O.V., VOROB'IEV, V.V., SERGEEV, V.V., 1987, The design PDO heat transfer in tubes, *Teploenergetika* **10**, 55–56 (in Russian).

Rep., 1976, Study of Heat Transfer in Rod Bundles after CHF, OKB Gidropress, No 213-0-084 (in Russian).

Rep., 1980, Study of Heat Transfer of Moistured and Superheated Steam at Low Mass Velocity, OKB Gidropress, No 431-0-047 (in Russian).

SAHA, P., 1980 A nonequilibrium heat transfer model for dispersed droplet post-dryout regime, *Int. J. Heat Mass Transfer* **23**, 483–492.

SAKURAI, G., 1990a, "Film boiling heat transfer", *Proc. 9th Int. Heat Transfer Conf.*, Jerusalem 1, 157–186.

SAKURAI, G., SHIOTSU, M., HATA, K., 1990b, A General correlation for Pool Film Boiling Heat Transfer, *J. Heat Transfer* **112** 2, 430–451.

SAKURAI, G., SHIOTSU, M., HATA, K., 1990c, Correlations for subcooled pool film boiling heat transfer from large surfaces with different configurations, *Nucl. Eng. Design* **120**, N 2–3, 271–280.

Seok, H., Chang, S.H., 1990, "Mechanistic model of the inverted annular film boiling", *Proc. 9th Int. Heat Transfer Conf.*, Jerusalem 3, 431–435.

SERGEEV, V.V., 1978, PDO Heat Transfer in Annulis and Rod Bundles, Analytical Review FEI OB-67, Institute of Physics and Power Engineering, Obninsk (in Russian).

SERGEEV, V.V., GALCHENKO, E.F., REMIZOV, O.V., 1985a, Engineering Method of Design PDO Heat Transfer, Preprint FEI-1649, Institute of Physics and Power Engineering, Obninsk (in Russian).

SERGEEV, V.V., 1985b, The Dynamic Entrainment of Liquid from Film Surface, Preprint FEI-1750, Institute of Physics and Power Engineering, Obninsk (in Russian).

SERGEEV, V.V., 1987, PDO Heat Transfer in Vertical Tubes, Preprint FEI-1836, Institute of Physics and Power Engineering, Obninsk (in Russian).

SHIRALKAR, B.S., HEIN, R.A., YADIGAROGLU, G., 1980, "The 'boiling curve' in high quality flow boiling", Proc.of ANS/ASME/NRC Int. Top. Mtg on Nucl. Reactor Thermal-Hydraulics, Saratoga Springs, NUREG/CP-0014 2, 1131–1141.

SIEGEL, R., HOWELL, J.R., 1972, Thermal Radiation Heat Transfer, McGraw Hill.

SLAUGHTERBECK, D.C., YBARRONDO, L.J., OBENCHAIN, C.F., 1973, Flow Film Boiling Heat Transfer Correlations: A Parametric Study with Data Comparison, ASME Rep.73-HT-50.

SMITH, T.A., 1976, Heat Transfer and Carryover of Low Pressure Water in a Heated Vertical Tube, M.Sc Thesis, MIT

STEWART, J.C., 1981, Low Quality Film Boiling at Intermediate and Elevated Pressures, MSc Thesis, University of Ottawa.

STEWART, J.C., GROENEVELD, D.C., 1982, Low quality and subcooled film boiling at elevated pressure, Nucl. Eng. Design **67**, 254–272.

SWENSON, H.S., CARVER, J.R., SZOEKE, G., 1961, The Effects of Nucleate Boiling Versus Film Boiling on Heat Transfer in Power Boiler Tubes, ASME Rep. 61-WA-201.

SWINNERTON, D., MOOD, M.L., PERSON, K.G., 1988, Steady State Post-Dryout Experiments at Low Quality and Medium Pressure, Rep. AEEW-R2267, Winfrith.

STYRIKOVICH, M.A., POLONSKIY, V.S., ZIKLAURI, G.V., 1982, Heat and mass transfer and hydrodynamic two-phase flow for nuclear power, Nauka **368**.

SUDO, Y., MURAO, Y., 1975, Study on Film Boiling Heat Transfer During Reflood Process, JAERI Rep. JPNRSR-15.

SUN, K.H., GONZALES-SANTALO, J.M., TIEN, C.L., 1976, Calculation of combined radiation and convection heat transfer in rod bundles under emergency cooling conditions", J. Heat Transfer **98** 3.

TAKENAKA, N., FUJII, T., AKAGAWA, K., NISHIDA, K., 1989, Flow pattern transition and heat transfer of inverted annular flow, Int. J. Multiphase Flow **15**, 767–785.

TONG, L.S., 1965, Boiling Heat Transfer Two-phase Flow, J. Wily & Sons Inc., London, Sidney, No. 4 (344).

TONG, L.S., YOUNG, J.D., 1974, "A phenomenological transition and film boiling heat transfer correlation", Proc. 5th Int. Heat Transfer Conf. Tokyo IV, B. 3.9.

TONG, L.S., 1978, "Heat transfer in reactor safety", Proc. 6th Int. Heat Transfer Conf., Toronto 6, 285–309.

TRUSHIN, I.M., BEZRUKOV, YU.A., LOGINOV, S.A., BRANTOV, V.G., 1978, "Investigations of heat transfer to damp and superheated steam at low mass fluxes and low pressures", Thermophysical Investigations Relevant to Ensuring of Reliability and Safety of Water Cooled Reactors, Seminar TF-78, Budapest 1, 305–318 (in Russian).

VARONE, A.F., ROHSENOW, W.M., 1984, "Post-dryout heat transfer prediction", Proc. 1st Int. Workshop on Fundamental Aspects of Post-dryout Heat Transfer, Salt Lake City, NUREG/CP-0060.

VOJTEK, J., 1982, "Investigation of transient CHF phenomena and forced convection film boiling heat transfer", Proc. 7th Int. Heat Transfer Conference Munich 4, 557–563.

VOROB'IEV, V.V., LOSCHININ, V.M., REMIZOV, O.V., SERGEEV, V.V., 1981. "Generalization of PDO heat transfer experimental data with using nonequilibrium model", Heat Transfer and Hydrodynamics at Steam Generation, Nauka, 181–187, (in Russian).

WACHTERS, L.H.J., 1965, De Warmte Overdracht van een Hete Wand Naar Druppels in de Sferoidale Toestand, PhD Thesis, Technological University, Delft.

WANG, B.X., PENG, X.F., 1987, An advanced study of forced turbulent flow film boiling for subcooled liquid with high velocity in a circular tube, *Warme-Stoffubertrag* **21**, 139–144.

WANG, B.X., LIN, Z.Z., PENG, X.E., YUAN, H.J., 1988, Experimental study of steady turbulent flow film boiling of subcooled liquid R 11 flowing upward in a vertical circular tube, *Sci. Sinica* **31**.

WEBB, S.W., CHEN, J.C., SUNDARAM, R.K., 1982, "Vapour generation rate in non-equilibrium convective film boiling", Proc. 7th Int. Heat Transfer Conf. Munich 4, 437–442.

WHALLEY, P.B., et al., 1982, "A physical model for two phase flows with thermo-dynamic and hydrodynamic non-equilibrium", Proc. 7th Int. Heat Transfer Conf. Munich 5, 181–188.

WINTERTON, R.S., 1982, Transition Boiling, Rep. AEEW-R1567.

YADIGAROGLU, G., ANDREANI, M., 1989, "Two-fluid modeling of thermal-hydraulic phenomena for best-estimate LWR safety analysis", Proc.NURETH-4, Karlsruhe, V.2, 980995 (Mueller, U., Rehme, K., Eds).

YAN, D.M., 1987, "Subcooled forced convection film boiling heat transfer", Heat Transfer Science and Technology, Hemisphere, Washington.

YAO SHI-CHUNE, HOCHREITER, L.E., LEECH, W.J., 1982, Heat transfer augmentation in rod bundles near grid spacers, J. Heat Transfer **104** 1.

YODER, G.L., MORRIS, D.G., MULLINS, G.B., 1983, Dispersed flow film boiling heat transfer data near spacer grids in a rod bundle, Nucl. Technol. **60** 2, 304.

YODER, G.L., Jr., ROHSENOW, W.M., 1983, A solution for dispersed flow heat transfer using equilibrium fluid, J. Heat Transfer **105** 1.

Chapter 5

PRESSURE DROP RELATIONSHIPS

NOMENCLATURE

A	flow area
A_r	flow area ratio (< 1)
A_g	projected grid cross section
C_f	friction coefficient
C_d	drag coefficient
C_v	modified loss coefficient
C_0	distribution coefficient
D, d	diameter
e	absolute roughness
F	correction coefficient
Fr	Froude Number
f	friction factor
f_l	laminar friction factor
f_t	turbulent friction factor
G	mass flux
G_{SL}	superficial liquid mass flux ($\rho_L j_L$)
g	gravitational acceleration
H	wire pitch
h	heat transfer coefficient
h_{fg}	latent heat
I	specific enthalpy
j	volumetric flux
K	loss coefficient
L	length
p_t	rod pitch
P, p	pressure
q	heat flux
Re	Reynolds Number
S	slip ratio
T	temperature
t	thickness
u	velocity
V	velocity
v	specific volume
v_{fg}	$v_G v_L$
W	mass flow rate
x	mass quality
Z	length, elevation

GREEK SYMBOLS

α	void fraction
θ	angle of direction of flow with vertical

β	homogeneous void fraction
Δ	difference
δ	thickness of annular film
ϕ^2	two phase friction multiplier
μ	dynamic viscosity
ρ	density
σ	surface tension
χ	Martinelli parameter

SUBSCRIPTS

a	acceleration
av	average
B	bundle
b	bulk
cir	circular
crit	critical
e	elevation
f	film, frictional
G	vapour
GO	gas only
h	hydraulic
i	inlet
L	liquid
LO	liquid only
l	local
m	mean
o	outlet
R	relative
s	spacer
SPF	single-phase flow
TP, TPF	two-phase flow
tot	total
w	wall

5.1. INTRODUCTION

In the nuclear industry, pressure drop correlations find extensive application for design and analysis of many systems and components. For example, validated pressure drop correlations (PDCs) are required to determine the extent of orificing needed to match the channel flow to the power, pumping power required, the riser height required to achieve a certain circulation rate in natural circulation BWRs, recirculation ratio in natural circulation type steam generators, stability analysis, transient and accident analyses, etc. Some of the above applications require correlations for both single-phase and two-phase flows. Two-phase flows are encountered during normal operation of BWRs, transients and accidents in PWRs and PHWRs, and in certain components like the steam generators.

Two-phase flow pressure drop depends on a large number of independent parameters like geometric configuration of the duct, mass and volume fractions of the individual phases, pressure, fluid properties, mass flux, orientation of the duct (i.e. horizontal, vertical or inclined), flow direction (i.e. vertical upflow, downflow or counter-current flow) and flow patterns. Further, in many engineering applications, two-phase flow systems can be adiabatic, diabatic, one-component, two-component or multi-component. To cater to the needs of these diverse applications, a very large number of two-phase flow pressure drop correlations are reported in literature. Many of these correlations, being empirical in nature, are applicable only for limited parameter ranges. Even mechanistic models are based on certain assumptions and careful examination of the particular application is necessary to ensure that the assumptions made in deriving the model hold good. For many practical situations, designers and analysts often require some guidance to choose the appropriate correlation.

The parameter ranges of two-phase flow in some of the above applications can be quite different. For example, natural circulation reactors are characterised by relatively low mass flux and driving pressure differential compared to forced circulation systems. Therefore, correlations chosen for the analysis of natural circulation systems require improved accuracy at low mass fluxes. For the analysis of critical flow, following a break in high pressure systems, pressure drop correlations valid for very high mass fluxes (10–20 Mg/m²s) are required. For investigations on the start-up procedure for natural circulation boiling water reactors, correlations valid over a wide range of pressures starting from atmospheric pressure are required.

In this document, some of the commonly used and often-cited pressure drop correlations are compiled along with their range of application. Later on assessments of these PDCs reported in literature are reviewed and their recommendations summarized. Limitations of the reported assessments are brought out and a rational assessment procedure for diabatic flow is proposed. As per this procedure assessment of pressure drop correlations cannot be carried out in isolation. For example, a rational assessment of diabatic flow pressure drop requires pre-assessment of models for the onset of nucleate boiling (ONB) and void fraction. Assessment of flow pattern specific pressure drop correlations also require pre-assessment of the criteria for flow pattern transitions.

5.2. SURVEY OF SITUATIONS WHERE PRESSURE DROP RELATIONSHIPS ARE IMPORTANT

In a nuclear reactor, the generated power, Q_G , is extracted from the core by means of a fluid coolant. The first purpose of the thermohydraulic design of the reactor is to ensure that, during the nominal steady state reactor operating conditions, the extracted power, Q_E , is equal to the generated one. Secondly, for accidental conditions, the evaluation of the difference between Q_G and Q_E is necessary for predicting the behaviour of the plant. The evaluation of the extracted power is performed by means of the well known relationship:

$$Q_E = W \Delta I \quad (5.1)$$

where

ΔI is the enthalpy difference between the core outlet and inlet and W is the mass flow rate.

For the evaluation of the extracted power, it is then necessary to know the flow rate. In some cases, it can be measured (total flow rate in the main loop) but generally at design level, it

has to be computed and this calculation requires a knowledge of the pressure loss through the different parts of the plant.

It is necessary to take into account the fact that the total pressure loss is due to different components, namely distributed pressure loss due to friction, local pressure losses due to sudden variations of shape, flow area, direction, etc. and pressure losses (the reversible ones) due to acceleration (induced by flow area variation or by density change in the fluid) and elevation (gravity effect).

A general purpose relationship for the evaluation of the pressure loss in any possible case does not exist up to now and thus it becomes necessary to collect a set of relationships applicable to the different configurations, conditions, etc. A list of the factors on which the pressure loss depends is shown in Table 5.1.

An important factor affecting the pressure loss is the geometry. In a reactor plant, we have to deal with several basic geometrical shapes (circular pipes, annuli, etc.) and with a number of special devices, like rod bundles, heat exchangers, valves, headers, plenums, pumps, pools, etc. Other factors are then concerned with the fluid status (single or two phase/one component, two-component or multi-component), the flow nature (laminar or turbulent), the flow pattern (bubbly, slug, annular, etc.), the flow direction (vertical upflow, downflow, inclined flow, horizontal flow, counter-current flow, etc.) and the operating conditions (transient or steady state).

TABLE 5.1. FACTORS ON WHICH THE PRESSURE DROP DEPENDS

Geometry	basic shapes	circular pipe, rectangular channel, annulus, etc.
	other shapes & rod bundle, spacer, valve, devices	heat exchanger, orifice, plenum, header, pump etc.
fluid status	single phase	
	two phase	one-component, two-component & multi-component
flow nature	laminar	
	turbulent	
flow patterns	bubbly, slug, annular, etc.	
flow direction	vertical upflow, downflow, inclined flow & horizontal flow	co-current & counter-current flow
operating conditions	steady state transient	
driving force	forced convection	
	natural convection	

A final, very important issue, is concerned with the driving force depending on whether the flow is sustained by a density difference in the fluid (natural convection) or by a pump (forced convection), or whether there will be feedback between the pressure loss and the extracted power or not. Once more, in case of natural convection, some differentiation could arise from what is called microscopic natural convection: normally the pressure loss inside a device does not depend on the fact that the flow is sustained by a pump or by a density difference (macroscopic natural convection); however, in some circumstances, local effects could happen and, as a consequence, the pressure loss will be influenced by the driving force.

By looking at Table 5.1, it appears clearly that it generates a very big matrix of conditions and to fill all the matrix cells is a very hard job. At the same time, it becomes immediately clear that the filling of the whole matrix is not necessary. For example, with respect to the geometry, mainly the basic geometrical shapes have to be taken into account. Some of the geometric conditions of interest are identified in the next section. The pressure loss correlation for special devices is usually given by the manufacturer.

5.2.1. Distinction between core and system approach

The term *thermohydraulic analysis* is often used to identify two widely different analytical approaches. The first one can be called *core approach* and is mainly concerned with the reactor core. In this case, a very detailed analysis is performed at subchannel level and, consequently, only the basic geometrical shapes are taken into account. For instance, the pressure drop in rod bundles is usually computed by subdividing them into subchannels of simple shape. The bundle pressure drop is then computed based on the pressure drop in single subchannel and, in principle, no special pressure drop correlation for bundles is needed. The special devices are limited to the spacers, a relatively limited class. Due to the fact that the analysis is a very detailed one, it is normally performed for steady state conditions or for slow transients, computed as subsequent steady states. This approach is the basic one for design purposes.

The second one can be called *system approach* and deals with the whole plant. In this case, each component is represented by a small number of mesh points. For instance, no detailed geometrical description of the core is considered. All the subassemblies are usually represented by means of one pin, from a thermal point, and the pressure drop is then computed by means of a bundle pressure drop correlation. Again, basic geometrical shapes are needed (circular pipe, annulus, etc.) but the several complex geometries of interest are represented by means of adhoc empirical relationships. This approach is mainly used in safety analysis and consequently deals with transient conditions.

5.2.2. Geometric conditions of interest

Geometric conditions of interest to nuclear power plants (NPPs) only are considered here. Emphasis is made on geometric conditions that are relevant to the primary loop of NPPs. The secondary loop of NPPs (the steam generator and the piping up to the main steam isolation valve (MSIV) and the feedwater valves in case of PWRs and PHWRs) is also important and is to be considered. In addition, the emergency core cooling (ECC) lines from the ECC pumps to the injection point along with the different types of valves may also be considered. Also, there are quite a few advanced designs to be dealt with (examples are SBWR, AP-600, CANDU-3, CANDU-9, EPR, AHWR, etc.). Again, it becomes a difficult task to cover typical geometries

relevant to all these designs. For the purpose of this report, the various geometries relevant to NPPs can be classified into two categories:

5.2.2.1. Simple geometry for steady state and design calculations

In case of NPPs, the attention is generally limited to the nuclear fuel. The geometries of interest for local pressure drop are the spacer grids, tie plates, etc. Similarly for distributed pressure drop the geometries of interest are the channel and subchannels (various types, i.e. central, lateral, middle-lateral) for the square and the triangular array.

TABLE 5.2. LOCATIONS IN A PWR WHERE LOCAL AND DISTRIBUTED PRESSURE LOSSES ARE IMPORTANT

Local pressure drop in the RPV: Cold leg to downcomer	
	Downcomer to lower plenum entry
	Core inlet
	Spacers
	Core outlet
	Upper plenum to hot leg
	Bypasses:
	Lower plenum to core bypass
	Core bypass to upper plenum
	Downcomer to hot leg
	Downcomer to upper head
	Upper head to upper plenum (direct)
	Upper head — Control Rod Guide (CRG)
	CRG-Upper Plenum (different positions)
Local pressure drops in the primary loop:	
	Hot leg bends
	Hot leg to steam generator inlet water box entry
	U-tube bends
	U-tube exit
	Steam generator outlet water box to cold leg entry
	Loop seal bends
	Pump inlet
	Pump (inside with various situations for the rotor)
	Pump outlet
	Pressurizer to surge line entry
	Hot leg to surge line connection
	Surge line bends if any
	Accumulator to pipe entry
	Accumulator pipe bends
	Accumulator line check valve
Similarly distributed (due to skin friction) pressure drops are important for the following locations in a PWR:	
Distributed pressure drops in the RPV:	
	Downcomer
	Core and Core bypass
	Upper Plenum
	CRG
Distributed pressure drops in the primary loop:	
Hot leg	Surge line
	U-Tubes
	Cold leg — loop seal
	Cold leg — horizontal

In addition, the reactor system consists of pipes of various sizes, annulus, etc. The flow paths on the secondary side of the steam generators and the water boxes could be considered separately.

5.2.2.2. *Complex geometry (or system) for safety — transient-analysis*

During a transient, both direct (i.e. the nominal direction of the flow) and reverse flow directions are relevant. Both transient and steady state knowledge is relevant (as already mentioned). Both single phase (liquid or steam only) and two phase flows are relevant. Flows with phase opposition including counter current flow limit (CCFL) may happen in any discontinuity.

A knowledge of local and distributed pressure drops is necessary for transient analysis, (e.g. LOCA calculations). For example, in a typical PWR, local loss coefficients for direct and reverse flow must be supplied by the code user for each of the locations identified in Table 5.2. Table 5.2 also identifies the locations where distributed pressure drops are important.

Similar tables can be prepared for other reactors. For example, in a pressure tube type heavy water reactor, additional local loss coefficients required are listed in Table 5.3.

TABLE 5.3. LOCATIONS IN A PHWR WHERE ADDITIONAL LOCAL PRESSURE LOSSES ARE IMPORTANT

Entry loss from steam generator outlet pipes to header
Header to feeder entry loss
Inlet feeder bends
Inlet grayloc
Inlet grayloc to Liner tube entry
Liner tube to channel entry
Fuel locator
Junction between two bundles
Channel to liner tube entry
Liner tube to outlet grayloc
Outlet grayloc
Outlet feeder bends
Feeder to header entry loss
Header to steam generator inlet pipe entry

5.3. CORRELATIONS FOR DESIGN AND ANALYSIS

5.3.1. Components of pressure drop

The overall static pressure drop, Δp , experienced by a fluid while flowing through a duct comprises of the following components:

$$\Delta p = \Delta p_f + \Delta p_l + \Delta p_a + \Delta p_e \quad (5.2)$$

where

ΔP_f , ΔP_l , ΔP_a and ΔP_e are the components of pressure drop due to skin friction, form friction (also known as local friction), acceleration and elevation respectively. The skin friction pressure drop is also known simply as friction pressure drop.

5.3.1.1. Friction pressure drop

This is the irreversible component of pressure drop caused by shear stress at the wall and can be expressed as:

$$\Delta p_f = \frac{fL}{D_h} \frac{W^2}{2\rho A^2} \quad (5.3)$$

where

D_h is equal to 4 times flow area/wetted perimeter.

The pressure drop occurs all along the length and hence referred to as distributed pressure drop sometimes. This equation is applicable for single-phase and homogeneous two-phase flows, although, the method of calculation of the friction factor, f , and density, ρ , differ in the two cases. Pressure drop across tubes, rectangular channels, annuli, bare rod bundle (i.e. without spacers), etc. are examples of this component.

5.3.1.2. Local pressure drop

This is the localized irreversible pressure drop component caused by change in flow geometry and flow direction. Pressure drop across valves, elbows, tee, spacer, etc. are examples. The local pressure drop is given by

$$\Delta p_l = K \frac{W^2}{2\rho A^2} \quad (5.4)$$

where

K is the local loss coefficient, the correlations for which differ for different geometries and for single-phase and two-phase flows.

5.3.1.3. Acceleration pressure drop

This reversible component of pressure drop is caused by a change in flow area or density. Expansion, contraction and fluid flowing through a heated section are the examples. The acceleration pressure drop due to area change for single-phase and two-phase flow can be expressed as

$$\Delta p_a = \frac{(1 - A_r^2) W^2 \phi}{2 A_0^2 \rho_L} \quad (5.5)$$

where A_0 = smaller flow area

$\phi = 1$ for single-phase flow and for two-phase flow ϕ is given by:

$$\phi = \left(\frac{x^3}{\rho_G^2 \alpha^2} + \frac{(1-x)^3}{\rho_L^2 (1-\alpha)^2} \right) \left(\frac{\rho_G \rho_L}{x \rho_L + (1-x) \rho_G} \right) \quad (5.6)$$

The acceleration pressure drop due to density change for single-phase and two-phase flows can be expressed as:

$$\Delta p_a = G^2 \left\{ \left(\frac{1}{(\rho_m)_o} \right) - \left(\frac{1}{(\rho_m)_i} \right) \right\} \quad (5.7)$$

For single-phase flows, this component is negligible, but can be significant in two-phase flows. For two-phase flow, the above equation can be used with ρ_m given by:

$$\frac{1}{\rho_m} = \left(\frac{x^2}{\rho_G \alpha} + \frac{(1-x)^2}{\rho_L (1-\alpha)} \right) \quad (5.8)$$

To evaluate the acceleration pressure drop due to density change, accurate prediction of the density of fluid is necessary. For single phase flow, density of fluid can be predicted reasonably well with established relationships for thermophysical properties of the fluid. For two phase flow, it is necessary to predict void fraction accurately to determine density and in turn acceleration pressure drop. Hence, correlation for void fraction needs to be chosen judiciously.

5.3.1.4. Elevation pressure drop

This reversible component of pressure drop is caused by the difference in elevation and can be expressed as:

$$\Delta p_e = \rho g \Delta z \cos \theta \quad (5.9)$$

where

θ is the angle with the vertical in the direction of flow. For two phase flow,

$$\rho = \rho_L (1-\alpha) + \rho_G \alpha \quad (5.10)$$

In many instances with vertical test sections, the elevation pressure drop is the largest component. For such cases, accurate prediction of the void fraction is essential which again calls for a judicious choice of the correlation for void fraction.

5.3.2. Configurations

For the purpose of design of advanced reactors, the required correlations mainly cover the following configurations. For friction pressure loss, circular pipe, annulus, rectangular channels and rod cluster and for local pressure loss, spacer, bottom and top tie plates, flow area changes like contraction, expansion, bends, tees, valves etc. are most common. For CANDU type fuel

bundles, the alignment of two adjacent fuel bundles also is important in estimating the pressure drop. In addition, in-core effects like radiation induced creep, blister formation, swelling, corrosion, etc. are also important factors affecting the pressure drop which are not dealt with here. Following is an account of the pressure drop correlations described configuration-wise and generally used for design.

5.3.3. Friction pressure drop correlations

The present compilation of pressure drop correlations is applicable to steady state fully developed flow. Fully developed flow conditions are expected to occur in long components like the steam generator U-tubes.

5.3.3.1. Circular pipe

5.3.3.1.1. Adiabatic single-phase flow

For fully developed laminar flow, the friction factor is given by:

$$f = 64/Re \quad (5.11)$$

which is valid for Reynolds number less than 2000. For turbulent flow in smooth pipes several friction factor correlations are proposed and in use. A few commonly used correlations for smooth pipe are given below.

Blasius (1913) proposed the following equation:

$$f = 0.316 Re^{-0.25} \quad (5.12)$$

valid in the range $3000 \leq Re \leq 10^5$. The following equation valid in the range of $3000 \leq Re \leq 10^6$ is also often used for design.

$$f = 0.184 Re^{-0.2} \quad (5.13)$$

Drew et al. (1932) proposed the following equation:

$$f = 0.0056 + 0.5 Re^{-0.32} \quad (5.14)$$

valid in the range $3000 \leq Re \leq 3 \times 10^6$. The following equation proposed by Nikuradse (1933)

$$\frac{1}{\sqrt{f}} = 0.86 \ln(Re \sqrt{f}) - 0.8 \quad (5.15)$$

is valid over the entire range of Reynolds number. Colebrook (1938) proposed the following equation

$$\frac{1}{\sqrt{f}} = 0.86 \ln \left(\frac{e/D}{3.7} + \frac{2.51}{Re \sqrt{f}} \right) \quad (5.16)$$

valid for smooth and rough pipes for the whole range of Reynolds number above 3000. The following explicit equation proposed by Filonenko (1948) is a good approximation of Colebrook equation for smooth tube in the range $4 \times 10^3 \leq Re \leq 10^{12}$.

$$f = [1.82 \log(Re) - 1.64]^{-2} \quad (5.17)$$

An explicit form of the Colebrook equation valid for smooth and rough tubes has been obtained by Selander (1978) for use in computer codes.

$$f = 4 [3.8 \log(10/Re + 0.2e/D)]^{-2} \quad (5.18)$$

It may be noted from the above that well established correlations for friction factor do not exist in the transition region between $2000 \leq Re \leq 3000$. Further, in many transients, the flow may change from laminar to turbulent, or vice versa, necessitating a switch of correlations. Numerical calculations, often encounter convergence problems when such switching takes place due to the discontinuity in the friction factor values predicted by the laminar flow and turbulent flow equations. A simple way to overcome this problem is to use the following criterion for switch over from laminar to turbulent flow equation.

$$\text{if } f_t > f_l \text{ then } f = f_t \quad (5.19)$$

where

f_t and f_l are friction factors calculated by turbulent and laminar flow equations respectively. This procedure, however, causes the switch over from laminar to turbulent flow equation at $Re \approx 1100$. Solbrig's (1986) suggestion to overcome the same is to use friction factor as equal to greater of $(f_t)_{4000}$ and f_l below Reynolds number of 4000. $(f_t)_{4000}$ is the friction factor calculated by the turbulent flow equation at $Re = 4000$. Effectively this leads to

$$f = (f_t)_{4000} \text{ for } 2000 \leq Re \leq 4000 \quad (5.20)$$

In addition, a condition to avoid infinite friction factor is required to take care of flow stagnation (i.e. $Re \approx 0$).

5.3.3.1.2. Diabatic single-phase flow

Generally isothermal friction factor correlations are used with properties evaluated at the film temperature $T_f = 0.4 (T_w - T_b) + T_b$, where T_w and T_b are the wall and bulk fluid temperatures [Knudsen & Katz (1958)]. Sometimes the friction factor for non-isothermal flow is obtained by multiplying the isothermal friction factor with a correction coefficient, F . The correction coefficient accounts for the temperature gradient in the laminar layer and the consequent variation in physical properties of the fluid. The correction coefficient can be expressed as a function of the temperature drop in the laminar layer, ΔT_f as given below:

$$F = 1 \pm C \Delta T_f \quad (5.21)$$

The negative sign shall be used for heat transfer from wall to the fluid, and

$$\Delta T_f = q/h \quad (5.22)$$

Different values of the constant C are given by different investigators. El-Wakil (1971) gives a value of 0.0025, while Marinelli and Pastori (1973) give a value of 0.001.

An alternative approach is to express the correction factor in terms of the viscosity ratio. This approach is more widely used and the following empirical equation proposed by Leung and Groeneveld (1993) is recommended.

$$F = (\mu_b/\mu_w)^{-0.28} \quad (5.23)$$

where

the subscripts b and w refer to the bulk fluid and wall respectively.

5.3.3.1.3. Adiabatic two-phase flow

A large number of two-phase flow pressure drop correlations can be found in literature. These correlations can be classified into the following four general categories.

- (1) Empirical correlations based on the homogeneous model,
- (2) Empirical correlations based on the two-phase friction multiplier concept,
- (3) Direct empirical models,
- (4) Flow pattern specific models.

In addition, computer codes based on the two-fluid or three-fluid models requires correlations for the partitioning of wall friction between the fluids and interfacial friction correlations.

Some of the widely used and often cited correlations in each of the above category are given below.

Homogeneous flow model

In the homogeneous flow model, the two-phase frictional pressure gradient is calculated in terms of a friction factor, as in single-phase flow. The friction factor is calculated using one of the equations given in Section 5.3.3.1.1, with the use of the two-phase viscosity in calculating the Reynolds number. Several models for two-phase viscosity are available some of which are given in Appendix VII.

Many of the models for mixture viscosity do not yield significantly different results. Further, homogeneous models are expected to give good results for high mass flux flows with low and high void fractions where the bubble diameter is small compared to the duct diameter. Hussain et al. (1974) recommend a value of $G = 2700 \text{ kg/m}^2\text{-s}$ ($\approx 2 \times 10^6 \text{ lb/h-ft}^2$) above which homogeneous models are applicable.

Correlations based on the multiplier concept

In this case, the two-phase pressure drop is calculated from the single-phase pressure drop by multiplying with a two-phase friction factor multiplier. The following definitions of two-phase friction multipliers are often used.

$$\begin{aligned}\phi_{LO}^2 &= \frac{(dp/dz)_{TPF}}{(dp/dz)_{LO}}; & \phi_{GO}^2 &= \frac{(dp/dz)_{TPF}}{(dp/dz)_{GO}}; \\ \phi_L^2 &= \frac{(dp/dz)_{TPF}}{(dp/dz)_L} & \text{and} & \quad \phi_G^2 = \frac{(dp/dz)_{TPF}}{(dp/dz)_G}\end{aligned}\tag{5.24}$$

where

the denominators refer to the single-phase pressure gradient for flow in the same duct with mass flow rates corresponding to the mixture flow rate in case of ϕ_{LO}^2 and ϕ_{GO}^2 and individual phases in case of ϕ_L^2 and ϕ_G^2 . Among these, ϕ_{LO}^2 is the most popular friction multiplier. Some of the multiplier based correlations are briefly described in Appendix VIII.

There are many more empirical correlations (other than those in Appendix VIII) given under the multiplier concept, inclusion of all of which is outside the scope of the present report. Care has been taken to include all those correlations which are of interest to current and advanced reactor designs. In passing, it may be mentioned that all of the homogeneous models given in the previous section can also be expressed in terms of a two-phase friction multiplier.

Direct empirical models

In this category, the two-phase friction pressure drop is directly expressed as a function of mass flux, mixture density, length, equivalent diameter, etc. without reference to single-phase pressure drop. Examples in this category are the models proposed by Lombardi-Pedrocchi (1972), Lombardi-Ceresa (1978), Bonfanti et al. (1982) and Lombardi-Carsana (1992). These correlations also specify the use of the homogeneous model for the calculation of the gravitational and accelerational pressure drop. Such correlations are expected to provide accurate values of the calculated total pressure drop rather than the individual components of the pressure drop. Since Lombardi-Carsana is the latest in this series only this correlation is given in Appendix IX.

Flow pattern specific models

In general, two methods are being used to generate flow pattern specific correlations. In the first, empirical correlations are obtained by correlating the data for each flow pattern. In the second method mechanistic models which take into account the distribution of phases in each flow pattern have been developed. Examples of the first approach are those due to Baker [see Govier and Aziz (1972) and Hoogendoorn (1959)] for horizontal flows and Hughmark (1965) for horizontal slug flow. Examples of mechanistic models are those due to Taitel and Dukler (1976a) and Agrawal et al. (1973) for stratified flow; Wallis and Dobson (1973) and Dukler and Hubbard (1975) for slug flow and Hewitt and Hall-Taylor (1970) for annular flow. Some of the empirical and mechanistic models for calculating pressure gradient for horizontal and vertical flows are given in Appendices X and XI respectively.

To apply flow pattern specific correlations, we must also have a method to identify flow patterns. This can be done by the use of flow pattern maps proposed by different authors for horizontal, vertical and inclined flows.

Interfacial friction models

The two-fluid model used in many of the advanced system codes require correlations for interfacial friction in addition to wall friction. Complete description of the models used in computer codes like TRAC-PFI/MOD1 [Liles and Mahaffy (1984)] and RELAP5/MOD3.2 [the RELAP5/MOD3 development team (1995)] are readily available in the open literature. For specific flow patterns, models are proposed by Wallis (1970), Couttris (1989), Putney (1991) and Stevanovic and Studovic (1995). For use in computer codes, it is also essential that such correlations for the various flow patterns be consistent. For example, when the flow pattern changes from bubbly to slug, the interface force predicted at the transition point by correlations for the bubbly and slug flow should be same. A consistent set of interfacial and wall friction correlations for vertical upward flow has been proposed by Solbrig (1986) along with a flow pattern map for use in two-fluid models (Appendix XII).

5.3.3.1.4. Diabatic two-phase flow

The correlations discussed so far are applicable to adiabatic two-phase flow. The effect of heat flux on two phase pressure drop has been studied by Leung and Groeneveld (1991), Tarasova (1966) and Koehler and Kastner (1988). Tarasova (1966) observed that two phase friction pressure drop is higher in a heated channel compared to that in an unheated channel for same flow condition. However, Koehler and Kastner (1988) concluded that two phase pressure drops are same for heated and unheated channels. Studies conducted by Leung and Groeneveld indicate that the surface condition is significantly influenced by heat flux. Effective surface roughness increases due to the formation of bubbles at heated surface leading to larger pressure drop. They concluded that for the same flow conditions, the two phase multiplier is larger for low heat flux than high heat flux. They further observed that maximum value of two phase multiplier is obtained when heat flux approaches critical heat flux value. In the absence of established procedure to take the affect of heat flux into account the following procedure for calculation of two phase diabatic pressure drop is generally followed.

For diabatic two-phase flow, the quality, void fraction, flow pattern, etc. change along the heated section. To calculate the pressure drop in such cases, two approaches are usually followed. In the first approach, the average ϕ_{LO}^2 is calculated as:

$$\phi_{LO}^2 = \frac{1}{L} \int_0^L [\phi_{LO}^2(z)] dz \quad (5.25)$$

The approach can be used in cases where the $\phi_{LO}^2(z)$ is an integrable function. Numerical integration is resorted to in other cases. An example of such an approach is proposed by Thom (1964). Thom has derived average values of $\phi_{LO}^2(z)$ which are reproduced in Table 5.4. Similar integrated multiplication factors for diabatic flow as a function of outlet quality are also available for the Martinelli-Nelson method. Thom has also obtained multiplication factors for calculating the acceleration and elevation pressure drops for diabatic flow in this way.

In the second approach the heated section is subdivided into a large number of small segments. Based on average conditions (i.e. x_i , α_i and flow pattern) in that segment, the pressure drop is calculated as in adiabatic two-phase flow using one of the models described previously.

TABLE 5.4. VALUES OF FRICTION MULTIPLIER FOR DIABATIC FLOW [THOM (1964)]

Outlet Quality	Pressure (bar)				
	17.24	41.38	86.21	144.83	206.9
0.000	1.00	1.00	1.00	-	-
0.010	1.49	1.11	1.03	-	-
0.015	1.76	1.25	1.05	-	-
0.020	2.05	1.38	1.08	1.020	-
0.030	2.63	1.62	1.15	1.050	-
0.040	3.19	1.86	1.23	1.070	-
0.050	3.71	2.09	1.31	1.100	-
0.060	4.21	2.30	1.40	1.120	-
0.070	4.72	2.50	1.48	1.140	-
0.080	5.25	2.70	1.64	1.190	1.050
0.100	6.30	3.11	1.71	1.210	1.060
0.150	9.00	4.11	2.10	1.330	1.090
0.200	11.40	5.08	2.47	1.460	1.120
0.300	16.20	7.00	3.20	1.720	1.180
0.400	21.00	8.80	3.89	2.010	1.260
0.500	25.90	10.60	4.55	2.320	1.330
0.600	30.50	12.40	5.25	2.620	1.410
0.700	35.20	14.20	6.00	2.930	1.500
0.800	40.10	16.00	6.75	3.230	1.580
0.900	45.00	17.80	7.50	3.530	1.660
1.000	49.93	19.65	8.165	3.832	1.740

In many cases, the pressure drop is to be calculated for a component with subcooled inlet flow (for example rod bundles in BWRs). For such cases a single-phase friction model is used in the non-boiling part of the test section and a two-phase model is used in the boiling zone. A model is also required to establish the onset of boiling in such cases. Usually, the thermal equilibrium model is used. But in many cases a model taking into account the effect of subcooled boiling is also used. The Saha and Zuber (1974) model is preferred by many investigators for this purpose [Marinelli & Pastori (1973), Vijayan et al. (1981), Snoek & Ahmad (1983)].

Comparison of diabatic two-phase pressure drop predictions with experimental data by Snoek and Leung (1989) showed that the Saha & Zuber model is not adequate to predict the onset of nucleate boiling (ONB) in 37-rod bundles with non-uniform heat flux due to enthalpy maldistribution in the subchannels. They found that the Saha and Zuber correlation overpredicted the single-phase region length by as much as 50%. They modified the Saha & Zuber correlation for the case of Peclet number $>70\,000$ as:

$$x_{\text{ONB}} = -568 \frac{q}{Gh_{fg}} \quad (5.26)$$

Knowing the thermodynamic quality, x_e , the true quality, x_t , is obtained as:

$$x_t = x_e - x_{\text{ONB}} \exp\left(\frac{x_e}{x_{\text{ONB}}} - 1\right) \quad (5.27)$$

They also tested this correlation with the available data and found that better agreement is obtained in the prediction of single-phase length in case of nonuniform heat flux. With uniform heat flux, however, the single-phase length is underpredicted to some extent.

5.3.3.2. Annulus

Correlations for circular pipe are normally used for the calculation of single phase pressure drop in annulus using the hydraulic diameter concept. For two-phase pressure drop, the same concept is expected to be applicable. The accuracy of this method can be checked by comparison with experimental data. Examples of available experimental data are those due to Adorni (1961), CISE (1963), Moeck (1970), etc.

5.3.3.3. Rod bundle

The rod bundle geometries used in advanced designs differ in several ways. In PWRs and BWRs, the fuel bundles are long ($\gg 1.8$ to 4.5 m) whereas in CANDU type heavy water reactors short fuel bundles of about 0.5 m are used. Generally grid spacers are used in PWRs and BWRs while split-wart spacers are used in CANDUs. In certain fast breeder reactors wire-wrapped bundles are still used. In PWRs and BWRs, the total pressure drop is obtained by summing up the pressure drop in bare rod bundle and the spacers. For wire-wrapped bundles empirical correlations for the pressure drop in the bundle considering the geometric details of the wire wraps are available. For prototype CANDU type bundles, the total pressure drop is sometimes expressed in terms of an overall loss coefficient due to the closeness of the spacers and the complex geometry of the end plates [Vijayan et al. (1984)] and alignment problem at the junction between two bundles [Pilkhwil et al. (1992)].

5.3.3.3.1. Pressure drop in wire wrapped rod bundles

In the case of wire wrapped rod bundles, the geometry and shape of the system is quite rigid and the development of a general correlation for predicting the pressure drop is a reasonable task. Such a correlation proposed by Rehme (1968 and 1969) is given below:

$$\Delta P = f_r \frac{L}{D_h} \frac{\rho u_R^2}{2} \frac{U_B}{U_G} \quad (5.28)$$

where

$U_B = U_S + U_D$ is the bundle perimeter

$U_G = U_S + U_D + U_K$ is the total perimeter

U_K , U_S and U_D are the shroud perimeter, pins perimeter and wire perimeter respectively. The reference velocity, u_R , is defined as:

$$u_R = u \sqrt{F} \quad (5.29)$$

where

u is the average velocity in the rod bundle

The geometrical factor F depends on the pitch to diameter ratio and on the ratio between the mean diameter and the wire pitch (H).

$$F = \left(\frac{p_t}{D}\right)^{0.5} + \left[7.6 \frac{d_m}{H} \left(\frac{p_t}{D}\right)^2\right]^{2.16} \quad (5.30)$$

where

d_m is the mean diameter of wire wraps. The reference friction factor f_R is calculated by means of the following correlation based on Rehme's experimental data.

$$f_R = \frac{64}{Re_R} + \frac{0.0816}{Re_R^{0.133}} \quad \text{for } 2 \times 10^3 \leq Re_R \leq 5 \times 10^5 \quad (5.31)$$

where

$$Re_R = Re \sqrt{F} \text{ and } Re = (u_R D_h)/\nu \quad (5.32)$$

These are valid in the range $1.12 < p_t/D < 1.42$ and $6 < H/d_m < 45$. Later on Dalle Donne and Hame (1982) extended the validity of the correlation to lower p_t/D ratios by multiplying F with a correction factor C for $p_t/D < 1.03$.

$$C = 1.6 - e^{-\frac{p_t/D - 1}{0.05873}} \quad (5.33)$$

The measurements on wire wrapped bundles performed in ENEA when compared with the general correlation were found to be in very good agreement for a wire pitch of 140 mm. The discrepancy in the whole Reynolds number range was about 4-5 per cent. The agreement for the 160 mm pitch was a little worse, up to 13 per cent which is attributed to measurement uncertainty. Later on, pressure drop measured by ENEA in prototype fuel elements of the PEC reactor were found to be in good agreement with the predictions of Rehme's correlation thus confirming its general validity [Cevolani (1996)].

5.3.3.3.2. Pressure drop in CANDU type fuel bundles

Several short bundles are stacked end to end in CANDU type PHWRs compared to a long single fuel bundle used in PWRs and BWRs. Due to the basic change in design concept some of the problems and geometries are unique to the design.

Snoek & Ahmad (1983)

Snoek & Ahmad suggested the following empirical correlation for friction factor based on experiments on a 6 m long electrically heated horizontal 37 rod cluster.

$$f = 0.05052 Re^{-0.05719} \quad \text{for } 108,000 \leq Re \leq 418,000 \quad (5.34)$$

Venkat Raj (1993)

Venkat Raj proposed the following equations based on a set of experiments with prototype horizontal 37 rod clusters for PHWRs with split-wart type spacer which includes the junction pressure drop.

$$f = 0.22 \text{ Re}^{-0.163} \quad 10,000 \leq \text{Re} \leq 1,40,000 \quad (5.35)$$

$$f = 0.108 \text{ Re}^{-0.108} \quad 1,40,000 \leq \text{Re} \leq 5,00,000 \quad (5.36)$$

5.3.3.3.3. Pressure drop in bare rod bundles

Single-phase

Correlations for circular pipes are commonly used to calculate pressure drop using hydraulic diameter of the rod bundle in the absence of experimental data. Some of the commonly used correlations are:

Kays (1979)

For rod clusters

$$f = f_{\text{cir}} K_1 \quad (5.37)$$

where

K_1 — is provided as a function of p/D (pitch to diameter ratio) based on the work by Diessler and Taylor (1956).

f_{cir} — can be calculated using correlations given for circular pipe.

Rehme (1980)

For non-circular channels

Laminar flow;

$$f \text{ Re} = K \quad (5.38)$$

where K is a geometry parameter that only depends on the configuration of the channel.

Turbulent flow;

$$\sqrt{(8/f)} = A[2.5 \ln \text{Re} \sqrt{(f/8)} + 5.5] - G^* \quad (5.39)$$

where

the empirical factors A & G^* can be determined from the diagrams given in Rehme (1973a)

Grillo and Marinelli (1970)

Grillo and Marinelli proposed the following equation based on their measurements on a 4×4 square array rod bundle with rod diameter of 15.06 mm and p/D of 1.283

$$f = 0.1626 \text{ Re}^{-0.2} \quad (5.40)$$

Two-phase

In the absence of experimental data, the method used for diabatic two phase flow in Section 5.3.3.1.4 can be used with hydraulic diameter of the bundle in place of pipe diameter. Lombardi-Carsana (1992) (CESNEF-2) correlation discussed in Appendix IX is also applicable for rod bundles. In addition, there are some empirical equations proposed for rod bundles some of which are given below.

CNEN correlation (1973)

$$\Delta p_{\text{TPF}} = 1.7205 \times 10^{-6} (L M^{0.852}) / D_h^{1.242} \quad (5.41)$$

where

M is given by:

$$M = [xv_G + (1 - x)v_L]G^2 \quad (5.42)$$

where

M is in $[N/m^2]$

L & D_h are in metres,

Δp_{TPF} is obtained in metres of water at 25°C .

This equation is applicable for square array fuel bundles with pitch to diameter ratio = 1.28, $D_h = 1.31$ cm, peripheral rod-channel gap = $0.55 \times \text{pitch}$, $8 < P < 70 \text{ kg/cm}^2$ and $680 < G < 2700 \text{ kg/m}^2\text{s}$.

Grillo and Marinelli (1970)

$$\xi(G) = \frac{\phi_{\text{LO}}^2}{(\phi_{\text{LO}}^2)_{M-N}} \quad (5.43)$$

$$\xi(G) = 0.56 + 0.315 \left(\frac{10^6}{G} \right) \quad (5.44)$$

where $(\phi_{\text{LO}}^2)_{M-N}$ is calculated using the Martinelli-Nelson method (Appendix VIII).

Unal (1994)

For rod cluster

$$f = 0.1 \text{ Re}_{av}^{-0.3} \quad (5.45)$$

$$\text{Re}_{av} = GD/\mu_{av} \quad (5.46)$$

where μ_{av} corresponds to average of inlet and outlet under post CHF dispersed flow condition.

5.3.3.4. Steam generator secondary side

Two-phase pressure drop calculations are important for natural circulation type steam generators. The driving force for natural circulation flow is resisted by pressure losses which oppose the flow. The natural circulation driving force is provided by the difference between the density of the water in the downcomer and that of the steam-water mixture in the heating zone and riser. Calculation of pressure losses in a steam generator is therefore an integral part of evaluating the circulation and flow rate through the heating zone. Pressure drop correlations specific to steam generator tube banks are not readily available. For design and analysis purposes, however, the frictional pressure losses can be calculated by the procedure listed for diabatic two-phase flow discussed in Section 5.3.3.1.4 with the hydraulic diameter of the tube bank used in place of the pipe diameter [ORNL-TM-3578 (1975)].

5.3.4. Local pressure drop

5.3.4.1. Grid spacers

Because of variation and complexity of geometry, it is extremely difficult to establish a pressure loss coefficient correlation of general validity for grid spacers. But methods of calculation reasonably accurate for design purpose can be achieved. For more precise determination of pressure drop across spacers, experimental studies are required. Some correlations used to determine pressure drop across grid spacers are discussed below.

5.3.4.1.1. Single-phase flow

Single-phase pressure drop is calculated using a spacer loss coefficient, K , as:

$$\Delta p = K \rho V_B^2 / 2 \quad (5.47)$$

In some cases, it may be possible to obtain a reasonable value of the spacer loss coefficient if its geometry can be approximated to one of those considered in Idelchik (1986). For other cases, the different empirical models for K , described below may be used.

Rehme (1973b)

$$K = C_v \varepsilon^2 \quad (5.48)$$

where

$$\varepsilon = A_g / A_B.$$

For $Re_B > 5 \times 10^4$, $C_v = 6$ to 7 and for $Re_B \leq 5 \times 10^4$ C_v values are given in graphical form as a function of Re_B . Subsequently Rehme (1977) studied the effect of roughness of rod surface on the pressure drop across spacers. Cevolani (1995) proposed $C_v = 5 + 6133Re^{-0.789}$ for square bundles and $\ln(C_v) = 7.690 - 0.9421 \ln(Re) + 0.0379 \ln^2(Re)$ for triangular bundles with an upper limit of $K = 2$ if the calculated value is greater than 2.

Mochizuki & Shiba (1986)

$$K = 2.7 - 1.55(\log Re_B - 4) \text{ for } Re_B \leq 8 \times 10^4 \quad (5.49)$$

$$K = 1.3 \quad \text{for } Re_B > 8 \times 10^4 \quad (5.50)$$

This correlation is valid only for the specific spacer used for the experimental studies with 37 rod cluster.

Kim et al. (1992)

$$K = (C_d + 2LC_f/t) \varepsilon / (1 - \varepsilon)^2 \quad (5.51)$$

where

C_d the drag coefficient varies from 0.8 to 1.0 for a thin rectangular plate depending on the aspect ratio of the plate,

C_f the friction coefficient can be obtained from the flat plate flow solution. For turbulent boundary layer preceded by laminar region.

$$C_f = 0.074 (Re_B L/D_h)^{-0.2} - 1740 (Re_B L/D_h)^{-1} \quad (5.52)$$

For fully laminar flow

$$C_f = 1.328(D_h/L)^{0.5} (Re_B)^{-0.5} \quad (5.53)$$

Transition Reynolds number is assumed to be 5×10^5 .

5.3.4.1.2. Two phase flow

In general, the homogeneous model or the slip model is used for the estimation of the two-phase pressure drop across grid spacers.

Homogeneous model

$$\Delta p = K(Re_{sat}) v G^2/2 \quad (5.54)$$

where

$K(Re_{sat})$ is the form loss coefficient for single phase flow estimated at the Reynolds number corresponding to the total flow in the form of saturated liquid and v is the specific volume given by

$$v = x v_G + (1-x) v_L \quad (5.55)$$

This model may be used when experimental data are not available. Beattie (1973) has provided the following equation to calculate the pressure drop in rod spacers, sudden expansion, etc. if the flow is churn-turbulent at the obstruction.

$$\phi_{LO}^2 = \left[1 + \left(x \frac{\rho_L}{\rho_G} - 1\right)\right]^{0.8} \left[1 + x \left(\frac{3.5 \rho_L}{\rho_G} - 1\right)\right]^{0.2} \quad (5.56)$$

Slip model

According to this model, the form loss coefficient for two phase flow can be obtained from

$$\Delta p_{TPF} = \frac{K_{SPF} G^2}{2\rho} = K_{SPF} \frac{\rho_L}{\rho} \frac{G^2}{2\rho_L} = K_{TPF} \frac{G^2}{2\rho_L} \quad (5.57)$$

where

ρ is given by

$$\rho = \alpha \rho_G + (1-\alpha) \rho_L ; \quad \alpha = \frac{1}{1 + \left(\frac{1-x}{x}\right) S \frac{\rho_G}{\rho_L}}$$

It may be noted that this equation reduces to the homogeneous model if $S = 1$. Grillo and Marinelli (1970) recommend a value of $S = 2$ for grid spacers.

Tie plate

Generally, tie plates are used at the ends of rod cluster fuel elements which structurally joins all the fuel pins. Unlike spacers, the flow areas at the downstream and upstream sides of the tie plates are different. Also, these are generally located in the unheated portion of the bundle. Reported studies on pressure drop for the tie plates are few in number. An approximate calculation for design purposes can be made using the contraction and expansion model for local pressure losses. In addition the friction losses in the thickness of the tie plates can be calculated using the hydraulic diameter concept. For two-phase pressure losses, the homogeneous or the slip model described above can be employed in the absence of experimental data.

5.3.4.2. Area changes

Single-phase

The pressure losses due to area changes are calculated by Equation 5.4 with loss coefficients calculated for the relevant geometry from Idelchik (1986).

Two-phase

In general, the irreversible pressure drop due to area changes is estimated from the knowledge of single-phase loss coefficient using the homogeneous model. When details of the slip ratio are available, then the slip model given above can be used.

Sudden expansion

Romey [see Lottes (1961)] expresses the two-phase pressure drop across sudden expansion by the following equation:

$$\Delta p = G^2 A_r^2 \frac{(1 - A_r)}{\rho_L} \left\{ 1 + x \left(\frac{\rho_L}{\rho_G} - 1 \right) \right\} \quad (5.58)$$

Beattie (1973) model given above can also be used (Eq. 5.56).

Fitzsimmons (1964) provides the following equation to calculate the pressure change across abrupt expansion

$$\Delta p = \frac{G^2 A_r^2}{\rho_L} \left\{ \frac{\rho_L}{\rho_G} x^2 \left(\frac{1}{\alpha_1 A_r} - \frac{1}{\alpha_2} \right) \right\} \left\{ (1 - x)^2 \left(\frac{1}{(1 - \alpha_1) A_r} - \frac{1}{(1 - \alpha_2)} \right) \right\} \quad (5.59)$$

where

subscripts 1 and 2 refer respectively to the upstream and downstream locations of the abrupt expansion. An assessment carried out by Husain et al. (1974) suggests that better agreement with data is obtained when α_1 and α_2 are calculated by assuming slip flow.

5.3.4.3. Bends and fittings

The single-phase pressure drop due to bends and fittings can be calculated using the appropriate loss coefficients from Idelchik (1986).

Two-phase pressure drop

Chisholm (1969) provides the following general equation for the calculation of two-phase pressure drop in bends and fittings.

$$\frac{\Delta p_{TP}}{\Delta p_L} = 1 + \left(\frac{\Delta p_G}{\Delta p_L} \right) + C \left(\frac{\Delta p_G}{\Delta p_L} \right)^{0.5} \quad (5.60)$$

$$C = \left\{ 1 + (C_2 - 1) \left(\frac{v_{fg}}{v_G} \right)^{0.5} \right\} \left\{ \left(\frac{v_G}{v_L} \right)^{0.5} \left(\frac{v_L}{v_G} \right)^{0.5} \right\} \quad (5.61)$$

where

$v_{fg} = v_G - v_L$, and
 C_2 is a constant.

Bends

For bends C_2 is a function of R/D , where R is the radius of curvature of the bend and D is the pipe diameter.

$R/D \rightarrow$	1	3	5	7
C_2 for normal bend	4.35	3.40	2.20	1.00
C_2 for bend with upstream disturbance within 50 L/D	3.10	2.50	1.75	1.00

Chisholm provided the above values of C_2 by fitting Fitzsimmons (1964) data.

Chisholm & Sutherland (1969)

$$\text{For } 90^\circ \text{ bends: } C_2 = I + 35 N \quad (5.62)$$

$$\text{For } 180^\circ \text{ bends: } C_2 = I + 20 N \quad (5.63)$$

N is the number of equivalent lengths used for calculating single-phase pressure drop.

Tees:

$$C_2 = 1.75$$

Valves:

$$\begin{aligned} C_2 &= 1.5 \text{ for gate valves} \\ &= 2.3 \text{ for globe valves} \end{aligned}$$

Alternatively the homogeneous model may be used.

Orifices:

For separated flow (stratified) at obstruction, Beattie (1973) obtained the following expression for ϕ_{LO}^2 .

$$\phi_{LO}^2 = \left\{ 1 + x \left(\frac{\rho_L}{\rho_G} - 1 \right) \right\}^{0.8} \left\{ 1 + x \left(\frac{\rho_L \mu_G}{\rho_G \mu_L} - 1 \right) \right\}^{0.2} \quad (5.64)$$

5.3.5. Importance of void fraction correlations

Void fraction plays an important role, not only in pressure drop calculation, but also in flow pattern determination and neutron kinetics. All the four components of pressure drop directly or indirectly depend on the void fraction. For certain situations of practical interest, accurate prediction of all the components are required. For example, steady state flow prevails in a natural circulation loop when the driving pressure differential due to buoyancy (i.e. the

elevation pressure drop) balances the opposing pressure differential due to friction and acceleration. For natural circulation loops, therefore, the largest contribution to pressure drop arises from the elevation pressure drop. Also, the acceleration pressure drop can be 10–15% of the total core pressure drop. For such cases, accurate estimation of each component of pressure drop is required. Therefore, it is very important to have a reliable relationship for the mean void fraction. Significant deviations are observed between the predicted flow rate using different models for friction and void fraction.

In many experiments with diabatic vertical test sections, the friction pressure loss is obtained as shown below:

$$\left(\frac{dp}{dz}\right)_{\text{TPF}} = \left(\frac{dp}{dz}\right)_m - g\left(\frac{\alpha}{v_G} + \frac{1-\alpha}{v_L}\right) - G^2 \frac{d}{dz}\left(\frac{x^2}{\alpha} v_G + \frac{(1-x)^2}{1-\alpha} v_L\right) \quad (5.65)$$

where

$(dp/dz)_m$ is the measured pressure drop.

It is observed from the above equation that the void fraction, α , and quality, x , play an important role in deducing the frictional term from the measured static pressure drops. Usually, the acceleration and elevation drops are calculated with the help of a void fraction value, which may not be measured but calculated by a correlation.

The stability predictions of natural circulation loops are also strongly influenced by the friction and mean void fraction model [see Furutera (1986)]. The use of certain friction models can completely mask the stability phenomenon. In coupled neutronic thermalhydraulic calculations, the void fraction plays an important role in the calculation of reactor power [Saphier and Grimm (1992)]. For such calculations, it is essential to use the best models for each component of pressure drop which indirectly also implies the use of the best void fraction model. Hence, it is necessary to make a judicious choice of the void fraction correlations. Some of the commonly used void fraction correlations are described briefly in the following section.

5.3.5.1. Void fraction correlations

In general, the void fraction correlations can be grouped into three; viz.,

- (a) slip ratio models,
- (b) $K\beta$ models and
- (c) correlations based on the drift flux model.

In addition, there are some empirical correlations, which do not fall in any of the three categories. Some of the commonly used correlations in all the above categories are described below.

5.3.5.1.1. Slip ratio models

These models essentially specify an empirical equation for the slip ratio, S ($=u_G/u_L$). The void fraction can, then be calculated by the following equation:

$$\alpha = \frac{1}{1 + \left(\frac{1-x}{x} \right) S \frac{\rho_G}{\rho_L}} \quad (5.66)$$

For homogeneous flow, $u_G = u_L$ and $S = 1$. At high pressure and high mass flow rates the void fraction approaches that of homogeneous flow, and can be calculated by setting $S = 1$ in the above equation. But usually, the slip ratio is more than unity for both horizontal and vertical flows. For vertical upward flows, the buoyancy also assists in maintaining $S > 1$. The common slip ratio models are given in Appendix XIII.

5.3.5.1.2. $K\beta$ models

These models calculate α by multiplying the homogeneous void fraction, β , by a constant K . Well-known models in this category are due to Armand (1947), Bankoff (1960) and Hughmark (1965) which are given in Appendix XIV.

5.3.5.1.3. Correlations based on the drift flux model

By far the largest number of correlations for void fraction reported in the literature are based on the drift flux model. The general drift flux formula for void fraction can be expressed as

$$\alpha = \frac{j_G}{C_0[j_G + j_L] + V_{Gj}} \quad (5.67)$$

where

V_{Gj} is the drift velocity ($= u_G - j$, where j is the mixture velocity) and for homogeneous flow $C_0 = 1$ and $V_{Gj} = 0$. The various models (see Appendix XV) in this category differ only in the expressions used for C_0 and V_{Gj} which are empirical in nature.

The Chexal and Lellouche (1996) correlation is applicable over a wide range of parameters and can tackle both co-current and counter-current steam-water, air-water and refrigerant two-phase flows. The correlation is used in RELAP5 [the RELAP5 Development Team (1995)] and RETRAN [Mcfadden et al. (1992)] and is given in Appendix XV for steam-water two-phase flow.

5.3.5.1.4. Miscellaneous correlations

There are a few empirical correlations which do not belong to the three categories discussed above. Some of the more common ones are given in Appendix XVI.

Significant differences exist between the void fraction values obtained using different correlations. This necessitates a thorough assessment of the void fraction correlations.

5.3.6. Review of previous assessments

Several assessments of pressure drop and void fraction correlations reported in literature are reviewed and their recommendations summarized in this section.

5.3.6.1. Pressure drop correlations

In general, two different approaches are followed while assessing the predictive capability of pressure drop correlations. In one of these, a particular correlation is chosen and compared with all available two-phase flow pressure drop data disregarding the flow pattern to which the data belong. This approach is adequate for adiabatic flows while assessing correlations valid for all flow patterns, and is followed by Idsinga et al. (1977), Friedel (1979 & 1980), Beattie and Whalley (1982), Snoek & Leung (1989) and Lombardi & Carsana (1992).

In the other approach correlations are chosen for a particular flow pattern and compared against data obtained for that flow pattern. Since flow pattern specific pressure drop data are limited, the flow pattern to which the data belong is identified with a flow pattern map to facilitate the selection of the correlation. This approach requires a pre-assessment of flow pattern maps. Examples of such assessments are those due to Mandhane et al. (1977), Hashizume & Ogawa (1987) and Behnia (1991). Some assessments like those of Dukler et al. (1964) and Weisman & Choe (1976) combine both these approaches.

Some limited assessments for investigating parametric effects are also reported. For example, Simpson et al. (1977) and Behnia (1991) assessed data from large diameter pipes while D'Auria and Vigni (1984) studied the effect of high mass velocity flows. Most assessments employed statistical methods, but the parameter and the correlations chosen for assessment are widely different. Some salient results of these assessments are presented here.

5.3.6.1.1. Homogeneous model

Beattie and Whalley (1982) compared 12 pressure drop correlations including 5 homogeneous models using the HTFS (Heat transfer and fluid flow services) databank containing about 13500 adiabatic data points for steam/water and non-steam water mixtures. This study used roughly about 8400 horizontal flow data points and 5100 vertical flow data points. They used the homogeneous void fraction model to calculate the elevation head for the homogeneous friction models whereas an unpublished void fraction correlation (HTFS-1981) was used for the other models. From this study Beattie and Whalley conclude that the homogeneous model is as good as the others in predicting the two-phase flow pressure drop over the range of parameters considered. The main results of Beattie and Whalley are summarized in Table 5.5.

Idsinga et al. (1977) compared 18 different correlations (4 homogeneous models) against 3500 steam-water pressure drop measurements under both adiabatic and diabatic flow conditions. Most of the data were from vertical pipes ranging in diameter from 0.23 to 3.3 cm. Also, the amount of low mass flux data (less than $300 \text{ kg/m}^2\text{s}$) was much less. They used the thermodynamic equilibrium model for the calculation of single-phase length in case of diabatic data. The void fraction model used is the homogeneous model for all homogeneous friction models and for other models, consistent void fraction correlations recommended by the original authors were used. Assessment by Idsinga et al. (1977) shows that best results are obtained from the homogeneous models proposed by Owens (1961) and Cicchitti (1960). Incidentally, these models were also considered for assessment by Beattie and Whalley (1982) and were found to give reasonable results for steam/water flow, although not as good as that of Beattie and Whalley model.

Assessment by Weisman and Choe (1976) showed that the homogeneous models of McAdams (1942) and Dukler et al. (1964) give better results in the homogeneous flow regime ($G > 2712.4 \text{ kg/m}^2\text{s}$). Interestingly, the homogeneous model by Dukler (1964) gave consistently good results for all flow regimes except the separated (stratified) flow regime.

5.3.6.1.2. Correlations based on the multiplier concept

Several comparisons of these correlations have been reported previously. One of the earliest assessment was carried out by Dukler et al. (1964). They also compiled a databank consisting of about 9000 data points. They have selected 5 correlations [Baker (1954), Bankoff (1960), Chenoweth and Martin (1955), Lockhart and Martinelli (1949) and Yagi (1954)] for assessment. Their assessment showed that the Lockhart and Martinelli correlation is the best out of the five correlations for two-component two-phase flow.

Idsinga et al. (1977) assessed 14 multiplier based models against 3500 steam-water pressure drop data. The multiplier based models recommended by Idsinga et al. (1977) are the ones due to Baroczy (1966) and Thom (1964).

Friedel (1980) compared 14 pressure drop correlations against 12 868 data points obtained by 62 authors from circular and rectangular channels. Both horizontal and vertical flow adiabatic data in pipes ranging from 1 to 15 cm in diameter were studied. While applying the correlations no distinction is made as to whether they were derived for horizontal or vertical two-phase flow. Overall, the Chisholm (1973) and the Lombardi-Pedrocchi (DIF-1) correlations were found to be the most accurate. However, these two correlations are equivalent and are unexpectedly inadequate for prediction of the measured values in gas/water and gas/oil flows.

TABLE 5.5. MAIN RESULTS OF BEATTIE AND WHALLEY

Fluid used	NDP ^(a)	Orientation	Recommended Correlation
Non steam-water	7168	horizontal	HTFS, L-M ^(b) & B-W ^(c)
Non steam-water	2011	vertical	L-M, HTFS & B-W
Steam-water	1236	horizontal	Dukler et al, B-W & Isbin
Steam-water	3095	vertical	B-W, HTFS, & Friedel

^(a) NDP: No. of data points,

^(b) L-M: Lockhart-Martinelli (1948),

^(c) B-W: Beattie and Whalley (1982).

Friedel (1979) derived two-phase friction pressure drop correlations for horizontal, vertical upflow and downflow based on his databank. He has also compared the predictions of these correlations with the Chisholm (1973) and DIF-2 correlations using an enhanced databank consisting of about 25 000 data points. The data pertain to one-component and two-component mixtures flowing in straight unheated sections with horizontal, vertical upflow and downflow in tubes, annular and rectangular ducts under widely varying conditions. The Friedel correlation was found to be better than the other two.

5.3.6.1.3. Flow pattern specific models

To assess flow pattern specific pressure drop correlations, the first step is to select a flow pattern map applicable to the geometry. Previous review of flow pattern specific pressure drop correlations have been carried out by Weisman and Choe (1976), Mandhane et al. (1977), Hashizume & Ogawa (1987) and Behnia (1991) for horizontal two-phase flow. In the reviews by Mandhane et al. and Behnia, the flow pattern to which the data belong has been obtained with the help of Mandhane's flow pattern map. Hashizume and Ogawa (1987) used a modified Baker map in their assessment. Weisman and Choe used their own flow pattern map.

Using the AGA-API databank (enhanced by the addition of Fitzsimmons (1964), Petrick (1961) and Miropolski (1965) data), Weisman and Choe made a flow pattern specific assessment for horizontal two-phase flow. Their assessment covers four basic flow patterns referred to as separated flow (Stratified flow), homogeneous flow, intermittent (slug) flow and annular flow. The transition criteria used by them are given in Table 5.6.

Based on their assessment the correlations recommended for different flow patterns are given in Table 5.7. Their assessment shows that the scatter obtained using the different correlations (11 in all) for separated flow is substantially large. Ten different correlations were assessed for the homogeneous flow pattern and in this regime, the homogeneous models give better predictions. Most of the correlations tested for the intermittent flow regime were found to give reasonably good values, although the best predictions are obtained with the Dukler et al. (1964) correlation followed by Lockhart-Martinelli correlation. These two correlations are also seen to give consistently good results for annular flow.

TABLE 5.6. TRANSITION CRITERIA FOR HORIZONTAL FLOW (WEISMAN & CHOE)

Flow pattern	Transition criteria
Separated flow	$J_G^* < 2.5 \exp [-12(1-\alpha)] + 0.03\alpha$ where $J_G^* = \rho_G^{0.5} J_G / [g D (\rho_L - \rho_G)^{0.5}]$
Annular flow	$G > 10(G_L)^{-0.285} (D/D_c)^{0.38}$ where G_L is in $\text{lb/ft}^2\text{hr}$ and $D_c = 1.5''$ (0.0381 m)
Homogeneous flow	$G \geq 2712.4 \text{ kg/m}^2\text{s} \text{ (} 2 \times 10^6 \text{ lb/h ft}^2\text{)}$

Mandhane et al. (1977) compared 16 pressure drop correlations against the University of Calgary Pipe Flow Data Bank containing about 10 500 data points. The data were grouped by predicted flow pattern using the Mandhane et al. (1974) flow pattern map. Each correlation was then tested against all the data points contained within each flow pattern grouping. The correlations recommended by Mandhane et al. are given in Table 5.8. Hashizume and Ogawa (1987) also carried out an assessment of 5 pressure drop correlations using selected data (only 2281 data) from the HTFS databank. This, however, contained some very low mass flux data. In this analysis they have used the modified Baker (1954) map for flow pattern identification. They concluded that their correlation gives the best prediction for refrigerant data.

TABLE 5.7. CORRELATIONS RECOMMENDED BY WEISMAN & CHOE (1976)

Flow pattern	Recommended correlation	No. of correlations tested
Separated flow	Agrawal et al. (1973) and Hoogendoorn (1959)	11
Homogeneous flow	McAdams (1942), Dukler et al. (1964) & Chisholm (1968)	10
Intermittent flow	Dukler (1964), Lockhart-Martinelli (1949) & Hughmark (1965)	7
Annular flow	Dukler (1964) & Lockhart-Martinelli (1949)	6

TABLE 5.8. CORRELATIONS RECOMMENDED BY MANDHANE ET AL. (1977)

Flow pattern	Correlation
Bubble, elongated bubble	Chenoweth and Martin (1956)
Stratified	Agrawal et al. (1973)
Stratified Wavy	Dukler et al (1964)
Slug	Mandhane et al. (1974)
Annular, annular mist	Chenoweth and Martin (1956)
Dispersed bubble	Mandhane et al. (1974)

5.3.6.1.4. Assessment for diabatic flow

With modified Saha and Zuber correlation for the onset of nucleate boiling and the Armand correlation for void fraction, Snoek & Leung (1989) carried out an assessment of 9 different correlations using diabatic pressure drop data from horizontal 37 and 41 rod clusters relevant to CANDU type reactors. The databank consisted of 1217 measurements using either water or refrigerant-12. The correlations compared are the Beattie model (1973), Levy model (1974), Lombardi and Pedrocchi correlation, Martinelli-Nelson separated flow model (1948, 1949), Chisholm and Sutherland model (1969), Chisholm (1983), Reddy et al. (1982) and Beattie and Whalley model (1982). The acceleration pressure drop was calculated using Eqs. 5.6 and 5.7 given in Section 5.3.1 Friedel (1979) correlation was found to predict the experimental results best. Either of the Beattie models were found to yield small errors. Levy model was found to be good for water, but poor for refrigerant-12 data. Results of similar studies for vertical clusters are not available in open literature.

5.3.6.1.5. Parametric effects

Effect of diameter

Simpson et al. (1977) compared six pressure drop correlations with data from large diameter (12.7 and 21.6 cm) horizontal pipes. None of the pressure gradient correlations predicted the measured pressure drop accurately, suggesting the need for considering the effect of pipe diameter. Behnia (1991) has compared seven pressure drop correlations with data generated from large diameter pipe lines ranging in diameter from 7.6 cm to 48.4 cm. In order to identify the flow pattern to which the data belong he has used the Mandhane et al. (1974) flow pattern map. He concludes that the best predictions are obtained using the Beggs and Brill (1973) correlation followed by Aziz et al. (1972) correlation. However, it may be noted that the majority of the data is from large oil pipe lines of about 0.5 m in diameter.

Effect of high mass velocity two-phase flow

An assessment to identify a correlation suitable for predicting friction pressure losses in high velocity two-phase flows (characteristic of critical flow in long channels) has been carried out by D'Auria and Vigni (1984). The pressure drop measurements obtained in the exit nozzle of a pressure vessel was used to assess different pressure drop correlations. The investigations were in the range of pressures from 0.1 to 7.0 MPa and flow rate between 500 to 20 000 kg/m²s. The assessments were carried out in two-phases; first 17 different correlations were compared with experimental data adopting a homogeneous equilibrium model. Later on a two-velocity model accounting for slip was considered and the correlations were compared with the same experimental data. Results from these studies indicate that practically none of the correlations is able to predict the measured $(\Delta p)_{tot}$ for high values of mass velocities ($G > 8000 \text{ kg/m}^2\text{s}$) while for low values of the same quantity ($G < 2000 \text{ kg/m}^2\text{s}$) nearly all correlations produce results which are within the experimental error band.

5.3.6.2. Assessment of void fraction correlations

Assessment of void fraction correlations are comparatively few in number. The reported assessments are due to Dukler et al. (1964), Friedel (1980), Chexal et al. (1991) Diener and Friedel (1994) and Maier and Coddington (1997). Dukler compared three holdup (i.e. $1 - \alpha$) correlations, viz., Hoogendoorn (1959), Hughmark (1962) and Lockhart-Martinelli (1949). Hughmark correlation was found to give the best agreement with data.

Friedel (1980) compared 18 different correlations for mean void fraction using a databank having 9009 measurements of void fraction in circular and rectangular channels by 39 different authors. In his assessment no distinction was made as to whether the correlations were derived for horizontal or vertical two-phase flow. The mean void fraction correlation of Hughmark (1962) and Rouhani (I and II) (1969) were found to reproduce the experimental results considerably better than the other relationships, regardless of the fluid and flow directions. However, Rouhani equation II was found to reproduce the measured values more uniformly over the whole range of mean density. Hence, Friedel recommends Rouhani II relationship.

Chexal, Horowitz and Lellouche (1991) carried out an assessment of eight void fraction models using 1500 steam-water data points for vertical configurations representative of several areas of interest to nuclear reactors such as: (1) high pressure — high flows, (2) high pressure —

low flows, (3) low pressure — low flow, (4) counter current flooding limitation, (5) natural circulation flows and (6) co-current downflows. The data were representative of PWR and BWR fuel assemblies and pipes up to 18 inches in diameter. The correlations assessed and statistical comparison are given in Table 5.9.

Diener and Friedel (1994) made an assessment of mean void fraction correlations using about 24000 data points. The data consists of single-component (mostly water & refrigerant 12) and two-component systems (mostly air-water). In this assessment, they had compiled 26 most often used and cited correlations. These correlations were then checked for the limiting conditions [i.e. zero and unity value of void fraction for single-phase liquid ($x = 0$) and single-phase vapor ($x = 1$)]. Only 13 correlations were found to fulfill the limiting conditions and were selected for further assessment. In this assessment they have not differentiated the data on the basis of flow direction, although, in vertical upward flow the mean void fraction is expected to be lower than in case of horizontal flow under identical conditions (due to larger velocities caused by buoyancy effect). Most of the void fraction correlations reproduce the data with a rather acceptable accuracy. The three best correlations in the order of decreasing prediction accuracy are listed in Table 5.10 for various fluid conditions.

Maier and Coddington (1997) carried out an assessment of 13 wide range void correlations using rod bundle void fraction data. The database consisted of 362 steam-water data points. The data is from level swell and boil-off experiments performed within the last 10–15 years at 9 experimental facilities in France, Japan, Switzerland, the UK and the USA. The pressure and mass flux of the data range from 0.1 to 15 MPa and from 1 to 2000 kg/m²-s respectively. Of the 13 correlations considered, 5 were based on tube data. The remaining correlations either are specific to rod bundles or include rod bundle option.

TABLE 5.9. STATISTICAL COMPARISON OF THE EIGHT VOID FRACTION MODELS [CHEXAL, HOROWITZ AND LELLOUCHE (1991)]

Void fraction model	Mean error	Standard deviation
Chexal-Lellouche (1986)	–0.0041	0.049
Liao, Parlos and Griffith (1985)	0.002	0.094
Yeh and Hochreiter (1980)	0.050	0.142
Wilson et al. (1965)	0.013	0.099
Ohkawa and Lahey (1980)	0.025	0.057
Dix (1971)	0.023	0.094
GE ramp (1977)	0.012	0.062
Katoka and Ishii (1982)	0.031	0.101

All 13 correlations except Gardner (1980) are based on drift flux model. Some of the correlations e.g. Ishii (1977), Liao, Parlos and Griffith (1985), Sonnenburg (1989), Takeuchi et al. (1992), Chexal-Lellouche (1992) require iterations to calculate the void fraction. The important results of this assessment are:

- (1) Two of the tube based correlations i.e. Liao, Parlos and Griffith (1985) and Takeuchi (1992), produce standard deviations which are as low as the best of the rod bundle correlations.
- (2) Complex correlations like Chexal et al. (1992), or others requiring iterative solutions produce no significant improvement in mean error or standard deviation compared to more direct correlations of Bestion (1990), Inoue et al. (1993) and Maier and Coddington (1997).

TABLE 5.10. VOID FRACTION CORRELATIONS RECOMMENDED BY DIENER & FRIEDEL (1994)

Fluid	Total number of Data points	Recommended Correlation
Water/air mixture	10991	Rouhani I, Rouhani II, HTFS-Alpha [@]
1-component mixtures	9827	HTFS-Alpha, HTFS [@] , Rouhani II
2-component mixtures	14521	HTFS-Alpha, Rouhani I, Rouhani II
2-component mixtures with $G > 100 \text{ kg/m}^2\text{s}$	11394	Rouhani II, Rouhani I, HTFS

[@] proprietary correlations belonging to HTFS.

5.3.6.3. Limitations of the previous assessment procedure

Most of the well documented assessments of pressure drop correlations have been reviewed in the Section 5.3.6.1. Some limitations of these assessments are given below:

- (1) To the best of our knowledge, none of the prior assessments of the two-phase friction correlations concentrate on low mass flux two-phase flows. Analysis using limited number of data (see Vijayan & Austregesilo) shows that there is considerable scatter in the predictions at the low mass fluxes typical of advanced designs. Hence it is desirable to assess the predictive capability of correlations reported in literature for use in the design of advanced reactors where better accuracy of prediction at low mass flux is the criterion of acceptability.
- (2) Most assessment of PDCs are based on statistical approach. The correlations selected by a statistical method need not necessarily reproduce the parametric trends as shown by Leung & Groeneveld (1991). Reliable reproduction of parametric trends by PDCs is important to capture certain thermalhydraulic phenomena. An example in this regard is the flow pattern transition instability occurring near slug flow to annular flow transition [Boure et al. (1971)].
- (3) Effect of pressure has not been studied separately. It is of interest to study this aspect for the advanced designs.
- (4) Effect of pipe diameter needs to be assessed as the pipe diameters in advanced designs can be large. In this case, there is a need to generate additional data as most of the available data on steam water mixture are for small diameter pipes.
- (5) Most assessments are for pipe flow data. The only assessment for rod bundles in the open literature is that reported by Snoek and Leung (1989) for CANDU type reactors.

- (6) The database for vertical downflow is less extensive.
- (7) In deriving certain empirical friction models, a specific void correlation is used to derive the experimental friction pressure drop data. Such empirical models, are to be used with the specified void correlation to predict the pressure drop. Such correlations may not be acceptable for natural circulation reactors where the flow rate is a dependent variable governed by the balance of the driving pressure differential due to elevation and the pressure losses. Therefore, applicability of such correlations needs to be assessed for natural circulation flow.
- (8) To our knowledge, assessment of flow pattern specific pressure drop correlations for vertical flow are not reported so far. For the assessment of flow pattern specific correlations, the flow pattern to which the data belong is identified with the help of a flow pattern map which is different for different orientations of the duct. Therefore, separate assessments are required for identifying the best flow pattern map.

5.3.7. Proposed assessment procedure for diabatic vertical flow

For adiabatic vertical flows, the gravitational pressure drop is significant and therefore a void fraction correlation is necessary to derive the experimental friction pressure drop from the measured total pressure drop. For diabatic vertical two-phase flows with subcooled inlet conditions, which is relevant to nuclear reactors, a model for the onset of nucleate boiling is necessary in addition to void fraction correlation. This suggests that the frictional Pressure Drop Correlations (PDCs) cannot be assessed in isolation. In fact, a rational assessment of PDCs for diabatic flow requires a preassessment of models for onset of nucleate boiling (ONB), void fraction and flow pattern transitions. Therefore, a rational assessment procedure consists of the following steps:

- (1) To review the literature and compile a set of correlations for ONB, void fraction, flow pattern and pressure drop,
- (2) To compile a databank consisting of raw data for ONB, void fraction, flow patterns and pressure drop for forced and natural circulation conditions of one-component two-phase flow,
- (3) Assessment of models for ONB, void fraction, flow pattern transitions and pressure drop.

This assessment also aims to investigate the parametric effects due to mass flux, pressure, quality, diameter, flow direction and geometry relevant to the advanced designs. An assessment is in progress in BARC. Some of the results available at this stage are given below.

5.3.8. Results of assessment

5.3.8.1. Compilation of databank

Several databanks exist for the pressure drop in two-phase flow. Examples are those due to Dukler et al. (1964), Friedel (1980), AGA-API, University of Calgary multiphase pipe flow databank, HTFS databank and MIDA [Brega et al. (1990)]. A databank has been compiled by Friedel (1994) for void fraction. Some databanks for flow patterns are also available. These databanks are not available to us at present and therefore a *two-phase flow data bank* (TPFDB) consisting of raw experimental data on the following phenomena is being compiled.

- (a) Adiabatic and diabatic pressure drop in ducts of various geometry,
- (b) Void fraction,
- (c) Flow patterns,
- (d) Flow pattern specific pressure drop.

In this compilation, special emphasis is given to steam-water flows although some data on air-water and refrigerant two-phase flows are included. The databank is being updated continuously. Currently, this databank consists of about 4000 data on pressure drop, 5000 data on void fraction, 3000 data on flow pattern and 500 data on flow pattern specific pressure drop. The sources from where the original data were compiled are shown in Appendix XVII.

5.3.8.2. Assessment of void fraction correlations

An assessment of the void fraction correlations given in Section 5.3.5.1 was carried out using a part of the void fraction data (about 3300 entries) contained in the TPFDB. The data used for assessment pertains to vertical upward flow of steam-water mixture in circular, annular and rectangular channels. Further details of the assessment are given in Appendix XVIII.

The present assessment showed that Chexal-Lellouche correlation performs better than other correlations. Clearly, all the statistical parameters considered above are minimum for this correlation, followed by Hughmark, Modified Smith and Rouhani correlations (Table 5.11). Previous assessments by Dukler et al. (1964) and Friedel (1980) have also shown that the Hughmark correlation to be the best. Assessment by Diener and Friedel (1994) have shown the Rouhani correlation to be among the best three correlations for predicting void fraction.

A generic problem of all good correlations mentioned above except Modified Smith correlation is that they overpredict the void fraction. This is clear from the mean error given in the table-11, which is positive for almost all the correlations (except Nabizadeh and Modified Smith correlations). Among the top four correlations only the Chexal-Lellouche and the modified Smith correlations satisfy the three limiting conditions (i.e. at $x = 0$, $\alpha = 0$; at $x = 1$, $\alpha = 1$ and at $P = P_{crit}$, $\alpha = x$) over a wide range of parameters (see also Appendix XVIII). Therefore, these correlations may be used in computer codes used for thermalhydraulic analysis.

5.3.8.3. Assessment of flow pattern maps for vertical upward two-phase flow

A large number of flow pattern maps are found in the literature. Many of these are based on experiments. Examples are those due to Griffith and Wallis (1961), Hosler (1967), Spedding and Nguyen (1980) and Weisman and Kang (1981). Since such flow pattern maps are based on limited data, these cannot be assumed to be of general validity. Therefore, theoretical flow pattern maps have been proposed by a few authors. In such maps, the transition criteria are physically based and can be considered to be of general validity. Examples of such maps are those proposed by Taitel et al. (1980), Mishima-Ishii (1984), Solbrig (1986), Bilicki and Kestin (1987) and McQuillan and Whalley (1985). In the present assessment, only three theoretical flow pattern maps for vertical upward flow, proposed by

Taitel et al. (1980), Mishima and Ishii (1984) and Solbrig (1986) are considered as they form the basis of the flow pattern maps used in computer codes for the thermal-hydraulic analysis of nuclear reactors.

A fairly large number of flow regimes are reported in literature. Examples are bubbly, dispersed bubbly, slug, churn, annular, wispy annular, wavy annular, annular mist, spray annular, droplet flow, etc. However, most investigators categorised the flow pattern data into mainly three regimes. These are the bubbly, slug and annular flow regimes. Even computer codes like RELAP5 consider only these as independent flow regimes. Therefore, in our assessment only these three flow patterns are considered. Corresponding to these three patterns the relevant transitions are bubbly-to-slug and the slug-to-annular.

Detailed results of this assessment are given in Appendix XVIII. Table 5.12 shows a summary of the comparison of the data with bubbly-slug together with slug — annular transition criteria. The characterization of bubbly flow data using the different transition criteria yield comparable results. Since it uses $\alpha = 0.52$, 95% of all bubbly flow data is characterized as bubbly by the Solbrig criterion. However, a large amount of slug flow data also fall in the bubbly flow regime.

The slug-annular transition criteria together with bubbly-slug transition criteria are required to assess the slug flow data. Table 5.13 shows the results of such an assessment. As seen all the criteria fare badly in characterizing slug flow data even though the Solbrig criterion I is somewhat better than others.

TABLE 5.11. COMPARISON OF VARIOUS VOID FRACTION CORRELATIONS

Correlation name	mean error (%)	absolute mean error (%)	r. m. s. error (%)	standard deviation (%)
Chexal-Lellouche	5.10	15.25	22.74	22.16
Hughmark	6.85	16.72	23.81	22.60
Modified Smith	-5.44	18.13	24.19	23.58
Rouhani	10.76	18.42	25.97	23.64
Zuber-Findlay	11.20	19.32	26.15	23.64
Bankoff	9.08	19.21	26.58	24.98
Osmachkin	1.32	18.91	26.59	26.56
Bankoff-Jones	12.50	20.78	27.95	25.00
Thom	6.72	21.11	28.88	28.08
Nabizadeh	-21.17	24.40	30.00	21.35
Armand	21.54	27.75	34.75	27.27
GE-Ramp	27.30	32.60	39.10	28.08
Bankoff-Malnes	30.98	36.57	44.15	31.45
Dix	17.81	39.92	48.52	45.14
Homogeneous model	44.90	49.03	55.51	32.65

TABLE 5.12. CHARACTERIZATION OF BUBBLY FLOW DATA USING THE VARIOUS TRANSITION CRITERIA

Item	Taitel et al.	Mishima-Ishii	Solbrig
PBB*	72.3	77.7	95.1
PBS ⁺	21.1	17.8	4.9
PBA**	6.7	4.6	0.0
PSB [@]	13.0	17.7	39.6
PAB [#]	0.7	1.6	4.0

*PBB: Percentage of bubbly data characterized as bubbly;
+PBS: Percentage of bubbly data characterized as slug;
** PBA: Percentage of bubbly data characterized as annular;
@PSB: Percentage of slug data characterized as bubbly;
PAB: Percentage of annular data characterized as bubbly.

TABLE 5.13. CHARACTERIZATION OF SLUG FLOW DATA USING VARIOUS TRANSITION CRITERIA

Item	Taitel et al.	Mishima-Ishii	Solbrig I	Solbrig II
PSS*	40.2	43.2	46.6	34.4
PSB	13.0	17.7	39.6	24.6
PSA**	47.0	39.2	13.5	40.5
PBS	21.1	17.8	4.9	11.8
PAS [#]	9.4	16.0	47.8	12.1

* PSS: Per cent of slug data characterized as slug;
PAS: % of annular data characterized as slug;
** PSA: Per cent of slug data characterized as annular.

TABLE 5.14. CHARACTERIZATION OF ANNULAR FLOW DATA WITH VARIOUS TRANSITION CRITERIA

Item	Taitel et al. (1980)	Mishima-Ishii (1984)	Solbrig I (1986)	Solbrig II (1986)
PAA*	90.1	82.7	48.1	85.5
PAS	9.4	16.0	47.8	12.1
PAB	0.7	1.6	4.0	2.4
PBA	6.7	4.6	0.0	0.7
PSA	47.0	39.2	13.5	40.5

* PAA: Percentage of annular data characterized as annular.

Limiting our attention to only the characterization of annular flow data shown in Table 5.14, Taitel et al. Mishima-Ishii and the Solbrig II criterion are found to perform well. However, an acceptable criterion shall not characterize slug flow data as annular and that is where all the three criteria fail.

5.3.8.4. Assessment of pressure drop correlations

A part of the pressure drop data from TPFDB for vertical upward two-phase flow in different geometries has been assessed against some of the correlations described earlier in this report. In the present assessment 2156 data points collected from literature for diabatic steam-water flow were assessed against the correlations listed in Table 5.15. Excepting Chisholm and Turner-Wallis the other correlations belong to the homogeneous model. The assessment is based on Colebrook equation for single-phase friction factor, Zuber-Findlay (1965) correlation for void fraction and Saha and Zuber (1974) model for the onset of nucleate boiling. The results are also given in Table 5.15. The table shows that the Chisholm correlation is the one with least R.M.S. error (37%) and least standard deviation (28%) followed by the homogeneous model given by Dukler et al. (1964) with 48% R.M.S. error and 46% standard deviation which suggests that the simple homogeneous models can give reasonable predictions for design purposes. Earlier assessment by Friedel (1980) had shown that the Chisholm (1973) correlation to be most accurate for adiabatic steam-water flow. Prior assessment by Weisman and Choe (1976) showed that the Dukler et al. (1964) gave consistently good results for all flow regimes.

5.4. COMPARISON OF CORRELATIONS AS THEY STAND IN CODES

Reference is made hereafter to system codes used in the safety and design analysis of nuclear power plants. The attention is focused toward RELAP5 and CATHARE owing to the direct experience gained in the use of these codes. The physical phenomenon addressed is the wall-to-fluid (steam and/or liquid) pressure drop excluding other phenomena that may contribute to the overall (steady state or transient) pressure drop.

TABLE 5.15. COMPARISON OF PRESSURE DROP CORRELATIONS

Correlation	Mean error (%)	R.M.S. error%	Standard Deviation %
Dukler et al. (1964)	12	48	46
McAdams (1942)	20	54	50
Beattie & Whalley (1982)	21	55	51
Cicchittie (1960)	31	65	57
Chisholm (1973)	24	37	28
Turner-Wallis (1965)	21	61	57

The comparison among correlations as they stand in the codes, implies two different steps:

- (a) description of the physical models or constitutive equations or closure equations implemented in the codes;
- (b) comparison among results produced by the code in terms of pressure drops, eventually including experimental data.

The item a) constitutes the objective of the Section 5.4.1, while item b) is addressed in the following discussion.

The calculation (better, the results of calculations) of pressure drop by system codes is a function of different types of parameters including :

- nodalization details,
- user assumptions,
- physical models for wall-to-fluid pressure drops (Section 5.4.1),
- general code hydraulic model and coupling with physical models other than pressure drops (e.g. heat transfer coefficient),
- numerical structure of the code.

The role of each set of parameters may be extremely different in the various code applications; i.e. user assumptions may be very important in one situation and (almost) not important in the another case; clearly, physical models are always important.

A huge amount of comparison among calculation results by system codes (including comparison with experimental data), is provided in the open literature (e.g. International Standard Problems organized by OECD/CSNI or Standard Problem Exercise organized by the IAEA). In the case of natural circulation, a detailed comparison among system codes, including evaluation of the effects of nodalization details, of boundary and initial conditions and of user choices can be found in D'Auria and Galassi (1992). In the framework of the present CRP some presentations focused on this item too [D'Auria and Frogheri (1996)].

Considering all of the above, it was preferred not to include results of time trends predicted by the code.

5.4.1. Physical models in system codes

The attention is focused hereafter to the two-phase wall-to-fluid friction in RELAP5/MOD3.2 [the RELAP5 Development Team (1995)] and CATHARE 2 v1.3 [Houdayer et al. (1982)] codes.

5.4.1.1. RELAP5

The wall friction model is based on the Heat Transfer and Fluid Flow Service (HTFS) modified Baroczy correlation, [see Chaxton et al (1972)]. The basic equation is

$$\left(\frac{dP}{dz}\right)_{2\phi} = \phi_L^2 \left(\frac{dP}{dz}\right)_L = \phi_G^2 \left(\frac{dP}{dz}\right)_G = \frac{1}{2D} \left\{ \lambda_L \rho_L (\alpha_L u_L)^2 + C \left[\lambda_L \rho_L (\alpha_L u_L)^2 \lambda_G \rho_G (\alpha_G u_G)^2 \right]^{1/2} + \lambda_G \rho_G (\alpha_G u_G)^2 \right\} \quad (5.68)$$

where

$$2 \leq C = -2 + f_1(G) T_1(\Lambda, G)$$

where

$$f_1(G) = 28 - 0.3\sqrt{G};$$

$$T_1(\Lambda, G) = \exp \left[\frac{\{\log_{10} \Lambda + 2.5\}^2}{\{2.4 - G(10^{-4})\}} \right], \text{ and}$$

$$\Lambda = (\rho_G/\rho_L)(\mu_L/\mu_G)^{0.2}$$

The same derivation implies the use of the Lockhart-Martinelli parameter, i.e. Eqs 1 to 3 in the Appendix VIII.

The partition between contributions to the total pressure drop due to liquid and steam is obtained following the theoretical basis proposed by Chisholm using the Z parameter defined as:

$$Z^2 = \frac{\lambda_L (Re_L) \rho_L u_L^2 \frac{\alpha_{LW}}{\alpha_L}}{\lambda_G (Re_G) \rho_G u_G^2 \frac{\alpha_{GW}}{\alpha_G}} \quad (5.69)$$

such that

$$\tau_L p_L = \alpha_L \frac{dP}{dz} \bigg|_{2\phi} \left\{ \frac{Z^2}{\alpha_G + \alpha_L Z^2} \right\} \quad (5.70)$$

$$\tau_G p_G = \alpha_G \frac{dP}{dz} \bigg|_{2\phi} \left\{ \frac{Z^2}{\alpha_G + \alpha_L Z^2} \right\} \quad (5.71)$$

In the last formulae (other than the already defined quantities) p_L and p_G are the section perimeters contacting with liquid and steam, respectively; in addition, α_{LW} and α_{GW} are the liquid and the vapor volume fraction respectively, in the wall film:

$$p_L/p = \alpha_{LW} \quad (5.72)$$

$$p_G/p = \alpha_{GW} \quad (5.73)$$

These are defined from the flow regime maps, on the basis of what can be referred as RELAP5 approach [the RELAP5 Development Team (1995)].

The single phase coefficient (Darcy-Weisbach friction factor) is computed from correlations for laminar and turbulent flows with interpolation in the transition regime. The laminar zone coefficient is obtained from the well known "64/Re" formula. The turbulent

friction factor is obtained from the Zigrang-Sylvester approximation, [Zigrang and Sylvester (1985)], that is introduced into the already discussed Colebrook correlation. The transition region is computed by a linear interpolation that, again, can be reported as RELAP5 approach. Finally the heated wall effect is accounted for, by introducing the correlation adopted in the VIPRE code [Stewart (1985)].

5.4.1.2. CATHARE

In relation to two-phase wall-to-fluid friction, a simpler approach is included in the CATHARE Code [Bestion (1990)]. The complex interaction of this model with terms included in other code models (e.g. dealing with momentum transfer : interfacial friction, stratification criterion, drift velocity, droplet diameter) should be recalled: the overall result of the code predicted pressure drop comes from the combination of the effects of all the above mentioned models.

The wall friction is computed from the following formula (the index "K" may indicate either the liquid phase, K = L, or the vapor phase, K = G):

$$\tau_{WK} = -C_K C_{FK} \rho_K \frac{u_K |u_K|}{2} \quad (5.74)$$

where

C_{FK} is the single-phase friction coefficient

$$C_{FK} = C_{FK}(Re_K) \text{ with } Re_K = \alpha_K \rho_K u_K D_H / \mu_K \quad (5.75)$$

and C_K is the two phase flow multiplier deduced from the experiments.

In the case of stratified flow, this is the relative fraction of the wettable perimeter occupied by the phase K; C_K is only a function of the void fraction. In the other flow patterns, the vapour friction is assumed as negligible and only the liquid-to-wall friction is computed. This is assumed true in all cases except the case of very high void fraction. Specifically, the Lockhart-Martinelli (Appendix VIII) correlation for liquid was adopted for pressure below 2 MPa; for pressure larger than this value a slightly different correlation was adopted which corrects the pressure effect.

This approach was demonstrated to be acceptable with the exception of the situation of high quality in the annular-mist flow regime. A special correlation for $C_{K=L}$ is developed in such a case. It should be mentioned that an extensive experimental database was utilized to demonstrate the validity of the approach.

5.5. FINAL REMARKS

The performed activity gave an idea of the difficulty in synthesizing the current understanding of a fundamental phenomenon in thermohydraulics: the occurrence and the modelling of various components of pressure drop. Making only reference to the modelling, different approaches can be pursued for calculating friction pressure drops. In addition, a number

of correlations, different from each other, have been developed and are currently in use. The areas and the modalities of application of the correlations are also different; in this context, system geometry (e.g. tubes, bundles), fluid status (single-phase, two-phase with or without interaction of phases), flow type (transient, steady state, fully developed or not), flow regime (e.g. in two-phase flow, bubbly or annular flow), can be distinguished. This makes it difficult to identify an 'agreeable' (or widely accepted) approach or to recommend a particular one.

The recommendations should also suit the objectives and the framework of the use of the correlations. Requirements of subchannel analysis codes and system codes should be distinguished. Detailed plans for future development are outside the purpose of the CRP, specifically the need to distinguish between the various applications. However, a few generic requirements that should be the basis of any future development are listed below.

- (a) To identify the conditions for a suitable experiment (i.e. quality of facility design, of test design, of instrumentation and of recorded data)
- (b) To identify "reference data sets"
- (c) To define acceptable errors (as a function of application)
- (d) To compare code and/or correlation results with selected "reference data sets".

In addition, a few specific requirements which need to be considered for future work are listed below.

The correlations selected based on assessment by statistical method need not necessarily reproduce the parametric trends. Therefore, future assessment should also examine the parametric trends for mass flux, pressure, quality and diameter.

Most of the reported assessments are for adiabatic pipe flow data. Assessment of pressure drop correlations for diabatic flow requires pre-assessment of the models for the on-set of boiling and void fraction. For flow pattern specific pressure drop correlations, a pre-assessment of flow pattern transition criteria is also required.

Only limited data are available for complex geometries like rod bundles, grid spacers, tie plates, etc. in the open literature. More data are required in this area.

The available database in the open literature is limited and further work is required to generate more pressure drop data for the following range of parameters:

Low ($<500 \text{ kg/m}^2 \text{ s}$) and high ($>8000 \text{ kg/m}^2 \text{ s}$) mass flux two-phase flow
Large diameter pipe ($>70 \text{ mm}$)
Low pressure ($<10 \text{ bar}$)
Vertical down flow.

Simultaneous void fraction measurement is required along with pressure drop measurement to calculate individual components of pressure drop. The availability of flow pattern specific pressure drop data is very limited. More data are required to be generated in this area.

As final remarks, from a methodological point of view, we can limit ourselves to list the following various approaches for modelling pressure drops that can be considered when developing advanced thermohydraulic models (capabilities intrinsic to CFD — Computational

Fluid Dynamics or DNS — Direct Numerical Simulation are excluded from the present review) suitable for system codes.

Two-phase flow multiplier (developed having a boiling channel as reference): An average value of the two-phase pressure drop can be calculated. Users must be aware of the conditions under which the correlations are developed or tested (e.g. length of the channel, consideration of acceleration pressure drops, etc.).

Interfacial drag: The lack of knowledge of the interfacial area may noticeably lower the quality of such an approach.

Use of drift flux: The calculation of void fraction, based on correlations not tuned to the calculation of pressure drops may limit the validity of the approach.

Use of 6-equation model: The same observations as above applies here.

Calculation of pressure drop considering subchannels: Lack of appropriate knowledge of two- or three-dimensional flows, may limit the validity of the approach.

REFERENCES TO CHAPTER 5

ADORNI, et al., 1961, Results of Wet Steam Cooling Experiments: Pressure Drop, Heat Transfer And Burnout Measurements in Annular Tubes with Internal and Bilateral Heating, CISE-R-31.

ADORNI, N., GASPARI, G.P., 1966, Heat Transfer Crisis and Pressure Drop with Steam-Water Mixtures, CISE-R-170.

AGRAWAL, S.S., GREGORY, G.A., GOVIER, G.W., 1973, An analysis of stratified two-phase flow in pipes, Can. J. Chem. Eng. **51**, 280-286.

ARMAND, A.A., TRESCHÉV, G.G., 1947, Investigation of the resistance during the movement of steam-water mixtures in heated boiler pipes at high pressure, Izv. Ves. Teplotekh. Inst. **4**, 1–5.

AZIZ, K., GOVIER, G.W. FOGARASI, M., 1972, Pressure drop in wells producing oil and Gas, J. Can. Petroleum Technol, 38–48.

BAKER, O., 1954, Simultaneous flow of oil and gas, Oil Gas J. **53**, 185.

BANKOFF, S.G., 1960, A variable density single-fluid model for two-phase flow with particular reference to steam-water flow, J. Heat Transfer **82**, 265–272.

BAROCZY, C.J., 1966, A systematic correlation for two-phase pressure drop, Chem. Eng. Progr. Symp. Ser. **62**, 232–249.

BEATTIE, D.R.H., 1973, “A note on calculation of two-phase pressure losses”, Nucl. Eng. Design, 25, 395–402.

- BEATTIE, D.R.H. WHALLEY, P.B., 1982, A simple two-phase frictional pressure drop calculation method, *Int. J. Multiphase Flow* **8**, 83–87.
- BECKER, K.M., HERNBORG, G., BODE, M., 1962, “An experimental study of pressure gradients for flow of boiling water in vertical round ducts”, (part 4) AE-86.
- BEGGS, H.D., BRILL, J.P., 1973, A study of two-phase flow in inclined pipes, *J. Petroleum Technol* **25**, 607–617.
- BEHNIA, M., 1991, Most accurate two-phase pressure drop correlation identified, *Oil & Gas J.*, 90–95.
- BENNETT, A.W., HEWITT, G.F., KEARSEY, H.A., KAY, R.K.F., LACEY, P.M.C., 1965, *Flow Visualisation Studies of Boiling at High Pressure*, UKAEA Rep. AERE-4874.
- BERGLES, A.E., CLAWSON, L.G., GOLDBERG, P., SUO, M., BOURNE, J.G., 1965b, *Investigation of Boiling Flow Regimes and Critical Heat Flux*, NYO-3304-5.
- BERGLES, A.E., DOYLE, E.F., CLAWSON; SUO, M., 1965a, *Investigation of Boiling Flow Regimes and Critical Heat Flux*, NYO-3304-4.
- BERGLES, A.E., GOLDBERG, P., CLAWSON, L.G., ROOS, J.P., BOURNE, J.G., 1965c, *Investigation of Boiling Flow Regimes and Critical Heat Flux*, NYO-3304-6.
- BERGLES, A.E., ROOS, J.P., ABRAHAM, S.C., GOUDA, S.C., MAULBETSCH, J.S., 1968a, *Investigation of Boiling Flow Regimes and Critical Heat Flux*, NYO-3304-11.
- BERGLES, A.E., ROOS J.P., 1968b, *Investigation of Boiling Flow Regimes and Critical Heat Flux*, NYO-3304-12.
- BERKOWITZ, L. et al., 1960, *Results of Wet Steam Cooling Experiments: Pressure Drop, Heat Transfer and Burnout Measurements with Round Tubes*, CISE-R-27.
- BESTION D., 1990, The physical closure laws in the CATHARE code, *J. Nucl. Eng. Design* **124**.
- BILICKI, Z., KESTIN, J., 1987, Transition criteria for two-phase flow patterns in vertical upward flow, *Int. J. Multiphase Flow* **13**, 283–294.
- BLASIUS, H., 1913, *Mitt. Forsch. Geb. Ing.-Wesen* **131**.
- BONFANTI, F., CERESA, I., LOMBARDI, C., 1982, “Two-phase densities and pressure drops in the low flow rate region for different duct inclinations”, *Proc. 7th Int. Heat Transfer Conf. Munich*.
- BOURE J.A., BERGLES, A.E., TONG L.S., 1971, Review of two-phase flow instability, *ASME Preprint* 71-HT-42.

BREGA, E., BRIGOLI, B., CARSANA, C.G., LOMBARDI, C., MARAN, L., 1990, "MIDA: Data bank of pressure and densities data of two-phase mixtures flowing in rectangular ducts", 8th Congresso UIT, Ancona.

CARLSON, K.E., et al., 1990, RELAP5/MOD3 Code manual, NUREG/CR-5535, EGG-2596.

CEVOLANI, S., Sept. 5–8, 1995, "ENEA Thermohydraulic data base for the advanced water cooled reactor analysis", 1st Research Co-ordination Meeting of IAEA CRP on Thermohydraulic Relationships for Advanced Water Cooled Reactors, Vienna.

CHAWLA, J.M., 1967, VDI-Forsch-Heft, No. 523.

CHAXTON K.T., COLLIER J.G., WARS J.A., 1972, "HTFS Correlation For Two-Phase Pressure Drop and Void Fraction in Tubes", AERE Rep. R7162.

CHENOWETH, J.M., MARTIN, M.W., 1956, Pressure drop of gas-liquid mixtures in horizontal pipes, *Petroleum Eng.* **28**, C-42-45.

CHEXAL, B., LELLOUCHE, G., 1986, A Full Range Drift Flux Correlation for Vertical Flows (Revision 1), EPRI-NP-3989-SR.

CHEXAL, B., et al., 1996, Understanding Void Fraction in Steady and Dynamic Environments, TR-106326/RP-8034-14, Electric Power Research Institute.

CHEXAL, B., LELLOUCHE, G., HOROWITZ, J., 1992, A void fraction correlation for generalized applications, *Progress in Nuclear Energy* **27** 4, 255–295.

CHEXAL, B., HOROWITZ, J., LELLOUCHE, G., 1991, An assessment of eight void fraction models, *Nucl. Eng. Design* **126**, 71–88.

CHISHOLM, D., 1973, Pressure gradients due to friction during the flow of evaporating two-phase mixtures in smooth tubes and channels, *Int. J. Heat Mass Transfer* **16**, 347–358.

CHISHOLM, D., 1968, "The influence of mass velocity on friction pressure gradient during steam-water flow", *Proc. Thermodynamics and Fluid Mechanics Conf.*, Institute of Mechanical Engineers, 182, 336–341.

CHISHOLM, D., SUTHERLAND, L.A., 1969, "Prediction of pressure gradient in systems during two-phase flow", *Proc. Inst. of Mechanical Engineers Symp. on Two-phase Flow Systems*, Univ. of Leeds.

CICCHITTI, A., LOMBARDI, C., SILVESTRI, M., SOLDAINI, G., ZAVATTARELLI, R., 1960, Two-phase cooling experiments: pressure drop, heat transfer and burnout experiments, *Energia Nucleare* **7**, 407–425.

CISE; 1963, A research programme in two-phase flow.

COLEBROOK, C.F., 1938, Turbulent flow in pipes with particular reference to the transition region between the smooth and rough pipe laws, *J. Inst. Civ. Eng. Lond.*, 133–156.

- COOK, W.W., 1956, Boiling Density in Vertical Rectangular Multichannel Sections with Natural Circulation, ANL-5621.
- COUTRIS, N., DELHAYE, J.M., NAKACH, R., 1989, Two-phase flow modelling: The closure issue for a two-layer flow, *Int. J. Multiphase Flow* **15**, 977–983
- DALLE DONNE, M., HAME, W., 1982, A Parametric Thermalhydraulic Study of an Advanced Pressurized Light Water Reactor with a Tight Fuel Rod Lattice, KfK 3453-WUR 7059e.
- D'AURIA, F., VIGNI, P., 1984, “The evaluation of friction pressure losses in two-phase high velocity flow using non-homogeneous models”, 1984 European Two-Phase Flow Group Meeting, Rome.
- D'AURIA, F., GALASSI, G.M., 1992, Relevant Results obtained in the analysis of LOBI/mod2 Natural Circulation Experiment A2-77A, US NRC, NUREG/IA-0084.
- DIESSLER, G., TAYLOR, M.F., 1956, Analysis of Axial Turbulent Flow Heat Transfer Through Banks of Rods or Tube, Reactor Heat Transfer Conference, TID-7529, Vol. 2.
- DIENER, R., FRIEDEL, L., 1994, Proc. German-Japanese Symp. on Multiphase Flow, Karlsruhe, Germany.
- DIX, G.F., 1971, Vapour Void Fraction for Forced Convection with Subcooled Boiling at Low Flow Rates, NEDO-10491.
- DREW, T.B., KOO, E.C., MCADAMS, W.H., 1932, *Trans. AIChE* **28**, 56.
- DUKLER, A.E., HUBBARD, M.G., 1975, A model for gas-liquid slug flow in horizontal and near horizontal tubes, *Ind. Engng. Chemistry Fundamentals* **14**, 337–347.
- DUKLER, A.E., WICKS, M., CLEVELAND, R.G., 1964, Frictional pressure drop and holdup in two-phase flow, Part A — A Comparison of existing correlations for pressure drop and holdup, B An approach through similarity analysis, *AIChE J.* **10**, 38–43 and 44–51.
- EL-WAKIL, M.M., 1971, Nuclear Heat Transport, International text book company, 233–34.
- EPRI, 1986, Advanced Recycle Methodology Program-02 Documentation, EPRI-NP-4574.
- FILONENKO, G.K., 1948, On Friction Factor for a Smooth Tube, All Union Thermotechnical Institute (Izvestija VTI, No 10), Russia.
- FITZSIMMONS, D.E., 1964, Two-phase Pressure Drop in Piping Components, Hanford Laboratory Rep., HW-80970.
- FRIEDEL, L., 1979, “Improved friction pressure drop correlations for horizontal and vertical two-phase flow”, European two-phase flow group mtg, Ispra.
- FRIEDEL, L., 1980, Pressure drop during gas/vapor-liquid flow in pipes, *Int. Chemical Engineering* **20**, 352–367.

GARDNER, G.C., 1980, Fractional vapour content of a liquid pool through which vapour is bubbled, *Int. J. of Multiphase Flow*, **6**, 399–410.

GENERAL ELECTRIC COMPANY, 1978, Qualification of the one-dimensional core transient model for boiling water reactors, NEDO-24154, 78 Nucl. Eng. Design **290**.

GOVIER, G.W., AZIZ, K., 1972, *The Flow of Complex Mixtures in Pipes*, Van Nostrand Reinhold Company, New York, 538.

GRIFFITH, P., 1963, The slug-annular flow regime transition at elevated pressure”, ANL-6796.

GRIFFITH, P., WALLIS, G.B., 1961, Two-phase slug flow, *J. Heat Transfer* **83** C (3), 307.

GRILLO, P., MARINELLI, V., 1970, Single and two-phase pressure drops on a 16-ROD bundle, *Nuclear Applications & Technol.* **9**, 682–693.

HASHIZUME, K., 1983, Flow pattern, void fraction and pressure drop of refrigerant two-phase flow in a horizontal pipe, *Int. J. Multiphase Flow* **9**, 399–410.

HASHIZUME, K., OGAWA, N., 1987, Flow pattern, void fraction and pressure drop of refrigerant two-phase flow in horizontal pipe — III Comparison of the analysis with existing pressure drop data on air/water and steam/water systems, *Int. J. Multiphase Flow* **13**, 261–267.

HASHIZUME, K., OGIWARA, H., TANIGUCHI, H., 1985, Flow pattern, void fraction and pressure drop of refrigerant two-phase flow in horizontal pipe — II: Analysis of frictional pressure drop, *Int. J. Multiphase Flow* **13**, 261–267.

HEWITT, G.F., HALL-TAYLOR, N.S., 1970, *Annular Two-Phase Flow*, Pergamon Press, New York.

HEWITT, G.F., OWEN, D.G., 1992, “Pressure and entrained fraction in fully developed flow”, *Multiphase Science and Technology*, Vol. 3 (G.F. Hewitt, J.M. Delhaye and N. Zuber, Eds), Hemisphere Publishing, New York.

HOGLUND, B., et al., 1958, Two-phase Pressure Drop in a Natural Circulation Boiling Channel, ANL-5760.

HOOGENDOORN, C.J., 1959, Gas-liquid flow in horizontal pipes, *Chem. Eng. Sci* **9**, 205–217.

HOSLER, E.R., 1967, Flow Patterns in High Pressure Two-Phase (Steam-Water) Flow with Heat Addition, WAPD-TM-658.

HOUDAYER G., et al., 1982, “The CATHARE code and its qualification on analytical experiments”, 10th Water Reactor Safety Information Mtg, Washington.

HUGHMARK, G.A., 1965, Holdup and heat transfer in horizontal slug gas-liquid flow, *Chemical Eng. Sci.* **20**, 1007–1010.

HUSSAIN, A., CHOE, W.G., WEISMAN, J., 1974, The applicability of the homogeneous flow model to pressure drop in straight pipe and across area changes, COO-2152-16.

IDELCHIK, I.E., 1979, Hand Book of Hydraulic Resistances, Hemisphere Publishing Company, New York.

IDSINGA, W., TODREAS, N., BOWRING, R., 1977, An assessment of two-phase pressure drop correlations for steam-water mixtures, Int. J. Multiphase Flow **3**, 401–413.

ISHII, M., 1977, One-dimensional Drift-flux Model and Constitutive Equations for Relative Motion Between Phases in Various Two Phase Flow Regimes, ANL-77-47.

INOUE, A., et al., 1993, “In bundle void measurement of a BWR fuel assembly by an X-ray CT scanner: Assessment of BWR design void correlation and development of new void correlation”, Proc. ASME/JSME Nuclear Engineering Conf., Vol. 1, 39–45.

ITO, A., MOWATARI, K., 1983, Ring Grid Spacer Pressure Loss Experimental Study and Evaluation Method, American Nuclear Society, 972–978.

JANSSEN, E., KERVINEN, J.A., 1971, Developing Two-phase Flow in Tubes and Annuli, Part-I: Experimental Results, Circular Tubes, GEAP-10341.

JANSSEN, E., KERVINEN, J.A., 1964, Two-phase Pressure Drop in Straight Pipes and Channels: Water-Steam Mixtures at 600 to 1400 psia, GEAP-4616.

JONES, A.B., DIGHT, D.G., 1962, Hydrodynamic Stability of a Boiling Channel, KAPL-2208, Knolls Atomic Power Laboratory.

KATAOKA, I., ISHII, M., 1982, Mechanism and Correlation of Droplet Entrainment and Deposition in Annular Two-Phase Flow, NUREG/CR-2885 and ANL-82-44.

KAYS, W.M., 1975, Convective Heat and Mass Transfer, Tata-McGraw Hill Publishing Company Ltd., New Delhi.

KHARE, R., VIJAYAN, P.K., SAHA, D., VENKAT RAJ, V., 1997, Assessment of Theoretical Flow Pattern Maps for Vertical Upward Two-Phase Flow, BARC/1997/E010.

KIM, NAE-HYUN; LEE, S.K., MOON K.S., 1992, Elementary model to predict the pressure loss across a spacer grid without a mixing vane, Nuclear Technol. **98**, 349–353

KING, C.H., OUYANG, M.S., PEI, B.S., WANG, Y.W., 1988, Identification of two-phase flow regimes by an optimum modeling method, Nuclear Technol. **82**, 211–226.

KOEHLER, W., KASTNER, W., 1988, Two Phase Pressure Drop in Boiler Tubes, Two-Phase Flow heat Exchangers: Thermalhydraulic Fundamentals and Design (S. Kakac, A.E. Bergles E.O. Fernandes, Eds), Kluwer Academic Publishers.

KNUDSEN, J.G., KATZ, D.L., 1958, Fluid Dynamics and Heat Transfer, McGraw-Hill, New York, 178.

- LAHEY, R.T., Jr., 1984, Two-phase Flow In Boiling Water Reactors, NEDO-13388, 59–70.
- LAHEY, R.T., Jr., LEE, S.J., 1992, “Phase distribution and two-phase turbulence for bubbly flows in pipes”, *Multiphase Science and Technology*, Vol. 3 (G.F. Hewitt, J.M. Delhaye, N. Zuber, Eds), Hemisphere Publishing, New York.
- LAHEY, R.T., Jr., SHIRALKAR, B.S., RADCLIFFE, D.W., 1970, Two-phase Flow and Heat Transfer in Multirod Geometries, Subchannel Flow and Pressure Drop Measurements in a 9-Rod Bundle for Diabatic and Adiabatic Conditions, GEAP-13040.
- LEUNG, L.K.H., GROENEVELD, D.C., 1991, “Frictional pressure gradient in the pre- and post-CHF heat-transfer regions”, *Multiphase flows' 91*, Tsukuba, 1991, Tsukuba, Japan.
- LEUNG, L.K.H., GROENEVELD, D.C., AUBE, F., TAPUCU, A., 1993 New studies of the effect of surface heating on frictional pressure drop in single-phase and two-phase flow, NURETH-3, Grenoble, France.
- LIAO, L.H., PARLOS, A., GRIFFITH, P., Heat Transfer Carryover and Fall Back in PWR Steam Generators During Transients, NUREG/CR-4376, EPRI NP-4298.
- LILES, D.R., MAHAFFY, J.H., 1984, TRAC PF1-MOD1 An advanced best-estimate computer program for pressurised reactor thermal-hydraulic analysis, Los Alamos National Laboratory.
- LOCKHART, R.W., MARTINELLI, R.C., 1949, Proposed correlation of data for isothermal two-phase, two-component flow in pipes, *Chem. Eng. Prog.* **45**, 39–48.
- LOMBARDI, C., CARSANA, C.G., 1992, A dimensionless pressure drop correlation for two-phase mixtures flowing upflow in vertical ducts covering wide parameter ranges, *Heat and Technol.* **10**, 125–141.
- LOMBARDI, C., CERESA, I., 1978, A generalized pressure drop correlation in two-phase flow, *Energia Nucleare* **25** 4, 181–198.
- LOMBARDI, C., PEDROCCHI, E., 1972, A pressure drop correlation in two-phase flow, *Energia Nucleare* **19** 2, 91–99.
- LORENZINI, E., SPIGA, M., TARTARINI, P., 1989, “Some notes on the two-phase flow friction multiplier”, 7th Seminar on Thermal Non-equilibrium in Two-Phase Flow, Roma.
- LOTTE, P.A., FLINN, W.S., 1956, A method of analysis of natural circulation boiling systems, *Nuclear Science Eng.* **19** 2, 91–99.
- LU ZHONGQI ZHANG XI, 1994, Identification of flow patterns of two-phase flow by mathematical modelling, *Nuclear Eng. and Design* **149**, 111–116.
- MAIER, D., CODDINGTON, P., 1997, “Review of wide range void correlations against an extensive database of rod bundle void measurements”, *Proc. ICONE*, 5th Int. Conf. on Nuclear Engineering, Nice.

MALNES, D., 1979 “Slip ratios and friction factors in the bubble flow regime in vertical tubes, KR-110, Kjeller Norway (1966) and A new general void correlation”, European two-phase flow group Mtg., Ispra (1979).

MANDHANE, J.M., GREGORY, G.A., AZIZ, K., 1977, Critical evaluation of friction pressure-drop prediction methods for gas-liquid flow in horizontal pipes, *J. Petroleum Technol.* **29**, 1348–1358.

MANDHANE, J.M., GREGORY, G.A., AZIZ, K., 1974, A flow pattern map for gas-liquid flow in horizontal pipes, *Int. J. Multiphase Flow* **1**, 537.

MARCHATERRE, J.F., 1956, The effect of pressure on boiling density in multiple rectangular channels, ANL-5522.

MARCHATERRE, J.F., PETRICK, M., LOTTES, P.A., WEATHELAND, R.J., FLINN, W.S., 1960, Natural and Forced Circulation Boiling Studies, ANL-5735.

MARTINELLI, R.C., NELSON, D.B., 1948, Prediction of pressure drop during forced-circulation boiling of water, *Trans. ASME* **70**, 695–702.

MARINELLI, V., PASTORI, L., 1973, AMLETO — A Pressure drop computer code for LWR fuel bundles, RT/ING(73)11, Comitato Nazionale Energia Nucleare (CNEN).

MCADAMS, W.H., WOODS, W.K., HEROMAN, R.H., Jr., 1942, Vaporization inside horizontal tubes. II. Benzene-oil mixtures, *Trans ASME* **64**, 193.

MCFADDEN, J.H., et al., 1992, RETRAN-03: A program for Transient Analysis of Complex Fluid Flow Systems, Volume 1: Theory and Numerics, Electric Power Research Institute, EPRI NP-7450.

MCQUILLAN, K.W., WHALLEY, P.B., 1985, Flow patterns in vertical two-phase flow, *Int. J. Multiphase flow* **11**, 161–175.

MIROPOLSKI, E.L., SHITSMAN, M.E., SHNEENOVA, R.I., 1965, *Thermal Eng.* **12** 5, 80.

MISHIMA, K., ISHII, M., 1984, Flow regime transition criteria for upward two-phase flow in vertical pipes, *Int. J. Heat Mass Transfer*, 723–739.

MOCHIZUKI, Y., ISHII, Y., 1992, “Study of thermalhydraulics relevant to natural circulation in ATR”, *Proc. 5th Int. Top. Mtg on Reactor Thermal Hydraulics*, Vol. I, Salt Lake City, 127-134.

MOCHIZUKI, H., SHIBA, K., 1986, “Characteristics of natural circulation in the ATR plant”, *2nd Int. Top. Mtg. Nuclear Power Plant Thermal Hydraulics and Operations*, Tokyo, 132–139.

MOECK, E.O., 1970, Annular Dispersed Flow and Critical Heat Flux, AECL-3656.

NABIZADEH, H., 1977, Modellgesetze and Parameteruntersuch fur den volumetrischen Dampfgehalt in einer zweiphasen Stroemung, EIR-Bericht, Nr. 323.

- NIKURADSE, J., 1932, Mitt. Forsch Geb. Ing.-Wesen, **356**, 1.
- OHKAWA, K., LAHEY, R.T., Jr., 1980, The analysis of CCFL using drift-flux models, Nucl. Eng. Design **61**.
- ORNL-TM-3578, 1975, Design Guide for Heat Transfer Equipment in Water Cooled Nuclear Reactor Systems, Oak Ridge National Laboratory and Burns and Roe Incorporated, Tenn.
- OSMACHKIN, V.S., BORISOV, V., 1970, Paper B4.9, IVth Int. Heat Transfer Conf., Versailles.
- OWENS, W.S., 1961, "Two-phase pressure gradient", Int. Developments in Heat Transfer, Part II, ASME.
- PETERSON, A.C., Jr., WILLIAMS, C.L., 1975, Flow patterns in high pressure two-phase flow: A visual study of water in a uniformly heated 4 — rod bundle, WAPD-TM-1199.
- PETRICK, M., 1961, Two-phase Water Flow Phenomena, ANL-5787.
- PETRICK, M., 1962, A Study of Vapour Carryunder and Associated Problems, ANL-6581.
- PILKHWAL, D.S., VIJAYAN, P.K., VENKAT RAJ, V., 1992, "Measurement of pressure drop across the junction between two 37 rod fuel bundles for various alignments of the bundles", Proc. 19th National Conf. on Fluid Mechanics and Fluid Power, IIT, Powai, Bombay.
- RANSOM, V.H., et al., 1987, RELAP5/MOD2 Code Manual, Volume 1: Code structure, System Models And Solution Methods, NUREG/CR-4312, EGG-2396, Rev. 1.
- REHME, K., 1968, Systematische experimentelle Untersuchung der Abhängigkeit des Druckverlustes von der geometrischen Anordnung für längs durchströmte Stabbündel mit Spiraldraht-Abstandshaltern, KfK, Rep. 4/68-16.
- REHME, K., 1969, Druckverlust in Stabbündeln mit Spiraldraht-Abstandshaltern, Forsh. Ing.-Wes.35 Nr.4.
- REHME, K., 1973a, Simple method of predicting friction factors of turbulent flow in non-circular channels, Int. J. Heat Mass Transfer **16**, 933–950.
- REHME, K., 1973b, Pressure drop correlations for fuel element spacers, Nuclear Technol. **17**, 15–23.
- REHME, K., 1977, Pressure drop of spacer grids in smooth and roughened rod bundles, Nuclear Technol. **33**, 313–317.
- REHME, K., TRIPPE, G., 1980, Pressure drop and velocity distribution in rod bundles with spacer grids, Nuclear Eng. Design **62**, 349–359.
- ROUHANI, S.Z., 1966, Void Measurements in the Regions of Sub-cooled and Low Quality Boiling, AE-238.

ROUHANI, S.Z., 1966, Void Measurements in the Regions of Sub-cooled and Low Quality Boiling, AE-239.

ROUHANI, S.Z., 1969, Subcooled Void Fraction, AB Atomenergi, Rep. AWE-RTV-841.

ROUHANI, S.Z., BECKER, K., 1963, Measurement of Void Fractions for Flow of Boiling Heavy Water in a Vertical Round Duct, AE-106.

SAHA, P., ZUBER, N., 1974, "Point of net vapour generation and void fraction in subcooled boiling", Paper B4.7, Proc. 5th Int. Heat Transfer Conf., 175–179.

SAPHIER, D., GRIMM, P., 1992, Bypass Channel Modelling and New Void Correlations for the BWR Option of the SILWER Code, PSI-Bericht Nr.-119.

SEKOGUCHI, K., SAITO, Y., HONDA, T., 1970, JSME Preprint No. 700-7, 83.

SELANDER, W.N., 1978, Explicit Formulas for the Computation of Friction Factors in Turbulent Pipe Flow, AECL-6354.

SIMPSON, H.C., et al., 1977, "Two-phase flow studies in large diameter horizontal lines", European two-phase flow meeting, Grenoble.

SNOEK, C.W., AHMAD, S.Y., 1983, A Method of Predicting Pressure Profiles in Horizontal 37-Element Clusters, AECL-8065, Chalk River, Ontario (1983).

SNOEK, C.W., LEUNG, L.K.H., 1989, A model for predicting diabatic pressure drops in multi-element fuel channels, Nucl. Eng. Design **110**, 299–312.

SOLBRIG, C.W., 1986, "Consistent flow regime map and friction factors for two-phase flow", AIChE Annual meeting, Miami Beach, Florida.

SONNENBURG, H.G., 1989, "Full-range drift-flux model based on the combination of drift flux theory with envelope theory", NURETH-4 Proceedings, Vol. 2 (1003–1009).

SPEDDING, P.L., NGUYEN, V.T., 1980, Regime maps for air-water two-phase flow, Chem. Eng. Sci. **35**, 779.

STEINER, D., 1987, Pressure drop in horizontal flows, Multiphase Science and Technology, Vol. 3 (G.F. Hewitt, J.M. Delhay, N. Zuber, Eds), Hemisphere Publishing, New York.

STEVANOVIC, V., STUDOVIC, M., 1995, A simple model for vertical annular and horizontal stratified two-phase flows with liquid entrainment and phase transitions: one-dimensional steady state conditions, Nucl. Eng. Design **154**, 357–379.

STEWART C.W., 1985, VIPRE-01: A Thermalhydraulic Code For Reactor Cores, EPRI NP-2511-CCM

SUO, M., BERGLES, A.E., DOYLE, E.F., CLAWSON, L., GOLDBERG, P., 1965, Investigation of Boiling Flow Regimes and Critical Heat Flux", NYO-3304-3.

TAITEL, Y., BORNEA, D., DUKLER, A.E., 1980, Modelling flow pattern transitions for upward gas-liquid flow in vertical tubes, *AIChE J.* **26**, 345–354.

TAITEL, Y., DUKLER, A.E., 1976, A model for predicting flow regime transitions in horizontal and near horizontal gas-liquid flow, *AIChE J.* **22**, 47–55.

TAITEL, Y., DUKLER, A.E., 1976a, A theoretical approach to the Lockhart-Martinelli correlation for stratified flow, *Int. J. Multiphase Flow* **2**, 591–595.

TAKEUCHI, K., YOUNG, M.Y., HOCHREITER, L.E., 1992, *Nucl. Sci. Eng.* **112**, 170–180.

TARASOVA, N.V., et al., 1966, “Pressure drop of boiling subcooled water and steam water mixture flowing in heated channels”, *Proc. of 3rd Int. Heat Transfer Conf.* 178, ASME.

TAKEUCHI, K., YOUNG, M.Y., HOCHREITER, L.E., 1992, Generalized drift flux correlation for vertical flow, *Nucl. Sci. and Eng.* **112**, 170–180.

RELAP5 DEVELOPMENT TEAM; 1995, RELAP5/MOD3 Code Manual, Vol. 1 Code Structure, System Models and Solution Methods, NUREG/CR-5535 or INEL-95/0174, Idaho National Engineering Laboratory, Idaho Falls.

THOM, J.R.S., 1964, Prediction of pressure drop during forced circulation boiling of water, *Int. J. Heat Mass Transfer* **7**, 709–724.

TIPPETS, F.E., 1962, Critical heat flux and flow pattern characteristics of high pressure boiling water in forced convection, GEAP-3766.

TURNER, J.M., WALLIS, G.B., 1965, The Separate Cylinders Model of Two-Phase Flow”, NYO-3114-6, Thayer School of Engg. Darmouth College, Hanover, New Hampshire.

TUTU, N.K., 1982, Pressure fluctuations and flow pattern recognition in vertical two-phase gas-liquid flows, *Int. J. Multiphase Flow* **8**, 443–447.

UNAL, C., BADR, O., TUZLA, K., CHEN, J.C., NETI, S., 1994, Pressure Drop at Rod Bundle Spacers in the Post-CHF Dispersed Flow Regime, *Int. J. of Multiphase Flow* **20**, 515–522.

VENKAT RAJ, V., 1993, “Experimental thermal hydraulics studies for pressurised heavy water reactors — An Update and Review, 3rd World Conf. on Experimental Heat Transfer, Fluid Mechanics and Thermodynamics, Hawaii.

VIJAYAN, P.K., PRABHAKAR, B., VENKAT RAJ, V., 1981, “Experimental measurement of pressure drop in diabatic two-phase flow and comparison of predictions of existing correlations with the experimental data”, H-13, 6th National heat and mass transfer conf. Madras.

VIJAYAN, P.K., SAHA, D., VENKAT RAJ, V., 1984, Measurement of Pressure Drop in PHWR Fuel Channel with 19 Rod Bundles (Wire-Wrap Type) at Low Reynolds Numbers’, BARC/I-811.

VIJAYAN P.K., AUSTREGESILO, H., 1993, Predictive Capability of the Models used in the ATHLET Code for the Estimation of Frictional Pressure Loss, Technical Note No. TN-VIJAYAN-93-1, Gesellschaft für Reaktorsicherheit, Garching.

WALLIS, G.B., 1970, J. Basic Eng. Trans ASME Ser. D. 92, 59.

WALLIS, G.B., 1969, One-Dimensional Two-Phase Flow, McGraw-Hill, New York.

WALLIS, G.B., DOBSON, J.E., 1973, The onset of slugging in horizontal stratified air-water flow, Int. J. Multiphase Flow **1**, 173–193.

WEISMAN, J., KANG, S.Y., 1981, Flow pattern transitions in vertical upwardly inclined lines, Int. J. Multiphase Flow **7**, 271.

WEISMAN, J., CHOE, W.G., 1976, “Methods for calculation of pressure drop in cocurrent gas-liquid flow”, Proc. Two-phase Flow and Heat Transfer Symp. Workshop, Fort Lauderdale, Two-Phase Transport and Reactor Safety. Vol. 1.

WILSON, S.F., LITTLETON, W.E., YANT, H.W., MAYER, W.C., 1965, Preliminary Separation of Steam from Water by Natural Separation, Part 1, Allis-Chalmers Atomic Energy Report No. ACNP-65002.

YEH, H.C., HOCHREITER, L., 1980, Mass effluence during FLECHT forced reflood experiments, Nucl. Eng. Design **60**, 413–429.

ZHAO, L., REZKALLAH, K.S., 1995, Pressure drop in gas-liquid flow at microgravity conditions, Int. J. Multiphase Flow **21** (1995) 837–849.

ZIGRANG, D.J., SYLVESTER N.D., 1985, A review of explicit friction factor equations, Trans. ASME, J. Energy Res. Technol. **107**.

ZUBER, N., FINDLAY, J.A., 1965, Average volumetric concentration in two-phase flow systems, J. Heat Transfer, Trans. ASME **87**, 453–468.

Chapter 6

REMARKS AND FUTURE NEEDS

The content of this TECDOC is based on work done and related activities carried out by the institutes within Member States contributing to the Co-ordinated Research Project (CRP) on Thermohydraulic Relationships for Advanced Water Cooled Reactors as well as information presented at two IAEA Technical Committee meetings [IAEA (1996 and 2000)]. During the process of preparing this TECDOC, the maturity of knowledge for thermohydraulic phenomena of advanced water-cooled reactors (AWCRs) and the wide degree of usage of the prediction methods for the phenomena have been considered. As a result, emphasis within this CRP has been on the following topics:

- CHF prediction methods for AWCRs;
- General film boiling heat transfer methods for AWCRs; and
- Pressure drop relationships for AWCRs.

While the CRP examined the above phenomena in detail, it is important to note that it was not possible within this CRP to examine in detail other very important thermohydraulic phenomena of interest to AWCRs. For example, transition film boiling, condensation with non-condensables, natural circulation, and heat transfer in large pools are very important phenomena but have not been reviewed in detail in this activity. The performed activity also gave an idea of the difficulty in synthesizing the current understanding of the above mentioned fundamental phenomena which were addressed.

The recommendations and future needs for the phenomena addressed in this TECDOC are provided in each of related chapters in some detail. Therefore the reader should refer to the individual chapters for the details of the conclusions and remarks. In this chapter recommendations for the most reliable prediction methods, and comments on future needs are provided in generic form. Detailed plans for future development are outside the purpose of the CRP.

The following are general remarks and comments on future needs:

Some years ago, it was considered that application of passive safety systems for advanced water cooled reactor designs was limited to small to medium size plants (less than about 700 MW(e)). Now, as a result of further design and testing activities, passive systems are being incorporated into designs of 1000 MW(e) and above [IAEA (1996, 1999 and 2000)]. Uncertainties in phenomenology typically result in incorporation of extra margins into system designs. Thorough knowledge of thermohydraulic phenomena for passive systems can help both to achieve economical designs and to assure that the passive systems will function as intended. For passive systems, developers of nuclear power plants need to assure that sufficient data exist for validation of thermohydraulic codes, and that the effects of degradation mechanisms on system performance are well understood.

For advanced water cooled reactors with passive systems, the importance of certain phenomena (e.g. tracking of non-condensable gases, condensation of steam in the presence of non-condensable gases, mixing and steam condensation in large pools, natural circulation, temperature stratification and turbulence) is greater than in current designs. For such phenomena, qualification of the associated thermohydraulic codes and methodologies relying on best-estimate predictions and uncertainty analyses is highly important.

A considerable base of data for condensation heat transfer in the presence of non-condensable gases has been accumulated over fifty years. Although there had been increased activity in recent years in this field, because of the importance of this phenomenon to advanced water cooled reactors, there remains a need for a thorough literature survey, and for a review and assimilation of the existing data. Because such data are very dependent on thermohydraulic conditions and system geometry, a proper review should start with plant design and anticipated operational and accident conditions. If it is found necessary, appropriate experiments could be carried out to extend the database for the relevant conditions where current data are insufficient.

For natural circulation phenomena (both single phase and two-phase natural circulation), there is a need for a thorough literature survey and a review and assimilation of the existing data for relevant geometries of the new designs. Specific aspects that should be addressed include both establishment of natural circulation and transition from forced flow to natural circulation.

For heat transfer in large pools of water, there is a need for a thorough literature survey and a review and assimilation of the existing data for conditions relevant to the new designs. Specific aspects that should be addressed include mixing, condensation, and stratification.

International standard problems (ISPs) are an effective way to assess thermohydraulic computer codes versus experimental data. Further work in this area is recommended, as some past ISPs have experienced large differences in predictions made with the same code. Factors which can be addressed within the frame of ISPs include “user effect”, analyses of code uncertainties, deficiencies in models, and needs for further experimental work. In order to use experimental data for code validation, it is important to have proper instrumentation to collect the needed data for important phenomena, and for use in performing uncertainty analyses of the experimental results.

Specifically as a result of the collaboration within the Co-ordinated Research Programme, the following remarks and comments on future needs are made:

- (1) The look up table (Appendix II) based on CHF in tubes is recommended as the reference method for predicting **critical heat flux** in advanced water cooled reactors; methods are presented for predicting CHF in rod bundles and in bundle sub-channels using these data for CHF in tubes together with correction factors obtained either from a sub-channel codes or from correlations which account for rod geometry and neutron flux distributions. As an alternative for fuel bundles in which the rods are arranged in a triangular array, the WWER-based look-up table of Appendix III is recommended. Further efforts are needed for combining these two cited methods to develop a prediction method for CHF in rod bundles of various shapes. Further work in CHF is also needed for predicting how the CHF spreads in the reactor core, which is necessary in predicting the coupled thermohydraulic — neutronic response of the core. Experimental work is needed to improve knowledge of CHF especially in low flow/low quality conditions and in high flow/high quality conditions.
- (2) The prediction methods for **film boiling** are less advanced than those for CHF. While this TECDOC reviews various methods for predicting film boiling, no recommendations for specific methods are given because important work on combining the most promising methods into a validated method is still in progress. The current proliferation of film boiling prediction methods, and their limited range of validity, indicate the need for universal prediction methods, e.g. look up tables based on

qualified experimental data. The current status of development of such methods is reflected in the methods presented in Appendices IV, V and VI.

- (3) Many prediction methods in use for the various components of **pressure drop** are reviewed and summarized in this TECDOC. No single unified method can be recommended due to the wide range of conditions (geometry, fluid status, flow type, flow regime) which must be addressed. It is to be noted that forced and natural circulation conditions should be clearly distinguished. In the latter case, the influence of pressure drops upon the system performance is much higher. Therefore, care must be exercised in selecting proper correlations for calculating the pressure drops of the individual components.
- (4) Areas in which future work should be considered include acquisition of data for complex geometries (e.g. new design rod bundles and grid spacers), and for conditions for which the current openly available database is limited (e.g. two phase flow at low and high mass flux; pressure drop in large diameter pipes; pressure drop at low pressure; and vertical down flow).
- (5) Supercritical water is currently being considered as a coolant medium for several advanced water cooled reactor concepts. The heat transfer characteristics of reactor cores cooled by supercritical water needs further investigation. Specifically the pseudo-CHF and post-CHF behaviour of supercritical water has received very little attention in the literature.
- (6) During the course of this CRP, there has been extensive experimental data exchange. Some of these data, including look-up tables for CHF and post-CHF are integrated into the database at the International Nuclear Safety Center (INSC) at the Argonne National Laboratory (ANL). A sizeable database is maintained at the Heat and Mass Transfer Information Center (HEMATIC) in the State Scientific Center of the Russian Federation — Institute for Physics and Power Engineering, Obninsk, Russian Federation. The establishment of a distributed database which can join the contents of local databases using standard network connections would be useful and convenient. The use of such databanks would contribute to the exchange of technical information and know-how, and to the sharing of research results among various organizations.

REFERENCES TO CHAPTER 6

IAEA, 1996, Progress in Design, Research and Development and Testing of Safety Systems for Advanced Water Cooled Reactors, IAEA-TECDOC-872, Vienna.

IAEA, 1997, Status of Advanced Light Water Cooled Reactor Designs, IAE-TECDOC-968, Vienna.

IAEA, 1999, Evolutionary Water Cooled Reactors: Strategic Issues, Technologies and Economic Viability, IAEA-TECDOC-1117, Vienna.

IAEA, 2000, Experimental Tests and Qualification of Analytical Methods to Address Thermohydraulic Phenomena in Advanced Water Cooled Reactors, IAEA-TECDOC-1149, Vienna.

APPENDICES I–XIX

Appendix I

ACTIVITIES CONTRIBUTED TO THE CRP BY THE RESEARCH GROUPS AT THE PARTICIPATING INSTITUTES

AECL, Canada

Atomic Energy of Canada Ltd (AECL) has performed experimental and analytical studies on CHF. They have combined the AECL and the IPPE databank of CHF up to 1993, and constructed the interim 1993 tube CHF lookup table. Since then additional CHF data have been added to the CHF databank. The expanded CHF databank has a total of 30 417 CHF points and covers a wider range of conditions.

Using the expanded CHF data, the AECL and IPPE have proposed a new CHF lookup table covering a wider range of thermohydraulic conditions. They incorporated a multidimensional (pressure, dryout quality, mass flux and inlet subcooling) smoothing procedure based on weighted polynomial fitting method in the CHF lookup table. The new CHF lookup table for tubes shows improved smoothness and accuracy.

In addition, the AECL has developed an interim post-dryout databank which contains a total of 21 525 post-dryout data for vertical upward flow in tubes, and a corresponding lookup table for post-dryout heat transfer using direct interpolation of experimental data because it usually provides good prediction accuracy and reduces computing time. The databank is being expanded by additional post CHF data from IPPE and CIAE.

CIAE, China

CIAE has conducted studies on film boiling, vapour convection and CHF. The film boiling experiments with flowing water have been performed at steady-state condition using the directly heated hot patch technique. A great number of wall heat transfer and vapour superheat data have been obtained in stainless steel tube and Inconel tube with different diameter, covering a wide range of thermohydraulic conditions. The data fill the gap of database which are interest for the reactor accidents. The experiments involved inverted annular flow and dispersed flow, showing complicated effects of pressure, mass flux, quality, heat flux, diameter and significant history-dependence. Based on the data of wall heat transfer and vapour superheat the mechanistic model has been proposed. An assessment of RELAP5/MOD2.5 has been made based on the CIAE data. The data have been used for the look-up table. The minimum film boiling temperatures were also measured using the same steady-state technique. The pressure and subcooling showed appreciable effects on this temperature, but the effect of mass flux was not appreciable. An empirical correlation was formulated on the basis of experiment.

The experiment on the vapour convection heat transfer has been performed in tubes with different diameter. The change of flow regime from turbulent to transition regime was evidenced by a substantial decrease of heat transfer coefficient. The Reynolds number at this transition was the function of Gr number, and varied significantly with the diameter and pressure. The correlation of heat transfer in fully developed turbulent flow and the criteria for the transition of regimes have been proposed.

Low pressure subcooled CHF experiment has been conducted in tubes with different diameter. The effect of diameter was found to be related to the flow condition. The subcooling and velocity had strong effects on the CHF, but the effect of pressure appeared not appreciable

NRI, Czech Republic

NRI activities have involved experimental research on CHF for water cooled rod bundles modelling WWER type reactors; CHF databank for tubes, annuli and rod bundles; a computational system based on CHF databank; and subchannel analysis code based on rod bundle data for coolant behaviour in the WWER type cores.

The SKODA Plzen a large water loop has been designed for research on CHF in water flow through a WWER fuel bundle.

The NRI collected CHF experimental data of tubes, annuli and rod bundles into NRI CHF databank. The number of data points in the NRI databank was more than 20 000. Besides, they have developed their original CHF correlations.

The NRI also develop a software enabling evaluation of CHF correlations with CHF databank by means of statistical methods.

The NRI has carried out system analyses covering axial distribution of DNBR (departure from nucleate boiling ratio) using their CHF correlations to compare the analytical results each other. They also compare results of subchannel analyses and isolated channel analyses.

FZK, Germany

FZK has conducted experimental and analytical investigations on critical heat flux (CHF) in circular tubes of different diameters, ranging from 2 mm to 16 mm, and in tight hexagonal 7 and 37 rod bundles. The model fluid Freon-12 was used as working fluid due to its low latent heat, low critical pressure, well known properties and intensively investigated fluid-to-fluid modelling for water and Freon-12. More than 1700 data points in tubes and 1300 data points in rod bundles have been obtained in a large range of parameters: pressure 1.0 MPa to 3.0 MPa, mass flux 1.0 Mg/m²s to 6.0 Mg/m²s and exit steam quality -0.75 to +0.60.

The effect of different parameters on CHF have been studied, especially the effect of tube diameter and spacers. The test data have been compared with different CHF prediction methods, e.g. CHF look-up table, and with the CHF data available in the literature. Comparison of the CHF data in Freon-12 with that in water was made, to investigate the fluid-to-fluid scaling laws for circular tubes as well as for rod bundles.

In the 7-rod bundles experimental investigations have also been performed on two-phase turbulent mixing. The effect of different parameters on the turbulent mixing has been studied.

BARC, India

BARC has performed studies on friction pressure drop under low mass flow conditions for advanced heavy water reactors (AHWR), which uses natural circulation in the primary and the safety systems. Extensive studies are being carried out on natural circulation flow as well as instability of natural circulation. Pressure drop experiments have been conducted on 19-rod and 37-rod fuel bundles of PHWRs and 52-rod fuel bundle of AHWR. Experimental investigations have been carried out to study the effect of alignment of bundles at junctions and creep of fuel channel on the pressure drop in PHWR fuel channels. Studies also covered various components of the fuel channel like the fuel locator, end fittings, and refueling tools.

Under this CRP, BARC has compiled correlations for single-phase and two-phase pressure drop, void fraction and flow pattern transitions. A two-phase flow databank has also been compiled using published data on pressure drop including flow pattern specific pressure drop, void fraction and flow patterns. Using this databank the compiled correlations have been assessed.

University of Pisa, Italy

Activities at University of Pisa have involved development and assessment of the special codes, large-system-code assessment, evaluation of experimental data, planning and conduct of experiments, code application to nuclear plants, and studies on uncertainties of CHF predictions.

They have developed and assessed three special codes which are used for integral thermohydraulic analyses of advanced water cooled reactors, for evaluation of "isolation condenser" performance, and for evaluation of fission product transport inside the primary circuit and the containment vessel. Assessment and evaluation of large-system-codes have been carried out by comparing with test results from integral test facilities (ITF) and separate effect test facilities (SETF). Accident analyses including severe accident are performed for advanced water cooled reactors. Besides, they have been planning and conducting experiments using their facilities.

Studies on uncertainties of CHF predictions have been also carried out at University of PISA. UMAE (Uncertainty Methodology based on Accuracy Extrapolation) was developed to evaluate uncertainties in prediction of transient and accident scenarios by thermohydraulic system codes. Since the use of UMAE is limited to only the ITF, UMAE-SETF is being developed to use vast data from the SETF. The UMAE-SETF considers only a specific phenomenon in a transient or an accident condition. Then similarity analyses and grouping of experimental data are performed to establish calculational database. Using the database and same methodology in the UMAE, extrapolation of accuracy and uncertainty are estimated for single phenomenon.

ENEA, Italy

ENEA activities have involved the development of computer codes for the thermohydraulic design of reactor cores and experimental researches supporting both the core design and the codes development.

The reference code is the ANTEO code, a subchannel model for the steady-state analysis of reactor core rod bundles. The wide experience available in the field of subchannel codes has allowed to develop a simple, fast and user-oriented code running on a PC machine. Due to its characteristics, the code can be used for comparison among different models, for instance for comparing different CHF models.

Experiments were performed mainly in the field of pressure drop and flow distribution in different geometries of interest for the reactor core design. Particularly, pressure drop in rod bundles with helical wire wraps system were measured. Part of the investigations were extended down to the low flow region, in order to cover the natural circulation range.

KAERI, Republic of Korea

KAERI has conducted experiments on CHF and on natural circulation including a single rod CHF test, a 3x3 bundle CHF test and a natural circulation test. Objectives of the single rod CHF test are to obtain fundamental CHF data and to understand thermal hydraulic phenomena under abnormal conditions such as LOCA and pump trip. In the 3×3 rod bundle test, two types of tests were made; steady state test under low flow and under boil off conditions, and test of power or flow rate transient. The objective of the natural circulation test is to understand fundamental characteristics of natural circulation, heat transfer capability of the heat exchanger and characteristics of boiling phenomena.

A study on hydraulic characteristics in rod bundles has been also carried out by the KAERI. Heat transfer improves near spacer grids in the rod bundles. To understand this behaviour, hydraulic characteristics near the spacer grids should be clarified before thermal characteristics. Besides, hydraulic characteristics are useful to develop the local thermal diffusion coefficient in a subchannel analysis code.

Furthermore, heat/mass transfer study has been performed using Naphthalene sublimation technique, which measures mass transfer coefficients in the complex geometry where the conventional heat transfer measurement is impossible. The objective of this study is to investigate mechanism and analogy of heat/mass transfer at the complicated flow conditions.

KAIST, Republic of Korea

CHF at low pressure and low flow (LPLF) conditions is a key thermohydraulic phenomenon which may limit thermal power under natural circulation and accident conditions. KAIST has performed a series of LPLF CHF experiment for both stable and oscillating flow conditions. Totally 523 stable CHF data have been obtained with vertical round tubes of various diameters and heated lengths for low pressure, low flow, and high quality conditions. Parametric trends were examined and existing prediction models were assessed against the data. KAIST also performed some tests to identify the effects of flow oscillations and circulation modes on LPLF CHF.

In addition to the LPLF CHF study, an independent assessment was conducted for the applicability of the AECL-IPPE CHF table to predicting CHF in round tubes and bundles. Some works on the development of a length correction factor was also conducted.

IPPE, Russian Federation

It is significantly important to know CHF for water flowing in various channels for safety analyses of water cooled reactors. An international collaboration with IPPE, AECL, Technical University of Branschweig and KfK has led to joint studies on CHF. In that way, a Joint International Data Bank (JIDB) on CHF in tubes has been established covering the most available data in the world. Then the lookup table 1996 version was proposed and contains about 30 000 data points for tubes.

The lookup table has been tested against the JIDB for the 8 mm tubes to show that the lookup table has satisfactory features of accuracy and smoothness. The CHF at low flow rate and low pressure, however, show complicated behaviour possibly due to complicated role of buoyancy, flow instability, geometry effects on flow stability, and near sound velocity. Besides, there are a few amounts of data in the regions so that accuracy of the CHF prediction is insufficient.

A post-dryout heat transfer table was developed and covers a wide range of thermohydraulic conditions. The number of data points is 42 800. The heat transfer coefficients are expressed as a function of pressure, mass flux, quality and heat flux. In IPPE has been developed Look-Up Table CHF WWER rod bundles for wide range parameters.

PSI, Switzerland

PSI has developed together with institutes in some other OECD countries a methodology to establish SET (Separate Effect Tests) validation matrix. The SET validation matrix is an information which collects the best set of test data available for calculational code validation, assessment and improvement. The SET validation matrix report can be used for code development and quantitative uncertainty analyses.

In the SET matrix, a particular attention has been paid in definition of each phenomenon since the level of the state of knowledge for different phenomenon varies. Internationally coordinated works are necessary to compensate the short of the knowledge. The first volume of the SET matrix report provides cross references between test facilities and thermal hydraulic phenomena, and list of tests classified by phenomena. Presently 67 phenomena and 2094 tests have been identified and selected in the matrix.

Different CHF correlations and CHF lookup tables have been examined and analyzed by the PSI. The correlations were tested in thermohydraulic analyses under low mass flow and low pressure conditions like small break LOCA, and under high mass flow and high pressure conditions like large break LOCA. The influences of major physical and geometrical parameters on CHF are investigated. The behaviour in a correlation based on local conditions was compared with that in the CHF lookup table.

Middle East Technical University, Turkey

Condensation heat transfer in the presence of a non-condensable gas such as air often dominates the cooling performance of the safety systems used in advanced water cooled reactors. Since there is a need for more experimental data on in-tube condensation in the presence of non-condensable gas, an experimental research has been carried out by Middle

East Technical University in collaboration with Turkish Atomic Energy Authority which was partially sponsored by International Atomic Energy Agency.

A test facility with a vertical single-tube, once-through type of heat exchanger was constructed to examine the non-condensable gas effect on heat transfer associated with in-tube condensation.

In this research work, in-tube condensation in the presence of air has been investigated experimentally for different operating conditions, and inhibiting effect of air is analyzed by comparing the experimental data of air/steam mixture with the data of corresponding pure steam cases, with respect to temperature, heat flux, and heat transfer coefficient. The test matrix covered the range of; $P_n = 2\text{--}6$ bar, $Re_v = 45000 - 94000$, and $X_i = 0\% - 52\%$.

The inhibiting effect of air manifests itself as a remarkable decrease in centerline temperature (10°C – 50°C), depending on inlet air mass fraction. However, the measured centerline temperature is suppressed compared to the predicted one, from the Gibbs-Dalton Law, which indicates that the centerline temperature measurements are highly affected by inner wall thermal conditions, possibly due to narrow channel and high vapour Reynolds number.

Even at the lowest air quality (10%) the reduction of the heat flux is 20% while it reaches up to 50% for the quality of 40%. Maximum percent decrease of the heat transfer coefficient was observed in runs with the system pressure of 2 bar; 45% and 65%, for the air mass fraction of 10% and 28%, respectively. The film Reynolds number of cases with pure vapour and air/vapour mixture lies in the range of turbulent region ($Re_f > 300$).

The RELAP5 code, using Shah-Colburn-Hougen model, overestimates the heat flux data from about 5% to 50%. However, the majority of the predicted values of the Nusselt number fall in the uncertainty band ($\pm 24\%$) of experimental data.

Argonne National Laboratory, USA

Argonne National Laboratory (ANL) hosts the US Department of Energy (DOE) International Nuclear Safety Center (INSC). One of the main goals of the INSC is to promote the international exchange of information and data to enhance the safety of nuclear installations. The INSC has developed a database, accessible on the World Wide Web, to support the Center activities and facilitate the exchange of information among international organizations. The database contains nuclear installation and nuclear safety information. Argonne National Laboratory contributes the INSC database facility, its support and maintenance structure to the present IAEA Coordinated Research Project. ANL has offered the INSC database to become a common repository of data on thermohydraulics of nuclear reactors-look-up tables, raw experimental data, software tools, correlations and prediction methods, and references - provided by organizations participating in the CRP that have experimental programs in this area. The data and information contributed by these organizations are stored in the INSC database and maintained by ANL. Data related to thermophysical material properties, in coordination with another IAEA Coordinated Research Project is already being stored in the INSC database (<http://www.insc.anl.gov>). The addition of thermohydraulics data complements the existing nuclear safety related information in the INSC database (<http://www.insc.anl.gov/thrmhydr/iaea/chf>).

Appendix II

THE 1995 CHF LOOK-UP TABLE FOR CRITICAL HEAT FLUX IN TUBES

Table II.I. has been published previously by Groeneveld et al. (1996). It contains CHF values in kW/m^2 as a function of pressure, mass flux and thermohydraulic quality. The shaded numbers refer to CHF values having a less sound basis (based either on questionable data or on extrapolation).

Pressure (kPa)	Mass Flux (kg.m ⁻² .s ⁻¹)
-------------------	---

¹ Note: shaded are denotes less reliable data.

TABLE II.I. THE 1995 CHF LOOK-UP TABLE FOR CRITICAL HEAT FLUX IN 8 mm TUBES (in kW.m⁻²). (Continued)

Pressure (kPa)		Mass Flux (kg.m ⁻² .s ⁻¹)		Quality																														
		-0.5	-0.4	-0.3	-0.2	-0.15	-0.1	-0.05	0	0.05	0.1	0.15	0.2	0.25	0.3	0.35	0.4	0.45	0.5	0.6	0.7	0.8	0.9	1										
1000	0			5619	4685	4058	3564	2859	2175	1910	1438	1030	717	519	389	312	286	270	256	198	188	181	175	0										
1000	50			6371	5523	4991	4436	3928	3323	2944	2469	2071	1752	1559	1414	1307	1230	1157	1076	876	806	804	700	0										
1000	100			6981	6252	5685	5281	4851	4268	3386	2799	2651	2531	2415	2292	2184	2041	1891	1703	1312	1291	1250	732	0										
1000	300			7492	7295	7089	6901	6766	6620	6215	5289	4760	4456	4120	3432	2600	2151	1924	1708	1343	1289	1215	660	0										
1000	500			7577	7464	7327	7177	7110	7048	6818	5771	5094	4660	4233	3856	2754	2284	1979	1659	1035	825	767	589	0										
1000	1000			7594	7466	7329	7192	7124	7022	6705	5694	5042	4634	3953	3264	2670	2035	1741	1516	958	592	452	338	0										
1000	1500			7700	7468	7349	7230	7153	7013	6604	5532	4989	4422	3952	3236	2429	1557	1145	930	637	411	370	266	0										
1000	2000			8187	7552	7424	7281	7192	7012	6401	5196	4720	4404	3952	3143	2259	1373	980	713	541	343	137	86	0										
1000	2500			8962	7788	7544	7314	7202	6979	6100	5028	4668	4397	3924	2999	2081	1281	925	690	512	306	84	25	0										
1000	3000			9731	8149	7728	7370	7206	6966	5900	4920	4647	4391	3898	2880	1955	1234	908	701	510	349	95	30	0										
1000	3500			10456	8659	8005	7450	7179	6910	5800	4849	4628	4385	3865	2765	1797	1252	1059	1000	595	356	108	36	0										
1000	4000			11146	9203	8342	7591	7143	6778	5752	4757	4584	4380	3794	2723	1891	1484	1292	1021	605	375	134	51	0										
1000	4500			11816	9746	8754	7750	7141	6500	5537	4627	4477	4304	3715	2689	1953	1498	1327	1034	643	401	159	65	0										
1000	5000			12447	10239	9182	7859	6988	5900	5107	4361	4211	3924	3338	2581	1978	1579	1363	1126	726	438	188	83	0										
1000	5500			13033	10745	9599	8124	6794	5800	4822	4239	4085	3729	3112	2523	2017	1703	1469	1235	816	484	227	104	0										
1000	6000			13573	11285	10064	8595	6647	5530	4654	4096	3966	3625	3050	2519	2063	1767	1555	1325	902	546	275	129	0										
1000	6500			14101	11770	10479	8933	6351	5228	4460	3913	3804	3484	2973	2497	2115	1852	1633	1406	983	616	326	155	0										
1000	7000			14608	12172	10857	9325	6654	4850	4232	3734	3547	3336	2867	2461	2178	1945	1707	1480	1057	681	375	180	0										
1000	7500			15109	12524	11194	9725	7272	5409	4227	3683	3525	3287	2851	2478	2246	2006	1774	1548	1126	744	423	204	0										
1000	8000			15629	12866	11463	9958	7773	6039	4447	3684	3536	3341	3061	2571	2306	2062	1834	1612	1190	802	470	227	0										
3000	0		6583	5927	5252	4544	4205	3891	3536	3022	2429	2009	1564	1145	892	699	568	502	452	413	321	275	266	256	0									
3000	50		7307	6575	5972	5386	5107	4857	4570	4135	3478	3061	2653	2266	2041	1865	1722	1614	1521	1418	1409	1400	1392	1000	0									
3000	100		7888	7106	6580	6114	5897	5708	5479	5057	4121	3502	3326	3186	3051	2926	2796	2625	2475	2367	2191	1936	1587	1015	0									
3000	300		8463	7476	7307	7303	7302	7300	7298	7255	6954	5922	5380	5211	4936	4635	3997	3322	3177	3173	2865	2078	1536	953	0									
3000	500		8655	7674	7578	7560	7554	7541	7627	7621	7496	7000	6400	5660	5269	4807	4297	3392	3376	3324	2745	1841	1320	835	0									
3000	1000		9003	7776	7660	7598	7560	7548	7518	7512	7444	6846	6208	5620	4728	4200	3745	3079	2910	2618	1925	1242	830	471	0									
3000	1500		9523	8313	7824	7647	7578	7560	7471	7436	7250	6661	5980	5043	4364	3792	3422	2691	2130	1728	1080	626	499	312	0									
3000	2000		10680	9563	8427	7706	7640	7567	7453	7298	6723	6026	5315	4507	3991	3485	2958	2279	1686	1211	608	373	330	216	0									
3000	2500		11975	10928	9397	8034	7681	7634	7441	7158	6226	5599	4880	4175	3702	3152	2369	1726	1252	867	431	308	89	25	0									
3000	3000		12932	11900	10414	8640	7947	7643	7439	7069	5966	5339	4712	4094	3619	2963	2085	1423	1037	772	520	374	129	45	0									
3000	3500		13887	12661	11230	9396	8434	7824	7437	6995	5829	5131	4586	4067	3540	2705	1715	1329	1127	1020	678	431	137	44	0									
3000	4000		14813	13379	11939	10174	9013	8028	7418	6832	5753	4966	4471	4021	3424	2463	1474	1234	1228	1118	699	440	147	54	0									
3000	4500		15714	14077	12608	10862	9586	8292	7365	6566	5570	4792	4348	3945	3273	2302	1514	1311	1306	1145	713	445	163	63	0									
3000	5000		16584	14778	13200	11500	10262	8818	7348	6039	5258	4610	4242	3867	3121	2196	1610	1505	1405	1173	766	466	179	72	0									
3000	5500		17426	15454	13765	12044	10824	9249	7402	6188	5134	4431	4136	3794	3006	2155	1712	1650	1500	1252	846	493	197	83	0									
3000	6000		18238	16101	14321	12489	11385	10063	7735	6382	5070	4332	4061	3753	3042	2265	1853	1738	1542	1311	876	532	234	103	0									
3000	6500		19035	16814	14849	12926	11946	10878	8193	6446	5002	4181	3931	3693	3067	2360	2043	1876	1622	1388	982	589	282	129	0									
3000	7000		19813	17464	15350	13332	12053	11351	8542	6507	4694	3888	3705	3557	3084	2530	2209	2008	1755	1514	1062	656	333	155	0									
3000	7500		20584	18107	15834	13724	12429	11527	8891	6526	4644	3817	3643	3459	3103	2699	2390	2073	1825	1588	1138	724	385	181	0									
3000	8000		21353	18730	16299	14090	12789	11585	9157	7075	4971	3980	3715	3548	3291	2904	2413	2112	1885	1654	1205	787	437	207	0									
5000	0		5951	5460	4941	4459	4230	4011	3762	3360	2628	2234	1791	1346	1083	877	731	638	571	515	405	345	341	323	0									
5000	50		6644	6095	5629	5224	5030	4840	4626	4294	3606	3225	2837	2450	2224	2047	1896	1774	1666	1553	1532	1512	945	830	0									
5000	100		7234	6636	6223	5891	5734	5573	5387	5065	4165	3609	3458	3315	3174	3061	2936	2803	2655	2476	2300	2148	1757	1080	0									
5000	300		7680	6990	6769	6737	6722	6686	6677	6619	6280	5401	5007	4907	4741	4509	4202	3881	3659	3315	2973	2543	1823	1215	0									
5000	500		7918	7164	6943	6900	6882	6819	6812	6739	6395	5734	5296	5178	5027	4588	4244	3975	3803	3503	3040	2459	1769	1118	0									
5000	1000		8364	7644	7171	7014	6948	6829	6743	6595	6107	5662	5289	4957	4676	4166	3759	3447	3322	3086	2066	1433	1034	763	0									
5000	1500		9068	8009	7470	7142	7025	6859	6707	6441	5779	5317	4899	4530	4074	3623	3337	2983	2569	2134	1194	913	899	744	0									
5000	2000		10362	9287	8159	7346	7139	6944	6593	6110	5262	4779	4405	3984	3610	3206	2865	2557	1973	1332	668	650	650	526	0									
5000	2500		11531	10599	9179	7837	7458	7195	6565	5849	4915	4515	3981	3594	3401	3067	2744	1861	1301	921	401	313	117	53	0									
5000	3000		12458	11530	10191	8483	7761	7353	6543	5654	4707	4321	3782	3428	3268	2855	2024	1406	948	793	584	420	132	53	0									
5000	3500		13348	12271	10990	9196	8178	7551	6527	5421	4581	4144	3693	3380	3109	2510	1688	1195	958	874	645	441	149	55	0									
5000	4000		14214	12958	11651	9917	8669	7764	6476	5139	4421	3916	3540	3317	2945	2421	1437	1140	1108	1049	688	441	151	58	0									
5000	4500		15045	13625	12254	10566	9102	7880	6502	5044	4317	3784	3457	3260	2799	2059	1425	1247	1242	1187	734													

Pressure (kPa)	Mass Flux (kg.m ⁻² .s ⁻¹)
-------------------	---

		Pressure (kPa)		Mass Flux (kg.m ⁻² .s ⁻¹)		Quality																			
						-0.5	-0.4	-0.3	-0.2	-0.15	-0.1	-0.05	0	0.05	0.1	0.15	0.2	0.25	0.3	0.35	0.4	0.45	0.5	0.6	0.7
6000	0	5626	5219	4798	4387	4185	3995	3777	3415	2669	2291	1859	1416	1150	941	787	686	608	547	439	348	344	327	0	
6000	50	6300	5838	5443	5092	4920	4760	4575	4272	3564	3191	2812	2431	2204	2023	1871	1749	1645	1537	1229	989	942	823	0	
6000	100	6873	6366	5999	5708	5567	5434	5273	4973	4079	3530	3377	3237	3089	2966	2854	2724	2598	2431	1833	1647	1511	1070	0	
6000	300	7318	6710	6451	6395	6379	6330	6310	6255	5942	5126	4783	4679	4496	4269	4066	3800	3584	3283	2663	2330	1766	1193	0	
6000	500	7573	6883	6586	6512	6480	6364	6316	6261	5978	5371	5005	4822	4683	4333	4077	3812	3707	3468	2874	2374	1636	1061	0	
6000	1000	8080	7185	6742	6576	6502	6256	6114	6008	5633	5334	4857	4429	4177	3788	3528	3418	3263	2964	1965	1257	803	735	0	
6000	1500	8817	7758	7023	6667	6585	6331	6146	5787	5138	4703	4326	3964	3637	3309	3056	2839	2550	2068	1029	785	714	707	0	
6000	2000	10109	9053	7842	6970	6796	6559	6167	5531	4716	4227	3875	3532	3229	2910	2640	2383	1789	1096	532	418	439	435	0	
6000	2500	11237	10324	8947	7698	7356	7038	6235	5383	4543	4030	3545	3244	3054	2797	2311	1632	930	519	370	305	107	52	0	
6000	3000	12123	11219	9913	8360	7693	7264	6241	5237	4449	3882	3340	3043	2876	2560	1887	1093	571	477	472	353	122	52	0	
6000	3500	12969	11949	10669	8979	7986	7458	6243	4962	4218	3651	3219	2961	2696	2235	1522	871	582	576	505	382	145	57	0	
6000	4000	13791	12626	11288	9594	8324	7679	6245	4590	3787	3318	3038	2893	2570	1995	1376	988	952	952	580	384	146	59	0	
6000	4500	14582	13274	11857	10119	8549	7682	6247	4578	3624	3133	2922	2814	2470	1863	1358	1154	1133	1124	622	386	147	60	0	
6000	5000	15341	13920	12372	10555	8820	7811	6336	4701	3674	3115	2918	2795	2432	1792	1319	1237	1183	1130	650	390	148	64	0	
6000	5500	16091	14489	12910	11165	9671	8416	6533	4793	3751	3148	2936	2816	2475	1877	1459	1363	1345	1149	698	411	167	74	0	
6000	6000	16823	15039	13396	12151	10623	9568	7356	5118	3824	3169	2946	2843	2506	2049	1755	1621	1405	1192	756	438	196	90	0	
6000	6500	17524	15635	13826	12525	11575	10720	8043	5370	3900	3211	2979	2886	2586	2247	2026	1760	1468	1250	818	472	223	105	0	
6000	7000	18210	16212	14268	12743	11838	11239	8441	5556	4010	3305	3095	2988	2795	2492	2169	1822	1545	1314	887	528	260	123	0	
6000	7500	18884	16771	14706	13013	12063	11299	8839	5779	4287	3660	3411	3187	2980	2635	2268	1901	1632	1394	960	587	299	142	0	
6000	8000	19548	17309	15140	13347	12447	11537	9144	6019	4481	3966	3675	3423	3262	2860	2359	1981	1717	1479	1034	646	341	162	0	
7000	0	5361	5010	4651	4293	4118	3954	3762	3426	2692	2336	1918	1485	1212	996	834	723	641	575	466	369	357	339	0	
7000	50	6002	5599	5236	4926	4778	4644	4483	4198	3498	3137	2769	2397	2165	1981	1826	1706	1604	1501	1200	984	940	774	0	
7000	100	6539	6094	5738	5474	5355	5245	5105	4818	3957	3401	3239	3093	2941	2820	2707	2595	2489	2302	1710	1515	1479	1060	0	
7000	300	6998	6441	6104	6015	6002	5947	5886	5865	5582	4834	4494	4247	4046	3862	3632	3430	3138	3065	2402	2144	1735	1179	0	
7000	500	7264	6617	6233	6123	6088	5953	5940	5887	5690	5134	4682	4316	4157	3900	3634	3469	3366	3157	2596	2213	1587	1029	0	
7000	1000	7798	6930	6386	6216	6135	5799	5604	5505	5318	5070	4472	3892	3626	3347	3136	3031	3028	2838	1774	1121	735	613	0	
7000	1500	8557	7520	6715	6339	6253	5886	5603	5145	4673	4301	3874	3486	3189	2964	2735	2523	2250	1728	805	488	273	259	0	
7000	2000	9793	8774	7597	6676	6480	6142	5684	4952	4275	3785	3407	3122	2890	2731	2451	2023	1445	844	432	322	196	190	0	
7000	2500	10882	9986	8709	7496	7142	6690	5806	4876	4104	3537	3147	2922	2723	2445	1983	1367	789	424	261	204	99	51	0	
7000	3000	11730	10850	9620	8170	7523	6953	5816	4724	3981	3369	2940	2714	2491	2133	1570	967	553	425	346	263	112	52	0	
7000	3500	12535	11558	10344	8740	7757	7135	5848	4567	3834	3199	2786	2565	2294	1896	1323	782	519	490	409	317	135	57	0	
7000	4000	13317	12216	10929	9320	8041	7398	5938	4372	3469	2928	2645	2490	2201	1730	1228	840	734	732	470	317	136	58	0	
7000	4500	14070	12839	11469	9769	8188	7399	6061	4410	3347	2743	2515	2418	2139	1640	1200	930	872	854	492	317	137	59	0	
7000	5000	14792	13465	11954	10124	8354	7427	6225	4552	3378	2696	2588	2380	2105	1591	1193	1010	949	888	521	326	138	63	0	
7000	5500	15509	14000	12474	10713	9223	8025	6409	4682	3454	2710	2471	2382	2146	1673	1308	1154	1102	952	582	348	153	70	0	
7000	6000	16208	14521	12931	11464	10460	9338	7226	4752	3483	2714	2470	2415	2123	1840	1539	1385	1228	1032	655	379	179	84	0	
7000	6500	16785	15091	13336	11264	10132	10650	7804	4867	3535	2784	2519	2466	2330	2140	1879	1599	1311	1108	725	422	210	99	0	
7000	7000	17529	15640	13763	12432	11718	11183	8065	5055	3745	3006	2708	2595	2464	2260	2014	1687	1401	1186	795	476	243	116	0	
7000	7500	18170	16174	14182	12682	11740	11185	8202	5208	3974	3339	3032	2913	2779	2541	2199	1773	1489	1269	866	530	277	132	0	
7000	8000	18806	16673	14610	12995	12067	11187	8424	5405	4172	3727	3483	3384	3259	2846	2288	1851	1576	1353	936	581	312	149	0	
8000	0	5101	4795	4484	4175	4022	3883	3716	3403	2547	2044	1674	1295	1195	994	838	731	653	591	542	456	423	364	0	
8000	50	5714	5359	5025	4744	4615	4503	4362	4081	3170	2622	2374	2169	2006	1871	1761	1667	1579	1490	1183	980	938	720	0	
8000	100	6229	5834	5487	5235	5132	5039	4916	4650	3796	3239	3086	2969	2837	2708	2601	2507	2417	2281	1678	1457	1449	1050	0	
8000	300	6685	6179	5792	5654	5637	5577	5512	5484	5250	4549	4207	3911	3759	3642	3458	3328	3212	2893	2144	1877	1538	1083	0	
8000	500	6958	6354	5920	5763	5718	5605	5597	5544	5324	4784	4306	3829	3583	3411	3248	3096	2964	2629	2068	1858	1427	917	0	
8000	1000	7518	6668	6140	5919	5765	5314	5072	5040	4997	4755	4106	3452	3103	2847	2749	2560	2331	2069	1413	944	554	511	0	
8000	1500	8280	7266	6556	6124	5911	5334	5042	4774	4459	4066	3562	3137	2863	2639	2355	2001	1661	1209	643	364	205	195	0	
8000	2000	9465	8470	7416	6490	6179	5626	5178	4623	4015	3483	3039	2749	2551	2345	2014	1559	1068	656	388	250	154	134	0	
8000	2500	10508	9633	8457	7323	6937	6335	5386	4575	3816	3144	2769	2551	2319	1899	1514	1099	655	396	237	178	96	49	0	
8000	3000	11320	10465	9316	7976	7376	6702	5426	4348	3609	2906	2535	2340	2093	1694	1253	811	524	397	307	225	111	50	0	
8000	3500	12091	11136	10017	8489	7576	6794	5461	4205	3479	2798	2381	2179	1947	1616	1128	696	501	470	385	258	122	55	0	
8000	4000	12839	11763	10584	9021	7836	7014	5626	4145	3241	2592	2238	2084	1893	1528	1063	702	603	577	401	258	122	56	0	
8000	4500	13559	12361	11093	9494	8078	7215	5921	4248	3137	2403	2116	2037	1867	1475	1066	783	738	676	425	259	122	57	0	
8000	5000	14251	12945	11568	9938	8351	7424	6106	4394	3169	2420	2120	2031	1821	1450	1147	923	859	756	470	275	125	59	0	
8000	5500	14934	13466	12056																					

Pressure (kPa)	Mass Flux (kg.m ⁻² .s ⁻¹)
-------------------	---

Pressure (kPa)		Mass Flow (kg.m ⁻² .s ⁻¹)		Quality																											
				-0.5	-0.4	-0.3	-0.2	-0.15	-0.1	-0.05	0	0.05	0.1	0.15	0.2	0.25	0.3	0.35	0.4	0.45	0.5	0.6	0.7	0.8	0.9	1					
9000	0	4836	4571	4301	4034	3902	3783	3639	3352	2503	1977	1637	1290	1179	992	843	739	660	608	560	471	431	349	0							
9000	50	5422	5114	4813	4547	4432	4335	4213	3960	3071	2528	2304	2110	1945	1810	1699	1610	1536	1457	1152	971	938	650	0							
9000	100	5916	5571	5251	4988	4892	4811	4704	4462	3658	3134	2976	2841	2697	2575	2458	2373	2317	2165	1554	1306	1300	1040	0							
9000	300	6366	5916	5527	5300	5260	5239	5236	5194	4944	4270	3692	3478	3344	3257	3065	2894	2713	2334	1672	1380	1197	899	0							
9000	500	6641	6100	5668	5412	5332	5250	5147	5114	4925	4243	3625	3364	3160	2999	2887	2741	2351	1983	1583	1282	904	626	0							
9000	1000	7221	6432	5947	5625	5398	4936	4705	4703	4697	4204	3520	3118	2854	2661	2545	2118	1553	1143	984	729	346	311	0							
9000	1500	7976	7023	6356	5856	5535	4958	4693	4467	4189	3730	3227	2850	2712	2495	2034	1429	1081	892	546	350	131	119	0							
9000	2000	9111	8171	7160	6258	5863	5299	4835	4196	3569	3097	2746	2448	2312	1931	1428	1027	745	603	345	186	97	48	0							
9000	2500	10108	9252	8185	7162	6749	6025	5004	4119	3339	2797	2521	2241	1942	1373	1028	809	570	348	211	136	96	48	0							
9000	3000	10887	10041	8998	7755	7210	6399	5097	4045	3240	2604	2289	2038	1724	1354	967	708	508	393	282	169	103	49	0							
9000	3500	11622	10683	9660	8227	7395	6453	5140	3995	3155	2487	2124	1896	1643	1276	952	650	457	419	305	184	107	49	0							
9000	4000	12336	11283	10200	8756	7669	6674	5266	3983	3066	2349	1931	1750	1604	1375	982	664	558	499	331	190	108	55	0							
9000	4500	13022	11857	10680	9235	7924	6936	5469	4047	3026	2245	1827	1719	1631	1385	1037	771	670	615	381	205	109	56	0							
9000	5000	13683	12418	11127	9685	8259	7305	5645	4183	3080	2249	1836	1755	1663	1416	1152	908	816	717	445	239	116	57	0							
9000	5500	14332	12927	11580	10180	8782	7818	5764	4272	3210	2355	1963	1856	1760	1542	1290	1071	935	801	512	281	130	62	0							
9000	6000	14961	13402	11998	10758	9759	8777	6149	4331	3303	2421	2126	2045	1937	1699	1500	1219	1072	892	578	329	157	73	0							
9000	6500	15570	13909	12387	11336	10230	9257	6353	4416	3344	2492	2346	2317	1977	1985	1710	1431	1170	977	646	378	186	88	0							
9000	7000	16165	14403	12779	11578	10702	9737																								

Pressure (kPa)	Mass Flux (kg.m ⁻² .s ⁻¹)
-------------------	---

Pressure		Mass Flux		Quality																								
(kPa)	(kg.m ⁻² .s ⁻¹)			-0.5	-0.4	-0.3	-0.2	-0.15	-0.1	-0.05	0	0.05	0.1	0.15	0.2	0.25	0.3	0.35	0.4	0.45	0.5	0.6	0.7	0.8	0.9	1		
12000	0	4022	3849	3671	3501	3419	3349	3259	3053	2397	1859	1535	1258	1130	988	859	766	706	660	565	494	376	224	0				
12000	50	4511	4309	4111	3909	3809	3729	3634	3462	2826	2360	2111	1910	1745	1598	1505	1436	1383	1309	1069	933	818	507	0				
12000	100	4924	4699	4488	4261	4147	4058	3957	3791	3213	2789	2599	2447	2293	2152	2088	2036	2008	1916	1415	985	946	708	0				
12000	300	5311	5011	4728	4435	4333	4239	4176	4057	3775	3404	3187	3099	2966	2695	2591	2227	2034	1389	1112	820	636	545	0				
12000	500	5533	5172	4848	4467	4300	4185	4097	3919	3659	3254	3004	2866	2685	2402	2057	1673	1341	940	716	537	263	228	0				
12000	1000	6063	5518	5083	4489	4119	3776	3577	3372	3118	2733	2496	2232	1947	1675	1318	815	619	514	338	262	128	96	0				
12000	1500	6852	6169	5458	4626	4129	3854	3569	3177	2823	2464	2101	1764	1474	1094	793	536	408	320	235	175	114	54	0				
12000	2000	7804	7104	6246	5206	4596	4089	3659	3172	2712	2281	1898	1497	1168	747	568	474	345	257	221	119	91	44	0				
12000	2500	8606	7926	7227	6161	5502	4523	3768	3225	2688	2203	1707	1262	949	640	457	363	275	221	176	107	87	44	0				
12000	3000	9263	8483	7798	6682	6060	4884	3885	3274	2659	2064	1477	1064	850	620	402	310	263	253	209	113	87	48	0				
12000	3500	9873	8929	8209	7076	6416	5166	4024	3319	2654	1983	1395	1053	900	682	485	376	335	309	220	116	88	49	0				
12000	4000	10395	9339	8589	7553	6877	5668	4293	3390	2687	1935	1384	1160	1038	867	687	559	419	342	260	145	94	50	0				
12000	4500	10866	9735	8953	7997	7296	6103	4504	3487	2735	1952	1450	1285	1176	1020	863	684	462	363	318	181	101	51	0				
12000	5000	11303	10049	9268	8306	7473	6374	4628	3605	2874	2068	1598	1465	1359	1211	995	777	540	433	376	226	109	52	0				
12000	5500	11820	10479	9523	8588	7674	6576	4720	3697	2952	2165	1738	1625	1501	1343	1135	914	650	518	424	265	123	55	0				
12000	6000	12614	11227	10153	9051	8222	7070	5076	3873	3098	2268	1877	1799	1673	1456	1281	1109	894	749	513	299	142	66	0				
12000	6500	13206	11751	10530	9514	8530	7357	5290	3991	3239	2429	2116	1091	2020	1664	1445	1280	1076	903	588	343	169	80	0				
12000	7000	13689	12152	10841	9715	8838	7643	5346	4035	3319	2652	2326	2225	2106	1800	1576	1390	1150	973	652	390	198	94	0				
12000	7500	14161	12534	11149	9952	8942	7712	5403	4054	3404	2855	2556	2423	2286	1948	1653	1433	1223	1037	714	437	228	109	0				
12000	8000	14662	12943	11474	10247	9213	7919	5460	4075	3533	3020	2664	2570	2496	2307	1914	1594	1374	1140	774	484	260	123	0				
13000	0	3766	3617	3465	3317	3247	3184	3111	2935	2352	1850	1530	1255	1115	987	865	775	720	677	588	518	373	187	0				
13000	50	4208	4039	3883	3712	3624	3555	3463	3302	2728	2293	2039	1827	1658	1496	1404	1326	1237	1143	1005	926	752	444	0				
13000	100	4575	4391	4236	4030	3947	3870	3762	3597	3067	2675	2463	2279	2106	1909	1830	1749	1618	1446	1234	940	933	636	0				
13000	300	4843	4613	4448	4050	4040	4018	3934	3831	3536	3175	2868	2663	2492	2124	1896	1746	1454	1179	931	746	622	506	0				
13000	500	4923	4655	4500	4070	4000	3803	3654	3560	3358	3019	2708	2485	2193	1864	1584	1320	1069	716	473	397	245	208	0				
13000	1000	5355	4921	4614	4095	3769	3369	3032	2832	2644	2307	1992	1724	1540	1361	1136	721	471	351	254	202	122	72	0				
13000	1500	6344	5777	5070	4197	3817	3594	3201	2766	2390	2013	1697	1396	1182	937	699	476	361	293	229	162	112	50	0				
13000	2000	7337	6773	5836	4656	4124	3820	3363	2852	2361	1983	1637	1277	962	638	455	387	307	243	206	113	86	44	0				
13000	2500	8056	7515	6896	5685	4865	4126	3471	2940	2403	1965	1567	1149	797	504	362	290	231	192	161	105	84	44	0				
13000	3000	8688	7876	7317	6269	5533	4509	3631	3022	2449	1962	1434	1031	777	562	385	309	235	228	186	111	84	45	0				
13000	3500	9210	8021	7365	6395	5766	4775	3802	3091	2491	1978	1413	1065	874	681	462	364	331	287	201	112	86	46	0				
13000	4000	9436	8108	7419	6533	5984	5113	4060	3223	2622	2024	1493	1222	1050	882	695	586	452	342	244	139	90	47	0				
13000	4500	9495	8197	7536	6741	6225	5464	4230	3342	2784	2106	1604	1362	1188	1023	866	712	526	387	298	178	97	48	0				
13000	5000	9545	8199	7622	7067	6480	5834	4420	3429	2879	2232	1789	1352	1324	1139	950	769	530	403	355	218	105	49	0				
13000	5500	10034	8609	7982	7400	6731	6064	4489	3515	2935	2324	1949	1726	1520	1303	1094	904	640	473	403	255	119	54	0				
13000	6000	11456	10012	9157	8347	7605	6635	4586	3609	3029	2384	2027	1894	1714	1449	1265	1098	890	735	499	292	139	65	0				
13000	6500	12458	11078	9915	8897	8120	6995	4727	3679	3121	2471	2174	2101	2016	1658	1431	1278	1053	882	578	336	165	78	0				
13000	7000	12882	11431	10179	9113	8280	7180	4812	3703	3206	2607	2298	2192	2090	1791	1573	1369	1137	955	641	383	194	93	0				
13000	7500	13246	11713	10405	9314	8405	7305	4870	3742	3310	2761	2431	2305	2191	1898	1640	1434	1217	1022	703	431	225	107	0				
13000	8000	13772	12145	10756	9606	8630	7448	4957	3776	3396	2923	2537	2427	2360	2161	1859	1592	1365	1126	763	477	257	122	0				
14000	0	3493	3365	3232	3106	3046	2994	2930	2779	2271	1812	1510	1248	1089	963	851	767	714	695	598	509	351	175	0				
14000	50	3895	3750	3620	3476	3402	3343	3266	3123	2618	2211	1958	1756	1588	1423	1327	1253	1168	1070	974	807	632	355	0				
14000	100	4229	4072	3948	3794	3708	3641	3551	3434	2933	2560	2336	2169	2005	1804	1708	1636	1509	1300	992	764	615	350	0				
14000	300	4448	4260	4142	3958	3862	3800	3706	3630	3411	3099	2800	2552	2404	1967	1669	1554	1263	986	757	563	378	246	0				
14000	500	4497	4278	4181	3970	3832	3618	3453	3399	3267	2963	2612	2295	1941	1605	1318	1124	950	626	381	322	224	164	0				
14000	1000	4928	4533	4349	4004	3659	3197	2864	2705	2530	2189	1791	1508	1359	1209	980	627	434	334	223	190	116	70	0				
14000	1500	5911	5399	4821	4046	3724	3394	3020	2650	2255	1886	1534	1287	1089	877	629	396	307	273	205	150	93	47	0				
14000	2000	6752	6229	5421	4413	3994	3672	3200	2739	2230	1847	1520	1188	902	629	425	316	248	220	195	109	80	41	0				
14000	2500	7369	6879	6351	5379	4639	4017	3363	2826	2300	1938	1477	1078	826	529	351	266	200	170	148	104	82	43	0				
14000	3000	8033	7236	6834	6001	5227	4390	3551	2931	2372	1959	1498	1089	826	589	388	285	218	202	166	108	83	43	0				
14000	3500	8543	7311	6865	6069	5420	4584	3679	3013	2439	2039	1546	1190	943	696	496	383	312	257	185	111	84	44	0				
14000	4000	8724	7332	6886	6137	5545	4794	3790	3086	2620	2184	1688	1356	1106	871	702	596	471	330	227	135	87	44	0				
14000	4500	8731	7377	6942	6292	5734	5054	3846	3189	2929	2368	1828	1489	1240	1067	874	746	586	394	282	172	94	45	0				
14000	5000	8733	7394	6999	6618	6103	5568																					

Pressure (kPa)	Mass Flux (kg.m ⁻² .s ⁻¹)
-------------------	---

181

Pressure (kPa)	Mass Flux (kg.m ⁻² .s ⁻¹)
-------------------	---

182

Appendix III

CHF PREDICTION FOR WWER-TYPE BUNDLE GEOMETRIES

The CHF look-up table for the WWER-type bundles has been derived at IPPE, Obninsk and is included in this appendix as an alternative to calculate CHF in bundles of the WWER-type. This look-up table is based on (i) experimental data for bundles, and (ii) predictions using a semi-empirical model described in detail by Bobkov (1993, 1995) and Bobkov et al. (1993, 1995a-b, 1997a-b) in which the data on CHF in other geometries (tubes, annuli) and the look-up table for CHF in tubes were used that helped to expand the ranges of applicability. More than 4000 CHF data were used, obtained for 22 bundle geometries that were taken from the unified Czech-Russian CHF data bank [Kostalek et al. (1990)] (3, 7, 19 and 37 rods, triangular shape with p/d ratio of 1.16-1.52, ranges of flow conditions are: $1.5 \leq P \leq 20$ MPa; $220 \leq G \leq 504$ kg/m²s; $-0.52 \leq X \leq 0.9$). A 3-dimensional smoothing procedure was applied to remove irregular trends.

This version of look-up table is derived for the WWER-type rod bundles with the following applicability conditions:

- bundle with triangular rod array ;
- smooth channel with no effect of spacers;
- uniform axial and radial heating;
- heated-equivalent diameter is 9.36 mm;
- pitch to rod diameter ratio is 1.4;
- pressure: from 0.1 to 20 MPa;
- mass flux: from 50 to 5000 kg/m²s;
- relative enthalpy (steam quality): from -0.5 to 0.9.

The range of application of the look-up table can be expanded by using the following correction factors:

$$\text{CHF} = \text{CHF}(P, G, X, D_{\text{he}} = 9.36 \text{ mm}) \cdot K_1 \cdot K_2 \cdot K_3 \cdot K_4$$

where

- CHF(...) refers to the look-up table value;
- $K_1 = (9.36/D_{\text{he}})^{1/3}$;
- for $p/d < 1.1$: $K_2 = 0.90 - 0.7 \exp[-35(p/d-1)]$;
- for $p/d \geq 1.1$: $K_2 = 0.26 + 0.57 p/d$;
- $K_3 = 0.95 + 0.6 \exp(-0.01 L_h/D_{\text{he}})$.
- $K_4 = 1 + 1.5 \cdot \xi^{0.5} (G/1000)^{0.2} \cdot \exp(0.1 L_{\text{gs}}/D_{\text{he}})$, where ξ is spacer grid friction factor, L_{gs} - distance from outlet to the nearest grid spacer.

These correction factors permit to expand the application range of look-up table presented in this appendix up to:

- heated-equivalent diameter range, D_{he} , - from 2.8 to 21 mm;
- heated length/diameter ratio, L/D_{he} , - from 40 to 300;
- pitch to rod diameter ratio, p/d , - from 1.02 to 1.52;
- effect of rod spacing devices.

In the look-up table, strongly shaded cells are connected with the data on bundles, lightly shaded - with the data on simpler geometries (tubes, annuli).

TABLE III.I. THE LOOK-UP TABLE FOR CHF IN REGULAR TRIANGULAR ROD BUNDLES OF WWER-TYPE (HEATED EQUIVALENT DIAMETER IS 9.36 mm, THE PITCH TO ROD DIAMETER RATIO IS 1.4), CHF IS IN kW/m²

P MPa	G kg/m ² s	X															
		-0.5	-0.4	-0.3	-0.2	-0.1	0.0	0.1	0.2	0.3	0.4	0.5	0.6	0.7	0.8	0.9	
100	50	-	-	-	628	242	136	123	126	130	131	124	101	77	61	45	
100	100	-	-	-	694	324	214	223	232	243	248	239	195	151	110	70	
100	200	-	-	-	747	417	279	287	292	291	275	255	207	171	124	77	
100	300	-	-	-	799	516	349	356	357	343	303	270	219	192	138	84	
100	500	-	-	-	902	652	434	457	449	441	421	355	238	185	133	81	
100	750	-	-	-	1039	764	531	552	539	497	494	433	278	179	129	80	
100	1000	-	-	-	1184	885	640	657	636	555	573	520	321	169	123	76	
100	1500	-	-	-	1432	1072	802	804	772	737	770	681	372	160	117	73	
100	2000	-	-	-	1660	1247	950	946	885	879	868	720	343	98	75	52	
100	3000	-	-	-	2136	1620	1278	1254	1064	930	797	528	220	41	37	33	
100	4000	-	-	-	2711	2024	1646	1614	1312	932	661	390	194	92	71	50	
100	5000	-	-	-	3461	2471	2083	1985	1685	1270	942	648	388	198	142	86	
200	50	-	-	-	632	292	196	152	140	140	140	134	111	90	70	50	
200	100	-	-	-	707	372	252	238	246	253	253	248	210	167	121	75	
200	200	-	-	-	770	471	321	316	318	312	295	274	223	184	133	81	
200	300	-	-	-	834	577	394	400	395	375	339	301	235	202	144	87	
200	500	-	-	-	943	724	501	512	491	452	419	351	240	189	136	83	
200	750	-	-	-	1081	845	603	605	579	510	485	410	265	183	132	81	
200	1000	-	-	-	1227	975	716	706	674	570	556	473	290	173	125	77	
200	1500	-	-	-	1475	1169	882	852	810	727	699	576	313	132	98	64	
200	2000	-	-	-	1710	1357	1038	999	939	840	770	614	297	87	68	49	
200	3000	-	-	-	2217	1759	1376	1309	1141	922	757	509	219	41	37	34	
200	4000	-	-	-	2903	2187	1753	1656	1342	954	679	408	209	93	72	51	
200	5000	-	-	-	3734	2648	2169	2028	1727	1289	958	657	395	197	141	85	
300	50	-	-	-	636	341	256	180	154	150	149	145	120	104	79	54	
300	100	-	-	-	720	421	291	253	259	264	259	257	225	183	132	81	
300	200	-	-	-	794	525	362	345	343	334	315	293	238	197	141	86	
300	300	-	-	-	869	637	439	444	433	408	374	331	252	212	151	90	
300	500	-	-	-	984	796	568	567	533	464	416	347	242	193	138	84	
300	750	-	-	-	1124	925	676	658	619	523	476	386	252	187	134	82	
300	1000	-	-	-	1270	1064	793	756	711	585	539	426	259	176	127	78	
300	1500	-	-	-	1517	1266	963	900	849	717	628	471	253	104	79	54	
300	2000	-	-	-	1760	1467	1125	1051	993	802	672	508	251	77	61	45	
300	3000	-	-	-	2297	1899	1475	1364	1218	914	718	490	217	42	38	34	
300	4000	-	-	-	3095	2350	1861	1699	1372	976	697	425	224	95	73	51	
300	5000	-	-	-	4009	2825	2256	2072	1769	1307	975	666	402	195	140	85	
400	50	-	-	-	648	375	283	200	172	165	161	147	123	115	87	58	
400	100	-	-	-	746	467	312	289	293	295	283	274	250	211	150	90	
400	200	-	-	-	834	585	415	400	392	359	332	302	265	228	162	96	
400	300	-	-	-	925	711	524	520	498	427	383	331	279	245	173	101	
400	500	-	-	-	1048	867	655	635	587	487	410	319	244	201	144	87	
400	750	-	-	-	1195	1007	762	726	674	546	460	354	250	192	138	84	
400	1000	-	-	-	1350	1157	876	821	766	606	511	389	252	178	128	79	
400	1500	-	-	-	1611	1377	1050	1028	935	710	575	432	248	117	88	59	
400	2000	-	-	-	1871	1595	1223	1218	1086	782	614	464	212	74	59	44	
400	3000	-	-	-	2459	2057	1658	1634	1315	871	654	426	201	42	38	34	
400	4000	-	-	-	3293	2547	2016	1961	1468	998	712	430	234	96	74	52	
400	5000	-	-	-	4276	3036	2351	2129	1828	1326	986	671	407	195	140	85	

TABLE III.I. (CONT.)

P MPa	G kg/m ² s	X															
		-0.5	-0.4	-0.3	-0.2	-0.1	0.0	0.1	0.2	0.3	0.4	0.5	0.6	0.7	0.8	0.9	
500	50	-	-	932	660	410	309	220	190	181	173	148	127	127	94	62	
500	100	-	-	1067	772	514	334	326	326	326	308	291	275	239	169	99	
500	200	-	-	1166	874	645	467	456	441	385	349	311	291	258	182	106	
500	300	-	-	1265	981	785	610	596	564	447	392	331	307	278	195	113	
500	500	-	-	1396	1111	938	741	703	642	512	405	291	247	209	149	89	
500	750	-	-	1552	1267	1089	848	792	729	569	444	321	248	197	141	85	
500	1000	-	-	1709	1430	1249	959	886	821	628	482	352	244	179	129	79	
500	1500	-	-	2025	1705	1487	1137	1156	1021	703	523	392	244	130	97	63	
500	2000	-	-	2351	1982	1723	1322	1384	1181	763	556	420	173	71	57	43	
500	3000	-	-	3243	2621	2216	1840	1904	1412	827	590	362	186	42	38	34	
500	4000	-	-	4521	3491	2744	2171	2223	1564	1020	727	435	245	98	75	53	
500	5000	-	-	6060	4542	3249	2445	2186	1888	1345	997	677	412	195	140	85	
600	50	-	-	931	678	440	336	244	210	198	188	161	143	145	106	68	
600	100	-	-	1072	802	559	372	362	359	353	328	299	289	259	183	106	
600	200	-	-	1183	925	717	533	512	480	407	365	320	305	278	195	112	
600	300	-	-	1296	1054	886	707	675	611	465	404	340	321	296	207	118	
600	500	-	-	1436	1195	1053	855	788	709	534	419	320	270	230	155	92	
600	750	-	-	1595	1353	1205	967	883	784	586	456	324	249	203	145	87	
600	1000	-	-	1756	1518	1365	1082	981	860	638	492	352	242	180	130	80	
600	1500	-	-	2079	1808	1621	1272	1233	1054	683	495	369	233	139	103	66	
600	2000	-	-	2418	2104	1876	1451	1463	1211	733	513	391	174	72	58	44	
600	3000	-	-	3337	2770	2402	1952	1978	1442	803	559	356	195	47	41	35	
600	4000	-	-	4645	3644	2950	2309	2336	1615	1029	735	444	258	102	78	54	
600	5000	-	-	6216	4684	3388	2585	2344	1925	1347	1001	679	416	195	140	85	
700	50			931	695	470	363	268	230	216	203	174	159	162	118	74	
700	100	-	-	1076	832	604	411	399	391	380	347	307	302	280	0.8	0.9	
700	200	-	-	1200	975	789	600	569	520	430	381	328	319	297	118	74	
700	300	-	-	1327	1126	987	805	754	658	483	415	349	336	314	197	113	
700	500	-	-	1475	1279	1166	969	875	776	556	433	300	254	228	208	119	
700	750	-	-	1637	1440	1320	1086	975	840	603	468	327	249	208	219	124	
700	1000	-	-	1802	1606	1481	1206	1076	900	647	501	352	239	181	162	96	
700	1500	-	-	2133	1912	1755	1407	1311	1087	664	467	346	223	149	149	89	
700	2000	-	-	2486	2225	2029	1581	1542	1241	704	470	361	176	73	130	80	
700	3000	-	-	3430	2917	2590	2064	2052	1472	780	527	349	204	52	109	69	
700	4000	-	-	4769	3796	3157	2447	2450	1666	1038	744	453	271	105	58	44	
700	5000	-	-	6372	4825	3527	2725	2504	1963	1349	1005	682	420	195	44	37	
800	50	-	-	930	712	500	391	291	251	234	218	187	175	180	80	55	
800	100	-	-	1080	862	649	449	435	424	407	366	315	316	301	140	85	
800	200	-	-	1217	1026	860	667	626	560	453	397	337	333	317	130	80	
800	300	-	-	1358	1199	1088	903	833	706	501	427	358	350	332	211	120	
800	500	-	-	1514	1363	1280	1083	961	845	579	447	305	258	237	221	125	
800	750	-	-	1680	1526	1435	1205	1066	896	620	480	329	250	214	231	130	
800	1000	-	-	1847	1693	1596	1329	1173	940	657	511	352	236	182	168	99	
800	1500	-	-	2187	2015	1888	1542	1389	1121	644	440	323	212	158	153	91	
800	2000	-	-	2552	2347	2182	1711	1622	1272	675	428	332	177	74	131	80	
800	3000	-	-	3522	3065	2777	2176	2127	1502	757	495	343	214	56	115	72	
800	4000	-	-	4892	3947	3364	2586	2564	1717	1047	752	462	284	109	59	44	
800	5000	-	-	6527	4965	3666	2865	2665	2001	1351	1009	684	425	195	47	39	

TABLE III.I. (CONT.)

P MPa	G kg/m²s	X															
		-0.5	-0.4	-0.3	-0.2	-0.1	0.0	0.1	0.2	0.3	0.4	0.5	0.6	0.7	0.8	0.9	
1000	50		1072	929	746	561	446	339	292	269	248	214	207	216	154	92	
1000	100	-	1217	1088	921	740	526	508	489	461	405	331	343	343	239	134	
1000	200	-	1336	1249	1125	1004	801	740	640	499	428	354	361	356	248	139	
1000	300	-	1456	1417	1342	1288	1100	991	802	538	451	376	378	369	256	143	
1000	500	-	1614	1590	1531	1505	1313	1133	983	623	476	315	265	256	181	105	
1000	750	-	1792	1763	1699	1665	1446	1250	1009	653	505	335	251	226	160	95	
1000	1000	-	1971	1937	1868	1824	1578	1366	1020	675	530	352	230	183	132	81	
1000	1500	-	2363	2292	2220	2152	1814	1546	1190	605	384	277	189	177	128	79	
1000	2000	-	2904	2684	2589	2486	1973	1783	1334	617	342	272	179	75	60	45	
1000	3000	-	4416	3706	3359	3154	2403	2278	1564	712	431	329	233	66	54	42	
1000	4000		6226	5138	4249	3778	2864	2793	1822	1065	769	480	309	116	87	58	
1000	5000	-	8320	6837	5245	3941	3143	2991	2077	1355	1017	689	433	195	140	85	
2000	50		1120	1044	924	788	634	504	339	312	289	279	283	296	207	118	
2000	100		1256	1186	1083	964	819	594	558	529	487	442	428	395	273	151	
2000	200		1361	1312	1248	1167	1076	872	817	750	607	566	513	461	410	283	
2000	300		1465	1439	1421	1383	1353	1173	1079	957	689	648	589	495	424	292	
2000	500		1636	1615	1602	1571	1566	1463	1261	1125	782	724	579	429	352	244	
2000	750		1827	1797	1779	1742	1728	1606	1393	1161	823	734	565	401	314	219	
2000	1000		2022	1981	1957	1916	1890	1748	1525	1180	857	731	537	359	263	185	
2000	1500		2553	2385	2322	2273	2221	2010	1665	1314	842	556	378	240	210	150	
2000	2000		3388	2957	2715	2642	2547	2142	1814	1434	838	466	293	191	131	97	
2000	3000		5411	4600	3834	3428	3205	2511	2215	1623	782	457	336	248	81	64	
2000	4000		7486	6491	5449	4393	3827	2931	2699	1774	983	816	524	344	125	93	
2000	5000		9876	8630	7316	5615	4021	3235	2996	1955	1335	1050	718	457	195	140	
3000	50		1032	939	848	765	655	520	413	359	329	305	318	332	347	241	
3000	100		1160	1074	999	933	831	620	596	582	555	528	515	479	413	286	
3000	200		1270	1207	1167	1132	1074	889	836	802	674	656	633	531	434	299	
3000	300		1421	1382	1380	1379	1372	1135	1058	1006	775	771	738	570	442	304	
3000	500		1609	1592	1579	1566	1533	1385	1240	1131	925	839	710	557	419	288	
3000	750		1813	1798	1778	1758	1716	1566	1401	1211	1011	852	700	522	383	261	
3000	1000		2023	2053	2019	1986	1926	1741	1525	1286	1031	840	638	456	325	223	
3000	1500		2588	2530	2417	2342	2230	1961	1668	1371	1024	735	504	338	253	179	
3000	2000		3476	3360	3063	2844	2606	2186	1817	1443	992	632	393	263	185	132	
3000	3000		5610	4975	4291	3716	3185	2550	2087	1564	986	615	409	271	152	96	
3000	4000		7829	6962	5965	4850	3822	2948	2432	1719	1109	806	561	364	182	110	
3000	5000		1039	9287	8101	6258	4305	3265	2924	1819	1287	1073	744	478	200	143	
5000	50		945	873	811	753	675	544	446	390	357	331	339	352	247	174	
5000	100		1084	1015	961	910	835	646	618	606	590	554	539	529	462	318	
5000	200		1216	1154	1120	1089	1043	881	833	819	771	710	674	600	470	325	
5000	300		1364	1317	1311	1307	1297	1086	1017	985	835	786	746	629	485	333	
5000	500		1571	1577	1559	1542	1500	1367	1278	1178	1078	940	821	657	501	342	
5000	750		1811	1818	1788	1757	1699	1576	1431	1332	1159	1015	825	634	462	314	
5000	1000		2058	2117	2065	2013	1924	1754	1587	1421	1214	1005	773	552	396	268	
5000	1500		2679	2658	2513	2398	2234	1979	1732	1507	1221	903	614	424	313	224	
5000	2000		3634	3598	3259	2960	2619	2183	1848	1544	1133	743	468	318	237	171	
5000	3000		5857	5291	4588	3895	3177	2506	2046	1600	1073	678	440	301	187	118	
5000	4000		8113	7288	6265	5037	3776	2858	2326	1710	1146	820	591	388	205	123	
5000	5000		1063	9521	8325	6417	4173	3091	2802	1848	1286	1133	796	511	212	152	

TABLE III.I. (CONT.)

P MPa	G kg/m ² s	X															
		-0.5	-0.4	-0.3	-0.2	-0.1	0.0	0.1	0.2	0.3	0.4	0.5	0.6	0.7	0.8	0.9	
6000	50	980	914	855	800	728	585	482	419	382	355	304	257	249	176	103	
6000	100	1131	1064	1011	964	893	693	655	639	624	592	484	443	425	293	161	
6000	200	1279	1212	1176	1144	1098	934	877	858	824	767	647	589	515	353	192	
6000	300	1470	1402	1383	1370	1354	1163	1090	1071	1018	938	809	735	601	410	220	
6000	500	1734	1707	1663	1626	1567	1453	1324	1272	1160	1047	889	751	591	409	237	
6000	750	2055	2000	1929	1863	1783	1636	1506	1379	1252	1090	907	716	537	366	208	
6000	1000	2378	2361	2253	2144	2004	1824	1641	1483	1317	1089	844	615	440	296	162	
6000	1500	3138	3001	2777	2571	2320	2012	1794	1602	1314	991	676	461	336	238	163	
6000	2000	4260	4056	3625	3200	2675	2189	1852	1587	1220	793	492	339	250	180	124	
6000	3000	6573	5793	5010	4149	3204	2409	1951	1575	1085	680	437	302	197	129	66	
6000	4000	8635	7599	6497	5145	3685	2612	2094	1596	1091	780	550	370	208	130	82	
6000	5000	10591	9447	8118	6088	3908	2465	2273	1707	1148	1104	738	461	209	149	89	
8000	50	1158	1087	1026	973	901	651	547	497	467	442	382	329	318	222	126	
8000	100	1338	1259	1198	1151	1083	838	774	754	737	717	587	511	516	354	192	
8000	200	1524	1429	1372	1336	1285	1107	998	971	946	908	735	644	601	410	220	
8000	300	1761	1645	1590	1567	1537	1365	1214	1181	1151	1094	881	775	678	462	246	
8000	500	2090	1982	1892	1822	1757	1604	1477	1348	1245	1072	890	746	605	426	266	
8000	750	2483	2329	2198	2083	1962	1823	1612	1452	1279	1071	868	689	525	363	222	
8000	1000	2872	2755	2569	2378	2178	1933	1708	1511	1270	1029	775	564	398	267	155	
8000	1500	3769	3487	3162	2836	2441	2090	1793	1539	1256	900	603	399	272	181	81	
8000	2000	4994	4618	4089	3491	2806	2195	1829	1524	1132	726	436	285	195	133	70	
8000	3000	7246	6286	5443	4448	3267	2374	1859	1457	1024	608	379	257	168	111	66	
8000	4000	8833	7693	6621	5228	3656	2446	1846	1419	960	653	451	304	182	119	76	
8000	5000	9819	8812	7648	5825	3855	2055	1645	1376	925	766	540	339	178	129	79	
10000	50	1398	1325	1253	1193	1126	839	697	626	581	557	494	433	406	280	155	
10000	100	1612	1526	1445	1384	1319	1050	949	911	883	876	734	616	581	397	213	
10000	200	1830	1721	1623	1561	1522	1336	1160	1145	1091	1023	786	623	584	399	214	
10000	300	2108	1968	1848	1785	1774	1610	1356	1372	1292	1157	819	612	569	389	209	
10000	500	2488	2300	2157	2040	1912	1760	1516	1408	1226	1010	766	601	485	339	189	
10000	750	2939	2680	2482	2295	2124	1891	1677	1442	1207	927	703	535	401	278	157	
10000	1000	3383	3147	2876	2591	2288	2013	1709	1429	1137	822	594	421	297	200	112	
10000	1500	4355	3931	3502	3034	2539	2073	1724	1398	1033	682	454	304	200	135	71	
10000	2000	5607	5064	4439	3712	2839	2202	1721	1333	930	558	346	227	152	103	59	
10000	3000	7637	6545	5686	4573	3288	2319	1737	1270	841	499	315	219	144	99	63	
10000	4000	8671	7451	6478	5139	3516	2326	1646	1223	828	533	376	255	159	107	66	
10000	5000	8671	7812	6935	5475	3301	1873	1208	1198	890	608	476	295	158	115	72	
12000	50	1617	1545	1473	1403	1332	1055	856	756	698	678	608	543	499	342	186	
12000	100	1851	1769	1686	1601	1523	1266	1113	1046	1019	1032	882	664	581	397	213	
12000	200	2076	1972	1867	1772	1696	1495	1345	1292	1217	1089	841	652	545	373	201	
12000	300	2366	2233	2099	1990	1915	1704	1566	1533	1408	1124	772	621	490	336	183	
12000	500	2738	2514	2348	2179	1991	1724	1522	1324	1156	887	646	479	361	248	115	
12000	750	3187	2874	2640	2377	2089	1833	1522	1309	1042	766	542	392	281	192	99	
12000	1000	3625	3328	3000	2630	2226	1873	1565	1260	936	623	427	301	211	145	77	
12000	1500	4661	4107	3595	3027	2429	1974	1571	1197	823	498	329	228	160	111	70	
12000	2000	5833	5144	4473	3605	2770	2100	1627	1159	743	425	270	196	135	95	60	
12000	3000	7445	6318	5455	4356	3122	2279	1647	1137	700	410	277	195	134	94	61	
12000	4000	7824	6673	5835	4676	3256	2243	1568	1090	719	454	322	227	146	101	65	
12000	5000	6913	6264	5685	4746	2890	1771	1102	994	755	436	354	266	152	111	70	

TABLE III.I. (CONT.)

P MPa	G kg/m ² s	X														
		-0.5	-0.4	-0.3	-0.2	-0.1	0.0	0.1	0.2	0.3	0.4	0.5	0.6	0.7	0.8	0.9
14000	50	1760	1699	1638	1573	1510	1249	1003	867	772	718	664	608	515	353	191
14000	100	1988	1923	1858	1782	1706	1456	1245	1137	1032	959	769	620	512	351	190
14000	200	2170	2097	2024	1937	1857	1678	1456	1326	1084	934	719	577	456	314	172
14000	300	2413	2330	2245	2141	2054	1883	1656	1508	1120	889	651	518	387	268	149
14000	500	2652	2498	2367	2190	1956	1715	1429	1235	982	753	533	388	284	196	101
14000	750	3014	2788	2584	2319	1957	1647	1388	1116	892	636	447	305	221	152	89
14000	1000	3362	3175	2895	2475	2040	1675	1363	1073	782	509	335	238	171	121	73
14000	1500	4469	3889	3392	2794	2191	1764	1400	1045	699	410	261	190	141	102	67
14000	2000	5472	4746	4066	3249	2459	1950	1503	1069	680	376	244	174	128	92	59
14000	3000	6614	5544	4778	3724	2774	2109	1602	1101	690	421	271	191	130	92	61
14000	4000	6263	5420	4762	3855	2816	2116	1559	1086	725	477	326	218	139	96	63
14000	5000	4740	4245	4016	3587	2380	1800	1248	929	702	511	324	228	135	100	65
16000	50	1748	1694	1643	1589	1536	1356	1094	932	760	661	581	490	376	261	145
16000	100	1950	1889	1835	1773	1708	1547	1323	1185	966	851	648	529	409	283	156
16000	200	2074	1995	1934	1867	1790	1678	1496	1332	1049	835	603	482	389	269	149
16000	300	2254	2152	2079	2006	1912	1794	1663	1473	1125	808	549	427	362	251	141
16000	500	2408	2173	2056	1914	1708	1478	1284	1061	855	648	456	328	254	180	100
16000	750	2649	2354	2193	1965	1664	1392	1144	938	739	547	375	262	192	139	86
16000	1000	2879	2642	2407	2107	1692	1391	1135	874	658	434	285	196	148	108	68
16000	1500	3633	3188	2818	2326	1865	1496	1202	896	621	358	219	158	121	90	59
16000	2000	4181	3818	3345	2686	2111	1704	1366	1007	656	380	224	160	116	86	57
16000	3000	5184	4423	3829	3050	2357	1903	1510	1100	743	450	300	202	132	91	62
16000	4000	5067	4256	3753	3089	2350	1910	1513	1126	774	536	361	241	144	94	59
16000	5000	3896	3318	3242	2980	1918	1665	1307	1015	752	547	356	227	117	88	59
18000	50	1496	1452	1411	1369	1328	1207	969	820	695	644	561	449	363	252	141
18000	100	1607	1554	1506	1457	1401	1286	1046	909	780	746	611	492	425	293	162
18000	200	1582	1509	1447	1386	1306	1205	1027	901	767	686	544	436	387	268	149
18000	300	1548	1454	1379	1306	1202	1116	1004	888	750	622	474	377	345	240	135
18000	500	1405	1282	1199	1140	1033	914	845	731	659	515	369	257	223	159	94
18000	750	1549	1394	1279	1202	1090	913	814	689	584	431	300	209	174	126	78
18000	1000	1687	1502	1353	1258	1142	906	776	642	502	342	227	158	121	90	60
18000	1500	2326	2082	1810	1544	1364	1059	927	748	526	252	165	102	79	63	46
18000	2000	2874	2590	2275	1905	1600	1244	1139	941	650	308	196	135	105	80	55
18000	3000	3735	3356	2970	2356	1774	1471	1421	1095	771	485	400	284	128	95	62
18000	4000	3661	3126	2728	2152	1634	1559	1403	1120	830	574	501	385	157	115	72
18000	5000	3650	3100	2628	1900	1534	1500	1403	1220	930	674	581	450	200	135	102
20000	50	1135	1115	1103	1081	1008	908	803	750	590	468	390	333	275	193	111
20000	100	1259	1244	1240	1216	1097	967	842	806	620	471	398	381	352	244	137
20000	200	1143	1123	1118	1104	993	871	717	663	552	420	345	335	317	221	125
20000	300	1027	1001	995	991	889	776	593	523	483	369	293	290	282	198	114
20000	500	749	701	666	647	609	532	452	438	413	342	228	193	179	129	79
20000	750	823	758	699	653	589	514	458	457	403	308	206	153	130	97	63
20000	1000	887	806	726	657	570	496	462	473	393	276	185	117	86	67	48
20000	1500	1257	1139	1022	907	743	643	658	526	424	312	160	99	74	59	44
20000	2000	1536	1354	1191	1034	831	709	673	612	525	309	167	110	81	64	47
20000	3000	1649	1417	1269	1068	830	699	602	624	570	416	290	198	94	72	51
20000	4000	1532	1386	1243	1046	840	765	788	666	569	459	346	276	122	91	60
20000	5000	1657	1561	1370	1138	966	906	855	755	678	494	381	315	1366	100	65

REFERENCES TO APPENDIX III

BOBKOV V.P.; 1993, "Burnout in Channels of Various Cross-Section", Preprint of IPPE - 2313, Obninsk (in Russian).

BOBKOV V.P., ZYATNINA O.A., KOZINA N.V., SUDNITSIN O.A., 1993, "Burnout in Channels of Various Cross-Section (Model and Statistical Results)". Preprint of IPPE - 2314, Obninsk (in Russian).

BOBKOV V.P.; 1994, "The Features of Burnout in Rod Bundles and Other Complex Channels", Proc. of Ist Russian Conference on Heat Transfer, Moscow, vol. 4, p.p. 32-37 (in Russian).

BOBKOV V.P., VINOGRADOV V.N., ZYATNINA O.A., KOZINA N.V.; 1995a, "Description of Critical Heat Flux in Rod Bundles and Other Complex Channels", Proc. of Intern. Conference on Thermophysical aspects of WWER's Safety, Obninsk, v.1, p.p.143-154 (in Russian).

BOBKOV V.P., VINOGRADOV V.N., ZYATNINA O.A., KOZINA N.V.; 1995b, "Method of Burnout Description in Channels of Complex Cross-Section", Teploenergetika, v.3, p.p. 37-46 (in Russian).

BOBKOV V.P., VINOGRADOV V.N., ZYATNINA O.A., KOZINA N.V.; 1997a, "Relative Description of Burnout in Rod Bundles and Other Complex Channels", Teploenergetika, v.3 p.p.1-7 (in Russian).

BOBKOV V.P., KIRILLOV P.L, SMOGALEV I.P., VINOGRADOV V.N.; 1997b, "Look-Up Tables Developing Methods for Critical Heat Flux in Rod Bundles", Proceedings, NURETH-8, Vol 3 pp. 1581-1589, 1997.

KOSTALEK YA., CIZEK J., LISTSOVA N.N., MAKHOV D.N., SUSLOV A.I.; 1990, "Data Bank on Burnout in Rod Bundles". Proc. of Seminar "Thermohydraulics-90", Obninsk, p.182, 1990 (in Russian).

Appendix IV

AECL LOOK-UP TABLE FOR FULLY DEVELOPED FILM-BOILING HEAT-TRANSFER COEFFICIENTS ($\text{kW m}^{-2} \text{K}^{-1}$)

This Appendix contains two tables. The first table contains the filmboiling heat transfer coefficients as a function of pressure, mass flux, quality and heat flux for a 8 mm ID tube. It has been described in Section 4.4.5 and should be used only with the following qualifications:

- the heat transfer coefficients at low flows and qualities are based on extrapolation from Hammouda's model (except for zero flow and $X < 0$ where the data are based on pool film boiling conditions).
- the conditions where data are available can be found in the second table of this appendix. This table also specifies the number of data points and the errors for each subset of flow conditions.

Legend:

Non-shaded	: Areas where data exist;
Lightly-shaded	: Areas where data are not available, values come from models;
Heavily-shaded	: Areas where data are not available, (predicted surface-temperature is greater than $1,450^{\circ}\text{C}$).

TABLE IV.I. AECL TABLE FOR FULLY-DEVELOPED FILM-BOILING HEAT TRANSFER COEFFICIENTS

P	G	Xe	q (kW m ⁻²)									
			50	100	150	200	400	600	800	1000	2000	3000
(kPa)	(kg m ⁻² s ⁻¹)	(-)	Heat Transfer Coefficient (kW m ⁻² K ⁻²)									
100	0	-0.20	0.174	0.205	0.237	0.269	0.400	0.531	0.664	0.803	1.502	2.189
100	0	-0.10	0.173	0.203	0.226	0.252	0.368	0.484	0.602	0.726	1.345	1.954
100	0	-0.05	0.161	0.185	0.218	0.238	0.347	0.463	0.580	0.704	1.324	1.934
100	0	0.00	0.142	0.162	0.192	0.218	0.320	0.440	0.560	0.687	1.321	1.931
100	0	0.05	0.101	0.124	0.153	0.182	0.294	0.422	0.546	0.674	1.319	1.929
100	0	0.10	0.069	0.096	0.130	0.157	0.284	0.410	0.537	0.667	1.316	1.926
100	0	0.20	0.046	0.065	0.097	0.130	0.264	0.394	0.524	0.654	1.307	1.920
100	0	0.40	0.046	0.065	0.090	0.128	0.259	0.389	0.518	0.649	1.303	1.918
100	0	0.60	0.068	0.094	0.125	0.155	0.279	0.403	0.527	0.657	1.305	1.922
100	0	0.80	0.079	0.107	0.137	0.166	0.288	0.409	0.532	0.661	1.305	1.939
100	0	1.00	0.071	0.101	0.133	0.162	0.286	0.408	0.530	0.660	1.300	1.937
100	0	1.20	0.057	0.078	0.109	0.139	0.266	0.392	0.519	0.649	1.299	1.936
100	50	-0.20	0.222	0.251	0.279	0.307	0.414	0.522	0.628	0.726	1.207	1.709
100	50	-0.10	0.218	0.243	0.271	0.295	0.382	0.471	0.559	0.643	1.051	1.477
100	50	-0.05	0.180	0.208	0.241	0.257	0.343	0.423	0.506	0.584	0.961	1.357
100	50	0.00	0.129	0.153	0.177	0.198	0.288	0.371	0.455	0.531	0.904	1.296
100	50	0.05	0.087	0.112	0.133	0.155	0.252	0.336	0.423	0.499	0.873	1.268
100	50	0.10	0.068	0.093	0.116	0.140	0.235	0.322	0.409	0.485	0.862	1.260
100	50	0.20	0.056	0.083	0.113	0.137	0.230	0.315	0.399	0.476	0.857	1.257
100	50	0.40	0.081	0.112	0.134	0.156	0.235	0.319	0.399	0.477	0.854	1.251
100	50	0.60	0.105	0.127	0.150	0.170	0.252	0.335	0.415	0.494	0.874	1.273
100	50	0.80	0.118	0.139	0.168	0.188	0.271	0.356	0.440	0.519	0.906	1.312
100	50	1.00	0.136	0.157	0.187	0.211	0.298	0.386	0.473	0.553	0.949	1.365
100	50	1.20	0.202	0.221	0.242	0.264	0.346	0.431	0.516	0.596	0.991	1.404
100	100	-0.20	0.303	0.347	0.375	0.385	0.447	0.547	0.644	0.730	1.154	1.595
100	100	-0.10	0.286	0.323	0.355	0.370	0.420	0.495	0.570	0.640	0.984	1.339
100	100	-0.05	0.257	0.290	0.338	0.354	0.398	0.445	0.494	0.555	0.849	1.158
100	100	0.00	0.134	0.165	0.205	0.226	0.306	0.368	0.417	0.472	0.745	1.036
100	100	0.05	0.091	0.122	0.152	0.169	0.259	0.303	0.371	0.425	0.692	0.978
100	100	0.10	0.093	0.120	0.149	0.165	0.236	0.293	0.360	0.414	0.685	0.967
100	100	0.20	0.114	0.139	0.166	0.179	0.241	0.299	0.357	0.412	0.682	0.966
100	100	0.40	0.137	0.170	0.185	0.199	0.253	0.312	0.367	0.423	0.692	0.976
100	100	0.60	0.155	0.175	0.189	0.205	0.264	0.330	0.391	0.449	0.733	1.033
100	100	0.80	0.162	0.184	0.209	0.228	0.297	0.368	0.435	0.496	0.794	1.110
100	100	1.00	0.215	0.233	0.265	0.289	0.361	0.433	0.503	0.564	0.871	1.195
100	100	1.20	0.378	0.391	0.406	0.422	0.480	0.543	0.605	0.663	0.950	1.254
100	200	-0.20	0.320	0.401	0.455	0.472	0.503	0.583	0.680	0.765	1.187	1.625
100	200	-0.10	0.311	0.391	0.445	0.463	0.488	0.535	0.603	0.672	1.013	1.365
100	200	-0.05	0.288	0.329	0.367	0.389	0.456	0.481	0.550	0.605	0.853	1.149
100	200	0.00	0.140	0.179	0.219	0.252	0.350	0.388	0.440	0.489	0.720	0.981
100	200	0.05	0.111	0.146	0.181	0.215	0.304	0.328	0.391	0.437	0.652	0.905
100	200	0.10	0.145	0.171	0.188	0.214	0.270	0.317	0.364	0.411	0.646	0.904
100	200	0.20	0.241	0.259	0.278	0.283	0.316	0.353	0.396	0.442	0.671	0.916
100	200	0.40	0.275	0.341	0.365	0.372	0.379	0.403	0.440	0.489	0.725	0.975
100	200	0.60	0.278	0.344	0.368	0.376	0.382	0.433	0.481	0.534	0.800	1.079

P	G	Xe	q (kW m-2)									
			50	100	150	200	400	600	800	1000	2000	3000
(kPa)	(kg m-2 s-1)	(-)	Heat Transfer Coefficient (kW m-2 K-2)									
100	200	0.80	0.319	0.349	0.373	0.381	0.444	0.504	0.560	0.617	0.904	1.204
100	200	1.00	0.496	0.505	0.523	0.542	0.600	0.656	0.711	0.767	1.048	1.345
100	200	1.20	0.804	0.814	0.823	0.832	0.874	0.916	0.958	1.005	1.239	1.495
100	500	-0.20	0.296	0.331	0.362	0.393	0.513	0.630	0.741	0.838	1.341	1.818
100	500	-0.10	0.277	0.357	0.417	0.445	0.501	0.562	0.647	0.728	1.131	1.524
100	500	-0.05	0.263	0.295	0.334	0.364	0.451	0.493	0.572	0.616	0.927	1.245
100	500	0.00	0.149	0.179	0.215	0.247	0.347	0.385	0.447	0.480	0.745	1.005
100	500	0.05	0.151	0.179	0.204	0.230	0.314	0.348	0.403	0.450	0.669	0.894
100	500	0.10	0.215	0.232	0.240	0.269	0.335	0.400	0.432	0.472	0.694	0.904
100	500	0.20	0.346	0.386	0.398	0.413	0.449	0.482	0.523	0.563	0.761	0.965
100	500	0.40	0.478	0.510	0.531	0.543	0.574	0.611	0.653	0.701	0.933	1.170
100	500	0.60	0.595	0.617	0.639	0.654	0.700	0.751	0.804	0.858	1.132	1.397
100	500	0.80	0.904	0.908	0.916	0.924	0.964	1.010	1.060	1.113	1.385	1.643
100	500	1.00	1.425	1.429	1.432	1.435	1.444	1.471	1.506	1.549	1.758	1.969
100	500	1.20	1.997	2.003	2.009	2.017	2.040	2.065	2.091	2.123	2.277	2.438
100	1000	-0.20	0.300	0.333	0.365	0.397	0.526	0.652	0.776	0.890	1.455	2.007
100	1000	-0.10	0.252	0.281	0.310	0.341	0.451	0.554	0.657	0.751	1.213	1.666
100	1000	-0.05	0.188	0.231	0.267	0.302	0.394	0.464	0.553	0.628	0.996	1.357
100	1000	0.00	0.162	0.185	0.217	0.247	0.345	0.419	0.474	0.533	0.814	1.090
100	1000	0.05	0.209	0.234	0.261	0.289	0.366	0.433	0.470	0.517	0.749	0.978
100	1000	0.10	0.319	0.349	0.371	0.395	0.473	0.528	0.561	0.604	0.822	1.038
100	1000	0.20	0.539	0.565	0.582	0.600	0.646	0.688	0.735	0.782	1.011	1.240
100	1000	0.40	0.894	0.904	0.917	0.926	0.963	1.016	1.066	1.122	1.402	1.672
100	1000	0.60	1.469	1.459	1.456	1.445	1.454	1.480	1.516	1.566	1.820	2.064
100	1000	0.80	2.345	2.321	2.304	2.274	2.235	2.219	2.216	2.244	2.382	2.521
100	1000	1.00	3.192	3.174	3.161	3.135	3.099	3.079	3.065	3.080	3.141	3.214
100	1000	1.20	3.669	3.680	3.690	3.702	3.745	3.786	3.825	3.861	4.042	4.217
100	1500	-0.20	0.341	0.371	0.401	0.430	0.551	0.672	0.793	0.910	1.493	2.073
100	1500	-0.10	0.265	0.291	0.318	0.347	0.453	0.555	0.656	0.748	1.208	1.669
100	1500	-0.05	0.190	0.214	0.240	0.268	0.367	0.461	0.551	0.622	0.981	1.350
100	1500	0.00	0.173	0.197	0.223	0.251	0.332	0.413	0.490	0.543	0.814	1.101
100	1500	0.05	0.262	0.282	0.303	0.327	0.389	0.455	0.516	0.561	0.793	1.039
100	1500	0.10	0.464	0.478	0.493	0.510	0.567	0.620	0.673	0.717	0.944	1.180
100	1500	0.20	0.867	0.874	0.882	0.887	0.923	0.961	1.004	1.052	1.287	1.518
100	1500	0.40	1.666	1.650	1.639	1.618	1.606	1.613	1.628	1.678	1.915	2.135
100	1500	0.60	2.678	2.641	2.611	2.566	2.495	2.453	2.428	2.463	2.616	2.748
100	1500	0.80	3.846	3.808	3.776	3.730	3.636	3.571	3.520	3.524	3.544	3.548
100	1500	1.00	4.782	4.765	4.750	4.727	4.682	4.646	4.620	4.625	4.635	4.637
100	1500	1.20	5.174	5.189	5.204	5.219	5.278	5.336	5.388	5.434	5.681	5.928
100	2000	-0.20	0.381	0.409	0.437	0.464	0.582	0.701	0.822	0.943	1.546	2.140
100	2000	-0.10	0.286	0.312	0.338	0.364	0.467	0.566	0.665	0.756	1.211	1.664
100	2000	-0.05	0.197	0.222	0.248	0.275	0.371	0.461	0.549	0.619	0.974	1.339
100	2000	0.00	0.187	0.210	0.232	0.257	0.341	0.419	0.494	0.547	0.819	1.108
100	2000	0.05	0.343	0.358	0.374	0.391	0.453	0.513	0.573	0.618	0.852	1.102
100	2000	0.10	0.664	0.672	0.682	0.690	0.733	0.776	0.823	0.866	1.087	1.314
100	2000	0.20	1.302	1.297	1.296	1.287	1.296	1.313	1.334	1.377	1.569	1.757
100	2000	0.40	2.544	2.511	2.484	2.442	2.372	2.329	2.296	2.327	2.459	2.564

P	G	Xe	q (kW m-2)									
			50	100	150	200	400	600	800	1000	2000	3000
(kPa)	(kg m-2 s-1)	(-)	Heat Transfer Coefficient (kW m-2 K-2)									
100	2000	0.60	3.863	3.815	3.772	3.714	3.590	3.499	3.428	3.439	3.465	3.465
100	2000	0.80	5.169	5.131	5.097	5.054	4.948	4.863	4.793	4.787	4.731	4.652
100	2000	1.00	6.178	6.167	6.156	6.143	6.110	6.085	6.082	6.080	6.079	6.066
100	2000	1.20	6.638	6.654	6.669	6.685	6.747	6.809	6.871	6.926	7.208	7.496
100	3000	-0.20	0.418	0.446	0.473	0.502	0.618	0.736	0.856	0.979	1.589	2.183
100	3000	-0.10	0.299	0.326	0.353	0.380	0.484	0.584	0.683	0.774	1.231	1.682
100	3000	-0.05	0.203	0.228	0.253	0.279	0.374	0.464	0.552	0.625	0.993	1.367
100	3000	0.00	0.230	0.250	0.270	0.293	0.372	0.448	0.522	0.579	0.869	1.175
100	3000	0.05	0.548	0.558	0.569	0.580	0.630	0.680	0.732	0.779	1.016	1.265
100	3000	0.10	1.085	1.087	1.090	1.090	1.112	1.138	1.168	1.208	1.401	1.595
100	3000	0.20	2.110	2.096	2.086	2.069	2.043	2.032	2.020	2.044	2.153	2.244
100	3000	0.40	4.003	3.966	3.931	3.890	3.784	3.704	3.635	3.628	3.581	3.506
100	3000	0.60	5.798	5.756	5.715	5.671	5.542	5.442	5.353	5.325	5.179	5.018
100	3000	0.80	7.460	7.432	7.406	7.379	7.297	7.230	7.171	7.148	7.025	6.892
100	3000	1.00	8.782	8.778	8.774	8.769	8.758	8.752	8.747	8.742	8.736	8.731
100	3000	1.20	9.477	9.492	9.506	9.522	9.582	9.643	9.704	9.764	10.066	10.373
100	4000	-0.20	0.435	0.464	0.491	0.522	0.634	0.749	0.862	0.974	1.532	2.080
100	4000	-0.10	0.296	0.325	0.353	0.383	0.489	0.590	0.689	0.778	1.222	1.661
100	4000	-0.05	0.205	0.231	0.256	0.283	0.378	0.470	0.558	0.632	1.007	1.387
100	4000	0.00	0.278	0.296	0.315	0.336	0.413	0.489	0.563	0.623	0.930	1.253
100	4000	0.05	0.749	0.757	0.766	0.774	0.816	0.861	0.908	0.956	1.197	1.448
100	4000	0.10	1.458	1.458	1.460	1.462	1.474	1.494	1.517	1.555	1.736	1.913
100	4000	0.20	2.770	2.759	2.749	2.737	2.711	2.709	2.690	2.703	2.770	2.823
100	4000	0.40	5.171	5.145	5.120	5.094	5.012	4.956	4.890	4.866	4.743	4.606
100	4000	0.60	7.452	7.422	7.393	7.365	7.270	7.190	7.118	7.080	6.882	6.684
100	4000	0.80	9.591	9.569	9.548	9.527	9.462	9.409	9.361	9.337	9.213	9.083
100	4000	1.00	11.310	11.304	11.299	11.291	11.277	11.268	11.262	11.250	11.244	11.230
100	4000	1.20	12.198	12.211	12.225	12.239	12.295	12.354	12.412	12.471	12.768	13.070
100	5000	-0.20	0.458	0.488	0.516	0.549	0.663	0.777	0.889	0.994	1.524	2.051
100	5000	-0.10	0.285	0.316	0.346	0.379	0.489	0.594	0.695	0.784	1.228	1.671
100	5000	-0.05	0.208	0.234	0.259	0.287	0.382	0.474	0.563	0.639	1.020	1.409
100	5000	0.00	0.334	0.350	0.367	0.388	0.460	0.534	0.607	0.669	0.985	1.318
100	5000	0.05	0.943	0.951	0.959	0.967	1.004	1.045	1.088	1.134	1.367	1.610
100	5000	0.10	1.798	1.800	1.803	1.804	1.820	1.840	1.862	1.896	2.059	2.221
100	5000	0.20	3.360	3.356	3.353	3.349	3.342	3.337	3.334	3.347	3.400	3.439
100	5000	0.40	6.234	6.221	6.209	6.199	6.157	6.120	6.085	6.060	5.935	5.805
100	5000	0.60	9.009	8.989	8.970	8.954	8.894	8.843	8.795	8.758	8.576	8.403
100	5000	0.80	11.648	11.628	11.609	11.590	11.532	11.486	11.446	11.424	11.314	11.201
100	5000	1.00	13.764	13.754	13.746	13.734	13.710	13.692	13.678	13.670	13.665	13.658
100	5000	1.20	14.832	14.845	14.858	14.872	14.926	14.982	15.039	15.096	15.382	15.670
100	6000	-0.20	0.505	0.535	0.565	0.599	0.719	0.840	0.960	1.076	1.658	2.250
100	6000	-0.10	0.277	0.310	0.341	0.375	0.493	0.605	0.712	0.807	1.285	1.767
100	6000	-0.05	0.212	0.238	0.263	0.291	0.387	0.480	0.569	0.645	1.032	1.432
100	6000	0.00	0.387	0.402	0.418	0.438	0.506	0.577	0.647	0.705	1.008	1.445
100	6000	0.05	1.117	1.124	1.132	1.140	1.174	1.212	1.251	1.290	1.491	1.708
100	6000	0.10	2.112	2.115	2.118	2.120	2.137	2.155	2.176	2.203	2.334	2.480
100	6000	0.20	3.940	3.939	3.938	3.935	3.935	3.937	3.942	3.953	4.010	4.064

P	G	Xe	q (kW m-2)									
			50	100	150	200	400	600	800	1000	2000	3000
(kPa)	(kg m-2 s-1)	(-)	Heat Transfer Coefficient (kW m-2 K-2)									
100	6000	0.40	7.335	7.323	7.312	7.300	7.266	7.238	7.214	7.200	7.132	7.068
100	6000	0.60	10.619	10.596	10.575	10.556	10.491	10.440	10.395	10.369	10.239	10.116
100	6000	0.80	13.716	13.692	13.669	13.647	13.578	13.524	13.476	13.453	13.340	13.220
100	6000	1.00	16.172	16.160	16.150	16.137	16.103	16.077	16.054	16.052	16.043	16.019
100	6000	1.20	17.406	17.419	17.432	17.446	17.500	17.557	17.614	17.671	17.959	18.251
100	7000	-0.20	0.546	0.577	0.608	0.641	0.771	0.904	1.038	1.175	1.860	2.554
100	7000	-0.10	0.267	0.301	0.333	0.368	0.492	0.612	0.729	0.838	1.382	1.929
100	7000	-0.05	0.217	0.242	0.267	0.295	0.394	0.492	0.588	0.674	1.109	1.559
100	7000	0.00	0.447	0.461	0.475	0.495	0.563	0.635	0.708	0.773	1.110	1.549
100	7000	0.05	1.284	1.292	1.300	1.309	1.347	1.388	1.431	1.476	1.703	1.951
100	7000	0.10	2.421	2.425	2.430	2.433	2.454	2.478	2.504	2.537	2.698	2.873
100	7000	0.20	4.522	4.521	4.520	4.517	4.518	4.522	4.529	4.547	4.630	4.717
100	7000	0.40	8.430	8.416	8.403	8.390	8.353	8.326	8.304	8.299	8.275	8.260
100	7000	0.60	12.204	12.179	12.156	12.135	12.066	12.015	11.969	11.947	11.840	11.743
100	7000	0.80	15.739	15.714	15.689	15.667	15.592	15.533	15.479	15.449	15.302	15.153
100	7000	1.00	18.520	18.509	18.498	18.486	18.449	18.418	18.390	18.379	18.319	18.246
100	7000	1.20	19.935	19.947	19.959	19.973	20.027	20.084	20.141	20.198	20.488	20.785
200	0	-0.20	0.198	0.222	0.252	0.282	0.408	0.534	0.662	0.795	1.462	2.121
200	0	-0.10	0.196	0.220	0.244	0.268	0.384	0.498	0.616	0.741	1.366	1.981
200	0	-0.05	0.180	0.204	0.235	0.256	0.363	0.479	0.596	0.721	1.350	1.965
200	0	0.00	0.161	0.181	0.209	0.235	0.338	0.458	0.576	0.704	1.343	1.969
200	0	0.05	0.120	0.142	0.172	0.201	0.313	0.440	0.561	0.691	1.338	1.975
200	0	0.10	0.089	0.112	0.148	0.175	0.302	0.428	0.552	0.682	1.334	1.977
200	0	0.20	0.050	0.077	0.119	0.147	0.281	0.410	0.538	0.669	1.324	1.970
200	0	0.40	0.066	0.079	0.116	0.143	0.274	0.404	0.531	0.662	1.318	1.964
200	0	0.60	0.099	0.126	0.150	0.174	0.297	0.418	0.541	0.671	1.323	1.966
200	0	0.80	0.102	0.129	0.162	0.186	0.306	0.425	0.547	0.676	1.324	1.968
200	0	1.00	0.094	0.124	0.155	0.183	0.304	0.424	0.546	0.675	1.321	1.955
200	0	1.20	0.068	0.097	0.128	0.159	0.285	0.409	0.533	0.664	1.317	1.954
200	50	-0.20	0.236	0.264	0.290	0.318	0.421	0.524	0.625	0.719	1.178	1.657
200	50	-0.10	0.229	0.253	0.279	0.302	0.389	0.478	0.566	0.649	1.058	1.482
200	50	-0.05	0.195	0.223	0.253	0.271	0.354	0.433	0.515	0.593	0.972	1.367
200	50	0.00	0.149	0.172	0.194	0.217	0.305	0.383	0.467	0.543	0.913	1.301
200	50	0.05	0.108	0.133	0.153	0.176	0.271	0.350	0.436	0.511	0.878	1.267
200	50	0.10	0.087	0.113	0.137	0.158	0.251	0.335	0.421	0.496	0.865	1.256
200	50	0.20	0.087	0.113	0.147	0.165	0.251	0.325	0.407	0.483	0.858	1.251
200	50	0.40	0.111	0.144	0.170	0.185	0.260	0.328	0.406	0.482	0.853	1.243
200	50	0.60	0.127	0.152	0.183	0.191	0.273	0.342	0.420	0.497	0.870	1.262
200	50	0.80	0.131	0.154	0.196	0.203	0.288	0.362	0.444	0.521	0.897	1.293
200	50	1.00	0.144	0.165	0.198	0.220	0.305	0.391	0.475	0.554	0.938	1.343
200	50	1.20	0.212	0.231	0.250	0.272	0.352	0.435	0.518	0.597	0.983	1.389
200	100	-0.20	0.288	0.323	0.349	0.356	0.451	0.546	0.638	0.718	1.116	1.530
200	100	-0.10	0.286	0.320	0.347	0.354	0.420	0.496	0.571	0.640	0.981	1.333
200	100	-0.05	0.262	0.293	0.336	0.353	0.402	0.450	0.500	0.560	0.855	1.162
200	100	0.00	0.152	0.182	0.216	0.240	0.318	0.376	0.429	0.483	0.755	1.042
200	100	0.05	0.110	0.143	0.172	0.189	0.277	0.317	0.386	0.440	0.702	0.982
200	100	0.10	0.106	0.139	0.167	0.179	0.250	0.306	0.373	0.427	0.689	0.969

P	G	Xe	q (kW m-2)									
			50	100	150	200	400	600	800	1000	2000	3000
(kPa)	(kg m-2 s-1)	(-)	Heat Transfer Coefficient (kW m-2 K-2)									
200	100	0.20	0.126	0.161	0.192	0.206	0.265	0.308	0.365	0.419	0.684	0.962
200	100	0.40	0.151	0.192	0.218	0.233	0.281	0.321	0.374	0.428	0.689	0.965
200	100	0.60	0.169	0.195	0.226	0.234	0.287	0.337	0.396	0.452	0.727	1.018
200	100	0.80	0.173	0.200	0.236	0.242	0.312	0.372	0.438	0.496	0.783	1.089
200	100	1.00	0.218	0.239	0.271	0.291	0.363	0.434	0.503	0.562	0.857	1.172
200	100	1.20	0.382	0.395	0.409	0.425	0.481	0.543	0.604	0.661	0.941	1.238
200	200	-0.20	0.309	0.343	0.370	0.397	0.493	0.585	0.675	0.752	1.142	1.552
200	200	-0.10	0.300	0.372	0.423	0.446	0.483	0.531	0.599	0.666	0.995	1.337
200	200	-0.05	0.286	0.322	0.358	0.383	0.455	0.484	0.551	0.604	0.847	1.137
200	200	0.00	0.156	0.193	0.229	0.263	0.359	0.406	0.450	0.497	0.723	0.980
200	200	0.05	0.135	0.174	0.206	0.239	0.322	0.357	0.410	0.454	0.660	0.904
200	200	0.10	0.152	0.192	0.206	0.239	0.287	0.337	0.383	0.428	0.653	0.900
200	200	0.20	0.207	0.256	0.273	0.306	0.352	0.382	0.416	0.461	0.681	0.907
200	200	0.40	0.239	0.321	0.365	0.406	0.428	0.430	0.464	0.510	0.737	0.962
200	200	0.60	0.274	0.325	0.368	0.410	0.436	0.442	0.490	0.541	0.797	1.067
200	200	0.80	0.308	0.329	0.370	0.415	0.445	0.506	0.566	0.621	0.899	1.192
200	200	1.00	0.499	0.502	0.521	0.536	0.596	0.655	0.713	0.767	1.040	1.332
200	200	1.20	0.810	0.820	0.827	0.835	0.871	0.912	0.955	1.001	1.232	1.484
200	500	-0.20	0.325	0.359	0.389	0.418	0.528	0.638	0.740	0.830	1.299	1.746
200	500	-0.10	0.289	0.332	0.400	0.441	0.505	0.563	0.649	0.726	1.113	1.490
200	500	-0.05	0.261	0.292	0.332	0.362	0.453	0.496	0.566	0.614	0.919	1.227
200	500	0.00	0.171	0.202	0.230	0.260	0.361	0.425	0.457	0.503	0.751	1.000
200	500	0.05	0.188	0.220	0.240	0.263	0.350	0.424	0.439	0.484	0.683	0.892
200	500	0.10	0.219	0.267	0.282	0.314	0.398	0.480	0.493	0.532	0.707	0.896
200	500	0.20	0.311	0.367	0.388	0.444	0.486	0.535	0.549	0.587	0.766	0.958
200	500	0.40	0.461	0.488	0.526	0.574	0.599	0.634	0.670	0.716	0.939	1.166
200	500	0.60	0.593	0.610	0.640	0.665	0.710	0.762	0.817	0.870	1.143	1.404
200	500	0.80	0.921	0.922	0.929	0.931	0.973	1.021	1.075	1.127	1.402	1.659
200	500	1.00	1.428	1.430	1.434	1.436	1.461	1.485	1.519	1.562	1.773	1.985
200	500	1.20	2.016	2.020	2.024	2.028	2.046	2.068	2.093	2.125	2.278	2.439
200	1000	-0.20	0.340	0.371	0.399	0.430	0.546	0.661	0.775	0.881	1.410	1.933
200	1000	-0.10	0.282	0.308	0.333	0.360	0.463	0.561	0.663	0.753	1.200	1.642
200	1000	-0.05	0.253	0.265	0.296	0.325	0.425	0.539	0.566	0.639	0.992	1.342
200	1000	0.00	0.210	0.238	0.268	0.300	0.423	0.537	0.542	0.590	0.825	1.073
200	1000	0.05	0.264	0.301	0.336	0.369	0.496	0.596	0.554	0.589	0.768	0.963
200	1000	0.10	0.335	0.370	0.404	0.453	0.598	0.674	0.638	0.672	0.840	1.025
200	1000	0.20	0.547	0.581	0.598	0.622	0.675	0.715	0.754	0.799	1.018	1.238
200	1000	0.40	0.913	0.917	0.938	0.952	0.974	1.018	1.075	1.131	1.408	1.680
200	1000	0.60	1.506	1.494	1.484	1.469	1.473	1.493	1.526	1.577	1.836	2.088
200	1000	0.80	2.426	2.395	2.373	2.336	2.283	2.253	2.240	2.267	2.411	2.557
200	1000	1.00	3.297	3.272	3.253	3.220	3.168	3.131	3.105	3.100	3.178	3.246
200	1000	1.20	3.703	3.713	3.723	3.735	3.775	3.813	3.852	3.886	4.056	4.223
200	1500	-0.20	0.394	0.421	0.447	0.472	0.578	0.683	0.790	0.897	1.427	1.972
200	1500	-0.10	0.298	0.321	0.345	0.370	0.470	0.567	0.663	0.752	1.195	1.648
200	1500	-0.05	0.226	0.248	0.272	0.298	0.385	0.474	0.562	0.631	0.980	1.343
200	1500	0.00	0.213	0.237	0.268	0.296	0.373	0.442	0.504	0.556	0.820	1.100
200	1500	0.05	0.304	0.328	0.360	0.391	0.442	0.493	0.534	0.577	0.800	1.037

P	G	Xe	q (kW m-2)									
			50	100	150	200	400	600	800	1000	2000	3000
(kPa)	(kg m-2 s-1)	(-)	Heat Transfer Coefficient (kW m-2 K-2)									
200	1500	0.10	0.479	0.492	0.511	0.529	0.598	0.649	0.689	0.732	0.951	1.179
200	1500	0.20	0.892	0.895	0.902	0.903	0.939	0.976	1.017	1.064	1.296	1.524
200	1500	0.40	1.704	1.685	1.672	1.643	1.628	1.625	1.641	1.691	1.933	2.157
200	1500	0.60	2.760	2.715	2.681	2.627	2.543	2.486	2.455	2.489	2.646	2.779
200	1500	0.80	3.994	3.948	3.909	3.853	3.738	3.648	3.579	3.577	3.574	3.581
200	1500	1.00	4.943	4.920	4.900	4.871	4.806	4.754	4.709	4.704	4.700	4.661
200	1500	1.20	5.215	5.231	5.246	5.262	5.321	5.378	5.435	5.481	5.712	5.949
200	2000	-0.20	0.446	0.471	0.495	0.518	0.617	0.718	0.821	0.929	1.466	2.014
200	2000	-0.10	0.328	0.352	0.376	0.400	0.494	0.585	0.677	0.764	1.198	1.639
200	2000	-0.05	0.225	0.249	0.273	0.299	0.390	0.477	0.561	0.630	0.976	1.335
200	2000	0.00	0.208	0.230	0.253	0.278	0.354	0.431	0.508	0.560	0.829	1.114
200	2000	0.05	0.355	0.371	0.388	0.405	0.460	0.519	0.582	0.626	0.859	1.106
200	2000	0.10	0.680	0.687	0.696	0.702	0.740	0.783	0.831	0.875	1.095	1.320
200	2000	0.20	1.332	1.325	1.323	1.310	1.316	1.327	1.348	1.389	1.588	1.775
200	2000	0.40	2.613	2.574	2.543	2.493	2.413	2.353	2.319	2.351	2.489	2.597
200	2000	0.60	3.998	3.941	3.891	3.824	3.679	3.568	3.483	3.493	3.511	3.515
200	2000	0.80	5.374	5.329	5.287	5.235	5.104	5.000	4.911	4.898	4.807	4.687
200	2000	1.00	6.384	6.368	6.353	6.334	6.282	6.240	6.203	6.200	6.166	6.104
200	2000	1.20	6.685	6.701	6.717	6.733	6.795	6.855	6.915	6.970	7.249	7.532
200	3000	-0.20	0.507	0.531	0.554	0.576	0.671	0.767	0.865	0.970	1.492	2.019
200	3000	-0.10	0.357	0.382	0.406	0.432	0.524	0.614	0.702	0.786	1.205	1.628
200	3000	-0.05	0.239	0.264	0.287	0.313	0.403	0.488	0.571	0.640	0.989	1.349
200	3000	0.00	0.250	0.270	0.289	0.312	0.391	0.467	0.540	0.596	0.881	1.183
200	3000	0.05	0.562	0.571	0.581	0.590	0.640	0.690	0.741	0.788	1.027	1.277
200	3000	0.10	1.115	1.114	1.112	1.113	1.130	1.153	1.181	1.221	1.417	1.612
200	3000	0.20	2.169	2.153	2.141	2.119	2.086	2.061	2.050	2.076	2.185	2.278
200	3000	0.40	4.134	4.092	4.052	4.003	3.880	3.781	3.698	3.694	3.639	3.552
200	3000	0.60	6.023	5.973	5.924	5.869	5.712	5.582	5.469	5.439	5.256	5.053
200	3000	0.80	7.768	7.733	7.699	7.661	7.547	7.451	7.364	7.329	7.135	6.923
200	3000	1.00	9.080	9.070	9.061	9.048	9.014	8.983	8.955	8.949	8.907	8.841
200	3000	1.20	9.544	9.558	9.572	9.586	9.641	9.699	9.757	9.817	10.117	10.420
200	4000	-0.20	0.553	0.577	0.600	0.623	0.711	0.799	0.887	0.979	1.436	1.902
200	4000	-0.10	0.367	0.395	0.420	0.448	0.541	0.630	0.717	0.795	1.188	1.587
200	4000	-0.05	0.247	0.272	0.296	0.322	0.412	0.498	0.581	0.651	0.998	1.358
200	4000	0.00	0.298	0.317	0.335	0.356	0.433	0.509	0.583	0.642	0.943	1.262
200	4000	0.05	0.773	0.780	0.787	0.793	0.833	0.876	0.922	0.970	1.212	1.463
200	4000	0.10	1.506	1.504	1.503	1.497	1.504	1.518	1.537	1.575	1.755	1.932
200	4000	0.20	2.862	2.848	2.835	2.817	2.780	2.748	2.731	2.750	2.818	2.865
200	4000	0.40	5.357	5.326	5.296	5.262	5.161	5.072	4.998	4.974	4.830	4.665
200	4000	0.60	7.753	7.715	7.678	7.640	7.516	7.410	7.312	7.263	7.004	6.738
200	4000	0.80	9.996	9.966	9.937	9.905	9.806	9.720	9.640	9.599	9.379	9.145
200	4000	1.00	11.701	11.689	11.679	11.663	11.623	11.587	11.554	11.547	11.493	11.416
200	4000	1.20	12.284	12.297	12.310	12.324	12.379	12.435	12.491	12.550	12.842	13.135
200	5000	-0.20	0.588	0.614	0.638	0.664	0.756	0.846	0.934	1.024	1.467	1.920
200	5000	-0.10	0.364	0.394	0.422	0.452	0.551	0.645	0.735	0.815	1.211	1.615
200	5000	-0.05	0.253	0.278	0.302	0.330	0.421	0.509	0.593	0.664	1.021	1.392
200	5000	0.00	0.355	0.371	0.388	0.409	0.482	0.556	0.630	0.690	1.003	1.334

P	G	Xe	q (kW m-2)									
			50	100	150	200	400	600	800	1000	2000	3000
(kPa)	(kg m-2 s-1)	(-)	Heat Transfer Coefficient (kW m-2 K-2)									
200	5000	0.05	0.976	0.982	0.990	0.996	1.029	1.068	1.110	1.157	1.391	1.633
200	5000	0.10	1.862	1.861	1.860	1.858	1.866	1.879	1.895	1.928	2.087	2.244
200	5000	0.20	3.481	3.473	3.466	3.456	3.434	3.417	3.404	3.414	3.453	3.477
200	5000	0.40	6.466	6.448	6.431	6.413	6.351	6.296	6.243	6.211	6.042	5.868
200	5000	0.60	9.375	9.349	9.323	9.298	9.211	9.133	9.060	9.008	8.745	8.487
200	5000	0.80	12.141	12.113	12.086	12.056	11.965	11.886	11.813	11.770	11.549	11.313
200	5000	1.00	14.237	14.223	14.210	14.189	14.140	14.093	14.051	14.039	13.960	13.857
200	5000	1.20	14.936	14.949	14.962	14.976	15.030	15.085	15.140	15.196	15.473	15.749
200	6000	-0.20	0.633	0.661	0.688	0.716	0.822	0.927	1.032	1.142	1.686	2.232
200	6000	-0.10	0.360	0.392	0.423	0.456	0.567	0.673	0.774	0.866	1.324	1.782
200	6000	-0.05	0.258	0.284	0.308	0.336	0.431	0.523	0.611	0.686	1.065	1.460
200	6000	0.00	0.406	0.421	0.437	0.457	0.528	0.600	0.672	0.731	1.041	1.479
200	6000	0.05	1.153	1.159	1.166	1.172	1.206	1.242	1.281	1.323	1.533	1.754
200	6000	0.10	2.186	2.187	2.188	2.189	2.196	2.210	2.226	2.252	2.382	2.514
200	6000	0.20	4.081	4.076	4.071	4.062	4.048	4.037	4.030	4.038	4.067	4.084
200	6000	0.40	7.606	7.588	7.572	7.552	7.496	7.447	7.403	7.379	7.250	7.114
200	6000	0.60	11.047	11.018	10.989	10.961	10.869	10.791	10.720	10.675	10.449	10.225
200	6000	0.80	14.289	14.258	14.228	14.196	14.095	14.008	13.927	13.881	13.639	13.383
200	6000	1.00	16.719	16.704	16.690	16.669	16.612	16.557	16.506	16.484	16.352	16.196
200	6000	1.20	17.526	17.539	17.552	17.566	17.620	17.676	17.731	17.787	18.066	18.345
200	7000	-0.20	0.663	0.692	0.721	0.750	0.867	0.986	1.105	1.232	1.864	2.501
200	7000	-0.10	0.348	0.382	0.415	0.448	0.569	0.684	0.796	0.900	1.420	1.937
200	7000	-0.05	0.261	0.287	0.313	0.341	0.440	0.537	0.631	0.715	1.141	1.582
200	7000	0.00	0.465	0.480	0.494	0.514	0.583	0.657	0.731	0.797	1.137	1.501
200	7000	0.05	1.325	1.332	1.339	1.346	1.383	1.423	1.466	1.512	1.746	1.991
200	7000	0.10	2.506	2.508	2.511	2.511	2.526	2.544	2.566	2.598	2.754	2.908
200	7000	0.20	4.681	4.676	4.672	4.663	4.652	4.644	4.640	4.651	4.702	4.740
200	7000	0.40	8.733	8.714	8.697	8.676	8.619	8.571	8.528	8.510	8.413	8.305
200	7000	0.60	12.687	12.656	12.625	12.595	12.498	12.417	12.344	12.301	12.085	11.864
200	7000	0.80	16.384	16.352	16.321	16.289	16.182	16.088	16.000	15.944	15.653	15.350
200	7000	1.00	19.128	19.115	19.101	19.080	19.021	18.962	18.904	18.870	18.678	18.464
200	7000	1.20	20.068	20.081	20.093	20.107	20.161	20.216	20.271	20.327	20.608	20.891
500	0	-0.20	0.246	0.272	0.299	0.324	0.439	0.553	0.670	0.796	1.425	2.043
500	0	-0.10	0.233	0.257	0.283	0.306	0.417	0.527	0.640	0.765	1.388	1.996
500	0	-0.05	0.214	0.238	0.266	0.289	0.401	0.510	0.625	0.751	1.384	2.001
500	0	0.00	0.198	0.221	0.247	0.269	0.383	0.496	0.611	0.739	1.380	2.005
500	0	0.05	0.173	0.197	0.226	0.252	0.369	0.485	0.603	0.731	1.374	2.003
500	0	0.10	0.152	0.176	0.211	0.238	0.358	0.476	0.594	0.724	1.369	2.000
500	0	0.20	0.122	0.150	0.186	0.215	0.338	0.456	0.578	0.708	1.357	1.992
500	0	0.40	0.124	0.145	0.178	0.206	0.328	0.446	0.567	0.698	1.349	1.985
500	0	0.60	0.147	0.173	0.194	0.218	0.340	0.454	0.572	0.702	1.350	1.987
500	0	0.80	0.155	0.182	0.209	0.234	0.348	0.461	0.577	0.706	1.350	1.988
500	0	1.00	0.148	0.177	0.204	0.231	0.347	0.460	0.575	0.705	1.349	1.974
500	0	1.20	0.118	0.147	0.178	0.207	0.329	0.447	0.568	0.697	1.344	1.973
500	50	-0.20	0.276	0.299	0.323	0.346	0.436	0.527	0.617	0.699	1.101	1.524
500	50	-0.10	0.258	0.279	0.300	0.322	0.404	0.488	0.571	0.650	1.036	1.440
500	50	-0.05	0.235	0.256	0.275	0.295	0.375	0.454	0.534	0.610	0.983	1.372

P	G	Xe	q (kW m ⁻²)									
			50	100	150	200	400	600	800	1000	2000	3000
(kPa)	(kg m ⁻² s ⁻¹)	(-)	Heat Transfer Coefficient (kW m ⁻² K ⁻²)									
500	50	0.00	0.203	0.225	0.241	0.261	0.340	0.419	0.500	0.576	0.945	1.331
500	50	0.05	0.167	0.190	0.213	0.233	0.314	0.394	0.475	0.549	0.908	1.287
500	50	0.10	0.142	0.165	0.189	0.212	0.293	0.372	0.452	0.526	0.885	1.263
500	50	0.20	0.120	0.148	0.171	0.189	0.266	0.343	0.420	0.496	0.865	1.251
500	50	0.40	0.125	0.153	0.177	0.194	0.265	0.338	0.412	0.487	0.852	1.233
500	50	0.60	0.133	0.155	0.192	0.211	0.278	0.354	0.429	0.504	0.866	1.246
500	50	0.80	0.150	0.172	0.196	0.215	0.294	0.375	0.455	0.529	0.893	1.278
500	50	1.00	0.178	0.199	0.220	0.243	0.323	0.406	0.488	0.564	0.934	1.326
500	50	1.20	0.242	0.260	0.278	0.297	0.372	0.451	0.531	0.608	0.983	1.377
500	100	-0.20	0.302	0.326	0.348	0.373	0.457	0.542	0.624	0.692	1.037	1.399
500	100	-0.10	0.283	0.304	0.324	0.346	0.419	0.494	0.567	0.630	0.949	1.281
500	100	-0.05	0.263	0.286	0.299	0.317	0.377	0.444	0.510	0.569	0.856	1.159
500	100	0.00	0.218	0.242	0.252	0.273	0.330	0.389	0.456	0.511	0.783	1.073
500	100	0.05	0.163	0.191	0.214	0.224	0.295	0.353	0.419	0.472	0.734	1.015
500	100	0.10	0.130	0.158	0.179	0.198	0.270	0.329	0.394	0.448	0.709	0.989
500	100	0.20	0.116	0.156	0.165	0.186	0.245	0.304	0.361	0.415	0.682	0.962
500	100	0.40	0.108	0.148	0.181	0.203	0.258	0.312	0.364	0.417	0.675	0.946
500	100	0.60	0.107	0.131	0.198	0.226	0.277	0.339	0.397	0.451	0.714	0.994
500	100	0.80	0.168	0.190	0.216	0.236	0.305	0.376	0.442	0.498	0.771	1.066
500	100	1.00	0.247	0.264	0.283	0.302	0.371	0.441	0.510	0.567	0.847	1.150
500	100	1.20	0.401	0.412	0.424	0.436	0.489	0.546	0.607	0.662	0.934	1.223
500	200	-0.20	0.342	0.369	0.392	0.419	0.506	0.586	0.666	0.728	1.048	1.402
500	200	-0.10	0.321	0.343	0.362	0.386	0.460	0.528	0.597	0.656	0.954	1.276
500	200	-0.05	0.303	0.322	0.334	0.357	0.416	0.466	0.527	0.579	0.843	1.128
500	200	0.00	0.216	0.238	0.248	0.275	0.358	0.411	0.455	0.502	0.743	1.005
500	200	0.05	0.162	0.197	0.220	0.241	0.326	0.375	0.417	0.461	0.684	0.929
500	200	0.10	0.122	0.158	0.185	0.208	0.291	0.361	0.405	0.448	0.666	0.908
500	200	0.20	0.148	0.182	0.195	0.214	0.289	0.333	0.391	0.435	0.657	0.900
500	200	0.40	0.172	0.234	0.264	0.282	0.329	0.374	0.423	0.469	0.698	0.947
500	200	0.60	0.180	0.238	0.313	0.349	0.387	0.438	0.480	0.530	0.781	1.052
500	200	0.80	0.293	0.311	0.344	0.368	0.429	0.497	0.569	0.623	0.890	1.181
500	200	1.00	0.506	0.511	0.529	0.543	0.597	0.656	0.720	0.773	1.036	1.325
500	200	1.20	0.827	0.831	0.834	0.836	0.860	0.897	0.944	0.991	1.224	1.478
500	500	-0.20	0.407	0.437	0.462	0.492	0.588	0.681	0.769	0.842	1.237	1.614
500	500	-0.10	0.361	0.386	0.412	0.439	0.519	0.599	0.679	0.747	1.104	1.446
500	500	-0.05	0.307	0.345	0.378	0.405	0.493	0.533	0.585	0.642	0.933	1.215
500	500	0.00	0.227	0.259	0.286	0.318	0.440	0.539	0.542	0.591	0.776	0.997
500	500	0.05	0.210	0.255	0.302	0.333	0.452	0.547	0.548	0.568	0.707	0.891
500	500	0.10	0.188	0.242	0.310	0.360	0.457	0.555	0.560	0.569	0.720	0.897
500	500	0.20	0.245	0.275	0.328	0.392	0.464	0.560	0.565	0.586	0.767	0.956
500	500	0.40	0.377	0.384	0.415	0.452	0.519	0.583	0.651	0.697	0.944	1.171
500	500	0.60	0.543	0.549	0.551	0.554	0.656	0.738	0.814	0.869	1.162	1.427
500	500	0.80	0.975	0.973	0.970	0.958	1.007	1.051	1.107	1.161	1.436	1.697
500	500	1.00	1.556	1.540	1.530	1.509	1.508	1.526	1.553	1.598	1.804	2.022
500	500	1.20	2.058	2.055	2.053	2.040	2.039	2.038	2.074	2.110	2.272	2.445
500	1000	-0.20	0.454	0.482	0.507	0.536	0.632	0.729	0.825	0.916	1.381	1.843
500	1000	-0.10	0.398	0.422	0.437	0.454	0.539	0.629	0.718	0.803	1.226	1.643

P	G	Xe	q (kW m-2)									
			50	100	150	200	400	600	800	1000	2000	3000
(kPa)	(kg m-2 s-1)	(-)	Heat Transfer Coefficient (kW m-2 K-2)									
500	1000	-0.05	0.348	0.383	0.400	0.414	0.534	0.590	0.626	0.693	1.021	1.347
500	1000	0.00	0.288	0.323	0.362	0.402	0.529	0.587	0.596	0.637	0.847	1.073
500	1000	0.05	0.291	0.340	0.397	0.452	0.572	0.625	0.606	0.635	0.789	0.964
500	1000	0.10	0.386	0.414	0.481	0.531	0.618	0.694	0.665	0.697	0.858	1.034
500	1000	0.20	0.567	0.590	0.623	0.654	0.711	0.754	0.793	0.834	1.040	1.246
500	1000	0.40	0.917	0.924	0.945	0.962	1.010	1.037	1.105	1.161	1.434	1.705
500	1000	0.60	1.587	1.569	1.546	1.523	1.525	1.529	1.554	1.606	1.875	2.140
500	1000	0.80	2.638	2.592	2.556	2.505	2.413	2.339	2.297	2.322	2.475	2.633
500	1000	1.00	3.562	3.519	3.484	3.434	3.325	3.231	3.166	3.164	3.242	3.309
500	1000	1.20	3.792	3.797	3.802	3.809	3.824	3.845	3.870	3.905	4.064	4.227
500	1500	-0.20	0.519	0.543	0.564	0.587	0.670	0.757	0.845	0.938	1.401	1.879
500	1500	-0.10	0.407	0.428	0.447	0.467	0.552	0.641	0.725	0.812	1.243	1.680
500	1500	-0.05	0.320	0.340	0.378	0.405	0.460	0.539	0.617	0.685	1.025	1.376
500	1500	0.00	0.308	0.330	0.377	0.404	0.455	0.506	0.551	0.600	0.852	1.118
500	1500	0.05	0.365	0.394	0.439	0.469	0.499	0.541	0.575	0.615	0.824	1.047
500	1500	0.10	0.535	0.553	0.577	0.602	0.644	0.692	0.727	0.768	0.976	1.189
500	1500	0.20	0.945	0.948	0.958	0.960	0.992	1.022	1.058	1.103	1.324	1.539
500	1500	0.40	1.789	1.768	1.756	1.725	1.707	1.691	1.708	1.755	1.984	2.193
500	1500	0.60	2.969	2.913	2.871	2.806	2.695	2.603	2.555	2.584	2.724	2.834
500	1500	0.80	4.369	4.304	4.247	4.171	4.001	3.849	3.732	3.730	3.726	3.657
500	1500	1.00	5.361	5.317	5.277	5.227	5.095	4.983	4.880	4.790	4.750	4.724
500	1500	1.20	5.362	5.339	5.351	5.366	5.409	5.454	5.505	5.554	5.767	5.985
500	2000	-0.20	0.583	0.603	0.621	0.640	0.714	0.791	0.870	0.960	1.408	1.870
500	2000	-0.10	0.438	0.460	0.479	0.501	0.579	0.659	0.739	0.822	1.238	1.660
500	2000	-0.05	0.312	0.334	0.356	0.381	0.459	0.537	0.614	0.681	1.023	1.374
500	2000	0.00	0.276	0.296	0.330	0.351	0.410	0.480	0.552	0.604	0.869	1.149
500	2000	0.05	0.406	0.419	0.440	0.455	0.499	0.554	0.613	0.657	0.886	1.129
500	2000	0.10	0.731	0.734	0.741	0.746	0.781	0.816	0.860	0.903	1.119	1.338
500	2000	0.20	1.411	1.400	1.394	1.377	1.373	1.373	1.389	1.424	1.623	1.793
500	2000	0.40	2.779	2.735	2.700	2.642	2.546	2.458	2.416	2.441	2.557	2.631
500	2000	0.60	4.338	4.268	4.206	4.122	3.936	3.781	3.664	3.661	3.626	3.544
500	2000	0.80	5.899	5.835	5.777	5.704	5.513	5.358	5.221	5.189	4.997	4.758
500	2000	1.00	6.918	6.886	6.855	6.818	6.710	6.615	6.528	6.509	6.368	6.180
500	2000	1.20	6.920	6.890	6.860	6.853	6.910	6.965	7.017	7.073	7.347	7.618
500	3000	-0.20	0.680	0.697	0.712	0.725	0.785	0.847	0.910	0.988	1.368	1.766
500	3000	-0.10	0.486	0.508	0.527	0.547	0.620	0.692	0.764	0.837	1.201	1.574
500	3000	-0.05	0.332	0.355	0.376	0.399	0.478	0.554	0.628	0.694	1.020	1.359
500	3000	0.00	0.316	0.335	0.352	0.373	0.450	0.522	0.593	0.649	0.934	1.233
500	3000	0.05	0.615	0.622	0.629	0.637	0.683	0.730	0.779	0.827	1.069	1.321
500	3000	0.10	1.192	1.189	1.188	1.180	1.191	1.209	1.234	1.271	1.462	1.650
500	3000	0.20	2.314	2.296	2.282	2.254	2.213	2.167	2.161	2.179	2.258	2.325
500	3000	0.40	4.464	4.414	4.368	4.306	4.153	4.018	3.909	3.892	3.774	3.613
500	3000	0.60	6.602	6.535	6.469	6.394	6.173	5.981	5.815	5.763	5.458	5.116
500	3000	0.80	8.565	8.510	8.456	8.396	8.206	8.042	7.890	7.816	7.424	6.999
500	3000	1.00	9.842	9.818	9.795	9.763	9.669	9.579	9.495	9.454	9.221	8.950
500	3000	1.20	9.845	9.820	9.800	9.770	9.798	9.848	9.902	9.960	10.254	10.551
500	4000	-0.20	0.782	0.796	0.809	0.819	0.866	0.912	0.960	1.022	1.322	1.640

P	G	Xe	q (kW m-2)									
			50	100	150	200	400	600	800	1000	2000	3000
(kPa)	(kg m-2 s-1)	(-)	Heat Transfer Coefficient (kW m-2 K-2)									
500	4000	-0.10	0.520	0.543	0.564	0.585	0.657	0.725	0.791	0.856	1.174	1.504
500	4000	-0.05	0.349	0.373	0.394	0.418	0.498	0.575	0.649	0.712	1.030	1.360
500	4000	0.00	0.369	0.387	0.403	0.424	0.499	0.573	0.645	0.704	1.007	1.323
500	4000	0.05	0.847	0.851	0.856	0.860	0.892	0.930	0.973	1.022	1.266	1.518
500	4000	0.10	1.628	1.622	1.618	1.608	1.602	1.609	1.624	1.656	1.820	1.987
500	4000	0.20	3.088	3.072	3.058	3.033	2.990	2.916	2.913	2.928	2.953	2.956
500	4000	0.40	5.829	5.790	5.752	5.705	5.571	5.426	5.337	5.294	5.059	4.789
500	4000	0.60	8.531	8.474	8.419	8.358	8.163	7.996	7.839	7.754	7.320	6.868
500	4000	0.80	11.041	10.988	10.937	10.880	10.693	10.528	10.369	10.280	9.804	9.298
500	4000	1.00	12.695	12.669	12.643	12.606	12.501	12.397	12.299	12.246	11.954	11.616
500	4000	1.20	12.700	12.680	12.650	12.615	12.591	12.642	12.695	12.751	13.029	13.306
500	5000	-0.20	0.852	0.867	0.881	0.892	0.943	0.992	1.042	1.106	1.418	1.732
500	5000	-0.10	0.535	0.560	0.584	0.607	0.687	0.761	0.832	0.899	1.229	1.564
500	5000	-0.05	0.364	0.387	0.410	0.435	0.519	0.599	0.676	0.742	1.073	1.416
500	5000	0.00	0.430	0.446	0.464	0.485	0.555	0.629	0.703	0.764	1.081	1.412
500	5000	0.05	1.073	1.076	1.081	1.084	1.109	1.142	1.180	1.227	1.463	1.703
500	5000	0.10	2.031	2.024	2.018	2.007	1.997	1.995	2.000	2.029	2.169	2.305
500	5000	0.20	3.791	3.775	3.761	3.739	3.690	3.651	3.620	3.617	3.596	3.564
500	5000	0.40	7.069	7.038	7.009	6.974	6.865	6.767	6.676	6.619	6.315	6.005
500	5000	0.60	10.331	10.285	10.241	10.193	10.034	9.891	9.754	9.659	9.175	8.687
500	5000	0.80	13.415	13.364	13.315	13.259	13.081	12.918	12.763	12.663	12.141	11.588
500	5000	1.00	15.445	15.417	15.389	15.346	15.230	15.111	14.999	14.936	14.582	14.179
500	5000	1.20	15.450	15.420	15.392	15.350	15.292	15.342	15.391	15.443	15.700	15.951
500	6000	-0.20	0.904	0.923	0.943	0.958	1.033	1.108	1.186	1.286	1.768	2.210
500	6000	-0.10	0.541	0.571	0.599	0.626	0.725	0.818	0.909	0.998	1.436	1.848
500	6000	-0.05	0.372	0.398	0.422	0.448	0.540	0.628	0.714	0.791	1.176	1.565
500	6000	0.00	0.481	0.497	0.512	0.533	0.604	0.679	0.753	0.816	1.142	1.484
500	6000	0.05	1.264	1.267	1.271	1.274	1.301	1.333	1.370	1.412	1.629	1.837
500	6000	0.10	2.389	2.382	2.377	2.368	2.357	2.353	2.354	2.376	2.479	2.554
500	6000	0.20	4.456	4.438	4.422	4.399	4.344	4.296	4.255	4.248	4.191	4.095
500	6000	0.40	8.320	8.287	8.255	8.215	8.100	7.995	7.898	7.840	7.526	7.180
500	6000	0.60	12.174	12.125	12.077	12.025	11.860	11.711	11.573	11.474	10.979	10.470
500	6000	0.80	15.786	15.734	15.683	15.625	15.439	15.266	15.104	14.991	14.403	13.792
500	6000	1.00	18.126	18.100	18.074	18.031	17.911	17.786	17.665	17.585	17.143	16.664
500	6000	1.20	18.130	18.105	18.080	18.040	17.928	17.979	18.030	18.081	18.337	18.588
500	7000	-0.20	0.922	0.946	0.969	0.988	1.078	1.167	1.258	1.364	1.881	2.376
500	7000	-0.10	0.528	0.560	0.591	0.620	0.732	0.834	0.934	1.030	1.502	1.953
500	7000	-0.05	0.376	0.402	0.427	0.454	0.551	0.645	0.737	0.819	1.235	1.655
500	7000	0.00	0.544	0.559	0.573	0.593	0.663	0.739	0.815	0.881	1.230	1.595
500	7000	0.05	1.453	1.457	1.461	1.466	1.495	1.530	1.569	1.613	1.840	2.052
500	7000	0.10	2.739	2.735	2.732	2.724	2.719	2.719	2.724	2.747	2.854	2.919
500	7000	0.20	5.106	5.091	5.077	5.054	5.004	4.958	4.919	4.908	4.839	4.707
500	7000	0.40	9.548	9.514	9.480	9.440	9.321	9.212	9.112	9.048	8.715	8.318
500	7000	0.60	13.980	13.927	13.877	13.823	13.645	13.486	13.338	13.233	12.698	12.127
500	7000	0.80	18.090	18.038	17.988	17.929	17.735	17.552	17.377	17.245	16.570	15.869
500	7000	1.00	20.713	20.689	20.665	20.625	20.504	20.372	20.243	20.146	19.621	19.066
500	7000	1.20	20.720	20.692	20.670	20.630	20.510	20.561	20.612	20.663	20.918	21.167

P	G	Xe	q (kW m-2)									
			50	100	150	200	400	600	800	1000	2000	3000
(kPa)	(kg m-2 s-1)	(-)	Heat Transfer Coefficient (kW m-2 K-2)									
1000	0	-0.20	0.329	0.353	0.378	0.401	0.507	0.613	0.722	0.839	1.423	1.997
1000	0	-0.10	0.296	0.320	0.345	0.367	0.474	0.579	0.689	0.810	1.413	2.001
1000	0	-0.05	0.270	0.293	0.319	0.341	0.450	0.556	0.669	0.794	1.419	2.027
1000	0	0.00	0.247	0.269	0.296	0.320	0.430	0.539	0.654	0.782	1.420	2.042
1000	0	0.05	0.228	0.250	0.277	0.307	0.420	0.531	0.647	0.775	1.415	2.039
1000	0	0.10	0.215	0.238	0.264	0.294	0.409	0.522	0.638	0.766	1.405	2.029
1000	0	0.20	0.176	0.202	0.232	0.264	0.382	0.497	0.615	0.743	1.385	2.010
1000	0	0.40	0.168	0.185	0.219	0.247	0.367	0.481	0.599	0.728	1.372	1.998
1000	0	0.60	0.191	0.215	0.236	0.259	0.379	0.488	0.603	0.732	1.374	2.000
1000	0	0.80	0.205	0.230	0.256	0.279	0.389	0.496	0.609	0.737	1.375	2.002
1000	0	1.00	0.201	0.228	0.255	0.281	0.393	0.502	0.616	0.743	1.375	2.002
1000	0	1.20	0.169	0.199	0.229	0.258	0.378	0.493	0.611	0.737	1.368	1.986
1000	50	-0.20	0.359	0.381	0.402	0.423	0.505	0.587	0.669	0.736	1.061	1.419
1000	50	-0.10	0.324	0.345	0.365	0.385	0.463	0.542	0.621	0.692	1.038	1.408
1000	50	-0.05	0.296	0.315	0.335	0.354	0.431	0.508	0.587	0.661	1.021	1.400
1000	50	0.00	0.268	0.288	0.298	0.316	0.397	0.475	0.555	0.632	1.008	1.399
1000	50	0.05	0.234	0.254	0.273	0.290	0.373	0.452	0.531	0.607	0.973	1.358
1000	50	0.10	0.203	0.222	0.245	0.266	0.345	0.422	0.499	0.573	0.930	1.305
1000	50	0.20	0.155	0.184	0.202	0.220	0.296	0.370	0.445	0.518	0.872	1.245
1000	50	0.40	0.144	0.168	0.196	0.212	0.282	0.352	0.424	0.496	0.844	1.209
1000	50	0.60	0.165	0.185	0.214	0.234	0.298	0.372	0.445	0.517	0.863	1.229
1000	50	0.80	0.180	0.200	0.221	0.242	0.317	0.396	0.473	0.545	0.896	1.269
1000	50	1.00	0.212	0.231	0.249	0.269	0.345	0.424	0.504	0.578	0.940	1.324
1000	50	1.20	0.274	0.289	0.305	0.321	0.391	0.465	0.542	0.618	0.988	1.375
1000	100	-0.20	0.385	0.407	0.429	0.452	0.530	0.609	0.684	0.739	1.015	1.320
1000	100	-0.10	0.352	0.373	0.392	0.413	0.481	0.551	0.619	0.675	0.951	1.250
1000	100	-0.05	0.324	0.342	0.355	0.373	0.437	0.503	0.567	0.623	0.895	1.186
1000	100	0.00	0.300	0.305	0.309	0.311	0.376	0.446	0.515	0.571	0.854	1.153
1000	100	0.05	0.245	0.264	0.265	0.265	0.336	0.409	0.478	0.533	0.807	1.097
1000	100	0.10	0.195	0.222	0.237	0.245	0.310	0.378	0.441	0.494	0.756	1.034
1000	100	0.20	0.139	0.183	0.199	0.208	0.259	0.320	0.377	0.428	0.678	0.947
1000	100	0.40	0.121	0.159	0.185	0.204	0.260	0.313	0.364	0.414	0.653	0.909
1000	100	0.60	0.154	0.174	0.221	0.248	0.287	0.349	0.406	0.457	0.704	0.970
1000	100	0.80	0.195	0.215	0.236	0.258	0.324	0.393	0.458	0.511	0.770	1.053
1000	100	1.00	0.274	0.289	0.303	0.319	0.381	0.447	0.514	0.570	0.848	1.147
1000	100	1.20	0.419	0.425	0.433	0.439	0.483	0.534	0.593	0.651	0.931	1.225
1000	200	-0.20	0.439	0.465	0.487	0.511	0.595	0.667	0.740	0.790	1.050	1.354
1000	200	-0.10	0.406	0.428	0.449	0.475	0.542	0.604	0.667	0.719	0.984	1.278
1000	200	-0.05	0.371	0.416	0.425	0.441	0.505	0.541	0.598	0.648	0.896	1.168
1000	200	0.00	0.325	0.345	0.351	0.357	0.405	0.457	0.517	0.565	0.809	1.072
1000	200	0.05	0.260	0.283	0.306	0.325	0.369	0.406	0.466	0.511	0.739	0.989
1000	200	0.10	0.178	0.222	0.259	0.271	0.337	0.377	0.435	0.478	0.698	0.940
1000	200	0.20	0.136	0.185	0.212	0.238	0.299	0.331	0.391	0.434	0.653	0.895
1000	200	0.40	0.156	0.236	0.275	0.295	0.335	0.367	0.418	0.462	0.684	0.928
1000	200	0.60	0.245	0.279	0.349	0.377	0.409	0.457	0.496	0.545	0.783	1.043
1000	200	0.80	0.345	0.363	0.388	0.414	0.502	0.564	0.598	0.651	0.904	1.183
1000	200	1.00	0.544	0.544	0.554	0.565	0.622	0.665	0.717	0.772	1.040	1.338
1000	200	1.20	0.790	0.794	0.798	0.800	0.814	0.826	0.872	0.926	1.196	1.488

P	G	Xe	q (kW m-2)									
			50	100	150	200	400	600	800	1000	2000	3000
(kPa)	(kg m-2 s-1)	(-)	Heat Transfer Coefficient (kW m-2 K-2)									
1000	500	-0.20	0.540	0.571	0.595	0.624	0.714	0.799	0.876	0.941	1.291	1.619
1000	500	-0.10	0.502	0.542	0.574	0.589	0.652	0.717	0.785	0.848	1.180	1.490
1000	500	-0.05	0.478	0.521	0.544	0.560	0.610	0.637	0.687	0.742	0.999	1.263
1000	500	0.00	0.320	0.339	0.359	0.384	0.457	0.500	0.542	0.589	0.820	1.051
1000	500	0.05	0.277	0.298	0.318	0.351	0.430	0.462	0.503	0.543	0.732	0.932
1000	500	0.10	0.224	0.268	0.309	0.348	0.421	0.457	0.498	0.536	0.734	0.929
1000	500	0.20	0.204	0.247	0.306	0.367	0.441	0.480	0.532	0.572	0.791	0.993
1000	500	0.40	0.343	0.361	0.410	0.454	0.552	0.594	0.660	0.710	0.986	1.216
1000	500	0.60	0.610	0.605	0.593	0.593	0.682	0.733	0.796	0.866	1.182	1.457
1000	500	0.80	1.124	1.114	1.100	1.152	1.154	1.156	1.159	1.166	1.443	1.719
1000	500	1.00	1.690	1.661	1.650	1.646	1.576	1.507	1.509	1.571	1.791	2.045
1000	500	1.20	2.074	2.050	2.029	2.020	1.918	1.861	1.925	1.975	2.206	2.459
1000	1000	-0.20	0.625	0.655	0.679	0.710	0.799	0.886	0.972	1.055	1.475	1.888
1000	1000	-0.10	0.584	0.622	0.648	0.673	0.724	0.791	0.866	0.945	1.341	1.660
1000	1000	-0.05	0.539	0.585	0.599	0.600	0.631	0.685	0.736	0.797	1.105	1.408
1000	1000	0.00	0.376	0.391	0.426	0.454	0.570	0.576	0.630	0.671	0.886	1.111
1000	1000	0.05	0.345	0.358	0.396	0.453	0.568	0.569	0.620	0.650	0.809	0.990
1000	1000	0.10	0.418	0.420	0.441	0.504	0.592	0.614	0.654	0.691	0.880	1.071
1000	1000	0.20	0.562	0.593	0.613	0.620	0.679	0.743	0.813	0.863	1.100	1.313
1000	1000	0.40	0.921	0.948	0.974	0.980	1.030	1.251	1.307	1.365	1.604	1.769
1000	1000	0.60	1.722	1.694	1.659	1.627	1.585	1.582	1.565	1.622	1.926	2.152
1000	1000	0.80	2.941	2.864	2.797	2.707	2.501	2.322	2.246	2.286	2.432	2.620
1000	1000	1.00	3.921	3.833	3.751	3.642	3.374	3.108	2.919	2.917	3.130	3.289
1000	1000	1.20	3.924	3.878	3.857	3.833	3.749	3.698	3.620	3.618	3.950	4.196
1000	1500	-0.20	0.677	0.702	0.723	0.752	0.830	0.911	0.991	1.076	1.501	1.935
1000	1500	-0.10	0.604	0.628	0.646	0.706	0.775	0.828	0.897	0.979	1.384	1.738
1000	1500	-0.05	0.504	0.538	0.563	0.628	0.686	0.715	0.778	0.840	1.146	1.456
1000	1500	0.00	0.409	0.425	0.458	0.519	0.587	0.600	0.663	0.707	0.928	1.162
1000	1500	0.05	0.430	0.444	0.480	0.533	0.596	0.597	0.643	0.680	0.871	1.074
1000	1500	0.10	0.615	0.597	0.617	0.669	0.716	0.726	0.771	0.810	1.008	1.210
1000	1500	0.20	0.999	0.997	1.004	1.012	1.045	1.086	1.126	1.165	1.351	1.535
1000	1500	0.40	1.866	1.857	1.853	1.839	1.838	1.979	1.980	2.001	2.075	2.140
1000	1500	0.60	3.225	3.159	3.107	3.030	2.876	2.803	2.679	2.696	2.801	2.806
1000	1500	0.80	4.866	4.761	4.666	4.541	4.239	3.984	3.870	3.875	3.877	3.880
1000	1500	1.00	5.938	5.837	5.740	5.620	5.286	4.852	4.638	4.686	4.807	4.809
1000	1500	1.20	5.940	5.840	5.745	5.624	5.413	5.389	5.251	5.321	5.710	5.950
1000	2000	-0.20	0.706	0.728	0.747	0.770	0.843	0.918	0.994	1.076	1.486	1.905
1000	2000	-0.10	0.586	0.608	0.627	0.658	0.728	0.802	0.874	0.957	1.367	1.660
1000	2000	-0.05	0.462	0.486	0.507	0.552	0.623	0.692	0.758	0.823	1.147	1.475
1000	2000	0.00	0.403	0.424	0.448	0.488	0.555	0.619	0.679	0.726	0.964	1.215
1000	2000	0.05	0.496	0.507	0.529	0.553	0.597	0.647	0.697	0.737	0.946	1.165
1000	2000	0.10	0.821	0.823	0.825	0.825	0.846	0.871	0.898	0.937	1.135	1.326
1000	2000	0.20	1.511	1.495	1.487	1.467	1.443	1.453	1.458	1.488	1.542	1.666
1000	2000	0.40	2.962	2.922	2.889	2.840	2.740	2.735	2.689	2.658	2.573	2.410
1000	2000	0.60	4.762	4.678	4.602	4.512	4.264	4.092	3.901	3.799	3.673	3.395
1000	2000	0.80	6.585	6.490	6.402	6.302	6.009	5.731	5.500	5.432	5.136	4.736
1000	2000	1.00	7.630	7.560	7.493	7.415	7.180	6.953	6.759	6.738	6.553	6.240
1000	2000	1.20	6.965	6.974	6.983	6.993	7.026	7.088	7.120	7.171	7.454	7.695

P	G	Xe	q (kW m-2)									
			50	100	150	200	400	600	800	1000	2000	3000
(kPa)	(kg m-2 s-1)	(-)	Heat Transfer Coefficient (kW m-2 K-2)									
1000	3000	-0.20	0.777	0.794	0.809	0.823	0.881	0.941	1.001	1.068	1.401	1.749
1000	3000	-0.10	0.593	0.614	0.633	0.654	0.724	0.795	0.864	0.936	1.295	1.659
1000	3000	-0.05	0.435	0.459	0.479	0.505	0.581	0.655	0.727	0.794	1.126	1.465
1000	3000	0.00	0.418	0.438	0.456	0.482	0.554	0.625	0.692	0.749	1.036	1.333
1000	3000	0.05	0.713	0.719	0.726	0.737	0.777	0.823	0.870	0.915	1.149	1.394
1000	3000	0.10	1.298	1.299	1.300	1.303	1.321	1.354	1.385	1.403	1.531	1.663
1000	3000	0.20	2.467	2.462	2.461	2.451	2.445	2.440	2.435	2.432	2.358	2.194
1000	3000	0.40	4.843	4.796	4.752	4.699	4.535	4.501	4.383	4.184	3.820	3.372
1000	3000	0.60	7.325	7.242	7.161	7.077	6.792	6.618	6.397	6.192	5.641	4.989
1000	3000	0.80	9.570	9.496	9.425	9.352	9.096	8.898	8.678	8.521	7.819	7.076
1000	3000	1.00	10.795	10.757	10.720	10.674	10.527	10.404	10.280	10.184	9.668	9.148
1000	3000	1.20	9.915	9.930	9.946	9.958	10.024	10.084	10.159	10.209	10.483	10.777
1000	4000	-0.20	0.881	0.892	0.903	0.910	0.951	0.991	1.035	1.087	1.344	1.614
1000	4000	-0.10	0.625	0.647	0.667	0.687	0.757	0.824	0.889	0.951	1.261	1.577
1000	4000	-0.05	0.453	0.475	0.496	0.520	0.597	0.670	0.741	0.806	1.129	1.458
1000	4000	0.00	0.477	0.494	0.512	0.534	0.605	0.676	0.746	0.807	1.115	1.435
1000	4000	0.05	0.964	0.968	0.971	0.979	1.004	1.043	1.086	1.131	1.371	1.630
1000	4000	0.10	1.766	1.771	1.779	1.783	1.813	1.857	1.910	1.914	1.990	2.100
1000	4000	0.20	3.307	3.322	3.339	3.347	3.406	3.675	3.740	3.745	3.750	3.090
1000	4000	0.40	6.378	6.350	6.324	6.289	6.190	6.180	6.173	5.954	5.290	4.732
1000	4000	0.60	9.503	9.428	9.356	9.280	9.015	8.791	8.554	8.427	7.666	6.888
1000	4000	0.80	12.357	12.277	12.199	12.117	11.835	11.585	11.361	11.166	10.320	9.469
1000	4000	1.00	13.932	13.886	13.841	13.782	13.600	13.423	13.253	13.139	12.527	11.875
1000	4000	1.20	12.775	12.787	12.799	12.810	12.862	12.915	12.972	13.020	13.273	13.538
1000	5000	-0.20	0.969	0.977	0.986	0.990	1.023	1.057	1.094	1.144	1.390	1.641
1000	5000	-0.10	0.652	0.674	0.695	0.715	0.787	0.855	0.920	0.980	1.281	1.588
1000	5000	-0.05	0.474	0.496	0.518	0.541	0.622	0.700	0.775	0.840	1.163	1.494
1000	5000	0.00	0.545	0.561	0.578	0.597	0.669	0.744	0.816	0.879	1.195	1.519
1000	5000	0.05	1.219	1.219	1.221	1.221	1.238	1.264	1.297	1.339	1.553	1.769
1000	5000	0.10	2.244	2.237	2.231	2.219	2.207	2.208	2.220	2.226	2.291	2.365
1000	5000	0.20	4.154	4.148	4.143	4.127	4.106	4.093	4.091	4.052	3.830	3.608
1000	5000	0.40	7.817	7.783	7.750	7.709	7.576	7.460	7.346	7.221	6.609	5.946
1000	5000	0.60	11.549	11.478	11.409	11.338	11.092	10.873	10.663	10.576	9.688	8.787
1000	5000	0.80	15.028	14.945	14.866	14.777	14.487	14.220	13.969	13.784	12.844	11.863
1000	5000	1.00	16.955	16.902	16.852	16.780	16.572	16.361	16.165	16.035	15.333	14.572
1000	5000	1.20	15.549	15.556	15.563	15.572	15.604	15.640	15.676	15.724	15.962	16.190
1000	6000	-0.20	1.050	1.059	1.068	1.071	1.108	1.149	1.196	1.266	1.607	1.937
1000	6000	-0.10	0.662	0.687	0.709	0.730	0.809	0.884	0.958	1.032	1.398	1.764
1000	6000	-0.05	0.478	0.503	0.526	0.552	0.640	0.725	0.807	0.879	1.240	1.600
1000	6000	0.00	0.600	0.617	0.633	0.656	0.729	0.805	0.879	0.938	1.244	1.542
1000	6000	0.05	1.449	1.447	1.446	1.446	1.455	1.467	1.481	1.498	1.582	1.627
1000	6000	0.10	2.686	2.666	2.648	2.626	2.566	2.514	2.468	2.451	2.404	2.307
1000	6000	0.20	4.964	4.926	4.891	4.846	4.720	4.607	4.504	4.422	4.187	3.880
1000	6000	0.40	9.252	9.195	9.140	9.077	8.880	8.696	8.521	8.360	7.672	6.971
1000	6000	0.60	13.628	13.550	13.475	13.397	13.135	12.894	12.665	12.521	11.542	10.517
1000	6000	0.80	17.695	17.612	17.531	17.444	17.148	16.872	16.608	16.403	15.347	14.256
1000	6000	1.00	19.894	19.848	19.802	19.737	19.536	19.328	19.125	18.977	18.176	17.335

P	G	Xe	q (kW m-2)									
			50	100	150	200	400	600	800	1000	2000	3000
(kPa)	(kg m-2 s-1)	(-)	Heat Transfer Coefficient (kW m-2 K-2)									
1000	6000	1.20	18.238	18.248	18.258	18.269	18.311	18.356	18.400	18.442	18.659	18.874
1000	7000	-0.20	1.074	1.087	1.100	1.107	1.157	1.208	1.263	1.337	1.695	2.054
1000	7000	-0.10	0.647	0.674	0.700	0.723	0.813	0.897	0.979	1.059	1.452	1.851
1000	7000	-0.05	0.483	0.507	0.531	0.558	0.650	0.739	0.826	0.901	1.284	1.668
1000	7000	0.00	0.674	0.688	0.702	0.725	0.794	0.869	0.942	1.000	1.310	1.608
1000	7000	0.05	1.671	1.669	1.667	1.668	1.673	1.682	1.691	1.699	1.740	1.742
1000	7000	0.10	3.087	3.069	3.051	3.030	2.969	2.913	2.859	2.827	2.699	2.501
1000	7000	0.20	5.695	5.657	5.621	5.575	5.440	5.310	5.186	5.112	4.701	4.160
1000	7000	0.40	10.637	10.571	10.508	10.438	10.204	9.980	9.765	9.597	8.743	7.779
1000	7000	0.60	15.679	15.591	15.507	15.422	15.123	14.848	14.584	14.366	13.267	12.092
1000	7000	0.80	20.296	20.213	20.130	20.042	19.731	19.439	19.156	18.922	17.739	16.527
1000	7000	1.00	22.726	22.684	22.643	22.582	22.386	22.179	21.973	21.806	20.926	20.028
1000	7000	1.20	20.886	20.896	20.906	20.916	20.960	21.004	21.050	21.088	21.288	21.489
2000	0	-0.20	0.531	0.551	0.572	0.592	0.686	0.780	0.877	0.981	1.502	2.090
2000	0	-0.10	0.428	0.450	0.474	0.494	0.595	0.695	0.800	0.915	1.488	2.088
2000	0	-0.05	0.373	0.388	0.412	0.435	0.539	0.644	0.753	0.874	1.483	2.084
2000	0	0.00	0.335	0.355	0.379	0.402	0.509	0.614	0.724	0.849	1.474	2.082
2000	0	0.05	0.329	0.351	0.368	0.391	0.500	0.606	0.717	0.843	1.469	2.078
2000	0	0.10	0.315	0.341	0.354	0.376	0.487	0.595	0.705	0.831	1.457	2.065
2000	0	0.20	0.245	0.262	0.304	0.324	0.441	0.556	0.670	0.795	1.419	2.028
2000	0	0.40	0.220	0.220	0.258	0.297	0.415	0.529	0.643	0.769	1.397	2.008
2000	0	0.60	0.251	0.272	0.300	0.325	0.433	0.537	0.646	0.772	1.399	2.003
2000	0	0.80	0.276	0.299	0.324	0.349	0.441	0.540	0.657	0.781	1.401	1.999
2000	0	1.00	0.280	0.306	0.331	0.357	0.457	0.558	0.673	0.796	1.405	1.996
2000	0	1.20	0.244	0.273	0.302	0.333	0.441	0.553	0.674	0.796	1.406	1.997
2000	50	-0.20	0.545	0.565	0.584	0.604	0.682	0.762	0.840	0.902	1.208	1.556
2000	50	-0.10	0.458	0.478	0.498	0.518	0.596	0.675	0.754	0.826	1.180	1.554
2000	50	-0.05	0.410	0.436	0.453	0.469	0.545	0.620	0.700	0.776	1.152	1.542
2000	50	0.00	0.372	0.387	0.403	0.420	0.496	0.572	0.651	0.731	1.126	1.530
2000	50	0.05	0.344	0.361	0.370	0.390	0.466	0.542	0.621	0.700	1.083	1.479
2000	50	0.10	0.309	0.330	0.337	0.357	0.429	0.500	0.577	0.652	1.019	1.398
2000	50	0.20	0.219	0.235	0.271	0.281	0.352	0.420	0.492	0.562	0.901	1.259
2000	50	0.40	0.173	0.177	0.211	0.243	0.311	0.381	0.450	0.518	0.844	1.190
2000	50	0.60	0.201	0.214	0.235	0.259	0.330	0.404	0.476	0.544	0.874	1.226
2000	50	0.80	0.231	0.249	0.267	0.281	0.369	0.447	0.511	0.581	0.919	1.280
2000	50	1.00	0.270	0.287	0.302	0.315	0.392	0.470	0.535	0.609	0.968	1.344
2000	50	1.20	0.329	0.341	0.354	0.363	0.436	0.504	0.566	0.642	1.010	1.391
2000	100	-0.20	0.561	0.583	0.604	0.625	0.704	0.784	0.860	0.914	1.193	1.494
2000	100	-0.10	0.484	0.506	0.527	0.549	0.619	0.691	0.761	0.820	1.114	1.425
2000	100	-0.05	0.445	0.482	0.492	0.504	0.569	0.627	0.693	0.751	1.041	1.347
2000	100	0.00	0.407	0.419	0.421	0.430	0.489	0.554	0.622	0.682	0.978	1.286
2000	100	0.05	0.374	0.385	0.386	0.394	0.441	0.506	0.574	0.632	0.918	1.216
2000	100	0.10	0.315	0.333	0.346	0.361	0.407	0.454	0.516	0.570	0.835	1.114
2000	100	0.20	0.206	0.227	0.263	0.270	0.327	0.357	0.414	0.461	0.689	0.935
2000	100	0.40	0.133	0.153	0.183	0.206	0.269	0.324	0.376	0.420	0.633	0.867

P	G	Xe	q (kW m-2)									
			50	100	150	200	400	600	800	1000	2000	3000
(kPa)	(kg m-2 s-1)	(-)	Heat Transfer Coefficient (kW m-2 K-2)									
2000	100	0.60	0.172	0.183	0.199	0.233	0.291	0.369	0.426	0.473	0.702	0.956
2000	100	0.80	0.242	0.259	0.276	0.292	0.395	0.466	0.490	0.541	0.786	1.056
2000	100	1.00	0.325	0.337	0.348	0.352	0.435	0.504	0.526	0.584	0.867	1.163
2000	100	1.20	0.458	0.457	0.459	0.454	0.522	0.561	0.578	0.639	0.934	1.232
2000	200	-0.20	0.605	0.628	0.650	0.671	0.754	0.826	0.900	0.947	1.197	1.484
2000	200	-0.10	0.558	0.600	0.616	0.617	0.683	0.748	0.811	0.862	1.127	1.417
2000	200	-0.05	0.545	0.610	0.616	0.632	0.677	0.690	0.736	0.787	1.043	1.308
2000	200	0.00	0.466	0.486	0.488	0.497	0.539	0.583	0.626	0.677	0.934	1.205
2000	200	0.05	0.365	0.384	0.400	0.417	0.458	0.508	0.549	0.597	0.841	1.105
2000	200	0.10	0.282	0.307	0.339	0.367	0.409	0.463	0.490	0.536	0.769	1.018
2000	200	0.20	0.186	0.217	0.253	0.279	0.331	0.369	0.404	0.447	0.670	0.912
2000	200	0.40	0.161	0.219	0.256	0.279	0.353	0.415	0.420	0.449	0.678	0.922
2000	200	0.60	0.267	0.300	0.325	0.348	0.433	0.481	0.511	0.561	0.794	1.050
2000	200	0.80	0.426	0.452	0.483	0.575	0.695	0.749	0.758	0.760	1.015	1.205
2000	200	1.00	0.593	0.594	0.599	0.599	0.700	0.750	0.769	0.820	1.076	1.369
2000	200	1.20	0.814	0.802	0.793	0.773	0.796	0.801	0.860	0.919	1.153	1.496
2000	500	-0.20	0.713	0.740	0.762	0.759	0.848	0.935	1.029	1.088	1.419	1.706
2000	500	-0.10	0.672	0.719	0.743	0.756	0.804	0.850	0.923	0.983	1.307	1.594
2000	500	-0.05	0.632	0.667	0.681	0.673	0.705	0.754	0.808	0.864	1.112	1.372
2000	500	0.00	0.448	0.463	0.476	0.485	0.534	0.573	0.632	0.680	0.918	1.161
2000	500	0.05	0.348	0.373	0.389	0.416	0.480	0.509	0.569	0.610	0.812	1.029
2000	500	0.10	0.293	0.328	0.360	0.396	0.466	0.493	0.553	0.597	0.797	1.011
2000	500	0.20	0.222	0.266	0.313	0.365	0.461	0.491	0.558	0.606	0.854	1.082
2000	500	0.40	0.331	0.379	0.408	0.463	0.590	0.663	0.779	0.832	1.112	1.308
2000	500	0.60	0.757	0.779	0.780	0.865	0.863	0.791	0.797	0.863	1.194	1.500
2000	500	0.80	1.395	1.393	1.394	1.636	1.473	1.253	1.255	1.260	1.421	1.709
2000	500	1.00	1.894	1.853	1.841	1.839	1.683	1.584	1.599	1.667	1.764	2.028
2000	500	1.20	2.061	2.018	1.985	1.983	1.768	1.679	1.776	1.846	2.117	2.466
2000	1000	-0.20	0.837	0.868	0.893	0.916	1.011	1.100	1.189	1.261	1.631	1.979
2000	1000	-0.10	0.823	0.861	0.886	0.902	0.958	1.045	1.089	1.156	1.500	1.828
2000	1000	-0.05	0.719	0.729	0.730	0.732	0.733	0.779	0.833	0.898	1.224	1.518
2000	1000	0.00	0.556	0.536	0.547	0.549	0.569	0.619	0.669	0.719	0.973	1.211
2000	1000	0.05	0.488	0.471	0.481	0.522	0.565	0.596	0.637	0.676	0.880	1.083
2000	1000	0.10	0.510	0.509	0.515	0.580	0.638	0.664	0.713	0.749	0.950	1.166
2000	1000	0.20	0.625	0.624	0.665	0.667	0.732	0.857	1.000	1.052	1.282	1.447
2000	1000	0.40	0.940	0.938	1.035	1.040	1.162	1.738	1.740	1.840	2.031	1.862
2000	1000	0.60	1.944	1.912	1.881	1.816	1.653	1.740	1.742	1.841	2.160	2.161
2000	1000	0.80	3.357	3.240	3.132	2.972	2.509	2.346	2.311	2.367	2.541	2.542
2000	1000	1.00	4.362	4.212	4.065	3.888	3.289	2.843	2.622	2.776	2.866	3.161
2000	1000	1.20	3.950	3.889	3.827	3.790	3.497	3.303	2.978	3.053	3.687	4.145
2000	1500	-0.20	0.881	0.911	0.936	0.971	1.062	1.150	1.233	1.306	1.680	2.059
2000	1500	-0.10	0.910	0.940	0.967	1.173	1.200	1.205	1.208	1.278	1.613	1.904
2000	1500	-0.05	0.888	0.899	0.929	1.037	1.074	1.113	1.133	1.177	1.383	1.550
2000	1500	0.00	0.704	0.705	0.717	0.815	0.881	0.896	0.942	0.971	1.114	1.235
2000	1500	0.05	0.630	0.631	0.643	0.739	0.801	0.805	0.843	0.873	1.017	1.135
2000	1500	0.10	0.760	0.764	0.765	0.847	0.884	0.886	0.906	0.940	1.111	1.247
2000	1500	0.20	1.107	1.138	1.140	1.141	1.167	1.347	1.439	1.445	1.445	1.485

P	G	Xe	q (kW m-2)									
			50	100	150	200	400	600	800	1000	2000	3000
(kPa)	(kg m-2 s-1)	(-)	Heat Transfer Coefficient (kW m-2 K-2)									
2000	1500	0.40	2.021	2.049	2.086	2.120	2.240	2.550	2.550	2.555	2.556	2.188
2000	1500	0.60	3.644	3.571	3.508	3.407	3.157	3.156	3.028	3.020	3.019	2.951
2000	1500	0.80	5.597	5.436	5.285	4.982	4.543	4.173	4.165	3.895	3.794	4.074
2000	1500	1.00	6.787	6.575	6.359	6.049	5.279	4.356	4.170	4.168	4.165	5.012
2000	1500	1.20	5.642	5.594	5.544	5.503	5.231	4.972	4.451	4.569	5.418	5.814
2000	2000	-0.20	0.873	0.901	0.924	0.955	1.044	1.131	1.215	1.286	1.656	2.032
2000	2000	-0.10	0.798	0.821	0.842	0.914	0.980	1.035	1.104	1.179	1.560	1.932
2000	2000	-0.05	0.692	0.700	0.732	0.961	0.970	0.972	1.006	1.063	1.347	1.625
2000	2000	0.00	0.621	0.642	0.666	0.836	0.919	0.920	0.922	0.945	1.137	1.334
2000	2000	0.05	0.689	0.706	0.714	0.801	0.853	0.855	0.862	0.894	1.074	1.249
2000	2000	0.10	1.030	1.027	1.025	1.023	1.020	0.983	0.973	1.040	1.125	1.284
2000	2000	0.20	1.752	1.728	1.713	1.704	1.703	1.700	1.600	1.590	1.414	1.549
2000	2000	0.40	3.326	3.307	3.305	3.304	3.303	3.302	3.300	3.169	2.743	2.188
2000	2000	0.60	5.491	5.382	5.282	5.153	4.795	4.658	4.349	4.194	3.997	3.154
2000	2000	0.80	7.734	7.568	7.405	7.215	6.663	6.122	5.867	5.576	5.359	4.488
2000	2000	1.00	8.768	8.625	8.484	8.317	7.826	7.136	6.755	6.750	6.649	6.223
2000	2000	1.20	7.189	7.192	7.194	7.199	7.209	7.219	7.147	7.235	7.501	7.738
2000	3000	-0.20	0.897	0.918	0.938	0.958	1.036	1.110	1.183	1.241	1.542	1.856
2000	3000	-0.10	0.722	0.744	0.766	0.785	0.867	0.954	1.033	1.102	1.458	1.817
2000	3000	-0.05	0.563	0.567	0.595	0.634	0.715	0.798	0.874	0.944	1.293	1.647
2000	3000	0.00	0.573	0.585	0.605	0.637	0.711	0.778	0.846	0.905	1.201	1.506
2000	3000	0.05	0.915	0.928	0.930	0.936	0.966	0.995	1.049	1.088	1.297	1.522
2000	3000	0.10	1.566	1.571	1.581	1.604	1.622	1.785	1.750	1.708	1.682	1.514
2000	3000	0.20	2.817	2.847	2.883	2.933	3.017	3.463	3.213	2.906	2.421	1.800
2000	3000	0.40	5.596	5.547	5.507	5.432	5.311	5.309	5.252	4.782	3.951	2.703
2000	3000	0.60	8.567	8.460	8.361	8.242	7.892	7.674	7.452	6.934	6.054	4.681
2000	3000	0.80	11.266	11.158	11.056	10.951	10.606	10.291	9.980	9.790	8.601	7.329
2000	3000	1.00	12.359	12.308	12.260	12.201	12.027	11.832	11.628	11.532	10.635	9.697
2000	3000	1.20	10.226	10.268	10.310	10.352	10.511	10.677	10.863	10.912	10.972	11.152
2000	4000	-0.20	0.967	0.981	0.996	1.009	1.070	1.127	1.186	1.232	1.473	1.723
2000	4000	-0.10	0.740	0.764	0.788	0.808	0.894	0.976	1.054	1.113	1.419	1.731
2000	4000	-0.05	0.587	0.607	0.627	0.647	0.723	0.798	0.871	0.940	1.287	1.637
2000	4000	0.00	0.648	0.663	0.678	0.694	0.756	0.820	0.888	0.957	1.287	1.626
2000	4000	0.05	1.201	1.205	1.207	1.208	1.229	1.240	1.302	1.349	1.577	1.817
2000	4000	0.10	2.066	2.089	2.116	2.138	2.241	2.527	2.704	2.547	2.257	1.995
2000	4000	0.20	3.636	3.753	3.898	3.995	4.406	5.655	5.586	4.982	3.660	2.556
2000	4000	0.40	7.302	7.315	7.347	7.348	7.359	8.060	7.736	7.096	5.510	3.970
2000	4000	0.60	11.205	11.088	10.975	10.861	10.452	10.241	10.001	9.261	7.973	6.541
2000	4000	0.80	14.582	14.466	14.354	14.237	13.846	13.481	13.189	12.881	11.410	9.868
2000	4000	1.00	15.975	15.909	15.845	15.764	15.511	15.229	14.985	14.785	13.661	12.528
2000	4000	1.20	13.221	13.239	13.258	13.278	13.352	13.434	13.514	13.544	13.698	13.909
2000	5000	-0.20	1.052	1.060	1.070	1.077	1.120	1.163	1.208	1.248	1.452	1.662
2000	5000	-0.10	0.768	0.792	0.815	0.842	0.922	0.991	1.063	1.118	1.401	1.694
2000	5000	-0.05	0.625	0.645	0.665	0.685	0.764	0.839	0.916	0.982	1.311	1.643
2000	5000	0.00	0.754	0.765	0.778	0.789	0.849	0.913	0.981	1.045	1.362	1.682
2000	5000	0.05	1.535	1.528	1.521	1.512	1.503	1.508	1.523	1.550	1.703	1.860
2000	5000	0.10	2.668	2.664	2.659	2.644	2.640	2.639	2.638	2.609	2.481	2.386

P	G	Xe	q (kW m-2)									
			50	100	150	200	400	600	800	1000	2000	3000
(kPa)	(kg m-2 s-1)	(-)	Heat Transfer Coefficient (kW m-2 K-2)									
2000	5000	0.20	4.818	4.816	4.814	4.812	4.810	4.809	4.805	4.656	3.917	3.375
2000	5000	0.40	9.135	9.078	9.020	8.957	8.714	8.618	8.445	7.902	6.508	5.345
2000	5000	0.60	13.665	13.542	13.423	13.303	12.868	12.490	12.136	11.558	9.916	8.211
2000	5000	0.80	17.764	17.635	17.511	17.376	16.927	16.535	16.166	15.803	14.049	12.285
2000	5000	1.00	19.451	19.367	19.285	19.178	18.851	18.520	18.226	17.983	16.680	15.353
2000	5000	1.20	16.115	16.112	16.109	16.109	16.108	16.117	16.113	16.154	16.388	16.586
2000	6000	-0.20	1.159	1.163	1.168	1.168	1.193	1.222	1.256	1.296	1.500	1.766
2000	6000	-0.10	0.768	0.790	0.811	0.829	0.906	0.977	1.047	1.110	1.425	1.765
2000	6000	-0.05	0.631	0.654	0.676	0.702	0.788	0.872	0.952	1.016	1.346	1.665
2000	6000	0.00	0.847	0.859	0.871	0.892	0.949	1.011	1.069	1.113	1.348	1.558
2000	6000	0.05	1.854	1.837	1.821	1.808	1.752	1.703	1.654	1.618	1.429	1.660
2000	6000	0.10	3.263	3.219	3.176	3.129	2.973	2.830	2.696	2.623	2.002	2.200
2000	6000	0.20	5.860	5.795	5.733	5.657	5.433	5.200	5.009	5.000	4.559	3.865
2000	6000	0.40	10.871	10.771	10.676	10.572	10.224	9.878	9.556	9.447	7.933	6.275
2000	6000	0.60	16.158	16.019	15.884	15.752	15.272	14.827	14.393	14.069	12.117	10.142
2000	6000	0.80	20.959	20.819	20.682	20.545	20.041	19.567	19.108	18.732	16.825	14.864
2000	6000	1.00	22.852	22.770	22.689	22.589	22.248	21.905	21.563	21.294	19.901	18.434
2000	6000	1.20	18.914	18.918	18.923	18.930	18.957	18.989	19.026	19.053	19.193	19.350
2000	7000	-0.20	1.197	1.202	1.208	1.210	1.235	1.264	1.296	1.337	1.539	1.795
2000	7000	-0.10	0.749	0.773	0.797	0.815	0.898	0.974	1.049	1.118	1.461	1.794
2000	7000	-0.05	0.642	0.665	0.687	0.713	0.800	0.886	0.968	1.035	1.377	1.709
2000	7000	0.00	0.950	0.959	0.969	0.988	1.038	1.095	1.148	1.188	1.399	1.579
2000	7000	0.05	2.135	2.116	2.097	2.083	2.015	1.953	1.888	1.830	1.541	1.585
2000	7000	0.10	3.761	3.713	3.666	3.616	3.437	3.269	3.102	2.987	2.173	2.042
2000	7000	0.20	6.751	6.675	6.602	6.516	6.237	5.950	5.671	5.514	4.658	3.730
2000	7000	0.40	12.537	12.419	12.304	12.186	11.758	11.328	10.915	10.589	8.776	6.929
2000	7000	0.60	18.628	18.479	18.334	18.198	17.678	17.195	16.719	16.300	14.219	12.112
2000	7000	0.80	24.071	23.932	23.794	23.658	23.145	22.656	22.177	21.774	19.728	17.650
2000	7000	1.00	26.106	26.033	25.959	25.869	25.548	25.222	24.889	24.604	23.141	21.630
2000	7000	1.20	21.673	21.679	21.686	21.696	21.728	21.763	21.805	21.821	21.910	22.030
5000	0	-0.20	1.223	1.223	1.224	1.225	1.253	1.283	1.330	1.403	1.757	2.089
5000	0	-0.10	0.845	0.853	0.863	0.867	0.933	0.993	1.070	1.171	1.671	2.148
5000	0	-0.05	0.661	0.668	0.679	0.688	0.768	0.847	0.937	1.052	1.617	2.159
5000	0	0.00	0.534	0.545	0.562	0.575	0.665	0.753	0.852	0.972	1.570	2.146
5000	0	0.05	0.518	0.530	0.545	0.562	0.653	0.739	0.838	0.958	1.555	2.128
5000	0	0.10	0.510	0.542	0.552	0.556	0.643	0.727	0.824	0.944	1.538	2.108
5000	0	0.20	0.413	0.459	0.479	0.492	0.584	0.675	0.773	0.892	1.481	2.046
5000	0	0.40	0.351	0.356	0.396	0.432	0.534	0.633	0.734	0.855	1.455	2.032
5000	0	0.60	0.405	0.421	0.445	0.461	0.555	0.644	0.743	0.862	1.454	2.024
5000	0	0.80	0.435	0.451	0.470	0.485	0.562	0.645	0.751	0.868	1.453	2.014
5000	0	1.00	0.433	0.452	0.470	0.486	0.571	0.656	0.761	0.878	1.459	2.017
5000	0	1.20	0.383	0.407	0.431	0.454	0.552	0.650	0.764	0.886	1.496	2.093
5000	50	-0.20	1.252	1.252	1.255	1.256	1.286	1.316	1.359	1.420	1.718	1.999
5000	50	-0.10	0.877	0.885	0.896	0.898	0.960	1.017	1.084	1.164	1.558	1.940
5000	50	-0.05	0.702	0.712	0.726	0.730	0.793	0.856	0.929	1.012	1.419	1.823
5000	50	0.00	0.584	0.595	0.605	0.613	0.676	0.742	0.815	0.897	1.298	1.701
5000	50	0.05	0.552	0.563	0.569	0.581	0.641	0.704	0.772	0.851	1.231	1.614

P	G	Xe	q (kW m-2)									
			50	100	150	200	400	600	800	1000	2000	3000
(kPa)	(kg m-2 s-1)	(-)	Heat Transfer Coefficient (kW m-2 K-2)									
5000	50	0.10	0.531	0.554	0.555	0.556	0.604	0.657	0.719	0.793	1.150	1.506
5000	50	0.20	0.411	0.443	0.451	0.452	0.498	0.543	0.597	0.659	0.959	1.268
5000	50	0.40	0.313	0.317	0.347	0.365	0.420	0.469	0.522	0.581	0.861	1.156
5000	50	0.60	0.324	0.332	0.348	0.366	0.420	0.471	0.531	0.596	0.895	1.208
5000	50	0.80	0.350	0.362	0.376	0.390	0.462	0.527	0.574	0.641	0.949	1.274
5000	50	1.00	0.405	0.416	0.427	0.445	0.503	0.567	0.615	0.685	1.009	1.347
5000	50	1.20	0.465	0.471	0.480	0.489	0.544	0.602	0.654	0.725	1.067	1.417
5000	100	-0.20	1.269	1.273	1.277	1.281	1.316	1.350	1.391	1.446	1.721	1.976
5000	100	-0.10	0.899	0.909	0.925	0.926	0.988	1.047	1.110	1.179	1.525	1.862
5000	100	-0.05	0.736	0.753	0.769	0.774	0.826	0.879	0.943	1.011	1.348	1.684
5000	100	0.00	0.627	0.645	0.645	0.651	0.696	0.753	0.811	0.875	1.188	1.506
5000	100	0.05	0.588	0.590	0.591	0.595	0.631	0.697	0.750	0.809	1.098	1.390
5000	100	0.10	0.563	0.588	0.590	0.592	0.593	0.634	0.678	0.731	0.990	1.250
5000	100	0.20	0.423	0.446	0.457	0.458	0.481	0.501	0.534	0.572	0.754	0.944
5000	100	0.40	0.291	0.308	0.330	0.345	0.398	0.421	0.455	0.488	0.642	0.809
5000	100	0.60	0.290	0.299	0.313	0.340	0.387	0.433	0.480	0.523	0.717	0.926
5000	100	0.80	0.351	0.364	0.376	0.397	0.488	0.550	0.553	0.601	0.817	1.049
5000	100	1.00	0.467	0.475	0.483	0.510	0.568	0.623	0.624	0.676	0.921	1.170
5000	100	1.20	0.600	0.602	0.603	0.605	0.649	0.686	0.688	0.744	1.014	1.280
5000	200	-0.20	1.296	1.303	1.309	1.318	1.351	1.382	1.416	1.450	1.622	1.786
5000	200	-0.10	0.937	0.952	0.967	0.998	1.052	1.084	1.140	1.192	1.452	1.715
5000	200	-0.05	0.814	0.860	0.871	0.878	0.907	0.941	0.982	1.037	1.313	1.590
5000	200	0.00	0.704	0.730	0.730	0.731	0.741	0.799	0.833	0.890	1.170	1.458
5000	200	0.05	0.625	0.650	0.650	0.652	0.656	0.715	0.747	0.802	1.071	1.345
5000	200	0.10	0.560	0.562	0.563	0.564	0.587	0.646	0.671	0.720	0.966	1.204
5000	200	0.20	0.434	0.434	0.434	0.440	0.475	0.512	0.538	0.576	0.784	0.976
5000	200	0.40	0.369	0.390	0.391	0.400	0.440	0.448	0.484	0.520	0.702	0.906
5000	200	0.60	0.390	0.413	0.423	0.454	0.531	0.693	0.716	0.717	0.828	1.042
5000	200	0.80	0.565	0.582	0.611	0.701	0.835	0.910	0.920	0.922	1.071	1.226
5000	200	1.00	0.789	0.790	0.793	0.858	0.876	0.913	0.945	0.969	1.158	1.395
5000	200	1.20	0.998	0.982	0.975	0.970	0.965	0.978	0.999	1.045	1.230	1.511
5000	500	-0.20	1.358	1.371	1.384	1.446	1.490	1.509	1.516	1.527	1.613	1.641
5000	500	-0.10	1.027	1.053	1.085	1.127	1.181	1.199	1.229	1.270	1.471	1.649
5000	500	-0.05	0.892	0.937	0.959	0.960	0.962	1.008	1.056	1.108	1.338	1.559
5000	500	0.00	0.725	0.766	0.769	0.770	0.783	0.844	0.891	0.931	1.206	1.449
5000	500	0.05	0.616	0.665	0.667	0.668	0.697	0.757	0.803	0.849	1.113	1.347
5000	500	0.10	0.532	0.589	0.590	0.595	0.642	0.692	0.734	0.787	1.040	1.263
5000	500	0.20	0.450	0.495	0.497	0.543	0.611	0.643	0.701	0.744	1.018	1.250
5000	500	0.40	0.487	0.530	0.535	0.552	0.638	0.758	0.842	0.879	1.223	1.280
5000	500	0.60	0.915	0.935	0.949	1.039	1.102	1.479	1.406	1.346	1.263	1.400
5000	500	0.80	1.731	1.707	1.687	1.686	1.685	1.680	1.671	1.655	1.584	1.580
5000	500	1.00	2.259	2.185	2.136	2.130	1.899	1.839	1.835	1.834	1.806	1.803
5000	500	1.20	2.192	2.145	2.101	2.197	1.939	1.870	1.869	1.867	1.865	1.860
5000	1000	-0.20	1.390	1.407	1.423	1.476	1.533	1.569	1.611	1.628	1.722	1.782
5000	1000	-0.10	1.109	1.116	1.144	1.188	1.208	1.257	1.296	1.342	1.580	1.783
5000	1000	-0.05	0.947	0.985	0.984	0.955	0.976	1.031	1.073	1.128	1.408	1.636
5000	1000	0.00	0.850	0.914	0.871	0.816	0.845	0.896	0.938	0.990	1.256	1.478

P	G	Xe	q (kW m-2)									
			50	100	150	200	400	600	800	1000	2000	3000
(kPa)	(kg m-2 s-1)	(-)	Heat Transfer Coefficient (kW m-2 K-2)									
5000	1000	0.05	0.784	0.854	0.814	0.777	0.815	0.856	0.898	0.945	1.188	1.396
5000	1000	0.10	0.771	0.835	0.825	0.800	0.846	0.877	0.922	0.969	1.205	1.431
5000	1000	0.20	0.813	0.880	0.879	0.859	0.888	1.027	1.134	1.199	1.480	1.626
5000	1000	0.40	1.143	1.250	1.249	1.212	1.278	1.907	1.917	1.993	2.129	2.130
5000	1000	0.60	2.634	2.553	2.469	2.272	1.970	1.950	1.953	1.994	2.170	2.399
5000	1000	0.80	4.362	4.142	3.934	3.475	2.768	2.435	2.457	2.461	2.665	2.700
5000	1000	1.00	5.294	5.030	4.780	4.340	3.534	2.854	2.714	2.823	2.825	2.826
5000	1000	1.20	3.917	3.807	3.702	3.653	3.302	2.984	2.980	2.830	2.913	2.920
5000	1500	-0.20	1.377	1.395	1.412	1.434	1.503	1.564	1.625	1.655	1.823	1.994
5000	1500	-0.10	1.206	1.229	1.250	1.414	1.440	1.442	1.443	1.488	1.711	1.898
5000	1500	-0.05	1.156	1.172	1.193	1.294	1.317	1.348	1.359	1.393	1.554	1.674
5000	1500	0.00	1.016	1.055	1.058	1.113	1.149	1.175	1.201	1.230	1.372	1.491
5000	1500	0.05	0.932	0.980	0.982	1.030	1.084	1.099	1.128	1.160	1.316	1.470
5000	1500	0.10	1.051	1.085	1.092	1.098	1.147	1.149	1.163	1.193	1.356	1.468
5000	1500	0.20	1.453	1.452	1.450	1.373	1.333	1.518	1.520	1.565	1.567	1.570
5000	1500	0.40	2.767	2.742	2.732	2.710	2.705	2.700	2.697	2.647	2.268	1.905
5000	1500	0.60	5.012	4.816	4.634	4.291	3.595	3.331	3.280	3.274	3.213	2.590
5000	1500	0.80	7.450	7.109	6.779	6.029	4.971	4.176	4.078	3.882	3.850	3.450
5000	1500	1.00	8.486	8.100	7.714	7.008	5.528	4.349	4.244	4.240	4.209	4.570
5000	1500	1.20	5.807	5.690	5.576	5.456	5.036	4.529	4.371	4.364	5.054	5.589
5000	2000	-0.20	1.361	1.380	1.397	1.416	1.488	1.555	1.622	1.663	1.884	2.110
5000	2000	-0.10	1.145	1.166	1.184	1.245	1.305	1.342	1.400	1.452	1.727	2.000
5000	2000	-0.05	0.979	1.027	1.034	1.209	1.265	1.265	1.266	1.311	1.553	1.797
5000	2000	0.00	0.870	0.882	0.902	1.066	1.113	1.114	1.130	1.173	1.388	1.611
5000	2000	0.05	0.953	0.935	0.936	1.044	1.090	1.092	1.095	1.132	1.353	1.479
5000	2000	0.10	1.427	1.398	1.376	1.361	1.331	1.218	1.183	1.180	1.179	1.288
5000	2000	0.20	2.463	2.397	2.339	2.231	2.020	1.954	1.789	1.661	1.324	1.479
5000	2000	0.40	4.617	4.493	4.385	4.223	3.854	3.711	3.420	3.190	2.542	2.100
5000	2000	0.60	7.503	7.211	6.928	6.339	5.132	4.627	4.399	4.423	4.175	3.300
5000	2000	0.80	10.475	10.075	9.673	8.882	7.310	6.015	5.876	5.734	5.353	4.449
5000	2000	1.00	11.389	11.056	10.720	10.264	9.103	7.393	6.917	6.900	6.248	5.573
5000	2000	1.20	7.822	7.731	7.627	7.565	7.203	6.472	6.082	6.302	6.262	6.764
5000	3000	-0.20	1.351	1.369	1.386	1.404	1.476	1.543	1.611	1.654	1.886	2.123
5000	3000	-0.10	1.087	1.111	1.131	1.151	1.227	1.302	1.375	1.430	1.729	2.029
5000	3000	-0.05	0.870	0.922	0.932	0.935	1.008	1.089	1.163	1.228	1.565	1.909
5000	3000	0.00	0.851	0.872	0.887	0.895	0.936	1.014	1.079	1.142	1.462	1.790
5000	3000	0.05	1.267	1.239	1.226	1.188	1.209	1.248	1.287	1.328	1.541	1.747
5000	3000	0.10	2.242	2.207	2.178	2.100	2.025	2.020	1.966	1.881	1.670	1.778
5000	3000	0.20	4.143	4.073	4.019	3.946	3.663	3.599	3.210	3.025	2.186	2.100
5000	3000	0.40	7.909	7.674	7.441	7.123	6.298	5.736	5.450	5.091	4.123	3.600
5000	3000	0.60	11.861	11.508	11.152	10.458	9.224	8.044	7.943	7.588	6.861	6.000
5000	3000	0.80	15.562	15.174	14.773	14.037	12.388	10.745	10.565	10.501	9.514	8.800
5000	3000	1.00	16.380	16.160	15.935	15.676	14.842	13.363	12.890	12.786	11.735	10.536
5000	3000	1.20	11.068	11.142	11.221	11.320	11.524	11.720	11.574	11.563	10.960	10.722
5000	4000	-0.20	1.354	1.369	1.385	1.400	1.469	1.533	1.598	1.637	1.849	2.064
5000	4000	-0.10	1.042	1.069	1.094	1.118	1.212	1.299	1.383	1.435	1.715	2.004
5000	4000	-0.05	0.868	0.885	0.901	0.915	0.991	1.067	1.144	1.213	1.573	1.940

P	G	Xe	q (kW m-2)									
			50	100	150	200	400	600	800	1000	2000	3000
(kPa)	(kg m-2 s-1)	(-)	Heat Transfer Coefficient (kW m-2 K-2)									
5000	4000	0.00	1.008	1.007	1.006	1.004	1.043	1.088	1.146	1.210	1.543	1.874
5000	4000	0.05	1.805	1.773	1.748	1.705	1.660	1.616	1.622	1.641	1.734	1.814
5000	4000	0.10	3.124	3.092	3.068	3.060	3.050	3.048	3.046	3.045	2.411	1.862
5000	4000	0.20	5.526	5.503	5.500	5.459	5.395	5.391	5.390	5.389	3.837	2.151
5000	4000	0.40	10.502	10.276	10.056	9.800	8.994	8.333	7.951	7.147	5.730	3.679
5000	4000	0.60	15.613	15.289	14.963	14.604	13.560	12.126	11.865	10.425	9.204	7.200
5000	4000	0.80	20.057	19.801	19.553	19.292	18.375	17.326	16.331	16.219	14.271	11.574
5000	4000	1.00	21.028	20.895	20.766	20.608	20.090	19.494	18.827	18.405	16.527	14.243
5000	4000	1.20	14.335	14.361	14.386	14.421	14.501	14.590	14.625	14.626	14.373	14.285
5000	5000	-0.20	1.375	1.386	1.399	1.412	1.471	1.527	1.584	1.616	1.797	1.977
5000	5000	-0.10	1.008	1.036	1.064	1.099	1.200	1.287	1.374	1.426	1.702	1.983
5000	5000	-0.05	0.908	0.921	0.936	0.951	1.025	1.098	1.176	1.245	1.605	1.974
5000	5000	0.00	1.218	1.205	1.197	1.186	1.201	1.232	1.276	1.345	1.684	2.027
5000	5000	0.05	2.390	2.341	2.297	2.237	2.124	2.046	2.000	2.042	2.158	2.248
5000	5000	0.10	4.047	3.985	3.928	3.860	3.667	3.501	3.377	3.172	2.784	2.455
5000	5000	0.20	7.059	6.953	6.847	6.723	6.295	5.958	5.644	5.393	4.309	3.056
5000	5000	0.40	12.883	12.634	12.380	12.141	11.180	10.161	9.465	8.740	7.023	5.700
5000	5000	0.60	19.006	18.706	18.407	18.141	16.860	15.666	14.856	12.519	10.641	9.772
5000	5000	0.80	24.437	24.199	23.967	23.745	22.909	22.156	21.327	20.565	17.478	14.234
5000	5000	1.00	25.547	25.414	25.283	25.118	24.565	24.043	23.491	22.872	20.299	17.681
5000	5000	1.20	17.443	17.430	17.418	17.408	17.379	17.407	17.411	17.438	17.522	17.540
5000	6000	-0.20	1.419	1.426	1.435	1.443	1.488	1.531	1.575	1.605	1.764	1.919
5000	6000	-0.10	0.957	0.991	1.023	1.055	1.172	1.277	1.377	1.439	1.763	2.070
5000	6000	-0.05	0.940	0.954	0.969	0.984	1.053	1.125	1.199	1.270	1.641	2.040
5000	6000	0.00	1.410	1.395	1.384	1.373	1.371	1.396	1.433	1.512	1.929	2.390
5000	6000	0.05	2.907	2.857	2.814	2.751	2.649	2.598	2.583	2.668	3.207	3.736
5000	6000	0.10	4.848	4.792	4.745	4.669	4.551	4.475	4.433	4.843	5.097	4.900
5000	6000	0.20	8.329	8.248	8.174	8.080	8.075	8.700	8.068	8.060	7.747	6.481
5000	6000	0.40	15.079	14.865	14.656	14.442	13.773	13.185	12.840	12.839	11.109	9.223
5000	6000	0.60	22.379	22.065	21.754	21.461	20.157	18.996	17.853	16.108	13.980	12.882
5000	6000	0.80	28.851	28.573	28.298	28.035	27.014	26.079	25.171	24.163	20.612	17.018
5000	6000	1.00	30.083	29.928	29.773	29.595	28.928	28.250	27.569	26.743	23.655	20.503
5000	6000	1.20	20.558	20.547	20.536	20.529	20.509	20.483	20.475	20.537	20.513	20.511
5000	7000	-0.20	1.447	1.452	1.458	1.465	1.498	1.534	1.571	1.604	1.773	1.934
5000	7000	-0.10	0.928	0.963	0.998	1.031	1.153	1.262	1.364	1.433	1.772	2.109
5000	7000	-0.05	0.974	0.987	1.001	1.016	1.085	1.159	1.235	1.313	1.709	2.139
5000	7000	0.00	1.589	1.570	1.554	1.540	1.527	1.546	1.580	1.666	2.097	2.589
5000	7000	0.05	3.343	3.291	3.245	3.181	3.067	3.008	2.984	3.097	3.631	4.154
5000	7000	0.10	5.600	5.531	5.469	5.381	5.199	5.071	4.979	5.050	5.605	6.057
5000	7000	0.20	9.595	9.498	9.406	9.288	8.964	8.666	8.452	8.450	7.938	9.120
5000	7000	0.40	17.260	17.097	16.939	16.770	16.223	15.734	15.268	15.114	13.817	12.389
5000	7000	0.60	25.708	25.454	25.206	24.973	24.117	23.356	22.584	21.970	19.319	16.765
5000	7000	0.80	33.145	32.882	32.622	32.373	31.412	30.486	29.617	28.826	25.009	21.198
5000	7000	1.00	34.395	34.237	34.080	33.902	33.222	32.502	31.785	31.094	27.625	24.031
5000	7000	1.20	23.579	23.573	23.567	23.568	23.557	23.544	23.538	23.531	23.467	23.451
7000	0	-0.20	1.570	1.546	1.529	1.503	1.487	1.466	1.472	1.530	1.803	2.160
7000	0	-0.10	1.073	1.064	1.061	1.046	1.079	1.106	1.157	1.250	1.700	2.158

P	G	Xe	q (kW m-2)									
			50	100	150	200	400	600	800	1000	2000	3000
(kPa)	(kg m-2 s-1)	(-)	Heat Transfer Coefficient (kW m-2 K-2)									
7000	0	-0.05	0.838	0.834	0.833	0.827	0.882	0.932	1.004	1.113	1.641	2.156
7000	0	0.00	0.668	0.667	0.673	0.675	0.751	0.822	0.908	1.026	1.604	2.155
7000	0	0.05	0.638	0.642	0.653	0.655	0.734	0.805	0.892	1.012	1.596	2.150
7000	0	0.10	0.629	0.641	0.655	0.658	0.723	0.790	0.875	0.993	1.570	2.115
7000	0	0.20	0.563	0.583	0.605	0.607	0.669	0.739	0.821	0.938	1.506	2.042
7000	0	0.40	0.504	0.515	0.532	0.545	0.621	0.698	0.785	0.903	1.482	2.038
7000	0	0.60	0.524	0.529	0.534	0.547	0.624	0.705	0.792	0.910	1.488	2.037
7000	0	0.80	0.537	0.546	0.558	0.562	0.635	0.709	0.795	0.911	1.488	2.035
7000	0	1.00	0.518	0.529	0.540	0.542	0.607	0.699	0.790	0.908	1.486	2.033
7000	0	1.20	0.478	0.494	0.510	0.515	0.605	0.699	0.795	0.914	1.503	2.062
7000	50	-0.20	1.761	1.741	1.726	1.693	1.666	1.625	1.614	1.648	1.787	1.890
7000	50	-0.10	1.185	1.175	1.172	1.153	1.173	1.182	1.216	1.279	1.575	1.850
7000	50	-0.05	0.907	0.897	0.895	0.885	0.921	0.953	1.006	1.079	1.426	1.767
7000	50	0.00	0.718	0.718	0.727	0.730	0.765	0.809	0.875	0.955	1.341	1.722
7000	50	0.05	0.683	0.690	0.696	0.699	0.738	0.783	0.847	0.926	1.307	1.681
7000	50	0.10	0.656	0.686	0.686	0.689	0.703	0.739	0.791	0.863	1.206	1.541
7000	50	0.20	0.556	0.596	0.596	0.599	0.600	0.616	0.655	0.714	0.986	1.261
7000	50	0.40	0.445	0.464	0.473	0.473	0.500	0.528	0.567	0.622	0.878	1.140
7000	50	0.60	0.403	0.409	0.417	0.437	0.479	0.512	0.562	0.621	0.901	1.188
7000	50	0.80	0.407	0.412	0.418	0.434	0.491	0.541	0.598	0.660	0.951	1.257
7000	50	1.00	0.471	0.476	0.486	0.544	0.580	0.614	0.666	0.727	1.023	1.332
7000	50	1.20	0.527	0.533	0.541	0.577	0.614	0.659	0.716	0.783	1.104	1.438
7000	100	-0.20	1.872	1.857	1.843	1.815	1.815	1.816	1.817	1.818	1.820	1.824
7000	100	-0.10	1.244	1.238	1.234	1.216	1.231	1.236	1.264	1.313	1.538	1.750
7000	100	-0.05	0.946	0.934	0.930	0.917	0.945	0.981	1.027	1.084	1.359	1.632
7000	100	0.00	0.754	0.761	0.760	0.759	0.787	0.827	0.882	0.944	1.252	1.556
7000	100	0.05	0.748	0.758	0.755	0.750	0.780	0.794	0.844	0.905	1.203	1.493
7000	100	0.10	0.746	0.757	0.754	0.749	0.761	0.765	0.781	0.833	1.079	1.315
7000	100	0.20	0.658	0.726	0.707	0.627	0.628	0.629	0.630	0.656	0.806	0.954
7000	100	0.40	0.477	0.509	0.511	0.512	0.514	0.516	0.521	0.548	0.673	0.799
7000	100	0.60	0.361	0.373	0.383	0.415	0.463	0.475	0.516	0.552	0.725	0.903
7000	100	0.80	0.381	0.381	0.384	0.420	0.468	0.526	0.577	0.619	0.816	1.030
7000	100	1.00	0.536	0.536	0.541	0.720	0.721	0.723	0.725	0.749	0.950	1.159
7000	100	1.20	0.665	0.667	0.671	0.776	0.778	0.780	0.793	0.847	1.114	1.373
7000	200	-0.20	1.953	1.945	1.940	1.938	1.937	1.877	1.806	1.802	1.761	1.717
7000	200	-0.10	1.268	1.267	1.266	1.265	1.298	1.324	1.325	1.359	1.520	1.675
7000	200	-0.05	0.973	0.994	1.020	0.978	0.996	1.053	1.078	1.127	1.373	1.609
7000	200	0.00	0.833	0.855	0.893	0.840	0.840	0.923	0.937	0.994	1.283	1.545
7000	200	0.05	0.767	0.806	0.813	0.780	0.790	0.866	0.884	0.939	1.217	1.465
7000	200	0.10	0.728	0.754	0.755	0.727	0.732	0.797	0.812	0.857	1.088	1.287
7000	200	0.20	0.616	0.629	0.630	0.606	0.616	0.648	0.661	0.691	0.853	0.988
7000	200	0.40	0.489	0.519	0.520	0.504	0.542	0.549	0.572	0.599	0.712	0.873
7000	200	0.60	0.459	0.467	0.494	0.589	0.622	0.698	0.752	0.753	0.840	1.007
7000	200	0.80	0.568	0.569	0.575	0.725	0.782	0.867	0.893	0.894	1.000	1.197
7000	200	1.00	1.057	1.057	1.079	1.310	1.315	1.325	1.330	1.331	1.334	1.369
7000	200	1.20	1.400	1.396	1.391	1.390	1.276	1.195	1.153	1.193	1.402	1.542
7000	500	-0.20	2.068	2.094	2.124	2.361	2.345	2.242	2.094	2.057	1.719	1.660

P	G	Xe	q (kW m-2)									
			50	100	150	200	400	600	800	1000	2000	3000
(kPa)	(kg m-2 s-1)	(-)	Heat Transfer Coefficient (kW m-2 K-2)									
7000	500	-0.10	1.297	1.324	1.347	1.384	1.426	1.444	1.443	1.473	1.521	1.600
7000	500	-0.05	1.022	1.080	1.114	1.115	1.137	1.238	1.210	1.268	1.450	1.610
7000	500	0.00	0.832	0.890	0.931	0.935	0.987	1.138	1.078	1.170	1.386	1.579
7000	500	0.05	0.727	0.780	0.814	0.818	0.918	1.055	1.016	1.092	1.304	1.494
7000	500	0.10	0.684	0.723	0.744	0.756	0.825	0.916	0.904	0.977	1.179	1.358
7000	500	0.20	0.655	0.689	0.690	0.720	0.764	0.820	0.819	0.858	1.071	1.236
7000	500	0.40	0.644	0.694	0.700	0.712	0.751	0.896	0.895	0.928	1.230	1.352
7000	500	0.60	0.940	0.981	0.990	1.021	1.122	1.596	1.494	1.394	1.264	1.501
7000	500	0.80	1.749	1.750	1.754	1.821	1.823	1.853	1.850	1.733	1.336	1.633
7000	500	1.00	2.647	2.556	2.475	2.470	2.300	1.969	1.967	1.960	1.680	1.894
7000	500	1.20	2.483	2.417	2.356	2.355	2.147	1.853	1.850	1.849	1.840	2.239
7000	1000	-0.20	1.993	1.997	2.000	2.117	2.087	2.009	1.926	1.889	1.721	1.698
7000	1000	-0.10	1.351	1.361	1.384	1.372	1.373	1.380	1.379	1.419	1.552	1.673
7000	1000	-0.05	1.105	1.149	1.202	1.155	1.225	1.284	1.283	1.315	1.488	1.640
7000	1000	0.00	0.892	0.973	1.018	0.994	1.157	1.261	1.236	1.266	1.432	1.584
7000	1000	0.05	0.846	0.930	0.950	0.948	1.122	1.217	1.194	1.222	1.381	1.528
7000	1000	0.10	0.885	0.963	0.964	0.951	1.069	1.124	1.139	1.155	1.326	1.514
7000	1000	0.20	1.001	1.064	1.075	1.031	1.049	1.162	1.224	1.254	1.494	1.608
7000	1000	0.40	1.331	1.424	1.427	1.362	1.460	1.943	1.960	2.135	2.181	1.820
7000	1000	0.60	3.068	2.971	2.864	2.593	2.651	2.256	2.103	2.137	2.235	2.073
7000	1000	0.80	5.149	4.866	4.600	3.952	3.442	2.633	2.509	2.449	2.427	2.229
7000	1000	1.00	6.092	5.761	5.442	4.805	4.022	3.002	2.950	2.936	2.728	2.721
7000	1000	1.20	4.181	4.028	3.884	3.771	3.241	2.911	2.906	3.152	3.655	3.236
7000	1500	-0.20	1.953	1.944	1.933	1.930	1.894	1.859	1.845	1.838	1.808	1.773
7000	1500	-0.10	1.320	1.321	1.330	1.329	1.343	1.358	1.400	1.438	1.631	1.821
7000	1500	-0.05	1.088	1.146	1.198	1.177	1.208	1.222	1.258	1.300	1.512	1.724
7000	1500	0.00	0.979	1.012	1.020	1.002	1.088	1.131	1.163	1.204	1.417	1.633
7000	1500	0.05	1.007	1.027	1.022	1.021	1.112	1.146	1.172	1.207	1.402	1.597
7000	1500	0.10	1.225	1.252	1.229	1.189	1.242	1.243	1.263	1.271	1.431	1.579
7000	1500	0.20	1.554	1.602	1.597	1.570	1.568	1.567	1.551	1.550	1.501	1.698
7000	1500	0.40	2.774	2.713	2.688	2.660	2.659	2.655	2.650	2.596	2.217	2.130
7000	1500	0.60	5.920	5.666	5.421	4.678	4.428	3.446	3.349	3.332	3.128	2.769
7000	1500	0.80	9.007	8.540	8.082	7.208	5.505	4.175	3.990	3.991	3.826	3.446
7000	1500	1.00	10.015	9.506	8.997	7.982	6.173	4.579	4.519	4.603	4.468	4.302
7000	1500	1.20	6.248	6.080	5.914	5.706	5.158	4.541	4.468	4.823	5.157	5.686
7000	2000	-0.20	1.955	1.944	1.936	1.926	1.900	1.883	1.872	1.880	1.920	1.952
7000	2000	-0.10	1.361	1.434	1.433	1.394	1.393	1.395	1.440	1.487	1.724	1.951
7000	2000	-0.05	1.220	1.342	1.322	1.222	1.234	1.244	1.285	1.337	1.590	1.838
7000	2000	0.00	0.943	1.001	0.985	0.920	0.939	1.001	1.048	1.108	1.422	1.759
7000	2000	0.05	0.968	0.971	0.970	0.944	0.979	1.063	1.120	1.163	1.440	1.729
7000	2000	0.10	1.437	1.411	1.381	1.281	1.264	1.305	1.333	1.484	1.486	1.570
7000	2000	0.20	2.345	2.314	2.239	2.245	2.105	2.122	2.132	2.188	1.715	1.700
7000	2000	0.40	4.514	4.391	4.288	3.919	3.611	3.546	3.340	3.280	2.601	2.200
7000	2000	0.60	8.688	8.298	7.915	7.060	5.528	4.519	4.379	4.313	3.716	3.026
7000	2000	0.80	12.476	11.953	11.427	10.405	8.352	6.641	6.280	5.972	4.847	4.000
7000	2000	1.00	13.540	13.060	12.566	11.889	10.014	7.814	7.350	7.116	5.864	5.223
7000	2000	1.20	8.414	8.249	8.069	7.924	7.204	5.842	5.205	5.539	5.513	5.400

P	G	Xe	q (kW m-2)									
			50	100	150	200	400	600	800	1000	2000	3000
(kPa)	(kg m-2 s-1)	(-)	Heat Transfer Coefficient (kW m-2 K-2)									
7000	3000	-0.20	1.947	1.937	1.931	1.930	1.911	1.900	1.894	1.914	2.009	2.092
7000	3000	-0.10	1.460	1.546	1.545	1.502	1.502	1.522	1.529	1.579	1.826	2.060
7000	3000	-0.05	1.307	1.434	1.414	1.326	1.340	1.342	1.379	1.435	1.706	1.957
7000	3000	0.00	1.072	1.131	1.118	1.063	1.075	1.136	1.172	1.235	1.556	1.886
7000	3000	0.05	1.215	1.200	1.227	1.182	1.204	1.281	1.330	1.367	1.609	1.847
7000	3000	0.10	2.130	2.073	2.032	1.859	1.813	1.851	1.865	2.056	1.909	1.905
7000	3000	0.20	4.129	4.031	3.829	3.744	3.497	3.363	3.212	3.200	2.689	2.300
7000	3000	0.40	8.359	8.097	7.857	7.236	6.292	5.855	5.585	5.399	4.345	3.500
7000	3000	0.60	13.767	13.280	12.792	11.854	9.849	8.402	8.133	7.817	6.931	5.770
7000	3000	0.80	18.454	17.863	17.243	16.088	13.354	10.802	10.535	10.347	9.547	8.225
7000	3000	1.00	19.355	18.930	18.478	17.942	16.166	13.215	12.614	12.205	11.288	9.844
7000	3000	1.20	11.887	11.874	11.862	11.899	11.687	11.358	10.587	10.285	9.752	9.736
7000	4000	-0.20	1.943	1.936	1.929	1.921	1.902	1.891	1.886	1.904	1.995	2.070
7000	4000	-0.10	1.456	1.466	1.474	1.486	1.509	1.534	1.572	1.618	1.845	2.042
7000	4000	-0.05	1.167	1.211	1.218	1.228	1.249	1.280	1.341	1.397	1.704	1.905
7000	4000	0.00	1.249	1.266	1.270	1.275	1.280	1.285	1.287	1.366	1.641	1.778
7000	4000	0.05	1.897	1.859	1.831	1.727	1.642	1.596	1.570	1.613	1.671	1.710
7000	4000	0.10	3.535	3.420	3.310	3.068	2.855	2.673	2.504	3.137	2.378	2.000
7000	4000	0.20	6.731	6.535	6.340	6.038	5.527	5.224	5.244	5.575	4.383	2.823
7000	4000	0.40	12.506	12.115	11.714	11.253	10.084	8.379	8.457	7.651	6.460	4.530
7000	4000	0.60	18.460	17.990	17.507	17.007	15.399	13.122	12.670	11.909	10.846	8.600
7000	4000	0.80	23.638	23.243	22.845	22.463	20.866	18.941	16.972	17.058	15.331	12.800
7000	4000	1.00	24.451	24.216	23.980	23.721	22.737	21.638	20.304	19.748	17.598	15.500
7000	4000	1.20	15.284	15.278	15.272	15.275	15.246	15.228	15.180	15.041	14.609	14.336
7000	5000	-0.20	1.945	1.937	1.929	1.918	1.899	1.886	1.880	1.894	1.965	2.025
7000	5000	-0.10	1.439	1.453	1.467	1.489	1.531	1.573	1.616	1.657	1.866	2.063
7000	5000	-0.05	1.174	1.175	1.198	1.233	1.266	1.315	1.376	1.436	1.761	2.091
7000	5000	0.00	1.460	1.461	1.467	1.468	1.470	1.472	1.476	1.532	1.870	2.212
7000	5000	0.05	2.517	2.454	2.392	2.267	2.127	2.054	2.026	2.136	2.424	2.399
7000	5000	0.10	4.748	4.591	4.441	4.063	3.784	3.552	3.383	3.659	3.235	2.818
7000	5000	0.20	8.845	8.606	8.373	8.035	7.360	6.520	6.289	6.738	5.097	3.327
7000	5000	0.40	15.614	15.251	14.883	14.524	13.287	11.759	11.265	10.617	8.904	6.423
7000	5000	0.60	22.437	22.049	21.656	21.325	19.918	18.288	17.192	15.646	14.992	13.493
7000	5000	0.80	28.665	28.342	28.020	27.727	26.526	25.285	23.841	23.169	20.114	17.100
7000	5000	1.00	29.532	29.350	29.168	28.943	28.128	27.385	26.504	25.596	22.575	19.600
7000	5000	1.20	18.563	18.546	18.531	18.517	18.482	18.512	18.561	18.561	18.301	17.997
7000	6000	-0.20	1.961	1.952	1.943	1.933	1.911	1.898	1.893	1.914	2.011	2.108
7000	6000	-0.10	1.352	1.378	1.402	1.429	1.515	1.593	1.667	1.716	2.064	2.342
7000	6000	-0.05	1.157	1.164	1.169	1.171	1.214	1.269	1.330	1.417	1.720	2.112
7000	6000	0.00	1.593	1.571	1.555	1.527	1.527	1.574	1.642	1.786	2.488	3.255
7000	6000	0.05	3.301	3.245	3.207	3.123	3.117	3.209	3.369	3.666	4.898	6.310
7000	6000	0.10	5.881	5.838	5.812	5.730	5.727	6.054	6.653	7.536	9.140	10.800
7000	6000	0.20	10.212	10.121	10.042	9.935	9.806	10.022	10.032	11.132	12.100	13.800
7000	6000	0.40	17.947	17.689	17.433	17.182	16.303	15.377	14.666	14.660	14.113	13.817
7000	6000	0.60	26.260	25.900	25.542	25.209	23.618	22.214	20.850	18.346	18.074	17.153
7000	6000	0.80	33.735	33.415	33.098	32.797	31.618	30.576	29.566	28.182	23.988	20.417
7000	6000	1.00	34.739	34.558	34.377	34.164	33.360	32.523	31.683	30.554	26.179	23.442
7000	6000	1.20	21.895	21.865	21.837	21.814	21.731	21.645	21.572	21.624	21.445	21.292

P	G	Xe	q (kW m-2)									
			50	100	150	200	400	600	800	1000	2000	3000
(kPa)	(kg m-2 s-1)	(-)	Heat Transfer Coefficient (kW m-2 K-2)									
7000	7000	-0.20	1.968	1.959	1.951	1.942	1.924	1.917	1.916	1.945	2.150	2.410
7000	7000	-0.10	1.300	1.333	1.364	1.394	1.499	1.589	1.673	1.729	2.101	2.350
7000	7000	-0.05	1.194	1.200	1.202	1.206	1.239	1.296	1.363	1.458	1.807	2.244
7000	7000	0.00	1.807	1.773	1.748	1.708	1.692	1.730	1.798	1.959	2.731	3.591
7000	7000	0.05	3.906	3.845	3.807	3.729	3.712	3.794	3.944	4.292	5.623	6.026
7000	7000	0.10	6.827	6.779	6.749	6.671	6.659	6.941	7.536	8.312	9.521	10.043
7000	7000	0.20	11.648	11.565	11.489	11.388	11.130	10.898	10.633	10.757	10.810	10.900
7000	7000	0.40	20.367	20.209	20.061	19.891	19.414	19.143	19.100	19.328	20.200	20.210
7000	7000	0.60	30.108	29.829	29.561	29.302	28.401	27.672	26.947	26.171	24.802	22.784
7000	7000	0.80	38.764	38.455	38.150	37.859	36.734	35.686	34.738	33.714	28.932	25.119
7000	7000	1.00	39.741	39.542	39.342	39.116	38.234	37.264	36.320	35.348	30.153	26.915
7000	7000	1.20	25.116	25.088	25.062	25.042	24.960	24.883	24.799	24.764	24.656	24.538
9000	0	-0.20	1.775	1.736	1.709	1.668	1.627	1.583	1.574	1.628	1.874	2.070
9000	0	-0.10	1.239	1.217	1.206	1.183	1.194	1.200	1.236	1.325	1.753	2.134
9000	0	-0.05	0.988	0.969	0.963	0.945	0.980	1.010	1.069	1.176	1.691	2.166
9000	0	0.00	0.799	0.789	0.785	0.775	0.836	0.889	0.966	1.083	1.656	2.194
9000	0	0.05	0.754	0.745	0.752	0.743	0.810	0.867	0.947	1.067	1.649	2.197
9000	0	0.10	0.732	0.731	0.743	0.733	0.794	0.848	0.929	1.045	1.618	2.154
9000	0	0.20	0.655	0.665	0.679	0.671	0.728	0.789	0.867	0.981	1.543	2.069
9000	0	0.40	0.604	0.604	0.620	0.617	0.682	0.750	0.830	0.945	1.515	2.046
9000	0	0.60	0.600	0.600	0.630	0.620	0.686	0.753	0.835	0.955	1.524	2.057
9000	0	0.80	0.595	0.598	0.637	0.632	0.689	0.762	0.846	0.961	1.527	2.057
9000	0	1.00	0.590	0.591	0.638	0.633	0.690	0.762	0.848	0.962	1.528	2.059
9000	0	1.20	0.589	0.590	0.640	0.634	0.693	0.772	0.857	0.969	1.529	2.060
9000	50	-0.20	2.215	2.191	2.170	2.134	2.079	2.006	1.961	1.983	2.046	2.059
9000	50	-0.10	1.495	1.475	1.462	1.424	1.421	1.399	1.409	1.463	1.702	1.908
9000	50	-0.05	1.129	1.106	1.096	1.062	1.077	1.085	1.121	1.191	1.518	1.827
9000	50	0.00	0.866	0.852	0.850	0.827	0.859	0.888	0.946	1.028	1.426	1.807
9000	50	0.05	0.806	0.801	0.800	0.783	0.822	0.856	0.915	0.998	1.399	1.784
9000	50	0.10	0.748	0.765	0.766	0.744	0.769	0.797	0.841	0.919	1.272	1.612
9000	50	0.20	0.598	0.635	0.635	0.613	0.618	0.637	0.669	0.729	0.996	1.265
9000	50	0.40	0.482	0.503	0.507	0.504	0.520	0.539	0.572	0.627	0.872	1.122
9000	50	0.60	0.457	0.460	0.465	0.482	0.511	0.541	0.582	0.632	0.899	1.170
9000	50	0.80	0.466	0.467	0.471	0.482	0.522	0.568	0.611	0.671	0.949	1.238
9000	50	1.00	0.520	0.521	0.526	0.553	0.590	0.628	0.674	0.733	1.017	1.312
9000	50	1.20	0.554	0.556	0.562	0.579	0.624	0.667	0.726	0.786	1.076	1.384
9000	100	-0.20	2.473	2.456	2.436	2.405	2.336	2.252	2.189	2.188	2.142	2.051
9000	100	-0.10	1.632	1.614	1.598	1.545	1.537	1.512	1.512	1.546	1.690	1.809
9000	100	-0.05	1.200	1.175	1.163	1.118	1.109	1.135	1.163	1.214	1.458	1.692
9000	100	0.00	0.904	0.886	0.884	0.881	0.880	0.910	0.957	1.022	1.339	1.646
9000	100	0.05	0.843	0.865	0.864	0.845	0.840	0.875	0.921	0.987	1.305	1.609
9000	100	0.10	0.831	0.894	0.880	0.853	0.829	0.830	0.835	0.894	1.152	1.392
9000	100	0.20	0.710	0.780	0.768	0.739	0.642	0.650	0.655	0.665	0.806	0.980
9000	100	0.40	0.516	0.560	0.568	0.561	0.522	0.523	0.525	0.544	0.655	0.871
9000	100	0.60	0.414	0.426	0.441	0.474	0.500	0.502	0.525	0.550	0.714	0.875
9000	100	0.80	0.439	0.430	0.434	0.453	0.488	0.539	0.570	0.611	0.802	1.005
9000	100	1.00	0.558	0.550	0.551	0.634	0.650	0.654	0.681	0.723	0.924	1.131
9000	100	1.20	0.628	0.625	0.629	0.677	0.705	0.709	0.757	0.804	1.037	1.281

P	G	Xe	q (kW m-2)									
			50	100	150	200	400	600	800	1000	2000	3000
(kPa)	(kg m-2 s-1)	(-)	Heat Transfer Coefficient (kW m-2 K-2)									
9000	200	-0.20	2.606	2.590	2.569	2.540	2.451	2.363	2.318	2.302	2.199	2.093
9000	200	-0.10	1.657	1.640	1.625	1.581	1.590	1.593	1.596	1.609	1.712	1.804
9000	200	-0.05	1.205	1.189	1.185	1.162	1.171	1.217	1.234	1.277	1.484	1.697
9000	200	0.00	0.957	1.012	1.010	0.965	0.960	1.036	1.038	1.093	1.360	1.625
9000	200	0.05	0.879	0.922	0.920	0.900	0.897	0.972	0.978	1.034	1.296	1.552
9000	200	0.10	0.829	0.878	0.865	0.839	0.826	0.881	0.897	0.930	1.139	1.342
9000	200	0.20	0.714	0.768	0.742	0.712	0.689	0.723	0.727	0.736	0.847	0.977
9000	200	0.40	0.577	0.610	0.605	0.600	0.599	0.613	0.636	0.640	0.730	0.871
9000	200	0.60	0.547	0.555	0.553	0.653	0.632	0.662	0.671	0.729	0.831	0.982
9000	200	0.80	0.666	0.611	0.608	0.724	0.723	0.713	0.841	0.842	0.970	1.171
9000	200	1.00	0.955	0.931	0.923	1.174	1.145	0.957	1.038	1.073	1.217	1.362
9000	200	1.20	1.032	1.019	1.011	1.141	1.088	1.002	1.010	1.045	1.320	1.544
9000	500	-0.20	2.675	2.660	2.643	2.656	2.606	2.497	2.452	2.414	2.192	2.015
9000	500	-0.10	1.623	1.624	1.630	1.636	1.654	1.680	1.674	1.663	1.723	1.779
9000	500	-0.05	1.211	1.249	1.280	1.284	1.345	1.462	1.397	1.446	1.586	1.710
9000	500	0.00	0.956	1.013	1.056	1.069	1.200	1.389	1.292	1.339	1.499	1.645
9000	500	0.05	0.861	0.904	0.936	0.971	1.102	1.264	1.203	1.231	1.403	1.554
9000	500	0.10	0.863	0.876	0.887	0.903	0.966	1.069	1.093	1.094	1.260	1.399
9000	500	0.20	0.852	0.877	0.878	0.880	0.888	0.980	0.990	0.995	1.125	1.288
9000	500	0.40	0.825	0.879	0.866	0.850	0.879	0.952	0.976	1.220	1.225	1.319
9000	500	0.60	1.087	1.059	1.030	1.029	1.025	1.097	1.139	1.225	1.338	1.555
9000	500	0.80	1.797	1.712	1.634	1.595	1.498	1.552	1.760	1.634	1.545	1.769
9000	500	1.00	2.294	2.205	2.107	2.146	1.889	1.727	1.962	1.876	1.793	2.074
9000	500	1.20	2.201	2.122	2.059	2.089	1.825	1.625	1.765	1.835	2.073	2.563
9000	1000	-0.20	2.579	2.550	2.520	2.459	2.410	2.339	2.307	2.269	2.091	1.917
9000	1000	-0.10	1.624	1.616	1.615	1.614	1.561	1.550	1.545	1.587	1.689	1.779
9000	1000	-0.05	1.257	1.294	1.320	1.313	1.390	1.457	1.437	1.459	1.584	1.708
9000	1000	0.00	0.936	1.025	1.068	1.063	1.292	1.443	1.374	1.396	1.529	1.657
9000	1000	0.05	0.948	1.020	1.032	1.025	1.228	1.327	1.328	1.343	1.480	1.600
9000	1000	0.10	1.078	1.125	1.131	1.098	1.230	1.338	1.340	1.346	1.451	1.548
9000	1000	0.20	1.303	1.333	1.345	1.304	1.285	1.406	1.446	1.459	1.467	1.566
9000	1000	0.40	1.601	1.720	1.657	1.531	1.511	1.600	1.671	2.014	2.016	1.800
9000	1000	0.60	2.922	2.916	2.766	2.251	1.962	1.982	2.040	2.325	2.519	2.270
9000	1000	0.80	4.814	4.559	4.323	3.713	3.063	2.794	2.726	2.663	2.552	2.550
9000	1000	1.00	5.507	5.162	4.880	4.171	3.312	3.185	3.175	3.023	3.020	3.019
9000	1000	1.20	4.245	4.069	3.895	3.549	2.996	2.940	3.226	3.385	3.878	3.510
9000	1500	-0.20	2.671	2.645	2.615	2.542	2.443	2.373	2.309	2.272	2.083	1.902
9000	1500	-0.10	1.548	1.522	1.497	1.462	1.382	1.445	1.472	1.504	1.681	1.895
9000	1500	-0.05	1.180	1.224	1.220	1.164	1.153	1.186	1.211	1.260	1.518	1.808
9000	1500	0.00	1.204	1.240	1.159	1.064	1.060	1.116	1.144	1.194	1.450	1.711
9000	1500	0.05	1.342	1.394	1.343	1.212	1.208	1.249	1.249	1.272	1.456	1.660
9000	1500	0.10	1.694	1.690	1.655	1.578	1.503	1.504	1.504	1.505	1.507	1.547
9000	1500	0.20	1.938	1.918	1.890	1.889	1.765	1.710	1.715	1.720	1.586	1.585
9000	1500	0.40	2.455	2.451	2.429	2.145	2.127	2.125	2.311	2.411	2.240	2.134
9000	1500	0.60	5.647	5.448	5.199	3.860	3.519	3.364	3.561	3.692	3.540	3.237
9000	1500	0.80	9.693	9.182	8.675	7.288	5.605	4.354	4.365	4.398	4.354	4.100
9000	1500	1.00	11.164	10.593	10.026	8.858	6.559	4.993	4.994	4.995	4.927	4.800

P	G	Xe	q (kW m-2)									
			50	100	150	200	400	600	800	1000	2000	3000
(kPa)	(kg m-2 s-1)	(-)	Heat Transfer Coefficient (kW m-2 K-2)									
9000	1500	1.20	6.942	6.743	6.541	6.251	5.517	4.789	4.882	5.275	5.270	5.265
9000	2000	-0.20	2.712	2.693	2.669	2.644	2.537	2.462	2.376	2.346	2.179	2.138
9000	2000	-0.10	1.568	1.539	1.538	1.515	1.406	1.407	1.480	1.527	1.767	2.025
9000	2000	-0.05	1.314	1.325	1.321	1.221	1.179	1.214	1.265	1.324	1.631	1.908
9000	2000	0.00	1.116	1.179	1.131	1.028	1.024	1.074	1.126	1.189	1.510	1.813
9000	2000	0.05	1.362	1.413	1.376	1.275	1.240	1.286	1.299	1.330	1.531	1.698
9000	2000	0.10	1.864	1.845	1.840	1.839	1.719	1.685	1.648	1.627	1.562	1.622
9000	2000	0.20	2.515	2.512	2.485	2.480	2.317	2.211	2.126	2.078	1.649	1.738
9000	2000	0.40	3.782	3.671	3.588	3.252	3.000	2.950	2.900	2.850	2.680	2.544
9000	2000	0.60	9.458	9.068	8.698	7.772	6.461	5.472	5.224	5.157	4.420	3.800
9000	2000	0.80	14.336	13.784	13.244	12.437	10.516	8.234	7.569	7.227	6.257	5.200
9000	2000	1.00	15.750	15.200	14.635	13.946	11.915	9.358	8.610	8.296	7.154	6.400
9000	2000	1.20	9.235	9.044	8.838	8.656	7.925	6.639	6.083	6.436	6.504	7.173
9000	3000	-0.20	2.705	2.686	2.664	2.649	2.555	2.488	2.411	2.394	2.289	2.170
9000	3000	-0.10	1.810	1.792	1.790	1.819	1.681	1.582	1.671	1.715	1.929	2.144
9000	3000	-0.05	1.483	1.486	1.485	1.434	1.392	1.392	1.458	1.513	1.796	1.950
9000	3000	0.00	1.225	1.261	1.247	1.169	1.160	1.213	1.262	1.328	1.654	1.820
9000	3000	0.05	1.526	1.563	1.560	1.502	1.466	1.519	1.530	1.550	1.726	1.660
9000	3000	0.10	2.535	2.465	2.410	2.400	2.293	2.212	2.132	2.133	1.856	1.700
9000	3000	0.20	3.909	3.828	3.630	3.629	3.405	3.144	3.034	3.123	2.481	2.300
9000	3000	0.40	8.187	7.811	7.427	6.283	5.457	5.400	5.390	5.744	4.697	4.091
9000	3000	0.60	15.841	15.277	14.731	13.697	11.912	9.569	9.201	8.977	8.035	6.382
9000	3000	0.80	21.528	20.904	20.260	19.552	17.205	13.594	12.428	11.837	10.730	8.341
9000	3000	1.00	22.605	22.054	21.438	20.967	18.643	14.864	13.864	13.220	12.171	10.084
9000	3000	1.20	13.004	12.925	12.849	12.758	12.413	11.839	11.247	11.039	10.613	10.510
9000	4000	-0.20	2.688	2.669	2.644	2.623	2.535	2.463	2.393	2.375	2.269	2.151
9000	4000	-0.10	1.982	1.966	1.965	1.964	1.910	1.855	1.856	1.884	2.027	1.995
9000	4000	-0.05	1.454	1.482	1.530	1.529	1.447	1.416	1.488	1.548	1.819	1.820
9000	4000	0.00	1.507	1.527	1.571	1.481	1.350	1.349	1.364	1.459	1.749	1.820
9000	4000	0.05	1.918	1.920	1.914	1.714	1.578	1.540	1.541	1.600	1.766	1.891
9000	4000	0.10	3.943	3.750	3.524	3.011	2.692	2.380	2.390	2.887	2.390	2.200
9000	4000	0.20	7.883	7.590	7.222	6.555	5.787	5.210	5.345	5.972	4.419	3.200
9000	4000	0.40	14.372	13.914	13.450	12.646	11.357	9.591	10.048	8.780	7.403	5.700
9000	4000	0.60	21.335	20.801	20.254	19.744	17.889	14.956	14.331	13.324	12.177	9.400
9000	4000	0.80	27.272	26.825	26.375	25.958	24.238	22.437	20.652	19.160	16.673	13.600
9000	4000	1.00	28.017	27.732	27.443	27.148	25.924	24.471	23.035	21.886	19.038	16.000
9000	4000	1.20	16.754	16.701	16.651	16.604	16.437	16.278	16.140	16.028	15.384	15.300
9000	5000	-0.20	2.683	2.660	2.633	2.611	2.524	2.454	2.389	2.371	2.262	2.145
9000	5000	-0.10	2.062	2.063	2.074	2.075	2.042	2.009	1.983	1.998	2.097	2.162
9000	5000	-0.05	1.484	1.516	1.568	1.624	1.542	1.540	1.594	1.640	1.899	2.170
9000	5000	0.00	1.737	1.753	1.791	1.735	1.577	1.564	1.600	1.682	1.997	2.310
9000	5000	0.05	2.300	2.274	2.262	2.049	1.916	1.915	1.935	2.049	2.517	2.512
9000	5000	0.10	5.216	4.934	4.607	3.704	3.362	3.163	3.117	3.592	3.306	2.951
9000	5000	0.20	10.961	10.540	10.105	9.290	8.185	6.502	6.225	7.784	5.221	4.300
9000	5000	0.40	18.466	18.067	17.663	17.248	15.785	13.986	13.524	12.756	10.613	8.800
9000	5000	0.60	25.880	25.480	25.074	24.687	23.220	21.666	20.362	19.145	18.106	15.000
9000	5000	0.80	32.836	32.485	32.134	31.798	30.453	29.178	27.803	26.558	22.493	19.600

P	G	Xe	q (kW m-2)									
			50	100	150	200	400	600	800	1000	2000	3000
(kPa)	(kg m-2 s-1)	(-)	Heat Transfer Coefficient (kW m-2 K-2)									
9000	5000	1.00	33.618	33.403	33.190	32.912	31.959	30.989	29.930	28.950	24.902	21.300
9000	5000	1.20	20.389	20.339	20.290	20.245	20.083	20.001	19.921	19.801	19.189	19.000
9000	6000	-0.20	2.705	2.683	2.659	2.637	2.555	2.492	2.436	2.434	2.416	2.692
9000	6000	-0.10	1.933	1.940	1.949	1.948	1.969	1.987	2.010	2.043	2.295	2.467
9000	6000	-0.05	1.352	1.352	1.355	1.352	1.379	1.422	1.472	1.554	1.995	2.344
9000	6000	0.00	1.639	1.622	1.612	1.596	1.601	1.655	1.735	1.872	2.554	2.951
9000	6000	0.05	3.606	3.525	3.457	3.329	3.277	3.381	3.549	3.831	4.677	4.467
9000	6000	0.10	7.155	7.070	6.999	6.823	6.680	6.860	7.355	8.279	9.135	7.734
9000	6000	0.20	12.511	12.368	12.235	12.116	11.769	11.468	11.051	11.994	9.136	7.735
9000	6000	0.40	21.059	20.798	20.545	20.317	19.482	18.723	18.040	18.031	15.973	14.928
9000	6000	0.60	30.305	29.947	29.598	29.289	27.991	26.894	25.851	24.495	22.606	20.248
9000	6000	0.80	38.767	38.418	38.073	37.749	36.468	35.285	34.147	32.976	27.758	26.500
9000	6000	1.00	39.641	39.429	39.216	38.965	38.018	37.027	36.039	34.930	29.742	28.840
9000	6000	1.20	23.990	23.934	23.881	23.833	23.656	23.485	23.326	23.239	22.635	22.084
9000	7000	-0.20	2.709	2.688	2.667	2.647	2.578	2.528	2.486	2.493	2.515	2.609
9000	7000	-0.10	1.906	1.905	1.900	1.895	1.956	2.000	2.045	2.088	2.381	2.608
9000	7000	-0.05	1.376	1.369	1.367	1.348	1.379	1.422	1.484	1.577	2.089	2.570
9000	7000	0.00	1.865	1.819	1.788	1.746	1.745	1.789	1.864	2.019	2.771	3.236
9000	7000	0.05	4.405	4.322	4.260	4.170	4.105	4.158	4.275	4.573	5.888	5.888
9000	7000	0.10	8.319	8.250	8.201	8.130	8.009	8.179	8.634	9.308	11.600	10.900
9000	7000	0.20	14.183	14.064	13.945	13.863	13.444	13.067	12.568	12.452	11.617	10.967
9000	7000	0.40	23.929	23.722	23.528	23.300	22.663	22.200	21.882	21.967	21.768	20.653
9000	7000	0.60	34.844	34.513	34.194	33.908	32.832	31.917	31.055	30.369	27.650	23.988
9000	7000	0.80	44.596	44.241	43.887	43.562	42.261	41.028	39.851	38.722	32.967	28.840
9000	7000	1.00	45.352	45.125	44.895	44.639	43.613	42.488	41.393	40.276	34.329	30.903
9000	7000	1.20	27.527	27.469	27.413	27.363	27.177	27.004	26.833	26.716	26.172	25.638
10000	0	-0.20	1.847	1.806	1.777	1.735	1.690	1.644	1.631	1.680	1.906	2.085
10000	0	-0.10	1.307	1.281	1.268	1.241	1.249	1.251	1.284	1.370	1.781	2.149
10000	0	-0.05	1.053	1.031	1.023	0.999	1.030	1.056	1.112	1.217	1.728	2.196
10000	0	0.00	0.862	0.848	0.847	0.829	0.883	0.930	1.004	1.122	1.696	2.232
10000	0	0.05	0.808	0.799	0.801	0.788	0.850	0.903	0.981	1.101	1.686	2.233
10000	0	0.10	0.776	0.770	0.774	0.764	0.826	0.879	0.958	1.074	1.649	2.186
10000	0	0.20	0.691	0.691	0.699	0.694	0.758	0.815	0.894	1.007	1.569	2.092
10000	0	0.40	0.640	0.642	0.650	0.647	0.715	0.775	0.854	0.968	1.534	2.066
10000	0	0.60	0.646	0.646	0.654	0.644	0.719	0.779	0.859	0.973	1.540	2.064
10000	0	0.80	0.654	0.656	0.664	0.663	0.729	0.788	0.869	0.980	1.541	2.060
10000	0	1.00	0.656	0.656	0.672	0.667	0.737	0.796	0.880	0.989	1.542	2.058
10000	0	1.20	0.641	0.650	0.669	0.664	0.746	0.812	0.898	1.003	1.542	2.048
10000	50	-0.20	2.426	2.405	2.387	2.356	2.298	2.221	2.170	2.185	2.203	2.175
10000	50	-0.10	1.655	1.633	1.619	1.583	1.569	1.535	1.534	1.584	1.795	1.967
10000	50	-0.05	1.251	1.222	1.209	1.176	1.175	1.173	1.202	1.274	1.610	1.914
10000	50	0.00	0.947	0.922	0.915	0.889	0.917	0.938	0.993	1.081	1.508	1.907
10000	50	0.05	0.862	0.845	0.845	0.824	0.863	0.892	0.951	1.040	1.469	1.873
10000	50	0.10	0.766	0.758	0.759	0.743	0.779	0.808	0.856	0.937	1.314	1.673
10000	50	0.20	0.558	0.559	0.559	0.554	0.579	0.609	0.649	0.712	0.995	1.284
10000	50	0.40	0.452	0.458	0.461	0.460	0.484	0.515	0.553	0.608	0.861	1.125
10000	50	0.60	0.480	0.483	0.492	0.490	0.511	0.543	0.581	0.640	0.901	1.171

P	G	Xe	q (kW m-2)									
			50	100	150	200	400	600	800	1000	2000	3000
(kPa)	(kg m-2 s-1)	(-)	Heat Transfer Coefficient (kW m-2 K-2)									
10000	50	0.80	0.517	0.513	0.517	0.513	0.548	0.584	0.625	0.687	0.954	1.235
10000	50	1.00	0.564	0.558	0.561	0.549	0.593	0.638	0.681	0.745	1.020	1.310
10000	50	1.20	0.573	0.572	0.576	0.576	0.617	0.669	0.719	0.785	1.065	1.364
10000	100	-0.20	2.767	2.755	2.738	2.713	2.638	2.549	2.478	2.468	2.356	2.210
10000	100	-0.10	1.849	1.829	1.813	1.773	1.743	1.694	1.677	1.705	1.807	1.874
10000	100	-0.05	1.356	1.325	1.309	1.270	1.262	1.247	1.262	1.315	1.561	1.781
10000	100	0.00	0.993	0.966	0.958	0.931	0.948	0.961	1.004	1.076	1.424	1.750
10000	100	0.05	0.894	0.878	0.878	0.856	0.884	0.905	0.952	1.025	1.376	1.704
10000	100	0.10	0.778	0.798	0.799	0.773	0.784	0.801	0.832	0.897	1.183	1.453
10000	100	0.20	0.530	0.583	0.584	0.549	0.552	0.556	0.575	0.614	0.780	0.954
10000	100	0.40	0.404	0.442	0.450	0.437	0.443	0.448	0.463	0.494	0.622	0.761
10000	100	0.60	0.449	0.467	0.472	0.479	0.489	0.493	0.509	0.548	0.706	0.869
10000	100	0.80	0.513	0.513	0.515	0.517	0.534	0.557	0.579	0.624	0.805	0.994
10000	100	1.00	0.600	0.590	0.591	0.575	0.606	0.640	0.666	0.716	0.914	1.125
10000	100	1.20	0.616	0.610	0.610	0.602	0.629	0.670	0.709	0.765	0.987	1.224
10000	200	-0.20	2.926	2.911	2.889	2.817	2.749	2.676	2.625	2.606	2.487	2.371
10000	200	-0.10	1.911	1.890	1.870	1.808	1.786	1.761	1.744	1.763	1.839	1.910
10000	200	-0.05	1.385	1.371	1.351	1.316	1.292	1.326	1.326	1.369	1.568	1.773
10000	200	0.00	1.002	1.001	1.019	0.987	1.000	1.060	1.065	1.125	1.401	1.683
10000	200	0.05	0.877	0.885	0.901	0.887	0.911	0.978	0.982	1.047	1.323	1.599
10000	200	0.10	0.764	0.781	0.792	0.788	0.793	0.825	0.875	0.905	1.135	1.367
10000	200	0.20	0.547	0.586	0.614	0.614	0.600	0.624	0.664	0.665	0.807	0.975
10000	200	0.40	0.488	0.518	0.552	0.555	0.550	0.566	0.586	0.565	0.696	0.838
10000	200	0.60	0.623	0.653	0.685	0.715	0.627	0.624	0.654	0.630	0.813	0.992
10000	200	0.80	0.797	0.782	0.757	0.943	0.766	0.753	0.794	0.743	0.966	1.174
10000	200	1.00	0.935	0.911	0.887	1.047	0.940	0.839	0.947	0.884	1.127	1.369
10000	200	1.20	0.917	0.891	0.872	0.844	0.882	0.819	0.926	0.919	1.221	1.546
10000	500	-0.20	2.953	2.930	2.906	2.818	2.834	2.756	2.741	2.712	2.537	2.402
10000	500	-0.10	1.871	1.868	1.859	1.868	1.868	1.870	1.869	1.880	1.880	1.902
10000	500	-0.05	1.413	1.452	1.440	1.461	1.461	1.565	1.494	1.531	1.648	1.760
10000	500	0.00	0.959	1.041	1.063	1.076	1.205	1.382	1.298	1.354	1.504	1.652
10000	500	0.05	0.817	0.876	0.884	0.902	1.038	1.207	1.144	1.220	1.396	1.559
10000	500	0.10	0.796	0.803	0.814	0.826	0.882	0.998	0.979	1.071	1.244	1.397
10000	500	0.20	0.819	0.827	0.850	0.864	0.827	0.928	0.916	0.966	1.080	1.211
10000	500	0.40	0.892	0.937	0.937	0.945	0.874	0.923	0.962	1.030	1.144	1.295
10000	500	0.60	1.175	1.152	1.132	1.245	1.153	1.150	1.268	1.268	1.333	1.552
10000	500	0.80	1.797	1.740	1.674	1.926	1.497	1.454	1.600	1.607	1.610	1.829
10000	500	1.00	2.139	2.068	1.995	2.089	1.736	1.586	1.880	1.886	1.889	2.193
10000	500	1.20	1.931	1.859	1.800	1.661	1.609	1.543	1.846	1.850	2.128	2.668
10000	1000	-0.20	2.962	2.928	2.890	2.791	2.722	2.651	2.615	2.578	2.399	2.225
10000	1000	-0.10	1.866	1.855	1.846	1.854	1.787	1.775	1.781	1.784	1.824	1.875
10000	1000	-0.05	1.397	1.437	1.431	1.450	1.477	1.560	1.513	1.533	1.642	1.756
10000	1000	0.00	1.001	1.093	1.092	1.085	1.269	1.431	1.363	1.389	1.533	1.672
10000	1000	0.05	1.040	1.103	1.077	1.027	1.174	1.330	1.283	1.306	1.474	1.606
10000	1000	0.10	1.213	1.246	1.232	1.156	1.202	1.331	1.332	1.333	1.448	1.533
10000	1000	0.20	1.458	1.484	1.482	1.469	1.407	1.442	1.467	1.482	1.520	1.520
10000	1000	0.40	1.712	1.839	1.754	1.626	1.622	1.664	1.709	1.846	1.683	1.803

P	G	Xe	q (kW m-2)									
			50	100	150	200	400	600	800	1000	2000	3000
(kPa)	(kg m-2 s-1)	(-)	Heat Transfer Coefficient (kW m-2 K-2)									
10000	1000	0.60	2.763	2.800	2.683	2.241	2.240	2.240	2.261	2.376	2.142	2.276
10000	1000	0.80	4.374	4.149	3.945	3.470	2.800	2.801	2.813	2.955	2.701	2.924
10000	1000	1.00	5.046	4.730	4.490	3.599	3.120	3.201	3.270	3.270	3.269	3.672
10000	1000	1.20	4.180	4.026	3.875	3.451	3.059	3.195	3.390	3.391	3.390	4.576
10000	1500	-0.20	3.072	3.045	3.013	2.962	2.821	2.731	2.655	2.603	2.330	2.071
10000	1500	-0.10	1.717	1.680	1.643	1.591	1.504	1.563	1.584	1.612	1.762	1.964
10000	1500	-0.05	1.266	1.265	1.239	1.190	1.168	1.237	1.257	1.306	1.567	1.848
10000	1500	0.00	1.315	1.314	1.232	1.095	1.094	1.149	1.174	1.224	1.481	1.737
10000	1500	0.05	1.513	1.512	1.458	1.301	1.273	1.318	1.318	1.329	1.487	1.672
10000	1500	0.10	1.888	1.885	1.847	1.745	1.612	1.613	1.593	1.592	1.591	1.516
10000	1500	0.20	2.141	2.127	2.089	2.085	1.959	1.959	1.884	1.857	1.694	1.530
10000	1500	0.40	2.353	2.508	2.525	2.526	2.656	2.821	2.798	2.682	1.944	1.870
10000	1500	0.60	5.570	5.399	5.176	3.819	3.799	3.691	3.690	3.687	3.235	2.890
10000	1500	0.80	9.629	9.151	8.680	7.246	5.688	4.797	4.689	4.688	4.543	3.999
10000	1500	1.00	11.252	10.747	10.252	9.168	7.000	5.837	5.680	5.678	5.677	5.171
10000	1500	1.20	7.275	7.113	6.956	6.753	5.970	5.723	5.685	5.888	6.126	5.530
10000	2000	-0.20	3.119	3.100	3.073	3.056	2.935	2.836	2.727	2.674	2.391	2.106
10000	2000	-0.10	1.708	1.636	1.580	1.550	1.449	1.467	1.542	1.587	1.821	2.068
10000	2000	-0.05	1.235	1.234	1.213	1.146	1.110	1.155	1.217	1.284	1.632	1.964
10000	2000	0.00	1.260	1.256	1.203	1.076	1.061	1.108	1.159	1.221	1.580	1.846
10000	2000	0.05	1.550	1.545	1.511	1.396	1.344	1.381	1.387	1.411	1.575	1.783
10000	2000	0.10	2.059	2.027	2.022	2.020	1.863	1.786	1.733	1.704	1.510	1.698
10000	2000	0.20	2.744	2.736	2.615	2.677	2.480	2.360	2.241	2.027	1.307	1.820
10000	2000	0.40	3.845	3.742	3.693	3.458	3.293	3.478	3.604	3.433	2.535	2.600
10000	2000	0.60	9.863	9.454	9.055	8.092	6.645	5.752	5.730	5.729	5.147	4.175
10000	2000	0.80	15.100	14.527	13.961	13.164	11.204	9.099	8.225	8.223	7.378	6.600
10000	2000	1.00	16.591	16.070	15.546	14.923	13.084	11.076	9.930	9.928	9.100	8.300
10000	2000	1.20	9.637	9.534	9.438	9.322	9.008	8.667	8.388	8.385	8.161	8.083
10000	3000	-0.20	3.110	3.091	3.067	3.054	2.947	2.856	2.757	2.715	2.489	2.252
10000	3000	-0.10	1.959	1.898	1.842	1.764	1.654	1.626	1.713	1.755	1.964	2.182
10000	3000	-0.05	1.358	1.381	1.365	1.309	1.249	1.280	1.346	1.413	1.766	2.120
10000	3000	0.00	1.302	1.322	1.306	1.224	1.184	1.245	1.283	1.352	1.693	2.027
10000	3000	0.05	1.702	1.735	1.734	1.681	1.603	1.645	1.647	1.661	1.727	1.998
10000	3000	0.10	2.804	2.717	2.685	2.680	2.475	2.349	2.235	2.189	1.729	2.089
10000	3000	0.20	4.225	4.122	3.960	3.958	3.672	3.358	3.265	2.985	1.810	2.630
10000	3000	0.40	8.652	8.253	7.835	6.379	6.350	6.325	6.300	6.242	4.663	4.500
10000	3000	0.60	16.833	16.288	15.778	14.739	13.224	11.430	10.893	11.010	10.154	7.300
10000	3000	0.80	22.829	22.288	21.754	21.197	19.334	17.090	15.333	15.082	13.900	10.600
10000	3000	1.00	23.806	23.402	22.975	22.739	21.125	18.862	17.105	16.525	15.100	12.000
10000	3000	1.20	13.755	13.679	13.612	13.500	13.280	13.054	12.818	12.557	12.500	12.000
10000	4000	-0.20	3.091	3.069	3.041	3.023	2.917	2.828	2.735	2.695	2.478	2.249
10000	4000	-0.10	2.239	2.213	2.199	2.190	2.090	2.009	2.010	2.025	2.122	2.193
10000	4000	-0.05	1.557	1.581	1.611	1.610	1.487	1.484	1.552	1.612	1.881	2.154
10000	4000	0.00	1.600	1.619	1.665	1.577	1.431	1.430	1.444	1.544	1.841	2.115
10000	4000	0.05	2.041	2.047	2.048	1.837	1.718	1.690	1.692	1.766	1.975	2.100
10000	4000	0.10	4.350	4.124	3.866	3.225	2.941	2.659	2.660	3.162	2.582	2.500
10000	4000	0.20	8.685	8.357	7.932	7.145	6.302	5.876	6.042	6.298	4.077	3.467

P	G	Xe	q (kW m-2)									
			50	100	150	200	400	600	800	1000	2000	3000
(kPa)	(kg m-2 s-1)	(-)	Heat Transfer Coefficient (kW m-2 K-2)									
10000	4000	0.40	15.444	14.965	14.479	13.597	12.186	10.683	10.533	9.401	7.566	5.700
10000	4000	0.60	22.769	22.244	21.717	21.207	19.384	17.111	16.383	15.373	13.878	9.400
10000	4000	0.80	29.057	28.628	28.201	27.809	26.242	24.737	23.400	22.038	18.600	14.000
10000	4000	1.00	29.793	29.523	29.251	28.978	27.841	26.716	25.408	24.487	20.529	15.976
10000	4000	1.20	17.798	17.725	17.656	17.585	17.354	17.141	16.977	16.829	16.007	15.600
10000	5000	-0.20	3.086	3.060	3.030	3.010	2.905	2.816	2.728	2.688	2.465	2.240
10000	5000	-0.10	2.385	2.380	2.378	2.354	2.276	2.224	2.190	2.186	2.229	2.232
10000	5000	-0.05	1.618	1.654	1.735	1.730	1.635	1.628	1.676	1.719	1.956	2.207
10000	5000	0.00	1.820	1.842	1.880	1.830	1.664	1.642	1.678	1.753	2.040	2.324
10000	5000	0.05	2.417	2.398	2.389	2.160	2.031	2.030	2.068	2.160	2.556	2.754
10000	5000	0.10	5.709	5.396	5.022	3.954	3.631	3.413	3.370	3.616	3.540	3.715
10000	5000	0.20	12.080	11.613	11.122	10.201	8.860	6.589	6.089	7.859	5.635	5.888
10000	5000	0.40	19.917	19.513	19.110	18.689	17.211	15.471	14.765	13.655	11.144	9.200
10000	5000	0.60	27.653	27.267	26.879	26.502	25.127	23.894	22.635	21.205	17.784	13.957
10000	5000	0.80	34.951	34.604	34.261	33.926	32.613	31.422	30.223	29.020	23.683	18.299
10000	5000	1.00	35.706	35.489	35.273	34.985	34.031	33.020	32.031	31.100	26.237	21.283
10000	5000	1.20	21.694	21.616	21.539	21.465	21.197	20.975	20.756	20.588	19.758	18.909
10000	6000	-0.20	3.113	3.088	3.060	3.038	2.933	2.846	2.760	2.725	2.541	2.359
10000	6000	-0.10	2.260	2.255	2.251	2.243	2.222	2.203	2.195	2.219	2.325	2.372
10000	6000	-0.05	1.443	1.442	1.441	1.439	1.467	1.505	1.552	1.624	1.979	2.372
10000	6000	0.00	1.644	1.631	1.624	1.615	1.621	1.665	1.730	1.836	2.375	2.979
10000	6000	0.05	3.809	3.711	3.621	3.488	3.342	3.343	3.392	3.575	4.434	4.467
10000	6000	0.10	7.917	7.789	7.672	7.448	7.095	6.870	6.721	6.786	7.872	7.079
10000	6000	0.20	13.813	13.629	13.454	13.298	12.627	11.930	11.372	11.507	9.235	10.000
10000	6000	0.40	22.769	22.500	22.241	22.010	21.051	20.202	19.286	18.897	15.824	13.612
10000	6000	0.60	32.465	32.103	31.750	31.441	30.176	29.049	27.954	26.970	22.676	18.417
10000	6000	0.80	41.375	41.008	40.644	40.303	38.945	37.654	36.380	35.196	29.313	23.456
10000	6000	1.00	42.197	41.966	41.733	41.459	40.435	39.346	38.261	37.193	31.754	26.198
10000	6000	1.20	25.498	25.425	25.354	25.290	25.044	24.822	24.607	24.418	23.490	22.576
10000	7000	-0.20	3.121	3.097	3.071	3.048	2.958	2.884	2.814	2.790	2.663	2.556
10000	7000	-0.10	2.198	2.196	2.195	2.193	2.210	2.225	2.247	2.284	2.456	2.555
10000	7000	-0.05	1.466	1.455	1.449	1.431	1.458	1.500	1.556	1.639	2.050	2.516
10000	7000	0.00	1.888	1.841	1.811	1.772	1.765	1.797	1.855	1.971	2.565	3.248
10000	7000	0.05	4.699	4.597	4.513	4.416	4.240	4.182	4.176	4.337	5.209	5.248
10000	7000	0.10	9.197	9.092	9.005	8.912	8.599	8.373	8.179	8.207	9.365	8.710
10000	7000	0.20	15.650	15.493	15.333	15.218	14.626	14.106	13.552	13.155	11.537	12.000
10000	7000	0.40	25.939	25.685	25.443	25.170	24.317	23.594	22.802	22.351	20.127	17.884
10000	7000	0.60	37.394	37.020	36.657	36.335	35.066	33.934	32.865	31.996	27.369	22.881
10000	7000	0.80	47.614	47.232	46.852	46.504	45.093	43.740	42.407	41.164	34.922	28.740
10000	7000	1.00	48.269	48.030	47.789	47.521	46.449	45.293	44.132	42.993	37.162	31.184
10000	7000	1.20	29.262	29.185	29.111	29.044	28.789	28.560	28.338	28.137	27.170	26.221
11000	0	-0.20	1.919	1.881	1.853	1.816	1.772	1.734	1.728	1.777	2.012	2.197
11000	0	-0.10	1.376	1.350	1.336	1.308	1.313	1.315	1.349	1.432	1.833	2.197
11000	0	-0.05	1.118	1.094	1.085	1.058	1.085	1.107	1.161	1.263	1.759	2.214
11000	0	0.00	0.925	0.907	0.905	0.885	0.933	0.973	1.044	1.159	1.720	2.241
11000	0	0.05	0.863	0.851	0.852	0.837	0.894	0.942	1.018	1.137	1.713	2.251
11000	0	0.10	0.824	0.816	0.819	0.807	0.867	0.917	0.993	1.111	1.684	2.217

P	G	Xe	q (kW m-2)									
			50	100	150	200	400	600	800	1000	2000	3000
(kPa)	(kg m-2 s-1)	(-)	Heat Transfer Coefficient (kW m-2 K-2)									
11000	0	0.20	0.737	0.735	0.742	0.735	0.797	0.852	0.927	1.040	1.592	2.106
11000	0	0.40	0.672	0.671	0.680	0.675	0.745	0.801	0.879	0.989	1.547	2.070
11000	0	0.60	0.649	0.647	0.654	0.621	0.725	0.786	0.870	0.982	1.546	2.069
11000	0	0.80	0.660	0.658	0.665	0.639	0.728	0.797	0.883	0.992	1.551	2.068
11000	0	1.00	0.687	0.685	0.694	0.687	0.760	0.825	0.910	1.016	1.559	2.066
11000	0	1.20	0.702	0.700	0.715	0.712	0.786	0.854	0.937	1.039	1.561	2.052
11000	50	-0.20	2.640	2.632	2.625	2.608	2.582	2.532	2.497	2.527	2.640	2.682
11000	50	-0.10	1.816	1.799	1.788	1.760	1.750	1.717	1.713	1.764	1.979	2.146
11000	50	-0.05	1.378	1.349	1.335	1.299	1.297	1.284	1.305	1.376	1.700	1.989
11000	50	0.00	1.035	1.007	0.996	0.962	0.982	0.995	1.041	1.129	1.550	1.941
11000	50	0.05	0.924	0.903	0.899	0.872	0.908	0.934	0.988	1.080	1.520	1.930
11000	50	0.10	0.787	0.773	0.773	0.754	0.795	0.827	0.883	0.967	1.374	1.760
11000	50	0.20	0.516	0.510	0.512	0.509	0.546	0.586	0.640	0.703	1.006	1.321
11000	50	0.40	0.431	0.430	0.434	0.437	0.461	0.499	0.541	0.601	0.857	1.127
11000	50	0.60	0.541	0.540	0.546	0.575	0.576	0.578	0.605	0.664	0.912	1.165
11000	50	0.80	0.595	0.592	0.599	0.620	0.622	0.631	0.656	0.718	0.967	1.224
11000	50	1.00	0.614	0.605	0.609	0.622	0.632	0.659	0.694	0.757	1.024	1.303
11000	50	1.20	0.584	0.579	0.582	0.587	0.624	0.664	0.712	0.778	1.061	1.359
11000	100	-0.20	3.075	3.080	3.078	3.074	3.041	2.985	2.933	2.932	2.930	2.860
11000	100	-0.10	2.072	2.057	2.046	2.019	1.990	1.942	1.916	1.942	2.036	2.085
11000	100	-0.05	1.522	1.491	1.472	1.435	1.413	1.386	1.389	1.440	1.669	1.867
11000	100	0.00	1.095	1.063	1.048	1.011	1.015	1.016	1.049	1.121	1.467	1.785
11000	100	0.05	0.956	0.934	0.928	0.898	0.922	0.938	0.982	1.058	1.425	1.762
11000	100	0.10	0.767	0.756	0.754	0.736	0.768	0.793	0.839	0.907	1.238	1.548
11000	100	0.20	0.402	0.402	0.405	0.406	0.438	0.475	0.520	0.562	0.771	0.999
11000	100	0.40	0.331	0.341	0.347	0.359	0.367	0.397	0.423	0.461	0.604	0.766
11000	100	0.60	0.557	0.571	0.588	0.685	0.691	0.699	0.712	0.718	0.720	0.851
11000	100	0.80	0.654	0.657	0.678	0.775	0.779	0.783	0.790	0.798	0.821	0.965
11000	100	1.00	0.647	0.648	0.649	0.670	0.675	0.679	0.683	0.715	0.907	1.104
11000	100	1.20	0.574	0.565	0.564	0.586	0.606	0.623	0.658	0.712	0.956	1.206
11000	200	-0.20	3.305	3.308	3.301	3.291	3.236	3.191	3.144	3.137	3.070	2.944
11000	200	-0.10	2.194	2.177	2.161	2.129	2.071	2.036	2.009	2.027	2.091	2.121
11000	200	-0.05	1.590	1.560	1.539	1.504	1.461	1.446	1.443	1.485	1.682	1.871
11000	200	0.00	1.120	1.091	1.078	1.048	1.039	1.052	1.075	1.135	1.424	1.714
11000	200	0.05	0.952	0.932	0.929	0.904	0.918	0.946	0.982	1.045	1.341	1.628
11000	200	0.10	0.746	0.738	0.740	0.729	0.750	0.786	0.825	0.880	1.143	1.402
11000	200	0.20	0.392	0.399	0.408	0.359	0.431	0.511	0.551	0.585	0.766	0.982
11000	200	0.40	0.432	0.448	0.460	0.512	0.565	0.582	0.583	0.584	0.684	0.846
11000	200	0.60	0.898	1.036	1.079	1.258	0.857	0.784	0.716	0.717	0.859	1.018
11000	200	0.80	1.056	1.155	1.167	1.234	0.941	0.936	0.878	0.880	1.055	1.192
11000	200	1.00	0.890	0.890	0.909	0.957	0.825	0.820	0.819	0.881	1.119	1.380
11000	200	1.20	0.700	0.686	0.686	0.690	0.692	0.750	0.816	0.844	1.198	1.555
11000	500	-0.20	3.453	3.439	3.419	3.351	3.293	3.247	3.235	3.218	3.122	3.015
11000	500	-0.10	2.262	2.238	2.215	2.157	2.112	2.073	2.059	2.070	2.110	2.149
11000	500	-0.05	1.615	1.609	1.585	1.608	1.535	1.562	1.537	1.569	1.726	1.858
11000	500	0.00	1.118	1.115	1.109	1.086	1.170	1.224	1.186	1.235	1.462	1.647
11000	500	0.05	0.929	0.927	0.912	0.888	0.982	1.068	1.054	1.105	1.351	1.527

P	G	Xe	q (kW m-2)									
			50	100	150	200	400	600	800	1000	2000	3000
(kPa)	(kg m-2 s-1)	(-)	Heat Transfer Coefficient (kW m-2 K-2)									
11000	500	0.10	0.854	0.833	0.818	0.802	0.824	0.913	0.974	1.001	1.209	1.346
11000	500	0.20	0.767	0.754	0.782	0.820	0.821	0.911	0.934	0.886	1.013	1.202
11000	500	0.40	0.914	0.932	0.950	1.144	1.234	1.162	1.265	1.209	1.210	1.212
11000	500	0.60	1.427	1.505	1.489	1.541	1.286	1.164	1.286	1.210	1.271	1.513
11000	500	0.80	1.693	1.722	1.691	1.779	1.386	1.288	1.504	1.449	1.542	1.851
11000	500	1.00	1.501	1.489	1.488	1.516	1.481	1.437	1.701	1.571	1.866	2.265
11000	500	1.20	1.341	1.316	1.303	1.265	1.415	1.471	1.730	1.671	2.133	2.741
11000	1000	-0.20	3.481	3.462	3.436	3.383	3.268	3.212	3.193	3.156	2.969	2.775
11000	1000	-0.10	2.267	2.238	2.212	2.162	2.075	2.042	2.039	2.044	2.070	2.091
11000	1000	-0.05	1.590	1.585	1.569	1.568	1.534	1.530	1.524	1.555	1.714	1.852
11000	1000	0.00	1.153	1.150	1.147	1.141	1.140	1.135	1.130	1.262	1.484	1.673
11000	1000	0.05	1.162	1.160	1.121	1.119	1.118	1.115	1.110	1.223	1.415	1.561
11000	1000	0.10	1.410	1.370	1.336	1.332	1.329	1.325	1.324	1.335	1.405	1.436
11000	1000	0.20	1.880	1.792	1.762	1.992	1.970	1.851	1.828	1.829	1.490	1.491
11000	1000	0.40	1.921	1.920	1.877	1.994	1.972	1.857	1.870	1.871	1.520	1.585
11000	1000	0.60	2.496	2.458	2.429	2.496	2.313	2.221	2.261	2.262	1.925	1.932
11000	1000	0.80	3.398	3.302	3.252	3.240	2.842	2.828	2.867	3.096	2.723	2.789
11000	1000	1.00	3.770	3.636	3.562	3.167	3.278	3.312	3.494	3.495	3.496	3.730
11000	1000	1.20	3.853	3.749	3.662	3.050	3.408	3.414	3.620	3.621	4.073	4.649
11000	1500	-0.20	3.522	3.511	3.490	3.479	3.383	3.300	3.215	3.152	2.827	2.499
11000	1500	-0.10	2.223	2.192	2.168	2.056	1.987	2.012	1.996	2.006	2.044	2.073
11000	1500	-0.05	1.539	1.517	1.490	1.389	1.361	1.414	1.439	1.480	1.688	1.895
11000	1500	0.00	1.247	1.264	1.229	1.144	1.137	1.157	1.189	1.241	1.499	1.750
11000	1500	0.05	1.506	1.521	1.482	1.358	1.320	1.321	1.319	1.350	1.511	1.663
11000	1500	0.10	2.035	2.035	1.995	1.981	1.852	1.856	1.743	1.691	1.618	1.518
11000	1500	0.20	2.805	2.815	2.810	2.800	2.786	2.787	2.420	2.313	1.897	1.660
11000	1500	0.40	3.378	3.421	3.420	3.419	3.154	3.154	2.902	2.681	1.898	1.790
11000	1500	0.60	4.478	4.333	4.206	3.910	3.827	3.973	3.877	3.748	3.147	2.754
11000	1500	0.80	7.268	6.926	6.618	5.598	5.280	5.410	5.147	5.200	4.775	4.252
11000	1500	1.00	9.787	9.365	8.962	7.793	6.415	6.466	6.023	6.385	6.300	5.806
11000	1500	1.20	7.717	7.568	7.421	7.427	6.753	6.473	6.208	6.461	6.485	6.682
11000	2000	-0.20	3.540	3.530	3.512	3.512	3.421	3.336	3.239	3.169	2.805	2.436
11000	2000	-0.10	2.207	2.170	2.141	2.029	1.925	1.917	1.955	1.975	2.067	2.143
11000	2000	-0.05	1.485	1.443	1.392	1.266	1.234	1.327	1.410	1.462	1.725	2.000
11000	2000	0.00	1.253	1.281	1.256	1.133	1.118	1.158	1.221	1.283	1.580	1.879
11000	2000	0.05	1.702	1.683	1.647	1.509	1.435	1.466	1.454	1.495	1.684	1.622
11000	2000	0.10	2.556	2.424	2.312	2.186	1.926	1.909	1.679	1.584	1.626	1.571
11000	2000	0.20	3.337	3.218	3.093	3.086	2.896	2.712	2.295	1.921	1.368	1.585
11000	2000	0.40	5.700	5.514	5.348	5.257	4.521	4.166	3.859	3.602	2.378	2.300
11000	2000	0.60	9.572	9.173	8.798	7.661	6.511	6.393	6.252	6.588	5.745	4.243
11000	2000	0.80	14.869	14.303	13.748	12.127	10.035	9.274	9.130	9.826	8.489	6.432
11000	2000	1.00	16.703	16.183	15.666	14.647	12.232	10.987	11.179	11.166	10.300	9.200
11000	2000	1.20	10.341	10.297	10.274	10.248	10.095	10.151	10.616	10.181	9.800	9.800
11000	3000	-0.20	3.533	3.522	3.504	3.504	3.419	3.339	3.249	3.186	2.857	2.514
11000	3000	-0.10	2.334	2.302	2.272	2.212	2.094	2.041	2.059	2.079	2.175	2.243
11000	3000	-0.05	1.517	1.492	1.461	1.375	1.325	1.427	1.501	1.561	1.854	2.160
11000	3000	0.00	1.356	1.350	1.345	1.290	1.243	1.309	1.374	1.442	1.800	1.905

P	G	Xe	q (kW m-2)									
			50	100	150	200	400	600	800	1000	2000	3000
(kPa)	(kg m-2 s-1)	(-)	Heat Transfer Coefficient (kW m-2 K-2)									
11000	3000	0.05	2.185	2.083	2.038	1.901	1.781	1.809	1.814	1.867	1.790	1.862
11000	3000	0.10	3.911	3.733	3.558	3.461	2.973	2.751	2.545	2.236	1.780	1.726
11000	3000	0.20	6.432	6.264	5.968	5.941	5.363	4.665	3.946	3.004	1.471	2.100
11000	3000	0.40	10.719	10.370	10.044	8.777	8.775	8.014	7.463	6.971	4.211	4.500
11000	3000	0.60	18.099	17.630	17.191	16.256	15.612	14.200	14.150	14.100	12.854	9.600
11000	3000	0.80	24.185	23.635	23.096	22.474	20.291	18.615	18.420	18.400	16.000	13.800
11000	3000	1.00	25.173	24.765	24.357	24.030	22.513	20.991	19.979	20.018	16.969	15.000
11000	3000	1.20	14.779	14.702	14.632	14.533	14.338	14.302	14.131	13.536	12.703	13.000
11000	4000	-0.20	3.522	3.511	3.492	3.489	3.402	3.321	3.230	3.168	2.842	2.506
11000	4000	-0.10	2.474	2.455	2.438	2.418	2.345	2.288	2.248	2.253	2.277	2.450
11000	4000	-0.05	1.583	1.572	1.568	1.564	1.548	1.562	1.594	1.657	1.954	2.400
11000	4000	0.00	1.559	1.556	1.554	1.553	1.497	1.502	1.531	1.621	1.933	2.350
11000	4000	0.05	2.757	2.668	2.570	2.348	2.155	2.158	2.159	2.258	2.322	2.322
11000	4000	0.10	5.695	5.542	5.390	5.076	4.610	4.860	4.575	3.901	2.623	2.455
11000	4000	0.20	9.734	9.619	9.542	9.473	9.170	9.458	8.319	6.380	3.110	3.800
11000	4000	0.40	16.778	16.325	15.871	15.035	13.953	12.819	12.505	10.507	7.970	6.800
11000	4000	0.60	24.295	23.801	23.311	22.685	21.285	19.650	19.630	19.600	17.076	11.695
11000	4000	0.80	30.916	30.498	30.090	29.702	28.259	26.884	25.785	25.412	21.000	17.500
11000	4000	1.00	31.670	31.402	31.137	30.863	29.827	28.772	27.615	26.970	22.389	18.800
11000	4000	1.20	19.138	19.037	18.941	18.843	18.514	18.222	17.969	17.674	16.599	16.800
11000	5000	-0.20	3.523	3.508	3.488	3.480	3.391	3.310	3.221	3.157	2.823	2.484
11000	5000	-0.10	2.568	2.555	2.544	2.540	2.475	2.420	2.370	2.369	2.368	2.343
11000	5000	-0.05	1.594	1.594	1.597	1.612	1.614	1.635	1.663	1.722	2.011	2.292
11000	5000	0.00	1.651	1.666	1.700	1.710	1.715	1.724	1.733	1.751	2.070	2.381
11000	5000	0.05	3.321	3.201	3.062	2.802	2.574	2.520	2.546	2.620	2.707	2.813
11000	5000	0.10	7.273	7.086	6.899	6.464	5.876	5.450	5.242	5.177	4.239	3.240
11000	5000	0.20	13.066	12.803	12.552	12.257	11.371	10.774	10.131	9.254	6.389	4.800
11000	5000	0.40	21.270	20.884	20.494	20.099	18.667	17.316	16.399	14.821	11.476	8.700
11000	5000	0.60	29.450	29.078	28.710	28.422	27.206	25.915	24.878	23.752	18.683	13.535
11000	5000	0.80	37.053	36.728	36.407	36.078	34.914	33.765	32.515	31.296	25.097	19.042
11000	5000	1.00	37.828	37.627	37.426	37.168	36.238	35.318	34.249	33.213	27.691	22.187
11000	5000	1.20	23.335	23.222	23.111	22.996	22.584	22.156	21.804	21.653	20.478	19.237
11000	6000	-0.20	3.536	3.518	3.498	3.487	3.398	3.316	3.229	3.163	2.825	2.482
11000	6000	-0.10	2.562	2.549	2.537	2.517	2.470	2.431	2.400	2.412	2.453	2.464
11000	6000	-0.05	1.511	1.506	1.505	1.504	1.529	1.570	1.617	1.685	2.032	2.381
11000	6000	0.00	1.650	1.635	1.626	1.622	1.636	1.677	1.727	1.803	2.192	2.598
11000	6000	0.05	4.138	4.043	3.957	3.874	3.658	3.521	3.418	3.419	3.424	3.452
11000	6000	0.10	8.795	8.647	8.506	8.324	7.827	7.385	6.992	6.812	5.794	4.689
11000	6000	0.20	15.206	14.982	14.763	14.493	13.664	12.855	12.156	11.724	9.216	6.600
11000	6000	0.40	24.647	24.333	24.028	23.739	22.581	21.502	20.457	19.608	15.354	11.075
11000	6000	0.60	34.769	34.370	33.977	33.615	32.157	30.852	29.548	28.347	22.712	17.154
11000	6000	0.80	44.061	43.664	43.269	42.903	41.405	39.983	38.605	37.279	30.758	24.276
11000	6000	1.00	44.833	44.581	44.328	44.029	42.930	41.759	40.616	39.496	33.825	27.986
11000	6000	1.20	27.410	27.317	27.225	27.142	26.816	26.530	26.237	25.941	24.580	23.249
11000	7000	-0.20	3.545	3.526	3.505	3.489	3.409	3.335	3.260	3.205	2.921	2.640
11000	7000	-0.10	2.523	2.522	2.520	2.508	2.492	2.477	2.468	2.493	2.594	2.638
11000	7000	-0.05	1.537	1.526	1.522	1.520	1.519	1.586	1.642	1.720	2.116	2.518

P	G	Xe	q (kW m-2)									
			50	100	150	200	400	600	800	1000	2000	3000
(kPa)	(kg m-2 s-1)	(-)	Heat Transfer Coefficient (kW m-2 K-2)									
11000	7000	0.00	1.872	1.837	1.814	1.793	1.782	1.809	1.854	1.931	2.338	2.775
11000	7000	0.05	4.967	4.853	4.756	4.665	4.401	4.223	4.079	4.051	3.946	3.896
11000	7000	0.10	10.122	9.972	9.833	9.655	9.141	8.668	8.230	8.009	6.824	5.554
11000	7000	0.20	17.322	17.100	16.880	16.612	15.744	14.843	14.061	13.606	10.841	7.970
11000	7000	0.40	28.216	27.893	27.578	27.241	26.089	24.993	23.901	23.098	18.434	13.899
11000	7000	0.60	40.110	39.680	39.257	38.859	37.336	35.952	34.586	33.416	27.486	21.710
11000	7000	0.80	50.735	50.314	49.896	49.519	47.945	46.446	45.018	43.674	36.982	30.332
11000	7000	1.00	51.298	51.039	50.777	50.482	49.353	48.138	46.962	45.824	40.040	34.061
11000	7000	1.20	31.459	31.362	31.267	31.180	30.845	30.552	30.250	29.919	28.445	27.028
13000	0	-0.20	2.124	2.082	2.050	2.013	1.951	1.901	1.880	1.916	2.082	2.211
13000	0	-0.10	1.548	1.519	1.501	1.470	1.460	1.450	1.471	1.545	1.901	2.214
13000	0	-0.05	1.271	1.242	1.228	1.197	1.209	1.216	1.258	1.353	1.811	2.223
13000	0	0.00	1.063	1.040	1.032	1.007	1.040	1.066	1.125	1.234	1.758	2.240
13000	0	0.05	0.989	0.971	0.969	0.947	0.993	1.028	1.094	1.206	1.750	2.252
13000	0	0.10	0.934	0.922	0.920	0.905	0.956	0.996	1.064	1.176	1.721	2.224
13000	0	0.20	0.826	0.824	0.823	0.817	0.873	0.921	0.990	1.098	1.621	2.105
13000	0	0.40	0.725	0.723	0.731	0.731	0.796	0.848	0.923	1.029	1.565	2.077
13000	0	0.60	0.664	0.612	0.621	0.628	0.718	0.807	0.893	1.002	1.557	2.076
13000	0	0.80	0.688	0.639	0.647	0.666	0.751	0.825	0.911	1.017	1.564	2.074
13000	0	1.00	0.741	0.735	0.737	0.740	0.810	0.875	0.954	1.056	1.578	2.066
13000	0	1.20	0.760	0.759	0.760	0.763	0.838	0.905	0.982	1.078	1.581	2.052
13000	50	-0.20	3.156	3.148	3.138	3.118	3.062	2.973	2.897	2.896	2.837	2.701
13000	50	-0.10	2.188	2.167	2.152	2.118	2.079	2.012	1.973	2.006	2.119	2.167
13000	50	-0.05	1.665	1.629	1.607	1.563	1.532	1.487	1.480	1.539	1.794	1.999
13000	50	0.00	1.241	1.204	1.184	1.140	1.135	1.121	1.148	1.230	1.610	1.949
13000	50	0.05	1.081	1.053	1.043	1.006	1.025	1.031	1.073	1.160	1.571	1.945
13000	50	0.10	0.891	0.871	0.867	0.842	0.876	0.897	0.947	1.029	1.421	1.789
13000	50	0.20	0.544	0.533	0.532	0.531	0.570	0.613	0.667	0.729	1.028	1.342
13000	50	0.40	0.479	0.479	0.481	0.472	0.498	0.533	0.572	0.630	0.875	1.133
13000	50	0.60	0.694	0.755	0.756	0.675	0.678	0.680	0.683	0.736	0.945	1.151
13000	50	0.80	0.759	0.810	0.810	0.725	0.728	0.730	0.735	0.792	1.001	1.210
13000	50	1.00	0.725	0.730	0.740	0.720	0.720	0.725	0.750	0.810	1.049	1.294
13000	50	1.20	0.683	0.673	0.672	0.671	0.690	0.711	0.751	0.813	1.070	1.338
13000	100	-0.20	3.796	3.799	3.791	3.780	3.699	3.585	3.470	3.426	3.139	2.788
13000	100	-0.10	2.575	2.555	2.535	2.501	2.426	2.325	2.246	2.241	2.154	2.170
13000	100	-0.05	1.894	1.854	1.823	1.775	1.710	1.637	1.600	1.631	1.746	1.814
13000	100	0.00	1.340	1.297	1.270	1.218	1.190	1.157	1.165	1.228	1.522	1.775
13000	100	0.05	1.128	1.096	1.082	1.040	1.045	1.048	1.065	1.137	1.467	1.767
13000	100	0.10	0.857	0.833	0.829	0.802	0.834	0.848	0.889	0.957	1.279	1.575
13000	100	0.20	0.374	0.365	0.362	0.358	0.412	0.458	0.511	0.555	0.776	1.024
13000	100	0.40	0.375	0.382	0.388	0.380	0.392	0.418	0.439	0.477	0.614	0.769
13000	100	0.60	0.830	1.066	1.111	1.018	0.871	0.715	0.672	0.703	0.768	0.812
13000	100	0.80	0.922	1.130	1.188	1.046	0.915	0.796	0.751	0.788	0.869	0.928
13000	100	1.00	0.797	0.798	0.863	0.825	0.775	0.729	0.727	0.774	0.931	1.085
13000	100	1.20	0.660	0.664	0.680	0.693	0.675	0.665	0.691	0.746	0.951	1.162
13000	200	-0.20	4.143	4.137	4.120	4.101	3.976	3.863	3.737	3.677	3.315	2.881
13000	200	-0.10	2.782	2.754	2.726	2.683	2.554	2.460	2.368	2.350	2.211	2.140

P	G	Xe	q (kW m-2)									
			50	100	150	200	400	600	800	1000	2000	3000
(kPa)	(kg m-2 s-1)	(-)	Heat Transfer Coefficient (kW m-2 K-2)									
13000	200	-0.05	2.011	1.965	1.926	1.875	1.767	1.701	1.651	1.672	1.755	1.818
13000	200	0.00	1.385	1.338	1.300	1.252	1.192	1.169	1.165	1.219	1.473	1.718
13000	200	0.05	1.134	1.096	1.081	1.039	1.019	1.023	1.044	1.105	1.390	1.660
13000	200	0.10	0.843	0.823	0.820	0.790	0.800	0.819	0.855	0.913	1.179	1.441
13000	200	0.20	0.315	0.316	0.320	0.321	0.327	0.433	0.494	0.553	0.761	1.090
13000	200	0.40	0.506	0.587	0.641	0.743	0.669	0.641	0.600	0.605	0.771	1.012
13000	200	0.60	1.689	2.242	2.224	1.873	1.445	1.169	0.966	0.971	1.030	1.044
13000	200	0.80	1.736	2.159	2.124	1.670	1.326	1.226	1.080	1.084	1.169	1.199
13000	200	1.00	1.031	1.220	1.214	1.064	0.950	0.947	0.946	0.983	1.170	1.370
13000	200	1.20	0.688	0.672	0.681	0.835	0.789	0.845	0.858	0.879	1.187	1.525
13000	500	-0.20	4.383	4.351	4.310	4.238	4.073	3.938	3.832	3.754	3.297	2.884
13000	500	-0.10	2.931	2.889	2.845	2.773	2.628	2.504	2.426	2.392	2.155	2.130
13000	500	-0.05	2.077	2.036	1.988	1.962	1.827	1.760	1.711	1.720	1.738	1.760
13000	500	0.00	1.398	1.360	1.326	1.279	1.254	1.230	1.217	1.260	1.462	1.635
13000	500	0.05	1.140	1.111	1.082	1.035	1.041	1.061	1.074	1.121	1.360	1.540
13000	500	0.10	0.991	0.963	0.940	0.872	0.879	0.918	0.953	1.011	1.188	1.325
13000	500	0.20	0.708	0.710	0.717	1.007	1.084	0.940	0.945	0.950	1.122	1.259
13000	500	0.40	1.158	1.227	1.258	1.496	1.293	1.161	1.200	1.220	1.226	1.300
13000	500	0.60	1.792	2.055	2.057	1.689	1.328	1.259	1.308	1.308	1.330	1.506
13000	500	0.80	1.864	2.053	2.055	1.744	1.414	1.402	1.523	1.533	1.671	1.863
13000	500	1.00	1.307	1.378	1.378	1.380	1.496	1.542	1.710	1.715	1.954	2.316
13000	500	1.20	0.929	0.972	1.041	1.116	1.422	1.619	1.795	1.798	2.221	2.817
13000	1000	-0.20	4.407	4.374	4.330	4.281	4.080	3.937	3.818	3.717	3.196	2.678
13000	1000	-0.10	2.954	2.909	2.865	2.795	2.634	2.520	2.433	2.385	2.137	2.200
13000	1000	-0.05	2.041	2.001	1.957	1.923	1.808	1.756	1.700	1.707	1.742	1.762
13000	1000	0.00	1.412	1.381	1.351	1.301	1.272	1.263	1.240	1.281	1.486	1.665
13000	1000	0.05	1.403	1.370	1.325	1.231	1.210	1.209	1.203	1.239	1.396	1.521
13000	1000	0.10	1.670	1.598	1.556	1.746	1.730	1.585	1.492	1.349	1.348	1.355
13000	1000	0.20	2.344	2.277	2.272	2.350	1.985	1.590	1.575	1.500	1.321	1.325
13000	1000	0.40	2.553	2.473	2.355	2.355	1.990	1.592	1.590	1.506	1.325	1.480
13000	1000	0.60	2.755	2.739	2.700	2.725	2.382	2.213	2.212	2.129	1.770	1.930
13000	1000	0.80	3.367	3.388	3.399	3.400	3.255	3.201	3.155	3.150	2.812	3.005
13000	1000	1.00	3.397	3.437	3.522	3.585	3.982	4.071	3.967	4.145	4.155	4.166
13000	1000	1.20	3.533	3.542	3.566	3.508	3.988	4.080	4.053	4.168	4.444	4.874
13000	1500	-0.20	4.411	4.387	4.352	4.336	4.172	4.021	3.857	3.738	3.116	2.443
13000	1500	-0.10	2.952	2.908	2.866	2.768	2.625	2.533	2.431	2.390	2.148	2.000
13000	1500	-0.05	1.975	1.936	1.895	1.814	1.731	1.702	1.669	1.681	1.740	1.779
13000	1500	0.00	1.452	1.431	1.399	1.337	1.289	1.275	1.273	1.321	1.545	1.752
13000	1500	0.05	1.816	1.769	1.720	1.620	1.515	1.459	1.423	1.467	1.610	1.731
13000	1500	0.10	2.689	2.564	2.475	2.418	2.346	2.101	1.927	1.888	1.699	1.641
13000	1500	0.20	3.686	3.495	3.404	3.741	3.461	2.886	2.566	2.459	1.850	1.600
13000	1500	0.40	4.323	4.184	4.079	4.202	3.615	3.135	2.849	2.685	2.300	2.000
13000	1500	0.60	4.873	4.813	4.773	5.044	4.577	4.580	4.366	4.360	3.574	3.200
13000	1500	0.80	6.259	6.195	6.180	6.418	6.383	6.865	6.530	6.525	6.426	5.346
13000	1500	1.00	8.876	8.778	8.714	9.013	8.311	9.103	8.390	8.385	8.090	7.334
13000	1500	1.20	8.906	8.905	8.919	9.581	8.993	9.038	8.580	8.530	7.493	7.200
13000	2000	-0.20	4.415	4.391	4.358	4.346	4.187	4.036	3.866	3.734	3.059	2.330

P	G	Xe	q (kW m-2)									
			50	100	150	200	400	600	800	1000	2000	3000
(kPa)	(kg m-2 s-1)	(-)	Heat Transfer Coefficient (kW m-2 K-2)									
13000	2000	-0.10	2.957	2.907	2.859	2.755	2.584	2.471	2.394	2.378	2.147	1.885
13000	2000	-0.05	1.914	1.854	1.800	1.719	1.655	1.666	1.669	1.658	1.766	1.842
13000	2000	0.00	1.490	1.464	1.438	1.367	1.331	1.339	1.363	1.414	1.673	1.698
13000	2000	0.05	2.180	2.098	2.035	1.932	1.776	1.699	1.659	1.881	1.982	1.698
13000	2000	0.10	3.615	3.404	3.219	2.874	2.552	2.159	1.832	2.268	2.154	1.738
13000	2000	0.20	4.870	4.630	4.406	4.219	3.734	2.887	2.295	2.078	1.422	1.862
13000	2000	0.40	6.739	6.517	6.317	6.305	5.563	4.801	4.239	3.862	2.072	2.800
13000	2000	0.60	9.087	8.783	8.519	8.096	7.174	7.870	7.869	8.641	7.450	6.660
13000	2000	0.80	14.402	13.930	13.488	11.463	9.447	11.010	12.172	14.272	13.647	11.419
13000	2000	1.00	17.265	16.807	16.352	15.289	13.245	13.541	14.219	15.901	15.200	13.600
13000	2000	1.20	12.430	12.380	12.327	12.556	12.648	12.805	13.765	13.459	12.300	12.400
13000	3000	-0.20	4.409	4.383	4.350	4.335	4.180	4.033	3.869	3.740	3.092	2.396
13000	3000	-0.10	3.024	2.978	2.932	2.864	2.684	2.550	2.465	2.474	2.269	2.007
13000	3000	-0.05	1.876	1.832	1.794	1.732	1.671	1.711	1.720	1.722	1.880	1.738
13000	3000	0.00	1.609	1.574	1.558	1.519	1.480	1.508	1.542	1.595	1.890	1.738
13000	3000	0.05	2.946	2.810	2.726	2.597	2.392	2.272	2.214	2.608	2.610	1.820
13000	3000	0.10	5.596	5.333	5.070	4.869	4.277	3.743	3.358	3.350	2.987	1.995
13000	3000	0.20	8.575	8.259	7.920	7.648	6.860	5.646	4.733	3.797	1.748	2.754
13000	3000	0.40	12.391	11.981	11.603	10.570	10.568	9.957	9.086	8.276	4.582	6.000
13000	3000	0.60	19.481	18.987	18.532	16.964	15.737	15.976	16.424	17.899	16.108	13.000
13000	3000	0.80	26.193	25.268	24.287	22.652	17.187	18.786	22.286	25.601	23.164	18.000
13000	3000	1.00	27.831	27.391	26.964	26.467	23.878	22.681	23.658	24.778	23.200	19.100
13000	3000	1.20	17.616	17.585	17.548	17.428	17.427	17.115	17.299	16.467	15.500	13.800
13000	4000	-0.20	4.400	4.376	4.342	4.328	4.175	4.032	3.873	3.764	3.183	2.555
13000	4000	-0.10	3.107	3.073	3.040	3.000	2.868	2.754	2.652	2.619	2.448	2.221
13000	4000	-0.05	1.881	1.855	1.834	1.810	1.769	1.757	1.756	1.750	1.740	1.735
13000	4000	0.00	1.754	1.730	1.721	1.707	1.666	1.663	1.660	1.620	1.580	1.738
13000	4000	0.05	3.644	3.528	3.418	3.267	3.055	2.888	2.850	2.845	2.794	2.188
13000	4000	0.10	7.473	7.311	7.154	6.902	6.315	6.310	6.285	5.356	3.453	3.236
13000	4000	0.20	12.177	12.004	11.870	11.775	12.004	11.959	10.563	8.049	3.890	5.495
13000	4000	0.40	19.260	18.844	18.464	17.695	17.368	16.123	15.312	13.224	10.274	9.600
13000	4000	0.60	27.447	26.846	26.236	25.115	23.939	23.751	23.748	23.740	23.515	16.000
13000	4000	0.80	34.409	33.989	33.593	33.099	31.377	30.299	30.250	30.180	28.065	19.900
13000	4000	1.00	35.459	35.206	34.963	34.642	33.750	32.327	32.273	32.119	29.800	23.000
13000	4000	1.20	22.716	22.607	22.495	22.357	21.931	21.606	21.055	20.256	18.117	18.400
13000	5000	-0.20	4.398	4.371	4.336	4.317	4.166	4.027	3.875	3.773	3.228	2.643
13000	5000	-0.10	3.166	3.140	3.115	3.086	2.975	2.878	2.785	2.761	2.622	2.188
13000	5000	-0.05	1.871	1.851	1.834	1.822	1.795	1.792	1.790	1.785	1.775	1.770
13000	5000	0.00	1.879	1.858	1.852	1.850	1.820	1.815	1.810	1.800	1.793	1.905
13000	5000	0.05	4.354	4.224	4.085	3.909	3.634	3.477	3.388	3.350	3.082	2.455
13000	5000	0.10	9.175	9.025	8.879	8.659	8.052	7.545	7.150	6.709	5.008	3.631
13000	5000	0.20	15.653	15.411	15.177	14.962	14.005	13.948	13.422	11.438	7.520	5.700
13000	5000	0.40	24.625	24.186	23.744	23.297	21.601	20.890	19.746	17.529	13.801	10.000
13000	5000	0.60	33.531	33.130	32.738	32.453	31.250	29.324	29.411	29.027	23.016	15.566
13000	5000	0.80	41.581	41.268	40.958	40.727	39.759	38.237	37.137	35.895	28.833	22.035
13000	5000	1.00	42.357	42.173	41.988	41.839	40.948	40.100	38.775	37.727	31.303	25.105
13000	5000	1.20	27.654	27.488	27.324	27.215	26.567	26.005	25.226	24.960	22.945	20.830

P	G	Xe	q (kW m-2)									
			50	100	150	200	400	600	800	1000	2000	3000
(kPa)	(kg m-2 s-1)	(-)	Heat Transfer Coefficient (kW m-2 K-2)									
13000	6000	-0.20	4.402	4.370	4.334	4.308	4.159	4.019	3.870	3.757	3.170	2.541
13000	6000	-0.10	3.204	3.178	3.151	3.113	3.008	2.913	2.828	2.811	2.683	2.089
13000	6000	-0.05	1.824	1.807	1.793	1.785	1.779	1.772	1.768	1.761	1.758	1.751
13000	6000	0.00	1.933	1.908	1.887	1.880	1.870	1.869	1.853	1.846	1.841	1.836
13000	6000	0.05	5.093	4.979	4.871	4.787	4.471	4.225	4.000	3.851	3.134	2.487
13000	6000	0.10	10.767	10.593	10.421	10.213	9.547	8.915	8.315	7.922	5.452	4.000
13000	6000	0.20	18.235	17.971	17.710	17.394	16.379	15.362	14.458	13.649	10.143	6.394
13000	6000	0.40	28.579	28.217	27.863	27.537	26.181	24.847	23.562	22.349	16.725	10.898
13000	6000	0.60	39.447	39.007	38.574	38.170	36.523	35.080	33.530	32.124	24.911	17.945
13000	6000	0.80	49.435	48.997	48.560	48.133	46.452	44.932	43.299	41.776	34.257	26.772
13000	6000	1.00	50.424	50.124	49.822	49.452	48.162	46.792	45.525	44.228	37.799	31.162
13000	6000	1.20	32.676	32.518	32.362	32.199	31.634	31.090	30.616	30.087	27.615	25.173
13000	7000	-0.20	4.408	4.371	4.334	4.300	4.154	4.017	3.877	3.763	3.179	2.555
13000	7000	-0.10	3.182	3.167	3.152	3.121	3.046	2.973	2.908	2.896	2.798	2.138
13000	7000	-0.05	1.846	1.828	1.814	1.807	1.803	1.800	1.792	1.786	1.779	1.762
13000	7000	0.00	2.162	2.122	2.091	2.080	2.075	2.058	2.049	2.036	2.030	1.862
13000	7000	0.05	5.984	5.854	5.733	5.637	5.274	4.988	4.723	4.533	3.622	2.812
13000	7000	0.10	12.310	12.122	11.939	11.715	10.995	10.292	9.623	9.192	6.391	4.467
13000	7000	0.20	20.840	20.555	20.269	19.913	18.777	17.514	16.408	15.749	11.547	7.186
13000	7000	0.40	32.817	32.421	32.031	31.619	30.183	28.650	27.245	26.122	19.487	13.061
13000	7000	0.60	45.512	45.017	44.530	44.055	42.248	40.710	38.896	37.376	29.991	22.904
13000	7000	0.80	56.906	56.427	55.953	55.480	53.604	52.025	50.421	48.956	41.473	33.972
13000	7000	1.00	57.712	57.400	57.089	56.707	55.392	53.982	52.734	51.440	45.153	38.601
13000	7000	1.20	37.488	37.339	37.191	37.037	36.496	35.961	35.506	34.892	32.159	29.478
17000	0	-0.20	2.536	2.481	2.433	2.387	2.282	2.197	2.146	2.172	2.282	2.346
17000	0	-0.10	1.949	1.909	1.878	1.841	1.792	1.749	1.740	1.798	2.069	2.290
17000	0	-0.05	1.646	1.606	1.579	1.539	1.511	1.483	1.494	1.570	1.930	2.239
17000	0	0.00	1.412	1.378	1.357	1.320	1.314	1.302	1.330	1.416	1.828	2.189
17000	0	0.05	1.315	1.287	1.272	1.237	1.246	1.244	1.279	1.371	1.809	2.150
17000	0	0.10	1.209	1.190	1.182	1.154	1.176	1.185	1.229	1.324	1.778	2.100
17000	0	0.20	1.015	1.010	1.012	0.999	1.039	1.069	1.122	1.216	1.671	2.084
17000	0	0.40	0.860	0.861	0.869	0.868	0.927	0.971	1.033	1.130	1.607	2.043
17000	0	0.60	0.808	0.753	0.760	0.763	0.846	0.927	0.996	1.098	1.599	2.060
17000	0	0.80	0.845	0.791	0.795	0.806	0.877	0.949	1.014	1.114	1.604	2.055
17000	0	1.00	0.891	0.888	0.877	0.862	0.923	0.990	1.050	1.147	1.615	2.047
17000	0	1.20	0.864	0.869	0.879	0.857	0.921	0.999	1.057	1.152	1.611	2.037
17000	50	-0.20	4.184	4.150	4.109	4.050	3.887	3.682	3.512	3.487	3.289	2.943
17000	50	-0.10	3.013	2.978	2.944	2.888	2.778	2.633	2.528	2.542	2.543	2.432
17000	50	-0.05	2.370	2.321	2.280	2.215	2.118	2.000	1.928	1.965	2.081	2.112
17000	50	0.00	1.814	1.761	1.723	1.657	1.586	1.501	1.466	1.517	1.719	1.862
17000	50	0.05	1.554	1.511	1.482	1.424	1.382	1.322	1.309	1.370	1.627	1.829
17000	50	0.10	1.265	1.234	1.216	1.175	1.162	1.137	1.145	1.207	1.480	1.716
17000	50	0.20	0.793	0.773	0.765	0.751	0.762	0.782	0.817	0.865	1.094	1.332
17000	50	0.40	0.668	0.659	0.655	0.639	0.643	0.658	0.687	0.727	0.920	1.125
17000	50	0.60	0.913	0.970	0.963	0.934	0.880	0.814	0.814	0.847	0.990	1.127
17000	50	0.80	1.006	1.051	1.042	0.998	0.948	0.884	0.885	0.917	1.060	1.193
17000	50	1.00	1.019	0.999	1.003	0.986	0.953	0.906	0.917	0.951	1.112	1.271
17000	50	1.20	0.982	0.962	0.946	0.945	0.927	0.886	0.910	0.946	1.118	1.290

P	G	Xe	q (kW m-2)									
			50	100	150	200	400	600	800	1000	2000	3000
(kPa)	(kg m-2 s-1)	(-)	Heat Transfer Coefficient (kW m-2 K-2)									
17000	100	-0.20	5.261	5.223	5.170	5.100	4.852	4.560	4.294	4.188	3.532	2.755
17000	100	-0.10	3.687	3.645	3.598	3.530	3.350	3.138	2.960	2.916	2.598	2.200
17000	100	-0.05	2.809	2.750	2.695	2.616	2.457	2.286	2.160	2.156	2.051	1.868
17000	100	0.00	2.052	1.988	1.936	1.857	1.740	1.617	1.546	1.573	1.648	1.659
17000	100	0.05	1.692	1.641	1.604	1.535	1.463	1.375	1.336	1.379	1.543	1.646
17000	100	0.10	1.304	1.269	1.246	1.200	1.165	1.123	1.112	1.156	1.342	1.487
17000	100	0.20	0.687	0.662	0.650	0.635	0.632	0.647	0.672	0.701	0.842	1.001
17000	100	0.40	0.621	0.615	0.608	0.585	0.556	0.550	0.557	0.574	0.653	0.745
17000	100	0.60	1.113	1.351	1.384	1.281	1.087	0.886	0.831	0.835	0.815	0.766
17000	100	0.80	1.234	1.439	1.486	1.347	1.188	0.994	0.944	0.948	0.938	0.898
17000	100	1.00	1.185	1.166	1.215	1.218	1.129	0.979	0.957	0.969	1.013	1.041
17000	100	1.20	1.117	1.089	1.065	1.113	1.058	0.924	0.927	0.944	1.018	1.081
17000	200	-0.20	5.910	5.847	5.771	5.688	5.331	5.031	4.720	4.581	3.793	2.898
17000	200	-0.10	4.078	4.019	3.953	3.874	3.602	3.387	3.175	3.108	2.697	2.310
17000	200	-0.05	3.043	2.971	2.903	2.814	2.579	2.413	2.265	2.249	2.114	1.929
17000	200	0.00	2.169	2.096	2.036	1.948	1.769	1.658	1.573	1.595	1.670	1.716
17000	200	0.05	1.753	1.697	1.652	1.577	1.452	1.380	1.330	1.367	1.511	1.623
17000	200	0.10	1.387	1.349	1.313	1.251	1.168	1.119	1.097	1.134	1.294	1.430
17000	200	0.20	0.819	0.739	0.714	0.706	0.657	0.653	0.615	0.675	0.855	1.054
17000	200	0.40	0.839	0.904	0.939	0.907	0.740	0.702	0.611	0.645	0.781	0.931
17000	200	0.60	2.055	2.597	2.590	2.142	1.698	1.450	1.115	1.166	1.183	1.029
17000	200	0.80	2.091	2.523	2.504	2.061	1.743	1.609	1.283	1.371	1.325	1.122
17000	200	1.00	1.471	1.597	1.694	1.650	1.477	1.428	1.267	1.355	1.358	1.267
17000	200	1.20	1.209	1.204	1.222	1.428	1.347	1.322	1.131	1.257	1.380	1.412
17000	500	-0.20	6.468	6.366	6.258	6.171	5.744	5.357	5.009	4.804	3.616	2.643
17000	500	-0.10	4.403	4.319	4.233	4.147	3.824	3.542	3.308	3.196	2.540	2.080
17000	500	-0.05	3.210	3.123	3.046	2.950	2.699	2.487	2.343	2.303	2.003	1.799
17000	500	0.00	2.253	2.174	2.108	2.023	1.830	1.689	1.622	1.635	1.641	1.689
17000	500	0.05	1.867	1.802	1.750	1.669	1.521	1.409	1.371	1.396	1.471	1.553
17000	500	0.10	1.666	1.611	1.555	1.426	1.290	1.179	1.155	1.204	1.281	1.356
17000	500	0.20	1.336	1.217	1.144	0.927	0.662	0.612	0.944	0.788	0.923	1.107
17000	500	0.40	1.440	1.453	1.434	1.488	1.061	1.013	1.171	1.090	1.012	1.212
17000	500	0.60	2.090	2.304	2.268	1.965	1.498	1.636	1.620	1.478	1.578	1.695
17000	500	0.80	2.108	2.313	2.348	2.136	1.971	2.164	2.113	1.832	2.019	1.981
17000	500	1.00	1.681	1.807	1.921	1.967	2.275	2.566	2.247	1.932	2.331	2.352
17000	500	1.20	1.534	1.634	1.754	2.028	2.408	2.635	2.550	2.446	2.596	2.791
17000	1000	-0.20	6.511	6.403	6.291	6.200	5.773	5.392	5.015	4.778	3.607	2.532
17000	1000	-0.10	4.460	4.374	4.286	4.196	3.868	3.587	3.326	3.189	2.620	2.153
17000	1000	-0.05	3.185	3.101	3.025	2.938	2.695	2.500	2.345	2.293	2.037	1.923
17000	1000	0.00	2.276	2.196	2.129	2.050	1.865	1.738	1.662	1.669	1.707	1.751
17000	1000	0.05	2.261	2.169	2.100	1.999	1.796	1.646	1.544	1.553	1.560	1.565
17000	1000	0.10	2.475	2.359	2.260	1.932	1.621	1.491	1.789	1.518	1.444	1.364
17000	1000	0.20	2.391	2.253	2.115	2.027	1.632	1.362	1.818	1.702	1.415	1.321
17000	1000	0.40	3.256	3.132	3.006	2.949	2.262	1.770	1.854	1.845	1.660	1.600
17000	1000	0.60	3.527	3.501	3.457	3.503	3.135	3.035	3.527	3.452	3.204	3.162
17000	1000	0.80	4.230	4.338	4.434	4.399	4.914	5.109	5.633	5.655	4.921	4.960
17000	1000	1.00	4.194	4.459	4.763	4.895	6.539	6.716	7.030	6.754	5.527	5.336
17000	1000	1.20	5.216	5.358	5.522	5.577	6.853	6.769	7.117	6.631	5.401	4.933

P	G	Xe	q (kW m-2)									
			50	100	150	200	400	600	800	1000	2000	3000
(kPa)	(kg m-2 s-1)	(-)	Heat Transfer Coefficient (kW m-2 K-2)									
17000	1500	-0.20	6.457	6.357	6.250	6.158	5.747	5.386	5.024	4.806	3.688	2.692
17000	1500	-0.10	4.505	4.421	4.335	4.254	3.929	3.638	3.373	3.255	2.616	2.291
17000	1500	-0.05	3.095	3.024	2.957	2.893	2.680	2.510	2.358	2.320	2.104	1.950
17000	1500	0.00	2.302	2.224	2.164	2.091	1.935	1.830	1.752	1.769	1.829	1.864
17000	1500	0.05	2.983	2.860	2.761	2.597	2.327	2.125	1.986	1.999	1.984	1.921
17000	1500	0.10	4.311	4.104	3.918	3.988	3.432	2.649	2.468	2.633	2.217	1.905
17000	1500	0.20	5.880	5.671	5.465	5.531	4.667	3.483	3.120	3.108	2.210	2.089
17000	1500	0.40	6.382	6.198	6.008	5.979	5.011	4.149	3.676	3.687	1.971	2.630
17000	1500	0.60	6.444	6.390	6.352	6.414	6.244	6.171	6.090	6.521	5.551	4.898
17000	1500	0.80	7.435	7.497	7.607	7.660	8.455	9.542	10.161	10.861	9.994	8.128
17000	1500	1.00	10.546	10.543	10.568	10.204	11.007	12.206	12.376	12.926	9.554	9.419
17000	1500	1.20	12.020	11.921	11.827	11.421	11.364	11.761	11.358	11.382	7.801	5.620
17000	2000	-0.20	6.444	6.345	6.241	6.147	5.748	5.394	5.042	4.817	3.672	2.476
17000	2000	-0.10	4.558	4.475	4.388	4.302	3.975	3.683	3.406	3.321	2.651	2.138
17000	2000	-0.05	3.024	2.966	2.912	2.858	2.677	2.532	2.393	2.312	2.127	1.903
17000	2000	0.00	2.383	2.311	2.253	2.203	2.059	1.968	1.899	1.914	1.999	2.073
17000	2000	0.05	3.826	3.679	3.550	3.418	3.008	2.711	2.530	2.863	2.708	2.138
17000	2000	0.10	6.545	6.238	5.935	5.438	4.742	3.859	3.171	3.601	3.256	2.344
17000	2000	0.20	8.577	8.192	7.837	7.553	6.658	5.184	4.322	3.932	2.415	2.818
17000	2000	0.40	9.385	9.112	8.878	8.821	8.383	7.931	7.332	6.768	3.841	4.169
17000	2000	0.60	11.622	11.388	11.210	10.698	10.558	11.514	11.649	11.960	9.928	8.574
17000	2000	0.80	17.044	16.634	16.253	13.748	12.500	14.867	16.116	16.940	15.970	14.176
17000	2000	1.00	20.483	20.336	20.254	19.602	17.730	19.935	18.450	19.558	16.159	14.300
17000	2000	1.20	17.814	17.909	18.040	18.057	17.587	19.359	17.755	18.095	12.288	11.000
17000	3000	-0.20	6.436	6.338	6.236	6.141	5.752	5.409	5.070	4.861	3.781	2.658
17000	3000	-0.10	4.607	4.527	4.443	4.350	4.040	3.756	3.489	3.392	2.779	2.455
17000	3000	-0.05	2.936	2.880	2.829	2.781	2.629	2.516	2.412	2.385	2.315	2.230
17000	3000	0.00	2.575	2.508	2.449	2.401	2.275	2.200	2.147	2.178	2.318	2.239
17000	3000	0.05	5.136	4.983	4.831	4.705	4.236	3.839	3.563	3.666	3.312	2.630
17000	3000	0.10	9.812	9.469	9.122	8.656	7.652	6.745	5.878	5.616	4.012	3.236
17000	3000	0.20	14.580	14.078	13.618	12.758	11.756	10.208	9.167	7.954	4.543	4.600
17000	3000	0.40	19.197	18.610	18.059	16.433	15.641	14.905	14.216	13.242	9.044	7.000
17000	3000	0.60	24.686	24.058	23.471	21.616	19.245	20.828	21.241	21.851	18.962	16.548
17000	3000	0.80	31.875	30.656	29.329	27.202	18.899	22.275	25.324	27.742	26.127	23.200
17000	3000	1.00	34.200	33.750	33.297	32.720	29.387	29.395	28.408	30.628	26.620	24.600
17000	3000	1.20	25.812	25.866	25.885	26.089	26.283	26.509	25.613	25.994	19.270	17.600
17000	4000	-0.20	6.421	6.326	6.226	6.135	5.758	5.435	5.118	4.949	4.080	3.147
17000	4000	-0.10	4.644	4.573	4.498	4.411	4.129	3.881	3.651	3.608	3.145	2.692
17000	4000	-0.05	2.858	2.796	2.739	2.680	2.526	2.430	2.354	2.337	2.477	2.597
17000	4000	0.00	2.731	2.658	2.593	2.537	2.415	2.346	2.307	2.338	2.528	2.727
17000	4000	0.05	6.209	6.059	5.920	5.807	5.396	5.025	4.724	4.896	4.042	3.164
17000	4000	0.10	12.282	12.043	11.809	11.546	10.765	10.545	10.253	9.888	6.483	4.000
17000	4000	0.20	19.109	18.756	18.438	17.837	17.150	17.059	16.177	14.523	9.313	6.000
17000	4000	0.40	27.353	26.654	25.956	24.752	22.363	20.885	20.318	19.474	15.372	10.278
17000	4000	0.60	35.417	34.644	33.840	32.784	30.455	28.582	28.945	29.307	25.604	18.000
17000	4000	0.80	42.475	42.004	41.553	41.011	38.516	37.301	37.287	37.874	32.993	26.000
17000	4000	1.00	44.100	43.869	43.640	43.383	42.337	41.228	39.962	39.517	33.614	27.066

P	G	Xe	q (kW m-2)									
			50	100	150	200	400	600	800	1000	2000	3000
(kPa)	(kg m-2 s-1)	(-)	Heat Transfer Coefficient (kW m-2 K-2)									
17000	4000	1.20	33.153	33.064	32.958	32.933	32.337	31.744	30.854	29.930	24.361	21.700
17000	5000	-0.20	6.411	6.318	6.222	6.132	5.778	5.478	5.188	5.047	4.302	3.496
17000	5000	-0.10	4.656	4.598	4.539	4.460	4.228	4.023	3.833	3.778	3.441	3.023
17000	5000	-0.05	2.814	2.753	2.696	2.641	2.499	2.417	2.360	2.410	2.637	2.842
17000	5000	0.00	2.946	2.866	2.794	2.737	2.608	2.546	2.512	2.548	2.746	2.954
17000	5000	0.05	7.366	7.211	7.068	6.949	6.510	6.176	5.873	5.649	4.647	3.642
17000	5000	0.10	14.605	14.437	14.276	14.099	13.422	12.706	11.951	11.359	7.980	4.411
17000	5000	0.20	23.318	23.013	22.708	22.494	21.114	20.334	19.765	18.518	12.222	7.200
17000	5000	0.40	33.650	33.097	32.540	32.115	29.902	27.610	26.100	25.225	19.405	13.100
17000	5000	0.60	43.217	42.701	42.187	41.821	39.904	37.228	36.138	35.532	28.801	21.476
17000	5000	0.80	51.672	51.317	50.958	50.697	49.572	47.520	45.971	45.254	36.821	28.995
17000	5000	1.00	53.017	52.815	52.608	52.412	51.443	49.880	49.017	47.642	39.840	32.526
17000	5000	1.20	40.402	40.138	39.879	39.579	38.601	37.405	36.665	35.770	31.212	26.920
17000	6000	-0.20	6.410	6.316	6.222	6.128	5.789	5.496	5.217	5.064	4.266	3.418
17000	6000	-0.10	4.674	4.628	4.581	4.511	4.313	4.130	3.961	3.902	3.544	3.113
17000	6000	-0.05	2.781	2.727	2.678	2.637	2.525	2.470	2.435	2.481	2.718	2.946
17000	6000	0.00	3.185	3.107	3.038	2.995	2.862	2.810	2.782	2.817	3.041	3.291
17000	6000	0.05	8.587	8.411	8.244	8.106	7.619	7.250	6.921	6.700	5.665	4.647
17000	6000	0.10	17.159	16.947	16.740	16.478	15.635	14.803	14.003	13.358	10.156	6.818
17000	6000	0.20	27.444	27.116	26.790	26.389	25.086	23.730	22.400	21.320	15.510	9.621
17000	6000	0.40	39.236	38.782	38.334	37.895	36.238	34.628	32.998	31.413	23.709	16.106
17000	6000	0.60	50.741	50.225	49.717	49.243	47.395	45.734	43.889	41.985	33.433	24.943
17000	6000	0.80	61.462	60.940	60.423	59.906	57.897	56.122	54.214	52.210	43.206	34.112
17000	6000	1.00	63.452	63.032	62.613	62.129	60.376	58.707	56.872	55.188	46.923	38.389
17000	6000	1.20	48.131	47.808	47.488	47.177	45.964	44.862	43.672	42.610	37.394	32.105
17000	7000	-0.20	6.415	6.323	6.234	6.139	5.817	5.533	5.265	5.085	4.178	3.228
17000	7000	-0.10	4.623	4.598	4.570	4.516	4.373	4.222	4.079	4.008	3.592	3.104
17000	7000	-0.05	2.801	2.753	2.709	2.680	2.593	2.563	2.550	2.590	2.826	3.071
17000	7000	0.00	3.537	3.449	3.371	3.335	3.190	3.142	3.118	3.144	3.357	3.622
17000	7000	0.05	9.902	9.720	9.544	9.408	8.888	8.488	8.124	7.854	6.582	5.342
17000	7000	0.10	19.491	19.265	19.042	18.767	17.847	16.924	16.036	15.327	11.691	7.917
17000	7000	0.20	31.456	31.094	30.731	30.264	28.819	27.258	25.694	24.470	18.130	13.000
17000	7000	0.40	45.296	44.792	44.298	43.779	41.996	40.363	38.641	36.848	28.494	20.307
17000	7000	0.60	58.564	57.985	57.419	56.863	54.837	53.177	51.242	49.264	40.447	31.734
17000	7000	0.80	70.658	70.092	69.534	68.966	66.705	64.888	63.007	60.990	52.075	42.972
17000	7000	1.00	72.570	72.151	71.732	71.258	69.489	67.834	65.909	64.250	55.934	47.280
17000	7000	1.20	55.134	54.860	54.583	54.352	53.252	52.239	51.069	49.922	44.199	38.357
20000	0	-0.20	2.690	2.638	2.592	2.550	2.459	2.394	2.361	2.387	2.507	2.605
20000	0	-0.10	2.254	2.212	2.177	2.139	2.081	2.034	2.021	2.067	2.276	2.454
20000	0	-0.05	1.989	1.941	1.904	1.858	1.804	1.754	1.746	1.804	2.071	2.292
20000	0	0.00	1.766	1.718	1.684	1.635	1.589	1.540	1.534	1.598	1.890	2.125
20000	0	0.05	1.644	1.602	1.574	1.526	1.494	1.452	1.454	1.525	1.854	2.123
20000	0	0.10	1.481	1.452	1.434	1.395	1.388	1.367	1.386	1.465	1.838	2.090
20000	0	0.20	1.192	1.183	1.181	1.161	1.190	1.204	1.246	1.332	1.742	2.109
20000	0	0.40	1.025	1.028	1.035	1.024	1.075	1.099	1.157	1.247	1.671	2.054
20000	0	0.60	1.010	1.010	0.956	0.938	1.056	1.081	1.145	1.235	1.664	2.054
20000	0	0.80	0.997	0.996	0.942	0.926	1.050	1.084	1.153	1.241	1.662	2.053

P	G	Xe	q (kW m-2)									
			50	100	150	200	400	600	800	1000	2000	3000
(kPa)	(kg m-2 s-1)	(-)	Heat Transfer Coefficient (kW m-2 K-2)									
20000	0	1.00	1.016	1.015	0.963	0.948	1.075	1.110	1.177	1.261	1.666	2.042
20000	0	1.20	1.085	1.087	1.092	1.099	1.137	1.161	1.206	1.285	1.657	1.993
20000	50	-0.20	4.750	4.741	4.722	4.681	4.616	4.498	4.418	4.477	4.698	4.757
20000	50	-0.10	3.646	3.628	3.607	3.561	3.508	3.409	3.352	3.416	3.660	3.774
20000	50	-0.05	3.032	2.986	2.945	2.876	2.777	2.646	2.568	2.612	2.758	2.795
20000	50	0.00	2.440	2.374	2.319	2.235	2.103	1.952	1.858	1.876	1.892	1.834
20000	50	0.05	2.086	2.023	1.974	1.892	1.779	1.643	1.564	1.590	1.657	1.646
20000	50	0.10	1.665	1.619	1.585	1.527	1.464	1.386	1.350	1.391	1.550	1.649
20000	50	0.20	1.008	0.979	0.961	0.941	0.927	0.927	0.945	0.983	1.169	1.354
20000	50	0.40	0.750	0.729	0.720	0.709	0.701	0.723	0.736	0.768	0.937	1.117
20000	50	0.60	0.968	0.939	1.000	0.980	0.866	0.853	0.835	0.864	0.999	1.127
20000	50	0.80	1.178	1.139	1.194	1.165	1.020	0.979	0.945	0.970	1.089	1.187
20000	50	1.00	1.302	1.259	1.300	1.267	1.111	1.062	1.023	1.047	1.158	1.247
20000	50	1.20	1.141	1.109	1.082	1.029	0.991	0.968	0.962	0.990	1.129	1.260
20000	100	-0.20	6.162	6.162	6.143	6.100	6.001	5.841	5.714	5.747	5.797	5.684
20000	100	-0.10	4.542	4.526	4.499	4.447	4.359	4.226	4.134	4.183	4.328	4.336
20000	100	-0.05	3.668	3.615	3.560	3.479	3.328	3.153	3.030	3.053	3.074	2.979
20000	100	0.00	2.843	2.762	2.690	2.589	2.394	2.190	2.044	2.033	1.887	1.665
20000	100	0.05	2.351	2.275	2.212	2.112	1.945	1.760	1.634	1.634	1.558	1.395
20000	100	0.10	1.802	1.745	1.701	1.632	1.531	1.420	1.350	1.367	1.410	1.383
20000	100	0.20	0.982	0.942	0.912	0.887	0.842	0.822	0.819	0.832	0.903	0.977
20000	100	0.40	0.710	0.674	0.655	0.642	0.590	0.592	0.574	0.581	0.637	0.704
20000	100	0.60	1.106	1.063	1.270	1.247	0.910	0.853	0.774	0.778	0.786	0.764
20000	100	0.80	1.473	1.417	1.648	1.610	1.190	1.082	0.966	0.966	0.955	0.883
20000	100	1.00	1.638	1.575	1.768	1.724	1.305	1.189	1.074	1.076	1.068	1.000
20000	100	1.20	1.274	1.228	1.186	1.096	1.026	0.968	0.934	0.948	1.016	1.059
20000	200	-0.20	7.170	7.150	7.116	7.065	6.882	6.746	6.601	6.606	6.533	6.279
20000	200	-0.10	5.107	5.070	5.025	4.959	4.781	4.666	4.556	4.598	4.715	4.689
20000	200	-0.05	4.014	3.945	3.874	3.782	3.545	3.391	3.253	3.280	3.331	3.293
20000	200	0.00	3.043	2.951	2.865	2.755	2.482	2.297	2.137	2.135	2.064	1.962
20000	200	0.05	2.494	2.405	2.329	2.220	1.973	1.802	1.656	1.651	1.572	1.441
20000	200	0.10	2.049	1.971	1.912	1.825	1.624	1.491	1.387	1.384	1.339	1.247
20000	200	0.20	1.468	1.388	1.279	1.181	1.068	0.962	0.824	0.864	0.873	0.869
20000	200	0.40	1.338	1.249	1.250	1.122	0.894	0.694	0.590	0.700	0.732	0.778
20000	200	0.60	2.110	2.050	2.540	2.302	1.550	1.322	0.868	1.004	1.028	1.004
20000	200	0.80	2.550	2.509	3.087	2.888	1.819	1.801	1.145	1.361	1.312	1.238
20000	200	1.00	2.541	2.520	3.119	2.936	1.844	1.784	1.272	1.486	1.459	1.419
20000	200	1.20	1.501	1.460	1.426	1.472	1.259	1.075	1.044	1.192	1.316	1.428
20000	500	-0.20	8.329	8.268	8.207	8.138	7.909	7.708	7.541	7.478	7.000	6.736
20000	500	-0.10	5.677	5.603	5.530	5.439	5.204	5.016	4.895	4.914	4.819	4.926
20000	500	-0.05	4.260	4.174	4.089	3.995	3.735	3.536	3.407	3.425	3.354	3.464
20000	500	0.00	3.167	3.069	2.977	2.870	2.594	2.378	2.236	2.234	2.100	2.114
20000	500	0.05	2.778	2.669	2.570	2.443	2.156	1.924	1.778	1.757	1.544	1.440
20000	500	0.10	2.860	2.726	2.607	2.417	2.070	1.823	1.659	1.648	1.449	1.276
20000	500	0.20	2.913	2.744	2.581	2.445	1.789	1.410	1.855	1.528	1.332	1.242
20000	500	0.40	3.139	2.979	2.834	3.050	2.044	1.546	2.524	1.831	1.509	1.420
20000	500	0.60	3.569	3.475	3.464	3.524	2.775	2.338	2.906	2.418	1.923	1.674

P	G	Xe	q (kW m-2)									
			50	100	150	200	400	600	800	1000	2000	3000
(kPa)	(kg m-2 s-1)	(-)	Heat Transfer Coefficient (kW m-2 K-2)									
20000	500	0.80	3.573	3.584	3.737	3.727	3.423	3.112	3.253	2.467	2.450	2.048
20000	500	1.00	3.258	3.350	3.683	3.658	3.631	3.624	3.470	3.148	2.840	2.413
20000	500	1.20	3.056	3.108	3.187	3.379	3.698	3.596	3.640	3.348	2.868	2.467
20000	1000	-0.20	8.670	8.587	8.512	8.430	8.169	7.950	7.753	7.648	7.139	6.747
20000	1000	-0.10	5.829	5.744	5.665	5.561	5.303	5.110	4.956	4.947	4.898	4.942
20000	1000	-0.05	4.237	4.145	4.060	3.972	3.718	3.537	3.390	3.391	3.404	3.502
20000	1000	0.00	3.247	3.139	3.042	2.934	2.658	2.458	2.296	2.285	2.237	2.260
20000	1000	0.05	3.584	3.431	3.293	3.093	2.711	2.424	2.193	2.166	1.960	1.793
20000	1000	0.10	4.438	4.235	4.050	3.627	3.093	2.874	2.904	2.635	2.188	1.971
20000	1000	0.20	4.689	4.509	4.358	4.431	3.835	3.801	4.161	3.672	2.823	2.214
20000	1000	0.40	6.274	6.209	6.137	6.316	5.739	5.294	5.905	4.756	3.623	2.625
20000	1000	0.60	6.129	6.207	6.281	6.288	6.924	6.828	8.063	6.200	5.063	3.872
20000	1000	0.80	5.452	5.813	6.240	6.310	8.738	9.353	10.122	8.609	6.175	4.631
20000	1000	1.00	5.491	5.952	6.559	6.654	10.274	11.031	11.320	9.893	6.601	4.807
20000	1000	1.20	8.818	8.911	9.091	8.712	11.217	11.003	11.167	9.588	6.348	4.259
20000	1500	-0.20	8.613	8.532	8.462	8.379	8.135	7.927	7.737	7.650	7.195	6.699
20000	1500	-0.10	5.779	5.708	5.641	5.543	5.320	5.145	4.998	5.005	4.988	4.883
20000	1500	-0.05	4.172	4.080	3.999	3.908	3.676	3.512	3.377	3.403	3.490	3.533
20000	1500	0.00	3.470	3.347	3.241	3.119	2.827	2.618	2.459	2.464	2.450	2.413
20000	1500	0.05	4.829	4.638	4.473	4.238	3.729	3.341	3.078	3.036	2.651	2.168
20000	1500	0.10	6.857	6.613	6.393	5.788	5.458	5.271	4.528	4.267	3.385	2.159
20000	1500	0.20	7.785	7.654	7.575	7.314	7.959	7.956	7.061	6.291	3.560	2.570
20000	1500	0.40	9.053	9.112	9.203	9.281	10.641	10.050	9.313	8.410	4.789	3.548
20000	1500	0.60	9.535	9.667	9.842	9.617	11.916	12.259	12.063	11.062	8.805	6.134
20000	1500	0.80	12.145	12.115	12.156	11.759	13.243	15.845	15.703	14.994	11.309	9.800
20000	1500	1.00	17.141	16.966	16.827	14.813	16.288	18.560	17.885	17.210	11.363	10.000
20000	1500	1.20	18.819	18.594	18.400	17.075	18.820	17.860	17.039	15.088	10.753	8.400
20000	2000	-0.20	8.568	8.493	8.426	8.345	8.113	7.914	7.733	7.646	7.187	6.685
20000	2000	-0.10	5.732	5.675	5.618	5.538	5.336	5.171	5.031	5.047	4.992	4.807
20000	2000	-0.05	4.115	4.022	3.942	3.845	3.631	3.486	3.375	3.390	3.507	3.632
20000	2000	0.00	3.748	3.611	3.498	3.360	3.055	2.841	2.681	2.684	2.668	2.636
20000	2000	0.05	6.199	5.985	5.803	5.565	4.948	4.459	4.067	4.113	3.467	2.394
20000	2000	0.10	9.919	9.646	9.391	9.012	8.588	8.270	7.678	6.632	4.685	2.360
20000	2000	0.20	13.368	13.189	13.058	12.605	13.673	13.215	12.002	9.874	4.555	3.236
20000	2000	0.40	16.127	15.828	15.570	13.868	15.128	15.664	15.153	13.673	7.705	6.300
20000	2000	0.60	19.748	19.296	18.875	15.788	16.682	17.865	18.406	17.984	14.382	11.800
20000	2000	0.80	26.162	25.541	24.913	22.533	20.069	21.098	21.614	21.698	19.025	15.684
20000	2000	1.00	28.919	28.436	27.965	26.828	24.662	24.978	24.652	23.714	19.678	16.500
20000	2000	1.20	24.627	24.492	24.390	24.071	23.998	24.673	24.454	22.212	17.082	13.800
20000	3000	-0.20	8.550	8.476	8.409	8.330	8.101	7.904	7.725	7.638	7.182	6.683
20000	3000	-0.10	5.796	5.750	5.699	5.633	5.440	5.273	5.125	5.127	4.993	4.760
20000	3000	-0.05	3.986	3.893	3.815	3.716	3.519	3.398	3.313	3.341	3.550	3.739
20000	3000	0.00	3.994	3.848	3.736	3.601	3.324	3.133	3.005	3.004	2.999	2.999
20000	3000	0.05	8.063	7.834	7.644	7.433	6.836	6.275	5.843	5.774	4.435	3.040
20000	3000	0.10	14.376	14.117	13.869	13.611	12.646	12.318	11.515	10.697	7.272	4.000
20000	3000	0.20	21.334	21.051	20.790	20.448	19.782	19.314	17.950	15.916	10.581	6.400
20000	3000	0.40	28.922	28.275	27.633	26.534	24.063	23.525	22.677	21.400	15.906	12.000

P	G	Xe	q (kW m-2)									
			50	100	150	200	400	600	800	1000	2000	3000
(kPa)	(kg m-2 s-1)	(-)	Heat Transfer Coefficient (kW m-2 K-2)									
20000	3000	0.60	35.285	34.497	33.682	32.397	28.852	28.547	27.806	28.394	24.177	19.998
20000	3000	0.80	40.509	39.900	39.251	38.780	35.756	32.801	30.237	33.131	29.833	24.407
20000	3000	1.00	41.121	40.764	40.365	40.301	38.097	36.191	32.191	34.994	29.722	25.500
20000	3000	1.20	33.556	33.484	33.385	33.480	32.872	32.797	32.033	31.851	24.426	20.000
20000	4000	-0.20	8.536	8.460	8.392	8.311	8.078	7.879	7.699	7.615	7.179	6.700
20000	4000	-0.10	5.951	5.905	5.854	5.785	5.586	5.411	5.252	5.262	5.093	4.804
20000	4000	-0.05	3.836	3.743	3.666	3.577	3.391	3.277	3.204	3.222	3.489	3.769
20000	4000	0.00	4.080	3.941	3.835	3.720	3.479	3.332	3.225	3.228	3.263	3.331
20000	4000	0.05	9.571	9.340	9.144	8.939	8.356	7.889	7.394	7.436	5.842	4.133
20000	4000	0.10	18.108	17.913	17.729	17.505	16.761	15.954	15.970	15.586	11.218	6.106
20000	4000	0.20	27.360	27.042	26.700	26.339	25.438	24.958	25.355	23.119	17.205	10.300
20000	4000	0.40	36.363	35.813	35.227	34.710	32.662	30.893	29.965	29.368	24.748	17.805
20000	4000	0.60	43.875	43.348	42.796	42.385	40.208	38.509	37.078	37.652	33.491	26.060
20000	4000	0.80	50.590	50.214	49.818	49.573	47.915	46.229	44.080	44.279	37.872	30.400
20000	4000	1.00	52.185	51.948	51.691	51.538	50.182	48.746	46.619	45.775	37.923	31.700
20000	4000	1.20	43.616	43.419	43.204	43.084	42.000	40.942	39.753	38.402	30.778	23.021
20000	5000	-0.20	8.523	8.449	8.382	8.304	8.075	7.880	7.702	7.618	7.172	6.683
20000	5000	-0.10	6.061	6.018	5.971	5.897	5.706	5.532	5.377	5.351	5.145	4.852
20000	5000	-0.05	3.713	3.631	3.562	3.494	3.338	3.253	3.202	3.264	3.570	3.862
20000	5000	0.00	4.247	4.123	4.023	3.941	3.728	3.615	3.543	3.544	3.609	3.713
20000	5000	0.05	11.166	10.928	10.713	10.508	9.874	9.372	8.930	8.559	6.804	5.141
20000	5000	0.10	21.716	21.515	21.321	21.035	20.138	19.177	18.229	17.431	12.657	7.785
20000	5000	0.20	32.806	32.533	32.248	31.958	30.552	29.047	28.089	27.082	19.715	11.805
20000	5000	0.40	43.074	42.665	42.232	42.010	40.319	38.225	35.792	35.146	27.701	18.321
20000	5000	0.60	52.002	51.590	51.164	50.930	49.380	47.266	44.669	43.769	35.561	25.467
20000	5000	0.80	60.475	60.114	59.748	59.397	57.871	56.422	53.943	52.641	42.936	33.239
20000	5000	1.00	63.129	62.821	62.513	62.075	60.703	59.139	57.249	55.798	46.460	37.535
20000	5000	1.20	53.729	53.353	52.980	52.549	51.183	49.524	48.058	46.668	39.478	32.652
20000	6000	-0.20	8.508	8.438	8.373	8.299	8.077	7.886	7.713	7.620	7.135	6.614
20000	6000	-0.10	6.078	6.047	6.013	5.944	5.783	5.625	5.483	5.454	5.228	4.911
20000	6000	-0.05	3.630	3.559	3.498	3.447	3.328	3.283	3.268	3.337	3.714	4.094
20000	6000	0.00	4.582	4.456	4.349	4.282	4.074	3.982	3.928	3.930	4.045	4.223
20000	6000	0.05	13.075	12.814	12.569	12.365	11.630	11.048	10.518	10.085	8.058	6.118
20000	6000	0.10	25.725	25.444	25.170	24.816	23.637	22.414	21.213	20.156	14.771	9.210
20000	6000	0.20	39.447	39.009	38.573	38.069	36.293	34.480	32.659	30.925	22.434	13.854
20000	6000	0.40	51.762	51.156	50.564	49.979	47.794	45.795	43.917	41.830	31.785	21.992
20000	6000	0.60	62.448	61.795	61.157	60.537	58.186	56.100	54.100	52.018	41.676	31.677
20000	6000	0.80	72.689	72.056	71.429	70.804	68.426	66.117	64.096	61.859	51.518	41.178
20000	6000	1.00	75.319	74.803	74.288	73.734	71.627	69.532	67.546	65.503	55.840	45.891
20000	6000	1.20	63.370	62.946	62.526	62.120	60.482	58.969	57.431	55.943	48.631	41.238
20000	7000	-0.20	8.504	8.439	8.376	8.309	8.096	7.911	7.742	7.632	7.080	6.501
20000	7000	-0.10	5.983	5.981	5.975	5.928	5.838	5.721	5.612	5.580	5.331	4.989
20000	7000	-0.05	3.637	3.571	3.513	3.478	3.382	3.367	3.379	3.450	3.863	4.311
20000	7000	0.00	5.084	4.943	4.819	4.761	4.527	4.441	4.392	4.388	4.522	4.766
20000	7000	0.05	15.001	14.738	14.486	14.294	13.528	12.918	12.353	11.863	9.574	7.401
20000	7000	0.10	29.085	28.803	28.525	28.182	26.961	25.681	24.406	23.270	17.425	11.348
20000	7000	0.20	45.234	44.765	44.295	43.761	41.831	39.893	37.852	35.933	26.757	17.384

P	G	Xe	q (kW m-2)									
			50	100	150	200	400	600	800	1000	2000	3000
(kPa)	(kg m-2 s-1)	(-)	Heat Transfer Coefficient (kW m-2 K-2)									
20000	7000	0.40	60.115	59.415	58.733	58.066	55.592	53.443	51.439	49.106	38.518	28.250
20000	7000	0.60	72.301	71.573	70.866	70.207	67.635	65.447	63.447	61.206	50.626	40.498
20000	7000	0.80	83.546	82.907	82.272	81.687	79.270	76.875	74.802	72.575	62.027	51.445
20000	7000	1.00	85.966	85.497	85.021	84.553	82.527	80.460	78.432	76.389	66.423	56.130
20000	7000	1.20	72.450	72.078	71.705	71.377	69.847	68.430	66.940	65.403	57.746	49.991

TABLE IV.II. DISTRIBUTION OF DATA AND ERRORS FOR WALL TEMPERATURES IN DEGREES C FOR THE AECL FILMBOILING LOOK-UP TABLE.

Pressure Range (kPa) = 100 to 1000													
Mass Flux Range (kg/(m ² -s))		50 to 500				500 to 2000				2000 to 4000			
Heat Flux Range (kW/m ²)		Quality Range				Quality Range				Quality Range			
		-0.20 to -0.05	0.00 to 0.10	0.10 to 0.40	0.40 to 1.00	-0.20 to -0.05	0.00 to 0.10	0.10 to 0.40	0.40 to 1.00	-0.20 to -0.05	0.00 to 0.10	0.10 to 0.40	0.40 to 1.00
50 to 200	No. of Data	0	770	1583	0	0	0	0	0	0	0	0	0
	Avg. Error (%)	0	-4.2	6.1	0	0	0	0	0	0	0	0	0
	RMS Error (%)	0	17.3	8.8	0	0	0	0	0	0	0	0	0
	No. of Data Set	0	1	1	0	0	0	0	0	0	0	0	0
200 to 600	No. of Data	0	145	87	0	0	0	0	0	0	0	0	0
	Avg. Error (%)	0	-1	1.6	0	0	0	0	0	0	0	0	0
	RMS Error (%)	0	12.6	6.9	0	0	0	0	0	0	0	0	0
	No. of Data Set	0	1	1	0	0	0	0	0	0	0	0	0
600 to 1000	No. of Data	0	0	0	0	0	0	0	0	0	0	0	0
	Avg. Error (%)	0	0	0	0	0	0	0	0	0	0	0	0
	RMS Error (%)	0	0	0	0	0	0	0	0	0	0	0	0
	No. of Data Set	0	0	0	0	0	0	0	0	0	0	0	0
1000 to 3000	No. of Data	0	0	0	0	0	0	0	0	0	0	0	0
	Avg. Error (%)	0	0	0	0	0	0	0	0	0	0	0	0
	RMS Error (%)	0	0	0	0	0	0	0	0	0	0	0	0
	No. of Data Set	0	0	0	0	0	0	0	0	0	0	0	0

TABLE IV.II. (CONT.)

Pressure Range (kPa) = 1000 to 5000																	
Mass Flux Range (kg/(m ² ·s))		50 to 500				500 to 2000				2000 to 4000				4000 to 7000			
Heat Flux Range (kW/m ²)	Quality Range				Quality Range				Quality Range				Quality Range				
	to		to		to		to		to		to		to		to		
	-0.20 to -0.05	0.00 to 0.10	0.10 to 0.40	0.40 to 1.00	-0.20 to -0.05	0.00 to 0.10	0.10 to 0.40	0.40 to 1.00	-0.20 to -0.05	0.00 to 0.10	0.10 to 0.40	0.40 to 1.00	-0.05 to 0.00	0.00 to 0.10	0.10 to 0.40	0.40 to 1.00	
50 to 200	No. of Data	0	2	273	332	9	0	53	205	33	0	0	0	0	0	0	0
	Avg. Error (%)	0	-4.9	2	-0.7	-6.8	0	-3.9	1.4	0.7	0	0	0	0	0	0	0
	RMS Error (%)	0	5.1	4	6.3	7	0	7.2	3.2	1.2	0	0	0	0	0	0	0
	No. of Data Set	0	2	2	2	2	0	2	2	2	0	0	0	0	0	0	0
200 to 600	No. of Data	0	2	9	13	42	2	131	173	37	5	0	0	0	0	0	0
	Avg. Error (%)	0	-4.2	0.9	-1.1	-2.3	-14.6	0.3	1.3	0.7	6.5	0	0	0	0	0	0
	RMS Error (%)	0	5	1.3	3.3	5.3	14.6	5.7	3.1	1.9	6.6	0	0	0	0	0	0
	No. of Data Set	0	2	2	2	2	2	2	2	2	2	0	0	0	0	0	0
600 to 1000	No. of Data	0	0	0	0	0	0	0	0	0	173	0	0	0	21	3	0
	Avg. Error (%)	0	0	0	0	0	0	0	0	0	-0.3	0	0	0	1	4.7	0
	RMS Error (%)	0	0	0	0	0	0	0	0	0	5.7	0	0	0	4.7	5.6	0
	No. of Data Set	0	0	0	0	0	0	0	0	0	2	0	0	0	2	2	0
1000 to 3000	No. of Data	0	0	0	0	0	0	0	0	0	41	0	0	0	17	9	0
	Avg. Error (%)	0	0	0	0	0	0	0	0	0	1.5	0	0	0	-1.9	-0.4	0
	RMS Error (%)	0	0	0	0	0	0	0	0	0	3	0	0	0	2.5	2.2	0
	No. of Data Set	0	0	0	0	0	0	0	0	0	2	0	0	0	2	2	0

TABLE IV.II. (CONT.)

Pressure Range (kPa) = 5000 to 9000

Mass Flux Range (kg/(m²-s))Heat Flux Range (kW/m²)

		50 to 500				500 to 2000				2000 to 4000				4000 to 7000			
		Quality Range				Quality Range				Quality Range				Quality Range			
50 to 200	No. of Data	0	6	63	113	26	0	38	71	22	0	0	38	20	0	0	0
	Avg. Error (%)	0	-1.2	0.7	1.8	-2.1	0	-2.1	0.8	3.6	0	0	0.2	-0.4	0	0	0
	RMS Error (%)	0	2.8	2.6	5.7	4.4	0	3.2	2.3	3.8	0	0	4.3	1.7	0	0	0
	No. of Data Set	0	2	2	4	3	0	2	2	2	0	0	2	2	0	0	0
		-0.20 to -0.05	0.00 to 0.10	0.10 to 0.40	0.40 to 0.70	0.70 to 1.00	1.00 to 1.30	-0.05 to 0.00	0.00 to 0.10	0.10 to 0.40	0.40 to 0.70	0.70 to 1.00	-0.05 to 0.00	0.00 to 0.10	0.10 to 0.40	0.40 to 0.70	0.70 to 1.00
200 to 600	No. of Data	9	38	64	116	50	70	100	170	106	40	0	45	43	0	4	0
	Avg. Error (%)	3	2.9	4.1	-2.2	0.8	0.05	-0.2	-1	-1.8	1.4	0	3.9	1.6	0	0.8	0
	RMS Error (%)	3.8	4.8	4.7	4.3	4	4.1	7.9	7.1	3.5	7.4	0	10.3	2.3	0	1.8	0
	No. of Data Set	2	2	2	5	3	2	2	2	4	2	0	2	2	0	1	0
		-0.20 to -0.05	0.00 to 0.10	0.10 to 0.40	0.40 to 0.70	0.70 to 1.00	1.00 to 1.30	-0.05 to 0.00	0.00 to 0.10	0.10 to 0.40	0.40 to 0.70	0.70 to 1.00	-0.05 to 0.00	0.00 to 0.10	0.10 to 0.40	0.40 to 0.70	0.70 to 1.00
600 to 1000	No. of Data	0	0	0	0	0	0	0	0	0	354	0	0	0	0	254	0
	Avg. Error (%)	0	0	0	0	0	0	0	0	0	0.9	0	0	0	0	-1.6	0
	RMS Error (%)	0	0	0	0	0	0	0	0	0	4.9	0	0	0	0	4.5	0
	No. of Data Set	0	0	0	0	0	0	0	0	0	4	0	0	0	0	4	0
		-0.20 to -0.05	0.00 to 0.10	0.10 to 0.40	0.40 to 0.70	0.70 to 1.00	1.00 to 1.30	-0.05 to 0.00	0.00 to 0.10	0.10 to 0.40	0.40 to 0.70	0.70 to 1.00	-0.05 to 0.00	0.00 to 0.10	0.10 to 0.40	0.40 to 0.70	0.70 to 1.00
1000 to 3000	No. of Data	0	0	0	0	0	0	0	0	0	199	0	0	0	96	419	0
	Avg. Error (%)	0	0	0	0	0	0	0	0	0	1.8	0	0	0	-0.9	-1.1	0
	RMS Error (%)	0	0	0	0	0	0	0	0	0	3.3	0	0	0	3.5	4	0
	No. of Data Set	0	0	0	0	0	0	0	0	0	3	0	0	0	3	3	0
		-0.20 to -0.05	0.00 to 0.10	0.10 to 0.40	0.40 to 0.70	0.70 to 1.00	1.00 to 1.30	-0.05 to 0.00	0.00 to 0.10	0.10 to 0.40	0.40 to 0.70	0.70 to 1.00	-0.05 to 0.00	0.00 to 0.10	0.10 to 0.40	0.40 to 0.70	0.70 to 1.00

TABLE IV.II. (CONT.)

Pressure Range (kPa) = 9000 to 11000

Mass Flux Range (kg/(m ² ·s))		50 to 500				500 to 2000				2000 to 4000				4000 to 7000			
Heat Flux Range (kW/m ²)		Quality Range				Quality Range				Quality Range				Quality Range			
		-0.20 to -0.05	0.00 to 0.10	0.10 to 0.40	0.40 to 1.00	-0.20 to -0.05	0.00 to 0.10	0.10 to 0.40	0.40 to 1.00	-0.20 to -0.05	0.00 to 0.10	0.10 to 0.40	0.40 to 1.00	-0.05 to 0.00	0.00 to 0.10	0.10 to 0.40	
50 to 200	No. of Data	0	0	0	0	0	31	190	141	0	0	31	78	7	0	0	
	Avg. Error (%)	0	0	0	0	0	1.2	-0.5	0.1	0	0	0.7	-0.9	2.6	0	-1.4	
	RMS Error (%)	0	0	0	0	0	2.4	2.7	4.2	0	0	2.3	4.42	3	0	3.4	
	No. of Data Set	0	0	0	0	0	2	2	4	0	0	2	2	1	0	2	
200 to 600	No. of Data	0	0	0	0	0	108	126	560	73	16	107	237	180	0	12	
	Avg. Error (%)	0	0	0	0	0	5.2	1.2	0.02	0.7	9.4	2.6	1.5	1.8	0	5.9	
	RMS Error (%)	0	0	0	0	0	7.9	8.6	6	4.7	11.5	10.4	5	4.7	0	6.3	
	No. of Data Set	0	0	0	0	0	2	2	4	3	2	2	2	3	0	2	
600 to 1000	No. of Data	0	0	0	0	0	0	0	84	295	0	0	19	84	26	0	
	Avg. Error (%)	0	0	0	0	0	0	0	1.7	-0.9	0	0	1.1	-2	0.2	0	
	RMS Error (%)	0	0	0	0	0	0	0	6.1	2.1	0	0	3	4.7	1.3	0	
	No. of Data Set	0	0	0	0	0	0	0	2	3	0	0	2	3	2	1	
1000 to 3000	No. of Data	0	0	0	0	0	0	0	2	25	0	0	0	73	93	0	
	Avg. Error (%)	0	0	0	0	0	0	0	-2.5	-2.9	0	0	0	3	0.6	0	
	RMS Error (%)	0	0	0	0	0	0	0	2.6	3.8	0	0	0	4.4	3.3	0	
	No. of Data Set	0	0	0	0	0	0	0	1	2	0	0	0	2	2	0	

TABLE IV.II. (CONT.)

Pressure Range (kPa) = 11000 to 17000													
Mass Flux Range (kg/(m ² ·s))		50 to 500				500 to 2000				2000 to 4000			
Heat Flux Range (kW/m ²)		Quality Range				Quality Range				Quality Range			
		-0.20 to 0.00		0.10 to 0.40		-0.05 to 0.10		0.00 to 0.10		-0.05 to 0.10		0.00 to 0.10	
		to		to		to		to		to		to	
		0.00 to -0.05		0.00 to 0.10		0.00 to -0.05		0.00 to 0.10		0.00 to -0.05		0.00 to 0.10	
50 to 200	No. of Data	0	0	0	0	0	0	0	0	0	0	0	0
	Avg. Error (%)	0	0	0	0	0	0	0	0	0	0	0	0
	RMS Error (%)	0	0	0	0	0	0	0	0	0	0	0	0
	No. of Data Set	0	0	0	0	0	0	0	0	0	0	0	0
200 to 600	No. of Data	0	0	0	0	0	0	0	0	0	0	0	0
	Avg. Error (%)	0	0	0	0	0	0	0	0	0	0	0	0
	RMS Error (%)	0	0	0	0	0	0	0	0	0	0	0	0
	No. of Data Set	0	0	0	0	0	0	0	0	0	0	0	0
600 to 1000	No. of Data	0	0	0	0	0	0	0	0	0	0	0	0
	Avg. Error (%)	0	0	0	0	0	0	0	0	0	0	0	0
	RMS Error (%)	0	0	0	0	0	0	0	0	0	0	0	0
	No. of Data Set	0	0	0	0	0	0	0	0	0	0	0	0
1000 to 3000	No. of Data	0	0	0	0	0	0	0	0	0	0	0	0
	Avg. Error (%)	0	0	0	0	0	0	0	0	0	0	0	0
	RMS Error (%)	0	0	0	0	0	0	0	0	0	0	0	0
	No. of Data Set	0	0	0	0	0	0	0	0	0	0	0	0

TABLE IV.II. (CONT.)

[illegible]

Appendix V

IPPE TABLE OF HEAT TRANSFER COEFFICIENTS FOR FILM BOILING AND SUPERHEATED STEAM FOR TUBES

TABLE V.1. IPPE TABLE OF HEAT TRANSFER COEFFICIENTS ($\text{kW/m}^2\cdot\text{K}$) FOR FILM BOILING AND SUPERHEATED STEAM FOR A TUBE OF DIAMETER 10 mm AT $q = 0.2 \div 1.0 \text{ MW/m}^2$; $T_{inlet} < T_s$; $[P]$ MPa; $[G]$ $\text{kg/m}^2\cdot\text{s}$, $x \leq 1$

Bold lines are approximate borderlines between film boiling and post-dryout regimes.

P MPa	G $\text{kg/m}^2\cdot\text{s}$	q MW/m^2	X															
			-0.2	-0.1	0.0	0.1	0.2	0.3	0.4	0.5	0.6	0.7	0.8	0.9	1.0			
0.1	250	0.2	0.42g	0.37g	0.24g	0.19g	0.19g	0.22g	0.25g	0.28g	0.32g	0.30a	0.28s	0.19s	0.14a			
		0.6	0.60g	0.53g	0.50g	0.45g	0.43g	0.45g	0.47g	0.49g	0.52g	0.56g	0.61g	0.56a	0.43a			
		1.0	1.18g	0.95g	0.75g	0.71g	0.72g	0.72g	0.72g	0.74g	0.76g	0.77g	0.82g	0.87g	0.71a			
0.1	500	0.2	0.42g	0.37g	0.24g	0.21g	0.26g	0.33g	0.42g	0.31s	0.18s	0.13a	0.11a	0.10a	0.09a			
		0.6	0.60g	0.53g	0.50g	0.45g	0.46g	0.53g	0.60g	0.68g	0.52a	0.37a	0.29a	0.24a	0.21a			
		1.0	1.18g	0.95g	0.75g	0.72g	0.72g	0.75g	0.78g	0.86g	0.85a	0.60a	0.47a	0.38a	0.33a			
0.1	750	0.2	0.42g	0.37g	0.24g	0.26g	0.40g	0.51g	0.26s	0.16s	0.13a	0.12a	0.11a	0.10a	0.10a			
		0.6	0.60g	0.53g	0.50g	0.46g	0.56g	0.69g	0.72a	0.41a	0.30a	0.25a	0.22a	0.20a	0.18a			
		1.0	1.16g	0.95g	0.75g	0.72g	0.77g	0.87g	0.97g	0.67a	0.48a	0.38a	0.33a	0.29a	0.26a			
0.1	1000	0.2	0.42g	0.37g	0.24g	0.32g	0.53g	0.34s	0.18s	0.15s	0.14s	0.14s	0.14s	0.14s	0.14s			
		0.6	0.60g	0.53g	0.50g	0.47g	0.66g	0.55a	0.44a	0.31a	0.26a	0.24a	0.22a	0.22a	0.21a			
		1.0	1.18g	0.95g	0.75g	0.72g	0.82g	0.99g	0.70a	0.48a	0.38a	0.33a	0.30a	0.29a	0.28a			
0.1	1500	0.2	0.50g	0.37g	0.24g	0.24a	0.23a	0.23s	0.21s	0.22s	0.23s	0.24s	0.25s	0.24s	0.24s			
		0.6	0.60g	0.53g	0.50g	0.49a	0.48a	0.48a	0.35a	0.32a	0.31a	0.32a	0.33a	0.33a	0.34a			
		1.0	1.18g	0.95g	0.74g	0.76g	1.06g	0.73a	0.49a	0.42a	0.39a	0.39a	0.39a	0.39a	0.40a			
0.1	2000	0.2	0.43g	0.37g	0.24g	0.30a	0.33s	0.34a	0.34a	0.35s	0.37s	0.38s	0.37s	0.36s	0.33s			
		0.6	0.60g	0.53g	0.50a	0.47a	0.45a	0.44a	0.41a	0.43a	0.45s	0.48s	0.49s	0.50s	0.50s			
		1.0	1.18g	0.95g	0.74g	0.65g	0.62a	0.58a	0.51a	0.50a	0.51a	0.54a	0.56a	0.57a	0.58a			
0.1	3000	0.2	0.43g	0.37g	0.24g	0.34a	0.44s	0.56s	0.65s	0.70s	0.72s	0.70s	0.66s	0.59s	0.51s			
		0.6	0.60g	0.53g	0.50g	0.55a	0.62s	0.64s	0.74s	0.82s	0.88s	0.91s	0.91s	0.88s	0.84s			
		1.0	1.18g	0.95g	0.74g	0.73a	0.73a	0.73a	0.79a	0.88s	0.95s	1.00s	1.03s	1.03s	1.02s			

g - Groeneveld

a - approximation

s - Sergeev

TABLE V.I. (CONT.)

P MPa	G kg/m ² s	q MW/m ²	X											
			1.1	1.2	1.3	1.4	1.5	1.6	1.7	1.8	1.9	2.0	2.1	2.2
0.1	250	0.2	0.12a	0.10a	0.09a	0.08a	0.07a	0.07a	0.06a	0.06a	0.05a	0.05a	0.05a	0.05a
		0.6	0.35a	0.29a	0.25a	0.22a	0.20a	0.18a	0.17a	0.15a	0.14a	0.13a	0.13a	0.12a
		1.0	0.58a	0.49a	0.42a	0.37a	0.33a	0.30a	0.27a	0.25a	0.23a	0.22a	0.20a	0.19a
0.1	500	0.2	0.08a	0.08a	0.07a	0.07a	0.07a	0.06a	0.06a	0.06a	0.06a	0.06a	0.06a	0.06a
		0.6	0.19a	0.17a	0.16a	0.15a	0.14a	0.13a	0.13a	0.12a	0.12a	0.12a	0.11a	0.11a
		1.0	0.29a	0.26a	0.24a	0.22a	0.21a	0.20a	0.19a	0.18a	0.17a	0.17a	0.16a	0.16a
0.1	750	0.2	0.10a	0.10a	0.10a	0.10a	0.09a	0.09a	0.09a	0.09a	0.08a	0.08a	0.08a	0.07a
		0.6	0.18a	0.17a	0.17a	0.16a	0.16a	0.16a	0.16a	0.15a	0.15a	0.15a	0.15a	0.15a
		1.0	0.25a	0.23a	0.22a	0.22a	0.21a	0.21a	0.20a	0.20a	0.20a	0.20a	0.20a	0.19a
0.1	1000	0.2	0.14s	0.14s	0.13s	0.13s	0.12s	0.12a	0.11a	0.10a	0.10a	0.09a	0.08a	0.08a
		0.6	0.21a	0.21a	0.21a	0.21a	0.21a	0.21a	0.20a	0.20a	0.20a	0.19a	0.19a	0.18a
		1.0	0.27a	0.27a	0.26a	0.26a	0.26a	0.26a	0.26a	0.26a	0.26a	0.25a	0.25a	0.25a
0.1	1500	0.2	0.22s	0.21s	0.19s	0.18s	0.14s	0.14s	0.13s	0.12s	0.10a	0.09a	0.08a	0.08a
		0.6	0.34a	0.34a	0.33a	0.33a	0.32a	0.31a	0.29a	0.28a	0.27a	0.25a	0.24a	0.23a
		1.0	0.40a	0.41a	0.41a	0.41a	0.40a	0.40a	0.39a	0.38a	0.37a	0.36a	0.35a	0.34a
0.1	2000	0.2	0.30s	0.27s	0.24s	0.20s	0.18s	0.15s	0.13s	0.12s	0.11a	0.10a	0.09a	0.08a
		0.6	0.49s	0.48s	0.46s	0.43s	0.41s	0.38s	0.35a	0.33a	0.30a	0.28a	0.26a	0.24a
		1.0	0.59a	0.58a	0.58a	0.56a	0.55a	0.53a	0.50a	0.48a	0.45a	0.43a	0.40a	0.38a
0.1	3000	0.2	0.42s	0.34s	0.27s	0.22s	0.18s	0.15s	0.13s	0.12s	0.11a	0.09a	0.09a	0.08a
		0.6	0.78s	0.71s	0.64s	0.57s	0.50s	0.44s	0.39s	0.35a	0.31a	0.28a	0.26a	0.24a
		1.0	0.98s	0.93s	0.87s	0.81s	0.74s	0.68s	0.62a	0.56a	0.51a	0.47a	0.43a	0.40a

g - Groeneveld

a - approximation

s - Sergeev

TABLE V.I. (CONT.)

P MPa	G kg/m ² s	q MW/m ²	X															
			-0.2	-0.1	0.0	0.1	0.2	0.3	0.4	0.5	0.6	0.7	0.8	0.9	1.0			
0.2	250	0.2	0.41g	0.37g	0.27g	0.23g	0.19g	0.22g	0.26g	0.29g	0.32g	0.37g	0.42g	0.35s	0.23s			
		0.6	0.66g	0.55g	0.52g	0.45g	0.44g	0.46g	0.47g	0.50g	0.52g	0.57g	0.62g	0.70g	0.70a			
		1.0	0.95g	0.84g	0.77g	0.72g	0.73g	0.73g	0.73g	0.75g	0.77g	0.80g	0.83g	0.88g	0.94g			
0.2	500	0.2	0.41g	0.37g	0.27g	0.24g	0.30g	0.36g	0.43g	0.49g	0.35s	0.22s	0.16s	0.13a	0.11a			
		0.6	0.66g	0.55g	0.52g	0.45g	0.47g	0.49a	0.51g	0.70g	0.76g	0.61a	0.44a	0.35a	0.29a			
		1.0	0.95g	0.84g	0.77g	0.72g	0.72g	0.75g	0.78g	0.87g	0.96g	1.01a	0.72a	0.56a	0.47a			
0.2	750	0.2	0.41g	0.37g	0.27g	0.28g	0.42g	0.52g	0.39a	0.27s	0.18s	0.15s	0.14s	0.13a	0.12a			
		0.6	0.66g	0.55g	0.52g	0.46g	0.57g	0.70g	0.82g	0.73a	0.47a	0.35a	0.30a	0.26a	0.24a			
		1.0	0.95g	0.84g	0.77g	0.73a	0.77g	0.88g	0.97g	1.11g	0.75a	0.56a	0.45a	0.39a	0.35a			
0.2	1000	0.2	0.41g	0.37g	0.27g	0.33g	0.54g	0.42a	0.30s	0.20s	0.18s	0.17s	0.17s	0.16s	0.16s			
		0.6	0.66g	0.55g	0.52g	0.47g	0.68g	0.86g	0.78s	0.47a	0.36a	0.31a	0.28a	0.27a	0.26a			
		1.0	0.95g	0.84g	0.77g	0.73g	0.82g	1.00g	1.17g	0.73a	0.54a	0.45a	0.40a	0.36a	0.34a			
0.2	1500	0.2	0.47g	0.37g	0.27g	0.47g	0.85g	0.34s	0.27s	0.27s	0.28s	0.28s	0.28s	0.28s	0.27s			
		0.6	0.66g	0.55g	0.52g	0.60g	0.96g	0.80s	0.48a	0.41a	0.39a	0.38a	0.39a	0.39a	0.39a			
		1.0	0.95g	0.84g	0.77g	0.76g	1.08g	1.26a	0.70a	0.55a	0.49a	0.47a	0.47a	0.47a	0.47a			
0.2	2000	0.2	0.56g	0.42g	0.27g	0.30a	0.33a	0.35s	0.38s	0.41s	0.44s	0.44s	0.43s	0.41s	0.38s			
		0.6	0.66g	0.55g	0.52g	0.55a	0.51a	0.51a	0.51s	0.52s	0.54s	0.56s	0.57s	0.58s	0.57s			
		1.0	0.95g	0.84g	0.77g	0.74a	0.71a	0.68a	0.66a	0.62a	0.62a	0.63a	0.65a	0.67a	0.67a			
0.2	3000	0.2	0.56a	0.48g	0.27g	0.40a	0.54s	0.66s	0.77s	0.83s	0.85s	0.83s	0.77s	0.69s	0.58s			
		0.6	0.66g	0.58g	0.52g	0.60a	0.68a	0.77s	0.87s	0.96s	1.03s	1.06s	1.05s	1.01s	0.96s			
		1.0	0.95g	0.84g	0.77g	0.81a	0.85a	0.90a	0.95s	1.03s	1.11s	1.17s	1.19s	1.19s	1.16s			

g - Groeneveld

a - approximation

s - Sergeev

TABLE V.I. (CONT.)

P MPa	G kg/m ² s	q MW/m ²	X											
			1.1	1.2	1.3	1.4	1.5	1.6	1.7	1.8	1.9	2.0	2.1	2.2
0.2	250	0.2	0.18s	0.14a	0.12a	0.11a	0.09a	0.08a	0.08a	0.07a	0.07a	0.06a	0.06a	0.06a
		0.6	0.53a	0.43a	0.36a	0.31a	0.27a	0.24a	0.22a	0.20a	0.18a	0.17a	0.16a	0.15a
		1.0	0.88a	0.71a	0.59a	0.51a	0.45a	0.40a	0.36a	0.33a	0.30a	0.28a	0.26a	0.24a
0.2	500	0.2	0.10a	0.09a	0.09a	0.08a	0.08a	0.08a	0.07a	0.07a	0.07a	0.07a	0.07a	0.06a
		0.6	0.25a	0.22a	0.20a	0.19a	0.18a	0.17a	0.16a	0.15a	0.15a	0.14a	0.14a	0.13a
		1.0	0.40a	0.35a	0.32a	0.29a	0.27a	0.25a	0.24a	0.22a	0.21a	0.20a	0.20a	0.19a
0.2	750	0.2	0.12a	0.12a	0.11a	0.11a	0.11a	0.10a	0.10a	0.09a	0.09a	0.08a	0.08a	0.08a
		0.6	0.22a	0.21a	0.20a	0.20a	0.19a	0.19a	0.18a	0.18a	0.18a	0.17a	0.17a	0.16a
		1.0	0.32a	0.30a	0.28a	0.27a	0.26a	0.25a	0.24a	0.24a	0.23a	0.23a	0.23a	0.22a
0.2	1000	0.2	0.16s	0.15s	0.15s	0.14s	0.13s	0.13s	0.12a	0.11a	0.10a	0.09a	0.09a	0.08a
		0.6	0.25a	0.25a	0.25a	0.24a	0.24a	0.23a	0.23a	0.23a	0.22a	0.21a	0.21a	0.20a
		1.0	0.33a	0.32a	0.31a	0.31a	0.30a	0.30a	0.30a	0.29a	0.29a	0.29a	0.28a	0.28a
0.2	1500	0.2	0.25s	0.23s	0.21s	0.19s	0.17s	0.15s	0.14s	0.14s	0.12s	0.11a	0.10a	0.09a
		0.6	0.39a	0.39a	0.38a	0.37a	0.35a	0.34a	0.32a	0.30a	0.29a	0.27a	0.25a	0.24a
		1.0	0.47a	0.47a	0.47a	0.46a	0.46a	0.45a	0.43a	0.42a	0.41a	0.39a	0.38a	0.36a
0.2	2000	0.2	0.34s	0.30s	0.26s	0.22s	0.19s	0.16s	0.14s	0.14s	0.12s	0.11a	0.10a	0.09a
		0.6	0.56s	0.54s	0.51s	0.48s	0.44s	0.41s	0.38a	0.34a	0.32a	0.29a	0.27a	0.25a
		1.0	0.67a	0.66a	0.65a	0.63a	0.60a	0.58a	0.55a	0.52a	0.48a	0.45a	0.42a	0.40a
0.2	3000	0.2	0.48s	0.38s	0.30s	0.24s	0.19s	0.16s	0.14s	0.14s	0.12s	0.11a	0.10a	0.09a
		0.6	0.88s	0.79s	0.70s	0.62s	0.54s	0.47s	0.41s	0.37s	0.33a	0.30a	0.27a	0.25a
		1.0	1.11s	1.05s	0.97s	0.89s	0.81s	0.73s	0.66s	0.59a	0.54a	0.49a	0.45a	0.41a

g - Groeneveld

a - approximation

s - Sergeev

TABLE V.I. (CONT.)

P MPa	G kg/mm ² s	q MW/m ²	x															
			-0.2	-0.1	0.0	0.1	0.2	0.3	0.4	0.5	0.6	0.7	0.8	0.9	1.0			
0.5	250	0.2	0.34g	0.32g	0.29g	0.26g	0.20g	0.23g	0.27g	0.31g	0.34g	0.39g	0.44g	0.55g	0.49a			
		0.6	0.57g	0.52g	0.46g	0.46g	0.45g	0.47g	0.49g	0.51g	0.54g	0.57g	0.64g	0.82g	0.82g			
		1.0	0.87g	0.81g	0.75g	0.74g	0.74g	0.74g	0.75g	0.77g	0.79g	0.82g	0.85g	0.91g	0.96g			
0.5	500	0.2	0.38g	0.34g	0.31g	0.26g	0.34g	0.39g	0.45g	0.52g	0.58g	0.56a	0.53s	0.32s	0.23s			
		0.6	0.62g	0.54g	0.46g	0.46g	0.48g	0.56g	0.64g	0.73g	0.82g	0.93g	1.04g	0.92s	0.65a			
		1.0	0.94g	0.84g	0.75g	0.74g	0.74g	0.78g	0.81g	0.90g	0.99g	1.10g	1.21g	1.39g	1.07a			
0.5	750	0.2	0.38g	0.34g	0.31g	0.31g	0.46g	0.56g	0.66g	0.78g	0.78s	0.36s	0.26s	0.21s	0.18s			
		0.6	0.62g	0.54g	0.47g	0.47g	0.59g	0.72g	0.85g	0.99g	0.99a	1.00s	0.66s	0.51a	0.42a			
		1.0	0.94g	0.84g	0.75g	0.75g	0.79g	0.91g	1.02g	1.16g	1.30g	1.17a	1.07a	0.81a	0.66a			
0.5	1000	0.2	0.38g	0.34g	0.31g	0.36g	0.58g	0.73g	0.87g	0.76s	0.36s	0.28s	0.24s	0.22s	0.21s			
		0.6	0.62g	0.54g	0.47g	0.48g	0.70g	0.88g	1.07g	1.25g	0.92s	0.62s	0.50a	0.43a	0.39a			
		1.0	0.94g	0.84g	0.75g	0.75g	0.84g	1.04g	1.23g	1.42g	1.47a	0.97a	0.75a	0.63a	0.55a			
0.5	1500	0.2	0.55g	0.42g	0.31g	0.50g	0.88g	1.19g	0.61s	0.40s	0.38s	0.37s	0.36s	0.35s	0.33s			
		0.6	0.62g	0.54g	0.48g	0.62g	0.99g	1.28g	1.52s	0.79s	0.62s	0.56s	0.53s	0.52s	0.50s			
		1.0	0.94g	0.84g	0.76g	0.78g	1.11g	1.41g	2.43s	1.18a	0.87a	0.74a	0.68a	0.65a	0.63a			
0.5	2000	0.2	0.67g	0.50g	0.31g	0.68g	1.30g	0.96s	0.55s	0.55s	0.57s	0.57s	0.55s	0.51s	0.46s			
		0.6	0.62g	0.56g	0.49g	0.77g	1.30g	1.71g	0.93s	0.76s	0.74s	0.74s	0.74s	0.73s	0.71s			
		1.0	0.94g	0.84g	0.76g	0.87g	1.40g	1.81g	1.33s	0.99s	0.90s	0.87s	0.86s	0.86s	0.85s			
0.5	3000	0.2	0.81g	0.59g	0.31g	0.50a	0.70a	0.90s	1.03s	1.11s	1.13s	1.08s	1.00s	0.87s	0.71s			
		0.6	0.79g	0.68g	0.49g	1.12g	1.16a	1.21s	1.23a	1.27s	1.33s	1.35s	1.32s	1.26s	1.17s			
		1.0	0.94g	0.84g	0.76g	1.22g	1.26a	1.30a	1.35s	1.39s	1.45s	1.50s	1.51s	1.48s	1.42s			

g - Groeneveld

a - approximation

s - Sergeev

TABLE V.I. (CONT.)

P MPa	G kg/m ² s	q MW/m ²	X											
			1.1	1.2	1.3	1.4	1.5	1.6	1.7	1.8	1.9	2.0	2.1	2.2
0.5	250	0.2	0.42s	0.29s	0.22s	0.18s	0.15s	0.13a	0.12a	0.10a	0.10a	0.09a	0.08a	0.07a
		0.6	0.82g	0.74a	0.66a	0.54a	0.45a	0.39a	0.34a	0.31a	0.28a	0.25a	0.23a	0.22a
		1.0	0.98g	0.97g	0.91a	0.89a	0.75a	0.65a	0.57a	0.51a	0.46a	0.42a	0.39a	0.36a
0.5	500	0.2	0.19s	0.16s	0.14s	0.12a	0.11a	0.10a	0.10a	0.09a	0.09a	0.08a	0.08a	0.07a
		0.6	0.51a	0.42a	0.36a	0.32a	0.29a	0.26a	0.24a	0.22a	0.21a	0.20a	0.19a	0.18a
		1.0	0.83a	0.69a	0.58a	0.51a	0.46a	0.41a	0.38a	0.35a	0.33a	0.31a	0.29a	0.27a
0.5	750	0.2	0.17s	0.15s	0.14s	0.14s	0.13s	0.12a	0.11a	0.11a	0.10a	0.09a	0.09a	0.08a
		0.6	0.37a	0.33a	0.30a	0.28a	0.26a	0.25a	0.24a	0.23a	0.22a	0.21a	0.21a	0.20a
		1.0	0.56a	0.50a	0.45a	0.41a	0.38a	0.36a	0.34a	0.33a	0.32a	0.30a	0.29a	0.28a
0.5	1000	0.2	0.20s	0.19s	0.18s	0.17s	0.15s	0.14s	0.13s	0.12a	0.11a	0.10a	0.09a	0.09a
		0.6	0.36a	0.34a	0.33a	0.31a	0.30a	0.29a	0.28a	0.27a	0.26a	0.25a	0.24a	0.23a
		1.0	0.50a	0.47a	0.44a	0.42a	0.41a	0.39a	0.38a	0.37a	0.36a	0.35a	0.34a	0.33a
0.5	1500	0.2	0.30s	0.27s	0.24s	0.22s	0.19s	0.17s	0.15s	0.13s	0.12a	0.10a	0.10a	0.09a
		0.6	0.49s	0.48s	0.46s	0.44s	0.41s	0.39a	0.37a	0.34a	0.32a	0.30a	0.27a	0.26a
		1.0	0.61a	0.60a	0.58a	0.57a	0.55a	0.53a	0.51a	0.49a	0.47a	0.44a	0.42a	0.40a
0.5	2000	0.2	0.40s	0.34s	0.29s	0.24s	0.20s	0.17s	0.15s	0.13s	0.12s	0.10a	0.10a	0.09a
		0.6	0.68s	0.64s	0.60s	0.55s	0.50s	0.46s	0.41s	0.37a	0.34a	0.31a	0.28a	0.26a
		1.0	0.83s	0.81s	0.78s	0.74s	0.70a	0.66a	0.62a	0.58a	0.53a	0.50a	0.46a	0.43a
0.5	3000	0.2	0.56s	0.43s	0.33s	0.25s	0.21s	0.17s	0.15s	0.13s	0.12a	0.10a	0.10a	0.09a
		0.6	1.05s	0.93s	0.80s	0.69s	0.59s	0.51s	0.44s	0.39s	0.35a	0.31a	0.28a	0.26a
		1.0	1.34s	1.24s	1.13s	1.01s	0.90s	0.80s	0.72s	0.64a	0.57a	0.52a	0.47a	0.43a

g - Groeneveld

a - approximation

s - Sergeev

TABLE V.I. (CONT.)

P MPa	G kg/m ² s	q MW/m ²	X															
			-0.2	-0.1	0.0	0.1	0.2	0.3	0.4	0.5	0.6	0.7	0.8	0.9	1.0			
1.0	250	0.2	0.55g	0.47g	0.36g	0.32g	0.25g	0.28g	0.31g	0.34g	0.36g	0.42g	0.48g	0.59g	0.70g			
		0.6	0.71g	0.61g	0.52g	0.50g	0.47g	0.49g	0.50g	0.53g	0.56g	0.61g	0.67g	0.74g	0.81g			
		1.0	0.88g	0.82g	0.78g	0.77g	0.77g	0.76g	0.76g	0.79g	0.81g	0.84g	0.87g	0.93g	0.99g			
1.0	500	0.2	0.84g	0.70g	0.40g	0.33g	0.44g	0.47g	0.50g	0.56g	0.61g	0.77g	0.69a	0.61s	0.37s			
		0.6	0.82g	0.69g	0.59g	0.52g	0.57g	0.62g	0.67g	0.76g	0.85g	0.98g	1.10g	1.08a	1.06s			
		1.0	1.02g	0.91g	0.82g	0.77g	0.80g	0.82g	0.83g	0.93g	1.02g	1.14g	1.27g	1.46g	1.35a			
1.0	750	0.2	0.84g	0.70g	0.42g	0.40g	0.55g	0.63g	0.71g	0.83g	0.96g	0.88s	0.43s	0.31s	0.25s			
		0.6	0.82g	0.68g	0.59g	0.66g	0.80g	0.95g	1.05g	1.15g	1.35g	1.26a	1.18s	0.79s	0.61s			
		1.0	1.02g	0.91g	0.82g	0.80g	0.84g	0.96g	1.07g	1.19g	1.32g	1.51g	1.38a	1.28a	0.97a			
1.0	1000	0.2	0.84g	0.70g	0.44g	0.46g	0.66g	0.79g	0.92g	0.86a	0.81s	0.43s	0.33s	0.29s	0.26s			
		0.6	0.82g	0.68g	0.59g	0.56g	0.75g	0.99g	1.23g	1.34g	1.20a	1.07s	0.74s	0.60s	0.52s			
		1.0	1.02g	0.91g	0.83g	0.81g	0.89g	1.10g	1.30g	1.46g	1.62g	1.38a	1.15a	0.90a	0.76a			
1.0	1500	0.2	0.84g	0.65a	0.44g	0.57g	0.94g	1.27g	0.96a	0.65s	0.50s	0.47s	0.45s	0.43s	0.40s			
		0.6	0.82g	0.68g	0.59g	0.64g	1.04g	1.40g	1.40a	1.35a	0.92s	0.76s	0.69s	0.65s	0.62s			
		1.0	1.02g	0.91g	0.83g	0.81g	1.15g	1.48g	1.43a	1.39a	1.34s	1.04a	0.91a	0.84a	0.79a			
1.0	2000	0.2	0.84g	0.65g	0.44g	0.72g	1.38g	1.10a	0.83s	0.72s	0.72a	0.72s	0.68s	0.62s	0.52s			
		0.6	0.82g	0.68g	0.59g	0.80g	1.37g	1.86a	1.60a	1.08s	0.96s	0.94s	0.92s	0.90s	0.86s			
		1.0	1.02g	0.91g	0.83g	0.90g	1.41g	1.88g	1.62a	1.46s	1.21s	1.13s	1.09s	1.07s	1.04s			
1.0	3000	0.2	0.84g	0.70g	0.44g	1.19g	1.21a	1.24s	1.34s	1.44s	1.46s	1.39s	1.26s	1.08s	0.87s			
		0.6	0.82g	0.69g	0.66g	1.18g	1.58a	1.57a	1.56s	1.63s	1.69s	1.70s	1.65s	1.55s	1.40s			
		1.0	1.02g	0.91g	0.86g	1.26g	2.10g	1.96a	1.84s	1.80s	1.85s	1.88s	1.87s	1.82s	1.72s			

g - Groeneveld

a - approximation

s - Sergeev

TABLE V.I. (CONT.)

P MPa	G kg/m ² s	q MW/m ²	x											
			1.1	1.2	1.3	1.4	1.5	1.6	1.7	1.8	1.9	2.0	2.1	2.2
1.0	250	0.2	0.63s	0.39s	0.29s	0.23s	0.19s	0.16s	0.14a	0.12a	0.11a	0.10a	0.09a	0.08a
		0.6	0.81g	0.79g	0.73a	0.67a	0.55a	0.47a	0.41a	0.36a	0.33a	0.30a	0.27a	0.25a
		1.0	1.01g	1.01g	0.98a	0.95a	0.92a	0.78a	0.68a	0.60a	0.54a	0.49a	0.45a	0.41a
1.0	500	0.2	0.27s	0.21s	0.18s	0.16a	0.14s	0.13a	0.12a	0.11a	0.10a	0.09a	0.09a	0.08a
		0.6	0.76s	0.59a	0.49a	0.42a	0.37a	0.33a	0.30a	0.28a	0.26a	0.24a	0.22a	0.21a
		1.0	1.25a	0.98a	0.80a	0.68a	0.60a	0.53a	0.48a	0.44a	0.41a	0.38a	0.35a	0.33a
1.0	750	0.2	0.21s	0.19s	0.18s	0.16s	0.15s	0.14s	0.13s	0.12s	0.11s	0.10s	0.10s	0.09s
		0.6	0.50a	0.44a	0.39a	0.36a	0.33a	0.31a	0.29a	0.27a	0.26a	0.25a	0.24a	0.23a
		1.0	0.79a	0.67a	0.59a	0.54a	0.49a	0.46a	0.43a	0.40a	0.38a	0.36a	0.35a	0.33a
1.0	1000	0.2	0.24s	0.23s	0.21s	0.19s	0.16s	0.16s	0.14s	0.13s	0.12a	0.11a	0.10a	0.09a
		0.6	0.46a	0.43a	0.40a	0.38a	0.36a	0.34a	0.33a	0.31a	0.29a	0.28a	0.27a	0.25a
		1.0	0.67a	0.61a	0.56a	0.53a	0.50a	0.48a	0.46a	0.44a	0.42a	0.41a	0.39a	0.37a
1.0	1500	0.2	0.36s	0.32s	0.29s	0.24s	0.21s	0.18s	0.16s	0.14s	0.12a	0.11a	0.10a	0.09a
		0.6	0.60s	0.57s	0.54s	0.51s	0.48s	0.44s	0.41a	0.38a	0.35a	0.32a	0.29a	0.27a
		1.0	0.76a	0.73a	0.71a	0.68a	0.65a	0.62a	0.59a	0.56a	0.52a	0.49a	0.46a	0.44a
1.0	2000	0.2	0.47s	0.39s	0.32s	0.26s	0.22s	0.18s	0.16s	0.14s	0.12a	0.11a	0.10a	0.09a
		0.6	0.81s	0.75s	0.69s	0.63s	0.56s	0.50s	0.45s	0.40a	0.36a	0.33a	0.30a	0.28a
		1.0	1.01s	0.97s	0.92s	0.87s	0.81s	0.75s	0.69a	0.63a	0.58a	0.53a	0.49a	0.45a
1.0	3000	0.2	0.66s	0.48s	0.36s	0.27s	0.22s	0.18s	0.16s	0.14s	0.12a	0.11a	0.10a	0.09a
		0.6	1.24s	1.07s	0.90s	0.76s	0.64s	0.54s	0.47s	0.41s	0.37a	0.33a	0.30a	0.26a
		1.0	1.59s	1.45s	1.29s	1.14s	1.00s	0.88s	0.77s	0.68a	0.61a	0.55a	0.50a	0.46a

g - Groeneveld

a - approximation

s - Sergeev

TABLE V.I. (CONT.)

P MPa	G kg/m ² s	q MW/m ²	x															
			-0.2	-0.1	0.0	0.1	0.2	0.3	0.4	0.5	0.6	0.7	0.8	0.9	1.0			
2.0	250	0.2	0.88g	0.75g	0.48g	0.39g	0.28g	0.34g	0.39g	0.41g	0.43g	0.54g	0.64g	0.71g	0.72a			
		0.6	0.90g	0.76g	0.63g	0.59g	0.53g	0.55g	0.56g	0.58g	0.59g	0.65g	0.72g	0.73g	0.74g			
		1.0	0.99g	0.90g	0.84g	0.82g	0.80g	0.80g	0.80g	0.82g	0.84g	0.89g	0.94g	0.98g	1.02a			
2.0	500	0.2	0.90g	0.77g	0.50g	0.42g	0.40g	0.49g	0.57g	0.67g	0.78g	0.90a	1.10a	1.02a	0.67s			
		0.6	0.90g	0.76g	0.70g	0.63g	0.63g	0.71g	0.78g	0.80g	0.82g	0.98g	1.14g	1.33g	1.27a			
		1.0	0.97g	0.91g	0.85g	0.84g	0.88g	0.93g	0.98g	1.02g	1.16g	1.29g	1.50g	1.71g	1.65g			
2.0	750	0.2	0.90a	0.76a	0.53g	0.49g	0.55g	0.66g	0.77g	0.94g	1.11g	1.04a	0.98s	0.52s	0.37s			
		0.6	0.90g	0.76g	0.70g	0.65g	0.75g	0.97g	1.10a	1.14g	1.21a	1.29g	1.34a	1.40s	0.95s			
		1.0	1.11g	0.97g	0.94g	0.90g	0.92g	1.08g	1.24g	1.25g	1.27g	1.45g	1.63g	1.58a	1.53a			
2.0	1000	0.2	0.19a	0.76a	0.55g	0.56g	0.70g	0.84g	0.97g	1.21g	1.07a	0.92s	0.54s	0.42s	0.37s			
		0.6	0.90g	0.76g	0.70g	0.66g	0.86g	1.23g	1.35a	1.48g	1.36g	1.33a	1.29s	0.92s	0.75s			
		1.0	1.11g	0.97g	0.97g	0.97a	1.00g	1.27g	1.44a	1.52g	1.61a	1.74g	1.57a	1.41s	1.12a			
2.0	1500	0.2	0.90a	0.77a	0.73g	0.76g	1.05g	1.42g	1.78g	1.32a	0.85s	0.71s	0.66s	0.60s	0.54s			
		0.6	0.90g	0.77g	0.74a	0.78g	1.17g	1.60a	1.90a	2.01a	1.71s	1.19s	1.00s	0.92s	0.86s			
		1.0	1.11g	0.97g	0.97g	1.00a	1.22g	1.64g	2.06g	2.36g	2.02a	1.68s	1.35s	1.19s	1.10s			
2.0	2000	0.2	0.90a	0.77a	0.73g	0.85g	1.30a	1.95a	1.70a	1.17s	1.11s	1.08s	1.00s	0.90s	0.77s			
		0.6	0.90g	0.77g	0.81g	0.88g	1.35a	2.00a	2.13a	1.91s	1.47s	1.36s	1.31s	1.25s	1.17s			
		1.0	1.11g	0.97g	0.97g	0.98g	1.38g	2.03g	2.68g	2.28a	1.88s	1.65s	1.55s	1.49s	1.43s			
2.0	3000	0.2	0.90a	0.78a	0.73g	1.35a	2.25a	2.34a	2.30a	2.28s	2.28s	2.16s	1.92s	1.59s	1.22s			
		0.6	0.90g	0.78g	0.81g	1.37g	2.30a	2.55a	2.55a	2.55a	2.55s	2.52s	2.40s	2.20s	1.94s			
		1.0	1.11g	0.97g	0.97g	1.37g	2.32g	2.60a	2.65a	2.71s	2.73s	2.75s	2.69s	2.55s	2.36s			

g - Groeneveld

a - approximation

s - Sergeev

TABLE V.I. (CONT.)

P MPa	G kg/m ² s	q MW/m ²	X											
			1.1	1.2	1.3	1.4	1.5	1.6	1.7	1.8	1.9	2.0	2.1	2.2
2.0	250	0.2	0.71g	0.54s	0.37s	0.28s	0.23s	0.19s	0.16s	0.14a	0.13a	0.12a	0.11a	0.09a
		0.6	0.72g	0.70g	0.69a	0.68a	0.68a	0.57a	0.49a	0.43a	0.38a	0.34a	0.31a	0.29a
		1.0	1.04a	1.05a	1.08a	1.11a	1.13a	0.94a	0.81a	0.71a	0.64a	0.57a	0.52a	0.48a
2.0	500	0.2	0.42s	0.31s	0.25s	0.21s	0.18s	0.16s	0.14s	0.13a	0.12a	0.11a	0.10a	0.10a
		0.6	1.21s	0.88s	0.69s	0.57a	0.49a	0.43a	0.38a	0.35a	0.32a	0.30a	0.27a	0.26a
		1.0	1.58g	1.44a	1.13a	0.93a	0.80a	0.70a	0.62a	0.56a	0.51a	0.47a	0.44a	0.41a
2.0	750	0.2	0.30s	0.26s	0.23s	0.21s	0.19s	0.17s	0.15s	0.14s	0.13a	0.12a	0.11a	0.10a
		0.6	0.74s	0.61s	0.53a	0.47a	0.43a	0.39a	0.37a	0.34a	0.32a	0.30a	0.28a	0.27a
		1.0	1.17a	0.96a	0.82a	0.72a	0.65a	0.59a	0.55a	0.51a	0.48a	0.45a	0.43a	0.41a
2.0	1000	0.2	0.33s	0.29s	0.26s	0.24s	0.21s	0.19s	0.17s	0.15s	0.13a	0.12a	0.11a	0.10a
		0.6	0.65s	0.58s	0.53s	0.49s	0.46a	0.43a	0.40a	0.38a	0.35a	0.33a	0.31a	0.29a
		1.0	0.95a	0.84a	0.76a	0.70a	0.65a	0.61a	0.58a	0.55a	0.52a	0.49a	0.47a	0.44a
2.0	1500	0.2	0.48s	0.41s	0.34s	0.29s	0.24s	0.20s	0.17s	0.15s	0.14s	0.12a	0.11a	0.10a
		0.6	0.80s	0.75s	0.69s	0.64s	0.58s	0.53s	0.48s	0.44a	0.39a	0.36a	0.33a	0.30a
		1.0	1.03s	0.98s	0.92s	0.87s	0.82a	0.77a	0.72a	0.67a	0.62a	0.57a	0.53a	0.49a
2.0	2000	0.2	0.63s	0.50s	0.39s	0.30s	0.25s	0.20s	0.17s	0.15s	0.14s	0.12a	0.11a	0.10a
		0.6	1.08s	0.98s	0.87s	0.77s	0.67s	0.59s	0.51s	0.45s	0.40a	0.36a	0.33a	0.30a
		1.0	1.36s	1.27s	1.18s	1.09s	0.99s	0.90s	0.81s	0.73a	0.66a	0.60a	0.55a	0.50a
2.0	3000	0.2	0.87s	0.60s	0.42s	0.31s	0.25s	0.20s	0.17s	0.15s	0.14s	0.12a	0.11a	0.10a
		0.6	1.65s	1.36s	1.10s	0.89s	0.73s	0.61s	0.52s	0.46s	0.41a	0.36a	0.33a	0.30a
		1.0	2.12s	1.86s	1.61s	1.37s	1.17s	1.00s	0.87s	0.76s	0.67a	0.61a	0.55a	0.50a

g - Groeneveld

a - approximation

s - Sergeev

TABLE V.I. (CONT.)

P MPa	G kg/m ² s	q MW/m ²	x															
			-0.2	-0.1	0.0	0.1	0.2	0.3	0.4	0.5	0.6	0.7	0.8	0.9	1.0			
3.0	250	0.2	0.98g	0.84g	0.56g	0.45g	0.32g	0.37g	0.42g	0.44g	0.46g	0.58g	0.70g	0.75a	0.76a			
		0.6	1.06g	0.88g	0.69g	0.64g	0.56g	0.57g	0.59g	0.60g	0.61g	0.68g	0.74g	0.77g	0.80g			
		1.0	1.20g	1.05g	0.88g	0.85g	0.82g	0.82g	0.83g	0.84g	0.86g	0.90g	0.94g	0.99g	1.04g			
3.0	500	0.2	1.00g	0.86g	0.58g	0.48g	0.45g	0.53g	0.61g	0.72g	0.83g	1.02a	1.10a	1.21a	1.04s			
		0.6	1.06g	0.88g	0.76g	0.68g	0.68g	0.75g	0.82g	0.86g	0.89g	1.02g	1.16g	1.34g	1.53g			
		1.0	1.28g	1.10g	0.96g	0.89g	0.88g	0.92g	0.97g	1.02g	1.07g	1.15g	1.23g	1.44g	1.65g			
3.0	750	0.2	1.06a	0.88a	0.60g	0.55g	0.61g	0.71g	0.82g	1.01g	1.19g	1.19a	1.19a	0.81s	0.51s			
		0.6	1.06g	0.88g	0.76g	0.70g	0.79g	1.02g	1.15a	1.22g	1.30a	1.40g	1.60g	1.47a	1.34s			
		1.0	1.28g	1.10g	0.98g	0.94g	0.96g	1.12g	1.29g	1.31g	1.34g	1.49g	1.64g	1.95g	1.75a			
3.0	1000	0.2	1.06a	0.88a	0.63g	0.63g	0.76g	0.89g	1.03g	1.28g	1.15a	1.00a	0.83s	0.58s	0.48s			
		0.6	1.06g	0.88g	0.76g	0.72g	0.91g	1.29g	1.55a	1.59g	1.52g	1.44a	1.36a	1.29s	0.99s			
		1.0	1.28g	1.10g	1.00g	1.00g	1.05g	1.33g	1.60g	1.61g	1.61g	1.81g	1.90a	1.99s	1.48s			
3.0	1500	0.2	1.06a	0.88a	0.78g	0.83g	1.16g	1.56g	1.97g	1.63a	1.29s	0.98s	0.88s	0.79s	0.69s			
		0.6	1.06g	0.88g	0.86g	0.83g	1.24g	1.82g	2.05a	2.20a	2.32a	1.64s	1.33s	1.19s	1.09s			
		1.0	1.28g	1.10g	1.00g	1.00g	1.29g	1.71g	2.13g	2.42g	2.37a	2.32s	1.78s	1.54s	1.40s			
3.0	2000	0.2	1.06a	0.88a	0.78g	0.95g	1.35a	1.90a	1.85a	1.78s	1.57s	1.50s	1.38s	1.20s	1.00s			
		0.6	1.06g	0.88g	0.86g	0.96g	1.40a	2.00a	2.70a	2.60a	2.07s	1.86s	1.75s	1.65s	1.52s			
		1.0	1.28g	1.10g	1.00g	1.05g	1.46g	2.11g	2.76g	2.71a	2.66s	2.22s	2.05s	1.94s	1.84s			
3.0	3000	0.2	1.06a	0.89a	0.78g	1.35a	2.30a	3.10a	3.15a	3.24s	3.23s	3.03s	2.66s	2.16s	1.60s			
		0.6	1.06g	0.89g	0.86g	1.40a	2.35a	3.35a	3.72s	3.62a	3.57s	3.50s	3.28s	2.94s	2.52s			
		1.0	1.28g	1.10g	1.02g	1.44g	2.39g	3.36g	3.80a	3.78s	3.78s	3.76s	3.63s	3.38s	3.05s			

g - Groeneveld

a - approximation

s - Sergeev

TABLE V.I. (CONT.)

P MPa	G kg/m ² s	q MW/m ²	X											
			1.1	1.2	1.3	1.4	1.5	1.6	1.7	1.8	1.9	2.0	2.1	2.2
3.0	250	0.2	0.77a	0.65s	0.43s	0.32s	0.26s	0.21s	0.18s	0.16a	0.14a	0.13a	0.12a	0.11a
		0.6	0.78g	0.75g	0.75a	0.75a	0.63a	0.54a	0.48a	0.42a	0.38a	0.34a	0.32a	
		1.0	1.06g	1.06g	1.06a	1.06a	1.06a	0.90a	0.79a	0.70a	0.63a	0.57a	0.52a	
3.0	500	0.2	0.56s	0.39s	0.30s	0.25s	0.21s	0.18s	0.16s	0.15s	0.14a	0.12a	0.11a	0.11a
		0.6	1.32a	1.12s	0.85s	0.69s	0.58a	0.50a	0.45a	0.40a	0.37a	0.34a	0.31a	0.29a
		1.0	1.58g	1.53g	1.39a	1.13a	0.95a	0.82a	0.72a	0.65a	0.59a	0.54a	0.50a	0.47a
3.0	750	0.2	0.39s	0.32s	0.28s	0.25s	0.22s	0.20s	0.18s	0.16s	0.14s	0.13a	0.12a	0.11a
		0.6	0.97s	0.78s	0.66s	0.58s	0.52a	0.47a	0.43a	0.40a	0.37a	0.35a	0.32a	0.30a
		1.0	1.55s	1.22a	1.02a	0.88a	0.79a	0.71a	0.65a	0.60a	0.56a	0.53a	0.50a	0.47a
3.0	1000	0.2	0.41s	0.36s	0.32s	0.28s	0.24s	0.21s	0.19s	0.16s	0.15s	0.13a	0.12a	0.11a
		0.6	0.83s	0.73s	0.66s	0.60s	0.55s	0.51s	0.47a	0.43a	0.40a	0.37a	0.34a	0.32a
		1.0	1.21s	1.05a	0.94a	0.86a	0.79a	0.74a	0.69a	0.64a	0.61a	0.57a	0.53a	0.50a
3.0	1500	0.2	0.59s	0.49s	0.39s	0.32s	0.26s	0.22s	0.19s	0.16s	0.14s	0.13a	0.12a	0.11a
		0.6	1.00s	0.92s	0.84s	0.75s	0.67s	0.60s	0.53s	0.48s	0.43a	0.39a	0.35a	0.32a
		1.0	1.29s	1.21s	1.13s	1.05s	0.97s	0.89s	0.82a	0.75a	0.69a	0.63a	0.58a	0.53a
3.0	2000	0.2	0.78s	0.59s	0.44s	0.34s	0.27s	0.22s	0.19s	0.16s	0.15s	0.13a	0.12a	0.11a
		0.6	1.37s	1.20s	1.04s	0.89s	0.76s	0.65s	0.56s	0.49s	0.44s	0.39a	0.36a	0.32a
		1.0	1.71s	1.58s	1.44s	1.29s	1.15s	1.02s	0.91s	0.81s	0.72a	0.65a	0.59a	0.54a
3.0	3000	0.2	1.08s	0.70s	0.47s	0.34s	0.27s	0.22s	0.19s	0.16s	0.15s	0.13a	0.12a	0.11a
		0.6	2.07s	1.64s	1.28s	1.00s	0.81s	0.67s	0.57s	0.49s	0.44s	0.39a	0.36a	0.32a
		1.0	2.67s	2.27s	1.90s	1.57s	1.31s	1.10s	0.94s	0.82s	0.73a	0.65a	0.59a	0.54a

g - Groeneveld

a - approximation

s - Sergeev

TABLE V.I. (CONT.)

P MPa	G kg/m ² s	q MW/m ²	X															
			-0.2	-0.1	0.0	0.1	0.2	0.3	0.4	0.5	0.6	0.7	0.8	0.9	1.0			
4	250	0.2	1.08g	0.85a	0.63g	0.50g	0.36g	0.40g	0.44g	0.47g	0.49g	0.62g	0.76g	0.78a	0.80a			
		0.6	1.22g	0.89g	0.75g	0.68g	0.59g	0.60g	0.61g	0.63g	0.64g	0.71g	0.78g	0.82g	0.85g			
		1.0	1.42g	1.20g	0.92g	0.88g	0.84g	0.85g	0.85g	0.87g	0.88g	0.91g	1.00g	1.07g	1.08g			
4	500	0.2	1.10g	0.96g	0.65g	0.53g	0.50g	0.58g	0.66g	0.77g	0.89g	0.95a	1.00a	1.30a	1.47s			
		0.6	1.22g	0.99g	0.82g	0.73g	0.72g	0.79g	0.86g	0.91g	0.96g	1.07g	1.17g	1.36g	1.55g			
		1.0	1.46g	1.22g	1.01g	0.93g	0.92g	0.96g	1.01g	1.06g	1.12g	1.14g	1.20a	1.38g	1.59g			
4	750	0.2	1.20g	0.99g	0.68g	0.61g	0.66g	0.76g	0.87g	1.07g	1.28g	1.31a	1.35g	1.17s	0.66s			
		0.6	1.22g	0.99g	0.82g	0.75g	0.84g	1.07g	1.30g	1.31g	1.32g	1.51g	1.60a	1.71a	1.73s			
		1.0	1.46g	1.22g	1.02g	0.99g	1.01g	1.17g	1.34g	1.37g	1.41g	1.53g	1.65g	1.95g	1.93a			
4	1000	0.2	1.30g	1.02g	0.70g	0.70g	0.82g	0.95g	1.08g	1.38g	1.50a	1.33a	1.18s	0.76s	0.60s			
		0.6	1.22g	0.99g	0.82g	0.78g	0.96g	1.34g	1.60a	1.62a	1.68g	1.95g	1.81a	1.68s	1.23s			
		1.0	1.46g	1.22g	1.03g	1.05g	1.11g	1.39g	1.67g	1.68g	1.70g	1.92g	2.14g	2.00a	1.85s			
4	1500	0.2	1.30g	1.03g	0.84g	0.90g	1.27g	1.71g	2.00a	2.15a	2.14s	1.34s	1.17s	1.03s	0.89s			
		0.6	1.22g	0.99g	0.90g	0.88g	1.32g	1.74a	2.10a	2.30a	2.53a	2.28s	1.74s	1.51s	1.37s			
		1.0	1.46g	1.22g	1.04g	1.05g	1.36g	1.77g	2.19g	2.49g	2.78g	3.26s	2.32s	1.94s	1.74s			
4	2000	0.2	1.30g	1.03g	0.84g	1.00a	1.45a	2.10a	2.72a	2.66s	2.12s	2.01s	1.83s	1.57s	1.27s			
		0.6	1.22g	0.99g	0.90g	1.03g	1.50a	2.15a	2.80a	3.09a	2.80s	2.44s	2.28s	2.11s	1.91s			
		1.0	1.46g	1.22g	1.04g	1.12g	1.54g	2.19g	2.83g	3.34g	3.59s	2.88s	2.63s	2.46s	2.29s			
4	3000	0.2	1.30g	1.03g	0.84g	1.40a	2.35a	3.30a	4.19s	4.40s	4.37s	4.08s	3.55s	2.84s	2.04s			
		0.6	1.22g	1.00g	0.90g	1.45a	2.40a	3.40a	4.35a	4.74s	4.80s	4.67s	4.33s	3.81s	3.19s			
		1.0	1.46g	1.22g	1.07g	1.50g	2.46g	3.45g	4.45g	5.08s	5.04s	4.98s	4.75s	4.36s	3.85s			

g - Groeneveld

a - approximation

s - Sergeev

TABLE V.I. (CONT.)

P MPa	G kg/m ² s	q MW/m ²	x															
			1.1	1.2	1.3	1.4	1.5	1.6	1.7	1.8	1.9	2.0	2.1	2.2				
4	250	0.2	0.78a	0.76s	0.49s	0.36s	0.28s	0.23s	0.20s	0.17s	0.15a	0.14a	0.12a	0.11a				
		0.6	0.88a	0.88a	0.94a	1.07a	0.84a	0.70a	0.59a	0.52a	0.46a	0.41a	0.37a	0.34a				
		1.0	1.09g	1.32a	1.55a	1.78a	1.40a	1.16a	0.99a	0.86a	0.76a	0.68a	0.62a	0.57a				
4	500	0.2	0.71s	0.47s	0.35s	0.28s	0.24s	0.21s	0.18s	0.16s	0.15a	0.14a	0.12a	0.11a				
		0.6	1.44g	1.35s	1.00s	0.79s	0.66s	0.57a	0.50a	0.45a	0.41a	0.37a	0.34a	0.32a				
		1.0	1.56g	1.52g	1.41a	1.30a	1.08a	0.93a	0.81a	0.73a	0.66a	0.60a	0.55a	0.51a				
4	750	0.2	0.48s	0.39s	0.33s	0.28s	0.25s	0.22s	0.19s	0.17s	0.15s	0.14a	0.13a	0.12a				
		0.6	1.20s	0.93s	0.77s	0.67s	0.60s	0.54a	0.49a	0.45a	0.41a	0.38a	0.36a	0.33a				
		1.0	1.91s	1.46s	1.20a	1.03a	0.91a	0.82a	0.74a	0.69a	0.64a	0.60a	0.56a	0.52a				
4	1000	0.2	0.51s	0.44s	0.37s	0.32s	0.27s	0.23s	0.20s	0.18s	0.16s	0.14a	0.13a	0.12a				
		0.6	1.01s	0.87s	0.78s	0.70s	0.64s	0.58s	0.53s	0.48a	0.44a	0.41a	0.37a	0.34a				
		1.0	1.47s	1.26s	1.11a	1.00a	0.92a	0.85a	0.79a	0.73a	0.68a	0.63a	0.59a	0.55a				
4	1500	0.2	0.73s	0.59s	0.46s	0.36s	0.29s	0.24s	0.20s	0.18s	0.16s	0.14s	0.13a	0.12a				
		0.6	1.24s	1.12s	1.00s	0.88s	0.77s	0.68s	0.59s	0.52s	0.47s	0.42a	0.38a	0.35a				
		1.0	1.59s	1.47s	1.35s	1.24s	1.13s	1.02s	0.93s	0.84a	0.76a	0.69a	0.63a	0.58a				
4	2000	0.2	0.96s	0.70s	0.50s	0.37s	0.29s	0.24s	0.20s	0.18s	0.16s	0.14s	0.13s	0.12s				
		0.6	1.68s	1.44s	1.22s	1.01s	0.85s	0.71s	0.61s	0.53s	0.47s	0.42a	0.38a	0.35a				
		1.0	2.11s	1.91s	1.70s	1.49s	1.30s	1.14s	0.99s	0.88s	0.78a	0.70a	0.63a	0.58a				
4	3000	0.2	1.31s	0.80s	0.52s	0.38s	0.29s	0.24s	0.20s	0.18s	0.16s	0.14s	0.13s	0.12a				
		0.6	2.54s	1.94s	1.46s	1.11s	0.88s	0.72s	0.61s	0.53s	0.47s	0.42a	0.38a	0.35a				
		1.0	3.28s	2.71s	2.20s	1.77s	1.44s	1.20s	1.02s	0.89s	0.78s	0.70a	0.64a	0.58a				

g - Groeneveld

a - approximation

s - Sergeev

TABLE V.I. (CONT.)

P MPa	G kg/m ² s	q MW/m ²	x															
			-0.2	-0.1	0.0	0.1	0.2	0.3	0.4	0.5	0.6	0.7	0.8	0.9	1.0			
6	250	0.2	1.56g	1.15g	0.77g	0.71g	0.48g	0.50g	0.53g	0.55g	0.58g	0.70g	0.82g	1.03g	1.05a			
		0.6	1.35g	1.10g	0.88g	0.79g	0.66g	0.67g	0.68g	0.69g	0.70g	0.78g	0.87a	0.94g	1.01g			
		1.0	1.53g	1.29g	1.01g	0.96g	0.90g	0.90g	0.90g	0.91g	0.91g	0.93g	0.97a	1.02g	1.12g			
6	500	0.2	1.57g	1.13a	0.81g	0.72g	0.64g	0.71g	0.78g	0.87g	0.96g	1.20g	1.42g	1.84g	1.42a			
		0.6	1.47g	1.26g	0.98g	0.85g	0.82g	0.83a	0.85g	1.02g	1.10g	1.17g	1.24g	1.47g	1.69g			
		1.0	1.55g	1.39g	1.14g	1.04g	1.01g	1.05g	1.09g	1.14g	1.19g	1.25a	1.30a	1.36g	1.40a			
6	750	0.2	1.62g	1.21g	0.85g	0.78g	0.80g	0.81g	1.02a	1.23g	1.45g	1.72g	2.00g	1.50a	1.00s			
		0.6	1.48g	1.27g	1.03g	0.91g	0.95g	1.17g	1.39g	1.46g	1.54g	1.69g	1.84g	2.15g	1.91a			
		1.0	1.56g	1.40g	1.18g	1.12g	1.12g	1.28g	1.44g	1.49g	1.55g	1.60g	1.66g	1.97g	2.28g			
6	1000	0.2	1.66g	1.25g	0.89g	0.85g	0.96g	1.11g	1.28g	1.60g	1.93g	2.00a	2.06s	1.15s	0.86s			
		0.6	1.49g	1.28g	1.07g	0.97g	1.08g	1.45g	1.83g	1.90g	1.98g	2.20g	2.43g	2.40a	1.73s			
		1.0	1.58g	1.42g	1.22g	1.20g	1.22g	1.50g	1.78g	1.85g	1.91g	2.06g	2.20g	2.58g	2.58s			
6	1500	0.2	1.66g	1.25g	0.95g	0.99g	1.51g	2.00g	2.49g	3.22g	2.68g	2.15s	1.80s	1.56s	1.31s			
		0.6	1.49g	1.28g	1.10g	1.02g	1.44g	2.02g	2.59g	2.89g	3.20g	3.30a	2.60s	2.19s	1.94s			
		1.0	1.58g	1.42g	1.22g	1.20g	1.49g	1.90g	2.32g	2.82g	2.93g	3.36g	3.43s	2.76s	2.41s			
6	2000	0.2	1.66g	1.25g	0.95g	1.21g	2.32g	3.22g	4.00a	3.75a	3.38s	3.17s	2.85s	2.41s	1.89s			
		0.6	1.49g	1.28g	1.10g	1.15g	2.01g	2.76g	3.52g	4.07g	4.12a	3.74s	3.43s	3.13s	2.77s			
		1.0	1.58g	1.42g	1.22g	1.25g	1.74g	2.38g	3.03g	3.59g	4.14g	4.33s	3.86s	3.56s	3.26s			
6	3000	0.2	1.66g	1.25g	0.98g	2.04g	4.16g	5.88g	6.84s	7.00s	6.94s	6.45s	5.59s	4.41s	3.09s			
		0.6	1.49g	1.28g	1.10g	1.77g	3.31g	4.51g	5.70g	6.93g	7.60s	7.33s	6.72s	5.81s	4.73s			
		1.0	1.58g	1.42g	1.25g	1.75g	2.71g	3.77g	4.82g	6.00g	7.17g	7.70s	7.26s	6.54s	5.64s			

g - Groeneveld

a - approximation

s - Sergeev

TABLE V.I. (CONT.)

P MPa	G kg/m ² s	q MW/m ²	x															
			1.1	1.2	1.3	1.4	1.5	1.6	1.7	1.8	1.9	2.0	2.1	2.2				
6	250	0.2	1.07g	0.94g	0.62s	0.44s	0.34s	0.28s	0.24s	0.20s	0.18s	0.16a	0.14a	0.13a				
		0.6	1.03a	1.08a	1.14a	1.08a	1.03a	0.83a	0.70a	0.61a	0.53a	0.48a	0.43a	0.39a				
		1.0	1.13g	1.14g	1.15a	1.15a	1.16a	1.16a	1.17a	1.01a	0.89a	0.79a	0.72a	0.65a				
6	500	0.2	1.00s	0.62s	0.45s	0.36s	0.29s	0.25s	0.22s	0.19s	0.17s	0.16s	0.14a	0.13a				
		0.6	1.54g	1.42g	1.27s	0.99s	0.81s	0.69s	0.60a	0.54a	0.48a	0.44a	0.41a	0.37a				
		1.0	1.47a	1.55g	1.57a	1.62a	1.33a	1.12a	0.98a	0.87a	0.78a	0.71a	0.65a	0.60a				
6	750	0.2	0.68s	0.52s	0.43s	0.36s	0.31s	0.27s	0.23s	0.20s	0.18s	0.16s	0.15a	0.13a				
		0.6	1.68s	1.25s	1.01s	0.86s	0.75s	0.67s	0.60s	0.55s	0.50a	0.46a	0.42a	0.39a				
		1.0	2.06g	1.87g	1.56s	1.31a	1.14a	1.02a	0.92a	0.84a	0.77a	0.72a	0.66a	0.62a				
6	1000	0.2	0.70s	0.59s	0.49s	0.40s	0.33s	0.28s	0.24s	0.21s	0.18s	0.16s	0.15a	0.13a				
		0.6	1.37s	1.16s	1.01s	0.90s	0.80s	0.72s	0.64s	0.58s	0.52s	0.47a	0.43a	0.40a				
		1.0	1.99s	1.65s	1.44s	1.28s	1.16s	1.06s	0.97a	0.89a	0.82a	0.76a	0.70a	0.65a				
6	1500	0.2	1.04s	0.80s	0.60s	0.45s	0.35s	0.29s	0.24s	0.21s	0.18s	0.16s	0.15s	0.13a				
		0.6	1.72s	1.51s	1.31s	1.13s	0.96s	0.82s	0.71s	0.61s	0.54s	0.49s	0.44a	0.40a				
		1.0	2.17s	1.97s	1.78s	1.59s	1.42s	1.27s	1.12s	1.00s	0.89s	0.80a	0.73a	0.66a				
6	2000	0.2	1.37s	0.94s	0.64s	0.46s	0.35s	0.29s	0.24s	0.21s	0.18s	0.16s	0.15s	0.13a				
		0.6	2.36s	1.96s	1.59s	1.28s	1.03s	0.85s	0.72s	0.62s	0.55s	0.49s	0.44a	0.40a				
		1.0	2.93s	2.58s	2.23s	1.91s	1.62s	1.38s	1.18s	1.03s	0.91s	0.81a	0.73a	0.67a				
6	3000	0.2	1.88s	1.07s	0.66s	0.46s	0.35s	0.29s	0.24s	0.21s	0.18s	0.16s	0.15s	0.13a				
		0.6	3.62s	2.63s	1.88s	1.38s	1.06s	0.86s	0.72s	0.62s	0.55s	0.49s	0.44a	0.40s				
		1.0	4.65s	3.69s	2.86s	2.22s	1.75s	1.43s	1.20s	1.03s	0.91s	0.81s	0.73a	0.67a				

g - Groeneveld

a - approximation

s - Sergeev

TABLE V.I. (CONT.)

P MPa	G kg/m ² s	q MW/m ²	x																
			-0.2	-0.1	0.0	0.1	0.2	0.3	0.4	0.5	0.6	0.7	0.8	0.9	1.0				
8	250	0.2	2.36g	1.54g	0.89g	0.75a	0.59g	0.60g	0.61g	0.64g	0.66g	0.73g	0.80g	0.84a	0.88a				
		0.6	1.64g	1.23g	0.98g	0.88g	0.73g	0.73g	0.73g	0.73a	0.75a	0.77g	0.83g	0.93g	1.95g				
		1.0	1.61g	1.33g	1.08g	1.02g	0.98a	0.95g	0.95g	0.94g	0.93g	0.93g	0.92g	1.01g	1.11g				
8	500	0.2	2.36g	1.54g	0.98g	0.89g	0.78g	0.84g	0.91g	0.95g	1.00g	1.10a	1.20a	1.30a	1.35a				
		0.6	1.77g	1.47g	1.17g	1.10a	0.93g	0.96g	0.99g	1.02g	1.04g	1.10g	1.16g	1.32a	1.45a				
		1.0	1.63g	1.48g	1.30g	1.16g	1.11g	1.14g	1.16g	1.18g	1.19g	1.25a	1.30a	1.36g	1.55a				
8	750	0.2	2.36g	1.56g	1.01g	0.94g	0.98g	1.09g	1.22g	1.42g	1.52a	1.62a	1.72a	1.80a	1.43s				
		0.6	1.78g	1.47g	1.24g	1.09g	1.07g	1.21g	1.36g	1.44g	1.52g	1.67g	1.82g	2.17g	2.30a				
		1.0	1.64g	1.52g	1.34g	1.21g	1.19g	1.34g	1.49g	1.55g	1.62g	1.66g	1.71g	2.06g	2.41g				
8	1000	0.2	2.36g	1.58g	1.03g	0.98g	1.14g	1.33g	1.52g	1.90g	2.00a	2.30a	2.25a	1.71s	1.26s				
		0.6	1.79g	1.51g	1.32g	1.18g	1.21g	1.47g	1.72g	1.86g	2.00g	2.24g	2.48g	2.46a	2.43s				
		1.0	1.66g	1.57g	1.38g	1.28g	1.29g	1.54g	1.78g	1.92g	2.05g	2.18g	2.31g	2.76g	2.72a				
8	1500	0.2	2.36g	1.58g	1.03g	1.19g	1.74g	2.09g	2.44g	3.00a	3.30a	3.32s	2.78s	2.38s	1.95s				
		0.6	1.79g	1.51g	1.32g	1.18g	1.50g	1.96g	2.42g	2.81g	3.20g	3.84g	3.89s	3.26s	2.85s				
		1.0	1.66g	1.57g	1.38g	1.31g	1.54g	1.95g	2.36g	2.78g	3.20g	3.62g	4.03g	3.99s	3.46s				
8	2000	0.2	2.36g	1.58g	1.03g	1.49g	2.53g	3.34g	4.14g	5.60a	5.24s	4.90s	4.38s	3.65s	2.80s				
		0.6	1.79g	1.51g	1.32g	1.36g	2.08g	2.72g	3.36g	4.28g	5.20g	5.81s	5.33s	4.79s	4.14s				
		1.0	1.66g	1.57g	1.38g	1.46g	1.94g	2.57g	3.20g	3.92g	4.64g	5.72g	5.90s	5.40s	4.85s				
8	3000	0.2	2.36g	1.58g	1.13g	2.33g	4.33g	5.92g	7.50g	10.3g	10.5s	9.73s	8.40s	6.59s	4.50s				
		0.6	1.79g	1.51g	1.32g	1.99g	3.24g	4.47g	5.69g	7.41g	9.13g	10.9g	10.4s	8.85s	7.02s				
		1.0	1.66g	1.57g	1.40g	2.04g	2.87g	4.14g	5.32g	6.65g	7.98g	9.05g	11.0g	10.0s	8.43s				

g - Groeneveld

a - approximation

s - Sergeev

TABLE V.I. (CONT.)

P MPa	G kg/m ² s	q MW/m ²	x															
			1.1	1.2	1.3	1.4	1.5	1.6	1.7	1.8	1.9	2.0	2.1	2.2				
8	250	0.2	0.92a	0.97g	0.78s	0.54s	0.41s	0.33s	0.28s	0.24s	0.21s	0.18s	0.17a	0.15a				
		0.6	1.00g	1.10a	1.30a	1.63a	1.23a	0.99a	0.83a	0.71a	0.62a	0.55a	0.50a	0.45a				
		1.0	1.15g	1.18g	1.94a	2.71a	2.05a	1.65a	1.37a	1.18a	1.03a	0.92a	0.83a	0.75a				
8	500	0.2	1.44s	0.84s	0.59s	0.45s	0.37s	0.31s	0.27s	0.23s	0.21s	0.18s	0.17s	0.15a				
		0.6	1.48g	1.35g	1.30a	1.25s	1.01s	0.85s	0.73s	0.65a	0.58a	0.52a	0.48a	0.44a				
		1.0	1.63g	1.64g	1.84a	2.04a	1.64a	1.37a	1.18a	1.04a	0.93a	0.84a	0.77a	0.71a				
8	750	0.2	0.94s	0.71s	0.57s	0.47s	0.39s	0.32s	0.28s	0.24s	0.21s	0.19s	0.17s	0.15s				
		0.6	2.26s	1.64s	1.30s	1.09s	0.94s	0.83s	0.74s	0.66s	0.60s	0.54a	0.49a	0.45a				
		1.0	2.24g	2.10g	1.99s	1.65s	1.42s	1.26a	1.13a	1.02a	0.93a	0.86a	0.79a	0.73a				
8	1000	0.2	1.01s	0.81s	0.65s	0.51s	0.41s	0.34s	0.28s	0.24s	0.21s	0.19s	0.17s	0.15s				
		0.6	1.88s	1.57s	1.34s	1.17s	1.02s	0.90s	0.79s	0.70s	0.62s	0.56s	0.50a	0.46a				
		1.0	2.68s	2.20s	1.89s	1.67s	1.49s	1.34s	1.21s	1.09s	0.99a	0.90a	0.82a	0.75a				
8	1500	0.2	1.50s	1.09s	0.77s	0.56s	0.42s	0.34s	0.28s	0.24s	0.21s	0.19s	0.17s	0.15s				
		0.6	2.47s	2.11s	1.76s	1.45s	1.20s	0.99s	0.84s	0.72s	0.63s	0.56s	0.50s	0.46a				
		1.0	3.08s	2.73s	2.40s	2.09s	1.81s	1.57s	1.36s	1.19s	1.04s	0.93s	0.84a	0.76a				
8	2000	0.2	1.95s	1.26s	0.81s	0.56s	0.42s	0.34s	0.28s	0.24s	0.21s	0.19s	0.17s	0.15s				
		0.6	3.42s	2.72s	2.10s	1.61s	1.26s	1.01s	0.84s	0.72s	0.63s	0.56s	0.50s	0.46a				
		1.0	4.24s	3.61s	3.00s	2.46s	2.01s	1.66s	1.40s	1.20s	1.05s	0.93s	0.84a	0.76a				
8	3000	0.2	2.60s	1.39s	0.82s	0.57s	0.43s	0.34s	0.28s	0.24s	0.21s	0.19s	0.17s	0.15s				
		0.6	5.16s	3.55s	2.40s	1.69s	1.27s	1.02s	0.84s	0.72s	0.63s	0.56s	0.50s	0.46s				
		1.0	6.70s	5.07s	3.73s	2.76s	2.12s	1.69s	1.41s	1.20s	1.05s	0.93s	0.84s	0.76s				

g - Groeneveld

a - approximation

s - Sergeev

TABLE V.I. (CONT.)

P MPa	G kg/m ² s	q MW/m ²	x															
			-0.2	-0.1	0.0	0.1	0.2	0.3	0.4	0.5	0.6	0.7	0.8	0.9	1.0			
10	250	0.2	3.16g	2.02g	0.86g	0.77g	0.46g	0.48g	0.50g	0.54g	0.58g	0.67g	0.75g	0.85g	0.90a			
		0.6	2.39g	1.54g	0.93g	0.82g	0.59g	0.60g	0.61g	0.61g	0.62g	0.66g	0.71g	0.83g	0.95g			
		1.0	2.06g	1.57g	1.07g	1.00g	0.88g	0.89g	0.90g	0.91g	0.93g	0.96g	0.99g	1.08g	1.17g			
10	500	0.2	3.16g	2.02g	1.08g	0.87g	0.77g	0.82g	0.86g	0.89g	0.89a	0.89a	0.90a	1.10a	1.20a			
		0.6	2.39g	1.58g	1.29g	1.03g	0.88g	0.89g	0.90g	0.87g	0.88a	0.89g	0.95g	1.12g	1.29g			
		1.0	2.06g	1.58g	1.36g	1.19g	1.08g	1.11g	1.14g	1.14g	1.16a	1.21g	1.29g	1.49g	1.69g			
10	750	0.2	3.16g	2.02g	1.08g	0.98g	1.10g	1.20g	1.30g	1.42g	1.55g	1.70a	1.80a	1.90a	1.83s			
		0.6	2.39g	1.60g	1.33g	1.14g	1.10g	1.18g	1.26g	1.33g	1.40g	1.54g	1.68g	1.94g	2.20g			
		1.0	2.06g	1.63g	1.41g	1.21g	1.18g	1.28g	1.38g	1.49g	1.60g	1.78g	1.96g	2.19g	2.43g			
10	1000	0.2	3.16g	2.02g	1.08g	1.10g	1.42g	1.58g	1.74g	1.95g	2.16g	2.30a	2.50a	2.42s	1.83s			
		0.6	2.39g	1.61g	1.38g	1.26g	1.32g	1.47g	1.62g	1.80g	1.98g	2.20g	2.42g	2.77g	3.12g			
		1.0	2.06g	1.68g	1.47g	1.23g	1.29g	1.46g	1.63g	1.85g	2.07g	2.35g	2.62g	2.89g	3.16g			
10	1500	0.2	3.16g	2.02g	1.08g	1.53g	2.02g	2.23g	2.44g	2.85a	3.30a	4.00a	4.17s	3.58s	2.88s			
		0.6	2.39g	1.61g	1.38g	1.33g	1.63g	2.06g	2.48g	2.90g	3.31g	4.10g	4.90g	4.87s	4.25s			
		1.0	2.06g	1.68g	1.47g	1.41g	1.64g	1.99g	2.34g	2.81g	3.28g	3.87g	4.45g	5.54g	5.08s			
10	2000	0.2	3.16g	2.02g	1.10g	1.90g	2.76g	3.48g	4.20g	6.45g	7.73s	7.27s	6.48s	5.38s	4.07s			
		0.6	2.39g	1.61g	1.38g	1.62g	2.22g	2.78g	3.34g	4.40g	5.46g	7.43g	8.18s	7.30s	6.19s			
		1.0	2.06g	1.68g	1.47g	1.69g	2.00g	2.62g	3.23g	4.15g	5.07g	6.39g	7.70g	8.27s	7.32s			
10	3000	0.2	3.16g	2.02g	1.26g	2.89g	4.56g	5.77g	6.99g	11.0g	15.0s	13.9s	12.0s	8.46s	6.43s			
		0.6	2.39g	1.61g	1.38g	2.40g	3.39g	4.63g	5.86g	8.43g	11.0g	14.0g	15.6s	13.2s	10.3s			
		1.0	2.06g	1.68g	1.47g	2.26g	2.88g	4.32g	5.76g	7.64g	9.52g	11.7g	14.0g	15.2s	12.6s			

g - Groeneveld

a - approximation

s - Sergeev

TABLE V.I. (CONT.)

P MPa	G kg/m ² s	q MW/m ²	X															
			1.1	1.2	1.3	1.4	1.5	1.6	1.7	1.8	1.9	2.0	2.1	2.2				
10	250	0.2	0.85a	0.82a	0.80a	0.68s	0.51s	0.40s	0.33s	0.28s	0.24s	0.22s	0.19s	0.18s				
		0.6	0.90g	0.86g	0.86a	0.86a	0.86a	0.86a	0.86a	0.84a	0.73a	0.64a	0.58a	0.52a				
		1.0	1.17g	1.18g	1.18a	1.18a	1.18a	1.18a	1.18a	1.18a	1.18a	1.07a	0.96a	0.87a				
10	500	0.2	1.15a	1.02a	0.76s	0.57s	0.46s	0.38s	0.32s	0.27s	0.24s	0.22s	0.19s	0.18s				
		0.6	1.16g	1.04g	1.04a	1.04a	1.04a	1.03s	0.88s	0.78s	0.69s	0.62a	0.56a	0.52a				
		1.0	1.66g	1.64g	1.64a	1.64a	1.64a	1.64a	1.42a	1.24a	1.11a	1.00a	0.91a	0.84a				
10	750	0.2	1.24s	0.94s	0.74s	0.66s	0.48s	0.39s	0.33s	0.28s	0.24s	0.22s	0.19s	0.18s				
		0.6	2.02g	1.86g	1.65s	1.38s	1.18s	1.03s	0.90s	0.80s	0.71s	0.64s	0.57s	0.52a				
		1.0	2.44g	2.45g	2.47s	2.05s	1.76s	1.55s	1.38s	1.24a	1.12a	1.02a	0.93a	0.86a				
10	1000	0.2	1.45s	1.14s	0.88s	0.67s	0.51s	0.41s	0.34s	0.29s	0.25s	0.22s	0.20s	0.18s				
		0.6	2.59s	2.15s	1.82s	1.55s	1.32s	1.13s	0.97s	0.84s	0.74s	0.65s	0.58s	0.53s				
		1.0	3.20g	2.94s	2.51s	2.19s	1.93s	1.70s	1.51s	1.34s	1.20s	1.07s	0.97a	0.88a				
10	1500	0.2	2.16s	1.50s	1.01s	0.71s	0.52s	0.41s	0.34s	0.29s	0.25s	0.22s	0.20s	0.18s				
		0.6	3.62s	3.00s	2.41s	1.91s	1.51s	1.22s	1.01s	0.86s	0.74s	0.65s	0.59s	0.53s				
		1.0	4.47s	3.88s	3.32s	2.80s	2.34s	1.96s	1.66s	1.42s	1.23s	1.09s	0.98s	0.88a				
10	2000	0.2	2.76s	1.70s	1.05s	0.71s	0.52s	0.41s	0.34s	0.29s	0.25s	0.22s	0.20s	0.18s				
		0.6	4.99s	3.81s	2.81s	2.07s	1.56s	1.23s	1.01s	0.86s	0.74s	0.65s	0.59s	0.53s				
		1.0	6.24s	5.14s	4.10s	3.22s	2.54s	2.04s	1.68s	1.43s	1.24s	1.09s	0.98s	0.88s				
10	3000	0.2	3.60s	1.83s	1.06s	0.71s	0.52s	0.41s	0.34s	0.29s	0.25s	0.22s	0.20s	0.18s				
		0.6	7.38s	4.85s	3.13s	2.13s	1.57s	1.23s	1.01s	0.86s	0.74s	0.66s	0.59s	0.53s				
		1.0	9.72s	7.06s	4.96s	3.52s	2.62s	2.06s	1.69s	1.43s	1.24s	1.09s	0.98s	0.88s				

g - Groeneveld

a - approximation

s - Sergeev

TABLE V.I. (CONT.)

P MPa	G kg/m ² s	q MW/m ²	x															
			-0.2	-0.1	0.0	0.1	0.2	0.3	0.4	0.5	0.6	0.7	0.8	0.9	1.0			
12	250	0.2	4.37g	2.78g	0.90g	0.80g	0.34g	0.42g	0.49g	0.62a	0.67a	0.70a	0.75a	0.78a	0.75a			
		0.6	3.49g	2.20g	0.88g	0.84g	0.57g	0.59g	0.61g	0.65g	0.68g	0.72g	0.76g	0.80g	0.83g			
		1.0	3.06g	2.11g	1.07g	1.02g	0.86g	0.88g	0.91g	0.93g	0.96g	0.98g	1.00g	1.06g	1.12g			
12	500	0.2	4.37g	2.78g	0.87a	0.83a	0.74g	0.79g	0.84g	1.03g	1.21g	1.44g	1.66g	1.70g	1.73g			
		0.6	3.49g	2.20g	0.90g	0.85g	0.76g	0.79g	0.82g	0.80g	0.77g	0.88g	0.99g	1.17g	1.36g			
		1.0	2.11g	1.07g	1.02g	0.95g	1.02g	1.10g	1.10g	1.10g	1.19g	1.29g	1.48g	1.68g	1.50g			
12	750	0.2	4.37g	2.78g	0.94g	1.06g	1.28g	1.33g	1.37g	1.64g	1.91g	2.23g	2.54g	2.70g	2.58s			
		0.6	3.49g	2.20g	0.93g	0.94g	1.03g	1.07g	1.11g	1.21g	1.32g	1.56g	1.81g	2.16g	2.51g			
		1.0	3.06g	2.11g	1.07g	1.07g	1.18g	1.24g	1.31g	1.42g	1.53g	1.80g	2.07g	2.49g	2.91g			
12	1000	0.2	4.37g	2.78g	0.95g	1.27g	1.83g	1.86g	1.90g	2.26g	2.62g	3.02g	3.42g	3.41s	2.69s			
		0.6	3.49g	2.20g	0.96g	1.04g	1.30g	1.34g	1.39g	1.63g	1.87g	2.25g	2.63g	3.15g	3.67g			
		1.0	3.06g	2.11g	1.08g	1.13g	1.42g	1.47g	1.52g	1.74g	1.96g	2.41g	2.86g	3.50g	4.14g			
12	1500	0.2	4.37g	2.78g	1.04g	2.05g	2.90g	3.30g	3.70g	4.18g	4.65g	5.68g	6.22s	5.35s	4.28s			
		0.6	3.49g	2.20g	1.02g	1.45g	1.79g	2.17g	2.55g	3.19g	3.84g	4.82g	5.81g	7.02g	6.53s			
		1.0	3.06g	2.11g	1.15g	1.42g	1.53g	1.90g	2.28g	3.03g	3.78g	4.73s	5.67g	7.11g	7.77s			
12	2000	0.2	4.37g	2.78g	1.15g	2.90g	3.78g	4.99g	6.20g	7.82g	9.44g	10.5s	9.41s	7.83s	5.91s			
		0.6	3.49g	2.20g	1.12g	1.88g	2.14g	3.06g	3.97g	5.28g	6.58g	8.29g	10.0g	11.2s	9.41s			
		1.0	3.06g	2.11g	1.26g	1.50a	1.71g	2.52g	3.32g	4.93g	6.53g	8.54g	10.5g	12.0g	11.3s			
12	3000	0.2	4.37g	2.78g	1.33g	5.11g	7.12g	8.49g	9.86g	13.6g	17.3g	19.3s	16.8s	13.3s	9.04s			
		0.6	3.49g	2.20g	1.30g	3.27g	4.58g	6.62g	8.67g	11.3g	13.9g	15.8g	17.6g	19.4s	15.1s			
		1.0	3.06g	2.11g	1.45g	2.30a	2.97g	4.98g	6.98g	10.2g	13.4g	16.2g	18.9g	20.2g	18.8s			

g - Groeneveld

a - approximation

s - Sergeev

TABLE V.I. (CONT.)

P MPa	G kg/m ² s	q MW/m ²	X															
			1.1	1.2	1.3	1.4	1.5	1.6	1.7	1.8	1.9	2.0	2.1	2.2				
12	250	0.2	0.73g	0.66g	0.66a	0.66a	0.65s	0.50s	0.41s	0.34s	0.30s	0.26s	0.23s	0.21s				
		0.6	0.80g	0.76g	0.76a	0.76a	0.76a	0.76a	0.76a	0.76a	0.76a	0.76a	0.69a	0.62a				
		1.0	1.12g	1.13g	1.13a	1.13a	1.13a	1.13a	1.13a	1.13a	1.13a	1.13a	1.13a	1.03a				
12	500	0.2	1.40g	1.15g	0.98s	0.74s	0.59s	0.48s	0.40s	0.34s	0.29s	0.26s	0.23s	0.21s				
		0.6	1.16g	0.96g	0.96a	0.96a	0.96a	0.96a	0.96a	0.95s	0.84s	0.75s	0.68s	0.61s				
		1.0	1.45a	1.32a	1.32a	1.32a	1.32a	1.32a	1.32a	1.32a	1.32a	1.20a	1.09a	1.00a				
12	750	0.2	1.80s	1.37s	1.06s	0.83s	0.64s	0.51s	0.42s	0.35s	0.30s	0.26s	0.23s	0.21s				
		0.6	2.18g	1.90g	1.90a	1.88s	1.59s	1.35s	1.16s	1.01s	0.88s	0.78s	0.70s	0.63s				
		1.0	2.68g	2.48g	2.43a	2.38a	2.34s	2.03s	1.79s	1.58s	1.41s	1.27a	1.14a	1.04a				
12	1000	0.2	2.14s	1.64s	1.22s	0.89s	0.66s	0.51s	0.42s	0.35s	0.30s	0.26s	0.23s	0.21s				
		0.6	3.15g	2.73g	2.57s	2.14s	1.77s	1.46s	1.22s	1.04s	0.89s	0.78s	0.70s	0.63s				
		1.0	3.73g	3.38g	3.19a	3.01s	2.59s	2.24s	1.93s	1.68s	1.47s	1.30s	1.16s	1.04a				
12	1500	0.2	3.15s	2.13s	1.38s	0.93s	0.67s	0.52s	0.42s	0.35s	0.30s	0.26s	0.23s	0.21s				
		0.6	5.48s	4.41s	3.42s	2.59s	1.98s	1.55s	1.25s	1.05s	0.90s	0.79s	0.70s	0.63s				
		1.0	6.78s	5.76s	4.78s	3.88s	3.12s	2.52s	2.07s	1.74s	1.50s	1.31s	1.16s	1.05s				
12	2000	0.2	3.94s	2.35s	1.41s	0.93s	0.67s	0.52s	0.42s	0.35s	0.30s	0.26s	0.23s	0.21s				
		0.6	7.43s	5.51s	3.90s	2.75s	2.01s	1.55s	1.25s	1.05s	0.90s	0.79s	0.70s	0.63s				
		1.0	9.46s	7.56s	5.80s	4.37s	3.31s	2.58s	2.09s	1.75s	1.50s	1.31s	1.16s	1.05s				
12	3000	0.2	4.99s	2.48s	1.42s	0.93s	0.67s	0.52s	0.42s	0.35s	0.30s	0.26s	0.23s	0.21s				
		0.6	10.6s	6.78s	4.21s	2.79s	2.02s	1.56s	1.26s	1.05s	0.90s	0.79s	0.70s	0.63s				
		1.0	14.3s	10.1s	6.78s	4.64s	3.36s	2.59s	2.09s	1.75s	1.50s	1.31s	1.16s	1.05s				

g - Groeneveld

a - approximation

s - Sergeev

TABLE V.I. (CONT.)

P MPa	G kg/m ² s	q MW/m ²	x																
			-0.2	-0.1	0.0	0.1	0.2	0.3	0.4	0.5	0.6	0.7	0.8	0.9	1.0				
14	250	0.2	3.53g	3.56g	1.13g	0.94g	0.42g	0.49g	0.56g	0.78g	1.00g	1.03g	1.05g	0.98g	0.90g				
		0.6	4.31g	2.68g	0.91g	0.89g	0.60g	0.61g	0.62g	0.70g	0.76g	0.83g	0.88g	0.91g	0.94g				
		1.0	3.47g	2.39g	1.21g	1.11g	0.88g	0.90g	0.93g	0.97g	1.01g	1.04g	1.07g	1.12g	1.18g				
14	500	0.2	5.53g	3.56g	1.13g	0.97g	0.87g	0.98g	1.08g	1.30g	1.53g	1.50e	1.40e	1.30e	1.30e				
		0.6	4.31g	2.68g	0.92g	0.90g	0.79g	0.80g	0.81g	0.88g	0.95g	1.12g	1.28g	1.50g	1.73g				
		1.0	3.47g	2.39g	1.21g	1.11g	0.99g	1.07g	1.15g	1.17g	1.19g	1.32g	1.45g	1.64g	1.83g				
14	750	0.2	5.53g	3.56g	1.13g	1.32g	1.45g	1.61g	1.76g	2.06g	2.35g	2.65g	2.95g	3.07g	3.20g				
		0.6	4.31g	2.68g	0.95g	1.04g	1.01g	1.05g	1.09g	1.31g	1.53g	1.89g	2.25g	2.69g	3.13g				
		1.0	3.47g	2.39g	1.21g	1.19g	1.26g	1.31g	1.36g	1.56g	1.75g	2.07g	2.39g	2.89g	3.39g				
14	1000	0.2	5.53a	3.56g	1.13g	1.66g	2.04g	2.24g	2.44g	2.81g	3.17g	3.57g	3.98g	4.21g	4.07s				
		0.6	4.31g	2.68g	0.99g	1.17g	1.22g	1.30g	1.37g	1.74g	2.10g	2.66g	3.22g	3.86g	4.54g				
		1.0	3.47g	2.39g	1.21g	1.27g	1.52g	1.55g	1.57g	1.94g	2.30g	2.82g	3.34g	4.14g	4.94g				
14	1500	0.2	5.53g	3.56g	1.22g	2.93g	3.74g	4.17g	4.60g	5.12g	5.64g	6.44g	7.24g	7.81s	6.28s				
		0.6	4.31g	2.68g	1.10g	1.79g	2.05g	2.48g	2.92g	3.77g	4.63g	5.88g	7.14g	8.33g	9.93g				
		1.0	3.47g	2.39g	1.26g	1.78g	1.92g	2.03g	2.69g	3.77g	4.86g	6.25g	7.64g	9.17g	10.7g				
14	2000	0.2	5.53g	3.56g	1.31g	4.23g	5.36g	6.52g	7.67g	9.20g	10.7g	12.8g	13.2s	11.1s	8.41s				
		0.6	4.31g	2.68g	1.23g	2.49g	2.74g	3.93g	5.12g	6.71g	8.29g	10.1g	11.9g	14.5g	14.2s				
		1.0	3.47g	2.39g	1.35g	2.00a	2.26g	3.28g	4.30g	6.40g	8.49g	10.9g	13.4g	15.0g	16.7g				
14	3000	0.2	5.53g	3.56g	1.54g	6.91g	9.29g	11.0g	12.7g	16.1g	19.5g	22.0g	22.5s	18.0s	12.4s				
		0.6	4.31g	2.68g	1.45g	4.64g	6.10g	8.60g	11.1g	13.9g	16.6g	18.2g	20.4g	25.0g	21.9s				
		1.0	3.47g	2.39g	1.57g	2.90a	4.25g	6.58g	8.91g	12.7g	16.6g	20.2g	23.9g	25.5g	27.1g				

g - Groeneveld

a - approximation

s - Sergeev

TABLE V.I. (CONT.)

P MPa	G kg/m ² s	q MW/m ²	X															
			1.1	1.2	1.3	1.4	1.5	1.6	1.7	1.8	1.9	2.0	2.1	2.2				
14	250	0.2	0.91e	0.84e	0.81e	0.78e	0.72a	0.66s	0.53s	0.44s	0.37s	0.32s	0.29s	0.26s				
		0.6	0.90g	0.86g	0.86a	0.86a	0.86a	0.86a	0.86g	0.86g	0.86a	0.86a	0.85a	0.76a				
		1.0	1.18g	1.19g	1.19a	1.19a	1.19a	1.19a	1.19a	1.19a	1.19a	1.19a	1.19a	1.19a				
14	500	0.2	1.30e	1.30e	1.20e	1.10e	0.82s	0.66s	0.53s	0.44s	0.38s	0.33s	0.29s	0.26s				
		0.6	1.46g	1.22g	1.22a	1.22a	1.22a	1.22a	1.22a	1.22a	1.08a	0.95a	0.85a	0.76a				
		1.0	1.74g	1.64g	1.64a	1.64a	1.64a	1.64a	1.64a	1.64a	1.64a	1.53a	1.38a	1.25a				
14	750	0.2	2.56g	2.04s	1.56s	1.18s	0.89s	0.68s	0.54s	0.45s	0.38s	0.33s	0.29s	0.26s				
		0.6	2.70g	2.32g	2.32a	2.32a	2.23s	1.85s	1.55s	1.31s	1.12s	0.98s	0.86s	0.77s				
		1.0	3.07g	2.78g	2.78a	2.78a	2.78a	2.78s	2.40s	2.08s	1.82s	1.60s	1.42s	1.28s				
14	1000	0.2	3.26s	2.47s	1.78s	1.25s	0.90s	0.69s	0.54s	0.45s	0.38s	0.33s	0.29s	0.26s				
		0.6	3.88g	3.33g	3.23a	3.12s	2.49s	1.99s	1.61s	1.34s	1.13s	0.98s	0.86s	0.77s				
		1.0	4.36g	3.86g	3.86a	3.86a	3.70s	3.10s	2.60s	2.19s	1.87s	1.63s	1.44s	1.28s				
14	1500	0.2	4.61s	3.06s	1.94s	1.28s	0.91s	0.69s	0.54s	0.45s	0.38s	0.33s	0.29s	0.26s				
		0.6	8.16g	6.67s	5.02s	3.67s	2.70s	2.06s	1.63s	1.34s	1.13s	0.98s	0.86s	0.77s				
		1.0	8.91g	7.52g	7.16s	5.61s	4.34s	3.39s	2.71s	2.23s	1.89s	1.63s	1.44s	1.28s				
14	2000	0.2	5.61s	3.32s	1.96s	1.28s	0.91s	0.69s	0.54s	0.45s	0.38s	0.33s	0.29s	0.26s				
		0.6	11.1s	8.11s	5.58s	3.82s	2.73s	2.06s	1.63s	1.34s	1.13s	0.98s	0.86s	0.77s				
		1.0	12.9g	10.3g	8.49s	6.16s	4.51s	3.43s	2.72s	2.23s	1.89s	1.63s	1.44s	1.28s				
14	3000	0.2	6.91s	3.44s	1.97s	1.28s	0.91s	0.69s	0.54s	0.45s	0.38s	0.33s	0.29s	0.26s				
		0.6	15.4s	9.65s	5.89s	3.85s	2.73s	2.06s	1.63s	1.34s	1.13s	0.98s	0.86s	0.77s				
		1.0	18.8g	13.8g	9.60s	6.40s	4.55s	3.44s	2.72s	2.24s	1.89s	1.63s	1.44s	1.28s				

g - Groeneveld

a - approximation

s - Sergeev

TABLE V.I. (CONT.)

P MPa	G kg/m ² s	q MW/m ²	x															
			-0.2	-0.1	0.0	0.1	0.2	0.3	0.4	0.5	0.6	0.7	0.8	0.9	1.0			
16	250	0.2	6.41g	4.25g	1.44g	1.12g	0.55g	0.62g	0.70g	0.92g	1.14g	1.15g	1.16g	1.14g	1.11g			
		0.6	4.63g	2.90g	0.96g	0.93g	0.64g	0.64g	0.64g	0.75g	0.86g	0.93g	0.98g	1.03g	1.06g			
		1.0	3.29g	2.43g	1.39g	1.21g	0.90g	0.93g	0.95g	1.00g	1.06g	1.10g	1.14g	1.20g	1.25g			
16	500	0.2	6.41s	4.25s	1.44g	1.13g	1.03g	1.24g	1.46g	1.68g	1.91g	2.10e	2.00e	2.00e	2.00e			
		0.6	4.63g	2.90g	0.97g	0.96g	0.81g	0.84g	0.88g	1.06g	1.24g	1.44g	1.63g	1.91g	2.00a			
		1.0	3.29g	2.43g	1.39g	1.21g	1.06g	1.13g	1.20g	1.27g	1.34g	1.49g	1.63g	1.82g	2.01g			
16	750	0.2	6.41g	4.25g	1.44g	1.50a	1.57g	1.93g	2.29g	2.63g	2.70a	2.80e	3.00e	3.20e	4.02g			
		0.6	4.63g	2.90g	1.01g	0.99a	0.96g	1.07g	1.19g	1.54g	1.89g	2.38g	2.87g	3.41g	3.86g			
		1.0	3.29g	2.43g	1.39g	1.34g	1.29g	1.40g	1.50g	1.81g	2.12g	2.54g	2.95g	3.43g	3.92g			
16	1000	0.2	6.41g	4.25g	1.44g	2.00a	2.11g	2.62g	3.13g	3.58g	4.04g	4.62g	5.20g	5.48g	5.75g			
		0.6	4.63g	2.90g	1.06g	1.08a	1.10g	1.30g	1.49g	2.01g	2.53g	3.32g	4.11g	4.92g	5.75g			
		1.0	3.29g	2.43g	1.39g	1.47g	1.52g	1.66g	1.80g	2.33g	2.90g	3.59g	4.27g	5.05g	5.82g			
16	1500	0.2	6.41g	4.25g	1.46g	4.05g	4.70g	5.31g	5.92g	6.36g	6.80g	7.51g	8.21g	10.4g	9.17s			
		0.6	4.63g	2.90g	1.21g	2.26g	2.56g	3.11g	3.66g	4.68g	5.70g	7.17g	8.65g	10.1g	11.6g			
		1.0	3.29g	2.43g	1.41g	2.27g	2.52g	2.99g	3.46g	4.88g	6.29g	8.07a	9.85g	11.1g	12.4g			
16	2000	0.2	6.41g	4.25g	1.52g	5.82g	7.46g	8.53g	9.60g	11.0g	12.4g	14.0g	15.5g	15.5s	11.9s			
		0.6	4.63g	2.90g	1.36g	3.38g	3.91g	5.43g	6.94g	8.74g	10.5g	12.6g	14.6g	18.5g	17.7a			
		1.0	3.29g	2.43g	1.46g	3.35g	3.19g	4.58g	5.97g	8.23g	10.7g	13.1g	15.6g	17.8g	20.0g			
16	3000	0.2	6.41g	4.25g	1.80g	9.04g	12.3g	14.4g	16.6g	19.4g	22.2g	24.5g	27.0a	24.1s	17.0s			
		0.6	4.63g	2.90g	1.63g	6.31g	6.54g	11.4g	14.4g	17.4g	20.5g	23.3g	26.1g	22.0a	31.5s			
		1.0	3.29g	2.43g	1.72g	3.90a	6.12g	8.86g	11.6g	15.7g	19.8g	24.2g	28.6g	31.8g	35.0g			

g - Groeneveld

a - approximation

s - Sergeev

TABLE V.I. (CONT.)

P MPa	G kg/m ² s	q MW/m ²	X															
			1.1	1.2	1.3	1.4	1.5	1.6	1.7	1.8	1.9	2.0	2.1	2.2				
16	250	0.2	1.08g	1.05g	1.05a	1.05a	1.05a	0.94s	0.74s	0.60s	0.50s	0.43s	0.37s	0.33s				
		0.6	1.01g	0.97g	0.97a	0.97a	0.97a	0.97a	0.97a	0.97a	0.97a	0.97a	0.97a	0.97a				
		1.0	1.26g	1.27g	1.27a	1.27a	1.27a	1.27a	1.27a	1.27a	1.27a	1.27a	1.27a	1.27a				
16	500	0.2	2.00e	1.90e	1.70e	1.60e	1.40e	1.20e	0.75s	0.61s	0.51s	0.43s	0.38s	0.33a				
		0.6	1.87g	1.58g	1.58a	1.58a	1.58a	1.58a	1.58a	1.58a	1.48s	1.28s	1.12s	0.99s				
		1.0	1.91g	1.82g	1.82a	1.82a	1.82a	1.82a	1.82a	1.82a	1.82a	1.82a	1.82a	1.63a				
16	750	0.2	3.50g	3.17s	2.42s	1.78s	1.30s	0.98s	0.76s	0.61s	0.51s	0.43s	0.38s	0.33s				
		0.6	3.38g	2.90g	2.90a	2.90a	2.90a	2.73s	2.22s	1.82s	1.52s	1.30s	1.13s	0.99s				
		1.0	3.59g	3.29g	3.29a	3.29a	3.29a	3.29a	3.29a	2.93s	2.49s	2.15s	1.87s	1.66s				
16	1000	0.2	4.64g	3.80s	2.70s	1.86s	1.32s	0.98s	0.76s	0.61s	0.51s	0.43s	0.38s	0.33s				
		0.6	4.87g	4.14g	4.14a	4.14a	3.75s	2.89s	2.27s	1.84s	1.53s	1.30s	1.13s	0.99s				
		1.0	5.23g	4.70g	4.70a	4.70a	4.70a	4.59s	3.71s	3.04s	2.54s	2.16s	1.88s	1.66s				
16	1500	0.2	6.79s	4.53s	2.87s	1.89s	1.32s	0.98s	0.76s	0.61s	0.51s	0.43s	0.38s	0.33s				
		0.6	9.94g	8.08g	7.72s	5.51s	3.96s	2.94s	2.28s	1.84s	1.53s	1.30s	1.13s	1.00s				
		1.0	10.6g	9.05g	8.83a	8.62s	6.45s	4.88s	3.80s	3.07s	2.54s	2.17s	1.88s	1.66s				
16	2000	0.2	8.06s	4.82s	2.89s	1.89s	1.33s	0.98s	0.76s	0.61s	0.51s	0.43s	0.38s	0.33s				
		0.6	16.9s	12.3s	8.39s	5.65s	3.98s	2.95s	2.29s	1.84s	1.53s	1.30s	1.13s	1.00s				
		1.0	16.2g	13.5g	13.1s	9.25s	6.61s	4.91s	3.81s	3.07s	2.55s	2.17s	1.88s	1.66s				
16	3000	0.2	9.64s	4.94s	2.90s	1.89s	1.33s	0.98s	0.76s	0.61s	0.51s	0.43	0.38s	0.33s				
		0.6	22.4s	14.2s	8.69s	5.68s	3.98s	2.95s	2.29s	1.84s	1.53s	1.30s	1.13s	1.00s				
		1.0	25.6g	19.6g	14.3s	9.46s	6.64s	4.92s	3.81s	3.07s	2.55s	2.17s	1.88s	1.66s				

g - Groeneveld

a - approximation

s - Sergeev

TABLE V.I. (CONT.)

P MPa	G kg/m ² s	q MW/m ²	x																
			-0.2	-0.1	0.0	0.1	0.2	0.3	0.4	0.5	0.6	0.7	0.8	0.9	1.0				
18	250	0.2	7.36g	4.92g	1.91g	1.41g	0.73g	0.79g	0.84g	1.03g	1.22g	1.25g	1.27g	1.34g	1.40g				
		0.6	5.29g	3.35g	1.14g	1.03g	0.70g	0.71g	0.72g	0.84g	0.86g	1.04g	1.12g	1.18g	1.24g				
		1.0	4.22g	3.16g	1.45g	1.24g	0.94g	0.97g	1.00g	1.06g	1.12g	1.17g	1.22g	1.28g	1.34g				
18	500	0.2	7.37g	4.92g	1.91g	1.47g	1.50g	1.72g	1.94g	2.21g	2.48g	2.68g	2.50g	2.50e	2.50e				
		0.6	5.79g	3.49g	1.15g	1.10g	0.94g	0.97g	1.01g	1.28g	1.54g	1.79g	2.04g	2.38g	2.72g				
		1.0	4.36g	3.16g	1.45g	1.29g	1.15g	1.22g	1.29g	1.41g	1.53g	1.69g	1.86g	2.06g	2.26g				
18	750	0.2	7.37g	4.92g	1.91g	2.05a	2.16g	2.79g	3.43g	3.45a	3.47a	3.50e	4.10e	4.60e	5.00e				
		0.6	5.79g	3.49g	1.18g	1.19a	1.21g	1.46g	1.72g	1.92a	2.16g	3.46g	4.16g	4.86g	5.56g				
		1.0	4.36g	3.16g	1.45g	1.48a	1.52g	1.77g	2.01g	2.43g	2.84g	3.23g	3.62g	4.34g	5.06g				
18	1000	0.2	7.37g	4.92g	1.91g	2.35a	2.81g	3.87g	4.92g	5.91g	6.20e	6.70e	9.27g	9.97g	10.6s				
		0.6	5.79g	3.49g	1.22g	1.35a	1.48g	1.96g	2.43g	3.20g	3.97g	5.12g	6.27g	7.33g	8.39g				
		1.0	4.36g	3.16g	1.45g	1.67a	1.90g	2.32g	2.73g	3.44g	4.15g	4.77g	5.39g	6.63g	7.87g				
18	1500	0.2	7.37g	4.92g	1.91g	5.40g	6.06g	7.60g	9.13g	10.3g	11.4g	12.9g	14.3g	16.5g	14.9s				
		0.6	5.79g	3.49g	1.36g	3.35g	4.42g	5.54g	6.66g	8.23g	9.80g	11.6g	13.4g	14.7g	16.0g				
		1.0	4.36g	3.16g	1.51g	3.07g	4.32g	5.24g	6.16g	7.87g	9.59g	11.2g	12.8g	13.9g	14.9g				
18	2000	0.2	7.37g	4.92g	1.95g	7.92g	10.3g	12.0g	13.7g	15.5g	17.2g	18.8g	20.3g	23.9s	18.8s				
		0.6	5.79g	3.49g	1.59g	5.33g	7.82g	10.1g	12.3g	14.9g	17.5g	19.9g	22.3g	25.6g	28.8g				
		1.0	4.36g	3.16g	1.64g	4.59g	6.10g	8.09g	10.1g	12.8g	15.6g	18.1g	20.5g	22.2g	24.0g				
18	3000	0.2	7.37g	4.92g	2.14g	12.0g	16.1g	19.0g	21.8g	24.5g	27.1g	29.1g	31.1g	34.0g	25.9s				
		0.6	5.59g	3.49g	1.94g	9.56g	15.2g	18.6g	22.1g	25.9g	29.7g	33.1g	36.4g	42.0g	47.6g				
		1.0	4.36g	3.16g	2.00g	7.36g	10.5g	13.5g	16.6g	21.1g	25.6g	30.6g	35.7g	38.4g	41.0g				

g - Groeneveld

a - approximation

s - Sergeev

TABLE V.I. (CONT.)

P MPa	G kg/m ² s	q MW/m ²	X															
			1.1	1.2	1.3	1.4	1.5	1.6	1.7	1.8	1.9	2.0	2.1	2.2				
18	250	0.2	1.36g	1.31g	1.31a	1.31a	1.31a	1.31a	1.21s	0.96s	0.79s	0.66s	0.56s	0.49s				
		0.6	1.21g	1.18g	1.18a	1.18a	1.18a	1.18a	1.18a	1.18a	1.18a	1.18a	1.18a	1.18a				
		1.0	1.35g	1.36g	1.36a	1.36a	1.36a	1.36a	1.36a	1.36a	1.36a	1.36a	1.36a	1.36a				
18	500	0.2	2.60e	2.50e	2.30e	2.00e	1.80e	1.60e	1.40e	1.20e	0.80s	0.66s	0.56s	0.49s				
		0.6	2.40g	2.10g	2.10a	2.10a	2.10a	2.10a	2.10a	2.10a	2.10a	1.97s	1.68s	1.46s				
		1.0	2.14g	2.02g	2.02a	2.02a	2.02a	2.02a	2.02a	2.02a	2.02a	2.02a	2.02a	2.02a				
18	750	0.2	4.50e	3.80e	3.00e	2.30e	2.00e	1.67s	1.26s	0.99s	0.80s	0.66s	0.56s	0.49s				
		0.6	4.89g	4.28g	4.28a	4.28a	4.28a	4.28a	3.73s	2.96s	2.40s	1.99s	1.69s	1.46s				
		1.0	4.69g	4.33g	4.33a	4.33a	4.33a	4.33a	4.33a	4.33a	3.96s	3.31s	2.81s	2.43s				
18	1000	0.2	8.72s	6.69s	4.78s	3.29s	2.30s	1.67s	1.27s	0.99s	0.80s	0.66s	0.56s	0.49s				
		0.6	7.20g	6.36g	6.36a	6.36a	6.36a	4.99s	3.79s	2.97s	2.40s	1.99s	1.69s	1.46s				
		1.0	7.19g	6.57g	6.57a	6.57a	6.57a	6.57a	6.25s	4.94s	4.00s	3.32s	2.81s	2.43s				
18	1500	0.2	11.3s	7.69s	4.98s	3.31s	2.31s	1.68s	1.27s	0.99s	0.80s	0.66s	0.56s	0.49a				
		0.6	13.7g	11.9g	10.8a	9.79s	6.91s	5.03s	3.80s	2.98s	2.40s	1.99s	1.69s	1.46s				
		1.0	13.0g	11.5g	11.5a	11.5a	11.4s	8.36s	6.33s	4.96s	4.00s	3.32s	2.82s	2.43s				
18	2000	0.2	13.1s	8.06s	5.01s	3.32s	2.31s	1.68s	1.27s	0.99s	0.80s	0.67s	0.56s	0.49s				
		0.6	23.4g	19.6g	14.7s	9.95s	6.93s	5.04s	3.81s	2.98s	2.41s	2.00s	1.69s	1.46s				
		1.0	20.4g	17.4g	16.9a	16.4s	11.5s	8.40s	6.35s	4.97s	4.01s	3.33s	2.82s	2.44s				
18	3000	0.2	15.2s	8.18s	5.02s	3.32s	2.31s	1.68s	1.27s	0.99s	0.80s	0.67s	0.56s	0.49s				
		0.6	35.1g	23.8s	15.0s	9.97s	6.94s	5.04s	3.81s	2.98s	2.41s	2.00s	1.69s	1.46s				
		1.0	32.3g	26.1g	24.9s	16.6s	11.6s	8.40s	6.35s	4.97s	4.01s	3.33s	2.82s	2.44s				

g - Groeneveld

a - approximation

s - Sergeev

TABLE V.I. (CONT.)

P MPa	G kg/m ² s	q MW/m ²	x																
			-0.2	-0.1	0.0	0.1	0.2	0.3	0.4	0.5	0.6	0.7	0.8	0.9	1.0				
20	250	0.2	8.40g	5.58g	2.56g	1.80g	0.97g	0.98g	0.99g	1.12g	1.24g	1.32g	1.40g	1.58g	1.76g				
		0.6	6.31g	4.04g	1.46g	1.17g	0.79g	0.82g	0.84g	0.95g	1.06g	1.16g	1.26g	1.37g	1.48g				
		1.0	6.25g	4.57g	1.38g	1.20g	1.00g	1.03g	1.07g	1.12g	1.19g	1.24g	1.29g	1.38g	1.46g				
20	500	0.2	8.41g	5.58g	2.56g	2.00g	2.28g	2.40g	2.52g	2.88g	3.24g	3.47g	3.71g	3.96g	4.21g				
		0.6	7.79g	4.44g	1.46g	1.26g	1.16g	1.19g	1.21g	1.54g	1.87g	2.18g	2.50g	2.92g	3.35g				
		1.0	6.67g	4.37g	1.38g	1.28g	1.25g	1.33g	1.40g	1.58g	1.76g	1.94g	2.12g	2.35g	2.58g				
20	750	0.2	8.41g	5.58g	2.56g	3.19g	3.22g	4.20g	5.17g	6.33g	7.47g	7.80a	8.20e	9.30e	9.30e				
		0.6	7.79g	4.44g	1.46g	1.60a	1.75g	2.23g	2.70g	3.42g	4.15g	5.13g	6.11g	7.02g	7.93g				
		1.0	6.67g	4.57g	1.38g	1.79g	1.94g	2.42g	2.89g	3.40g	3.90g	4.15g	4.40g	5.62g	6.83g				
20	1000	0.2	8.41g	5.58g	2.56g	3.36a	4.15g	5.99g	7.82g	9.76g	11.7g	14.0g	16.2g	17.7g	19.2g				
		0.6	7.79g	4.44g	1.46g	1.90a	2.35g	3.26g	4.18g	5.31g	6.43g	8.07g	9.71g	11.1g	12.5g				
		1.0	6.67g	4.57g	1.38g	2.30g	2.64g	3.31g	4.38g	5.21g	6.05g	6.37g	6.68g	8.88g	11.1g				
20	1500	0.2	8.41g	5.58g	2.56g	6.96g	7.83g	11.0g	14.2g	16.9g	19.6g	22.5g	25.4g	27.3g	29.1g				
		0.6	7.79g	4.44g	1.56g	5.09g	7.69g	9.80g	11.9g	14.4g	16.9g	19.1g	21.3g	22.2g	23.1g				
		1.0	6.67g	4.57g	1.56g	4.18g	7.29g	9.03g	10.8g	12.8g	14.7g	15.6g	16.5g	17.4g	18.2g				
20	2000	0.2	8.41g	5.58g	2.59g	10.6g	14.0g	17.0g	20.0g	22.7g	25.3g	27.2g	29.2g	30.4g	31.8g				
		0.6	7.79g	4.44g	1.90g	8.33g	14.4g	17.9g	21.3g	25.2g	29.2g	32.1g	34.9g	35.7g	36.4g				
		1.0	6.67g	4.57g	1.91g	6.36g	11.0g	13.8g	16.6g	20.0g	23.3g	25.6g	27.9g	28.4g	28.8g				
20	3000	0.2	8.41g	5.58g	2.56g	15.8g	20.8g	24.6g	28.4g	31.4g	34.4g	35.9g	37.4g	39.2g	41.0g				
		0.6	7.79g	4.44g	2.39g	14.4g	26.1g	30.2g	34.4g	39.3g	44.3g	47.8g	51.4g	51.9g	52.4g				
		1.0	6.67g	4.57g	2.41g	10.3g	17.7g	20.6g	23.8g	28.8g	33.8g	39.5g	45.1g	45.2g	45.3g				

g - Groeneveld

a - approximation

s - Sergeev

TABLE V.I. (CONT.)

P MPa	G kg/m ² s	q MW/m ²	x															
			1.1	1.2	1.3	1.4	1.5	1.6	1.7	1.8	1.9	2.0	2.1	2.2				
20	250	0.2	1.68g	1.59g	1.59a	1.59a	1.59a	1.70e	1.50e	1.40e	1.40a	1.40a	1.33s	1.09s				
		0.6	1.48g	1.49g	1.49a	1.49a	1.49a	1.49a	1.49a	1.49a	1.49a	1.49a	1.49a	1.49a				
		1.0	1.47g	1.47g	1.47a	1.47a	1.47a	1.47a	1.47a	1.47a	1.47a	1.47a	1.47a	1.47a				
20	500	0.2	4.15a	4.10e	3.80e	3.30e	2.80e	2.40e	2.40a	2.40a	2.14s	1.67s	1.33s	1.09s				
		0.6	3.08g	2.82g	2.82a	2.82a	2.82a	2.82a	2.82a	2.82a	2.82a	2.82a	2.82a	2.82a				
		1.0	2.42g	2.27g	2.27a	2.27a	2.27a	2.27a	2.27a	2.27a	2.27a	2.27a	2.27a	2.27a				
20	750	0.2	8.10e	6.40e	5.10e	4.10e	3.40e	2.90e	2.60e	2.10e	1.80e	1.60e	1.30e	1.20e				
		0.6	7.28g	6.65g	6.65a	6.65a	6.65a	6.65a	6.65a	6.65a	6.45s	5.01s	4.00s	3.28s				
		1.0	0001g	6.00g	6.00a	6.00a	6.00a	6.00a	6.00a	6.00a	6.00a	6.00a	6.00a	5.47s				
20	1000	0.2	16.8g	14.8g	13.5a	12.3s	8.28s	5.64s	3.95s	2.87s	2.15s	1.67s	1.34s	1.10s				
		0.6	11.4g	10.4g	10.4a	10.4a	10.4a	10.4a	10.4a	8.60s	6.46s	5.02s	4.01s	3.29s				
		1.0	10.4g	9.68g	9.68a	9.68a	9.68a	9.68a	9.68a	9.68a	9.68a	8.36s	6.68s	5.48s				
20	1500	0.2	24.1g	20.3g	18.1s	12.3s	8.30s	5.65s	3.96s	2.87s	2.16s	1.67s	1.34s	1.10s				
		0.6	20.2g	17.6g	17.6a	17.6a	17.6a	17.0s	11.9s	8.61s	6.47s	5.02s	4.01s	3.29s				
		1.0	16.7g	15.2g	15.2a	15.2a	15.2a	15.2a	15.2a	14.4s	10.8s	8.37s	6.69s	5.48s				
20	2000	0.2	25.5g	20.8g	18.2s	12.4s	8.31s	5.66s	3.96s	2.87s	2.16s	1.68s	1.34s	1.10s				
		0.6	31.6g	27.4g	26.5a	25.7a	24.9s	17.0s	11.9s	8.62s	6.48s	5.03s	4.02s	3.29s				
		1.0	25.6g	22.6g	22.6a	22.6a	22.6a	22.6a	19.8s	14.4s	10.8s	8.38s	6.69s	5.49s				
20	3000	0.2	32.7g	26.7s	18.2s	12.4s	8.32s	5.66s	3.97s	2.88s	2.16s	1.68s	1.34s	1.10s				
		0.6	46.3g	41.1g	39.1a	37.1s	24.9s	17.0s	11.9s	8.63s	6.48s	5.03s	4.02s	3.29s				
		1.0	39.4g	34.0g	34.0a	34.0a	34.0a	28.3s	19.8s	14.4s	10.8s	8.38s	6.70s	5.49s				

g - Groeneveld

a - approximation

s - Sergeev

Appendix VI

CIAE METHOD FOR DETERMINING FILMBOILING HEAT TRANSFER

The non-equilibrium factor is defined as [Plummer (1976)]:

$$k = \frac{X_a - X_c}{X_e - X_c}$$

and

$$k = k_0 k_d k_q k_x$$

where

k_d, k_q and k_x are the correction factors to account for the effects of tube diameter, heat flux and local quality, respectively.

$$k_d = \left(\frac{D}{0.008} \right)^{0.26}$$

The k_0 is a function of P, G and X_0 and its values are obtained from the calculation on the mechanistic model [Chen and Chen (1994)] and provided in this appendix in tabular form.

Then the vapour temperature is calculated by the heat balance equation:

$$T_v = T_s + \left[\frac{X_e}{X_a} - 1 \right] \frac{H_{fg}}{c_{p_g}}$$

Finally, the wall temperature is obtained by:

$$T_w = T_v + \frac{q}{(h_c + h_r)}$$

with

$$h_c = Nu_{f0} F \frac{\lambda_g}{D}$$

and

$$Nu_{f0} = 0.0175 \cdot Re_f^{0.812} Pr_f^{0.333} \text{ [Chen and Chen (1996a)]}.$$

$$F = 1 + 2.32(1 + 0.01P)e^{-12X_a}$$

where the subscript f refers to properties evaluated at the film temperature, $T_f = \frac{1}{2}(T_w + T_v)$ and P is in bar.

The non-equilibrium is primarily determined by the inlet flow condition, as accounted by the k_0 , but the effect of P and X are less important. With $K_q = 1$ and $K_x = 1$ and without considering the radiation heat transfer ($h_r = 0$). 2192 CIAE film boiling data ($L > 0.1m$ and

$We = \frac{(G \cdot X)^2 D}{\rho_g \sigma} > 10$) are calculated for the wall temperature with an average error of 1.4% and a RMS error of 7.2%.

TABLE VI.I. THE TABLE OF NON-EQUILIBRIUM FACTORS “ k_0 ” OF CHEN AND CHEN (1998)

P	G	X_{cr}							
(MPa)	(kg/m ² s)	0.0	0.05	0.1	0.2	0.4	0.6	0.8	1.0
0.1	25	0.68	0.58	0.44	0.31	0.28	0.26	0.18	0.0
	50	0.69	0.59	0.45	0.42	0.48	0.36	0.25	0.0
	100	0.74	0.63	0.60	0.64	0.68	0.56	0.44	0.0
	200	0.78	0.73	0.75	0.78	0.77	0.74	0.60	0.0
	400	0.81	0.81	0.86	0.89	0.90	0.89	0.81	0.0
	600	0.82	0.88	0.92	0.94	0.96	0.95	0.90	0.0
	1000	0.83	0.92	0.96	0.98	0.98	0.98	0.97	0.0
	1500	0.84	0.96	0.98	0.99	0.99	0.99	0.98	0.0
0.3	25	0.72	0.60	0.45	0.40	0.31	0.17	0.10	0.0
	50	0.74	0.61	0.46	0.43	0.36	0.30	0.16	0.0
	100	0.76	0.64	0.54	0.57	0.52	0.47	0.33	0.0
	200	0.78	0.71	0.66	0.70	0.68	0.63	0.47	0.0
	400	0.80	0.78	0.79	0.81	0.83	0.75	0.63	0.0
	600	0.82	0.80	0.84	0.88	0.90	0.86	0.75	0.0
	1000	0.83	0.86	0.89	0.92	0.93	0.92	0.87	0.0
	1500	0.83	0.90	0.95	0.96	0.98	0.97	0.95	0.0
0.5	25	0.74	0.56	0.44	0.35	0.29	0.23	0.12	0.0
	50	0.76	0.58	0.45	0.38	0.33	0.22	0.14	0.0
	100	0.78	0.60	0.50	0.44	0.40	0.36	0.26	0.0
	200	0.79	0.62	0.63	0.64	0.61	0.56	0.40	0.0
	400	0.80	0.67	0.65	0.77	0.74	0.70	0.54	0.0
	600	0.81	0.80	0.81	0.83	0.83	0.80	0.67	0.0
	1000	0.82	0.84	0.86	0.89	0.90	0.88	0.78	0.0
	1500	0.82	0.87	0.92	0.94	0.95	0.94	0.89	0.0
1.0	25	0.76	0.62	0.53	0.42	0.25	0.10	0.08	0.0
	50	0.77	0.63	0.56	0.46	0.28	0.14	0.09	0.0
	100	0.79	0.66	0.58	0.53	0.33	0.22	0.13	0.0
	200	0.80	0.66	0.60	0.50	0.45	0.38	0.25	0.0
	400	0.80	0.68	0.66	0.65	0.62	0.56	0.40	0.0
	600	0.80	0.77	0.74	0.73	0.71	0.63	0.45	0.0
	1000	0.81	0.80	0.79	0.82	0.80	0.73	0.57	0.0
	1500	0.82	0.84	0.85	0.87	0.84	0.82	0.70	0.0
2.0	25								
	50	0.81	0.68	0.65	0.54				
	100	0.81	0.71	0.68	0.62	0.32	0.16	0.08	0.0
	200	0.81	0.69	0.65	0.53	0.35	0.28	0.16	0.0
	400	0.81	0.70	0.68	0.56	0.52	0.44	0.29	0.0
	600	0.82	0.73	0.71	0.64	0.61	0.53	0.36	0.0
	1000	0.83	0.74	0.74	0.74	0.71	0.65	0.47	0.0
	1500	0.83	0.81	0.80	0.80	0.80	0.71	0.55	0.0
4.0	25								
	50								
	100	0.81	0.72	0.62	0.45	0.30	0.21	0.08	0.0
	200	0.81	0.72	0.63	0.50	0.34	0.26	0.14	0.0
	400	0.82	0.72	0.63	0.55	0.49	0.41	0.26	0.0
	600	0.83	0.77	0.73	0.61	0.56	0.48	0.33	0.0
	1000	0.83	0.78	0.76	0.71	0.70	0.60	0.42	0.0
	1500	0.84	0.79	0.78	0.78	0.77	0.69	0.53	0.0
6.0	25								
	50								
	100	0.81	0.72	0.63	0.45	0.35	0.20	0.11	0.0
	200	0.82	0.73	0.64	0.52	0.42	0.25	0.14	0.0
	400	0.82	0.76	0.67	0.55	0.51	0.39	0.26	0.0
	600	0.83	0.77	0.70	0.60	0.58	0.48	0.31	0.0
	1000	0.84	0.78	0.74	0.69	0.68	0.61	0.43	0.0
	1500	0.84	0.80	0.77	0.76	0.74	0.68	0.53	0.0

Appendix VII

TWO-PHASE VISCOSITY MODELS FOR USE IN THE HOMOGENEOUS MODEL FOR TWO-PHASE PRESSURE DROP

McAdams (1942)

$$\frac{1}{\mu} = \frac{x}{\mu_G} + \frac{(1-x)}{\mu_L} \quad (1)$$

Cicchitti (1960)

$$\mu = x \mu_G + (1-x) \mu_L \quad (2)$$

Owens (1961)

$$\mu = \mu_L \quad (3)$$

Dukler (1964)

$$\mu = (1-\beta) \mu_L + \beta \mu_G \quad (4)$$

Weisman and Choe (1976)

suggested the following equation for a frothy mixture

$$\mu = \mu_L \exp \left\{ \frac{2.5}{1 - 39\beta / 64} \right\} \quad (5)$$

and

$$\mu = \mu_G + (\mu_C - \mu_G) \left(\frac{1}{\beta} - 1 \right)^k \quad (6)$$

for a misty mixture at high void fraction. Choe (1975) suggested a value of 3 for the constant k and μ_C is the mean of μ_G and μ_L .

Beattie and Whalley (1982)

$$\mu = \mu_L (1 - \beta)(1 + 2.5 \beta) + \mu_G \beta \quad (7)$$

Beattie and Whalley also proposed some flow pattern specific models. For example, for bubbly flow

$$\mu = \mu_L (1 + 2.5\beta) \quad (8)$$

and for annular flow

$$\mu = \mu_L (1 - \beta) + \mu_G \beta \quad (9)$$

Appendix VIII

TWO-PHASE PRESSURE DROP CORRELATIONS BASED ON THE MULTIPLIER CONCEPT

Martinelli-Nelson (1948)

Based on tests conducted using steam-water mixture, values of ϕ_{LO}^2 are presented in graphical form as a function of pressure and quality by Martinelli and Nelson. Table VIII.I has been obtained from these graphs.

Accuracy of this correlation at high mass fluxes, i.e. $G > 1500 \text{ kg/m}^2\text{s}$ is not good.

Lockhart-Martinelli (1949)

The authors defined a parameter χ , generally known as the Martinelli parameter, as below.

$$\chi^2 = \frac{\phi_G^2}{\phi_L^2} = \frac{(dp/dz)_L}{(dp/dz)_G} \quad (1)$$

The following expressions were obtained for the two phase multiplier

$$\phi_L^2 = 1 + \frac{C}{\chi} + \frac{1}{\chi^2} \quad (2)$$

$$\phi_G^2 = 1 + C\chi + \chi^2 \quad (3)$$

Values of C are dependent on the nature of flow (i.e. laminar or turbulent) of individual phases and are given below:

- C = 20 for turbulent flow of both phases
- = 12 for laminar liquid and turbulent gas flow
- = 10 for turbulent liquid and laminar gas flow
- = 5 for laminar flow of both phases.

This correlation is mainly based on tests conducted at near atmospheric pressure with mass velocities less than $1500 \text{ g/m}^2\text{s}$.

Lottes-Flinn (1956)

Correlation for annular upward flow through heated channels is

$$\phi_{LO}^2 = \left(\frac{1-x}{1-\alpha} \right)^2 \quad (4)$$

Thom (1964)

Thom presented the two-phase friction multiplier, ϕ_{LO}^2 , in tabular and graphical form as a function of quality and pressure for water-steam mixtures (Table VIII.II).

TABLE VIII.I. VALUES OF THE TWO-PHASE FRICTIONAL MULTIPLIER ϕ_{LO}^2 FOR STEAM-WATER SYSTEM FROM THE MARTINELLI-NELSON MODEL

Steam Quality	Pressure (bar)								
	1.01	6.89	34.4	68.9	103.0	138.0	172.0	207.0	221.2
0.01	5.6	3.5	1.8	1.6	1.35	1.20	1.10	1.05	1.00
0.05	30.0	15.0	5.3	3.6	2.4	1.75	1.43	1.17	1.00
0.10	69.0	28.0	8.9	5.4	3.4	2.45	1.75	1.30	1.00
0.20	150.0	56.0	16.2	8.6	5.1	3.25	2.19	1.51	1.00
0.30	245.0	83.0	23.0	11.6	6.8	4.04	2.62	1.68	1.00
0.40	350.0	115.0	29.2	14.4	8.4	4.82	3.02	1.83	1.00
0.50	450.0	145.0	34.9	17.0	9.9	5.59	3.38	1.97	1.00
0.60	545.0	174.0	40.0	19.4	11.1	6.34	3.70	2.10	1.00
0.70	625.0	199.0	44.6	21.4	12.1	7.05	3.96	2.23	1.00
0.80	685.0	216.0	48.6	22.9	12.8	7.70	4.15	2.35	1.00
0.90	720.0	210.0	48.0	22.3	13.0	7.95	4.20	2.38	1.00
1.00	525.0	130.0	30.0	15.0	8.6	5.90	3.70	2.15	1.00

Turner-Wallis (1965)

The following relationships are provided by Turner-Wallis for annular two-phase flow

$$\phi_G^2 = \left[1 + \chi^{\frac{4}{5-n}} \right]^{\frac{5-n}{2}} ; \quad \phi_L^2 = \left[1 + \left(\frac{1}{\chi} \right)^{\frac{4}{5-n}} \right]^{\frac{5-n}{2}} \quad (5)$$

where

n is the exponent of Re in the single-phase friction factor correlation and χ is the Martenelli parameter.

Tarasova (1966)

The correlation applicable for adiabatic flow in the range of $49 \leq P \leq 195.9$ bar and $515 \leq G \leq 2575$ kg/m²s is:

$$\phi_L^2 = A \frac{Fr^{\frac{-7.35}{P}} 10^5}{(1 - \alpha)} \quad (6)$$

where

$Fr = u_L^2/gD$. SI units are used for the various parameters and A is a constant dependent on P.

P (bar)	49.0	98.000	147.000	196.00
A	3.1	1.628	1.313	1.14

Baroczy introduced a "physical property index" which is given below:

$$\frac{\rho_G}{\rho_L} \left(\frac{\mu_L}{\mu_G} \right)^{0.2}$$

TABLE VIII.II. VALUES OF FRICTION MULTIPLIER ϕ_{LO}^2 FOR FLOW OF WATER AND STEAM IN UNHEATED TUBES, REPRODUCED FROM THOM (1964)

Steam Quality	Pressure (bar)				
	17.24	41.38	86.21	144.83	206.9
0.000	1.00	1.00	1.00	-----	-----
0.010	2.12	1.46	1.10	-----	-----
0.015	2.71	1.60	1.16	-----	-----
0.020	3.22	1.79	1.22	1.060	-----
0.030	4.29	2.13	1.35	1.110	-----
0.040	5.29	2.49	1.48	1.160	-----
0.050	6.29	2.86	1.62	1.210	1.020
0.060	7.25	3.23	1.77	1.260	1.030
0.070	8.20	3.61	1.92	1.310	1.040
0.080	9.15	3.99	2.07	1.370	1.050
0.090	10.10	4.38	2.2	1.420	1.060
0.100	11.10	4.78	2.39	1.480	1.080
0.150	15.80	6.60	3.03	1.750	1.160
0.200	20.60	8.42	3.77	2.020	1.240
0.300	30.20	12.10	5.17	2.570	1.400
0.400	39.80	15.80	6.59	3.120	1.570
0.500	49.40	19.50	8.03	3.690	1.730
0.600	59.10	23.20	9.49	4.270	1.880
0.700	68.80	26.90	10.19	4.860	2.030
0.900	88.60	34.50	13.80	6.050	2.330
1.000	98.86	38.30	15.33	6.664	2.480

Baroczy supplied ϕ_{LO}^2 at a reference mass velocity of 1356.2 kg/m²s (10⁶ lb/h ft²) in tabular form as a function of steam quality and property index (Table VIII.III). Using this, $\phi_{LO}^2(G)$ (i.e. ϕ_{LO}^2 at any mass velocity G) is calculated by multiplying with a correction factor. Correction factors for different mass velocities are provided in graphical form as a function of quality and property index and are reproduced in Tables VIII.IV to VIII.VII. The method is valid in the range of $340 \leq G \leq 4070$ kg/m²s.

TABLE VIII.III. VARIATION OF FRICTION MULTIPLIER ϕ_{LO}^2 AT $G = 1356 \text{ kg/m}^2\text{s}$ ($10^6 \text{ lb/ft}^2\text{h}$) WITH PROPERTY INDEX AND QUALITY REPRODUCED FROM BAROCZY (1966)

Property index x 100	Quality (%)														
	0.1	0.5	1	2	3.5	5	7.5	10	15	20	30	40	60	80	100
0.01	2.2	5.8	9.2	16.0	26.5	47	99	163	376	630	1300	2050	4300	6600	10000
0.10	2.15	5.60	8.80	14.8	22.8	34.2	48.2	70.0	108	148	86.0	330	538	760	1000
0.40	2.08	4.90	7.80	11.9	16.3	22.8	29.0	36.0	49.5	63.0	86.5	110	155	203	250
1.00	1.59	3.30	4.80	7.00	9.60	12.4	16.0	20.0	27.0	33.5	43.5	53.0	69.0	85.0	100
3.00	1.12	1.55	1.81	2.57	3.45	4.70	6.10	7.90	11.0	13.2	17.3	21.2	26.0	30.0	33.3
10.0	1.04	1.12	1.22	1.48	1.78	2.05	2.50	2.80	3.60	4.20	5.50	6.5	8.00	9.10	10.0
30.0	1.01	1.02	1.06	1.13	1.26	1.36	1.50	1.59	1.77	1.93	2.25	2.48	2.86	3.20	3.33

TABLE VIII.IV. TWO-PHASE MULTIPLIER CORRECTION FACTOR FOR MASS FLUX OF $339 \text{ kg/m}^2\text{s}$ ($0.25 \times 10^6 \text{ lb/ft}^2\text{h}$) REPRODUCED FROM BAROCZY (1966)

Property index (ρ_G/ρ_L). (μ_L/μ_G) ^{0.2}	Quality (%)								
	0.1	1	5	10	20	40	60	80	100
0.000461	1.6690	1.6688	1.6000	1.5850	1.5851	1.4938	1.3587	1.1745	1.0
0.0065	1.1717	1.1717	1.0319	1.4212	1.4212	1.2404	1.1489	1.0979	1.0
0.055	1.2000	1.2702	1.2957	1.3723	1.3723	1.3128	1.1570	1.0830	1.0
0.0775	1.2130	1.2915	1.3864	1.5340	1.5340	1.3362	1.1574	1.0819	1.0
0.3551	1.1180	1.1532	1.5532	1.7750	1.7750	1.4106	1.1872	1.0681	1.0
1.0	1.0000	1.0000	1.0000	1.0000	1.0000	1.0000	1.0000	1.0000	1.0

TABLE VIII.V. TWO-PHASE MULTIPLIER CORRECTION FACTOR FOR MASS FLUX OF $678.1 \text{ kg/m}^2\text{s}$ ($0.5 \times 10^6 \text{ lb/ft}^2\text{h}$) REPRODUCED FROM BAROCZY (1966)

Property index (ρ_G/ρ_L).(μ_L/μ_G) ^{0.2}	Quality (%)								
	0.1	1	5	10	20	40	60	80	100
0.000461	1.3000	1.3316	1.3000	1.3000	1.3105	1.2474	1.2000	1.1030	1.0
0.0065	1.1289	1.2479	1.1289	1.2692	1.2362	1.1567	1.1103	1.0722	1.0
0.055	1.1051	1.1705	1.1895	1.2284	1.2400	1.2158	1.1158	1.0737	1.0
0.0775	1.1000	1.1516	1.2160	1.2263	1.2645	1.2316	1.3116	1.0790	1.0
0.3551	1.0737	1.0895	1.3105	1.4277	1.5610	1.3105	1.1579	1.0526	1.0
1.0	1.0000	1.0000	1.0000	1.0000	1.0000	1.0000	1.0000	1.0000	1.0

TABLE VIII.VI. TWO-PHASE MULTIPLIER CORRECTION FACTOR FOR MASS FLUX OF 2712.4 kg/m²s (2.0 × 10⁶ lb/ft²h) REPRODUCED FROM BAROCZY (1966)

Property index (ρ _G /ρ _L). (μ _L /μ _G) ^{0.2}	Quality (%)								
	0.1	1	5	10	20	40	60	80	100
0.000461	0.4526	0.4526	0.7526	0.7526	0.7326	0.7716	0.9126	0.9084	1.0
0.0065	0.7737	0.6737	0.6926	0.7268	0.7567	0.8053	0.8611	0.9316	1.0
0.055	0.9000	0.8368	0.7790	0.7947	0.7684	0.7263	0.7474	0.8474	1.0
0.0775	0.9095	0.8632	0.8000	0.8137	0.7632	0.7053	0.7147	0.8179	1.0
0.3551	0.9674	0.9158	0.7657	0.7152	0.6400	0.5895	0.5895	0.7150	1.0
1.0	1.0000	1.0000	1.0000	1.0000	1.0000	1.0000	1.0000	1.0000	1.0

TABLE VIII.VII. TWO-PHASE MULTIPLIER CORRECTION FACTOR FOR MASS FLUX OF 4068.6 kg/m²s (3.0 × 10⁶ lb/ft²h) REPRODUCED FROM BAROCZY (1966)

Property index (ρ _G /ρ _L). (μ _L /μ _G) ^{0.2}	Quality (%)								
	0.1	1	5	10	20	40	60	80	100
0.000461	0.6368	0.6105	0.6368	0.6368	0.6000	0.6526	0.7211	0.8389	1.0
0.0065	0.7842	0.5000	0.5211	0.5947	0.6211	0.7053	0.7737	0.8720	1.0
0.055	0.8526	0.7326	0.6591	0.6796	0.6424	0.5842	0.6000	0.7326	1.0
0.0775	0.8768	0.8000	0.7000	0.7000	0.6324	0.5474	0.5474	0.6889	1.0
0.3551	0.9474	0.8968	0.7158	0.6586	0.5700	0.4823	0.4823	0.6000	1.0
1.0	1.0000	1.0000	1.0000	1.0000	1.0000	1.0000	1.0000	1.0000	1.0

Sekoguchi (1970)

$$\phi_{LO}^2 = 0.38 \text{ Re}_{LO}^{0.1} \left[1 + \frac{x}{1-x} \frac{v_G}{v_L} \right]^{0.95} \quad (7)$$

Lystsova Correlation [Osmachkin & Borisov (1970)]

$$\phi_{LO}^2 = \psi \left\{ 1 + x \left(\frac{\rho_L}{\rho_G} - 1 \right) \right\} \quad (8)$$

ψ, the in-homogeneity parameter is defined as

$$\psi = \left[1 + x \left(\frac{\mu_L}{\mu_G} - 1 \right) \right]^{-0.2x} (1 + 0.57 x^{0.125}) \left\{ \frac{(1-x)^2}{0.2 + u_0 \rho_G / (\rho_L \sqrt{gD})} \right\} - 5.2 x^2 \quad (9)$$

where

$$u_0 = G/\rho_L$$

Becker (1973)

$$\phi_{LO}^2 = 1 + 10 \left(\frac{P_{crit}}{P} \right) x \quad (10)$$

The correlation is valid up to 70 bar.

Chisholm (1973)

Chisholm suggested that the equation

$$\Phi_L^2 = 1 + C/\chi + 1/\chi^2 \quad (11)$$

is rather unsatisfactory for use with evaporating flows where the liquid flow rate varies along the flow path. He suggested that the equation can be transformed with sufficient accuracy for engineering purposes to

$$\phi_{LO}^2 = 1 + (\Gamma^2 - 1) \left[B x^{\frac{2-n}{2}} \left(1 - x^{\frac{2-n}{2}} \right) + x^{2-n} \right] \quad (12)$$

where n is the exponent in Blasius equation; the following formulae apply for B

Γ	G (kg/m ² s)	B
≤ 9.5	≤ 500	4.8
	$500 < G < 1900$	$2400/G$
	> 1900	$55/G^{0.5}$
$9.5 < \Gamma < 28$	≤ 600	$520/(\Gamma G^{0.5})$
	> 600	$21/\Gamma$
≥ 28		$15\,000/(\Gamma^2 G^{0.5})$

and $\Gamma = (\Delta P_{GO}/\Delta P_{LO})^{0.5}$, which for turbulent flow can be written as

$$\Gamma = \left\{ \frac{\rho_L}{\rho_G} \right\}^{0.5} \left\{ \frac{\mu_G}{\mu_L} \right\}^{n/2} \quad (13)$$

Friedel (1979)

The correlation valid for horizontal and vertical upward flow in circular, rectangular and annular ducts has the form

$$\phi_{LO}^2 = E + F H / (Fr^{m1} We^{m2}) \quad (14)$$

where

$$E = (1-x)^2 + x^2 \rho_L f_{GO}/(\rho_G f_{LO}); F = 3.24 x^{0.78} (1-x)^{0.224}$$

$$H = (\rho_L/\rho_G)^{0.91}(\mu_G/\mu_L)^{0.19}(1-\mu_G/\mu_L)^{0.7} ; Fr = G^2/(\rho^2 g D)$$

$$We = DG^2/(\rho\sigma) ; m_1 = 0.0454 \text{ and } m_2 = 0.035$$

f_{GO} and f_{LO} are the friction factors computed for single-phase gas and liquid flows of mass flow equal to the two-phase flow and ρ is the density computed from the homogeneous model. For vertical downward flow F , H , m_1 and m_2 are to be replaced by the values given below:

$$F = 48.6 x^{0.5} (1-x)^{0.29} ; H = (\rho_L/\rho_G)^{0.9}(\mu_G/\mu_L)^{0.73}(1-(\mu_G/\mu_L))^{7.7} ;$$

$$m_1 = 0.03 \text{ and } m_2 = 0.12$$

Appendix IX

DIRECT EMPIRICAL TWO-PHASE PRESSURE DROP CORRELATIONS

CESNEF-2 [Lombardi-Carsana (1992)]

This correlation is the last version of four different correlations [Lombardi-Pedrocchi (1972) DIF-1, Lombardi-Ceresa (1978) DIF-2, Bonfanti et al. (1982) DIF-3 and the present one] developed first at the CISE laboratories and then at the Department of Nuclear Energy — CESNEF of Polytechnic of Milan. This correlation is the result of a wide research work carried out at CISE with different fluids, geometries and boundary conditions and assessed with a data bank, named MIDA, prepared at the Department of Nuclear Energy — CESNEF. Here only the CESNEF-2 correlation will be presented, because it is the logical generalization of the previous ones. This correlation is fully dimensionless, continuous between two-phase and single-phase flow and is valid only for vertical upflow (both for adiabatic and diabatic conditions). It calculates the total pressure drop as the sum of the elevation, acceleration and friction terms obtained by an energy balance instead of a momentum balance approach. Therefore in this approach the elevation term is proportional to the homogeneous density of the two-phase mixture and not to the actual density in the vertical duct, as in the case of a momentum balance approach. The acceleration term is obtained by the assumption of homogeneous flow. The friction term is given by an equation similar to that for single-phase flow, where the friction coefficient (Fanning type) is empirically correlated and the specific volume is assumed equal to the homogeneous value. By defining dimensionless numbers as follows:

$$l_o = \{(G^2 v_m D) / \sigma\} (\mu_G / \mu_L)^{0.5} \quad (1)$$

$$C_e = \{\rho_L g (D - D_o)^2 / \sigma\} (\mu_G / \mu_L) \quad \text{where } D_o = 0.001 \text{ m} \quad (2)$$

$$C_e = 0 \text{ for } D \leq D_o \quad (3)$$

where

$v_m = x v_G + (1-x) v_L$. One obtains the friction coefficient of the two-phase mixture, f_{TP} , as follows:

$$f_{TP} = \begin{cases} 0.046(l_o)^{-0.25} & \text{for } l_o \geq 30C_e \\ 0.046(30C_e)(l_o)^{-1.25} & \text{for } l_o < 30C_e \end{cases} \quad (4)$$

and the total friction coefficient is obtained as

$$f = f_G b_G + f_L b_L + f_{TP} b_{TP} \quad (5)$$

where

f_G and f_L are the single-phase friction coefficients (Fanning type), calculated at the same total flow rate by usual correlations, b_G , b_L and b_{TP} are the weight functions as follows:

$$b_G = x^{600 \left(\frac{v_L}{v_G} \right)} ; \quad b_L = (1-x)^{2 \left(\frac{v_G}{v_L} \right)} ; \quad b_{TP} = 1 - b_G - b_L \quad (6)$$

Then

$$\Delta P_f = \frac{2f}{D} G^2 v_m \Delta z \quad ; \quad \Delta P_e = \frac{g}{v_m} \Delta z \quad ; \quad \Delta P_a = G^2 (\Delta v_m) \quad (7)$$

where

ΔP_f , ΔP_e and ΔP_a are the friction, elevation and acceleration terms respectively. The total pressure drop is given by

$$\Delta p = \Delta P_f + \Delta P_e + \Delta P_a \quad (8)$$

To calculate the pressure drop, the channel is subdivided into sections, the number of which is problem dependent: diabatic or adiabatic conditions, high or low pressures, etc. Starting with a given subdivision (typically two sections), the above terms are calculated for each section, assuming average data for friction and elevation terms and true specific volume variations across the section for the acceleration term. Then all these terms for the different sections are summed up to obtain the channel overall pressure drop. The channel is then subdivided into a larger number of sections till the overall pressure drop converges to a definite value. The total pressure drop, when $l_0 < C_e$, is limited to the liquid weight of the channel ($g\Delta z/v_L$).

Appendix X

FLOW PATTERN SPECIFIC PRESSURE DROP CORRELATIONS FOR HORIZONTAL FLOW

(a) Stratified flow

The empirical model for the pressure gradient for stratified flow as given by *Baker* [Govier & Aziz (1972)] is as follows:

$$\phi_G = \frac{15400 \chi}{G_{SL}^{0.8}} \quad (1)$$

where

$G_{SL} = \rho_L j_L$ and χ is the Martinelli parameter. No separate equation is provided by Baker for the stratified wavy flow pattern.

Hoogendoorn (1959) proposed the following relation for $x < 0.8$ in case of stratified smooth and wavy flow patterns.

$$\frac{\Delta p}{\Delta z} = C \frac{x^{1.45} G^2}{2D \rho_G} \quad (2)$$

The constant C depends weakly on the diameter and the fluid used. For the purpose of engineering calculations, C can be given a value of 0.024 for smooth tubes (if $0.05 \text{ m} < D < 0.14 \text{ m}$). For rough pipes, the following table shall be used to calculate C .

Relative roughness, e/D	0.0012	0.0039	0.0190	0.0300
C	0.0260	0.0320	0.0450	0.0520

Dukler et al. [see Govier & Aziz (1972)] gave the following mechanistic model for stratified flow

$$\left\{ \frac{\Delta p}{\Delta z} \right\}_{TPF} = \frac{f_{TP} G^2}{2D \rho_m} \quad (3)$$

where

$$f_{TP} = F \eta f; f = 0.0056 + 0.5 \text{Re}^{-0.32}; \text{Re} = DG/\mu_m;$$

$$F = 1 + \gamma/[1.281 - 0.478\gamma + 0.444\gamma^2 - 0.094\gamma^3 + 0.00843\gamma^4]$$

$$\text{and } \gamma = -\ln(1 - \beta); \eta = (\rho_L/\rho_m)(1 - \beta)^2/(1 - \alpha) + (\rho_G/\rho_m)\beta^2/\alpha; \mu_m = \mu_L(1 - \beta) + \mu_G\beta; \rho_m = \rho_L(1 - \beta) + \rho_G\beta$$

Chawla (1967)

$$\left\{ \frac{\Delta p}{\Delta z} \right\}_{\text{TPF}} = \frac{0.3164}{(\text{GD} / \mu_G)^{0.25}} \frac{G^2 x^{7/4}}{2D \rho_G} \left(1 + \frac{(1-x)\rho_G}{x \varepsilon_c \rho_L} \right)^{19/8} \quad (4)$$

where

$$\varepsilon_c = 9.1[(1-x)/x](\text{Re}_L \text{Fr}_L)^{-1/6} (\rho_G/\rho_L)^{0.9} (\mu_G/\mu_L)^{0.5};$$

$$\text{Re}_L = \text{DG}(1-x)/\mu_L \text{ and } \text{Fr}_L = G^2(1-x)^2/(\rho_L^2 g D)$$

In addition, mechanistic models for stratified flow are provided by Agrawal et al. (1973) and Taitel and Dukler (1976a).

Agrawal et al. (1973)

$$\left\{ \frac{\Delta p}{\Delta z} \right\}_L = (\tau_{\text{WG}} p_G + \tau_i W_i) / A_G \quad (5)$$

p_G is the perimeter of the portion of the wall that is in contact with the gas phase.

$$\left\{ \frac{\Delta p}{\Delta z} \right\}_G = (\tau_{\text{WL}} p_L + \tau_i W_i) / A_L \quad (6)$$

where

$\tau_{\text{WG}} = f_G \rho_G u_G^2 / 2$; $\tau_{\text{WL}} = f_L \rho_L u_L^2 / 2$ with f_G and f_L calculated by Blasius equation using Re_G and Re_L defined as

$$\text{Re}_G = \rho_G u_G D_{\text{hG}} / \mu_G; \text{Re}_L = \rho_L u_L D_{\text{hL}} / \mu_L \text{ with } D_{\text{hG}} = 4A_G / (p_G + W_i) \text{ and } D_{\text{hL}} = 4A_L / p_L$$

where

W_i is the width of the gas-liquid interface.

$$\tau_i = (0.804 \text{Re}_G^{-0.285})^2 \rho_G u_G^2 \quad (7)$$

The calculations can be carried out if the geometric quantities appearing in the above equations are calculated. The following equations can be used to evaluate the geometric quantities.

$$h_L/D = 0.5 \{1 - \cos(\gamma/2)\}; \alpha = A_G/A = 1 - (\gamma \sin \gamma) / (2\pi); \text{ and}$$

$$W_i/D = 2 \{h_L/D - (h_L/D)^2\}^{0.5}; p_L/p = \gamma/2\pi; p_G/p = 1 - p_L/p;$$

where

γ , is the angle subtended by the interface at the pipe central line and h_L , is the depth of liquid phase at the pipe central line.

$$D_{\text{hG}}/D = 4A_G / \{D(p_G + W_i)\} = \alpha p / (p_G + W_i) \text{ and } D_{\text{hL}}/D = 4A_L / (p_L D) = (1 - \alpha)p/p_L$$

Computations can be made for laminar or turbulent liquid layer. Also, the average velocity in the liquid layer is calculated using the velocity distribution corresponding to the laminar or turbulent flow regime.

Taitel & Dukler (1976a)

This procedure assumes the pressure drop in the liquid and gas phase to be equal. Further it requires the calculation of the nondimensional liquid level, $\bar{h}_L (= h_L/D$, where, h_L is the depth of liquid phase at the pipe central line), in the horizontal pipe, which can be calculated knowing the Lockhart-Martinelli parameter from the following equation;

$$-\chi^2 \frac{(\bar{u}_L \bar{D}_L)^{-n}}{(\bar{u}_G \bar{D}_G)^{-m}} \frac{\bar{p}_L}{\bar{A}_L} \bar{u}_L^2 + \left[\frac{\bar{p}_G}{\bar{A}_G} + \frac{f_i}{f_G} \left(\frac{\bar{p}_i}{\bar{A}_L} + \frac{\bar{p}_i}{\bar{A}_G} \right) \right] \bar{u}_G^2 = 0 \quad (8)$$

where

$$\chi^2 = [C_L(D j_L/v_L)^{-n}] / [C_G(D j_G/v_G)^{-m}] (\rho_L/\rho_G)(j_L/j_G)^2$$

$$\bar{u}_L = \frac{\bar{A}}{\bar{A}_L}; \quad \bar{u}_G = \frac{\bar{A}}{\bar{A}_G}; \quad \bar{A}_L = \frac{A_L}{D^2}; \quad \bar{A}_G = \frac{A_G}{D^2}; \quad \bar{D}_G = \frac{D_G}{D}; \quad D_G = \frac{4A_G}{p_G + p_i}$$

$$\bar{A} = \frac{A}{D^2}; \quad \bar{D}_L = \frac{D_L}{D}; \quad D_L = \frac{4A_L}{p_L}$$

$$\bar{A}_L = 0.25[\pi - \cos^{-1}(2\bar{h}_L - 1) + (2\bar{h}_L - 1)\sqrt{1 - (2\bar{h}_L - 1)^2}]; \quad \bar{h}_L = \frac{h_L}{D}$$

$$\bar{A}_G = 0.25[\cos^{-1}(2\bar{h}_L - 1) - (2\bar{h}_L - 1)\sqrt{1 - (2\bar{h}_L - 1)^2}]$$

$$\bar{p}_L = \pi - \cos^{-1}(2\bar{h}_L - 1); \quad \bar{p}_G = \cos^{-1}(2\bar{h}_L - 1); \quad \bar{p}_i = \sqrt{1 - (2\bar{h}_L - 1)^2}$$

$$f_i = C_i \left(\frac{u_G D_G}{v_G} \right)^{-n}; \quad f_G = C_G \left(\frac{u_G D_G}{v_G} \right)^{-m}; \quad f_L = C_L \left(\frac{u_L D_L}{v_L} \right)^{-m}$$

Equation 8 can be solved for laminar or turbulent flow by specifying the values of C_i , C_L , C_G , n and m .

Knowing \bar{h}_L , the pressure drop can be calculated using the following equation;

$$\phi_G^2 = \frac{1}{4} \bar{u}_G^2 \left\{ \frac{(\bar{u}_G \bar{D}_G)^{-m}}{\bar{A}_G} \right\} \left\{ \bar{p}_G + \frac{f_i}{f_G} \bar{p}_i \right\} \quad (9)$$

(b) Bubbly flow

$$\frac{\Delta p}{\Delta z} = \frac{f \rho_m V_m^2}{2D} \quad (10)$$

where

$V_m = G/\rho_m$ and f is calculated from single-phase correlation using $Re = DV_m \rho_L / \mu_L$ and

$$\rho_m = (1 - \alpha) \rho_L + \alpha \rho_G.$$

(c) Elongated bubbly flow

Baker [Govier & Aziz(1972)] gave the following empirical equation for elongated bubble

$$f_G = 27.315 \chi^{0.855} / G_{SL}^{0.17} \quad (11)$$

Hoogendoorn gave the following equation valid for elongated bubble, slug and froth flow patterns

$$\frac{\Delta p}{\Delta z} = \frac{f_{TP} G^2}{2D \rho_L} \quad (12)$$

Hoogendoorn and Buitelaar (1961) provided a graphical correlation for f_{TP}/f as function of quality and density ratio where f is the friction factor calculated using single-phase liquid Reynolds number given by $Re = DG/\mu_L$.

(d) Slug flow:

Baker [Govier & Aziz (1972)]

$$f_G = 1190 \chi^{0.815} / G_{SL}^{0.5} \quad (13)$$

Hughmark (1965)

$$\left(\frac{\Delta p}{\Delta z} \right)_{TPF} = \frac{f \rho_L V_L^2}{2D} \quad (14)$$

f is the single-phase friction factor based on $Re = Du_L \rho_L / \mu_L$

where

$u_L = j_L (1 - \alpha)$, $\alpha = j_G / \{(1 + K) j\}$ and K is a function of $Re_m (= D j \rho_L / \mu_L)$. A graph of K vs. Re_m is given by Hughmark from which the following table has been obtained.

Re_m	10^3	10^4	5×10^4	10^5	2×10^5	3×10^5	$\geq 4 \times 10^5$
K	0.92	0.63	0.40	0.33	0.25	0.23	0.22

Dukler and Hubbard (1975)

$$\left\{ \frac{\Delta p}{\Delta z} \right\}_{TPF} = \frac{f_{TP} \rho_m j^2 (1 + C)}{2D \omega} \left\{ \frac{(j_L / \omega) - \xi}{1 - (\xi \omega / j)} \right\} \quad (15)$$

f_{TP} is calculated using the following single-phase correlation.

$$f_{TP} = 0.0056 + 0.5 Re_m^{-0.32} \quad (16)$$

where

$$\text{Re}_m = \frac{Dj\rho_m}{\mu_m}; \quad \rho_m = \rho_G\alpha + \rho_L(1-\alpha); \quad j = j_L + j_G; \quad \mu_m = \mu_G\alpha + \mu_L(1-\alpha)$$

Gregory and Scott (1969) proposed the following correlation for ω

$$\omega = 0.0226 \left[\frac{j_L}{gD} \left(\frac{19.75}{j} + j \right) \right]^{1.2} \quad (17)$$

For the constant C a value of 0.25 was proposed by Hubbard and Dukler whereas 0.35 was proposed by Gregory and Scott (1969).

$$\zeta = \left\{ \frac{1-\alpha}{B} \right\} \ln \left\{ 1 + \frac{j}{\omega} \right\} \quad (18)$$

where

$B = 0.2$. No equation for the void fraction, α , was proposed by Hubbard and Dukler.

(e) Annular mist flow:

Baker [Govier & Aziz (1972)]

$$\phi_G = (4.8 - 0.3125D) \chi^{0.343-0.021D} \quad (19)$$

FPS units are used in all the equations given by Baker.

Hoogendoorn (1959)

$$\left\{ \frac{\Delta p}{\Delta z} \right\}_{\text{TPF}} = \frac{f_{\text{TP}} G_{\text{GS}}^2}{2D\rho_G} \quad (20)$$

where

$f_{\text{TP}} = 0.025 (G_{\text{GS}})^{-0.025}$ with $G_{\text{GS}} (= \rho_G j_G)$ given in $\text{kg/m}^2\text{s}$.

Appendix XI

FLOW PATTERN SPECIFIC PRESSURE DROP CORRELATIONS FOR VERTICAL UPWARD FLOW

(a) Bubbly flow:

The pressure gradient in bubbly flow is calculated by essentially single phase methods

$$\left\{ \frac{\Delta p}{\Delta z} \right\}_{\text{TPF}} = \frac{f_L \rho_L j^2}{2D} \quad (1)$$

where

f_L is given by conventional single-phase friction factor with $Re = Dj\rho_L/\mu_L$. The homogeneous model is expected to give good results for bubbly flow.

Beattie (1973)

$$\phi_{LO}^2 = \left\{ 1 + x \left(\frac{\rho_L}{\rho_G} - 1 \right) \right\}^{0.8} \left\{ 1 + x \left(\frac{(3.5 \mu_G + 2 \mu_L) \rho_L}{(\mu_G + \mu_L) \rho_G} - 1 \right) \right\}^{0.2} \quad (2)$$

(b) Slug flow:

The pressure gradient in slug flow is calculated by

$$\left\{ \frac{\Delta p}{\Delta z} \right\}_{\text{TPF}} = \frac{(1 - \alpha) f_L \rho_L j^2}{2D} \quad (3)$$

where

f_L and Re are as defined for bubbly flow above.

(c) Froth flow (churn flow):

No equations are reported for this flow regime. The pressure gradient in this regime can be calculated using the homogeneous model as described for bubbly flow above.

(d) Pure annular flow (without entrainment):

Chawla (1967)

$$\left\{ \frac{\Delta p}{\Delta z} \right\}_{\text{TPF}} = \frac{0.3164}{(DG / \mu_G)^{0.25}} \frac{G^2 x^{7/8}}{2D \rho_G} \left(1 + \frac{1-x}{x} \alpha_c \frac{\rho_G}{\rho_L} \right)^{19/8} \quad (4)$$

where

$$1/\alpha_c^3 = 1/\alpha_1^3 + 1/\alpha_2^3$$

$$\log \alpha_1 = 0.960 + \log B; \quad \log \alpha_2 = \left[0.168 - 0.055 \log \frac{e}{D} \right] \log B - 0.67$$

$$B = \frac{(1-x)}{x} (\text{Re}_L \text{Fr}_L)^{-1/6} \left\{ \frac{\rho_L}{\rho_G} \right\}^{-0.9} \left\{ \frac{\mu_L}{\mu_G} \right\}^{-0.5} ; \text{Re}_L = G(1-x)D/\mu_L ; \text{Fr}_L = (G^2(1-x)^2)/(\rho_L^2 g D).$$

The correlation is valid in the range $0.006 \leq D \leq 0.154$ m, $5.9 \cdot 10^{-6} < (e/D) < 6.8 \cdot 10^{-2}$, $10^2 \leq \text{Re}_L \leq 3 \cdot 10^5$, $10^{-5} \leq \text{Fr}_L \leq 10^2$, $30 \leq (\rho_L/\rho_G) \leq 850$, $40 \leq (\mu_L/\mu_G) \leq 7000$ and $10^{-4} < x < 0.98$.

Wallis (1970)

$$\left\{ \frac{\Delta p}{\Delta z} \right\}_{\text{TPF}} = \frac{f \rho_G j_G^2}{2D \alpha^{2.5}} \quad (5)$$

where

$f = 0.005[1 + 75(1 - \alpha)]$ and j_G is the superficial velocity of gas.

Beattie (1973)

$$\phi_{\text{LO}}^2 = \left\{ 1 + x \left(\frac{\rho_L}{\rho_G} - 1 \right) \right\}^{0.8} \left\{ 1 + x \left(\frac{\mu_G \rho_L}{\mu_L \rho_G} - 1 \right) \right\}^{0.2} \quad (6)$$

(e) Dry wall (post dryout flow):

Beattie (1973)

$$\phi_{\text{LO}}^2 = \left\{ \frac{\mu_G}{\mu_L} \right\}^{0.2} \left\{ \frac{\rho_G}{\rho_L} \right\}^{0.8} \left\{ 1 + x \left(\frac{\rho_G}{\rho_L} - 1 \right) \right\}^{1.8} \quad (7)$$

Lorenzini et al. (1989)

This correlation applicable for the transition between annular and fog flow pattern is given by

$$\phi_{\text{LO}}^2 = k R^* \quad (8)$$

where

$k = 0.45 \ln(100 x_e)$, the subscript “e” refers to the final conditions in the section and R^* is given by

$R^* = GR_3$ if $\alpha_e > \alpha_T$,

$R^* = GR_2$ if $\alpha_e < \alpha_T$ and $x_e > x_T$,

$R^* = GR_1$ if $\alpha_e < \alpha_T$ and $x_e < x_T$;

where

$$GR_1 = \frac{\left\{ 0.5(1 - A^2) + (1 - A) \left\{ \frac{\rho_L}{\rho_G S} \right\} - B \left\{ \frac{\rho_L}{\rho_G S} \right\}^2 \right\}}{x_e}; \quad GR_2 = (1 - A^2) CD \left\{ \frac{S^2}{2\sqrt{\alpha_e}} \right\};$$

$$GR_3 = \left(1 - \frac{x_T}{x_e} \right) \left\{ 1 + \left(\frac{\rho_L - \rho_G}{2\rho_G} \right) (x_e + x_T) \right\}; \quad A = \frac{\rho_L}{\rho_L - \alpha_e \rho_L - \alpha_e \rho_G S}$$

$$B = \frac{(\alpha_e - 1)\rho_L}{\rho_L - \alpha_e \rho_L - \alpha_e \rho_G S}; \quad C = \frac{\rho_G S}{\rho_G S - \rho_L}; \quad D = \frac{f_{LG}(S-1)^2}{f_{LO}}$$

$$\alpha_T = \frac{1}{\left\{ 1 + \frac{1 - x_T}{x_T} \frac{v_L}{v_G} S \right\}}$$

$$x_T = \left\{ \frac{1067.622413}{G} - 0.308424 \right\} \{ 0.476615 - 0.442864 \exp(-0.014721P) \} \text{ where}$$

P is in bar.

If $G > 3461 \text{ kg/m}^2\text{s}$, then $x_T = 1/G$. Friction factors f_{LO} and f_{LG} are calculated corresponding to Re_{LO} and Re_{LG} respectively. Re_{LO} is the Reynolds number of the saturated liquid and Re_{LG} is given by

$$Re_{LG} = Re_{LO} \left\{ \frac{x_T}{\sqrt{\alpha_T}} \right\} \left\{ \frac{\mu_L}{\mu_G} \right\} (S-1) \quad \text{if } \alpha_e > \alpha_T \quad (9)$$

$$Re_{LG} = Re_{LO} \left\{ \frac{x_e}{\sqrt{\alpha_e}} \right\} \left\{ \frac{\mu_L}{\mu_G} \right\} (S-1) \quad \text{if } \alpha_e < \alpha_T \quad (10)$$

Appendix XII

INTERFACIAL FRICTION MODELS GIVEN BY SOLBRIG (1986)

(a) Bubbly flow:

$$F_i = -A_i B_i (u_G - u_L) \quad (1)$$

where

F_i is the interface force, A_i is interface area per unit volume and B_i is the coefficient of interface friction.

$$A_i = 3 \alpha / r_b,$$

where

$r_b = r_{b,we} (1 - P) + r_{b,m} P$; $P = \exp [(- D_b / r_{b,we}) / x_t]$ and x_t is normalized liquid induced bubble oscillation distance,

$$x_t = 1 \quad \text{if} \quad Re_L \leq 2,000;$$

$$x_t = \exp (1 - 2,000 / Re_L) \quad \text{if} \quad Re_L > 2,000;$$

$$r_{b,we} = 0.06147 \{ (We_{b,crit} / 2) (\sigma / (\rho u_R^2)) \}$$

where

$$u_R = u_G - u_L \text{ and } We_{b,crit} = 1.24$$

$$r_{b,m} = r_{b,we} / 0.06147$$

$B_i = f [\rho_L | u_G - u_L |] / 8$, f is obtained from the Colebrook equation, with Re defined as:

$$Re = D_h u_R \rho_L / \mu_L ;$$

$$D_h = 2 r_b x \quad \text{if} \quad r_b x < R ;$$

$$D_h = 2R \quad \text{if} \quad r_b x \geq R,$$

R is tube radius and $x = D_b / 2 r_{b,we}$. The roughness is set by setting $e = r_b$.

(b) Slug flow

Since the slugs are assumed to be made up of a combination of hemispherical end caps and a cylindrical center section, contributions to the interface friction are obtained by summing both of the components, i.e.

$$F_i = (A_{i,he} B_{i,he} + A_{i,ac} B_{i,ac}) u_R, \quad (2)$$

where

$$A_{i,he} = (\alpha/D)(4/\pi)^{0.5} [4/\{(2/3) + K\}],$$

$$A_{i,ac} = (\alpha/D)(4/\pi)^{0.5} [4K/\{(2/3) + K\}]$$

where subscripts “he” and “ac” refer to hemispherical ends and annular center portion respectively and $K = \{(2/3)K_1^2 - \alpha\}/\{\alpha - K_1^2\}$; $K_1 = (\pi/4)^{0.5} \approx 0.886$.

The friction coefficient of the hemispherical ends is calculated as $B_{c,he} = f [\rho_L |u_R|]/8$, where f is calculated using Moody friction factor correction with $D_h = 2 r_{b,m}$ and the roughness defined as $e = r_{b,m}$; i.e. calculation of friction coefficient $B_{c,he}$ is carried out by the same equations used for bubbly flow.

The friction coefficient for the annular center section based on the gas phase friction term is $B_{c,ac} = f_G [\rho_G |u_R|]/8$, where the friction is assumed to be that of annular flow plus an entrance length correction due to the developing velocity profile in the gas and liquid phase to give $f_G = f_{G,fd} + f_e$, where the fully developed friction factor $f_{G,fd}$ is obtained from Moody friction factor correlation with Reynolds number defined as $Re = D_h \rho_G u_R / \mu_G$ with $D_h = 2 r_{b,m}$ and the roughness is given by $e = 4 \delta$, where δ is the thickness of the liquid film. The thickness of film in Solbrig(1986) model is $\delta = 0.114 R$, where R is the tube radius. The entrance length friction factor is given as $f_e = 10 e^{-K/10}$.

(c) Annular flow regimes

c1. Annular flow

$$F_i = A_i B_{i,u_R}, \quad A_i = (4\sqrt{\alpha})/D, \quad B_i = f_G [\rho_G |u_R|]/8 \quad (3)$$

where

f_G calculated from the Moody diagram with $Re = D_h \rho_G u_R / \mu_G$; $D_h = \sqrt{\alpha} D$ and the roughness is given by $e = 4 \delta = 2(1 - \sqrt{\alpha})D$, The maximum value of film thickness is limited to $0.1R$, i.e. if e calculated is greater than this value, then $e = 0.1 R$ is used.

c2. Annular mist regime

The interface force for annular mist flow is

$$F_{i,am} = A_{i,am} B_{i,am} u_R \quad (4)$$

where

$$A_{i,am} = 4\sqrt{\{1 - (1 - \alpha)(1 - E)\}}/D$$

where E is the entrainment fraction given by

$$E = \tanh(4.5 \times 10^{-7} We^{1.25} Re_L^{0.25})$$

where We is the Weber number for entrainment and Re_L is the total liquid Reynolds number defined as

$$We = (\rho_G \alpha_G^2 u_R^2 D / \sigma) \{(\rho_L - \rho_G) / \rho_G\}^{0.33}, Re_L = \rho_L \alpha_L u_R D / \mu_L \quad (5)$$

In both of these definitions, the liquid velocity to be used in the calculation of u_R is that of the liquid film and not of the droplets. The friction coefficient is obtained from Moody diagram with the hydraulic diameter given by:

$$D_h = D \sqrt{\{1 - (1 - \alpha)(1 - E)\}}.$$

The roughness is defined as $e = 2 [1 - \sqrt{\{1 - (1 - \alpha)(1 - E)\}}]D$ with the maximum value limited to $0.1R$.

c3. Droplet regime

The interface force between the gas phase and the droplets is calculated in a manner similar to that of bubbles in the liquid phase except that the role of the continuous and discontinuous phases are reversed.

$$F_{i,d} = A_{i,d} B_{i,d} u_R \quad (6)$$

where

$$A_{i,d} = \{3(1 - \alpha)E/D ; B_{i,d} = f_G \rho | u_R | / 8 \text{ and}$$

$u_R = u_G - u_L$ in a two-fluid model,

$= u_G - u_D$ in a three-fluid model where u_D is the droplet velocity.

Appendix XIII

SLIP RATIO MODELS FOR CALCULATION OF VOID FRACTION

Osmachkin (1970)

$$S = 1 + \frac{(0.6 + 1.5\beta^2) \left(1 - \frac{P}{P_{\text{crit}}}\right) \left(\frac{G}{\rho_L}\right)^{0.5}}{(gD_h)^{0.25}} \quad (1)$$

Bankoff and Jones (1962)

$$S = \frac{1 - \alpha}{K - \alpha + (1 - K)\alpha^r} \quad (2)$$

where

$K = 0.71 + 0.00131 P$ and $r = 3.33 + 2.61 \times 10^{-5} P + 9.67 \times 10^{-3} P^2$, P is in bar.

Bankoff and Malnes (1979)

$$S = (1 - \alpha)/(C - \alpha) \text{ for } \alpha \leq C - 0.02 \quad (3)$$

and

$$S = 50[1.02 - C + 50(\alpha - C + 0.02)(1 - C)] \text{ for } \alpha > C - 0.02 \quad (4)$$

where

$u_G = Su_L + u_0$ with $u_0 = 0.174$ m/s and $C = 0.904$.

Modified Smith [Mochizuki and Ishii (1992)]

$$S = K + (1 - K) \left\{ \frac{\left(\frac{\rho_L}{\rho_G} + K \left(\frac{1}{x} - 1 \right) \right)}{1 + K \left(\frac{1}{x} - 1 \right)} \right\}^{0.5} \quad (5)$$

where

$K = 0.95 \tanh(5.0 x) + 0.05$

Appendix XIV

K β MODELS FOR THE CALCULATION OF VOID FRACTION

Armand (1947)

$$K = 0.833 + 0.167x \quad (1)$$

Bankoff (1960)

$$K = 0.71 + 0.00131 P \quad (2)$$

where

$$4.9 \leq P \leq 206.2 \text{ bar}$$

Hughmark (1961)

$$K = -0.16367 + 0.31037 Y - 0.03525 Y^2 + 0.0013667 Y^3 \quad \text{for} \quad Y < 10 \quad (3)$$

$$K = 0.75545 + 0.00358Y - 0.1436 \cdot 10^{-4} Y^2 \quad \text{for} \quad Y \geq 10 \quad (4)$$

$$Y = \text{Re}^{1/6} \text{Fr}^{1/8} (1 - \alpha)^{-1/4} \quad (5)$$

$$\text{Re} = G D / [\alpha \mu_G + (1 - \alpha) \mu_L] \quad (6)$$

$$\text{Fr} = (G^2 / gD)(x / \rho_G + (1 - x) / \rho_L)^2 \quad (7)$$

Appendix XV

DRIFT FLUX MODELS FOR THE CALCULATION OF VOID FRACTION

Zuber-Findlay (1965)

$$C_0 = 1.13 \quad \text{and} \quad V_{Gj} = 1.41 \left\{ \frac{(\rho_L - \rho_G) \sigma g}{\rho_L^2} \right\}^{0.25} \quad (1)$$

Rouhani (1969)

$$C_0 = 1 + 0.2(1 - x) \left\{ \frac{g D_h \rho_L^2}{G^2} \right\}^{0.25} \quad (2)$$

$$V_{Gj} = 1.18(1 - x) \left\{ \frac{(\rho_L - \rho_G) \sigma g}{\rho_L^2} \right\}^{0.25} \quad (3)$$

Dix (1971)

$$C_0 = \beta \left[1 + \left\{ \frac{1}{\beta - 1} \right\}^b \right]; \quad b = \left\{ \frac{\rho_G}{\rho_L} \right\}^{0.1} \quad (4)$$

$$V_{Gj} = 2.9 \left\{ \frac{(\rho_L - \rho_G) \sigma g}{\rho_L^2} \right\}^{0.25} \quad (5)$$

Nabizadeh (1977)

$$C_0 = \beta \left\{ 1 + \frac{1}{n} \text{Fr}^{0.1} \left(\frac{\rho_G}{\rho_L} \right)^n \left(\frac{1 - x}{x} \right)^{1.22n} \right\} \quad (6)$$

where

$$\text{Fr} = \frac{G^2}{\rho_L^2 g D_h}; \quad n = \sqrt{0.6 \left\{ \frac{\rho_L - \rho_G}{\rho_L} \right\}}; \quad V_{Gj} = 1.18 \left\{ \frac{(\rho_L - \rho_G) \sigma g}{\rho_L^2} \right\}^{0.25}$$

GE-Ramp (1970)

$$\begin{aligned} C_0 &= 1.1 \text{ for } \alpha \leq 0.65 \\ &= 1 + 0.1(1 - \alpha)/0.35 \text{ for } \alpha > 0.65 \end{aligned} \quad (7)$$

and the drift flux velocity is given by,

$$V_{Gj} = R \left\{ \frac{(\rho_L - \rho_G) \sigma g}{\rho_L^2} \right\}^{0.25} \quad (8)$$

and $R = 2.9$ for $\alpha \leq 0.65$

$$= 2.9 (1 - \alpha) / 0.35 \text{ for } \alpha > 0.65 \quad (9)$$

EPRI (1986)

$$C_0 = \frac{L(\alpha, P)}{K_0 + (1 - K_0) \alpha^r} \quad (10)$$

$$L(\alpha, P) = \frac{1 - \exp(C_1 \alpha)}{1 - \exp(-C_1)} \quad (11)$$

where the constants are given by,

$$C_1 = \frac{4 P_{crit}^2}{[P (P_{crit} - P)]} ; K_0 = B_1 + (1 - B_1) \left(\frac{\rho_G}{\rho_L} \right)^{1/4} ; r = (1 + 1.57 \frac{\rho_G}{\rho_L}) (1 - B_1) ;$$

$$B_1 = \min (0.8, A_1) ; A_1 = \frac{1}{[1 + \exp(-Re / 10^5)]}$$

and the drift velocity is given by

$$V_{Gj} = 1.41 \left\{ \frac{(\rho_L - \rho_G) \sigma g}{\rho_L^2} \right\}^{0.25} \frac{(1 - \alpha)^{0.5}}{1 + \alpha} \quad (12)$$

Chexal-Lellouche (1996)

The correlation valid for steam-water flow is presented here. For refrigerant two-phase flow or Air-water two-phase flow reference may be made to the original report.

1. Distribution parameter (C_0)

The distribution parameter, C_0 , for a two-phase mixture flowing at any angle, where the angle is measured from the vertical axis, is the weighted average of values for horizontal and vertical flow.

$$C_0 = F_r C_{ov} + (1 - F_r) C_{oh} \quad (13)$$

where

C_{ov} and C_{oh} are the distribution parameters evaluated for vertical and horizontal flow and F_r is a flow orientation parameter defined as

for $Re_G > 0$

$$F_r = \frac{(90^\circ - \theta)}{90^\circ} \quad \text{for} \quad (0^\circ \leq \theta \leq 90^\circ) \quad (14a)$$

for $Re_G < 0$

$$F_r = \begin{cases} 1 & \text{for} \quad (\theta \leq 80^\circ) \\ \frac{(90^\circ - \theta)}{10^\circ} & \text{for} \quad (80^\circ < \theta < 90^\circ) \end{cases} \quad (14b)$$

where

θ = pipe orientation angle measured from the vertical axis

$Re_G = D_h W_G / (\mu_G A)$ local vapour superficial Reynolds number

Note that in all cases, the pipe orientation angle $\theta = 0^\circ$ for a vertical pipe and $\theta = 90^\circ$ for a horizontal pipe. The angle is always in the limits of $(0 \leq \theta \leq 90^\circ)$.

1.1. Vertical flow

For vertical pipe ($\theta = 0^\circ$), the volumetric fluxes, j_L and j_G , are taken as positive if both phases are flowing upward and negative if both phases are flowing downward. For countercurrent flow, the vapour velocity is always positive (upward) and the liquid velocity is always negative (downward). Countercurrent flow is only considered for vertical flows. The distribution parameter for vertical flow is given by

for $Re_G \geq 0$

$$C_{ov} = \frac{L}{[K_o + (1 - K_o)\alpha^r]} \quad (15a)$$

for $Re_G < 0$

$$C_{ov} = \max \left\{ \begin{array}{l} \frac{L}{[K_o + (1 - K_o)\alpha^r]} \\ \frac{V_{Gj}^o (1 - \alpha)^{0.2}}{(|j_L| + |j_G|)} \end{array} \right. \quad (15b)$$

where

V_{Gj}^o = defined later by Eq. (30)

L = Chexal-Lellouche fluid parameter.

Different forms of L are used with different fluids. For *steam-water* mixtures the form of L is selected to ensure proper behavior as the pressure approaches the critical pressure,

$$L = \frac{1 - \exp(-C_1 \alpha)}{1 - \exp(-C_1)} \quad (16)$$

where

$$C_1 = \frac{4 P_{\text{crit}}^2}{[P (P_{\text{crit}} - P)]} \quad (17)$$

Other variables in the distribution parameter correlation are defined as,

$$K_o = B_1 + (1 - B_1) \left(\frac{\rho_G}{\rho_L} \right)^{1/4} \quad (18)$$

$$r = \frac{(1.0 + 1.57 \rho_G / \rho_L)}{(1 - B_1)} \quad (19)$$

$$B_1 = \min (0.8, A_1) \quad (20)$$

$$A_1 = \frac{1}{[1 + \exp(-\text{Re} / 60,000)]} \quad (21)$$

$$\text{Re} = \begin{cases} \text{Re}_G & \text{if } \text{Re}_G > \text{Re}_L \quad \text{or} \quad \text{Re}_G < 0.0 \\ \text{Re}_L & \text{if } \text{Re}_G \leq \text{Re}_L \end{cases} \quad (22)$$

$$\text{Re}_L = \text{local liquid Reynolds number} = \frac{W_L D_h}{\mu_L A} \quad (23)$$

$$\text{Re}_G = \text{local vapour Reynolds number} = \frac{W_G D_h}{\mu_G A} \quad (24)$$

The sign convention for all Reynolds numbers, Re , Re_L , and Re_G is the same as the sign convention for the individual flows.

1.2. Horizontal flow

For horizontal flow ($\theta = 90^\circ$), the void fraction correlation considers only cocurrent flows. Horizontal countercurrent flow has not yet been included in the database. The volumetric fluxes for horizontal flow are always taken as positive; negative volumetric fluxes should not be used. The distribution parameter for horizontal flow is given by

$$C_{oh} = \left[1 + \alpha^{0.05} (1 - \alpha)^2 \right] C_{ov} \quad (25)$$

where

C_{ov} is defined by Eq. (15a) above, and is evaluated with positive vapour Reynolds numbers, using the *horizontal* fluid parameter, L_h , defined as follows:

$$\text{steam water} \quad L_h = \frac{1 - \exp(-C_1 \alpha)}{1 - \exp(-C_1)} \quad (26)$$

All other parameters are defined as for vertical flows, with positive fluxes.

For both vertical and horizontal flows, the steam-water parameter is a function of pressure and void fraction.

2. Drift velocity (V_{Gj})

The drift velocity, V_{Gj} , for cocurrent upflow and pipe orientation angles ($0^\circ < \theta < 90^\circ$) is defined as:

$$V_{Gj} = F_r V_{gfv} + (1 - F_r) V_{gjh} \quad (27)$$

where

V_{gfv} and V_{gjh} are the drift velocities for vertical and horizontal flow and F_r is the flow orientation parameter defined by Eqs (14a) and (14b). For cocurrent downflow, the drift velocity is defined as:

$$V_{Gj} = F_r V_{gfv} + (F_r - 1) V_{gjh} \quad (28)$$

2.1. Vertical flow

Like the distribution parameter, the drift velocity for a vertical pipe ($\theta = 0^\circ$), V_{gfv} , covers cocurrent upflow and downflow and countercurrent flow. The drift velocity for vertical flow is given by:

$$V_{gfv} = V_{Gj}^0 C_9 \quad (29)$$

where

$$V_{Gj}^0 = 1.41 \left[\frac{(\rho_L - \rho_G) \sigma g}{\rho_L^2} \right]^{0.25} C_2 C_3 C_4 \quad (30)$$

$$C_9 = (1 - \alpha)^{B_1} \text{ for } Re_G > 0 \quad (31)$$

$$C_9 = (1 - \alpha)^{0.5} \text{ for } Re_G < 0 \quad (32)$$

Other parameters are defined as:

$$\text{for } \left(\frac{\rho_L}{\rho_G} \right) \leq 18 \quad C_2 = 0.4757 \left[\ln \left(\frac{\rho_L}{\rho_G} \right) \right]^{0.7} \quad (33)$$

$$\text{for } \left(\frac{\rho_L}{\rho_G} \right) > 18 \quad C_2 = \begin{cases} 1 & \text{if } C_5 \geq 1 \\ \frac{1}{\left\{ 1 - \exp \left[\frac{-C_5}{(1 - C_5)} \right] \right\}} & \text{if } C_5 < 1 \end{cases} \quad (34)$$

where:

$$C_5 = \sqrt{\frac{150}{\left(\frac{\rho_L}{\rho_G} \right)}} \quad (35)$$

$$C_4 = \begin{cases} 1 & \text{if } C_7 \geq 1 \\ \frac{1}{1 - \exp(-C_8)} & \text{if } C_7 \leq 1 \end{cases} \quad (36)$$

$$C_7 = (D_2/D_h)^{0.6} \quad (37)$$

$$C_8 = \frac{C_7}{1 - C_7} \quad (38)$$

$$D_2 = \text{Normalizing diameter, 0.09144 m} \quad (39)$$

The parameter C_3 is determined based on the direction of the gas and liquid flows. It is continuous as the two directional boundaries are crossed, but has a particularly strong derivative when coming across the j_L equals zero plane. The values of C_3 for the three types of flows (cocurrent upflow, cocurrent downflow, and countercurrent flow) are given as:

The upflow C_3 expression has been modified to decrease the rate of change of C_3 in the 1st Quadrant¹ as it approaches zero liquid flow rate. This change improves the ability of the system dynamic models to utilize the inferred interface friction factor. From a steady state standpoint, the expression can be modified as long as the proper end point characteristics are maintained and good statistical compositions with the data result.

The upflow C_3 expression is as follows:

$$C_3 = \max \left\{ \begin{array}{l} 0.5 \\ 2 \exp(-|Re_L|/300,000) \end{array} \right\} \quad (40)$$

¹ water and steam both flowing upwards.

A single C_3 expression covers the 2nd quadrant² and 3rd quadrant³ and the CCFL⁴ line. Only a portion of the original C_3 expression has been modified, C_3 , B_2 , and D_1 remain as designed in NSAC-139. The original NSAC-139 countercurrent/downflow C_3 expression is as follows:

$$C_3 = 2 \left(\frac{C_{10}}{2} \right)^{B_2} \quad (41)$$

$$C_{10} = 2 \exp \left\{ \frac{|\text{Re}_L|}{350,000} \right\}^{0.4} - 1.75 \{ |\text{Re}_L| \}^{0.03} \exp \left\{ \frac{-|\text{Re}_L|}{50,000} \left(\frac{D_1}{D_h} \right)^2 \right\} + \left(\frac{D_1}{D_h} \right)^{0.25} |\text{Re}_L|^{0.001} \quad (42)$$

where

$$B_2 = \left[\frac{1}{(1 + 0.05(|\text{Re}_L| / 350,000))} \right]^{0.4} \text{ and} \quad (43)$$

$$D_1 = \text{Normalizing diameter} = 0.0381 \text{ m}$$

For clarity, the revised expression for C_{10} is broken into the three constituent terms which are summed to form C_{10} .

$$C_{10}(\text{Term 1}) = 2 \exp \left\{ \frac{|\text{Re}_L| + Y}{350,000} \right\}^{0.4} \quad (44)$$

$$C_{10}(\text{Term 2}) = -1.7 \{ |\text{Re}_L| \}^{0.035} \exp \left\{ \frac{-|\text{Re}_L|}{(35,000 J_{Lrx} + 25,000)} \left(\frac{D_1}{D_h} \right)^2 \right\} \quad (45)$$

$$C_{10}(\text{Term 3}) = [0.26 J_{Lrx} + 0.85(1.0 - J_{Lrx})] \left(\frac{D_1}{D_h} \right)^{0.1} |\text{Re}_L|^{0.001} \quad (46)$$

where

$$Y = \begin{cases} 8.0^{(0.5D_1/D_h)} \text{Re}_G J_{Lrx} \exp \left\{ \frac{-10}{|\text{Re}_L|} \right\} & \text{in the 2}^{\text{nd}} \text{ Quadrant} \\ 0 & \text{in the 3}^{\text{rd}} \text{ Quadrant} \end{cases} \quad (47)$$

and

$$J_{Lrx} = \begin{cases} \left(1 - \frac{j_L}{j_{L(ccfl)}} \right)^Z & \text{in the 2}^{\text{nd}} \text{ Quadrant} \\ 1 & \text{in the 3}^{\text{rd}} \text{ Quadrant} \end{cases} \quad (48)$$

$j_{L(ccfl)}$ is the superficial liquid velocity at CCFL for vapour velocity j_G , and

² water flowing downwards and steam flowing upwards.

³ water and steam both flowing downwards.

⁴ counter current flow limit.

$$Z = \begin{cases} 0.8 & \text{for } \frac{j_L}{j_{L(ccfl)}} < 0.3 \\ 0.8 - \left(\frac{j_L}{j_{L(ccfl)}} - 0.3 \right) & \text{for } \frac{j_L}{j_{L(ccfl)}} \geq 0.3 \end{cases} \quad (49)$$

The new terms Y, Z, and J_{Lrx}^{rd} work together in the countercurrent quadrant to fit both the data and the CCFL line. In the 3rd quadrant, term 1 reduces to its original form and term 2 has only slight differences in the coefficients. The magnitude of Term 3 is small relative to the other two in the 3rd quadrant.

2.2. Countercurrent flow

For countercurrent flow, a large hydraulic diameter model is included to accommodate the behavior of the large diameter blowdown tests. The large diameter model is applicable when hydraulic diameter is greater than 0.3048 m (1 ft). A transition from the normal to the large diameter model is made from D_1 (0.0381 m/0.125 ft) to 0.3048 m. The following equations illustrate the large diameter model:

$$C_3 = \begin{cases} 0.6 X_T S + C_{3N} (1.0 - X_T) & \text{for } 0.3048\text{m} > D_h > D_1 \\ \left[0.6 - 0.27 \left(\frac{D_h - 0.3048}{0.3048} \right) \right] \times S & \text{for } 0.9144\text{m} > D_h \geq 0.3048\text{m} \\ 0.06S & \text{for } D_h \geq 0.9144\text{m} \end{cases} \quad (50)$$

where

C_{3N} = the normal C_3 as defined by Eq. (41)

$$S = J_{Lrx} + (1.0 - J_{Lrx}) \left(\frac{D_h}{D_1} \right)^{0.5}, \text{ and}$$

$$X_T = (D_h - D_1) / (0.3048 - D_1)$$

2.3 Horizontal flow

For horizontal flow only cocurrent flows are considered. The drift velocity for horizontal flow, V_{gjh} , is evaluated with Eq. 29, using positive values of the volumetric fluxes.

3. Units

The correlation is the same in either British or SI units. C_o has no units and V_{gj} has the units of a velocity and should be consistent with the units used for the volumetric flux.

Appendix XVI

MISCELLANEOUS EMPIRICAL CORRELATIONS FOR VOID FRACTION

Thom (1964)

$$\alpha = \gamma x / \{1 + x(\gamma - 1)\} \quad (1)$$

γ is a constant at any pressure and assumes the following values for water.

P (bar)	1.014	17.24	41.38	86.21	144.83	206.9	221.1
γ	246.0	40.0	20.0	9.8	4.95	2.15	1.0

Martinelli-Nelson (1948)

$$\alpha = \frac{C\sqrt{x}}{(1-x) + C\sqrt{x}} \quad (2)$$

where

$$C = (\rho_L / \rho_G)^{0.5}$$

Baroczy (1966)

Baroczy has expressed in graphical form, the void fraction as a function of the Martinelli parameter, χ_{tt} , and the property index:

$$\chi_{tt} = \left(\frac{1-x}{x} \right)^{0.9} \left(\frac{\rho_G}{\rho_L} \right)^{0.5} \left(\frac{\mu_L}{\mu_G} \right)^{0.1} \quad (3)$$

Based on these graphs Marinelli and Pastori (1973) have obtained the following best fit equation valid only for 70 kg/cm²

$$\alpha = 0.1800285 + 4.2049x - 11.523x^2 + 14.856x^3 - 6.7624x^4 \quad (4)$$

Appendix XVII

COMPILATION OF DATA

The compiled data are shown in Tables XVII.I, XVII.II, XVII.III and XVII.IV respectively for pressure drop, void fraction, flow pattern and flow pattern specific pressure drop.

TABLE XVII.I. TWO-PHASE FLOW PRESSURE DROP DATA — A COMPILATION

Author (year)	Test sec- tion	Flow direc- tion	adiabatic/ diabatic	Forced/ Natural	Fluid used	No. of Data pts.	Hydra- ulic- dia (mm)	Pres- sure range (MPa)	Mass Flux (kg/ m ² s)	Quality range
Adorni (1961)	A	V-U	adiabatic	forced	S-W	97	3.23	6.83- 7.07	961- 3799	0.0- 0.75
-do-	A	V-U	diabatic	forced	S-W	376	3.23	6.83- 7.58	976- 3828	0.0- 0.85
Hoglund (1958)	P	V-U	diabatic	natural	S-W	87	11.65	1.14- 4.24	717- 935	0.01- 0.065
Hashizume (1983)	P	H	adiabatic	natural	R-12	85	10.0	0.57- 1.22	88- 354	0.1- 0.81
Hashizume (1983)	P	H	adiabatic	natural	R-22	85	10.0	0.92- 1.96	88- 354	0.08- 0.81
Cicchitti (1960)	P	V-U	adiabatic	forced	S-W	52	5.1	2- 7.8	2000- 6000	0.05- 0.8
Cicchitti (1960)	P	V-U	diabatic	forced	S-W	18	5.1	3.6- 5.2	2200- 4000	0.4- 0.7
Janssen (1964)	P	V-U	adiabatic	forced	S-W	37	19.7& 11.1	4.1- 9.6	271- 1492	0.09- 0.9
Janssen (1964)	P	H	adiabatic	forced	S-W	65	18.8, 24.3 &32.3	4.1- 9.6	271- 2306	0.09- 0.9
Janssen (1964)	P	V-D	adiabatic	forced	S-W	37	24.3	4.1- 9.6	271- 1492	0.09- 0.9
Janssen (1964)	RC	V-U	adiabatic	forced	S-W	67	19.7& 11.1	4.1- 9.7	678- 2848	0.02- 0.99
Janssen (1964)	RC	V-U	adiabatic	forced	S-W	87	19.7& 11.1	4.1- 7.0	678- 2848	0.05- 0.92
Janssen (1964)	RC	V-U	adiabatic	forced	S-W	26	19.7&	4.1- 6.9	271- 2848	0.02- 0.79

TABLE XVII.I. (CONT.)

Author (year)	Test sec- tion	Flow direc- tion	adiabatic/ diabatic	Forced/ Natural	Fluid used	No. of Data pts.	Hydra- ulic- dia (mm)	Pres- sure range (MPa)	Mass Flux (kg/ m ² s)	Quality range
Lahey (1970)	RB	V-U	diabatic	forced	S-W	36	12.0	7.0	271- 2984	0.03- 0.45
Steiner (1988)	P	H	adiabatic	forced	R-12	158	14.0	0.15- 0.31	50- 240	0.1- 0.81
Berkowitz (1960)	P	V-U	diabatic	forced	S-W	920	5.2- 10.1	4- 8.36	1044- 4088	0.018- 0.97
Adorni (1966)	RB	V-U	diabatic	forced	S-W	314	5.07- 11.61	5- 6.96	80- 3800	0.0- 0.5
CISE (1963)	P	V-U	adiabatic	forced	S-W	525	5.2- 10.1	4- 7.06	1038- 4398	0.018- 0.8
CISE (1963)	A	V-U	adiabatic	forced	S-W	280-	3.23- 7.0	6.8- 7.13	961- 4570	0.001- 0.836
CISE (1963)	A	V-U	diabatic	forced	S-W	843	3.23- 7.0	6.8- 7.58	976- 4581	0.0- 0.98
Marchat (1956)	RC	V-U	diabatic	natural	S-W	30	16.23	0.79- 4.24	366- 500	0.019- 0.461
Cook (1956)	RC	V-U	diabatic	natural	S-W	62	16.23	4.23	173- 443	0.016- 0.087
Moeck (1970)	A	V-U	diabatic	forced	S-W	972	4.06	3.47- 7.25	150- 3350	0.066- 0.69
Vijayan (1981)	P	V-U	diabatic	forced	S-W	22	6.2	7.2	2740- 4044	0.01- 0.28

P - Pipe; A - Annulus; RC - rectangular channel; RB - rod bundle; V-U - vertical upward; V-D - vertical downward; H - horizontal; S-W - steam-water; R-12 - Refrigerant-12; R-22 - Refrigerant-22.

TABLE XVII.II. DETAILS OF STEAM-WATER VOID FRACTION DATA

Author (year)	Test sec- tion	Flow direc- tion	adiabatic/ diabatic	Forced/ Natural	Fluid used	No. of Data pts.	Hydra- ulic- dia (mm)	Pres- sure range (MPa)	Mass Flux (kg/ m ² s)	Quality range
Rouhani (1963)	P	V-U	diabatic	forced	S-W	149	6.1	0.7- 6.0	650- 2050	0.0- 0.38
Merchattere (1956)	RC	V-U	diabatic	natural	S-W	675	16.2	0.8- 4.3	360- 502	0.082- 0.0
Cook et al. (1956)	RC	V-U	diabatic	natural	S-W	1077	19.9	4.2	173- 457	0.0- 0.141
Petrack (1962)	P	V-U	diabatic	forced	S-W	108	49.3	4.1- 10.3	163- 1256	0.0- 0.11
Merchattere (1960)	RC	V-U	diabatic	natural	S-W	292	11.3	1.12- 4.23	490- 1112	0.0- 0.076
Merchattere (1960)	RC	V-U	diabatic	forced	S-W	237	11.3	1.12- 4.23	490- 1455	0.0- 0.0.65
Merchattere (1960)	RC	V-U	diabatic	natural	S-W	567	20.3	1.12- 4.23	289- 744	0.0- 0.076
Rouhani (1966)	A	V-U	diabatic	forced	S-W	535	13.0	1.0- 5.0	650- 1450	0.0- 0.12

A — Annulus; V-U — vertical upward; S-W — steam-water; P — pipe; RC — Rectangular Channel.

TABLE XVII.III. DETAILS OF THE FLOW PATTERN DATA COMPILED FOR STEAM-WATER

Author	Test section Geometry	Pressure (MPa)	hydraulic dia.(mm)	Method of identification of flow pattern	No. of data points
Bennett et. al. (1965)	Tube	3.44 & 6.9	12.638	High speed cine- photography x- ray photography	109
Hosler (1967)	Rectangular channel	1.034 to 13.79	6.003	High speed photography	683
Griffith (1963)	Tube	1.483 to 2.862	9.525 to 22.225	Electrical resistance probe	344
Suo et al. (1965)	Tube	6.9	10.16	Electrical resistance probe	67
Janssen & Kerivinen (1971)	Tube	7	17.06	Electrical conductance probe	94
Peterson & Williams (1975)	Rod bundle	2.758 to 13.79	7.06	Visual observations	98
Bergles et al. (1965a)	Tube	3.45	101.6	Electrical resistance probe	56
Bergles et al. (1965b)	Tube	3.45 & 6.89	9.652	Electrical resistance probe	65
Bergles et al. (1965c)	Tube	6.89	10.31	Electrical resistance probe	55
Bergles et al. (1968a)	Tube	3.45 & 6.89	20.93	Electrical resistance probe	88
Bergles et al. (1968b)	Rod bundle	6.89	14.2	Electrical resistance probe	301
Tippets (1962)	Rectangular channel	6.9	20.6	High speed motion picture	25

TABLE XVII.IV. COMPILATION OF FLOW PATTERN SPECIFIC PRESSURE DROP DATA

Author (year)	Test sec- tion	Flow direc- tion	adiabatic/ diabatic	Forced/ Natural	Fluid used	No. of Data pts.	Hy- draulic- dia (mm)	Pres- sure range (MPa)	Mass Flux (kg/ m ² s)	Quality range
Hashi-Zume (1983)	P	H	adiabatic	natural	R-12	78	10	0.57- 1.22	80- 320	0.1- 0.8
Hashi-Zume (1983)	P	H	adiabatic	natural	R-22	78	10	0.92- 1.96	80- 320	0.1- 0.8
Steiner C (1979)	P	H	adiabatic	forced	R-12	136	10	0.151- 0.309	80- 320	0.1- 0.8
Suo et al. (1965)	P	V-U	adiabatic	forced	S-W	68	10.2	6.89	510- 2800	0.01- 0.322
Zhao & Rezkallah (1994)	P	V-U	adiabatic	forced	A-W	53	9.7	0.1	-	-
Tutu (1982)	P	H	adiabatic	forced	A-W	8	52.2	0.1	-	-
Hewitt& Owen (1992)	P	V-U	adiabatic	forced	A-W	42	31.8	0.24	300- 460	-
Lahey & Lee (1992)	P	V-U	adiabatic	forced	A-W	16	57	0.1	-	-
Lahey & Lee (1992)	P	V-D	adiabatic	forced	A-W	16	57	0.1	-	-

V-U — vertical upward; V-D — vertical downward; H — horizontal; S-W — steam-water; R-12 — Refrigerant-12; R-22 — Refrigerant-22; P — pipe.

Appendix XVIII

DETAILED RESULTS OF ASSESSMENT OF VOID FRACTION CORRELATIONS

The assessment was carried out by standard statistical procedure. The error (e_i), mean error (\bar{e}), mean of absolute error ($|\bar{e}|$), R.M.S. error (e_{rms}) and standard deviation (σ) are calculated as follows:

$$e_i = \frac{\alpha_c - \alpha_m}{\alpha_m} \times 100 \quad (1)$$

where

the subscripts c and m refer to calculated and measured values respectively.

$$\bar{e} = \frac{1}{N} \sum_{i=1}^N e_i \quad (2)$$

$$|\bar{e}| = \frac{1}{N} \sum_{i=1}^N |\bar{e}_i| \quad (3)$$

$$e_{rms} = \left(\frac{\sum_{i=1}^N e_i^2}{N} \right)^{0.5} \quad (4)$$

$$\sigma = \left(\frac{\sum_{i=1}^N (\bar{e} - e_i)^2}{N - 1} \right)^{0.5} \quad (5)$$

Table XVIII.I shows the range of parameters of the data used for the assessment which formed a part (about 3292 data points) of the TPFDB data bank. The data used for the assessment was screened by deleting those data with predicted errors exceeding $\pm 100\%$ by any of the four correlations [i.e. Chexal-Lellouche, Rouhani, Modified Smith (modified by Mochizuki and Ishii) and Hughmark]. Number of data points deleted is about 2.7% of the total data in the original data bank. It is found that the erroneous data are not concentrated in a single dataset but present in almost all the datasets used in this data bank.

TABLE XVIII.I. RANGE OF PARAMETERS OF VOID FRACTION DATA USED FOR ASSESSMENT

Parameter	Minimum	Maximum
Quality (%)	0.01	22
Mass-Flux (kg/m ² s)	125	2950
Hydraulic Diameter (mm)	10	38
Measured Void fraction (%)	40	90
Pressure (bar)	7	51

From the frequency distribution given in Figures XVIII.I to XVIII.III only the Modified Smith correlation shows a skewness towards the negative side (Fig. XVIII.III) which indicates an underprediction to some extent. A comparison of the measured and predicted void fractions are given in Figures XVIII.IV to XVIII.VI which show predicted void fraction, α_c to be consistently more than the measured void fraction α_m except in the case of modified Smith correlation. For the modified Smith correlation, the predictions are more or less evenly distributed around the zero line. It may be noted that while Chexal-Lellouche and Rouhani are drift flux models, Hughmark is a $k\beta$ model and Modified Smith correlation is a slip ratio based model.

Assessment of correlations for the limiting conditions:

Void fraction correlations have to satisfy the following limiting conditions:

- (1) As x tends to 0, α tends to 0 (lower limiting condition)
- (2) As x tends to 1, α tends to 1 (upper limiting condition)
- (3) As P tends to P_{crit} , α tends to x (critical limiting condition).

To check for the compliance of the correlations with the lower and upper limiting conditions, void fractions predicted by different correlations are studied over a wide range of mass fluxes and pressures for $x = 0$ and $x = 1$. In order to allow for the round-off errors and approximations made in the computation of void fractions using various correlations, the following allowances are made to the limiting conditions. It is assumed that a correlation satisfies the limiting conditions if it satisfies the following conditions:

- (1) At $x = 0.000001$, α is less than 0.001 (approximation of lower limiting condition)
- (2) At $x = 1$, α is greater than 0.999 (approximation of upper limiting condition)
- (3) At $P = 218.3$ bar, Maximum deviation of predicted void fraction from the mass quality.

over the entire range of mass flux, *i.e.* 0 to 10 000 kg/m²s, is less than 1% (approximation of critical limiting condition).

The results of the observations are listed in Table XVIII.II.

TABLE XVIII.II. LIMITING CONDITIONS

Correlation	$G \leq 100.0 \text{ kg/m}^2\text{s}$			$G > 100.0 \text{ kg/m}^2\text{s}$		
name	$at\ x = 0;$ $\alpha = 0$	$at\ x = 1;$ $\alpha = 1$	$at\ P=P_{cr};$ $\alpha = x$	$at\ x = 0;$ $\alpha = 0$	$at\ x = 1;$ $\alpha = 1$	$at\ P=P_{cr};$ $\alpha = x$
Chexal et al. (1996)	yes	no	yes for $G > 10$	yes	yes for G > 140	yes
Modified Smith	yes	yes	yes	yes	yes	yes
Rouhani	yes	yes	no	yes	yes	yes for G > 2050
Zuber- Findlay	yes	no	no	yes	no	no
Bankoff	yes	no	yes	yes	no	yes
Bankoff- Jones	yes	yes	yes	yes	yes	yes
GE-Ramp	yes	yes for $G > 10$	no	yes	yes	no
Bankoff- Malnes	yes	yes	no	yes	yes	no
Homogene- ous model	yes	yes	yes	yes	yes	yes
Martinelli- Nelson	yes	yes	no	yes	yes	no
Hughmark	yes	no	no	yes	no	no
Osmachkin - Borisov	yes	yes	yes	yes	yes	yes
Thom	yes	yes	no	yes	yes	no
Nabizadeh	yes	no	no	yes	no	no
Armand	yes	yes	no	yes	yes	no
Dix	yes	no	no	yes	no	no

It is observed that the homogeneous model and the slip ratio based models satisfy all the three limiting conditions for all mass fluxes. Among the top four correlations only the modified Smith correlation satisfies all the three limiting conditions. The Chexal-Lellouche correlation satisfies all the three limiting conditions for $G > 140 \text{ kg/m}^2\text{s}$ whereas Rouhani correlation satisfies all the three limiting conditions only for $G > 2000 \text{ kg/m}^2\text{s}$. From these considerations, the Chexal-Lellouche and the modified Smith correlations may be used in computer codes for reactor analysis.

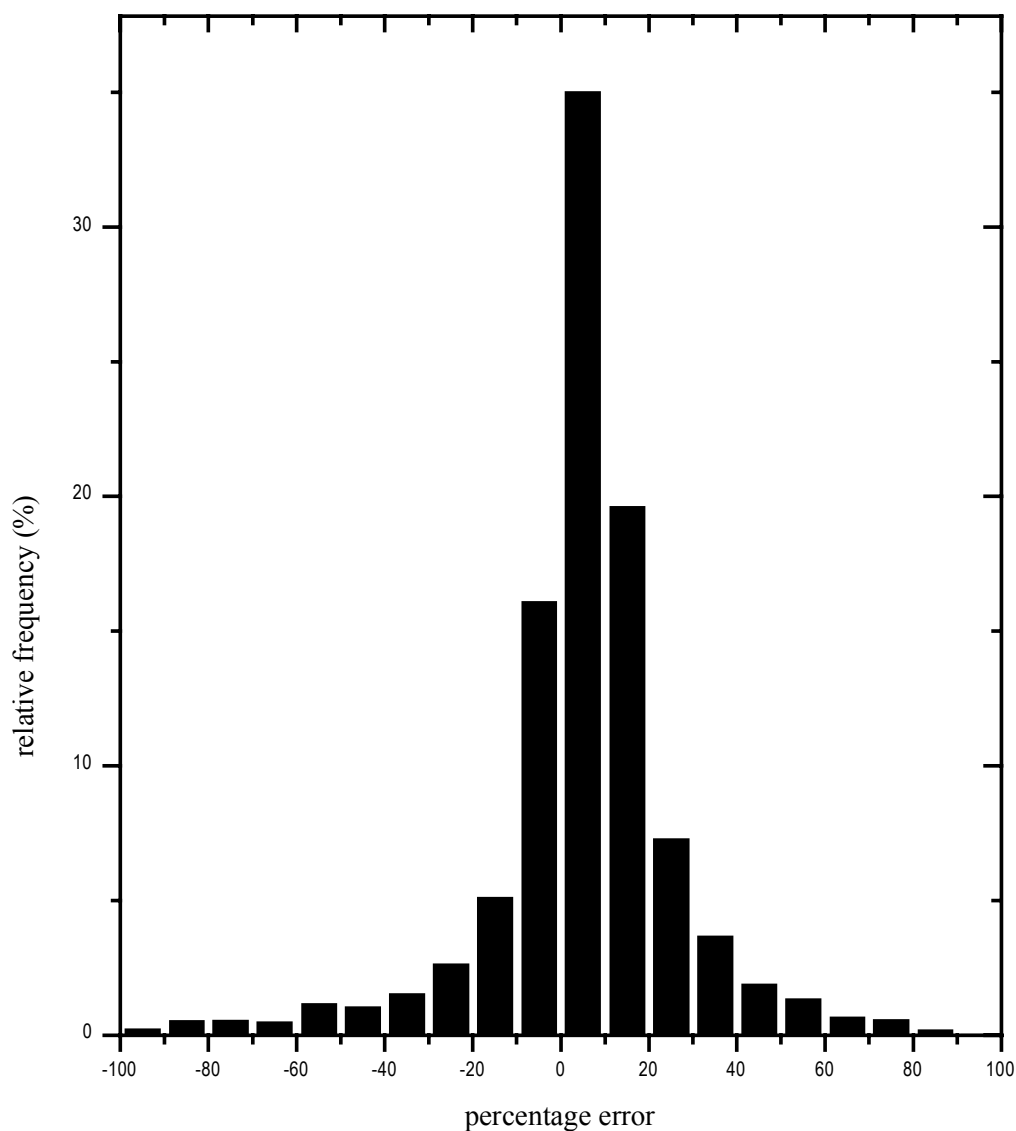


FIG. XVIII.1. Error distribution in predicted void fractions using Chexal-Lellouche correlation.

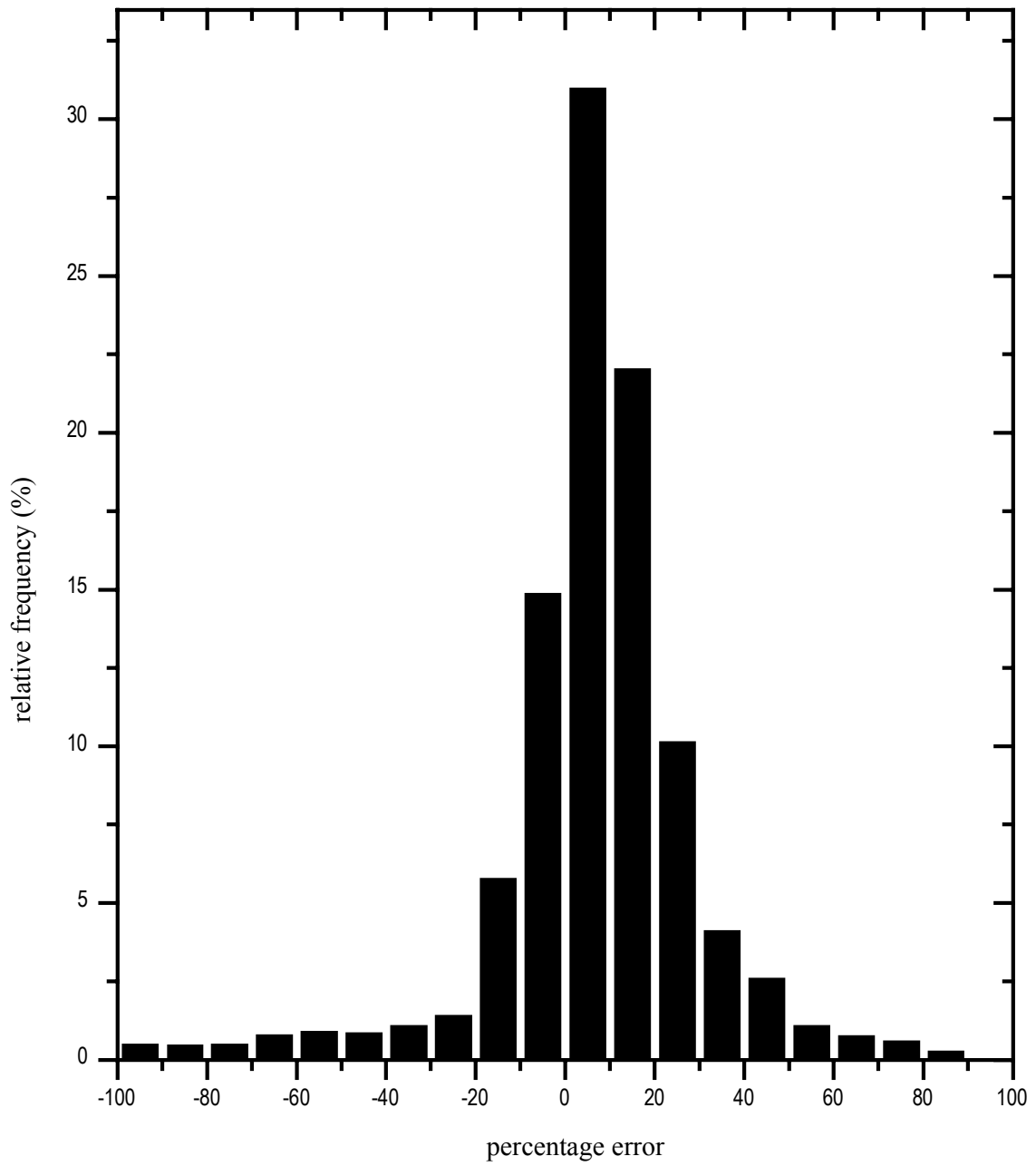


FIG. XVIII.II. Error distribution in predicted void fractions using Hughmark correlation.

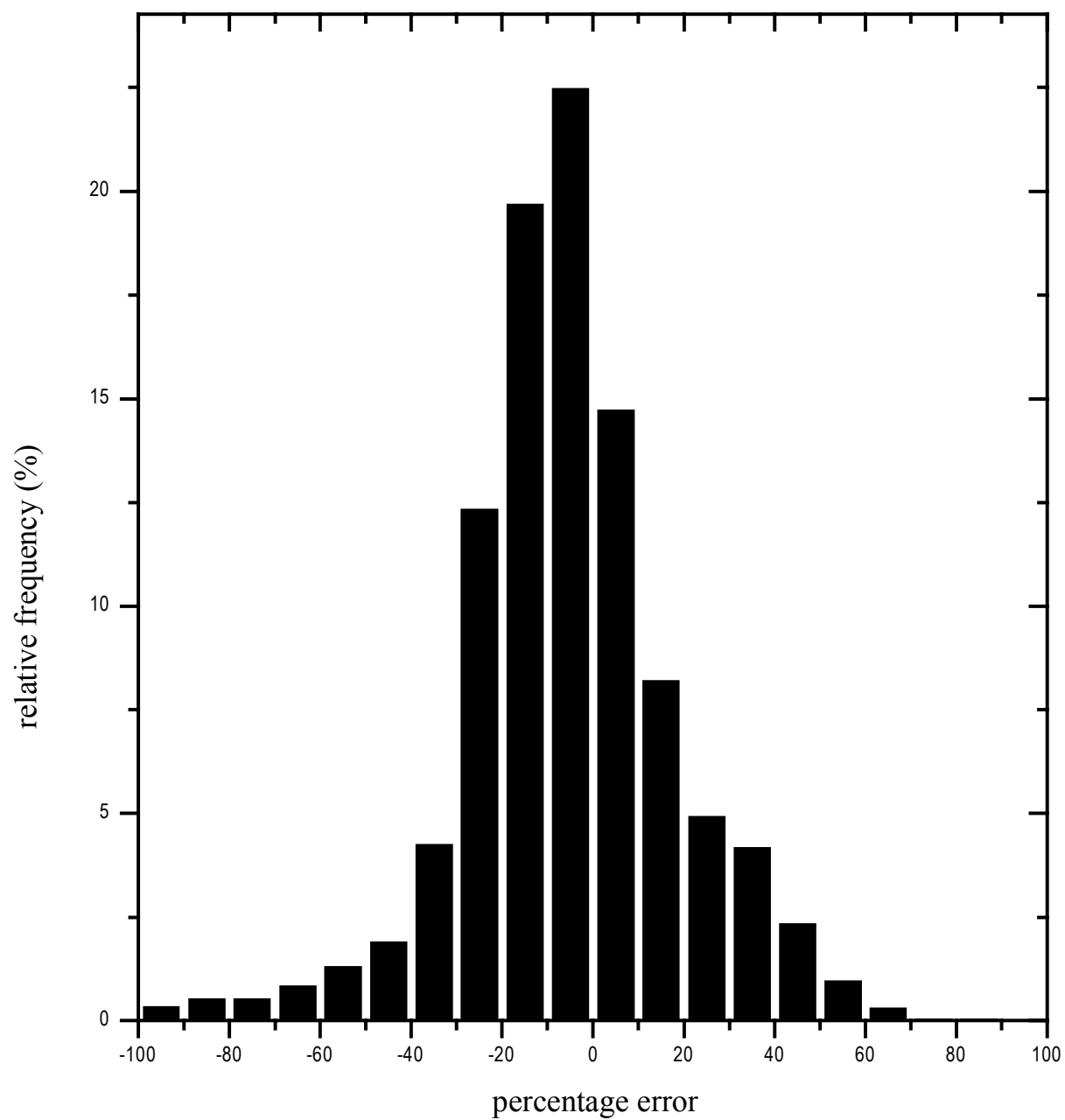


FIG. XVIII.III. Error distribution in predicted void fractions using modified Smith correlation.

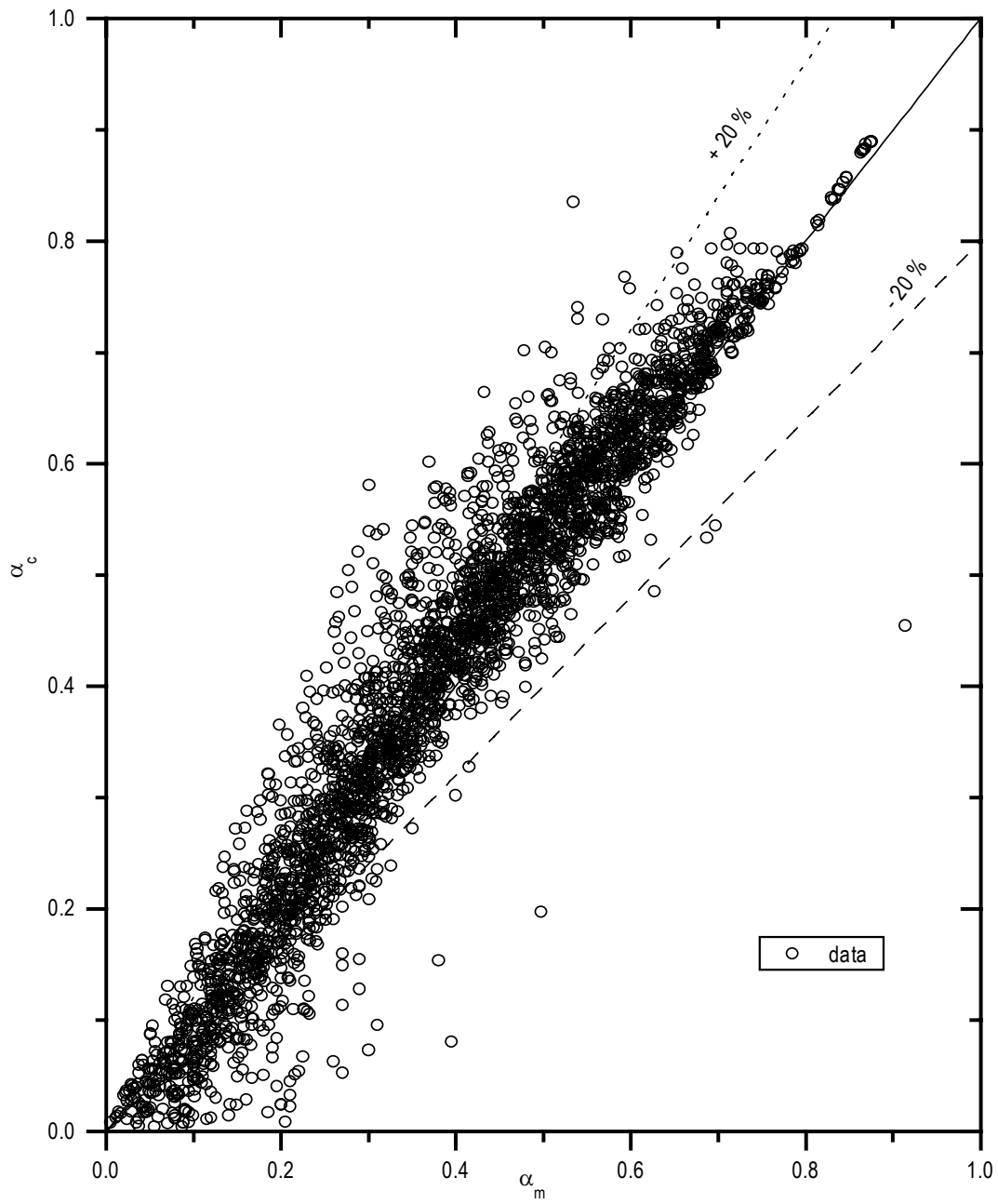


FIG.

XVIII.IV. Comparison of measured and predicted void fractions using Chexal-Lellouche correlation.

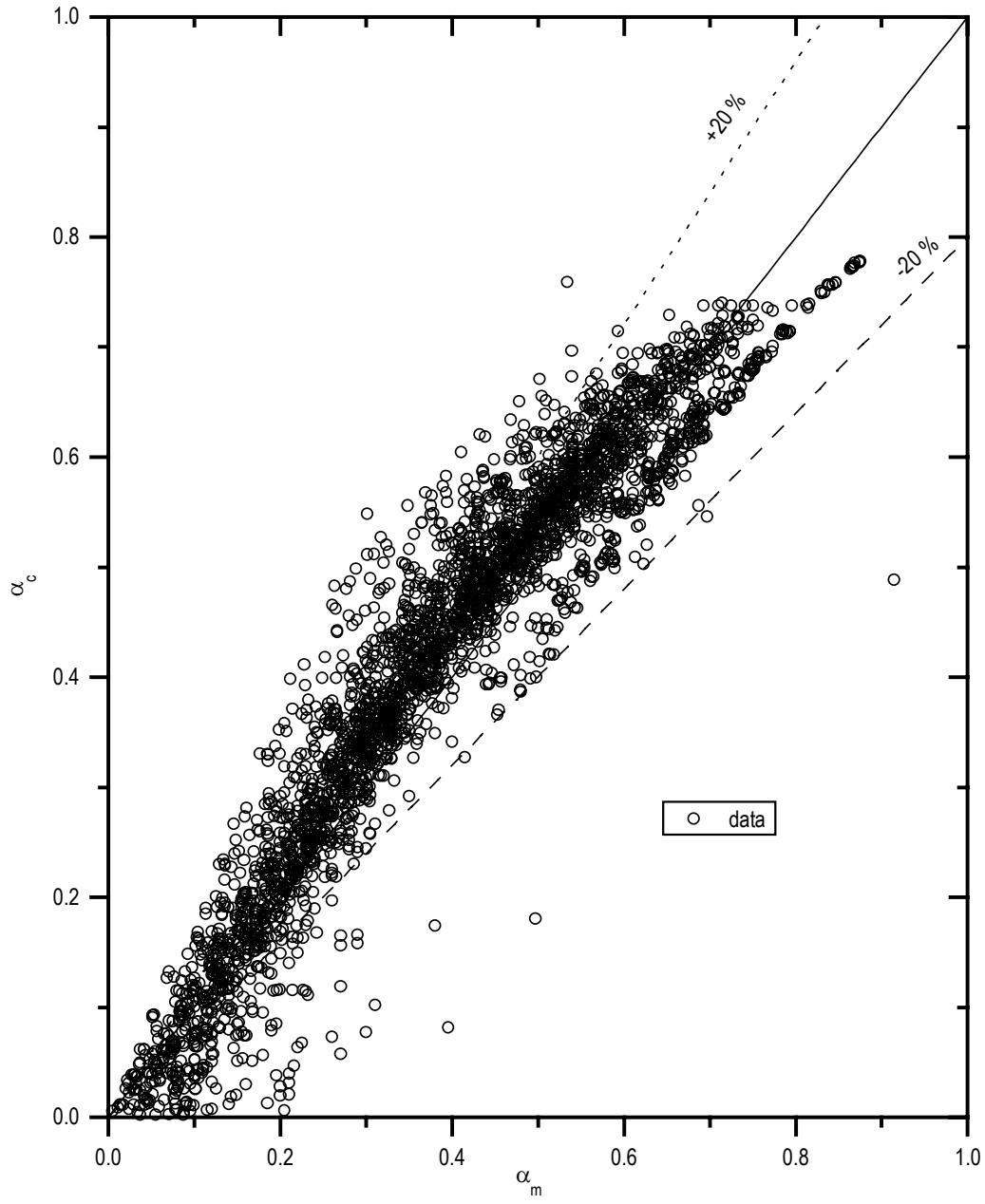


FIG. XVIII.V. Comparison of measured and predicted void fraction using Hughmark correlation.

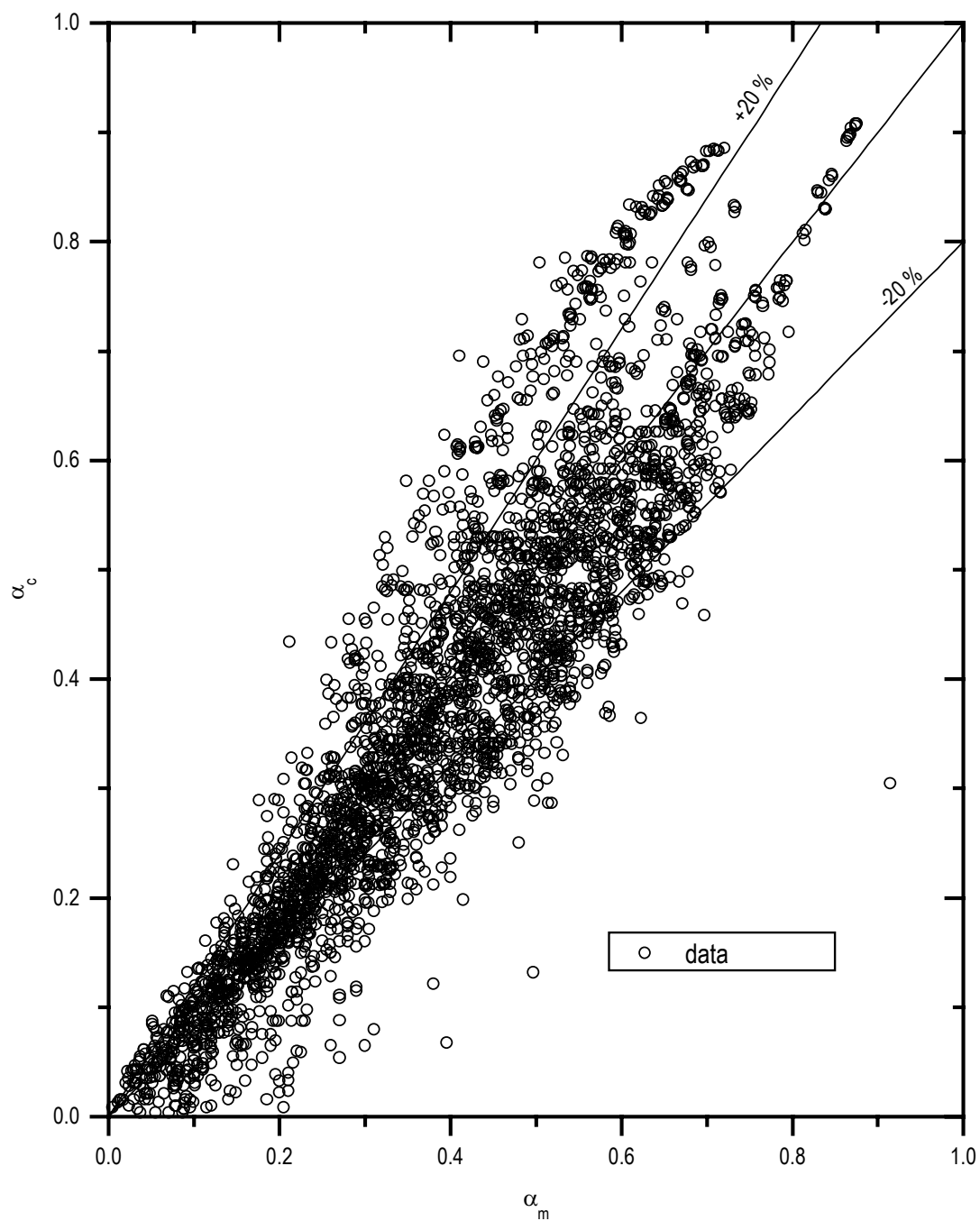


FIG. XVIII.VI. Comparison of measured and predicted void fractions using modified Smith correlation.

Appendix XIX

DETAILED RESULTS OF ASSESSMENT OF FLOW PATTERN DATA

The criteria proposed by Taitel et al. (1980), Mishima and Ishii (1984) and Solbrig (1986) are given in Tables XIX.I and XIX.II for bubbly-slug and slug-annular transitions respectively. The bubbly-slug criteria proposed by Taitel et al. consists of three criteria designated as Taitel et al. I, II and III. Taitel et al. III is an upper limit beyond which bubbly flow cannot exist whereas criterion II demarcates dispersed bubbly and slug flow.

Only Solbrig has provided a criterion for slug-annular transition. His recommended criterion is Solbrig I. However, Solbrig also discusses another criterion denoted as Solbrig II in Table XIX.II. Mishima and Ishii have proposed two different criteria for the transition to annular flow. The criterion corresponding to annular flow with entrainment is considered here for assessment. Taitel et al. proposed an upper limit of j_G beyond which only annular flow is possible.

1. Comparison of the various transition criteria

Figure XIX.I shows a comparison of the criteria for bubbly-slug and slug-annular transitions in j_G - j_L plane. Corresponding plots in α - j_R plane is shown in Fig. XIX.II. The following observations can be made from these figures:

- (i) The bubbly — slug transition criteria proposed by Taitel et al. and Mishima-Ishii are close to each other.
- (ii) Both Taitel et al. and Mishima-Ishii criteria for transition to annular flow are found to be independent of the liquid superficial velocity (Fig. XIX.I). While Mishima-Ishii suggest that the criterion for annular flow transition should not be extended beyond the j_L value corresponding to bubbly- slug transition, no such upper limit is specified by Taitel et al. Plotting these criteria in α - j_R plane (Fig. XIX.II) shows that at higher values of j_L the void fraction can go below that specified for bubbly to slug transition. This suggests that an upper limit of j_L needs to be specified for this criterion although no such limit is specified by Taitel et al. and Mishima-Ishii.

2. Data used for assessment of flow pattern maps

For assessment, a part of the flow pattern data contained in TPFDB data bank was used. Currently, this data bank consists of 811 bubbly, 818 slug and 762 annular flow points. In addition, it has 64 bubbly-slug and 62 slug-annular transition data points (Table XIX.III). It consists mainly of steam-water flow data at reasonably high pressure (>10 bar). Some refrigerant and air-water data are also included in the data bank. The data bank includes flow pattern data for diabatic and adiabatic two-phase flow. The range of parameters of the flow pattern data for vertical upward flow are given in Table XIX.IV. Since the amount of dispersed bubbly flow data in the present data bank are very few Taitel et al. criterion I only is considered for the assessment.

TABLE XIX.I. BUBBLY FLOW TO SLUG FLOW TRANSITION CRITERIA

Author	Criteria in j_G - j_L plane	Criteria in α - j_R plane
Taitel et al. I	$j_L = 3j_G - 1.15 [g(\rho_L - \rho_G)\sigma/\rho_L^2]^{1/4}$	$\alpha = 0.25$
Taitel et al. II	$j_L + j_G = 4 \left\{ \frac{D^{0.429} (\sigma / \rho_L)^{0.089} \left[\frac{g(\rho_L - \rho_G)}{\rho_L} \right]^{0.446}}{\nu_L^{0.072}} \right\}$	$\alpha = 0.25 - 0.52$
Taitel et al. III	$j_G = 1.083 j_L$	$\alpha = 0.52$
Mishima-Ishii	$j_L = (3.33 / C_0 - 1)j_G - (0.76 / C_0)(\sigma g \Delta \rho / \rho_L^2)$ $C_0 = 1.2 - 0.2(\rho_G / \rho_L)^{1/2}$ for round tubes $C_0 = 1.35 - 0.35(\rho_G / \rho_L)^{1/2}$ for rectangular tubes	$\alpha = 0.3$
Solbrig	$j_G = 1.083 j_L$	$\alpha = 0.52$

TABLE XIX.II. CRITERIA FOR TRANSITION TO ANNULAR FLOW

Author	Transition criterion
Taitel-Dukler	$\frac{j_G \rho_G^{0.5}}{\left[\sigma g (\rho_L - \rho_G)^{0.25} \right]} = 3.1$
Mishima-Ishii	$j_G = \left\{ \frac{\sigma g \Delta \rho}{\rho_G^2} \right\}^{0.25} N_{\mu L}$ $N_{\mu L} = \frac{\mu_L}{\left\{ \rho_L \sigma g \left(\frac{\sigma}{g \Delta \rho} \right)^{0.5} \right\}^{0.5}}$ <p>for annular flow with entrainment</p>
Solbrig I	$\alpha = \pi/4$
Solbrig II	$\alpha = 2/3$

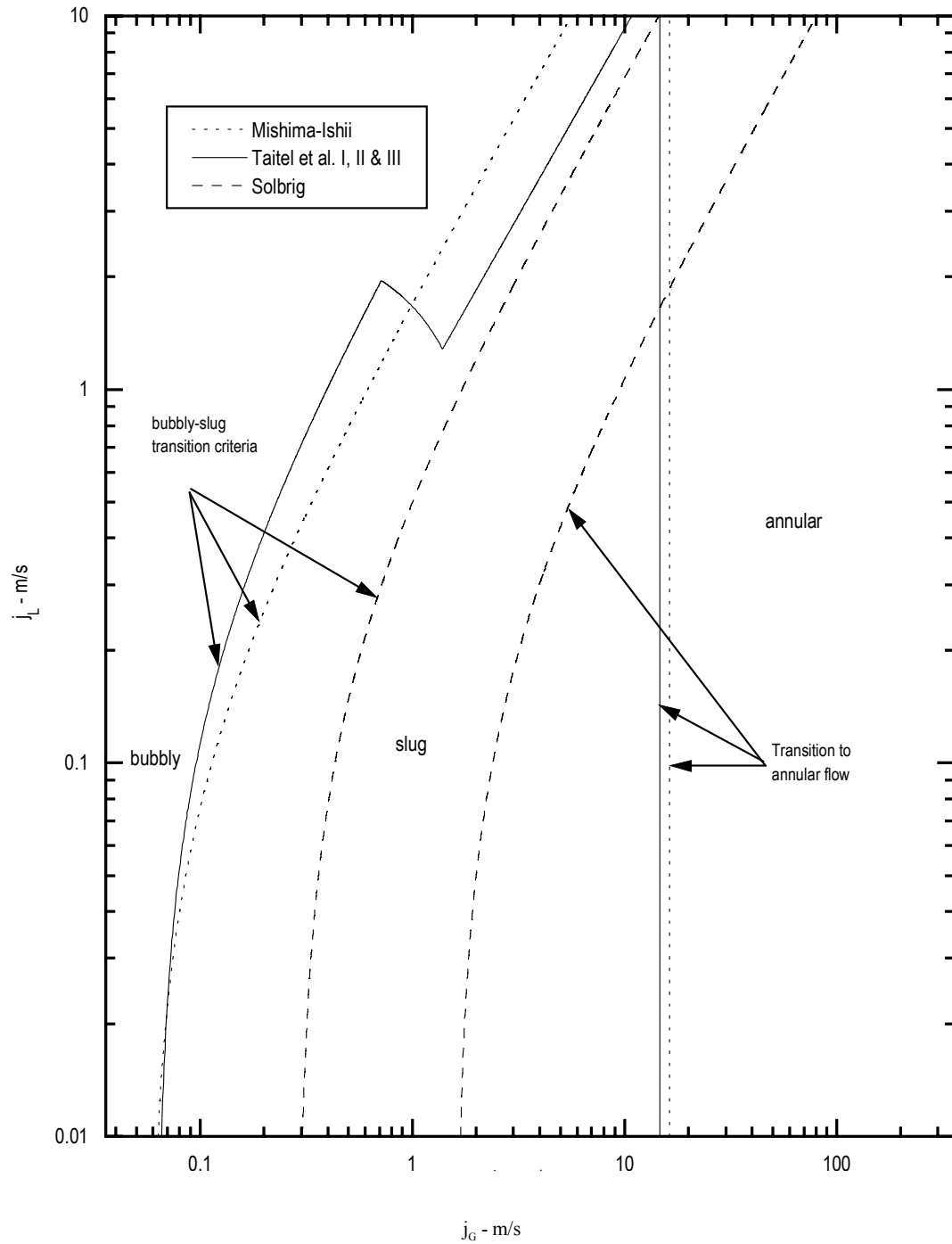


FIG. XIX.I. Comparison of the various flow pattern maps for air-water flow at 25 °C in a 25.4 mm i.d. tube.

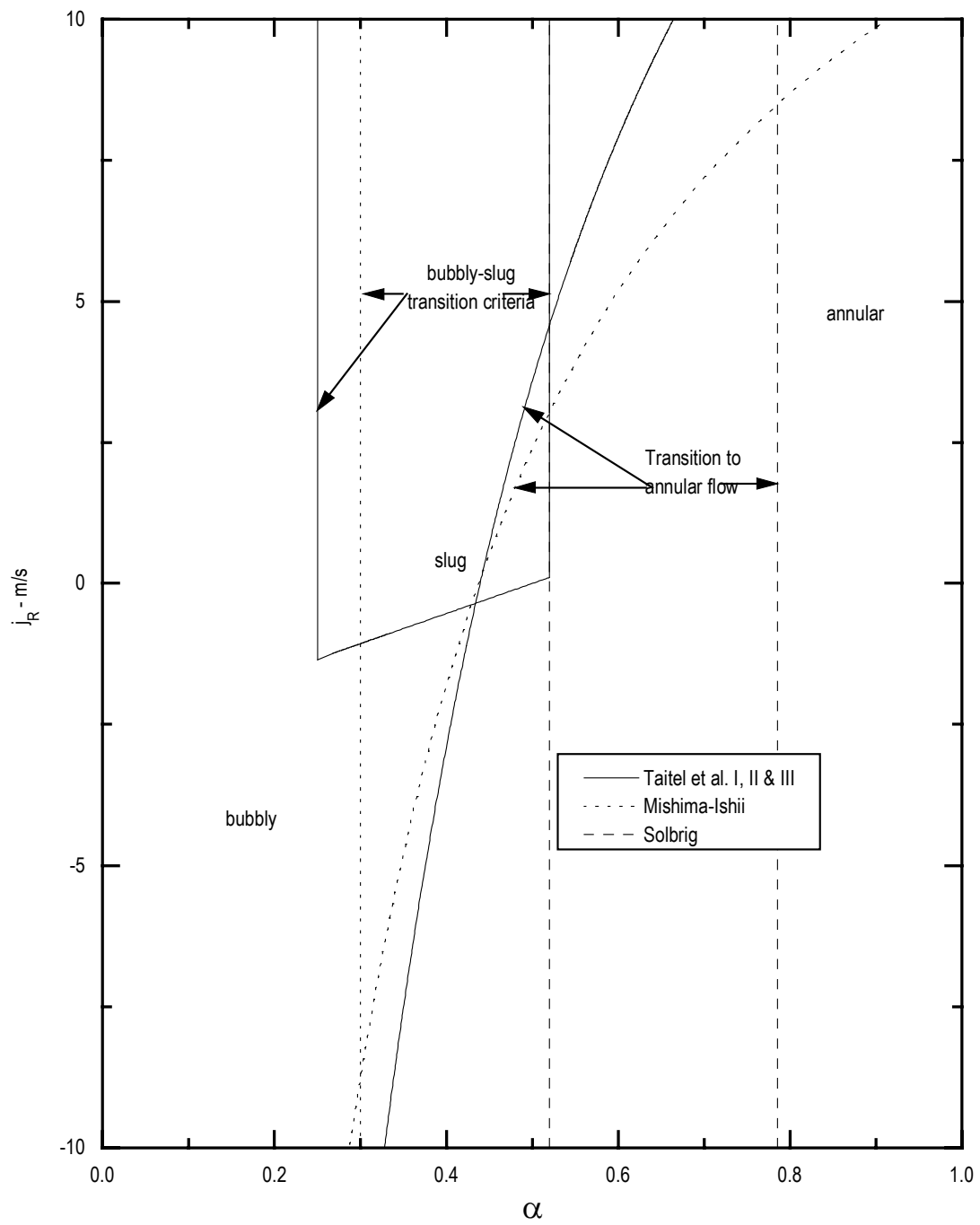


FIG. XIX.II. Comparison of the different flow pattern maps for air-water flow at 25°C and 0.1 MPa in a 25.4 mm i.d. tube.

TABLE XIX.III. FLOW PATTERN DATA

Geo- metry	Fluid	Flow Pattern													
		B	B-S	S	C	S - A	A	A - W	W - A	F	D - B	F - A	B - A	B - F	T
tube	Air Water	157	-	106	74	7	49	-	24	-	5	-	-	-	422
tube	Steam Water	84	28	303	13	26	366	22	31	34	-	2	51	4	863
tube	R-12	68	-	181	-	-	94	-	-	-	-	-	-	-	343
Rectan gular channel	Steam Water	413	-	158	-	-	222	-	-	-	-	-	-	-	793
Rod Bundle	Steam Water	89	36	70	-	29	31	10	-	36	-	-	-	-	301
Total	-	811	64	818	87	62	762	32	55	70	5	-	-	-	2822

B: bubbly flow; B-S: bubbly to slug transition; S: slug flow; C: churn flow; S-A: slug to annular transition; A: annular; AW: annular wavy; WA: Wispy annular; F: froth; DB: dispersed bubble; F-A: froth to annular transition; B-A: bubbly to annular transition; B-F: bubbly to froth transition; T: total data points.

TABLE XIX.IV. RANGE OF PARAMETERS FOR FLOW PATTERN DATA

Serial No.	Parameter	Range
1	pressure (MPa)	0.1–14
2	mass flux ($\text{kg/m}^2\text{s}$)	50–5000
3	hydraulic diameter (mm)	5–51
4	quality (fraction)	–0.03–0.5
5	j_L (m/s)	0.05–11
6	j_G (m/s)	0.0–80
7	fluid used	water, R-12 and air-water
8	geometry of test section	round tubes, rectangular channels and rod bundles

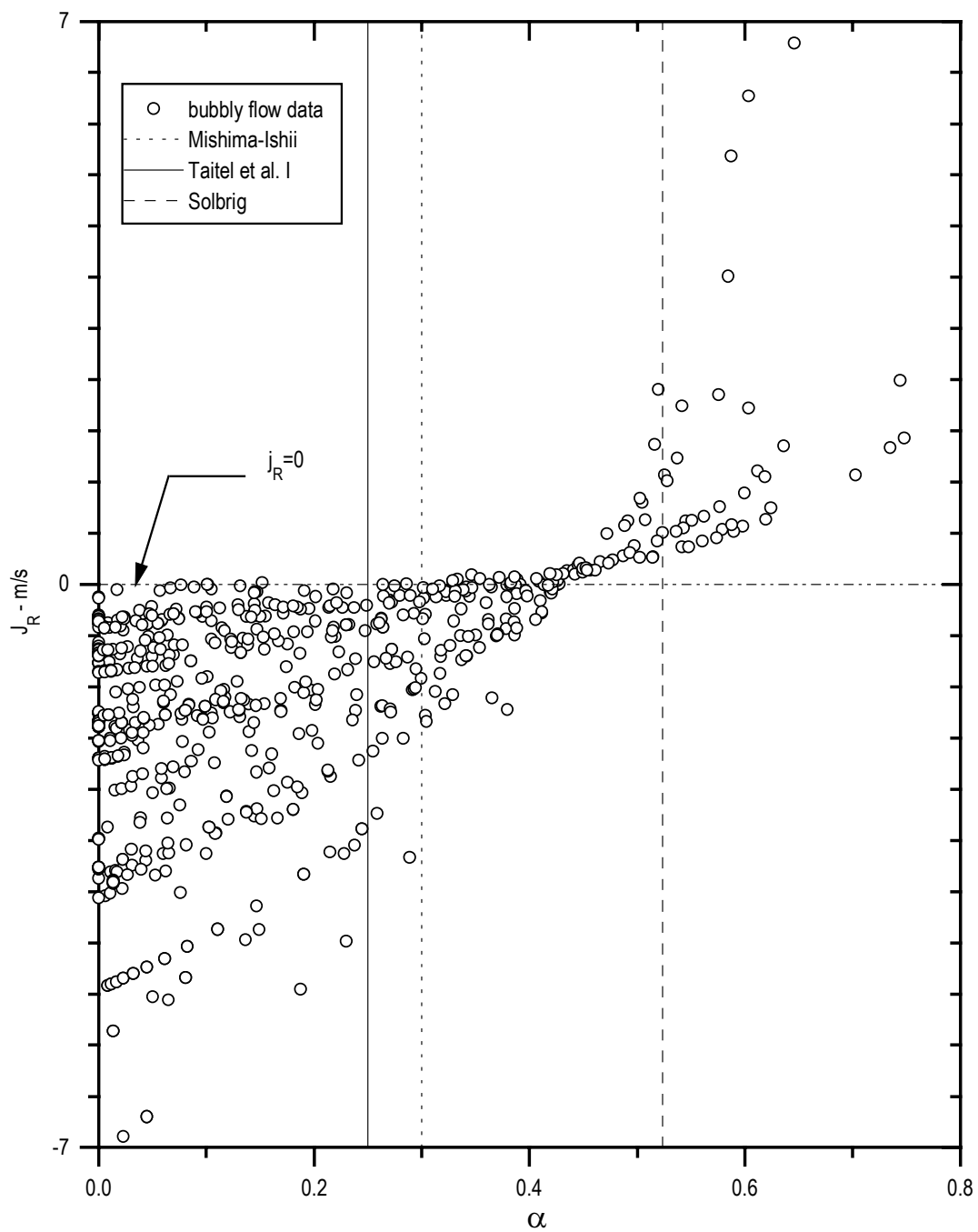


FIG. XIX.IIIa. Comparison of bubbly flow data with various bubbly-slug transition criteria.

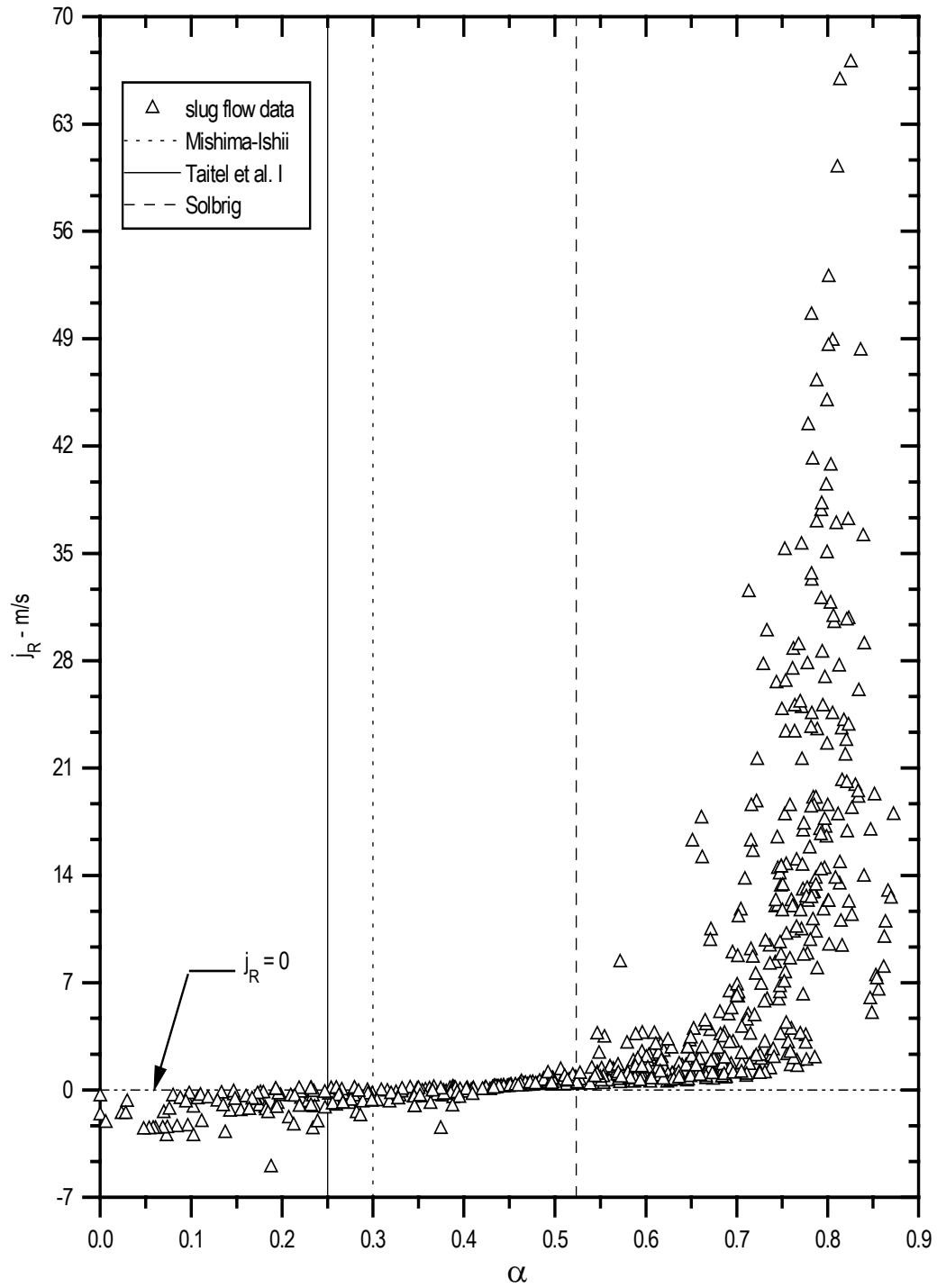


FIG. XIX.IIIb. Comparison of slug flow data with various bubbly-slug transition criteria.

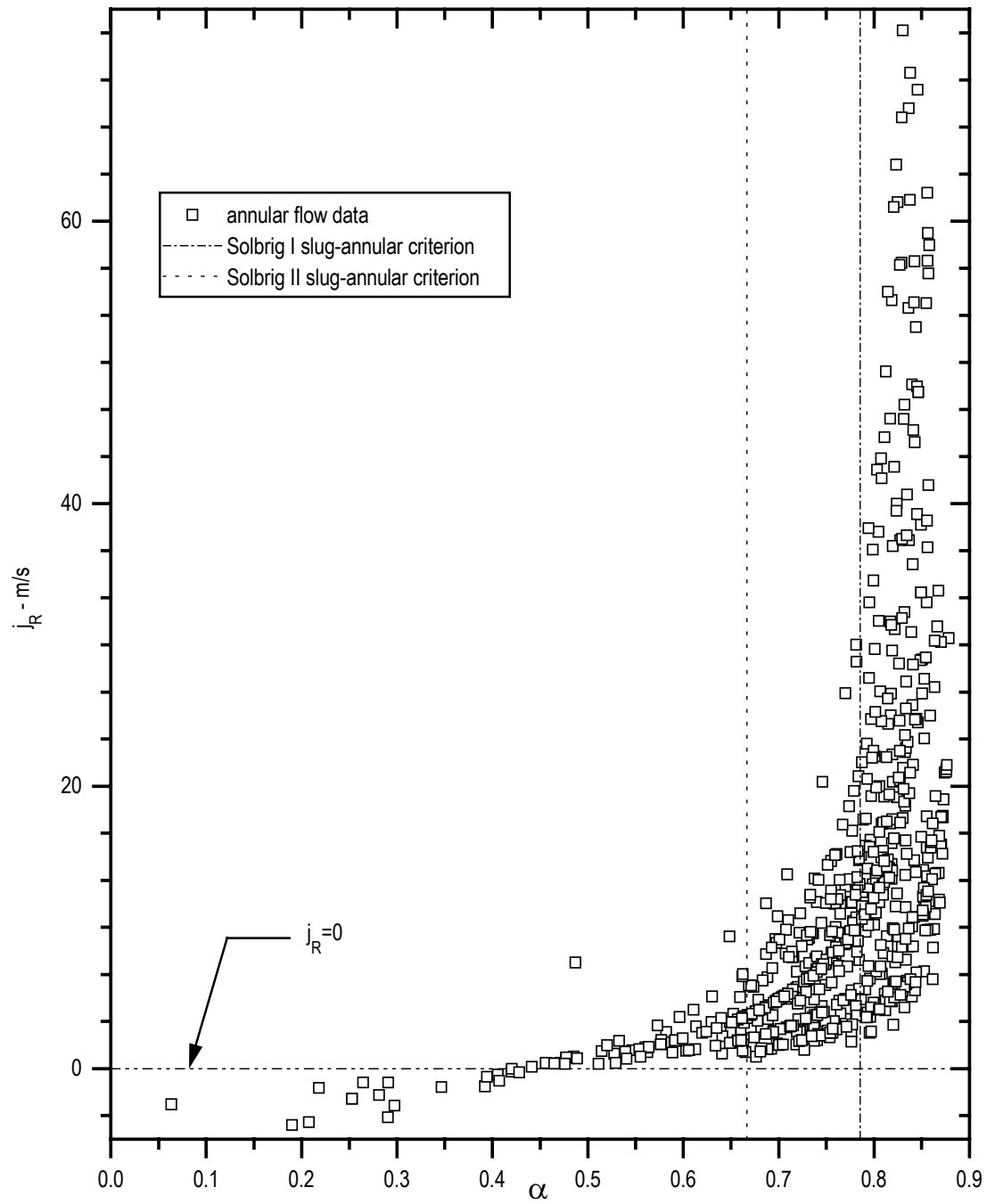


FIG. XIX.IIIc. Comparison of annular flow data with various slug-annular transition criteria.

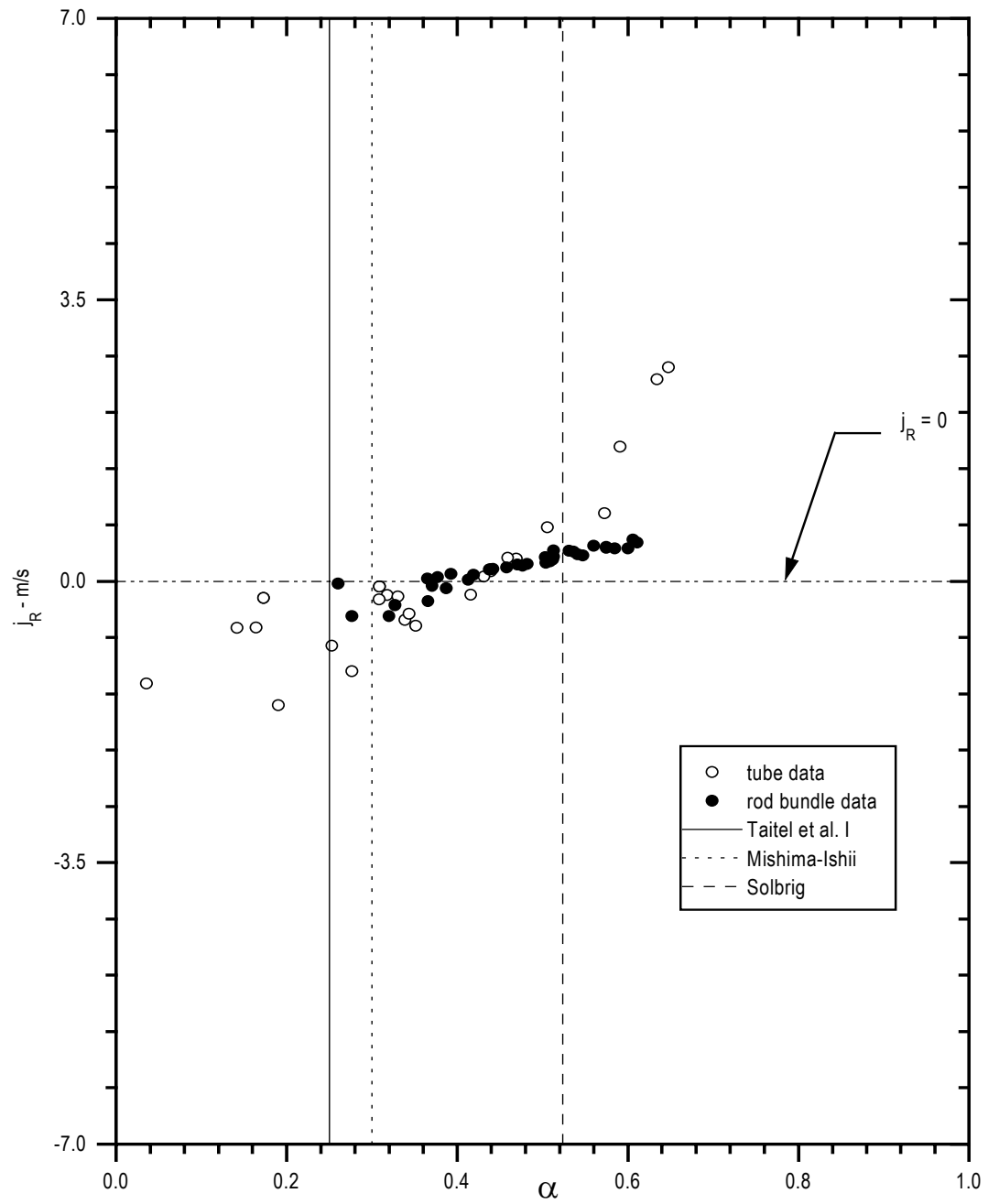


FIG. XIX.IV. Comparison of bubbly-slug transition data with various bubbly-slug transition criteria.

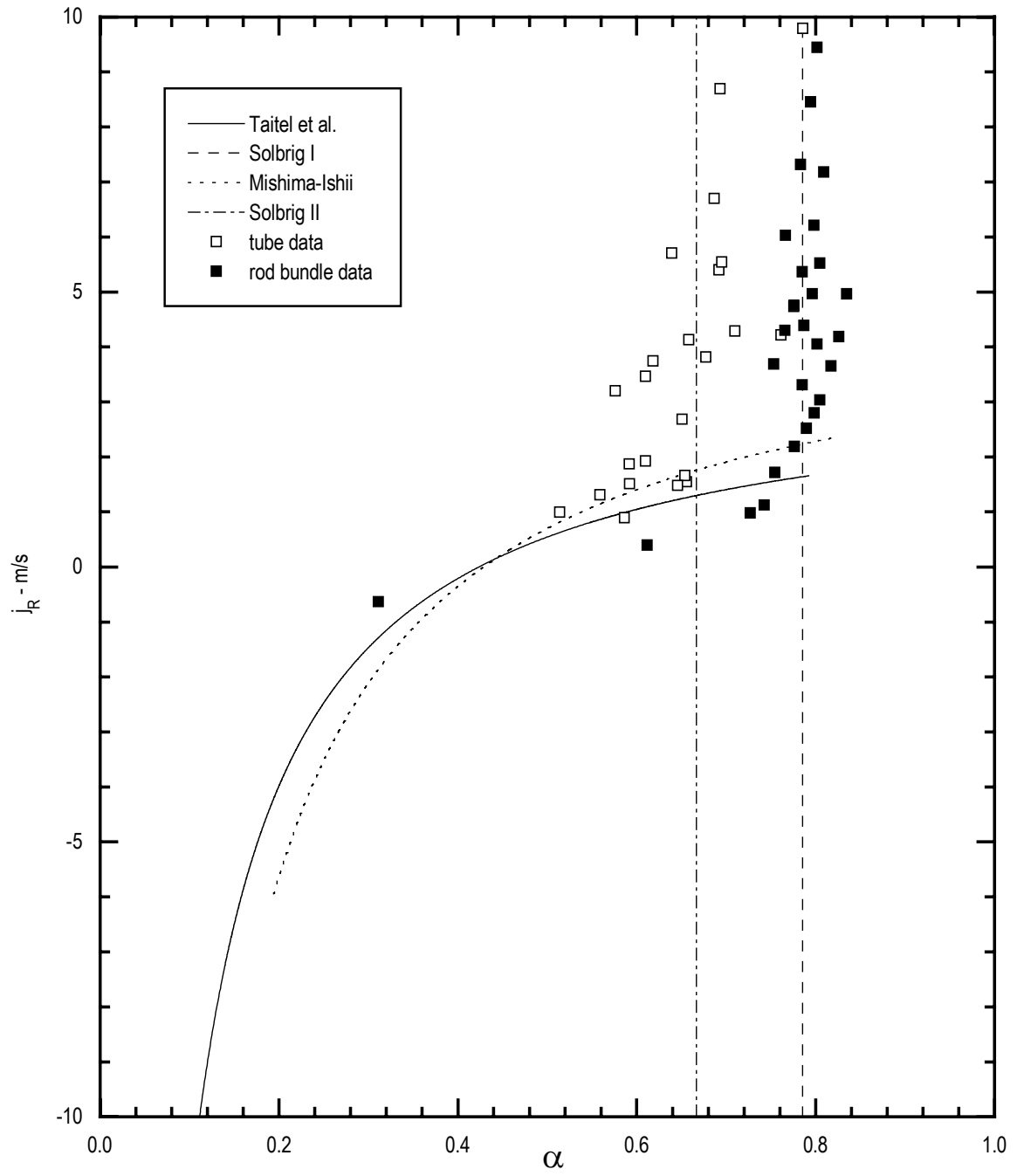


FIG. XIX.V. Comparison of the slug-annular transition data with various transition criteria at 7 MPa.

It must be mentioned that no filtering/screening of the raw data was done for the steam-water and refrigerant two-phase flow. These data were obtained at relatively high system pressure and the errors due to specific volume change is not significant. However, most air-water data are obtained at near atmospheric pressure and errors due to specific volume change are significant in some cases. Such data are excluded from the data bank. A large body of available air-water data do not qualify for inclusion in the data bank.

3. Assessment procedure

In principle, the flow pattern transition criteria must be assessed against flow pattern transition data. However, since the amount of transition data are limited, each transition criterion is tested with the flow pattern data before and after the transition. For example, the bubbly-slug transition criterion is tested with bubbly and slug flow data. Such an approach is followed while testing the transition criteria by Taitel et al. and Mishima-Ishii. However, this approach is only an approximate test of the transition criteria as the flow pattern data can be located far away from the transition point.

The flow pattern transition criteria when plotted in the j_G - j_L plane, will depend on the tube diameter, pressure and fluid used. Therefore, flow pattern transition criteria need to be assessed for each tube diameter, pressure and fluid. However, Khare et al. (1997) showed that if the experimental data are plotted in α - j_R plane, then a single graph can be used for the entire data, irrespective of the fluid, tube diameter, pressure, etc. for the assessment of the bubbly-slug transition criteria proposed by the different authors. Also, the flow pattern data showed a definite trend when plotted in the α - j_R plane. Therefore, the α - j_R plane was chosen for the assessment of the bubbly-slug transition criteria.

For the above assessment procedure, the void fraction and relative velocity are to be calculated for each flow pattern data. In cases, where the data are available in terms of j_G and j_L , the j_R is calculated as $j_R = j_G - j_L$. For calculating the void fraction, the Zuber-Findlay (1965) correlation is made use of. It may be noted that j_R is always obtained directly from measured data whereas α is not measured but calculated. In cases, where the data are given in terms of the mass flux and quality, the j_G and j_L are estimated as $j_G = Gx / \rho_G$ and $j_L = G(1 - x) / \rho_L$.

The results of this analysis are shown in Figs. XIX.IIIa, b and c for bubbly, slug and annular flow. The trends of the bubbly and slug flow data given in Figs. XIX.IIIa and b suggest that an essential requirement for the bubbly to slug flow transition is a near zero relative superficial velocity. This is further confirmed by the experimental bubbly-slug transition data plotted in Fig. XIX.IV. The transition data also clearly shows that there is no unique value of α for bubbly to slug flow transition. The transition from bubbly flow to slug flow depends on the relative superficial velocity and void fraction. None of the criteria used in the present assessment reproduces the trend of the transition data well.

Fig. XIX.V compares the experimental slug-annular transition data contained in the data bank with various slug-annular transition criteria. Clearly, none of the proposed criteria reproduces the trend of the transition data. However, the Solbrig I criterion is closer to the pipe data whereas Solbrig II criterion is closer to the rod bundle data indicating that the slug-annular transition criterion can be geometry dependent.

Annex A

INTERNATIONAL NUCLEAR SAFETY CENTER DATABASE

A.1. DATABASE PURPOSE AND CONTENTS

The United States Department of Energy (USDOE) and the Russian Ministry of Atomic Energy (MINATOM) signed a joint statement in September 1995 to establish International Centers for Nuclear Safety. As a result, in October 1995 the International Nuclear Safety Center (INSC) was established at Argonne National Laboratory (ANL). The Russian INSC was established in Moscow in July 1996. Initially hosted at the Research and Development Institute of Power Engineering, the Russian INSC is currently an independent organization within MINATOM.

The main goal of the International Nuclear Safety Center is to collaborate with other nations to advance the development and use of nuclear safety technology and the dissemination of nuclear safety information.

A key element for the INSC to accomplish its main goal is the development of an International Nuclear Safety database accessible electronically through the World Wide Web. The main purpose of the INSC database is to foster the international exchange of nuclear safety-related information with the aim of supporting worldwide improvements in civilian nuclear safety.

The International Nuclear Safety Center Database is a comprehensive World Wide Web- based resource for safety analysis and risk evaluation of nuclear power plants and other nuclear facilities all over the world. The readily available World Wide Web technology allows easy access to the database from anywhere in the world. Although most of the provided information is available to the public, mechanisms have been put in place to restrict access to proprietary information only to selected individuals or sites.

Although the scope of the database is worldwide, the current focus is on Soviet-designed nuclear power plants in Russia and Eastern Europe, and on reactor types in China and India. This and the pages referenced hereon provide an outline for the database and serve as a core for further development.

The database is being implemented by the Reactor Analysis Division at Argonne National Laboratory using the division's Unix-based workstation network. Information cataloging and database maintenance is performed with the Oracle[®] database management system providing controlled access to database elements based on user identity and access level authorization. The database and its content are verified and maintained in compliance with applicable quality assurance standards and practices.

Currently, the INSC database maintained at ANL contains the following information:

- Basic information on about 600 Power Reactors in 35 countries.
- Links to the US NRC database for plant technical documentation of 113 operable US reactors.

- Basic Plant Parameters for other selected reactors.
- Information for 590 Research Reactors in 74 countries.
- Information for 560 Fuel Processing Facilities in 44 countries.
- Bibliography of Reports and Documents.
- Computational Tools and Input Data Sets.
- The database provides access to Material Properties to meet the needs of analysts using computer codes and doing experiments for safety evaluation of nuclear reactors and other facilities. The focus is on LWRs, with an initial emphasis on materials unique to Soviet nuclear reactor designs. Categories are Fuel, Cladding, Absorber Materials, Structural Materials, Coolant, Concretes, and Severe Accident Mixtures. Part of this database has been established in collaboration with the IAEA.
- Descriptions, summaries, and results of the joint projects between the US and Russian International Nuclear Safety Centers.
- Collaboration clipboards are implemented to serve as an electronic forum to facilitate structured interorganizational communication among the participants of INSC related activities.
- Links to other information resources and databases allow access to additional sources of information interesting for the typical INSC Database user, such as the INSP Database at the Pacific Northwest National Laboratory.
- Currently under development: thermohydraulics data provided through the IAEA's Coordinated Research Programme (CRP) on Thermohydraulics Relationships for Advanced Water-Cooled Reactors.

Through the collaboration between the US and Russian International Nuclear Safety centers it has been possible to expand the resources of the INSC database, by adding additional data sources on remote Web sites such as the Russian INSC in Moscow, or other Russian organizations. The database architecture is such that the resources of the databases at the US and Russian Centers can be linked together transparently, allowing for a flexible and scalable platform for future development.

There are several institutes in other countries that perform work in collaboration with the US International Nuclear Safety Center. The database provides links to those institutes and their network resources and may hold additional materials regarding collaboration between the US and other countries in the future.

- A new Lithuanian INSC Web Site was established at the Lithuanian Energy Institute in Kaunas, Lithuania. This web site is under development and will provide access to detailed data on Lithuanian nuclear facilities.
- The Nuclear Safety Institute of the Russian Academy of Sciences (IBRAE) maintains a Web Site and provides access to detailed information on the Kola nuclear power plant and especially its Reactor #4. This data was collected and installed using USDOE funds and in collaboration with the US INSC. Other projects resulted in the establishment of a materials properties database for high temperatures to be used for the simulation of reactor accidents.

The INSC Database can be reached at:

<http://www.insc.anl.gov>

or, by e-mail, the database manager can be contacted:

inscdb@anl.gov or by Fax, at (630) 252-6690

A.2. THERMOHYDRAULICS DATA IN THE INSC DATABASE

The database on thermohydraulics data within the INSC database has been initiated as a result of the Coordinated Research Programme (CRP) on Thermohydraulic Relationships for Advanced Water-Cooled Reactors established under the auspices of the International Atomic Energy Agency (IAEA).

Organizations participating in the CRP are providing their experimental data for its storage on the INSC database. The thermohydraulics database can be currently reached at the following Web address:

<http://www.insc.anl.gov:/thrmhydr/iaea>

After the data providers review the contents, the database will be accessible through a subsection in the home page of the INSC database (www.insc.anl.gov).

The current contents of the database are as follows:

- Look-up table for Critical Heat Flux (CHF) in 8-mm tubes, developed by the Atomic Energy of Canada Limited (AECL) and the Institute of Physics and Power Engineering (IPPE) in Obninsk, Russia.

Look-up tables available provide values of CHF at discrete values of pressure, quality, and mass flux. The ranges of the three parameters are from 0.1 to 20 MPa of pressure, 50% to 100 % of vapor quality, and 0 to 7500 kg m⁻² s⁻¹ of mass flux.

The database contains multiple tables and graphic representations that permit finding the CHF value for any fix value of one of the three parameters, as a function of the other two parameters. The CHF Look-up table is also included in the TECDOC, Chapter 6.

- CHF databank for WWER reactor applications, contributed by the Nuclear Research Institute (NRI), Rez, Czech Republic. This section contains experimental CHF data for WWER fuel bundles, obtained with the SKODA Large Water Loop Test facility. 166 CHF data points are provided, along with a description of the facility and experimental equipment.
- Look-up table for the post-dryout (PDO) heat transfer in tubes, provided by the Institute of Physics and Power Engineering in Obninsk (IPPE), Russian Federation.

The look-up table was developed for PDO heat transfer in 10-mm tubes. It provides values of the PDO heat transfer coefficient for a range of pressures between 4 and

20 MPa, mass flux between 250 to 2000 kg m⁻² s⁻¹, quality between -0.2 to 2.2, and heat fluxes between 0.2 and 1 Mw m⁻². The PDO heat transfer look-up table is also included in the TECDOC, Chapter 5.

- Look-up table for CHF in WWER rod bundles, contributed by the Institute of Physics and Power Engineering (IPPE) in Obninsk, Russia.

The look-up table is applicable to rod bundles with triangular lattice, a heated diameter of 9.36 mm, and a pitch-to-diameter ratio of 1.4. The CHF values in the table are based on experimental bundle CHF data and predictions based on a semi-empirical model. The range of applicability of the look-up table is for pressures between 1.5 and 20 MPa, mass fluxes between 220 and 5040 kg m⁻² s⁻¹, and qualities between -0.52 and 0.9. The look-up table is also included in the TECDOC, Chapter 4.

In preparation — CHF data from low power and low flow experiments, provided by the Korea Advanced Institute of Science and Technology (KAIST).

In preparation — CHF data for high flow and low pressure conditions, provided by the China Institute of Atomic Energy (CIAE).

In preparation — PDO data for high flow and low pressure conditions, provided by the China Institute of Atomic Energy (CIAE).

Future additions — Documentation of other thermohydraulics relationships in use in nuclear reactor safety analyses.

Annex B

PREPARED METHODOLOGY TO SELECT RANGES OF THERMOHYDRAULIC PARAMETERS

B.1. INTRODUCTORY REMARKS

The thermalhydraulic phenomena of interest for the study of transient behaviour of existing water cooled reactors and for advanced concepts have been discussed in Chapter 2, respectively. An overall view of the foreseeable system behaviour has been given in that respect, [see also Aksan and D'Auria (1993 and 1995)].

In the present chapter the attention is addressed towards the phenomena of direct interest to the CRP, i.e. CHF, film boiling and pressure drops. These are described into detail in Chapters 3, 4 and 5, respectively, where aspects like phenomenology, experiments, modelling, and code capabilities are considered. Before such an evaluation, it is worthwhile to consider the parameters affecting the CHF, the film boiling heat transfer and the pressure drops together with the respective ranges of interest from a reactor design, operation and safety analysis point of view.

The activity should be considered as a pilot study: a systematic and final evaluation, specifically including an optimized selection of relevant combinations among ranges, would require resources that are well beyond the limits of the present activity. However, the objective can be reached in the present framework of making available ranges of parameters suitable for evaluating the existing data base, for deriving a more objective judgement about code capabilities and for planning further activities in the area.

With reference to each of the three phenomena, four groups of quantities are distinguished: this is considered as sufficient information to characterize the phenomenon (Section B.2). Ranges of variations are identified in Section 3B, making reference to the variables selected in the previous section and to the situations expected to be of interest to water cooled reactors (both current generation and advanced concepts).

B.2. QUANTITIES CHARACTERIZING THE PHENOMENA

Each thermalhydraulic phenomenon, specifically if it occurs during a complex transient, depends upon a large number of parameters. The "importance" on the phenomenon of the various parameters is clearly different among each other; a detailed ranking implies the use of subjective judgement; the "importance" may be a function of the range of variation of the parameter.

In this context, with the aim of characterizing as far as possible each phenomenon, an attempt is made to select a necessary/sufficient number of parameters suitable for such a purpose. Four groups of parameters are identified, connected, respectively with:

- (a) geometry (local and system geometry including microscopic surface geometry);
- (b) thermalhydraulic boundary and initial conditions (e.g. thermal flux distribution in the case of CHF and film boiling), including flow conditions;
- (c) material properties/constitutive laws;
- (d) transient effects (i.e. time variations of any quantity).

B.2.1. CHF

Critical heat flux is important in different conditions of a nuclear plant and may occur in different locations (see also Chapter 3): typical conditions are accident (e.g. DBA), operational transient, coupled neutronic thermalhydraulic instabilities (in BWR); typical locations are core and steam generators (in PWR). However during a LOCA, CHF may occur in the majority of the structures of the primary circuit also affecting the heat release to the fluid. In addition, the knowledge of CHF is of fundamental importance for the fuel design. A review of the present state of the art including identification of important parameters affecting the phenomena and predictive capabilities of the models and of associated system codes can be found in Ninokata and Aritomi (1992) and NED Issue dedicated to the Memory of Prof. K. Becker (1996).

With reference to the four groups of parameters identified above, the considerations and the choices below are made.

a) Geometry.

The investigation is limited to vertical rod bundles, i.e. at least a 2×2 configuration, though other configurations like single rod, single tube, tube bundles, plate, large unheated cylinder, horizontal or inclined fuel bundle, etc., are of interest in the technology.

In this assumption, the considered geometric parameters are:

- g1) rod diameter;
- g2) channel equivalent diameter (including the effects of surface roughness, pitch/diameter ratio, distance from unheated wall, etc.);
- g3) heated length.

It may be noted that parameters like array type (square or triangular), presence and configuration of the fuel box, configuration of the fluid entrance, presence and configuration of spacer grids, presence of oxide layer, roughness, etc., are not directly considered (see the previous discussion). In addition, equivalent diameter is assumed to include the information connected with different geometry related parameters.

b) Thermalhydraulic boundary and initial conditions.

The following parameters are selected:

- t1) pressure;
- t2) liquid temperature at channel inlet;
- t3) linear power (uniform/constant axial distribution);
- t4) power shape;
- t5) channel inlet flow/fluid velocity (i.e. mass flux, assumed to be single phase subcooled liquid);
- t6) rod surface temperature.

It is assumed that the values of parameters like channel exit equilibrium quality, flow pattern, local void fraction, etc., can be calculated as a function of the parameters above and

below. Rod surface temperature (item t6), has been added for completeness; it depends also upon heat transfer coefficient (i.e. from a number of parameters not explicitly reported here) and upon parameters directly considered here. Radial flux distribution in the bundle is assumed flat; so element flux tilt is not considered.

c) Material properties/constitutive laws.

It is assumed that only the fluid and the cladding base material affect the phenomenon. Aspects like oxide/crud formation are neglected together with the internal configuration of the rod (cladding thickness, gap conductivity, etc.).

In these assumption the following parameters are considered:

- m1) cladding material thermal capacity;
- m2) latent heat of vaporization;
- m3) liquid/steam density ratio;
- m4) surface tension.

d) Transient effects.

Most of the information (both experiments and correlations) connected with CHF is directly related to stationary conditions. However, in practical situations, "quasi" steady state and unsteady conditions must be distinguished. It is assumed that "quasi" steady conditions can be dealt with stationary conditions as characterized above. In order to stress the importance of unsteady situations the following parameters are introduced (not exhaustive list; individual time variations of parameters like pressure, flow, etc. can be important, as well as combinations of simultaneous transients involving flow-pressure-power, etc.; in addition, for the sake of simplicity, conditions including oscillatory flows are not taken into account):

- v1) time variations (slope and duration of the power excursion) of local linear power;
- v2) oscillations characteristics of local linear power.

B.2.2. Film boiling

In the case of film boiling the same quantities considered for CHF are important and should be used for defining the Phenomenological Areas (Ph. A.— see below); an exception to this is represented by the parameter m3 that seems uninfluent for the film boiling phenomenon. with main reference to the groups of parameters a to d, the following quantities should be added, [see also Hewitt and Delhay (1992)].

- g4) aspect ratio (geometry related parameter assumed representative for simulating radiation heat transfer phenomena);
- t7) fluid temperatures inside the channel (both steam and liquid if present or applicable);
- t8) temperature (including spatial distribution) of the structural materials heat sink;
- m5) thermal radiation emissivity and absorption coefficient for the fluid;
- m6) thermal radiation emissivity and absorption coefficient for the structural material.

B.2.3. Pressure drops

Pressure drops are clearly important in different (all) the parts of the nuclear power plants, including primary and secondary loop: their characterization is of fundamental interest for steady state and transient situations. With regard to both local pressure drop and distributed pressure drop types, the system geometry plays a decisive role together with the condition of "fully developed" flow. Strictly speaking, no zone of a typical water cooled reactor can be identified where the "fully developed" flow situation applies, with the possible partial exception represented by parts of the tubes in steam generator primary side in Western PWR equipped with U-Tubes or with Once-Through steam generators.

A systematic and comprehensive search of all the parameters affecting the pressure drop in all the situations of interest in a Water Cooled Reactor, is again well outside the purpose of the present activity.

In addition, the consideration of transient situations may imply the introduction of parameters like the flashing delay, the number of nucleation sites, etc. on the experimental side, and the consideration of the time derivative terms on the code side.

Considering the above, the field of investigation has been dramatically restricted making reference to the situation of steady state in a vertically heated boiling channel without internal restrictions (i.e. spatial grids, obstructions, etc.).

Reference is made hereafter to the total pressure drop per unit length (i.e. Pa/m) in a situation where the "fully developed" flow condition is applicable. It must be noted that the wall-to-fluid friction, the gravity and the "spatial" acceleration, contribute to the considered quantity. In the following, parameters affecting the pressure drop per unit length are identified.

a) Geometry.

The drastic assumptions made, bring to these parameters (the "span", characterizes the distance along the flow direction between two pressure taps that are connected to a pressure transducer):

- g1) channel equivalent diameter;
- g2) length of the considered span divided by the channel length;
- g3) bottom elevation of the span divided by the channel length.

Equivalent diameter is assumed, again, to include information connected with different geometry related parameters.

b) Thermalhydraulic boundary and initial conditions.

The following parameters are selected:

- t1) absolute pressure (at channel inlet);
- t2) liquid temperature at channel inlet;
- t3) linear power (uniform/constant axial distribution);
- t4) channel inlet flow/fluid velocity (i.e. mass flux, assumed to be single phase subcooled liquid);
- t5) rod surface temperature.

It might be noted that power shape is assumed to have a second order effect if the selected span length over channel length is sufficiently small. Rod surface temperature may significantly affect pressure drop specifically in cases where it separates wetted from unwetted zones. The information about parameters t_1 , t_2 , t_3 and t_4 allows the evaluation of local void fraction, local velocities and flow regimes that may have a strong impact on the calculation of pressure drop (clearly there may be a feedback between these values and the pressure drop value).

c) Material properties/constitutive laws.

In these assumption the following parameters are considered:

- m1) liquid viscosity;
- m2) steam viscosity;
- m3) liquid/steam density ratio;
- m4) surface tension.

It should be noted that a number of parameters connected with the interaction between liquid and steam at the interface (e.g. interfacial drag, interfacial area, bubble or droplet sizes, etc., including those causing a flow regime instead of another) may largely affect the pressure drop. Measurement difficulties suggest not to include these parameters in the list.

B.3. RANGES OF VARIATION

When a reference phenomenon is assigned in reactor safety and design technologies (i.e. one of the 67 phenomena in Chapter 2), the definition of *ranges of variations* may be important in different frameworks:

- a) ranges of validity of a correlation;
- b) ranges of availability of experimental data;
- c) expected ranges of variations in nuclear power plants.

The ranges of validity of a correlation (item a), imply the knowledge of the ranges of variations of relevant quantities considered by the "independent" assessment of the correlation. If the correlation (or the model) is implemented in a system code, this also implies the verification of the built-up model including the possible influence from other parts of the code. The ranges of validity also signify suitable ranges of availability (next item).

The ranges of availability (item b), imply the knowledge of the experimental researches carried out in the scientific community all over the world; suitable data are needed, so aspects like experimental facility design criteria, boundary conditions for the tests, sources and quantification of errors, quality of instrumentation and of recorded data, must be evaluated. In addition, once the ranges needed for the investigation are known (next item), preliminary scaling studies should be carried out: this could avoid the need of systematically covering, in the experiments, the whole ranges of selected parameters.

The expected ranges of variations in the plants (item c), imply the knowledge of plant transient scenarios and the deep understanding of phenomena; this, necessarily, also depends upon activities leading to items a) and b). These links must be recognized. when searching for

the ranges of variations in the plants, attentions should also be paid to the interactions among the ranges. For instance, in the case of CHF, hypothetical ranges for linear power, pressure and flowrate could be 0.1–50 kW/m, 0.1–20 MPa and 5–30000 kg/m²s, respectively; in this case a power of 50 Kw/m may not occur at low pressure; again, the occurrence of the low flow condition (i.e. 5 kg/m²s) might have very low probability when extreme (high) values of pressure or power are of interest. As a summary, ranges intersections should be considered.

In addition, Phenomenological Areas (Ph. A.) are introduced in the present analysis considering relevant intersections of the parameters ranges (parameters are those defined in Section B.2).

The identification of parameter ranges and, as a consequence, of phenomenological areas, include engineering judgement connected with:

- (1) choice of relevant parameters: e.g. steam or liquid velocities can be selected instead of liquid velocity and slip ratio, channel inlet quantities can be selected instead of local quantities;
- (2) the consideration of the mutual interactions between various phenomena: CHF may be affected by pressure drop, so parameters relevant for pressure drop are inherently relevant for CHF;
- (3) level of detail of the analytical or of the experimental investigation: the bubble diameters or bubble density may be important parameters to be used in addition to (or instead of) void fraction; 2-D or 3-D local system behaviour including cross section parameter distributions (e.g. velocity profiles in a cross section) may also be important.

Owing to all of the above the present one must be considered as a pilot study; as such the ranges of parameters and the phenomenological areas are limited to the CHF phenomenon.

Assuming that zircaloy and water are the only materials involved, in the case of CHF, the characterization of the ranges of parameters becomes simpler; in this case, material properties (parameters m1 to m6), are implicitly identified and depend upon other parameters here considered: their ranges of variations are not reported here.

B.3.1. Ranges of parameters for CHF

The following ranges apply:

g1) 0.006–0.013	m	(1)
g2) 0.002–0.015	m	(1)
g3) 1.0–4.5	m	(11)
tl) 0.1–20.	MPa	(2)
t2) 0–150.	K	(3)
t3) 0. 1–20.	kW/m	(4)

t4) 1–2. 5	-	(5)
t5) 0–15000.	kg/m ² s	(6)
t6) 0–40.	K	(7)
v1) 0–20.	kW/ms	(8)
1–2.	S	(9)
v2) 0.1–2.	Hz	
5–200%	-	(10)

- (1) this also includes advanced reactor and advanced fuel design;
- (2) four sub-ranges identified (these are needed for the definition of the Phenomenological areas, see below):
t1a) 0.1–2.5 MPa; t1b) 2.5–7.5 MPa; t1c) 7.5–16. MPa; t1d) 16–20 MPa;
- (3) subcooling value;
- (4) only the maximum values of the average linear power are considered here; absolute maximum linear power should be obtained by multiplying this value with the value at item t4; maximum "transient" power value (i.e. power excursion) needs consideration of item v1;
- (5) three power shapes identified: t4a (chopped) cosine with central peak; t4b bottom peaked: chopped cosine in the bottom 1/3 of the active length and uniform power in the upper 2/3 of the active length; t4c top peaked: uniform power in the bottom 2/3 of the active length and chopped cosine in the upper 1/3 of the active length. It is important to add that all the above is related to a vertical bundle and is not directly applicable to the CANDU geometry;
- (6) or 0–15 m/s;
- (7) 0. and 40 K are the minimum and the maximum temperature difference expected between the rod surface and the fluid, respectively;
- (8) linear variation of the generated power;
- (9) duration of the assumed triangular peak power trend;
- (10) amplitude of the power oscillation related to the actual linear power;
- (11) in the case of CANDU the upper limit must be extended to 6.0 m.

B.4. PHENOMENOLOGICAL AREAS

The definition of Phenomenological Areas (Ph. A.) constitutes the final step of the activity and requires additional assumptions. One parameter is assumed as the leading parameter.

B.4.1. CHF

The system pressure (parameter t1) is assumed as leading parameter and four sub-ranges are identified as given in Section B.3.1 on this basis the following Ph. A. are identified (e.g. PA.1 = Phenomenological Area 1; in addition "X" means that the overall range must be considered as reported in Section B.3.1):

	t1	t2	t3	t4	t5	t6	g1	g2	g3	v1	v2
PA.1	t1a	0-50	0.1-2	t4a	0-2000	X	X	X	X	X	X
PA.2	t1b	0-100	1-20	t4a,b,c	1000-15000	X	X	X	X	X	X
PA.3	t1c	0-150	1-20	t4a,b,c	1000-15000	X	X	X	X	X	X
PA.4	t1d	0-150	10-20	t4a	5000-15000	X	X	X	X	X	X

B.5. FURTHER ACTIVITIES

The comparison between the ranges of phenomena available from experimental programs, [Aksan and D'Auria (1993)] and the boundaries of the phenomenological areas, might give a direct information about the need for future experiments.

The phenomenological areas can be used to define ranges of validity (or of the best suitability) for correlations or codes and, as a follow up of the evolution of codes/correlation deficiencies, eventually for planning improvements or new developments.

Large amounts of resources can be envisaged for finalizing the systematic approach here proposed in the areas of planning of new experiments, advanced correlation or new codes.

REFERENCES TO ANNEX B

AKSAN, S.N., et al., 1993, Separate Effect Test Matrix for Thermalhydraulic Codes Validation: Phenomena Characterization and Selection of Facilities and Tests — Vol. III, OECD/CSNI Rep. OCDE/GD(94)82, Paris (F).

AKSAN, S.N., et al., 1994, Thermalhydraulic Phenomena in the CSNI Separate Effect Validation Matrix, Int. Conf. on New Trends in Nuclear System Thermalhydraulics, Pisa (I).

AKSAN, S.N., et al., 1995, Overview of the CSNI Separate Effects Tests Validation Matrix, NURETH-7, Saratoga Springs.

HEWITT, G.F., DELHAYE, J.M., ZUBER, N., (Eds), 1992, "Post-dryout heat transfer", Multiphase Science and Technology, CRC Press.

NINOKATA, H., ARITOMI, M., (Eds), 1992, Subchannel Analysis in Nuclear Reactors; Proc. Int. Sem. on Subchannel Analysis, Tokyo.

NED ISSUE DEDICATED TO THE MEMORY OF PROF. K. BECKER, 1996, J. Nucl. Eng. Design **163** 1–2.

CONTRIBUTORS TO DRAFTING AND REVIEW

Akimoto, H.	Japan Atomic Energy Research Institute, Japan
Baek, W.P.	Korea Advanced Institute of Science and Technology, Republic of Korea
Bobkov, V.P.	Institute of Physics and Power Engineering, Russian Federation
Cevolani, S.	ENEA, ERG/FISS, Italy
Chang, S.H.	Korea Advanced Institute of Science and Technology, Republic of Korea
Chen, Y.Z.	China Institute of Atomic Energy, China
Cheng, X.	Kernforschungszentrum Karlsruhe, Germany
Chung, M.K.	Korea Atomic Energy Research Institute, Republic of Korea
Ivashkevitch, A.A.	Institute of Physics and Power Engineering, Russian Federation
Leung, K.H.	Chalk River Laboratories, Canada
Macek, J.	Nuclear Research Institute, Czech Republic
Pilkhwal, D.S.	Bhabha Atomic Research Centre, India
Roglans-Ribas, J.	Argonne National Laboratory, United States of America
Smogalev, I.P.	Institute of Physics and Power Engineering, Russian Federation
Tanrikut, A.	Turkish Atomic Energy Authority, Turkey
Venkat Raj, V.	Bhabha Atomic Research Centre, India
Vijayan, P.K.	Bhabha Atomic Research Centre, India
Vinogradov, V.N.	Institute of Physics and Power Engineering, Russian Federation
Yesin. O.	Middle East Technical University, Turkey

